VNIVERSITAT DE VALÈNCIA Facultat de Química

Tesis Doctoral

Desarrollo y evaluación de metodologías de microextracción para el análisis de volúmenes pequeños de muestra

José Grau Escribano

Programa de Doctorado en Técnicas Experimentales en Química (3158)

Directores:

Alberto Chisvert Sanía

Amparo Salvador Carreño

Octubre 2022

La realización de esta tesis doctoral ha sido posible gracias a la ayuda predoctoral concedida por la Conselleria d'Educació, Investigació, Cultura i Esport de la Generalitat Valenciana y el Fondo Social Europeo (ACIF 2017/328).

Prólogo

Soy consciente de que aquí deberían incluirse todos los agradecimientos, pero no va a ser el caso. Y no se equivoquen, tengo mucho que agradecer a muchas personas, es solo que no creo poder expresar lo afortunado que soy de que estén a mi lado.

También soy consciente, como no podría ser de otra forma, de que esta tesis no es perfecta. Ya que, por suerte, siempre cometemos errores que nos ayudan a crecer.

Pero sí hay algo que le puedo asegurar, queridx investigadorx. Y es que estas páginas han sido escritas con sangre, sudor y muchas lágrimas; con largas noches de insomnio y con miedo a caer. Pero también con cariño e ilusión; con risas en el laboratorio y con ganas de volver a levantarse.

Ojalá pueda disfrutar de estas hojas como yo lo he hecho escribiéndolas o, por lo menos, que encuentre esa frase, esa referencia o esa figura que lleva todo el día buscando y aún no ha logrado encontrar. Eso es lo de menos, lo importante es que no deje de buscar.

A usted, queridx investigadorx, gracias.

ÍNDICE

RESUMEN/ABSTRACT

El empleo de técnicas de microextracción ha permitido el desarrollo de métodos analíticos de elevada sensibilidad. Además, ha conseguido reducir el empleo de disolventes orgánicos y otros compuestos tóxicos, permitiendo así trabajar acorde con los principios de la denominada Química Analítica 'Verde' en general (***Green Analytical Chemistry***, **GAC**) y, en particular, en la etapa de preparación de la muestra (***Green Sample Preparation*, GSP).**

No obstante, la miniaturización de estas técnicas, en ocasiones, descuida la miniaturización del volumen de muestra, a pesar de las múltiples ventajas que esta aporta, como son la reducción, todavía mayor, de volúmenes de disolvente, cantidad de sorbente y de residuos. Sin olvidar la limitación que, a veces, se tiene cuando se lleva a cabo el análisis de fluidos biológicos, ya sea por la naturaleza de la muestra, o por el paciente sometido a estudio.

Por ello, el objetivo de esta tesis es el estudio de estos beneficios, no solo en relación a la etapa de preparación de muestra, sino también en el muestreo, donde al utilizar un menor volumen de muestra, este será menos invasivo; y la síntesis del sorbente, ya que se disminuirá la cantidad de sorbente a utilizar, permitiendo con una misma síntesis realizar más análisis. Para ello, se han desarrollado y evaluado métodos analíticos que hacen uso de técnicas de microextracción desarrolladas por el grupo de investigación presente en el contexto de esta Tesis Doctoral, reduciéndose cada vez más el volumen de muestra necesario. Estos métodos han sido evaluados y comparados desde el punto de vista de sostenibilidad y seguridad para el operador.

La tesis se ha dividido en 4 secciones que engloban un total de 7 capítulos

En la **Sección 1** se incluye un capítulo de introducción (**Capítulo 1**) en el que se da una visión general de las técnicas de microextracción, tanto basadas en sorbentes como en disolventes, estudiando sus ventajas e inconvenientes y la evolución de las mismas para su acercamiento a los principios de la GSP y la GAC. Además, se estudia la adaptación de las técnicas de microextracción para su empleo con volúmenes de muestra reducidos y los beneficios que ello aporta.

En la **Sección 2** se incluyen los **Capítulos 2, 3** y **4** en los que se desarrollan y aplican métodos analíticos en los que el volumen de muestra analizado es relativamente elevado (en torno a los 20 mL). En concreto, en el **Capítulo 2**, se muestra la determinación de trifenilfosfato y difenilfosfato en muestras de orina utilizando la microextracción en fase sólida dispersiva sobre barra

agitadora (***Stir Bar Sorptive Dispersive Microextraction*, SBSDME**). En el **Capítulo 3** se aplica la SBSDME para la determinación de almizcles en muestras medioambientales. En el **Capítulo 4** se presenta un nuevo ferrofluido basado en un disolvente eutéctico profundo de baja toxicidad compuesto por mentol y timol para la determinación de trazas de filtros UV en aguas medioambientales, derivadas del uso de productos cosméticos para la protección solar.

La **Sección 3** se compone de los **Capítulos 5** y **6**, en los que se proponen métodos diseñados específicamente para el trabajo con volúmenes bajos de muestra (en torno a 500 µL). En concreto, en el **Capítulo 5**, se muestra una modificación de la extracción en fase sólida dispersiva asistida por disolvente (***Solvent Assisted Dispersive Solid Phase Extraction*, SA-DSPE**) para la determinación de cortisol y cortisona en muestras de saliva. En el **Capítulo 6** se presenta la técnica microextracción en punta de pipeta basada en sorbentes magnéticos ***(Magnetic-based Pipette Tip Microextraction,* M-PTME)** mostrando la determinación de testosterona en muestras de saliva como prueba de concepto.

La **Sección 4** la compone únicamente el **Capítulo 7,** en el que se emplea una versión miniaturizada de la técnica introducida en el **Capítulo 6** donde se lleva a cabo la determinación de cortisol en suero y orina de recién nacidos prematuros como prueba de concepto.

Por último, se muestran las conclusiones de la presente Tesis Doctoral y se incluyen los artículos publicados que dieron lugar.

The use of microextraction techniques has allowed the development of sensitive analytical approaches. Moreover, these miniaturized techniques has achieved the reduction of organic solvents and other toxic compound,. in accordance with the principles of Green Analytical Chemistry and Green Sample Preparation.

However, the miniaturization of these techniques tend to forget the miniaturization of the sample, despite their multiple advantages that it presents, such are the reduction, even more, of the amount of organic solvents, sorbent and wastes. Not forgetting the limitation when biological samples are analysed due to the nature of the sample or the patient under study.

For that reason, the objective of these PhD is to study these benefits, not only in the sample preparation steps, but also in sampling, where the reduction of the sample volume allows to perform less invasive sampling; and synthesis stages, since the reduction of the sorbent amount allows to perform more analysis with just one synthesis. In that aim, different analytical methods based on microextraction techniques have been developed by our research group during the realization of this thesis, reducing the sample volume needed for the analysis. These methods have been evaluated and compared from a sustainability and safety perspective.

Thus, the thesis have been organized in 4 sections with 7 chapters. In the **Section 1**, is included an unique introduction chapter (**Chapter 1**). This one includes an overview of the most common microextraction approaches either liquid or sorbent-based, including the pros and cons and their evolution. Moreover, it is discussed how some of these microextraction techniques have been adapted to perform analysis of small sample volumes.

Section 2 includes the **Chapters 2, 3 and 4,** which are focused on the use of analytical methods for the analysis of relatively high sample volumes (around 20 mL). In **Chapter 2**, it is shown the determination of triphenyl phosphate and diphenyl phosphate in urine by the employment of stir-bar sorptive dispersive microextraction (SBSDME). **Chapter 3** is also an application of SBSDME for the determination of nitro-musks in environmental waters. In **Chapter 4**, it is presented a new ferrofluid based on a low toxicity deep eutectic solvent composed by thymol and menthol that was employed for the determination of UV filters in environmental waters.

Section 3 is composed by **Chapters 5 and 6**, with new methodologies that have been designed for the analysis of small sample volumes (around 500 µL). **Chapter 5**, presents a modification of the solvent assisted-dispersive solid phase extraction (**SA-DSPE**) that is employed to extract cortisol and cortisone from saliva samples. In **Chapter 6**, is presented a new pipette-tip based extraction technique called magnetic-based pipette tip microextraction **(M-PTME)** that was tested on the determination of testosterone also in saliva samples.

In **Section 4,** an unique chapter (**Chapter 7**) includes a miniaturization of the technique introduced in **Chapter 6** for the determination of cortisol in serum and urine of preterm new-borns as a proof-of-concept.

Finally, conclusions of this thesis are shown besides the articles that have been published.

SECCIÓN 1

Capítulo 1: Introducción

Parte del contenido de este capítulo ha sido publicado en dos revisiones bibliográficas:

Use of nanomaterial-based (micro)extraction techniques for the determination of cosmetic-related compounds, **Molecules 25 (2020) 2586**

Use of green alternative solvents in dispersive liquid-liquid microextraction: A review**, J. Sep. Sci. 45 (2022) 210-222**

1.1. Preparación de muestra

Uno de los principales objetivos de la Química Analítica siempre ha sido el desarrollo de métodos analíticos que permitan alcanzar límites de detección cada vez más bajos, con el fin de poder analizar trazas de compuestos presentes en diferentes tipos de muestras. Sin embargo, con el reciente aumento de la preocupación medioambiental, estos métodos de análisis han tenido que adaptarse y buscar alternativas más sostenibles para reducir su impacto, no solo medioambiental, sino también en la salud del operador [1,2].

Como consecuencia, nace la **Química Analítica 'Verde' (*Green Analytical Chemistry*, GAC)**. La GAC se encuentra vertebrada en doce principios basados en la reducción de la toxicidad de los compuestos empleados y en su cantidad, para minimizar su impacto [3]. Estos doce principios son:

1. Evitar las etapas de preparación de muestra favoreciendo el **análisis directo**
2. Reducir el **tamaño de muestra**
3. Favorecer la preparación de muestra ***in situ***
4. Reducir el **número de etapas** necesarias para el análisis
5. Promover la **automatización** y **miniaturización** de los métodos
6. Evitar los procesos de **derivatización**
7. Reducir el volumen de **residuos** generados
8. Favorecer el **análisis multicomponente** en lugar de realizar un análisis independiente para cada analito.
9. Reducir el **consumo** energético
10. Emplear reactivos obtenidos de **fuentes renovables**
11. Reducir o eliminar el empleo de **reactivos tóxicos**
12. Garantizar **la seguridad** de la persona encargada del análisis

El análisis directo de la muestra es la opción menos perjudicial para el medioambiente, reduciendo completamente el uso de compuestos químicos peligrosos y minimizando el tiempo total del análisis [4]. No obstante, en la mayoría de ocasiones, el análisis directo resulta inviable debido a la complejidad de las muestras y/o la necesidad de preconcentrar analitos que se encuentren a nivel de trazas, por lo que es indispensable llevar a cabo una etapa de preparación de la muestra para su limpieza y/o preconcentración de los analitos [5,6].

En este sentido, se introdujo el concepto de **preparación 'verde' de muestra (*Green Sample Preparation*, GSP)** [7], cuyos principios son muy similares a los de la GAC, pero están más enfocados a la etapa de preparación de muestra. Estos son:

1. Favorecer la preparación de muestra ***in situ***, en el lugar de muestreo
2. Emplear disolventes y reactivos más **'verdes'** y **seguros**
3. Emplear materiales de extracción **reutilizables** y **simples**
4. Minimizar la cantidad de **residuos**
5. Minimizar la cantidad de **muestra**, **compuestos químicos** y **material de extracción**
6. Reducir el **tiempo de análisis** y/o permitir análisis de varias muestras al mismo tiempo
7. Promover la **automatización**
8. Minimizar el **consumo** de energía
9. Utilizar **metodologías post extracción** lo más 'verdes' posibles
10. Emplear **procedimientos seguros** para el operador

Es importante destacar que existe una fuerte correlación entre todos los principios, y la mejoría en uno de ellos puede conllevar ventajas en otros. Así, por ejemplo, la preparación de muestras *in situ* permite la disminución de los tiempos de análisis, y del consumo de energía. O, por otro lado, la reducción de compuestos tóxicos permite mejorar la seguridad del operador y minimizar la cantidad de residuos, entre otros ejemplos.

De acuerdo a estos principios, el empleo de técnicas de microextracción es preferible al uso de técnicas de extracción convencionales, como son la **extracción en fase sólida (*Solid Phase extraction*, SPE)** y la **extracción líquido-líquido** (***Liquid-Liquid Extraction*, LLE**). Estas técnicas de microextracción se pueden entender como una miniaturización de las convencionales, lo que posibilita la reducción de las cantidades de disolventes orgánicos, muestra y material extractante, a la vez que se reducen los tiempos de preparación de muestra [8]. La miniaturización de las técnicas favorece también el transporte, facilitando el análisis de muestras *in situ* u *on site* (esto es, realizar la preparación de muestra en el lugar de muestreo, aunque el análisis se realice en otro lugar [9]).

Estas ventajas se suman a la gran sensibilidad y simplicidad que poseen las técnicas de microextracción, permitiendo alcanzar límites de detección y cuantificación muy bajos a la vez que se reducen su impacto y la

manipulación de la muestra respecto a las técnicas de extracción convencionales [10].

Las técnicas de microextracción se pueden clasificar en función de diferentes parámetros. La división más común es la que se realiza en función del tipo de fase empleada en la extracción. De acuerdo a esta clasificación, encontramos principalmente dos grandes grupos, tal y como se resume en la **Figura 1.1**:

- **Microextracción en fase líquida:** se emplean disolventes como fase de extracción.

- **Microextracción basada en sorbentes sólidos:** se emplean sólidos (sorbentes) como fase de extracción.

Por otro lado, otra división menos frecuente es la que se realiza en función del comportamiento entre el material extractante y la muestra. En este caso, dentro de cada grupo, se establecen otros dos:

-**Técnicas dispersivas:** el sorbente o el disolvente se dispersa en la (disolución de) muestra durante la extracción.

-**Técnicas no dispersivas:** el sorbente o disolvente suele permanecer en el mismo lugar durante la extracción y no se dispersa en (disolución de) muestra.

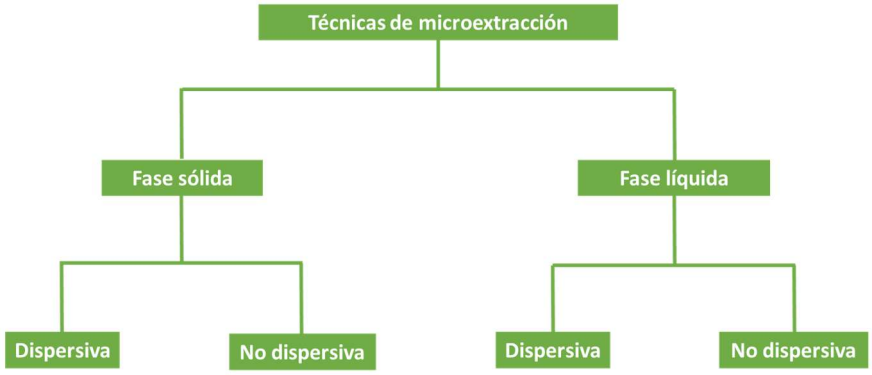

Figura 1.1. Clasificación de las técnicas de microextracción

En los siguientes apartados se describen algunas de las técnicas de microextracción más relevantes, así como algunas de las técnicas emergentes en la actualidad, comparando sus ventajas e inconvenientes

desde un punto de vista práctico y de impacto medioambiental y para el operador. Además, se comentará la utilidad de algunos de los materiales sorbentes y disolventes más empleados en este tipo de técnicas.

1.2. Microextracción basada en sorbentes

1.2.1. Materiales sorbentes

Las técnicas basadas en sorbentes, como se ha indicado anteriormente, son aquellas en las que se utiliza un material sólido como fase extractante. Una de las mayores ventajas de trabajar con materiales sólidos es la gran variedad de tipos de sorbentes disponibles, lo que permite una mayor versatilidad de cara a la planificación de un análisis respecto a las técnicas basadas en disolventes [11,12].

En los últimos años, dentro de los materiales sólidos, los que mayor interés han despertado son aquellos que presentan tamaños nanométricos [13]. Esto es debido a que su reducido tamaño se traduce en una elevada área superficial en relación a la de los materiales macroscópicos, lo que permite una mayor eficiencia de extracción y menores tiempos de análisis [14].

Cabe indicar que el empleo de materiales nanométricos, a pesar de sus mencionadas ventajas, puede implicar una serie de problemas para la salud de las personas que los manipulan, debido a su fácil penetración en la capas internas de los pulmones [15]. Por eso, es necesario el empleo de material de protección, como mascarillas, siempre que el operador se encuentre en contacto con este tipo de materiales.

Entre los materiales nanométricos, las nanopartículas han sido foco de atención para los investigadores de multitud de campos, incluida la Química Analítica. Estas partículas son esferas de metales u óxidos de metales que cuentan con un tamaño entre los 10 y los 100 nm. Dentro de este grupo, las **partículas magnéticas (*Magnetic Nanoparticles,* MNPs)** presentan un particular interés, ya que no solo cuentan con una gran área superficial propia de su pequeño tamaño, sino que además son capaces de interaccionar con campos magnéticos, lo que permite una mayor manejabilidad [16].

Salvo contadas excepciones, las MNPs no presentan una elevada eficacia de extracción, por lo que se suelen emplear funcionalizadas superficialmente con un material sorbente que presenta cualidades

extractantes frente a uno o varios analitos, obteniendo así materiales sorbentes magnéticos [17]. También se pueden obtener materiales sorbentes magnéticos mediante la incrustación de las MNPs en la estructura del material sorbente [18]. La primera opción resulta en materiales más estables, sin embargo, suele requerir de síntesis más largas y complejas.

El tipo de sorbente empleado depende del analito a determinar. De este modo, el investigador dispone de un enorme abanico de sorbentes con propiedades magnéticas que, como se discutirá en el **Apartado 1.2.2**, aportan grandes ventajas a las técnicas de microextracción.

Dentro de estos materiales sorbentes, los polímeros han sido tradicionalmente los más utilizados [19]; son microestructuras sintetizadas por la unión de uno o más tipos de monómeros. Los polímeros cuentan con extraordinarias capacidades de extracción, además, se les puede conferir propiedades magnéticas de forma muy simple incrustando las MNPs en su estructura.

Recientemente han surgido otro tipo de (nano)materiales, entre los que destacan los compuestos carbonáceos, como son el **óxido de grafeno** (***Graphene Oxide,* GO**) y el **óxido de grafeno reducido** (***Reduced Graphene Oxide*, rGO**). Para obtener el GO, es necesario oxidar el grafito y separar sus capas. Posteriormente, el rGO se obtiene a partir de la reducción del GO. Debido a que el GO cuenta con grupos funcionales como alcoholes o ácidos carboxílicos, suele ser empleado para la determinación de compuestos polares, mientras que el rGO es muy útil para analitos apolares y aromáticos [20].

Paralelamente, también se ha potenciado el uso de redes metal-orgánicas (***Metal Organic Frameworks*, MOFs**) [21]. Estas se caracterizan por ser estructuras cristalinas orgánicas-inorgánicas basadas en la combinación de centros metálicos con distintos ligandos orgánicos. La elección del ligando permite la modificación de la naturaleza del MOF en función de los analitos a determinar [22].

Si bien es cierto que todos los materiales anteriormente mencionados pueden ser modificados con el fin de adaptarse a la naturaleza de los analitos a determinar, estos materiales no son específicos y tienden a extraer gran variedad de compuestos en mayor o menor medida. Esto hace que se precise de una etapa cromatográfica para separar los analitos de los compuestos no deseados, incluso, el empleo de técnicas instrumentales de

análisis altamente selectivas como la espectrometría de masas (***Mass Spectrometry*, MS**) o la espectrometría de masas en tándem (MS/MS) para llevar a cabo una determinación selectiva.

Alternativamente, existen materiales que pueden considerarse específicos. Los más conocidos son los anticuerpos [23], que son proteínas que cuentan con unos centros de unión que reconocen (en la mayoría de casos) exclusivamente a un único compuesto (antígeno). Por otra parte, una alternativa cada vez más utilizada, es el empleo de polímeros de impresión molecular (***Molecularly Imprinted Polymers*, MIPs**) [24]. Estos son sintetizados por la formación de una red polimérica alrededor de las moléculas de los analitos a determinar. Posteriormente, se retiran las moléculas de analitos, obteniéndose así un molde específico para un único tipo de analito, o en el caso de usar más de un molde, varios analitos [25].

1.2.2. Técnicas de microextracción basadas en sorbentes

En lo referente a las técnicas de microextracción basadas en sorbentes, tradicionalmente se han empleado técnicas no dispersivas como la **microextracción en fase sólida (*Solid Phase Microextration,* SPME)** y la **extracción sobre barra agitadora (*Stir Bar Sorptive Extraction*, SBSE).** Ambas técnicas permiten una manipulación sencilla, así como la obtención de límites de detección bajos, empleando además muy poca cantidad de material y de disolventes orgánicos.

La SPME fue introducida en 1990 por Pawliszyn y colaboradores [26]. Se basa en el empleo de una microfibra de un material sorbente que puede introducirse en la disolución de muestra para producir la extracción de los analitos (inmersión directa). Para el caso de analitos volátiles, la fibra puede suspenderse sobre la parte superior de la disolución (espacio de cabeza), lográndose eliminar gran parte del efecto matriz [27]. Posteriormente, se lleva a cabo la desorción, bien sea introduciendo la fibra en un disolvente orgánico (desorción líquida) o mediante la aplicación de temperatura elevada para volatilizar los analitos (desorción térmica). En **la Figura 1.2** se muestra un esquema de ambas metodologías.

Desde su inicio, se han desarrollado una gran variedad de fibras con distintos materiales para su empleo en SPME [28] y poder llevar a cabo la

determinación de analitos de naturaleza variada, incrementando así la versatilidad de esta técnica.

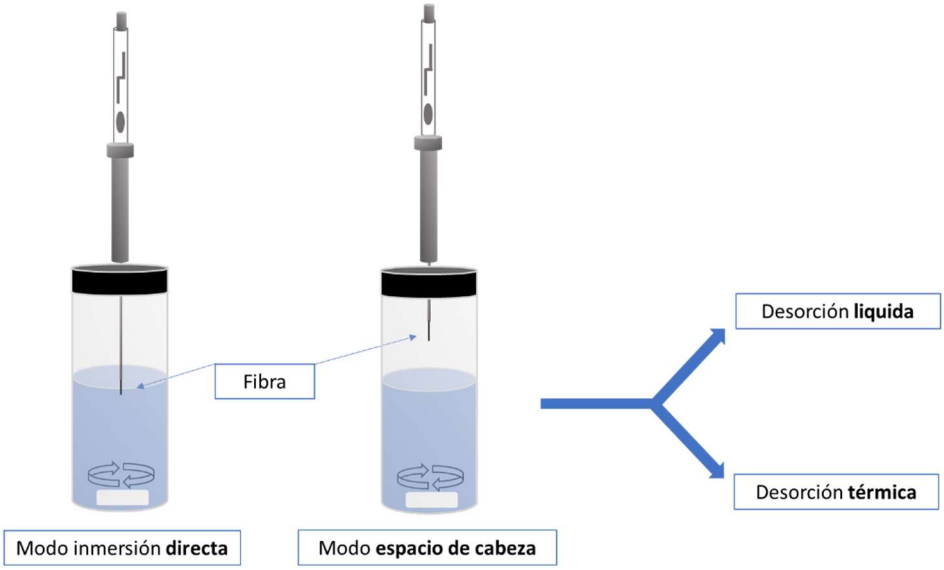

Figura 1.2. Esquema de la SPME

La simplicidad de la SPME, su fácil manipulación y su adaptación para procesos automáticos [29], han hecho que la SPME sea ampliamente utilizada tanto en trabajos de investigación como en análisis de rutina en empresas.

Por otro lado, la SBSE [30] consiste en una barra agitadora en cuya superficie se encuentra el material sorbente, como se muestra en la **Figura 1.3**. De este modo, para realizar la extracción basta con agitar la disolución. Una vez terminada la extracción, el imán de agitación puede introducirse en un disolvente orgánico para una desorción líquida o bien en un tubo de vidrio para realizar la desorción térmica de analitos volátiles [30].

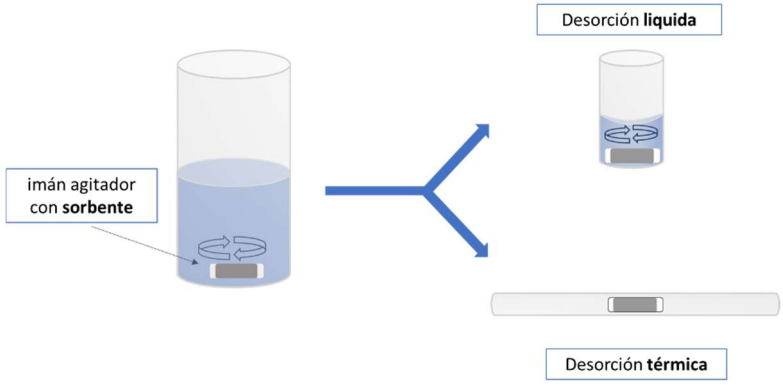

Figura 1.3. Esquema de la SBSE

Los imanes de SBSE suelen emplear **polidimetilsiloxano** (***polydimethylsiloxane***, **PDMS**) como material sorbente. El PDMS es muy útil para analitos apolares, sin embargo, no se recomienda para compuestos polares. Existen también otras opciones comerciales, como los imanes agitadores con etilenglicol para analitos más polares Por otro lado, se puede recurrir a la preparación en el laboratorio de barras agitadoras con el sorbente deseado [31]. Esta opción permite una mejora en la versatilidad de la técnica, ya que el sorbente puede ser seleccionado a medida, en función del tipo de analitos a determinar [32].

A pesar de sus dificultades para la automatización, la SBSE también se ha implementado en los laboratorios de rutina debido a su gran rendimiento, ya que mediante un agitador multiplaca se pueden procesar numerosas muestras de forma simultánea.

Sin embargo, pese a sus numerosas ventajas, tanto la SPME como la SBSE presentan algunos inconvenientes, ya que al tratarse de técnicas no dispersivas, la transferencia de masa es lenta. Por esta razón, los tiempos de extracción requeridos en estas dos técnicas suelen ser superiores a 30 minutos, incluso de varias horas [33].

Con el objetivo de reducir los tiempos de extracción en técnicas con sorbentes sólidos, en el año 2003, Anastassiades y colaboradores [34] realizaron la primera extracción en **fase sólida dispersiva (*Dispersive Solid Phase Extraction,* DSPE).** En esta técnica, como se puede apreciar en la **Figura 1.4**, se introduce un sorbente en la muestra. Posteriormente, se agita para producir su dispersión en el seno de la misma. De este modo,

se consigue incrementar el área de contacto sorbente-muestra, favoreciendo la transferencia de masa y, por lo tanto, reduciendo el tiempo necesario para la extracción [35]. Una vez realizada la extracción, se centrifuga para separar ambas fases, retirando después el sobrenadante y llevando a cabo las etapas de lavado y desorción, con sus respectivas etapas de centrifugación.

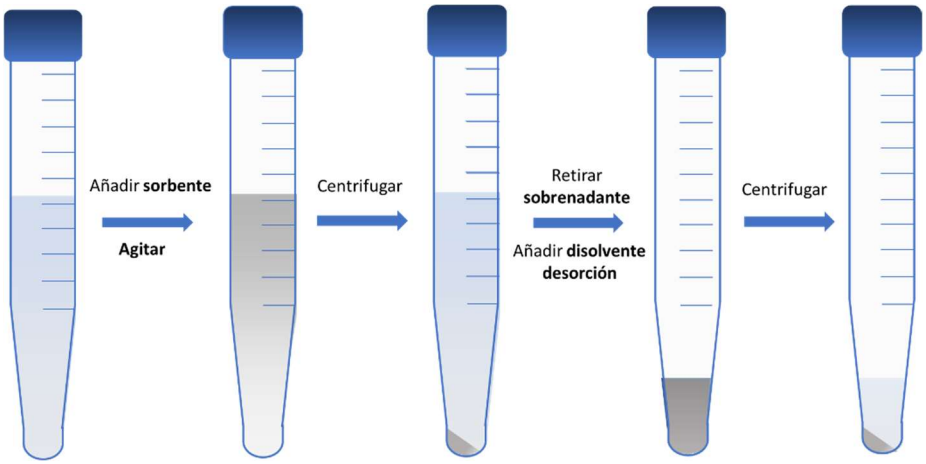

Figura 1.4. Esquema de la DSPE

No obstante, la DSPE también presenta algunas desventajas. A pesar de su mejora en los tiempos de extracción respecto a las técnicas no dispersivas, su manipulación es más tediosa y se requiere una etapa de centrifugación tras cada etapa (extracción, lavado y desorción) para separar el sólido [36]. Esto implica que, aunque la etapa de extracción sea más corta, el tiempo total de análisis puede ser elevado, incluso comparable al de las técnicas estáticas.

Como alternativa, se propuso el empleo de sorbentes magnéticos para ayudar a aliviar, en mayor o menor medida, este inconveniente [37]. De este modo, una vez finalizadas las etapas de extracción, lavado y desorción, el material puede separarse fácilmente de la disolución empleando un campo magnético externo, como se muestra en la **Figura 1.5**, eliminando así las etapas de centrifugación y reduciendo significativamente el tiempo total del análisis [38].

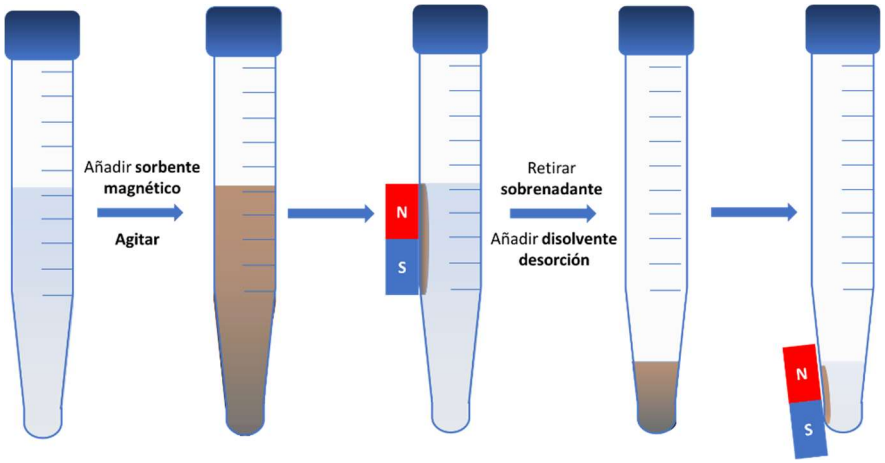

Figura 1.5. Esquema de la DSPE con sorbentes magnéticos

La sencillez de la síntesis de la mayoría de materiales magnéticos, sumada a los grandes beneficios en cuanto a tiempo de análisis y manipulación, han contribuido a que el uso de estos materiales en técnicas dispersivas se haya incrementado ampliamente en los últimos años, tal y como se observa en la **Figura 1.6,** superando al empleo de materiales no magnéticos [39].

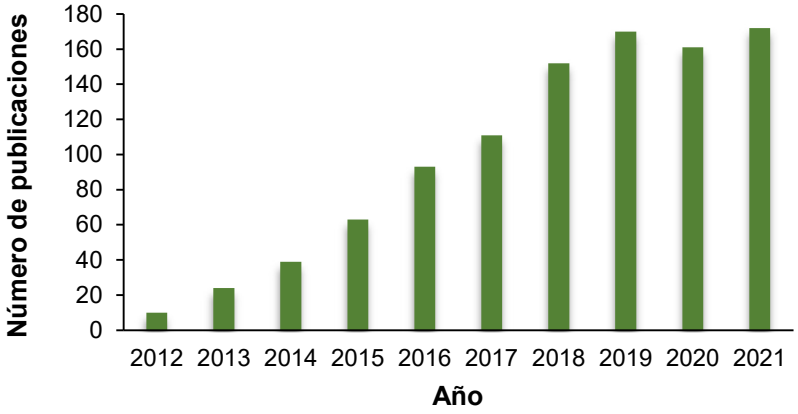

Figura 1.6. Evolución de las publicaciones con materiales magnéticos en DSPE desde 2012 hasta 2021

Sin embargo, el empleo de partículas magnéticas puede tener una serie de desventajas desde el punto de vista de la GAC [40]. Para empezar, su síntesis y su posterior funcionalización son dos etapas extra que pueden implicar el empleo de grandes cantidades de disolventes y/o compuestos químicos de elevada toxicidad [41]. Por esa razón, es necesario encontrar estrategias que permitan reducir el impacto de esta etapa. Por un lado, es indispensable encontrar métodos de síntesis más simples, rápidos y seguros. En el caso de las MNPs, en la última década se han publicado diversos métodos basados en el empleo de té verde como agente reductor, permitiendo así una elaboración más respetuosa con el medio ambiente y el operador, a la par que más económica [42]. Por otro lado, se debería rentabilizar más cada síntesis encontrando procesos que permitan obtener la máxima cantidad de material con el menor número de etapas y compuestos químicos utilizados. De esta forma, de una sola síntesis se podrían realizar un mayor número de extracciones. Finalmente, reducir la cantidad de sorbente necesario en cada análisis también minimizaría el impacto de la etapa de síntesis.

A raíz del empleo de los materiales magnéticos en técnicas de microextracción, comenzaron a surgir nuevas estrategias analíticas como alternativas a la DSPE. Entre ellas, una de las más destacadas y, que se ha empleado en la presente tesis doctoral, es la **microextracción en fase sólida dispersiva sobre barra agitadora (*Stir-bar Sorptive Dispersive Microextraction,* SBSDME)** introducida en 2014 por el grupo de investigación en el que se ha realizado la presente tesis doctoral [43].

En esta técnica, se añade una cantidad de sorbente magnético sobre una pequeña barra agitadora de neodimio inmersa en la disolución a extraer, quedando magnéticamente adherido. A velocidades de agitación bajas, la fuerza centrífuga resultante no es capaz de vencer a las interacciones magnéticas entre el imán y el material, por lo que este continúa anclado sobre el imán de neodimio. De esta forma, no se produce la dispersión y el sistema se comporta como una SBSE. Sin embargo, al incrementar la velocidad de agitación, la fuerza centrífuga supera a las interacciones magnéticas y permite separar el sorbente del imán dispersándolo en la muestra, incrementando el área de contacto sorbente/muestra al igual que sucede en la DSPE [44].

Una vez terminada la extracción, la agitación se detiene permitiendo al material magnético regresar a la barra agitadora tras un breve periodo de

deposición, sin necesidad de ninguna intervención por parte del operador. Una vez recogido el material, puede ser introducido en un pequeño volumen de disolvente orgánico para una desorción líquida o, en caso de analitos volátiles, ser introducido directamente en un equipo de desorción térmica [44]. La **Figura 1.7** muestra un esquema de la SBSDME.

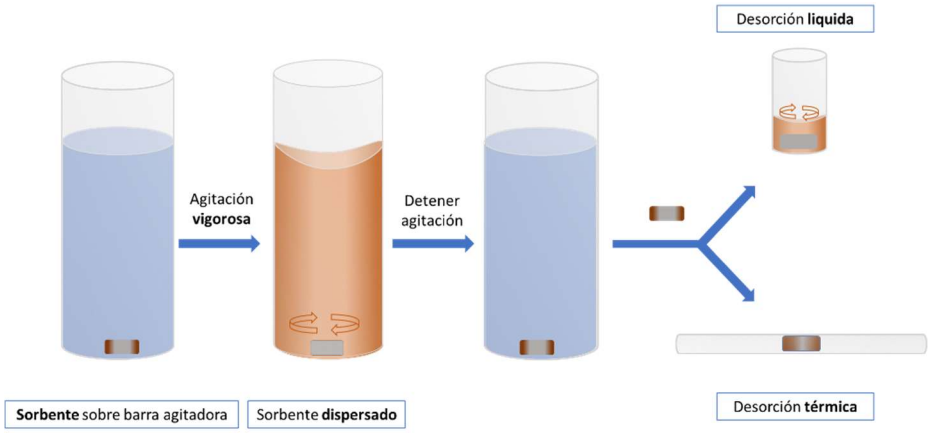

Figura 1.7. Esquema de la SBSDME

El empleo de la SBSDME presenta varias ventajas respecto a la DSPE con sorbentes magnéticos. En primer lugar, en la SBSDME el campo magnético se encuentra presente en todo momento dentro de la disolución a extraer, por lo que no es necesario acercar un campo magnético externo después de cada etapa, bastando simplemente con disminuir la velocidad de agitación para recoger el sorbente. Con esta simple modificación, es posible igualar los cortos tiempos de análisis de la DSPE con sorbentes magnéticos, pero reduciendo todavía más la manipulación por parte del operador.

Por otro lado, una vez terminada la agitación, el material queda unido a la barra agitadora, por lo que la manipulación es más sencilla que con el sorbente sin adherir. De esta forma puede ser fácilmente introducido en un tubo de desorción para su desorción térmica.

Por último, a diferencia de la DSPE, la agitación se produce únicamente por la agitación del imán. Esta (semi)automatización es preferible a las agitaciones manuales o mediante otros agitadores externos, como agitador *vortex*, requiriendo menor manipulación por parte de la persona encargada del análisis. Además, la utilización de agitadores multiplaca permite procesar varias muestras a la vez, reduciendo el tiempo total de análisis.

En la presente tesis doctoral se exponen dos aplicaciones de la SBSDME en dos tipos diferentes de muestra (orina y aguas medioambientales) que se discutirán con más detalle en los **Capítulos 2** y **3**.

1.2.3. Volúmenes pequeños de muestra

Hasta ahora, las técnicas de microextracción se han centrado en la reducción del volumen de disolventes orgánicos y cantidades de sorbente, mientras que la miniaturización de la cantidad de muestra se ha relegado a un segundo plano.

Es cierto que en algunos casos en los que el tratamiento de muestra tiene un impacto bajo, por ejemplo en análisis directos o cuando se emplean disolventes o sorbentes muy poco nocivos, y el tipo de muestra es de fácil acceso, como es el caso de aguas ambientales, la reducción de muestra no es una prioridad [45]. Al contrario, se apuesta por el empleo de una mayor cantidad de muestra con el fin de alcanzar mayor preconcentración y, por tanto, menores límites de detección [46,47].

No obstante, en muchas ocasiones no es necesario llegar a esos límites extremadamente bajos y merece la pena reducir la cantidad de muestra empleada debido a los beneficios que se obtienen desde el punto de vista de la GSP. Esto es, una disminución en el volumen de disolventes orgánicos, en el caso de ser empleados, y en la cantidad de material sorbente necesario para producir la extracción. Esto implica directamente una menor cantidad de residuos y un menor impacto para la persona encargada de llevar a cabo los análisis. Además, también puede contribuir a una reducción en el tiempo de análisis, permitiendo realizar un mayor número análisis en la misma cantidad de tiempo. Finalmente, la miniaturización de la muestras implica también una disminución en el tamaño de los dispositivos de preparación de la misma. Esto favorece su transporte, de forma que se facilita la preparación de muestra en el mismo lugar de muestreo (análisis *on site*) [48], aunque la medida no se realice allí. Así, se evitan también transportes innecesarios de muestra que puedan alterar el contenido de la misma y la necesidad de conservarla.

Pero no solo las etapas de muestreo y preparación de muestra se benefician de esta miniaturización. Al reducir la cantidad de material sorbente es posible realizar muchos más análisis con una única síntesis de material, por

lo que se reduce en gran medida el impacto de esta etapa, que suele ser una de las más perjudiciales a nivel ambiental y de toxicidad, al mismo tiempo que se disminuye el coste.

En la **Figura 1.8** se resumen estos beneficios.

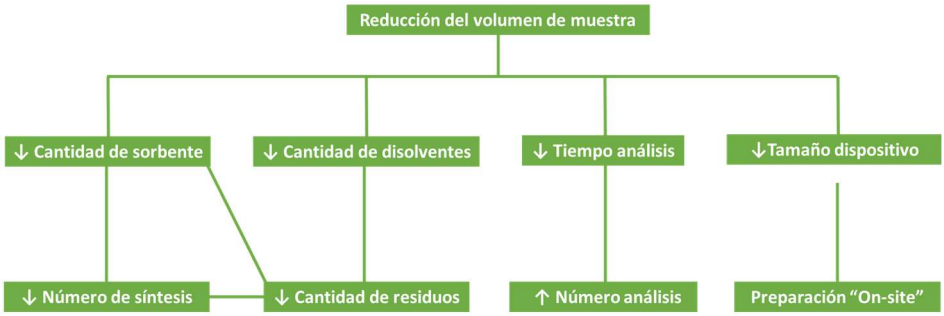

Figura 1.8. Beneficios a consecuencia de la reducción de muestra

Por otra parte, la disminución de la cantidad de muestra a analizar cobra especial importancia en muestras biológicas, en las que la cantidad de muestra a utilizar está, a menudo, limitada. Muestras como la sangre, requieren de un muestreo invasivo [49] basado en la extracción mediante aguja y jeringa que suele ser incómoda para la persona a la que se le va a hacer el estudio. Además, una retirada importante de sangre puede tener efectos perjudiciales para su salud y requiere de personal cualificado para su extracción [50]. En este sentido, la saliva es una alternativa muy atractiva debido a su bajo nivel de invasividad y mayor comodidad para el muestreo [51], aunque hay que tener en cuenta que las concentraciones de los analitos suelen ser más bajas en saliva que en sangre [52]. Además, la cantidad de muestra habitualmente tomada es inferior a los 2 mL para evitar un malestar en el paciente además de posibles contaminaciones con sangre [53].

Por estas razones, se han desarrollado diferentes estrategias analíticas para trabajar con volúmenes pequeños de muestra. En este aspecto, en las últimas décadas, las técnicas en puntas de pipeta 'funcionalizadas' con sorbentes, han atraído un gran interés [54].

Este tipo de técnicas, englobadas con el nombre de **(micro)extracción en fase sólida basada en puntas de pipeta (*Pipette Tip-Solid Phase***

***Extraction*, PT-SPE)** [55], pueden considerarse la miniaturización más "fiel" de la SPE convencional. En la PT-SPE, el material sorbente se introduce y se inmoviliza en el interior de la punta de la pipeta con el empleo de dos fritas. De este modo, al aspirar la muestra con la pipeta (semi)automática, esta pasa a través del sorbente, produciéndose la extracción. Al terminar la extracción, se puede realizar el lavado fácilmente con agua y, a continuación, proceder a la desorción con el disolvente apropiado. Se muestra un esquema de la PT-SPE en la **Figura 1.9**.

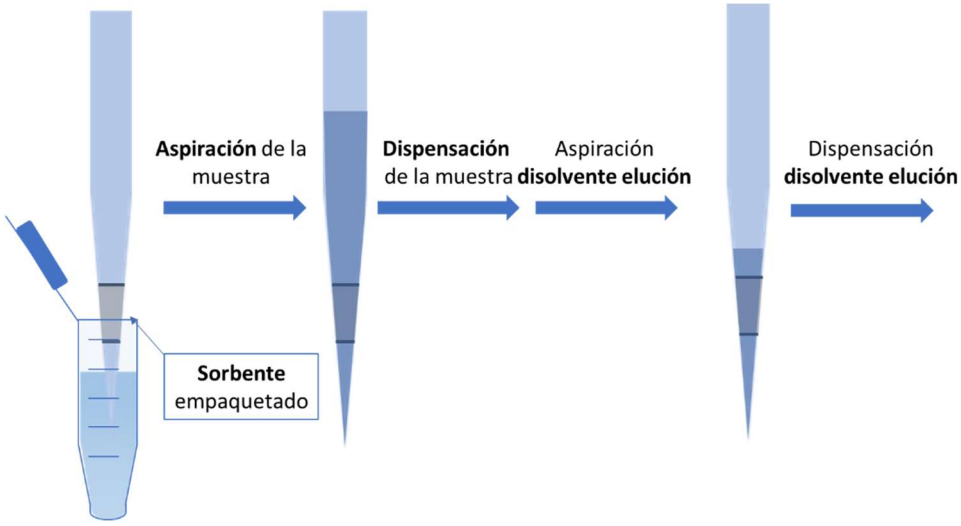

Figura 1.9. Esquema general de la PT-SPE

La PT-SPE cuenta con la ventaja de ser muy sencilla, ya que únicamente se basa en ciclos de aspiración/dispensación con una pipeta (semi)automática. Además, el análisis de varias muestras a la vez puede realizarse fácilmente empleando una pipeta multicanal [56,57]. Sin embargo, también presenta una serie de inconvenientes relacionados con la manipulación del operador que limitan su aplicación en análisis rutinario. Al tratarse de un método no dispersivo, el intercambio de masa es lento, lo que hace necesarios muchos ciclos de aspiración/dispensación para producir una extracción cuantitativa de los analitos [58]. Esto conlleva que el operador tenga que repetir el mismo movimiento de carga y descarga de la pipeta muchas veces en un solo día. Si esto se alarga durante semanas puede llegar a causar problemas graves en los flexores de la mano [59]. Es cierto que, al igual que la SPME, la PT-SPE puede ser automatizada de modo que se elimine este problema [60,61]. Sin embargo, el equipamiento requerido para su uso no es asumible por la

mayoría de laboratorios, por lo que se han ido proponiendo otras opciones. Además, en PT-SPE son frecuentes los problemas de obstrucción, así como de pérdida de material [62].

Una de las alternativas más populares, consistió en la dinamización de la PT-SPE, para conseguir una mejor eficiencia de extracción en un menor número de ciclos. Así surgió la **extracción dispersiva en fase sólida con pipeta** (***Disposable/Dispersive Pipette Extraction*, DPX**). En la que el material extractante del interior de la pipeta no se encuentra empaquetado, sino suelto. Ahora bien, para evitar que el material se pierda durante la microextracción, la punta de pipeta se encuentra delimitada a ambos lados por filtros, de forma que la muestra líquida puede entrar y salir, pero el sorbente siempre se encuentra dentro de la punta. El hecho de que el material esté suelto, hace que al aspirar la muestra, el sorbente se disperse en esta. De este modo, como se ha señalado en la DSPE, esta dispersión produce un incremento en el área de contacto muestra-sorbente incrementando la velocidad de transferencia de masa entre ambos. Así, la extracción se produce en menor tiempo que empleando PT-SPE, lo que permite reducir el número de ciclos de carga y descarga tanto de la fase de extracción como de la desorción, mejorando la ergonomía del trabajador [63,64].

Sin embargo, esta técnica cuenta con varios inconvenientes. En primer lugar, la DPX no permite el empleo de materiales nanométricos, ya que estos no serían retenidos por los filtros y se perderían con el resto de la muestra [62]. Además, aunque respecto a la PT-SPE se consigue una reducción del número de ciclos de carga y descarga, suelen ser necesarios varios ciclos para obtener una dispersión correcta del material en la muestra [65–70]. Esto se debe, por un lado, a la falta de afinidad entre muestra y sorbente y, por otro, a que la dispersión se produce durante la acción de carga de la pipeta y no durante la descarga, donde se puede aplicar más fuerza. Hay que añadir también el factor económico, ya que el precio de estas puntas está muy por encima de lo que costarían unas puntas de pipeta convencionales de laboratorio.

Desde el punto de vista de un laboratorio de investigación, estos dos hechos pueden tener una repercusión mínima o despreciable. Sin embargo, en un laboratorio de rutina, donde una misma persona puede realizar cientos de análisis el mismo día, estos dos problemas se acentúan en gran medida,

pudiendo tener graves repercusiones en la salud de la persona encargada de realizar los análisis y, por otro lado, suponer un gasto excesivo.

Recientemente, los propios inventores de la técnica han propuesto el uso de una pieza adicional llamada 'dispersador' [71], cuya función se esquematiza En la **Figura 1.10**. Este produce una variación del flujo el cual va a provocar una agitación vigorosa en el interior de la punta de pipeta, mejorando sustancialmente la dispersión del sorbente, pudiendo contribuir a reducir el número de ciclos. No obstante, aunque el empleo de este 'dispersador' soluciona el problema del número de ciclos, agrava el problema económico al incrementar, todavía más, el precio de las puntas.

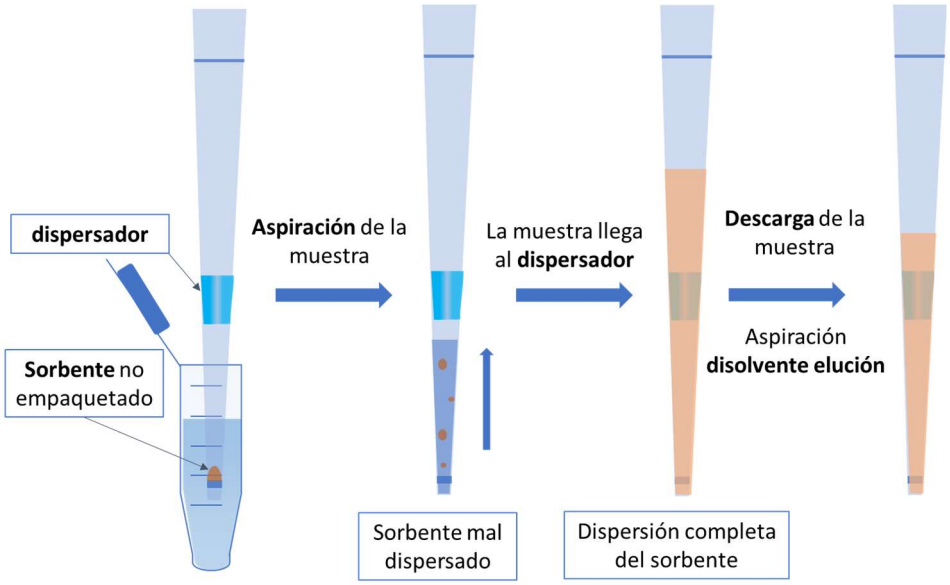

Figura 1.10. Esquema de la DPX empleando puntas con dispersador

Una alternativa más económica a estas puntas con dispersador, consiste en el empleo de un disolvente orgánico a modo de agente dispersante. La función de este agente dispersante es la de mejorar la afinidad entre dos fases inmiscibles entre sí, mejorando así la dispersión del sorbente en la muestra. El empleo de un agente dispersante ha sido ampliamente utilizado en la microextracción dispersiva líquido-líquido que se discutirá en más detalle en el **Apartado 1.3.** Sin embargo, su uso estaba menos extendido en técnicas de microextracción basadas en sorbentes, habiendo sido publicados muy pocos artículos con esta estrategia.

El empleo de este agente dispersante produce una reducción total de los ciclos de carga y descarga. Este tipo de técnicas, agrupadas bajo el nombre de **extracción dispersiva en fase sólida asistida por disolvente (*Solvent Assisted Dispersive Solid Phase Extraction,* SA-DSPE)** [72], permiten además una dispersión producida en el movimiento de descarga del disolvente y no de aspiración (como ocurre en la DPX y la PT-SPE), lo que permite aplicar más fuerza para producir una mejor dispersión y, en consecuencia, el número de ciclos se reduce. Además, la SA-DSPE puede combinarse con el uso de materiales magnéticos, eliminando las etapas de centrifugación y minimizando la manipulación, lo que la convierte en una técnica de interés para volúmenes de muestra reducidos. Hasta ahora, esta técnica se había empleado utilizando agitador *vortex* [73] o baño de ultrasonidos [74], con el gasto energético que esto conlleva, además de incrementar los tiempos de extracción y dificultar el tratamiento de muestras *in situ* y *on site*. Por esa razón, se ha propuesto una modificación que permita dispersar el sorbente sin necesidad de ningún dispositivo de agitación externa. Esta estrategia de microextracción se discutirá con más detalle en el **Capítulo 5.**

Si bien la SA-DSPE cuenta con ciertas ventajas sobre la PT-SPME y la DPX, también cuenta con inconvenientes. Debido a que el sorbente no está acotado dentro de la punta, se pierde la ausencia de manipulación y simplicidad de estas dos metodologías, aunque se utilicen materiales magnéticos. Por esta razón, ambas ventajas se han fusionado para obtener una técnica que combina la simpleza y manipulación de la PT-SPE con la velocidad de dispersión que permite la SA-DSPE. Esta nueva técnica, denominada **microextracción en punta de pipeta basada en sorbentes magnéticos** (***Magnetic-based Pipette Tip Microextraction,* M-PTME**) y desarrollada en el contexto de esta Tesis Doctoral, se presentará en el **Capítulo 6**.

1.2.4. Microvolúmenes de muestra

Tal y como se mencionó anteriormente, los fluidos biológicos requieren un muestreo más crítico, siendo necesario limitar la cantidad de muestra con el fin de garantizar la salud y la comodidad de la persona donante. En el caso de personas adultas suele ser asequible tomar muestras con un volumen adecuado para su análisis. No obstante, cuando se trata de pacientes

enfermos o en el caso de los recién nacidos, los volúmenes de muestra están más limitados [75,76]. También existen tipos de muestras como el semen, fluido folicular o fluido cerebroespinal donde la cantidad a obtener está también muy restringida.

Por esa razón, en estas situaciones es necesario realizar una miniaturización aún más drástica de las metodologías de microextracción, de forma que se pueda trabajar con muestras de pocos microlitros. Esto supone un reto extra, ya que volúmenes de muestra tan pequeños son más difíciles de manipular y los factores de preconcentración a los que se puede llegar son bajos, si es que se consigue realizar alguna preconcentración. Por ello, para estos casos es necesario disponer de técnicas instrumentales de análisis muy potentes que permitan alcanzar bajos límites de detección, tales como la espectrometría de masas.

A pesar de las dificultades que puede presentar el trabajo con volúmenes de muestra tan reducidos, también presenta una serie de ventajas. Como se ha discutido en el apartado anterior, la disminución del volumen de muestra presenta multitud de beneficios en relación con la generación de residuos en las etapas de análisis y síntesis. Así, el empleo de microvolúmenes permite que el impacto que ocasiona la preparación de muestra sea todavía más reducido.

En la presente Tesis Doctoral se ha desarrollado una nueva metodología que permite realizar análisis simples en microvolúmenes de muestra. Esta técnica está basada en los mismos principios que la M-PTME, explicada al final del apartado anterior, únicamente que modificada para trabajar con cantidades todavía más pequeñas. Esta se describe con detalle en el **Capítulo 7.**

1.3. Microextracción en fase líquida

En lo referente a la microextracción en fase líquida, dos técnicas han sido históricamente las predominantes. Primero la **microextracción en gota (*Single-Drop Microextraction*, SDME)** y más recientemente la **microextracción líquido-líquido dispersiva (*Dispersive Liquid-Liquid Microextraction*, DLLME)**.

En la SDME, introducida por Jeannot y Cantwell [77], una microgota de un disolvente de extracción es suspendida en la punta de una jeringa e introducida en la muestra, generalmente, de naturaleza acuosa (modalidad de inmersión directa). Posteriormente, se agita la disolución de muestra para producir la extracción de los analitos. Tras la extracción, la gota se recoge en la microjeringa para su medida en el instrumento adecuado. La SDME también permite trabajar en modalidad de espacio de cabeza [78] para la extracción de compuestos volátiles. En este caso, la gota se encuentra en el espacio de cabeza del recipiente en el que se introduce la muestra. En la **Figura 1.11** se representan ambos modos de trabajo.

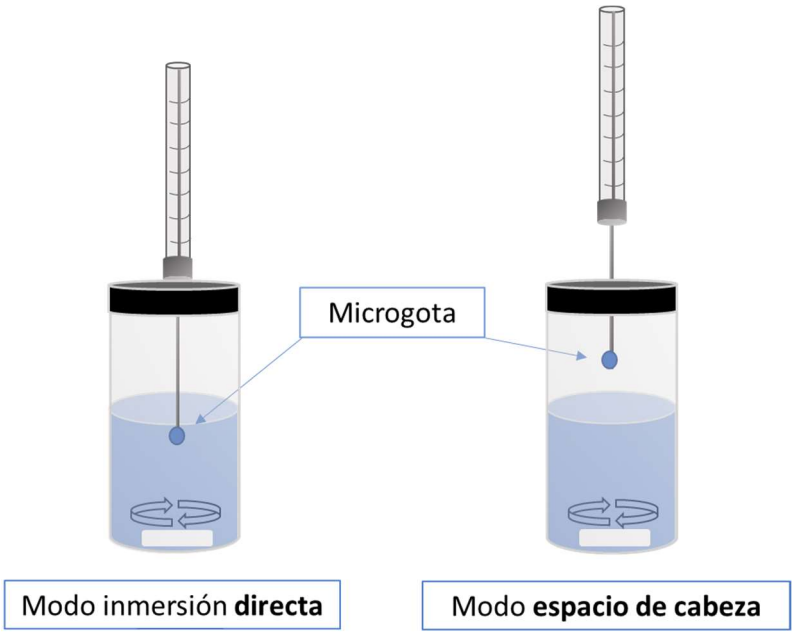

Figura 1.11. Esquema de la SDME

La poca estabilidad de la gota y su fácil evaporación hacen que el trabajo con esta técnica resulte tedioso, por lo que su popularidad cayó en detrimento de otras modalidades, siendo sustituida, en la mayoría de ocasiones, por la DLLME.

La DLLME fue propuesta en 2006 por Rezaee et al. [79]. En esta técnica, el disolvente de extracción se dispersa en el seno de la muestra con ayuda de, generalmente, un disolvente dispersante (disolvente orgánico miscible tanto

en la muestra como en el disolvente extractante).La microemulsión resultante hace que incremente el área de contacto entre las fases dadora y aceptora, consiguiéndose así que la microextracción se produzca de forma instantánea [80]. Una vez finalizada la extracción, ambas fases se separan mediante una etapa de centrifugación y se recoge la fase extractante empleando una jeringa para su posterior medida. En la **Figura 1.12**, se muestra un esquema de la DLLME.

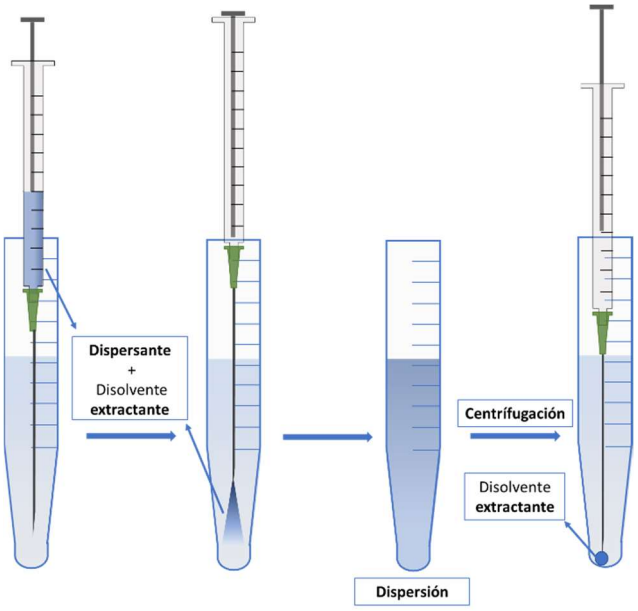

Figura 1.12. Esquema de la DLLME empleando un agente dispersante

La dispersión también se puede conseguir sin disolvente dispersante, ya sea por agitación por *vortex* o por ultrasonidos [81]. Estas dos últimas presentan la ventaja de no requerir, normalmente, disolventes orgánicos. Sin embargo, suele ser necesario un mayor tiempo para conseguir la dispersión y, por tanto, un mayor tiempo total de análisis.

La DLLME es una de las técnicas de microextracción más populares debido a su sencillez y eficacia. A pesar de esto, no está libre de inconvenientes. El problema principal de la DLLME 'clásica', es el uso de disolventes halogenados [82]. Este tipo de disolventes se utilizan debido a que son más densos que el agua, por lo que al terminar la extracción y separar ambas fases, el disolvente halogenado queda recogido como una gota en el fondo

del vial cónico, lo que permite recoger volúmenes muy pequeños y conseguir elevados factores de preconcentración de forma sencilla. Sin embargo, se trata de disolventes altamente tóxicos y, por tanto, han sido paulatinamente sustituidos por alternativas más 'verdes' de acuerdo a los principios de la GSP.

El uso de disolventes orgánicos de baja densidad (como alcoholes grasos), fue propuesto como alternativa y, si bien es cierto que son mucho menos tóxicos [83], tienen el inconveniente de ser menos densos que agua. Por ello, al separar las dos fases, la fase orgánica queda en la parte superior del recipiente , donde hay más área que en el fondo, dificultando en gran medida la recogida del disolvente y necesitando emplear mayores volúmenes. Alternativas como la **solidificación de gota orgánica flotante (*Solidified Floating Organic Drop*, SFOD)** [84], permite solidificar la fase extractante disminuyendo considerablemente la temperatura. Una vez sólida, la fase extractante puede retirarse con más facilidad. Sin embargo, estas estrategias conllevan un aumento en el número de etapas y en la complejidad del método. Por otra parte, tanto estos disolventes como los halogenados, cuentan con una baja selectividad en comparación con los sorbentes sólidos.

Por esta razón, en los últimos años se han propuesto una serie de disolventes 'hechos a medida' [85,86], los cuales pueden ser modificados en función de los analitos a extraer mejorando la selectividad.

Los primeros disolventes propuestos, y los más populares hasta la fecha, fueron los **líquidos iónicos (*Ionic Liquids*, ILs)** [87]. Los ILs son sales líquidas compuestas por la combinación de un catión orgánico con un anión que puede ser orgánico o inorgánico. Estos disolventes supusieron una revolución en el campo de la microextracción en fase líquida por sus propiedades, tales como elevada estabilidad térmica, baja inflamabilidad y baja presión de vapor, que son una ventaja con respecto a los disolventes tradicionales. Pero además, la gran variedad de cationes y aniones disponibles permite obtener numerosos ILs con diferentes afinidades, mejorando la selectividad y las eficiencias de extracción respecto al resto de disolventes [88].

Sin embargo, pese a que los ILs, cuentan con grandes capacidades analíticas, sus síntesis suelen ser complicadas y los componentes en los que se basan suelen tener una toxicidad elevada. Por lo que, aunque el producto final pueda ser inocuo, si el procedimiento para su obtención no es

'verde', el producto final no se puede considerar como tal [89]. Además, su acoplamiento a técnicas cromatográficas está muy limitado debido a su baja presión de vapor y baja volatilidad, por lo que no es posible trabajar en **cromatografía de gases (*Gas Chromatography,* GC)** a no ser que se emplee desorción térmica [90,91] u otras estrategias [92–95]. Por otro lado, su elevada viscosidad y baja volatilidad tampoco permiten su uso en técnicas como la cromatografía de **líquidos acoplada de espectrometría de masas (*Liquid Chromatography-Mass Spectrometry*, LC-MS)** ya que interfieren en la formación del *electrospray* [96,97].

Por todo ello, como alternativa, se propuso el empleo de **disolventes eutécticos profundos (*Deep Etutectic Solvents*, DESs)** [98]**.** Estos disolventes suelen formarse por interacciones de puente de hidrógeno producidas por un **dador de puente de hidrógeno (*Hydrogen Bond Donor,* HBD)** y un **aceptor de puente de hidrógeno (*Hydrogen Bond Acceptor,* HBA)** [99]. Estas interacciones hacen que, aunque los componentes iniciales sean sólidos, la mezcla resultante se comporte como un líquido a temperatura ambiente [100]. Las síntesis de estos disolventes es muy sencilla, de modo que, generalmente, basta con mezclar los componentes y mantenerlos en agitación durante un corto periodo de tiempo. Además, los DESs comparten muchas de las propiedades de los ILs [101]. No obstante, su obtención es mucho más simple, pudiendo realizarse en cuestión de minutos simplemente calentando en un baño de agua [102]. De este modo, se pueden conseguir disolventes más 'verdes' de forma más fácil y por un precio mucho menor. Por esta razón, su popularidad ha crecido enormemente desde su primera propuesta como disolvente de extracción en DLLME, tal y como se observa en la **Figura 1.13**.

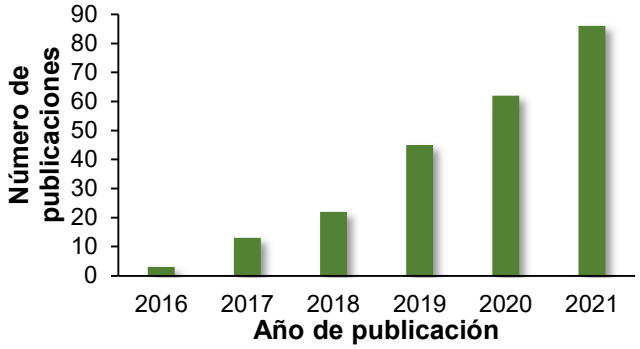

Figura 1.13. Evolución del número de publicaciones de DLLME utilizando DESs en el intervalo 2016-2021

Es importante señalar que, aunque los DESs cuenten con un gran potencial como disolventes 'verdes', eso no implica (como parece señalar parte de la bibliografía) que todos los DESs lo sean. Si los DESs se preparan a partir de componentes tóxicos, como pueden ser los fenoles, no pueden considerarse como 'verdes'. Comúnmente se denominan **DESs naturales (*Natural Deep Eutectic Solvents,* NADESs)** a aquellos DESs compuestos por componentes derivados del metabolismo celular [103,104]. Estos NADESs suelen caracterizarse por ser poco tóxicos y biodegradables. No obstante, esta terminología no es totalmente válida por diferentes motivos. En primer lugar, parece partir de la idea preconcebida de que todo lo natural es bueno mientras que lo sintético es tóxico. Y en segundo término, porque aunque un componente se encuentre de forma natural, su obtención suele requerir de procesos químicos de purificación y síntesis, de modo que la obtención de los componentes no es 'natural'. Además, la definición de NADES dejaría fuera a aquellos DESs cuyos componentes no entraran en la definición de natural. Por esta serie de razones, otras definiciones como **DESs de baja toxicidad (*Low Toxicity DES,* LT-DES)** o DESs 'verdes', podrían ajustarse mejor que NADES [105].

Pese a esto, los DESs no están exentos de inconvenientes. Por un lado, la elevada viscosidad [105,106] de algunos de ellos obliga a una etapa de dilución previa antes de ser introducidos en un cromatógrafo. Por otro lado, la mayoría de los DESs cuentan con una densidad menor que el agua, por lo que, como ocurre con el resto de disolventes de baja de densidad, requiere emplear más volumen de disolvente lo que entra en conflicto con los principios de la GSP. Como se había indicado en el caso de los disolventes convencionales, existen estrategias como la SFOD, pero que incrementan en gran medida el tiempo total de análisis.

Recientemente, han aparecido alternativas a la SFOD mucho más sencillas y que requieren menor manipulación. Como se indicó en **el Apartado 1.2.1** sobre sorbentes sólidos, el empleo de materiales magnéticos permite reducir enormemente el tiempo de análisis. En las técnicas de microextracción en fase líquida, el empleo de disolventes magnéticos está adquiriendo popularidad en los últimos años. De entre todos, lo más empleados hasta la fecha son los **líquidos iónicos magnéticos (*Magnetic Ionic Liquids*, MILs)** [107]**.** Estos son como los ILs tradicionales, pero incorporando a su síntesis un componente paramagnético para proporcionarle las propiedades magnéticas.

Como en el caso de los ILs, los MILs han demostrado ser una herramienta analítica eficaz y versátil [108], pero al igual que en el caso de los ILs, sus propiedades 'verdes' están cada vez más en duda, por lo que otros tipos de líquidos magnéticos empiezan a resonar con más fuerza. Este es el caso de los ferrofluidos, que se forman mediante la dispersión estable y uniforme de un material magnético, normalmente MNPs, en el seno de un disolvente [109]. Para mejorar la estabilidad de esta suspensión, se puede emplear un agente estabilizador o dispersante para evitar la aglomeración de las MNPs. En la mayoría de casos suelen ser surfactantes como el ácido oleico, que provocan una repulsión estérica entre las MNPs favoreciendo su dispersión [110]. La formación de estos ferrofluidos se consigue fácilmente introduciendo el disolvente transportador y las MNPs en un baño de ultrasonidos el tiempo suficiente para producir una suspensión estable. Como disolvente transportador se puede utilizar todo tipo de líquidos, sin embargo, los basados en DESs han sido los más utilizados hasta el momento [111]. Todas las propiedades antes mencionadas de los DESs, sumadas a la mejora de manipulación en el empleo de materiales magnéticos, los convierten en disolventes 'verdes' de gran potencial para aplicaciones analíticas. Hasta la fecha, la mayoría de estas aplicaciones se han basado en la DLLME, pero, como ocurría con la DSPE, ahora el material puede ser fácilmente recogido mediante el uso de un campo magnético, evitando así etapas extras de centrifugación y permitiendo su separación de la muestra sin necesidad de SFOD u otros procesos adicionales.

Del mismo modo que ocurría con los sorbentes sólidos, una vez introducidos los disolventes magnéticos, comenzaron a surgir nuevas estrategias. Entre ellas, cabe destacar la **microextracción en fase líquida dispersiva sobre barra agitadora** (***Stir-Bar Dispersive Liquid Microextraction*, SBDLME**) desarrollada por el grupo de investigación en el que se ha desarrollado la presente Tesis Doctoral [112]. Esta técnica se puede entender como la análoga a la SBSDME, detallada en la sección anterior, pero modificada para trabajar con líquidos magnéticos. El procedimiento es similar al de la SBSDME por lo que cuenta con todas sus ventajas, como son la mínima manipulación, la (semi)automatización y la posibilidad de realizar múltiples análisis a la vez con un agitador multiplaca.

Al tratarse de una técnica relativamente reciente, no existen muchas aplicaciones y en la mayoría de ellas se utilizan los MILs [91,112,113]. También se utilizó un ferrofluido basado en un DES de cloruro de colina y resorcinol [114], siendo este último componente altamente tóxico. Por eso,

como se estudiará en detalle en el **Capítulo 4**, se desarrolló un método en el que se emplea la SBDLME con un ferrofluido basado en un LT-DES formado por mentol y timol.

1.4. Evaluación de la sostenibilidad y la seguridad de los métodos

Para evaluar, desde el punto de vista del impacto ecológico y hacia el operador, los métodos analíticos desarrollados en la presente tesis doctoral y compararlos entre sí, se ha empleado la herramienta **'Analyticial GREEnes metric for sample preparation' (AGREEprep)** [115] desarrollada por Wojnowski y colaboradores, que es una modificación de **'Analytical GREEnes metric' (AGREE)** [116] desarrollada por Pena y colaboradores.

La principal diferencia radica en que AGREE se basa en los principios de la GAC mientras que la reciente AGREEprep está más enfocada a la etapa de preparación de muestra. Estas aplicaciones permiten, mediante la introducción de una serie de parámetros de un método analítico, obtener una puntuación entre 0 y 1, donde 0 será un método poco 'verde' mientras que 1 será un método muy 'verde'.

Esta herramienta presenta además un código de colores desde el rojo al verde, tal como se muestra en la **Figura 1.14**, el cual indica a simple vista el impacto medioambiental y los peligros de un determinado método.

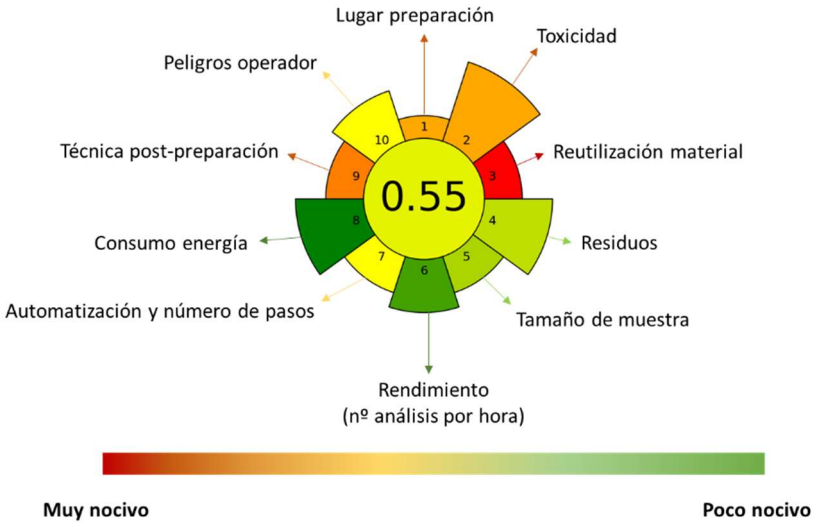

Figura 1.14. A modo de ejemplo, esquema de un resultado obtenido con AGREEprep

Dado que los principios de la GSP se adaptan mejor a las muestras complejas, se ha seleccionado AGREEprep para evaluar y comparar los distintos trabajos realizados en esta tesis doctoral.

AGREEprep se divide en diez apartados, uno por cada principio de la GSP. Cada uno de estos apartados viene, por defecto, con un valor de impacto determinado entre 1 y 5, donde 1 es poco influyente y 5 muy influyente. Aunque es posible modificar manualmente el impacto de cada apartado, se ha decidido mantener el formato por defecto, para mantener una mayor cohesión con el resto de trabajos fuera de la presente Tesis Doctoral.

Esta influencia se puede observar gráficamente viendo el tamaño del trapecio de cada apartado. Como se aprecia en la figura anterior, la influencia del volumen de muestra (punto 5) no es, a priori, muy elevada (2 sobre 5). Esto supone que un cambio en el volumen de muestra no causa un efecto importante en la evaluación final del método. Sin embargo, las mejoras indirectas que se obtienen en otros factores sí que son determinantes para el resultado final de la evaluación.

Por otro lado, aunque la app AGREEprep permite una evaluación muy detallada de la etapa de preparación de muestra, un procedimiento analítico

puede tener etapas mucho más dañinas para el medioambiente o las personas implicadas en el análisis, como puede ser la etapa de síntesis del disolvente o sorbente de extracción.

Por esa razón, de forma complementaria se utilizará, en algunas partes de la presente tesis doctoral, la herramienta ComplexGAPI [117] esquematizada en la **Figura 1.15**, para comparar la síntesis de algunos de los materiales aquí empleados.

ComplexGAPI emplea un código de colores idéntico al visto en AGREEprep. Este se compone principalmente de dos partes. Por un lado, cinco pentágonos que evalúan el método de preparación de muestra y medida (GAPI simple [118]), donde cada uno de los triángulos que lo forman corresponderían a un apartado de evaluación del método. Por otro lado, en la parte inferior hay un hexágono compuesto por varios trapecios. Este hexágono permite la evaluación de la etapa del proceso de síntesis y cada uno de los trapecios corresponde a cada uno de los apartados.

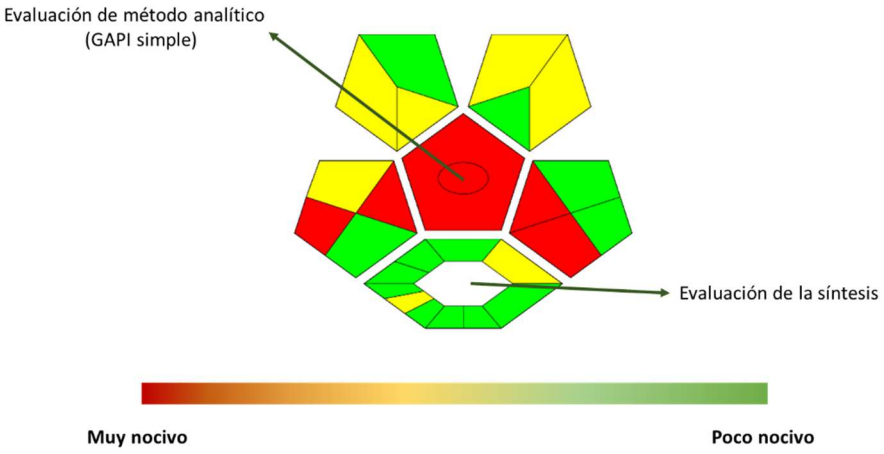

Figura 1.15. A modo de ejemplo, esquema de un resultado obtenido con ComplexGAPI

SECCIÓN 2

Capítulo 2: Microextracción en fase sólida dispersiva sobre barra agitadora para la determinación de trifenilfosfato y difenilfosfato en orina a nivel de trazas

El contenido de este capítulo ha sido publicado en el artículo: Stir bar sorptive-dispersive microextraction for trace determination of triphenyl and diphenyl phosphate in urine of nail polish users, **Journal of Chromatography A 1593 (2019) 9-16** y presentado en formato póster en el congreso "*20th International Symposium on Advances in Extraction Technologies"* Iowa, 2018

Objetivo

Desarrollo de un método analítico para la determinación de trazas de trifenilfosfato y difenilfosfato en muestras de orina.

Resumen

El **trifenilfosfato (*Triphenyl Phosphate,* TPP)** se emplea como plastificante en algunos productos cosméticos como esmalte de uñas. Sin embargo, se sospecha que el TPP se comporta como disruptor endocrino [119], penetrando en el organismo a través de la cutícula [120] y siendo metabolizado para ser expulsado a través de la orina, siendo su metabolito principal el **difenilfosfato (*Dyphenil Phosphate*, DPP**).

Para la determinación de TPP y DPP en muestras de orina, se empleó como técnica de microextracción la SBSDME, utilizando MNPs de $CoFe_2O_4$ incrustadas en un polímero de intercambio aniónico débil (***Strata™ X-Anion Weak Exchanger,* Strata™ X-AW***)* y se realizaron los análisis mediante LC-MS/MS.

Tras la optimización del método se obtuvieron buenos límites de detección (1.9 ng L^{-1} para TPP y 6.3 para DPP ng L^{-1}), valores de desviación estándar relativa (RSD) por debajo del 8 % y valores de coeficiente de recuperación entre 81 y 112 % .

Finalmente, se aplicó el método a muestras de orina de voluntarios tras la aplicación de esmalte de uñas que contenían TPP.

Datos de interés del método

- Material sorbente: $CoFe_2O_4$-Strata™ X-AW

- Volumen de muestra: 25 mL

- Técnica de microextracción empleada: SBSDME

- Tiempo extracción-desorción: 12 min

- Técnica de medida: LC-MS/MS

Compuestos estudiados

Tabla 2.1. Información sobre los compuestos estudiados

Analito	Estructura Química	Número CAS	Log P_{ow}	pK_a
TPP	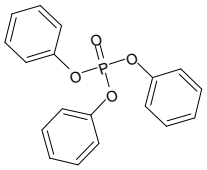	115-86-6	4.59	-
DPP	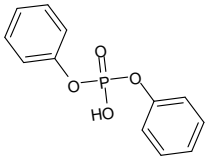	838-85-7	1.34	1.12

Como patrón interno se seleccionó el **dibencilfosfato (*Dibenzyl Phosphate*, DBP)** para corregir los errores de imprecisión derivados de la extracción.

Selección y síntesis del material

El material Strata™ X-AW permite interacciones de tipo aromático e interacciones hidrofóbicas con el TPP como con el DPP. Además, presenta propiedades de intercambiador aniónico débil, lo que mejora las interacciones con el DPP.

La síntesis del material se divide en dos etapas:

Por un lado, la **síntesis de las MNPs** de $CoFe_2O_4$ se llevó a cabo mediante un procedimiento descrito en la bibliografía [121] que se modificó para adaptarlo al problema analítico. En primer lugar, se calentó una mezcla de cloruro de hierro (III) (0.4 M) y cloruro de cobalto (II) (0.2 M) hasta una temperatura de 80 ºC. Posteriormente, se añadió NaOH (3 M) hasta pH básico, observándose la formación de un sólido negro en la suspensión. Esta mezcla se mantuvo en agitación a 80 ºC durante una hora. A continuación, se dejó decantar empleando un imán externo y se descartó el sobrenadante. Las partículas formadas se suspendieron en HCl (1 M) a 4 ºC

durante dos horas. Transcurrido este tiempo, se descartó nuevamente el sobrenadante y las MNPs se volvieron a suspender en agua durante 3 días. Con este proceso se consigue que las partículas más grandes sean depositadas en el fondo del vaso, mientras que las más pequeñas quedan en suspensión. Más adelante, se filtró (nylon, 0.45 µm) y el sólido se mantuvo en estufa a 100 ºC durante toda la noche. Finalmente se pesaron las MNPs para estimar la cantidad y se suspendieron nuevamente en agua.

Después de sintetizar las MNPs, se procedió a su incrustación en la red polimérica. Para ello 0.25 g del polímero Strata™ X-AW se suspendieron en 25 mL de agua. Después se añadió el volumen necesario de la suspensión de MNPs para obtener un relación polímero:MNPs de 1:1 (m/m) y se mantuvo en agitación durante 36 h. El sólido resultante se filtró (nylon, 0.45 µm) y se mantuvo toda la noche a 100 ºC para su secado.

Caracterización del material $CoFe_2O_4$-Strata™ X-AW

- **Estudio de las curvas de histéresis**

El procedimiento de síntesis descrito anteriormente se seleccionó después de estudiar cuatro metodologías:

-**Síntesis #1**: Se hinchó el polímero durante un día en una disolución de pirrolidona, previamente a la adición de la disolución de partículas magnéticas.

-**Síntesis #2:** Se mezcló el polímero directamente con las partículas magnéticas sin llevar a cabo la etapa de hinchado.

-**Síntesis #3 :** Se prepararon *in-situ* las partículas magnéticas en la disolución con el polímero hinchado por pirrolidona.

-**Síntesis #4:** Se prepararon *in-situ* las partículas magnéticas en la disolución con el polímero sin llevar a cabo la etapa de hinchado.

Los cuatro métodos se compararon estudiando sus curvas de histéresis (**Figura 2.1),** seleccionándose la síntesis #2 como método de síntesis al proporcionar un material más magnético (con una **saturación magnética** (***Magnetic Saturation*, Ms**) de 25 emu g^{-1}), y no necesitar de pirrolidona ni de etapa previa de hinchado del polímero.

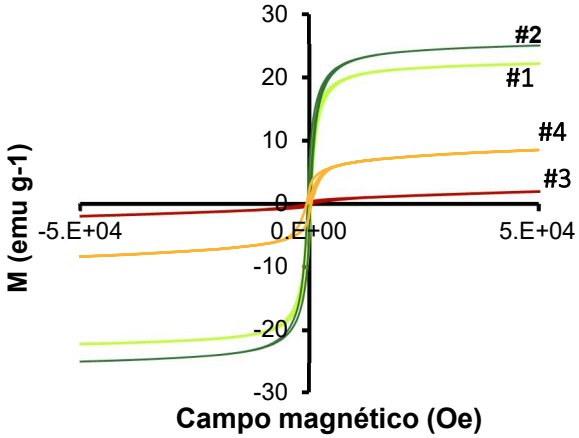

Figura 2.1. Curvas de histéresis de las cuatro estrategias de síntesis ensayadas

- **Tamaño de partícula**

El tamaño medio del composite, estudiado mediante dispersión dinámica de luz, fue de 32 ± 1 µm. En la **Figura 2.2**, se puede observar una pequeña población de partículas de entre 1 y 10 µm debidas, seguramente, a aglomeraciones de partículas magnéticas desprendidas del polímero.

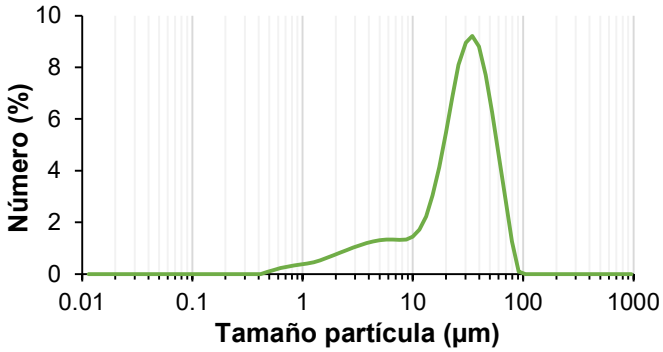

Figura 2.2. Distribución del tamaño de partícula de $CoFe_2O_4$-Strata™ X-AW

- **Potencial Z**

Se estudió la variación del potencial Z con el pH. Como se puede ver en la **Figura 2.3,** a pH ácido el polímero se mantiene cargado positivamente. Sin embargo, a pH superior a 6 el polímero empieza a cargarse negativamente afectando a su capacidad como intercambiador aniónico, lo que afecta negativamente a la extracción del DPP.

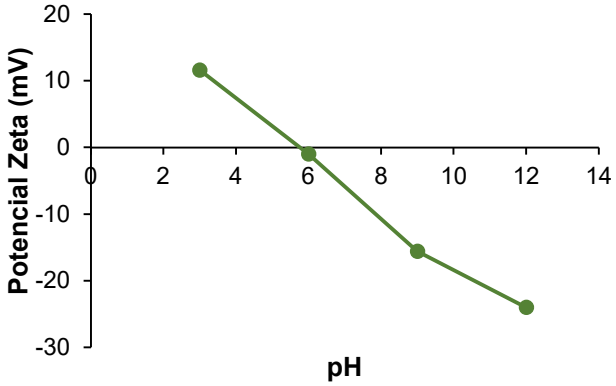

Figura 2.3. Potencial Zeta para $CoFe_2O_4$-Strata^{TM} X-AW

- **Isoterma de adsorción/desorción y tamaño de poro**

Se realizaron las medidas de la isoterma de adsorción/desorción del material, para comprobar su capacidad adsorbente. En la **Figura 2.4,** se observa un comportamiento de tipo IV caracterizado por la existencia de mesoporos y un ciclo de histéresis.

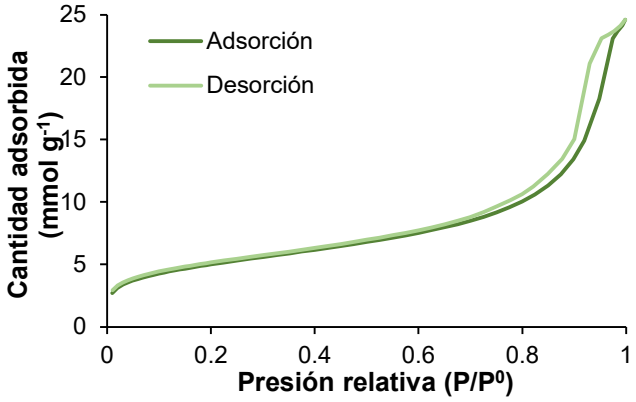

Figura 2.4. Isoterma de adsorción/desorción para $CoFe_2O_4$-Strata™ X-AW

En cuanto al área superficial, el resultado fue de 406 ± 0.7 $m^2\,g^{-1}$.

También se hicieron medidas del tamaño de poro (**Figura 2.5)**, encontrándose un tamaño de mesoporo medio de 29.54 nm.

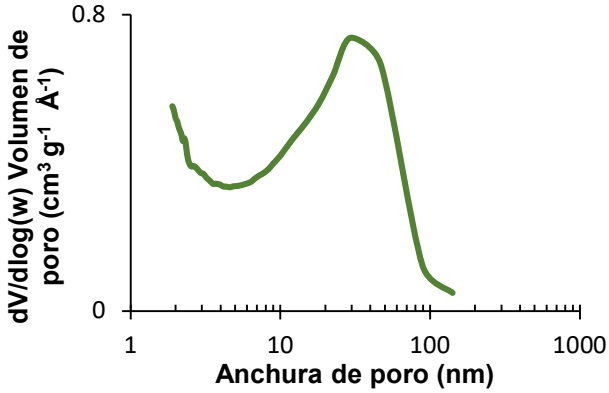

Figura 2.5. Distribución del tamaño de poro para $CoFe_2O_4$-Strata X™-AW

- **Imágenes SEM**

Se realizaron medidas mediante microscopía electrónica de barrido (***Scanning Electron Microscopy*, SEM**) del material $CoFe_2O_4$-Strata™ X-AW. En la **Figura 2.6,** se aprecia el polímero irregular recubierto por pequeñas esferas de $CoFe_2O_4$.

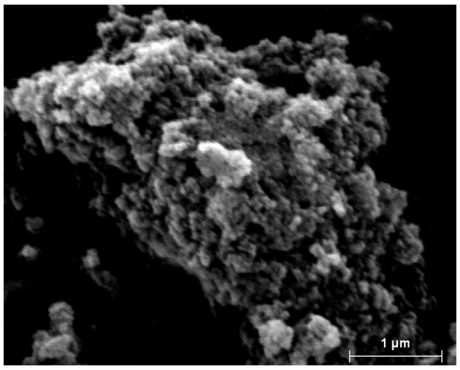

Figura 2.6. Imagen obtenida por SEM para $CoFe_2O_4$-Strata^{TM} X

Esquema del método analítico propuesto

En la **Figura 2.7** se muestra un esquema del método analítico propuesto. Primeramente, 10 mg de $CoFe_2O_4$-Strata ^{TM} X-AW se añaden sobre el imán de neodimio para que el material quede unido a este.

Posteriormente, se acondiciona produciendo la dispersión en 2 mL de MeOH agitando durante 3 min a alta velocidad.

Seguidamente, se introduce el imán con el material magnético en 25 mL de muestra o patrón (conteniendo 100 ng L^{-1} de DBP), agitando nuevamente a alta velocidad durante 5 min para producir la extracción de los analitos.

Transcurrido este tiempo, la agitación se detiene permitiendo al material magnético depositarse nuevamente sobre el imán de neodimio. El imán con el material se lava con una pequeña cantidad de agua ultrapura.

Finalmente, el imán con el material se introducen en un vial de desorción con 0.5 mL de MeOH (0.02 M de NH_3), donde se agita nuevamente para producir la desorción de los analitos. Previo a su introducción en el vial cromatográfico, el extracto se filtró (PTFE, 0.45 µm) para evitar la llegada de material al equipo de LC-MS/MS.

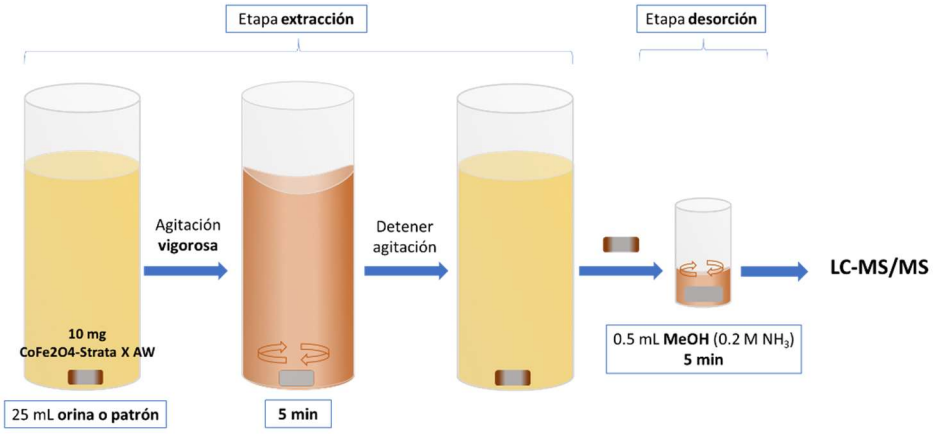

Figura 2.7. Método SBSDME-LC-MS/MS para la determinación de TPP y DPP en muestras de orina

Condiciones cromatográficas

- Columna: Zorbax SB-C18, 50 mm longitud, 2.1 mm de diámetro interno y 1.8 µm de tamaño de partícula

- Fase móvil: H_2O 0.01 acetato amónico y MeOH (20:80 v/v)

- Flujo: 0.3 mL min^{-1}

- Temperatura de columna: 45 ºC

- Modo operacional MS/MS: ESI+/ESI-

- Voltaje: 2000 V (ESI+), 3000 V (ESI-)

- Temperatura de gas: 350 ºC

- Flujo del gas nebulizador: 11 mL min^{-1}

- Presión de nebulizador: 50 psi

- Tiempo de cromatograma: 2 min

Tabla 2.2. Relaciones masa/carga (m/z) de los iones precursores y producto, energías de colisión (CE) y fragmentador para el TPP, DPP y DBP (patrón interno)

	Ion precursor (m/z)	Ion producto (m/z)	CE (V)	Fragmentador (V)
TPP	327	**152**	53	100
DPP	249	**179**	5	100
DBP	255	**105**	29	100

A modo de ejemplo, se muestran a continuación (**Figura 2.8)** el cromatograma obtenido para los analitos:

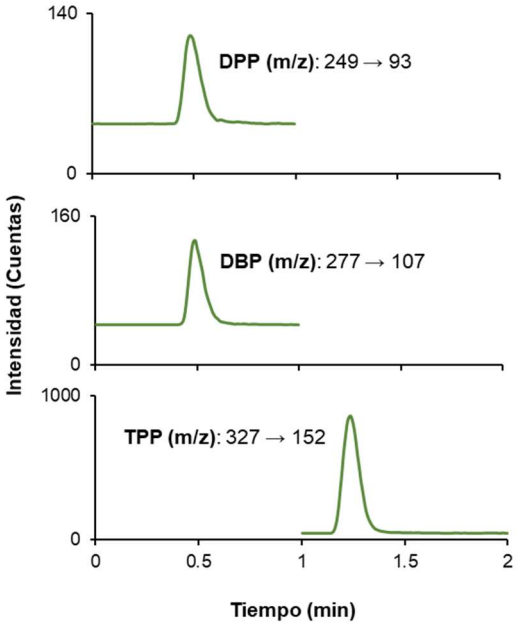

Figura 2.8. Cromatograma obtenido para un patrón de TPP (40 ng L^{-1}), DPP (400 ng L^{-1}) y DBP (1000 ng L^{-1})

Estudio de las variables implicadas en la etapa de extracción y desorción

Para el estudio se utilizó como señal analítica el área de los picos. Las variables estudiadas de las etapas de extracción y de desorción fueron:

- **Cantidad de sorbente:** 5-50 mg
- **Tiempo de extracción:** 1-30 min
- **Tiempo de deposición:** 1-30 min
- **pH de la fase dadora:** 3-12
- **Fuerza iónica de la fase dadora:** 0-2.5 %
- **Tiempo de desorción:** 1-10 min

▪ Cantidad de sorbente

En la **Figura 2.9** se observa una tendencia descendente a medida que aumenta la masa del composite. Esto se puede deber a que no se recupere completamente el material sorbente durante la etapa de deposición y, por tanto, se pierdan cantidades de analito. Además, a mayor cantidad de material, se dificulta la dispersión durante la etapa de desorción. Con estos datos, se seleccionaron **10 mg** ya que proporcionaron los resultados más satisfactorios.

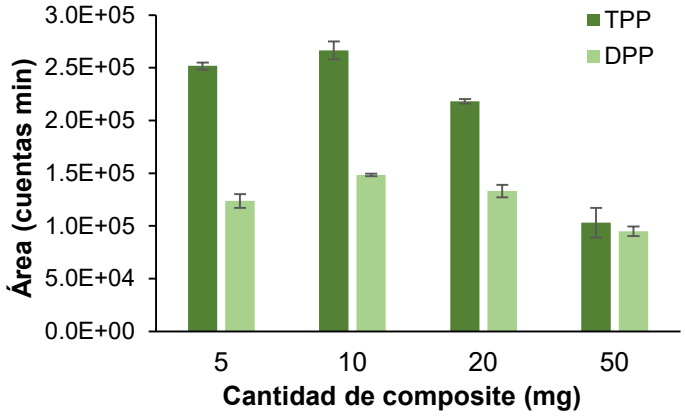

Figura 2.9. Estudio de la cantidad de sorbente. Las barras de error muestran la desviación estándar de los resultados (N=3)

- **Tiempo de extracción**

En la **Figura 2.10** no se observan grandes diferencias entre los distintos tiempos de extracción estudiados. Se seleccionó un tiempo de **5 min** ya que la extracción fue ligeramente superior para el caso del TPP.

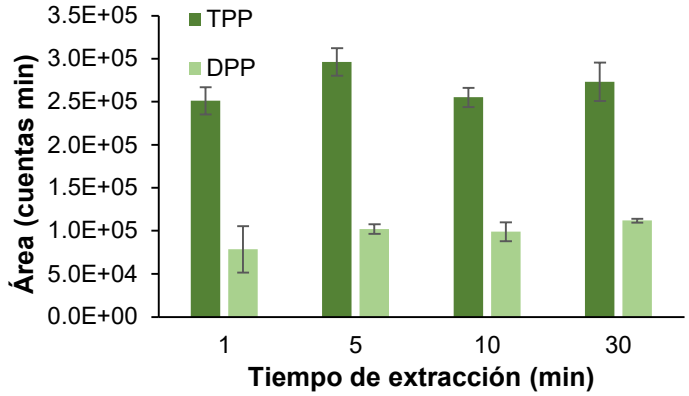

Figura 2.10. Estudio del tiempo de extracción. Las barras de error muestran la desviación estándar de los resultados (N=3)

- **Tiempo de deposición**

Como se observa en la **Figura 2.11**, la señal aumenta con el tiempo de deposición, ya que a tiempos por debajo de 5 min no se lograba recoger todo el material magnético tras la extracción. En cambio, tiempos superiores a 10 minutos no producían incrementos significativos de la señal, por lo que se decidió trabajar con **10 min** con el fin de reducir el tiempo del análisis.

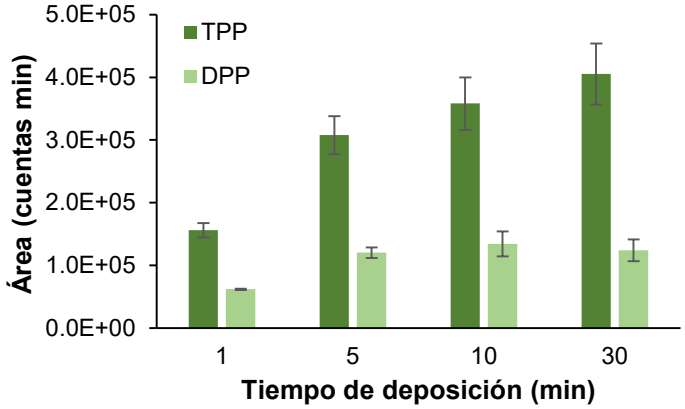

Figura 2.11. Estudio del tiempo de deposición. Las barras de error muestran la desviación estándar de los resultados (N=3)

- **pH de la fase dadora**

Dadas las propiedades ácido-base del DPP y del sorbente, se estudió el pH de la fase dadora. Los resultados se muestran en la **Figura 2.12,** observándose una clara reducción de la señal a pH básico. A estos pH, el polímero se encuentra, como se mostraba en la **Figura 2.3**, cargado negativamente, afectando a sus propiedades como intercambiador aniónico. Por ello se seleccionó **pH 6** que, además, corresponde al pH fisiológico de la orina.

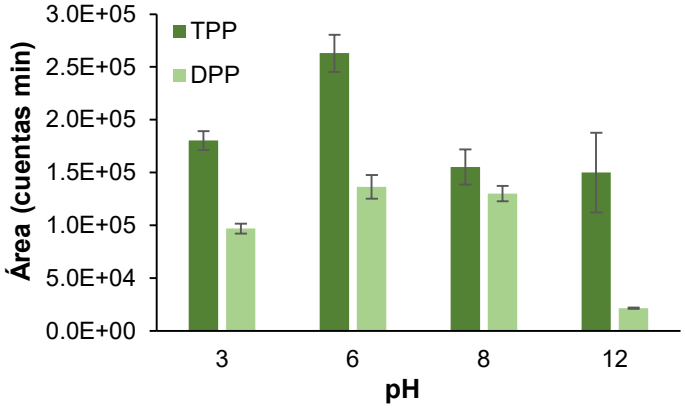

Figura 2.12. Estudio del pH de la fase dadora. Las barras de error muestran la desviación estándar de los resultados (N=3)

- **Tiempo de desorción**

En la **Figura 2.13** se observa una tendencia ascendente del tiempo necesario para llevar a cabo la desorción de los analitos. No se observan diferencias significativas entre desorber en 5 o en 10 min, por lo que se seleccionó un tiempo de **5 min** para reducir el tiempo total de análisis.

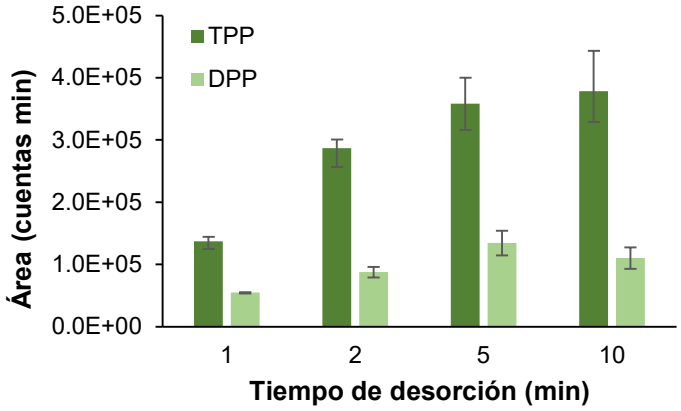

Figura 2.13. Estudio del tiempo de desorción. Las barras de error muestran la desviación estándar de los resultados (N=3)

- **Fuerza iónica**

Por último, se estudió la influencia de la fuerza iónica sobre la eficacia de extracción, ya que las muestras de orina tienen un porcentaje considerable de sales. Se observó que la señal para el DPP se veía afectada, probablemente debido a la competencia de los aniones presentes. Ante este resultado, se decidió realizar un estudio del efecto matriz.

Estudio del efecto matriz

Para determinar el posible efecto matriz se compararon las pendientes de un calibrado para DPP y TPP empleando disoluciones acuosas y orina fortificada, obteniéndose diferencias significativas, probando la existencia de efecto matriz.

El paso posterior consistió en comparar la pendiente de un calibrado obtenido con una mezcla de distintas muestras de orina, con la pendiente

de calibrado obtenida de cada una de las orinas. Como se observa en la **Tabla 2.3**, no se encontraron diferencias significativas, por lo que se puede trabajar empleando calibración en presencia de matriz.

Tabla 2.3. Comparación de las pendientes de calibrado obtenidas con orina de diferentes voluntarios con la pendiente de calibrado obtenida con una mezcla de orinas

Compuesto	Matriz	Pendiente ± desviación[a] (Cuentas min^{-1} ng^{-1} mL)	Test t de Student[b]	
			t_{exp}	Comparables
TPP	Mezcla	10.5 ± 0.1	-	-
	Voluntario A	11.5 ± 0.4	2.20	Sí
	Voluntario B	11.0 ± 0.3	1.45	Sí
	Voluntario C	10.3 ± 0.3	0.76	Sí
	Voluntario D	10.3 ± 0.3	0.72	Sí
DPP	Mezcla	0.098 ± 0.003	-	-
	Voluntario A	0.094 ± 0.004	0.67	Sí
	Voluntario B	0.092 ± 0.005	0.91	Sí
	Voluntario C	0.089 ± 0.003	1.68	Sí
	Voluntario D	0.108 ± 0.004	2.00	Sí

[a]Intervalo de concentración: 0.5 – 5 ng mL^{-1}. Número de puntos de calibración: 6

[b]Test t de Student para la comparación de pendientes entre muestras individuales de orina y la mezcla ($t_{crit}(0.05,8) = 2.31$)

Validación del método y análisis de muestras reales

Para realizar la validación del método, se estudiaron parámetros como la linealidad, los **factores de enriquecimiento** (***Enrichment Factor*, Ef**), los **límites de detección** (***Limit of Detection*, LOD**) y de **cuantificación** (***Limit of Quantification*, LOQ**) y la repetibilidad a través del cálculo de la **desviación estándar relativa** (***Relative Standard Deviation*, RSD**) empleando patrones acuosos sometidos al proceso de extracción. Los resultados se muestran en la **Tabla 2.4.**

Tabla 2.4. Parámetros analíticos del método propuesto

	LOD (ng L^{-1})	LOQ (ng L^{-1})	EF	Repetibilidad (% RSD)[a]					
				Intradía			Interdía		
				Nivel 1	Nivel 2	Nivel 3	Nivel 1	Nivel 2	Nivel 3
TPP	1.9	6.3	30	2.1	4.3	2.8	5.9	8.0	7.5
DPP	17.1	57.1	17	2.2	2.2	2.4	3.6	3.6	5.3

[a] Nivel 1: 0.05 ng mL^{-1}; Nivel 2: 0.5 ng mL^{-1}; Nivel 3: 2 ng mL^{-1}

- **Linealidad**

El método resultó ser lineal, al menos, hasta 100 ng mL^{-1}. Sin embargo, debido a las concentraciones esperadas en orina, se seleccionó un intervalo de trabajo entre 0.05 y 5 ng mL^{-1} para el TPP y 0.5 y 5 ng mL^{-1} para el DPP. Los coeficientes de determinación (R^2) fueron superiores a **0.99** para ambos analitos.

- **Factor de enriquecimiento**

Para establecer los EFs, se calculó el cociente entre la concentración de un patrón de cada analito después de la extracción y antes de realizarla. El resultado fue de **30 ± 1** para el TPP y **17 ± 1** para el DPP.

- **Límites de detección y cuantificación**

Los LODs y LOQsse establecieron estimando la concentración mediante la que se obtenía una relación señal ruido (S/N) de 3 y de 10 respectivamente. Los resultados de LOD fueron **6.7 ng L^{-1}** para el caso del TPP y **77.2 ng L^{-1}** para el DPP. En cuanto a los LOQs, se obtuvieron **22.1 ng L^{-1}** para el TPP y **254.8 ng L^{-1}** para el DPP.

- **Repetibilidad**

La repetibilidad se estableció calculando la RSD para tres niveles de concentración. Se midieron 5 réplicas de cada nivel un mismo día (repetibilidad intradía) y 5 réplicas en distintos días (repetibilidad interdía). Se obtuvieron RSDs inferiores al **8 %**, indicando una buena precisión del método.

- **Análisis de muestras reales**

Se fortificaron tres muestras de orina procedentes de tres voluntarios que no habían estado en contacto con TPP a tres niveles de concentración (0.05, 0.5 y 2.5 ng mL^{-1}). Se les aplicó el método propuesto empleando calibración en presencia de matriz y, posteriormente, se determinó el coeficiente de recuperación. En la **Tabla 2.5** se muestran los resultados obtenidos, mostrando excelentes coeficientes de recuperación.

Tabla 2.5. Coeficientes de recuperación obtenidos tras la aplicación del método propuesto empleando calibración en presencia de matriz para muestras de orina exentas de analito fortificadas a tres niveles de concentración

Voluntario	Cantidad añadida (ng mL^{-1})	Cantidad encontrada (ng mL^{-1})		Coeficientes de recuperación (%)	
		TPP	DPP	TPP	DPP
1	0.050	0.046	-	91 ± 6	-
	0.50	0.44	0.51	88 ± 3	103 ± 3
	2.50	2.13	2.47	85 ± 5	99 ± 2
2	0.050	0.044	-	88 ± 4	-
	0.50	0.40	0.51	81 ± 4	103 ± 7
	2.50	2.02	2.78	81 ± 8	111± 2
3	0.050	0.056	-	112 ± 7	-
	0.50	0.53	0.46	105 ± 8	93 ± 5
	2.50	2.60	2.60	104 ± 5	104 ± 5

Finalmente, se analizaron cuatro muestras de orina de distintos voluntarios tomadas a diferentes horas tras la aplicación de un esmalte de uñas que contenía un 4 % de TPP. Los resultados obtenidos para dos hombres (H) y dos mujeres (M) se muestran en la **Figura 2.14.**

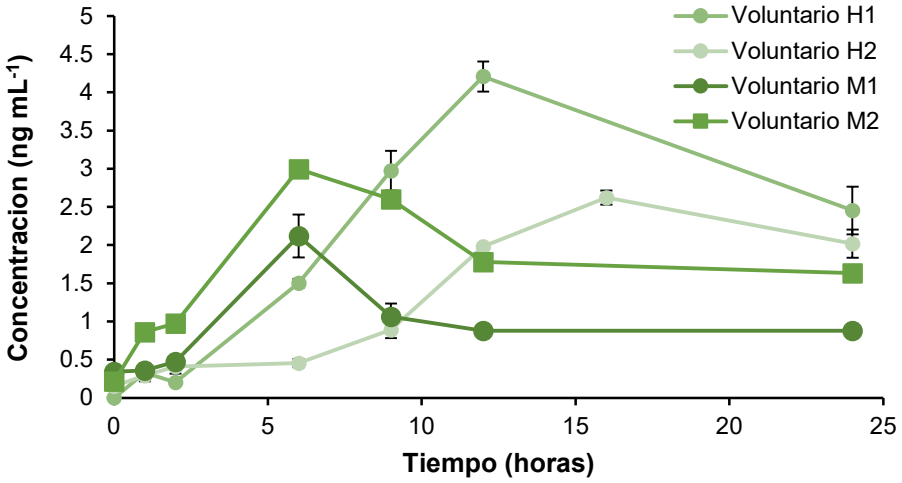

Figura 2.14. Perfiles de DPP en muestras de orina de cuatro voluntarios tras la aplicación de esmalte de uñas conteniendo TPP

Como se observa en la figura, las concentraciones de DPP aumentaron durante las primeras horas tras la aplicación para posteriormente ir disminuyendo a lo largo del día.

Para el TPP, se detectaron señales por debajo del LOQ durante las dos primeras horas, disminuyendo rápidamente hasta no ser detectable en las siguientes horas.

Comparación con otros métodos de la bibliografía

El método propuesto se comparó con métodos publicados en la bibliografía en los que se emplea SPE con diferentes materiales y medida mediante LC-MS/MS. Como se aprecia en la **Tabla 2.6**, el método propuesto permitía obtener LODs inferiores sin necesidad de derivatización y empleando muy poca cantidad de sorbente.

Tabla 2.6. Comparación del método propuesto con otros métodos empleando LC-MS/MS para la determinación de DPP en muestras de orina.

Técnica extracción	Fase extracción	LOD (ng mL^{-1})	Coeficiente de recuperación (%)	Ref
SPE	Strata-X^{TM}-AW	0.20	71 – 97	[122]
SPE[a]	Oasis Wax	0.09	102 – 105	[123]
SPE[a]	Isolute aminopropyl	0.05	95 – 108	[124]
SPE	Oasis Wax	0.13	108	[125]
SPE	Strata-X^{TM}-AW	0.2	-	[126]
SBSDME[b]	$CoFe_2O_4$-StrataX^{TM}-AW	0.08	93 – 111	[127]

[a]Métodos con derivatización

[b]Trabajo presentado en este capítulo

Evaluación de la seguridad y sostenibilidad del método

En la **Figura 2.15** se puede observar el diagrama AGREEprep para el método propuesto. El empleo de altos volúmenes de muestra, sumado al alto empleo de disolventes orgánicos como el MeOH, provoca una penalización muy grande en los puntos 2, 4 y 5 relacionados con la toxicidad y la cantidad de residuos. Esto, sumado a la dificultad de portabilidad de la técnica para el análisis *on site,* hace que su valoración final sea de tan solo 0.38 sobre 1.

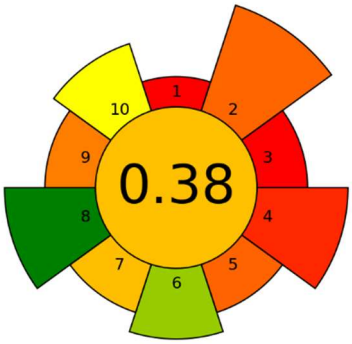

Figura 2.15. Evaluación del método propuesto empleando AGREEprep

Conclusiones

Se ha desarrollado con éxito un método para la determinación de TPP y DPP en muestras de orina.

El método se aplicó con éxito a muestras reales obteniendo valores de coeficiente de recuperación próximos al 100 % demostrando que la calibración en presencia de matriz resultó útil para corregir el efecto matriz.

Los bajos LODs permiten detectar y cuantificar DPP hasta un día después de haberse aplicado una laca de uñas con TPP.

En relación a los antecedentes bibliográficos, el método propuesto ofrece buenos resultados sin necesidad de una etapa de derivatización y reduciendo el volumen de disolventes.

Este método permite extender la aplicabilidad de la SBSDME al análisis de muestras biológicas.

Capítulo 3: Microextracción en fase sólida dispersiva sobre barra agitadora para la determinación de almizcles sintéticos en aguas ambientales

El contenido de este capítulo ha sido publicado en el artículo Polydopamine-coated magnetic nanoparticles for the determination of nitro musks in environmental water samples by stir bar sorptive-dispersive microextraction, **Talanta 231 (2021) 122375**

Objetivo

Desarrollo de un método analítico para la determinación de almizcles sintéticos en muestras de agua de origen ambiental

Resumen

Los almizcles sintéticos son una familia de compuestos de olor agradable que han sido ampliamente utilizados en productos cosméticos. Sin embargo, pueden tener efectos nocivos tanto para la salud de las personas como para el medioambiente. Por esto, algunos de ellos han sido recientemente prohibidos en el Anexo II del Reglamento Europeo sobre productos cosméticos [128].

Estos almizcles pueden llegar al medioambiente acuático a través de las aguas residuales de los hogares o vertidos industriales. Una vez allí, tardan mucho tiempo en degradarse, llegando incluso a bioacumularse [129].

Debido a las bajas concentraciones a las que se pueden encontrar estos compuestos en las aguas, es necesario el desarrollo de técnicas de microextracción para su correcta determinación. Por esa razón, se utilizó la SBSDME como técnicas de extracción, empleando MNPs de $CoFe_2O_4$ recubiertas con **polidopamina (*Polydopamine,* PDA)**. Tras la extracción, los analitos se desorbieron mediante un equipo de desorción térmica (***Thermal Desorption,* TD)** acoplado a un equipo de GC-MS.

Se estudiaron las variables del método y bajo las condiciones más favorables se obtuvieron límites de detección del orden de ng L^{-1}, valores de RSD inferiores al 15 % y coeficientes de recuperación entre el 91 y el 120 %. Por último, se aplicó el método a diversas muestras de agua para estudiar los niveles de almizcles sintéticos.

Datos de interés del método

- **Material sorbente:** $CoFe_2O_4$@polydopamine ($CoFe_2O_4$@PDA)
- **Volumen de muestra:** 25 mL
- **Técnica de microextracción empleada:** SBSDME
- **Tiempo extracción-desorción:** 15 min
- **Técnica de medida:** TD-GC-MS

Compuestos estudiados

Tabla 3.1. Información sobre los compuestos objeto de estudio en este capítulo

Almizcle	Estructura	Fórmula molecular	Nº CAS	T ebullición (ºC)
Almizcle ambreta (MA)	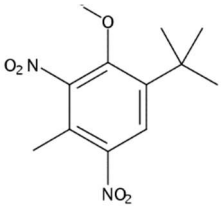	$C_{12}H_{16}N_2O_5$	83-66-9	369
Almizcle xileno (MX)	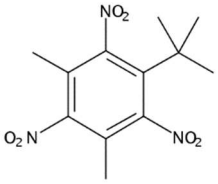	$C_{12}H_{15}N_3O_6$	81-15-2	392
Almizcle muscado (MM)	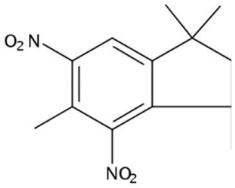	$C_{14}H_{18}N_2O_4$	116-66-5	351
Almizcle tibetano (MT)	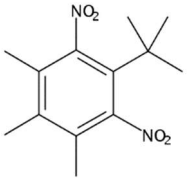	$C_{13}H_{18}N_2O_4$	145-39-1	391
Almizcle cetona (MK)	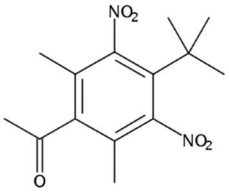	$C_{14}H_{18}N_2O_5$	81-14-1	369

Se empleó **hexaclorobenceno (*Hexachlorobenzene*, HCB)** como patrón interno para corregir los errores durante las etapas de microextracción y desorción térmica.

Selección y síntesis del material

Se eligió PDA como material sorbente, ya que cuenta con anillos aromáticos que pueden interaccionar con los anillos de los almizcles y, también, mediante interacciones hidrofóbicas. Por otro lado, la PDA se dispersa muy bien en agua, lo que es muy útil para cualquier técnica basada en la dispersión del sorbente.

Como en el capítulo anterior, la síntesis consistió en dos partes. Por un lado, la síntesis de las MNPs se llevó a cabo de forma similar a la realizada en el **Capítulo 2**. Sin embargo, las etapas de lavado en medio ácido y de resuspensión se eliminaron ya que no se consideran necesarias para esta aplicación.

Se mezclaron 250 mg de las MNPs con 500 mg de dopamina junto con 100 mL de una disolución amortiguadora de tris(hidroximetil) aminometano (en adelante, Tris) (10 mM, pH=8.5). La mezcla se agitó durante 12 horas. Finalmente, el sólido resultante se lavó con agua y etanol y se mantuvo a 80ºC durante toda la noche.

Caracterización del material $CoFe_2O_4$@PDA

- **Estudio de las curvas de histéresis**

Se comparó la curva de histéresis del material sorbente $CoFe_2O_4$@PDA con la de las MNPs de $CoFe_2O_4$ (**Figura 3.1)**. Como era de esperar, la Ms de $CoFe_2O_4$@PDA (28.5 emu g^{-1}) es menor que la del $CoFe_2O_4$ (65.0 emu g^{-1}) pero, aun así, el material presenta unas propiedades magnéticas suficientes para su empleo en SBSDME.

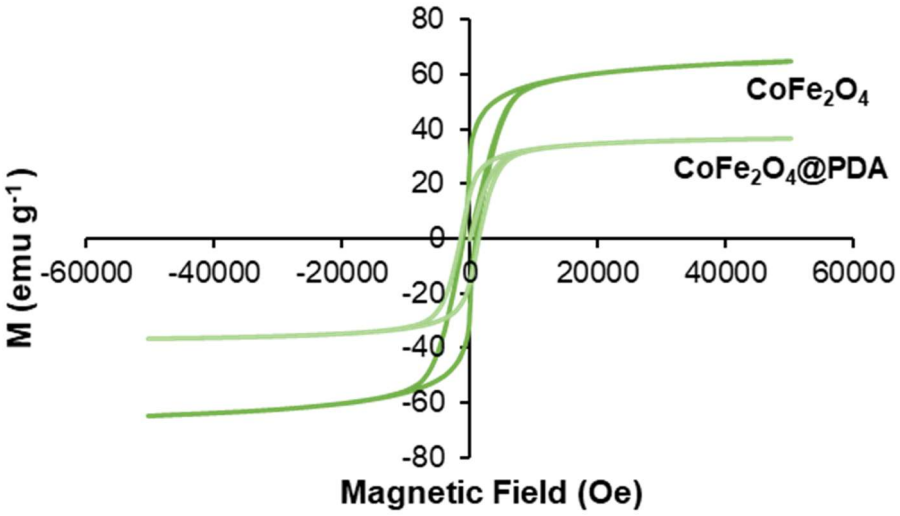

Figura 3.1. Curvas de histéresis del sorbente $CoFe_2O_4$@PDA y de las MNPs de $CoFe_2O_4$

- **Imágenes TEM y SEM**

Se realizaron medidas mediante SEM y microscopía electrónica de transmisión (***Transmission Electron Microscopy,* TEM**). Las imágenes incluidas en **la Figura 3.2** muestran la forma esférica del $CoFe_2O_4$@PDA, con diámetros en torno a los 50 nm. Las imágenes obtenidas por TEM muestran, además, el núcleo de las partículas magnéticas recubiertas por la capa polimérica.

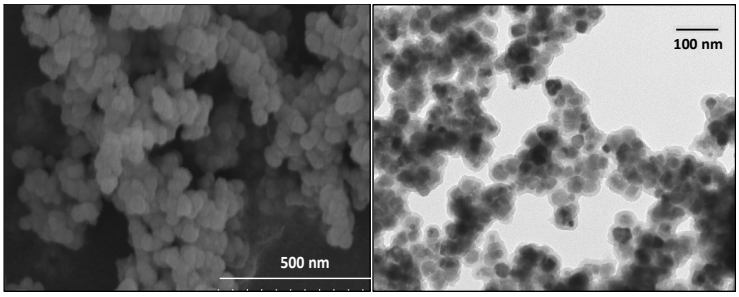

Figura 3.2. Imágenes obtenidas por SEM y TEM para $CoFe_2O_4$@PDA

- **Isoterma de adsorción/desorción**

Se realizaron las medidas de la isoterma de adsorción/desorción del material (**Figura 3.3)** mostrando un comportamiento de tipo IV y mesoporos en torno a los 7.5 nm. En cuanto al área superficial, se obtuvo un valor de 10.544 ± 0.008 $m^2\ g^{-1}$.

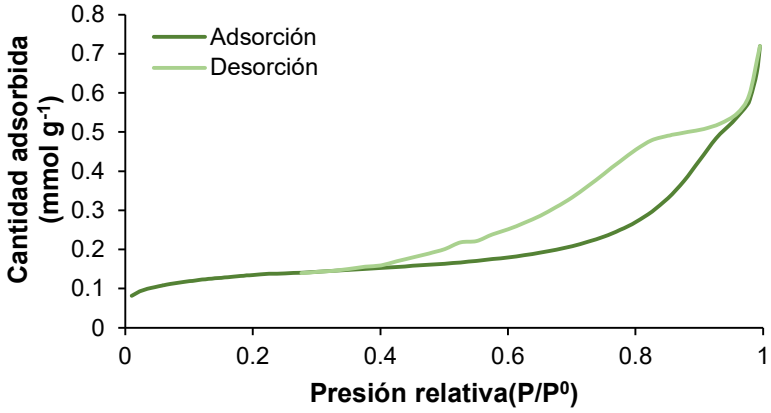

Figura 3.3. Isoterma de adsorción/desorción para $CoFe_2O_4$@PDA

- **TGA**

El **análisis termogravimétrico (*Thermogravimetric Analysis,* TGA),** representado en la **Figura 3.4**, muestra buena estabilidad térmica del composite a temperaturas inferiores a 300 ºC. A partir de esta temperatura, se produce la destrucción de la materia orgánica quedando solo las partículas magnéticas. En este sentido, el material presenta suficiente estabilidad térmica para poderse utilizar durante la etapa de desorción térmica, en la que se alcanzan temperaturas máximas de 275 ºC.

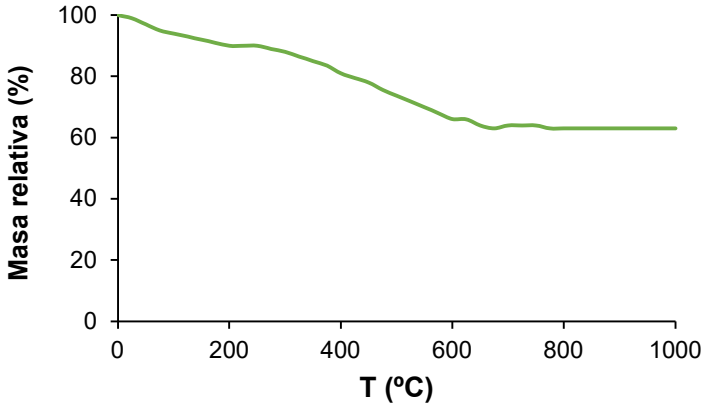

Figura 3.4. Análisis termogravimétrico para el $CoFe_2O_4$@PDA

Esquema del método analítico propuesto

En la **Figura 3.5** se muestra un esquema del método analítico propuesto. Primero se acondiciona el material con 10 mL de agua desionizada agitando a alta velocidad durante 5 min.

Posteriormente, el imán con el $CoFe_2O_4$@PDA se introduce en 25 mL de patrón o de muestra de agua (conteniendo 200 ng L^{-1} de HCB) y se agita vigorosamente durante 10 min para producir la extracción de los analitos.

Transcurrido este tiempo, se detiene la agitación y el material se deposita nuevamente en el imán de neodimio. A continuación, el imán con el material magnético se limpia con agua ultrapura para eliminar los posibles restos de muestra o patrón.

Finalmente, el imán se introduce en un tubo de desorción sellado con lana de vidrio para su introducción directa en el TD-GC-MS/MS.

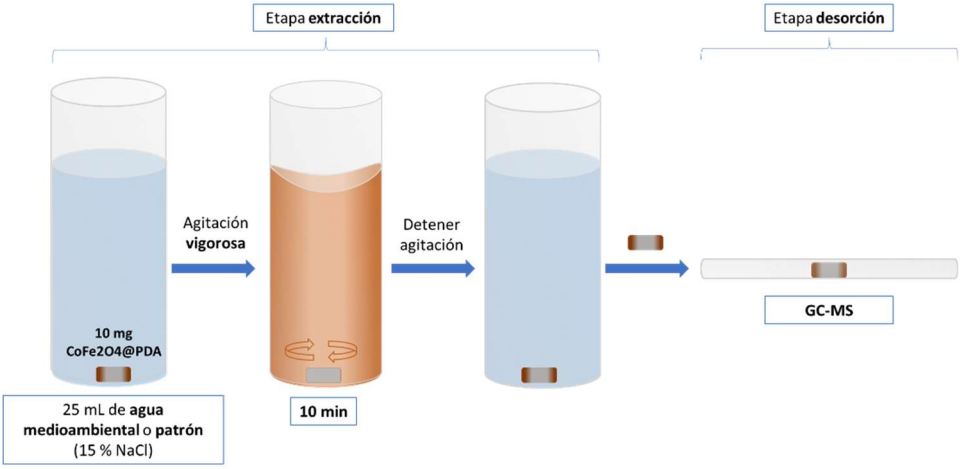

Figura 3.5. Método SBSDME-TD-GC/MS para la determinación de almizcles sintéticos en aguas medioambientales

Condiciones cromatográficas

- Programa TD: 50ºC (2 min) para eliminar los restos de agua que podrían quedar en el imán; Desorción: 275 ºC (10 min); Trampa fría: -10 ºC; Desorción trampa fría: Calentar hasta 275 ºC a 16 ºC s^{-1}

- Temperatura línea transferencia: 200 ºC

- Columna: HP-5MS (30 m longitud, 0.25 mm diámetro interno y 0.25 µm espesor de relleno)

- Programa temperatura GC: 60ºC (1 min); 120 ºC a 20 ºC min^{-1}; 180 ºC a 10 ºC min^{-1}; 280 ºC (1 min) a 25 ºC min^{-1}

Tabla 3.2. Relaciones masa/carga (m/z) para los almizcles sintéticos estudiados en este capítulo y para el patrón interno

	m/z[a]
MA	**253**, 263, 282
MX	253, 263, **282**
MM	253, **263**, 282
MT	**251**, 279
MK	251, **279**
HCB	**284**

[a] Señalados en negrita la m/z para la cuantificación

A modo de ejemplo, en la **Figura 3.6** se muestra el cromatograma obtenidos para los analitos y el patrón interno tras aplicar el método a una disolución patrón.

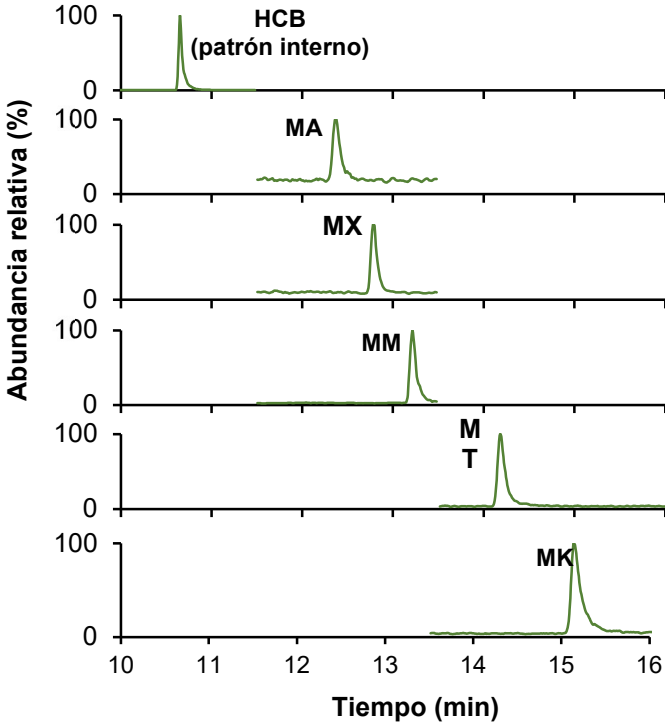

Figura 3.6. Cromatograma obtenido para una disolución patrón conteniendo 100 ng L^{-1} de los analitos estudiados y el patrón interno extraída según el método propuesto

Estudio de las variables implicadas en la etapa de extracción y desorción

Para el estudio se utilizó como señal analítica el área de los picos. Las variables estudiadas de las etapas de extracción y de desorción fueron:

- Cantidad de sorbente: 5-20 mg

- Tiempo de extracción: 1-30 min

- Fuerza iónica: 0-25 %

- Temperatura desorción térmica: 225-275 ºC

- Tiempo desorción térmica: 5-15 min

▪ Cantidad de sorbente

Como se aprecia en la **Figura 3.7**, se produce un aumento de la señal al incrementar la cantidad de sorbente de 5 a 10 mg. Sin embargo, las diferencias no son significativas entre 10 y 20 mg. Por esa razón, se seleccionaron finalmente **10 mg,** para reducir así la cantidad de sorbente empleado.

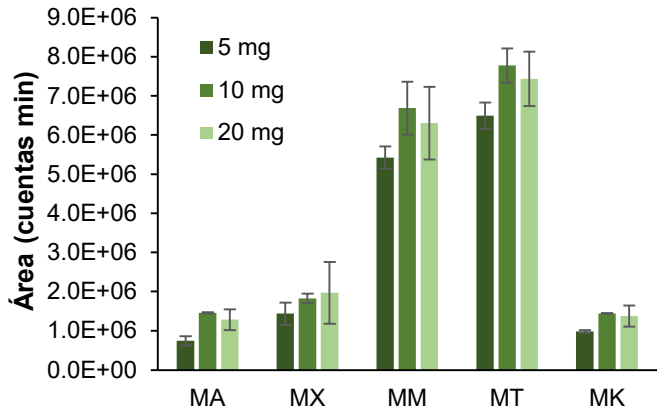

Figura 3.7. Estudio de la cantidad de sorbente. Las barras de error muestran la desviación estándar de los resultados (N=3)

- **Tiempo de extracción**

Al aumentar el tiempo de extracción cabría esperar un aumento progresivo de la señal seguido de una estabilización. Sin embargo, al analizar la **Figura 3.8.** se observa una disminución a tiempos de 20 y 30 min. Al tratarse de una técnica que busca una dispersión muy eficiente en volúmenes elevados de muestra, la agitación debe de ser suficientemente agresiva, por lo que a tiempos muy largos se puede dar, en menor o mayor medida, el fenómeno conocido como *leaching,* en el cual las MNPs se separan del sorbente. De este modo, al acabar la agitación, se recoge la parte magnética mientras que la parte sorbente con los analitos se mantiene en la disolución, perdiendo así parte de los analitos y disminuyendo así la señal [44]. Atendiendo a estos resultados, se seleccionó un tiempo de **10 minutos.**

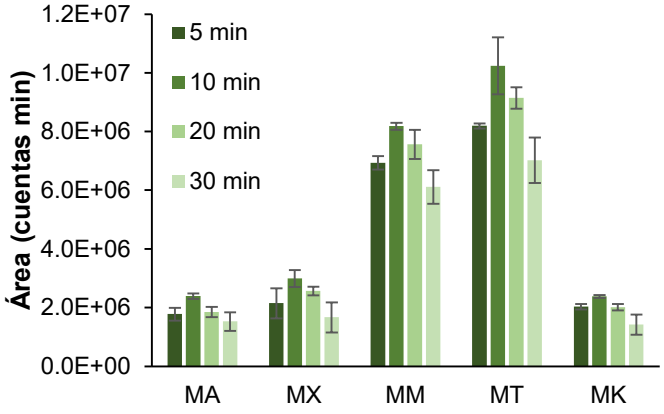

Figura 3.8. Estudio del tiempo de extracción. Las barras de error muestran la desviación estándar de los resultados (N=3)

- **Fuerza iónica**

Para verificar el posible efecto salino y la influencia de la salinidad en el análisis de las muestras, se estudió el efecto de la adición de distintas cantidades de NaCl. Tal y como muestra la **Figura 3.9**, se produce un aumento de la señal hasta el 15 %, seguido de una brusca disminución. Esto es debido al gran incremento de la viscosidad, sumado a la elevada concentración de iones, que disminuye la afinidad del sorbente por la muestra. De este modo, se seleccionaron finalmente **15 % de NaCl.**

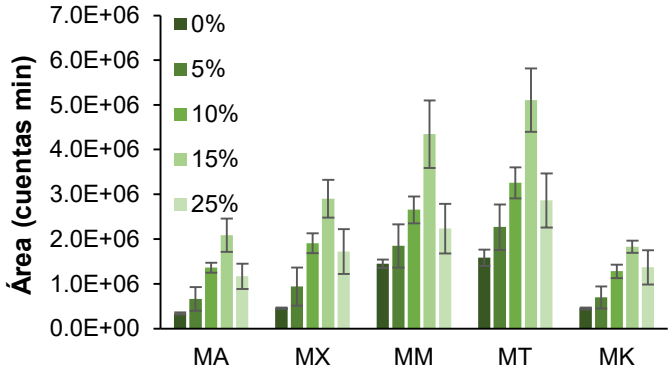

Figura 3.9. Estudio de la fuerza iónica (como concentración de NaCl %) de la fase dadora. Las barras de error muestran la desviación estándar de los resultados (N=3)

- **Temperatura de desorción térmica**

Se estudiaron diferentes temperaturas de desorción tras la retención de los analitos por la trampa fría. Los resultados se muestran en la **Figura 3.10**. Pese a no encontrar grandes diferencias en la señal obtenida, las mejores condiciones se obtuvieron a una temperatura de **275 ºC.** No se ensayaron temperaturas superiores, para no sobrepasar los límites de estabilidad térmica del sorbente.

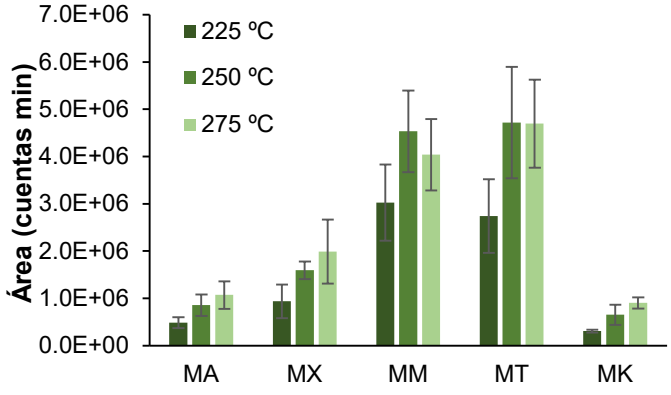

Figura 3.10. Estudio de la temperatura de desorción. Las barras de error muestran la desviación estándar de los resultados (N=3)

- **Tiempo de desorción**

Del mismo modo, se estudiaron diferentes tiempos de desorción. En este caso, como se puede apreciar en la **Figura 3.11**, sí que se observan diferencias muy significativas para algunos analitos como el MX y el MT. Por esta razón, se seleccionó un tiempo de **10 min**.

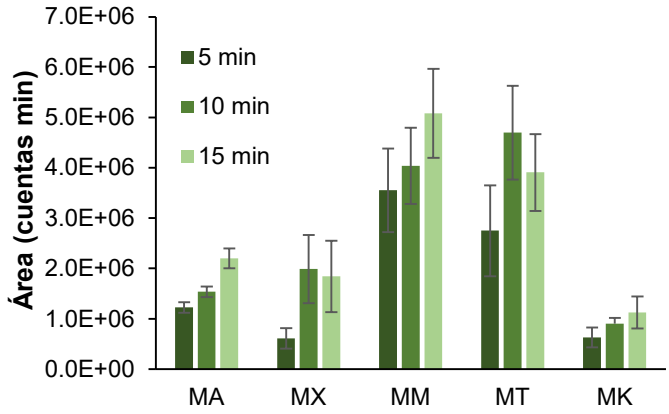

Figura 3.11. Estudio del tiempo de desorción. Las barras de error muestran la desviación estándar de los resultados (N=3)

Validación del método y análisis de muestras reales

Para realizar la validación del método, se estudiaron la linealidad, los EFs, LODs y LOQs, además de la repetibilidad a partir de patrones acuosos. Para el estudio del coeficiente de recuperación, se seleccionaron una muestra de agua de mar y una de agua de río que se fortificaron a dos niveles de concentración. Los resultados se muestran en la **Tabla 3.3.**

Tabla 3.3. Parámetros analíticos del método propuesto

	LOD ($ng\ L^{-1}$)	LOQ ($ng\ L^{-1}$)	EF	Repetibilidad (% RSD)[a]			
				Intradía		Interdía	
				Nivel 1	Nivel 2	Nivel 1	Nivel 2
MA	5.6	18.6	284 ± 10	3.9	4.5	9.7	10.2
MX	3.8	13.0	178 ± 10	4.8	5.4	8.6	9.6
MM	0.3	1.0	640 ± 70	3.5	3.7	7.8	12.3
MT	1.8	6.0	303 ± 30	5.8	6.6	9.8	11.5
MK	0.6	2.0	378 ± 30	5.3	5.9	10.5	10.1

[a] Nivel 1: 20 $ng\ L^{-1}$; Nivel 2: 40 $ng\ L^{-1}$

- **Linealidad**

El método es lineal al menos hasta 20 $\mu g\ L^{-1}$. Sin embargo, debido a la baja concentración en la que se encuentran estos compuestos en aguas ambientales, se decidió emplear un intervalo de trabajo entre 20 y 100 $ng\ L^{-1}$. Los coeficientes de determinación (R^2) fueron superiores a **0.995** para todos los analitos.

- **Factor de enriquecimiento**

Para el cálculo del EF, se inyectó 1 µL, dado que suele ser el volumen de inyección típico en GC, de una disolución patrón de una determinada concentración y se obtuvo su área. Posteriormente extrajo un patrón de la misma concentración y tras realizar la desorción térmica, se obtuvo su área. Los EFs se calcularon como el cociente entre las áreas obtenida con y sin la etapa de microextracción. Los resultados se encontraron entre **178** y **640** en función del analito.

- **Límites de detección y cuantificación**

Los LOD y LOQ se establecieron estimando la concentración mediante la que se obtenía una relación S/N de 3 y 10 respectivamente. Los LODs

obtenidos varían entre **0.3** y **5.6 ng L^{-1}** mientras que los LOQs entre **1.0** y **18.6 ng L^{-1},** según el analito.

- **Repetibilidad**

La repetibilidad se estableció calculando la RSD de 5 réplicas medidas el mismo día (repetibilidad intradía) y 5 réplicas medidas en distintos días (repetibilidad interdía). Las medidas se realizaron a dos niveles de concentración (20 y 40 ng L^{-1}), obteniéndose resultados de RSD entre **4** y **12 %.**

- **Análisis de muestras reales**

Una muestra de agua de mar y otra de río libres de analito se fortificaron a dos niveles de concentración (20 y 40 ng L^{-1}) para calcular los coeficientes de recuperación. Los resultados, mostrados en la **Tabla 3.4,** varían entre **91** y **120 %,** probando así la inexistencia de efecto matriz. De este modo, es posible trabajar con calibración externa con empleo de patrón interno.

Tabla 3.4. Coeficientes de recuperación obtenidos tras la aplicación del método propuesto a dos muestras de agua fortificadas a dos niveles de concentración

Almizcle	Coeficiente de recuperación (%)			
	Agua de mar		Agua de río	
	20 ng L^{-1}	40 ng L^{-1}	20 ng L^{-1}	40 ng L^{-1}
MA	103 ± 12	114 ± 6	111 ± 12	101 ± 9
MX	106 ± 10	102 ± 6	101 ± 5	98 ± 7
MM	118 ± 10	97 ± 10	101 ± 3	109 ± 14
MT	91 ± 2	99 ± 8	108 ± 6	110 ± 4
MK	110 ± 14	110 ± 10	108 ± 11	90 ± 11

Finalmente, se analizaron cuatro muestras de agua, dos medioambientales (una de mar y una de río), una muestra de vertidos de una industria cosmética y una muestra de una planta de tratamiento de aguas. Las concentraciones de todos los analitos resultaron inferiores a los LODs. Esto puede ser debido a la disminución del uso de estos almizcles sumado a que

el estudio se realizó durante la etapa más crítica del confinamiento debido a la pandemia de la COVID-19.

Estudio de la repetibilidad de la síntesis

Para verificar la repetibilidad de la síntesis del composite se realizaron tres síntesis independientes del material. Con cada síntesis se realizó una extracción de disolución de los diferentes analitos. Bajo las condiciones óptimas, obteniendo una RSD inferior al 15 % para todos los analitos.

Reutilización del $CoFe_2O_4$@PDA

Se comprobó que el material magnético se puede reutilizar al menos una vez, obteniendo resultados de RSD entre el 3 y el 6 % entre el primero y el segundo uso. No obstante la dificultad de la separación de tan poca cantidad de masa del imán hace el proceso tedioso. Precisamente, el empleo de tan poca cantidad hace que pueda prescindir de su reutilización.

Comparación con otros métodos de la bibliografía

En la **Tabla 3.5** se compara el método propuesto con otros encontrados en la bibliografía, hacen uso de diferentes técnicas de microextracción.

Tabla 3.5. Comparación del método propuesto con otros métodos para la determinación de almizcles sintéticos en aguas medioambientales.

Técnica de extracción	Tiempo de extracción (min)	EF	LOD (ng L^{-1})	Coeficiente de recuperación (%)	Ref
SPME	900	n.r.[b]	0.05-60	42-119	[130]
SBSE	240	n.r.[b]	0.02-1.4	n.r.[b]	[131]
DSPE	10	n.r.[b]	0.5-2.0	70-97	[132]
DLLME	-	230-314	4-33	87-116	[133]
BID-SDME	20	65-92	12-42	92-105	[134]
USAEME	10	n.r.[b]	9.2-10	80-114	[135]
MASE	240	n.r.[b]	4-25	47-138	[136]
SBSDME[a]	10	172-640	0.1-2.8	92-120	[137]

[a] Trabajo presentado en este capítulo

[b]n.r. no reportado

Como se puede apreciar en la tabla, con el método propuesto se obtienen excelentes resultados sin requerir los elevados tiempos de extracción de las técnicas en fase sólida no dispersiva (SPME y SBSE) y sin ningún tipo de disolvente orgánico.

Evaluación de la seguridad y sostenibilidad del método

En la **Figura 3.12.** se puede observar el diagrama AGREEprep del método propuesto en la que se aprecia una mejoría respecto a la toxicidad respecto al método del **Capítulo 2.** Esto se debe a la ausencia total de empleo de disolventes orgánicos. No obstante, este método se encuentra lastrado por el volumen tan alto de muestra empleado y por el uso de desorción térmica,

lo que, además de incrementar los tiempos y, por tanto, reducir el número de análisis por hora, también supone un incremento en el consumo energético. Por su parte, la alta generación de residuos continúa siendo un problema a mejorar.

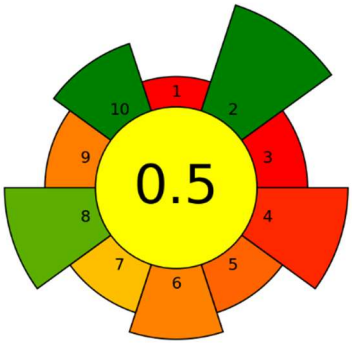

Figura 3.12. Evaluación del método propuesto empleando AGREEprep

Conclusiones

Se ha desarrollado y validado un método rápido y sensible para la determinación de una familia de almizcles sintéticos empleando SBSDME.

Este método no utiliza ningún tipo de disolvente orgánico en ninguna de sus etapas, reduciendo enormemente el impacto del mismo.

Empleando este método se consiguen tiempos de extracción cortos y sin necesidad de una elevada manipulación por parte del operador.

La presente aplicación evita el uso de compuestos tóxicos en todas las etapas, permitiendo una mejora significativa en el carácter 'verde' del método y de la SBSDME. No obstante, su elevado consumo energético y el limitado número de análisis por hora, lo convierten en un método todavía mejorable.

Capítulo 4: Microextracción en fase líquida dispersiva sobre barra agitadora para la determinación de filtros UV en aguas ambientales empleando un ferrofluido basado en un disolvente eutéctico de baja toxicidad

El contenido de este capítulo ha sido publicado en el artículo **Low toxicity deep eutectic solvent-based ferrofluid for the determination of UV filters in environmental waters by stir bar dispersive liquid microextraction, Talanta 243 (2022) 123378** y presentado en formato póster en el congreso "*XXIII Meeting of the Spanish Society of Analytical Chemistry*" Oviedo, 2022

Objetivo

Desarrollo de un nuevo ferrofluido basado en componentes de baja toxicidad para su empleo como disolvente de extracción en técnicas de microextracción en fase líquida dispersivas.

Aplicación de este ferrofluido a la determinación de filtros UV en aguas medioambientales mediante SBDLME.

Resumen

En este capítulo se presenta el desarrollo de un nuevo ferrofluido compuesto por un DES de baja toxicidad (LT-DES) formado por mentol y timol en proporción 1:5 y MNPs de $CoFe_2O_4$ recubiertas por **ácido oleico (*Oleic Acid*, OA)** ($CoFe_2O_4$@OA) como agente dispersante para evitar la aglomeración de las MNPs.

Este material se caracterizó y se empleó como extractante para la determinación de filtros UV en aguas ambientales de diferente procedencia utilizando SBDLME. Cabe indicar que los filtros UV empleados como ingrediente en productos cosméticos de protección solar, pueden acumularse en el medioambiente afectando a la fauna y la flora, por lo que es necesario el desarrollo de métodos analíticos para determinar trazas de estos compuestos en muestras medioambientales [47].

Se realizó un estudio multivariante para la optimización de las distintas variables implicadas en la etapa de extracción. Se validó el método obteniendo EFs entre 46 y 101, LODs entre 7 y 83 ng L^{-1} y RSDs inferiores al 15 %. Se analizaron muestras reales así como muestras fortificadas a diferentes concentraciones para calcular los coeficientes de recuperación, obteniéndose valores entre el 80 y el 117 %.

Datos de interés del método

- **Material sorbente:** $CoFe_2O_4$@OA-mentol:timol (1:5)
- **Volumen de muestra:** 15 mL
- **Técnica de microextracción empleada:** SBDLME
- **Tiempo extracción-desorción:** 15 min
- **Técnica de medida:** LC-MS/MS

Compuestos estudiados

Tabla 4.1. Información sobre los compuestos objeto de estudio en este capítulo

Compuesto	Estructura química	CAS	Log P_{ow}	pK_a
Benzofenona-3 (BZ3)	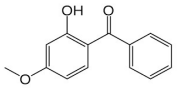	131-57-7	3.79	7.1
Isoamil p-metoxicinamato (IMC)	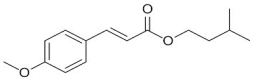	71617-10-2	3.25	-
4-metilbenciliden canfor (MBC)	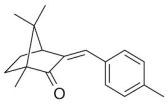	36861-47-9	4.95	-
Dietilamino hydroxibenzoil hexil benzoato (DHHB)	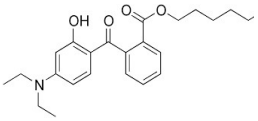	302776-68-7	6.20	7.6
Octocrileno (OC)	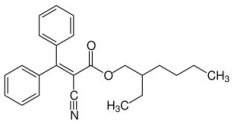	6197-30-4	7.04	-
Etillhexil dimetil PABA (EHDP)	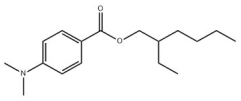	21245-02-3	5.77	2.9
Butil metoxidibenzoilmetano (BMDM)	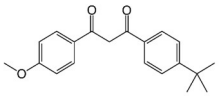	70356-09-1	4.51	9.7
Etilhexil salicilato (EHS)	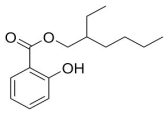	118-60-5	5.77	8.1

Como patrón interno se utilizó el octocrileno deuterado (OC-d15) para corregir los posibles errores durante la etapa de extracción.

Selección y síntesis del material

La combinación de mentol y timol para formar el DES hace que este pueda establecer interacciones hidrofóbicas, dipolo-dipolo e interacciones aromáticas debido a los anillos del timol, por lo que constituye un disolvente idóneo para la determinación de filtros UV de carácter liposoluble. La adición de MNPs de $CoFe_2O_4$ permite formar un ferrofluido que reduce sustancialmente la manipulación durante el análisis.

La síntesis de las MNPs se realizó de forma similar a lo descrito en el **Capítulo 3**. En este caso, una vez adicionado el NaOH (3 M), se añadieron 2 mL de OA y se mantuvo en agitación durante una hora para su funcionalización. Transcurrido este tiempo se realizaron lavados con agua y etanol y se mantuvo en estufa a 100 ºC durante una noche para su secado.

Para la preparación del DES se pesaron 0.47 g de mentol y 2.76 g de timol en tubos de centrífuga de 15 mL. Se introdujeron los tubos en un baño de agua que se mantuvo a 60 ºC durante 10 min. Seguidamente, se mezclaron y se mantuvieron en un agitador *vortex* durante un minuto. Transcurrido este tiempo, la mezcla se dejó enfriar a temperatura ambiente. Finalmente, para la síntesis del ferrofluido, se mezclaron 25 mg de las MNPs de $CoFe_2O_4$ y 1 mL del DES, y la mezcla se mantuvo en agitación en un baño de ultrasonidos durante 40 min.

▪ Proporción mentol:timol

Se estudiaron diferentes proporciones de mentol:timol (1:1, 1:2 y 1:5). La proporción 1:1 se descartó debido a que no se obtenía un líquido estable.

Para seleccionar entre las relaciones 1:2 y la 1:5, se realizaron extracciones de una mezcla de los filtros UV y se compararon las señales. Para ello se tomaron 5 mL de una disolución patrón de los analitos, a los que se añadieron 50 µL de ferrofluido y se agitó durante 5 min empleando SBDLME. Como se observa en la **Figura 4.1**, la relación 1:5 permitió obtener los

mejores resultados. Esto es debido al incremento de las interacciones aromáticas producidas por una mayor proporción de timol en el DES.

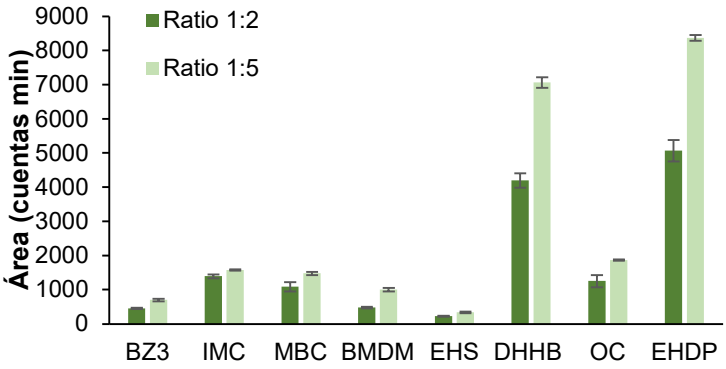

Figura 4.1. Evaluación del porcentaje de mentol y timol en la mezcla de ambos. Las barras de error muestran la desviación estándar de los resultados (N=3)

Caracterización del material $CoFe_2O_4$@OA-mentol:timol (1:5)

Se procedió a la caracterización tanto del ferrofluido como de sus componentes individuales (el DES mentol:timol 1:5 y las MNPs de $CoFe_2O_4$), mediante diferentes metodologías.

▪ Caracterización del DES mentol:timol (1:5)

Para estudiar la formación del DES, se realizaron medidas de absorción mediante espectroscopía infrarroja de los componentes iniciales (mentol y timol) y del producto final.

Como se observa en la **Figura 4.2**, los espectros de timol (**Figura 4.2.a**) y mentol (**Figura 4.2.b**) comparten las señales de extensión debidas a los enlaces O-H (3156 cm^{-1}), C-H (2866-2956 cm^{-1}), y para el caso del timol también se pueden observar unas bandas debidas al anillo aromático (1584-1619 cm^{-1}).

En la **Figura 4.2.c** se muestra el espectro del DES, donde se observan las señales debidas a los anillos aromáticos del timol así como un ensanchamiento de la banda del O-H que prueba la correcta formación del DES [138].

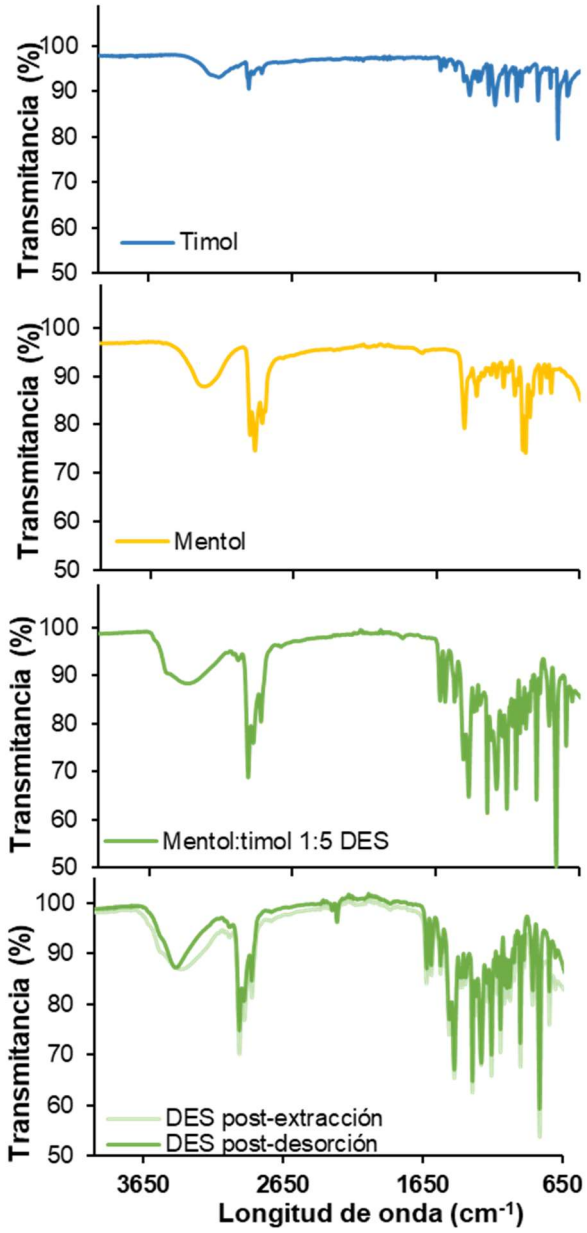

Figura 4.2. Espectros de infrarrojo para a) timol b) mentol c) DES mentol:timol 1:5 d) DES después de los procesos de extracción y desorción

Adicionalmente, como se pretendía emplear el DES en conjunto con acetonitrilo para las etapas de extracción y desorción (como se verá más

adelante), se llevó a cabo un estudio de estabilidad comparando el espectro IR del DES tras su dispersión en agua y acetonitrilo (aproximadamente 99:1, como en la etapa de extracción) y posterior separación, y el obtenido en una disolución del DES en acetonitrilo (etapa de desorción). Como se aprecia en la **Fig. 4.2.d**, tras mezclarse con agua y acetonitrilo, el DES mantiene su integridad y no se descompone. Por otro lado, cuando se mezcla con acetonitrilo puro, el DES se rompe en sus componentes individuales, como se puede apreciar en el estrechamiento de la banda del IR.

Paralelamente, se obtuvo el valor de densidad del DES, que fue 0.905 g mL^{-1}.

- **Caracterización de $CoFe_2O_4$@OA**

Se realizaron medidas mediante SEM de las MNPs de $CoFe_2O_4$@OA, observando en la **Figura 4.3** su forma esférica de un tamaño en torno a los 50 nm.

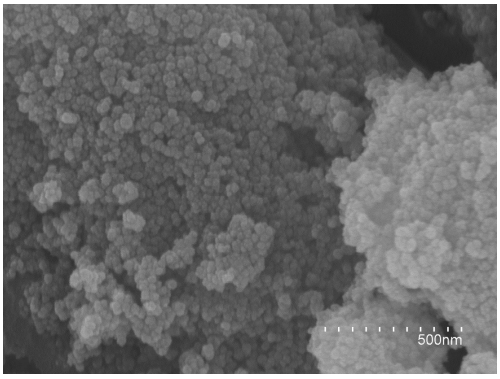

Figura 4.3. Imágenes obtenidas por SEM de las partículas de $CoFe_2O_4$@OA

- **Caracterización del ferrofluido $CoFe_2O_4$@OA-mentol:timol (1:5)**

Se obtuvieron las curvas de histéresis del ferrofluido $CoFe_2O_4$@OA-mentol:timol (1:5) y se compararon con las del $CoFe_2O_4$@OA (**Figura 4.4).**

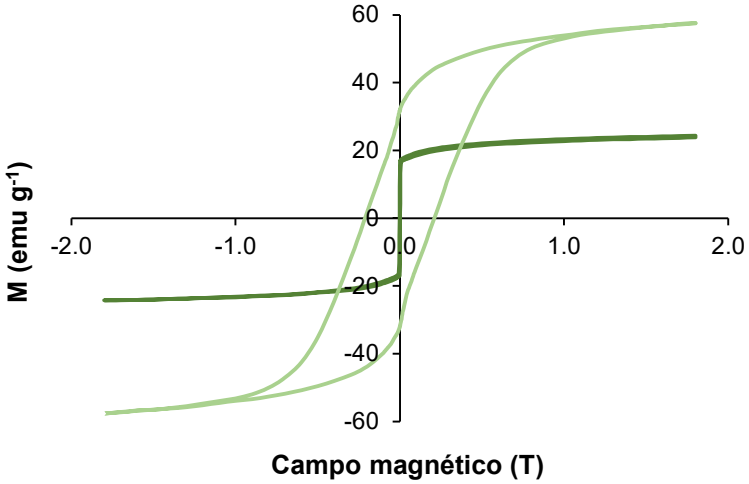

Figura 4.4 Curvas de histéresis del ferrofluido $CoFe_2O_4$@OA-mentol:timol 1:5 y del $CoFe_2O_4$@OA

Se observó que para el ferrofluido se produce una reducción en la Ms y la coercitividad respecto al material inicial, posiblemente producido por la menor cantidad de MNPs por masa de material o por el apantallamiento que el DES puede ocasionar en las MNPs tras la formación del ferrofluido. En cualquier caso, el ferrofluido formado posee una Ms de 28 emu g^{-1}que es suficiente para la SBDLME.

Esquema del método analítico propuesto

En la **Figura 4.5** se muestra un esquema del método analítico propuesto. Primeramente, se añaden 100 µL del ferrofluido $CoFe_2O_4$@OA-mentol:timol directamente sobre 15 mL de muestra o patrón (conteniendo 150 ng L^{-1} de OC-d_{15}) junto con 200 µL de ACN para mejorar la dispersión del ferrofluido. Posteriormente, se produce una agitación vigorosa durante 10 min para producir la extracción de los analitos.

Como en los **Capítulos 2 y 3,** transcurrido este tiempo, la agitación se detiene para producir la deposición del ferrofluido en el imán. Después, el imán con el ferrofluido se limpia con una pequeña cantidad de agua desionizada para eliminar los restos de muestra o patrón.

Finalmente, se introduce en un imán de desorción con 100 µL de ACN y se agita durante 2 min para producir la completa disolución del DES y de los

analitos. Previo a su introducción en el equipo de LC-MS/MS el extracto se filtra (nylon, 0.22 µm) para evitar la introducción de MNPs en este.

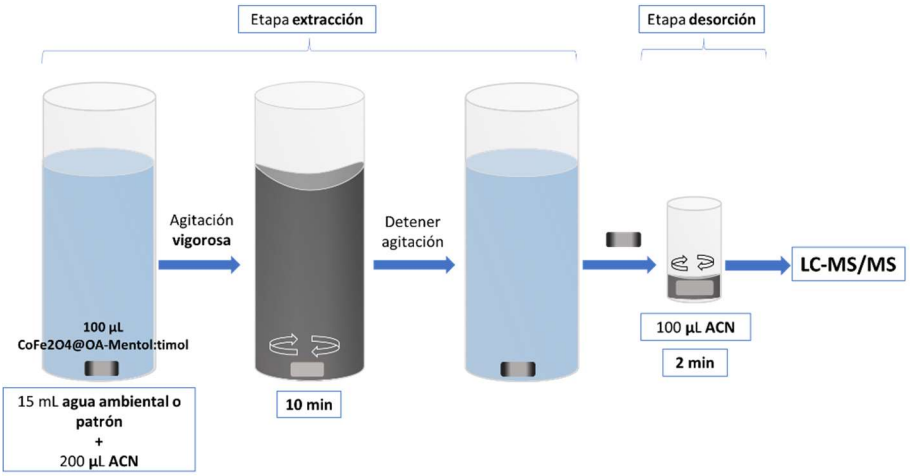

Figura 4.5. Método SBDLME-LC-MS/MS para la determinación de filtros UV en aguas medioambientales

Condiciones cromatográficas

- Columna: Zorbax SB-C18, 50 mm longitud, 2.1 mm de diámetro interno y 1.8 µm de tamaño de partícula

- Fase móvil: H_2O 0.1 % ácido fórmico y MeOH 0.1 % ácido fórmico (15:85 v/v)

- Flujo: 0.2 mL min^{-1}

- Temperatura de columna: 35 ºC

- Modo operacional MS/MS: ESI+

- Voltaje: 6000 V (ESI+)

- Temperatura de gas: 250 ºC

- Flujo del gas nebulizador: 13 L min^{-1}

- Presión de nebulizador: 35 psi

- Tiempo de cromatograma: 6 min

Tabla 4.2. Relaciones masa/carga (m/z) de los iones precursores y producto, energías de colisión y fragmentador para los distintos filtros UV determinados en este capítulo y el patrón interno

Compuesto	Ion precursor (m/z)	Ion producto (m/z) [a]	CE (V)	Fragmentador (V)
BZ3	229	**151**	17	100
		105	17	
IMC	249	**179**	5	100
		161	13	
MBC	255	**105**	29	100
		91	53	
DHHB	398	**149**	13	100
		93	69	
OC-d_{15}	377	**251**	21	100
OC	362	**250**	21	100
		232	21	
EHDP	278	**166**	21	150
		151	33	
BMDM	311	**161**	25	100
		135	25	
EHS	251	**139**	1	100
		121	21	

[a] Marcado en negrita el ion empleado para la cuantificación

En la **Figura 4.6** se muestran, a modo de ejemplo, los cromatogramas obtenidos para los analitos en una muestra de agua de mar tras aplicar el método propuesto:

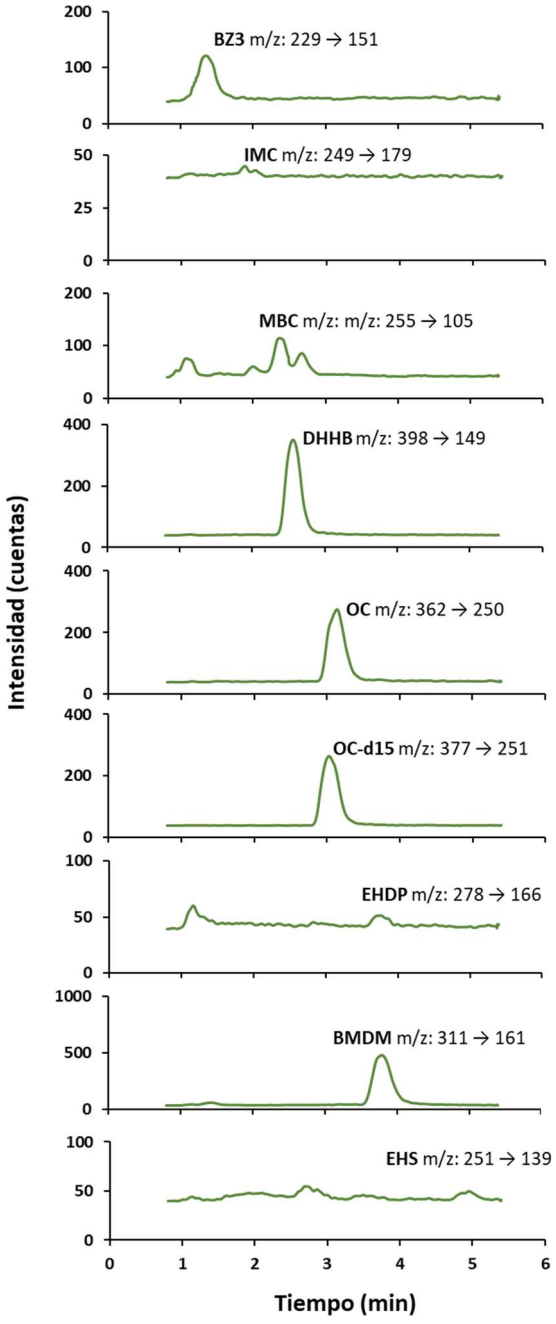

Figura 4.6. Cromatograma de una muestra obtenida tras la aplicación del método de SBDLME-LC-MS/MS propuesto

Estudio de las variables implicadas en la etapa de extracción y disolución

Para el estudio se utilizó como señal analítica el área de los picos.

- **Experimentos previos**

- **Disolvente desorción:** metanol, etanol, acetonitrilo

- **Volumen de fase dadora:** 5, 10, 15 y 20 mL

En cuanto al tipo de disolvente, tal y como se muestra en la **Figura 4.7,** se seleccionó el acetonitrilo, ya que proporcionó los mejores resultados para algunos de los filtros UV cuya determinación presenta menor sensibilidad, como son el BZ3, IMC, BMDM y EHS.

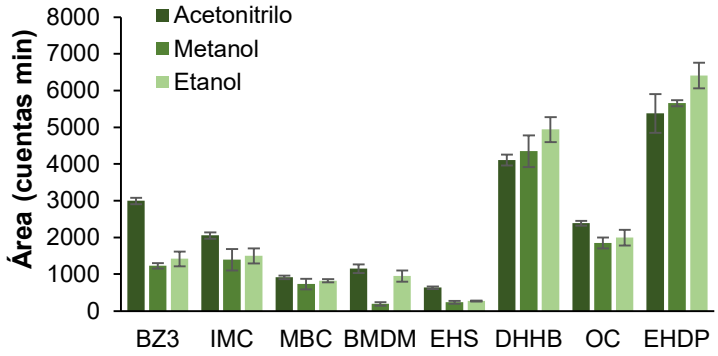

Figura 4.7. Estudio del disolvente de desorción. Las barras de error muestran la desviación estándar de los resultados (N=3)

Para el volumen de muestra, se seleccionaron 15 mL ya que, como se observa en la **Figura 4.8,** el empleo de volúmenes superiores no parece ofrecer mejora. Seguramente se debe a que el campo magnético no es capaz de atraer parte del ferrofluido que queda en la parte superior de la disolución debido a su baja densidad y, en consecuencia, se pierden parte de los analitos.

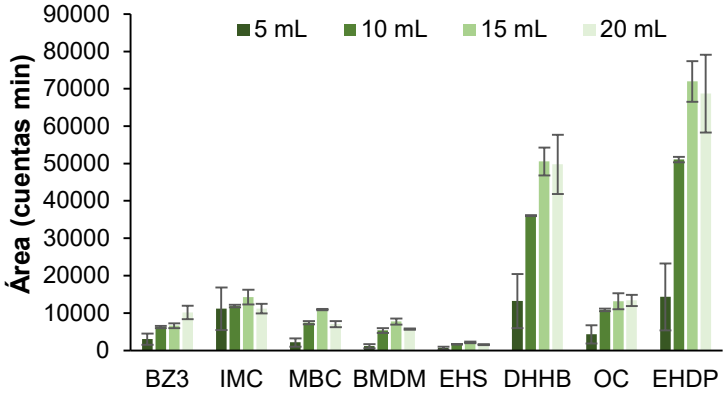

Figura 4.8. Estudio del volumen de fase dadora. Las barras de error muestran la desviación estándar de los resultados (N=3)

- **Optimización multivariante de las variables implicadas en la SBDLME**

Para este trabajo se escogió un modelo de optimización multivariante. Para ello se utilizó un diseño Box-Benhken en el que se estudiaron simultáneamente diferentes variables. El coeficiente de determinación corregido (R^2) fue > 81 % para todos los analitos. Los resultados se muestran en la **Figura 4.9**. Las variables estudiadas fueron:

- Volumen de ferrofluido: 20-200 µL

- Tiempo de extracción: 2-20 min

- Fuerza iónica: 0–20 %

- pH: 2-10

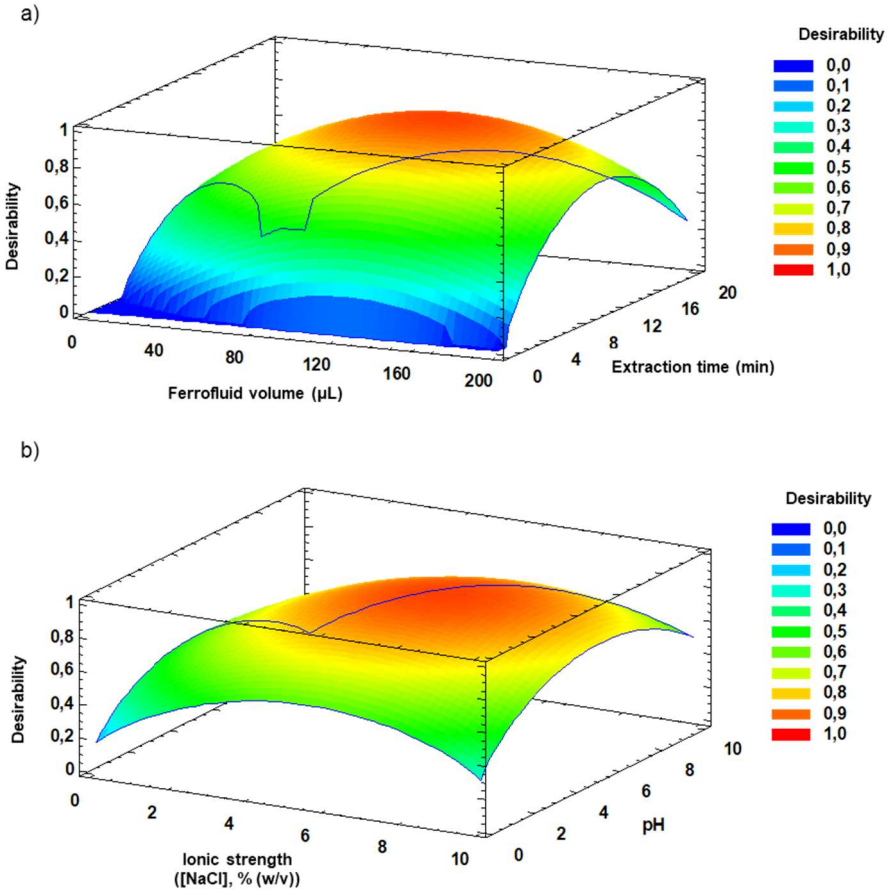

Figura 4.9. Superficie de respuesta (deseabilidad) representando la relación entre a) volumen de ferrofluido y tiempo de extracción, y b) fuerza iónica y pH

En la **Figura 4.9.a** se puede observar que el intervalo óptimo de cantidad de ferrofluido se encuentra entre 100 y 140 µL. A volúmenes superiores a 140 µL parte del ferrofluido no se ancla al imán, ya que este se encuentra saturado. De este modo, parte del ferrofluido con los analitos permanece en la disolución de muestra y no se recoge para la etapa de desorción, disminuyendo así la señal obtenida.

En lo referente al tiempo de extracción, la señal aumenta hasta los 10 min. A tiempos mayores, se produce el efecto *leaching,* explicado en capítulos anteriores, produciendo la separación del ferrofluido en el DES y las MNPs.

Por otro lado, en la **Figura 4.9.b**, se observa que el pH óptimo se encuentra entre 4 y 6, intervalo en el que todos los filtros UV se encuentran en su forma neutra.

Finalmente, para la fuerza iónica, se puede comprobar un aumento de la señal al incrementar la concentración de NaCl hasta el 6% debido al fenómeno de efecto salino. Sin embargo, a concentraciones superiores se produce un incremento de la viscosidad de la disolución que dificulta la correcta dispersión del ferrofluido, reduciéndose así la señal.

En función de los resultados obtenidos, se seleccionaron **100 µL** como volumen de ferrofluido, **10 min** como tiempo de microextracción, y un **6 %** de NaCl. No fue necesario ajustar el pH, ya que el pH normal de las aguas medioambientales está habitualmente dentro del intervalo óptimo.

- **Estudio de las variables de disolución**

Como se observó en la **Figura 4.2.d**, el acetonitrilo es capaz de separar el DES de mentol:timol en sus dos componentes, disolviéndolos. Por esta razón en lugar de desorción, se hablará de disolución El estudio de las variables de la etapa de disolución se llevó a cabo mediante un modelo univariante:

Tiempo de disolución: 0-10 min

Volumen disolución: 100-500 µL

El estudio del tiempo de disolución, tal y como se observa en la **Figura 4.10.a**, muestra que en menos de 2 min se disuelven todos los analitos. La razón es que el DES es altamente soluble en ACN, por lo que no son necesarios tiempos tan altos como ocurría en los **Capítulos 2 y 3**

En cuanto al volumen de disolvente de disolución, en la **Figura 4.10.b** se puede observar que los mejores resultados se obtienen, como era de esperar, con el menor volumen de acetonitrilo (100 µL).

De este modo se seleccionaron **2 min** como tiempo de disolución y **100 µL** de ACN como volumen de disolución.

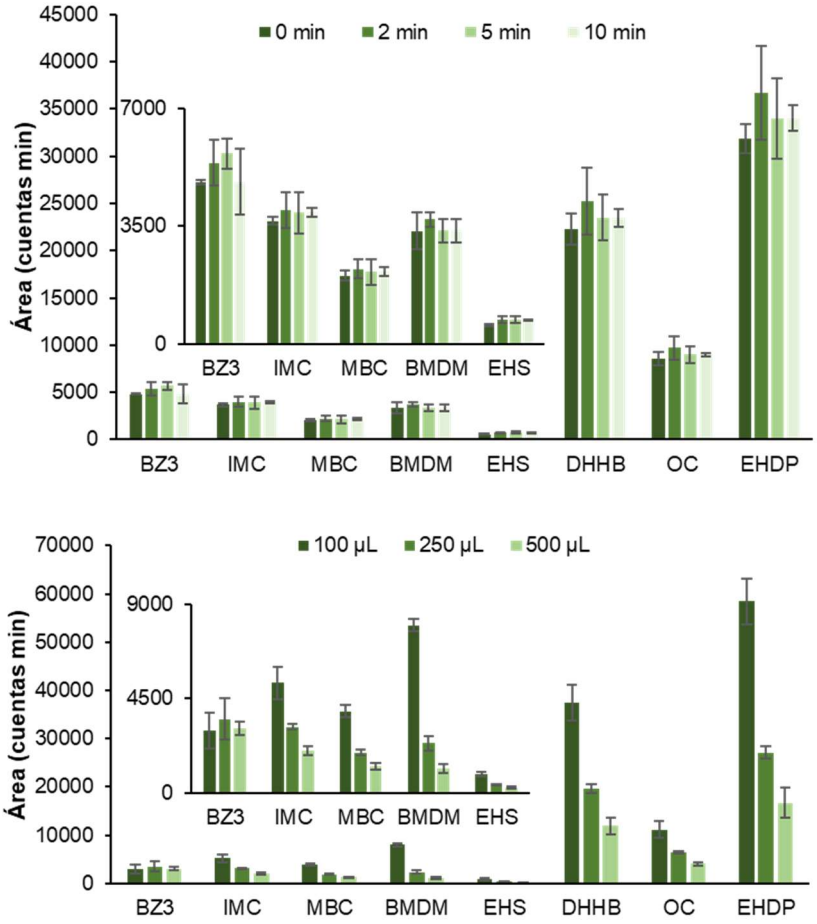

Figura 4.10. Estudio de las variables de disolución a) tiempo de disolución b) volumen de disolución

Validación del método y análisis de muestras reales

Para la validación del método, se estudiaron la linealidad, los EFs, LODs y LOQs, así como la repetibilidad a partir de patrones acuosos salinos. Para el cálculo del coeficiente de recuperación se seleccionaron tres muestras de aguas medioambientales (un río y dos playas) que contenían algunos de los analitos. Los resultados se muestran en la **Tabla 4.3.**

Tabla 4.3. Parámetros analíticos del método propuesto

	LOD (ng L^{-1})	LOQ (ng L^{-1})	EF	Repetibilidad (%RSD) [a]					
				Intradía			Interdía		
				Nivel 1	Nivel 2	Nivel 3	Nivel 1	Nivel 2	Nivel 3
BZ3	20	67	93	4.5	13.8	9.6	12.2	12.7	5.6
IMC	16	54	75	6.6	6.1	5.0	9.9	12.8	14.2
MBC	39	130	80	5.2	9.3	5.0	12.5	8.0	4.8
DHHB	8	25	73	8.3	8.8	2.7	12.8	14.9	10.7
OC	18	60	46	10.8	9.5	3.2	7.3	2.8	4.5
EHDP	7	24	101	12.8	10.1	1.8	8.6	11.1	9.1
BMDM	36	116	71	8.6	9.1	4.5	13.0	4.9	8.6
EHS	83	276	78	6.0	10.7	3.4	12.5	11.1	10.8

[a] **Nivel 1**: 30 ng L^{-1} para DHHB y EHDP; 70 ng L^{-1} para BZ3, IMC y OC; 130 ng L^{-1} para MBC y BMDM; 300 ng L^{-1} para EHS; **Nivel 2**: 190 ng L^{-1} para DHHB y EHDP; 340 ng L^{-1} para BZ3, IMC y OC; 690 ng L^{-1} para MBC y BMDM; 1875 ng L^{-1} para EHS; **Nivel 3**: 750 ng L^{-1} para DHHB y EHDP; 1350 ng L^{-1} para BZ3, IMC y OC; 2750 ng L^{-1} para MBC y BMDM; 7500 ng L^{-1} para EHS.

- **Linealidad**

El método resultó ser lineal hasta 20 ng mL^{-1}. No obstante, debido a la baja concentración esperada para los filtros UV en estas aguas, se decidió emplear un intervalo de trabajo de 20 a 100 ng L^{-1}. En este intervalo, el coeficiente de determinación (R^2) fue superior a **0.995** para todos los analitos.

- **Factor de enriquecimiento**

Para establecer los EFs, se calculó el cociente entre la señal de un patrón de los analitos después de la extracción y antes de realizarla. Los resultados variaron entre **46** y **101** según el analito.

- **Límites de detección y cuantificación**

Los LODs y LOQs se establecieron estimando la concentración mediante la cual se obtenía una relación S/N de 3 y 10 respectivamente. Los LODs variaron entre **7** y **83 ng L^{-1}** y los LOQs entre **25** y **276 ng L^{-1},**según el analito.

- **Repetibilidad**

La repetibilidad se estableció calculando la RSD de 5 réplicas medidas el mismo día (repetibilidad intradía) y 5 réplicas medidas en distintos días (repetibilidad interdía) a tres niveles de concentración que se establecieron en función de los LODs de los analitos. Los resultados obtenidos se encontraban por debajo del **15 %** de RSD.

- **Análisis de muestras reales**

Se analizaron tres muestras de agua medioambiental obtenidas de zonas con mucha afluencia recreativa de bañistas (dos de playa y una de río), encontrándose diferentes cantidades de algunos de los filtros UV analizados. Los resultados se muestran en la **Tabla 4.4.**

Tabla 4.4. Concentraciones de filtros UV obtenidas tras la aplicación del método propuesto a tres muestras de agua ambiental

Analito	Concentración encontrada (ng L^{-1})		
	Playa 1	Playa 2	Río
BZ3	225 ± 25	< 67[b]	< 20[a]
IMC	< 16[a]	< 16[a]	< 16[a]
MBC	148 ± 13	< 130[b]	< 39[a]
DHHB	58 ± 6	< 25[b]	< 25[b]
OC	78 ± 9	84 ± 7	208 ± 2
EHDP	< 24[b]	< 24[b]	< 7[a]
BMDM	240 ± 20	< 116[b]	< 36[a]
EHS	< 276[b]	< 276[b]	< 83[a]

[a] Límite de detección
[b] Límite de cuantificación

Las mismas muestras del apartado anterior se fortificaron a tres niveles de concentración para calcular los coeficientes de recuperación. Los resultados se muestran en la **Tabla 4.5.** Todos los coeficientes de recuperación se encontraron entre el **80** y el **117 %**, por lo que no se consideró la existencia de efecto matriz. De este modo, es posible trabajar con calibración externa con empleo de patrón interno.

Tabla 4.5 Coeficientes de recuperación obtenidos tras la aplicación del método propuesto a muestras de aguas ambientales fortificadas a tres niveles de concentración.

		Coeficiente de recuperación (%)		
Filtro UV	**Nivel de concentración[a]**	**Playa 1**	**Playa 2**	**Río**
BZ3	1	104 ± 13	113 ± 15	100 ± 4
	2	105 ± 9	83 ± 2	109 ± 16
	3	91 ± 9	87 ± 7	91 ± 12
IMC	1	96 ± 15	83 ± 3	84 ± 1
	2	112 ± 11	80 ± 3	85 ± 6
	3	94 ± 7	93 ± 7	98 ± 14
MBC	1	120 ± 1	109 ± 10	116 ± 4
	2	91 ± 8	84 ± 7	80 ± 2
	3	80 ± 8	82 ± 6	96 ± 5
DHHB	1	109 ± 7	89 ± 7	114 ± 8
	2	115 ± 4	104 ± 8	107 ± 3
	3	111 ± 10	101 ± 3	96 ± 6
OC	1	96 ± 6	107 ± 1	91 ± 3
	2	107 ± 1	112 ± 9	86 ± 10
	3	98 ± 4	112 ± 8	98 ± 2
EHDP	1	116 ± 4	97 ± 3	115 ± 6
	2	101 ± 5	107 ± 4	100 ± 4
	3	88 ± 7	102 ± 3	91 ± 8
BMDM	1	104 ± 8	107 ± 14	106 ± 3
	2	94 ± 16	112 ± 13	115 ± 3
	3	97 ± 13	104 ± 3	102 ± 6
EHS	1	80 ± 7	81 ± 1	98±9
	2	90 ± 10	103 ± 14	97±11
	3	84 ± 12	102 ± 2	96±8

[a] **Nivel 1**: 30 ng L^{-1} para DHHB y EHDP; 70 ng L^{-1} para BZ3, IMC y OC; 130 ng L^{-1} para MBC y BMDM; 300 ng L^{-1} para EHS; **Nivel 2**: 190 ng L^{-1} para DHHB y EHDP; 340 ng L^{-1} para BZ3, IMC y OC; 690 ng L^{-1} para MBC y BMDM; 1875 ng L^{-1} para EHS; **Nivel 3**: 750 ng L^{-1} para DHHB y EHDP; 1350 ng L^{-1} para BZ3, IMC y OC; 2750 ng L^{-1} para MBC y BMDM; 7500 ng L^{-1} para EHS.

Estudio de la repetibilidad de la síntesis

Para verificar la repetibilidad de la síntesis del material se realizaron tres síntesis independientes del ferrofluido. Los resultados de la **Figura 4.11.** muestran valores muy similares, probando así la buena repetibilidad de esta etapa.

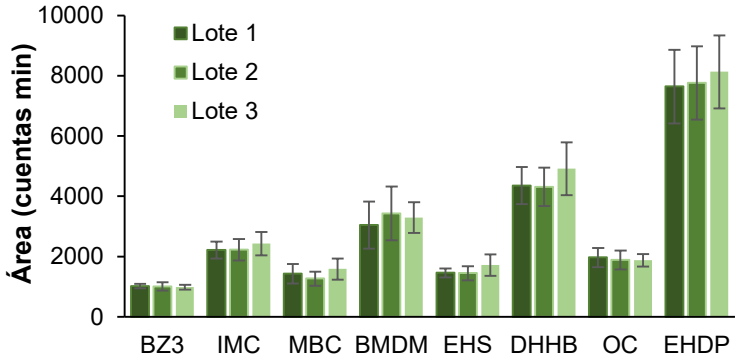

Figura 4.11. Comparación de las áreas obtenidas para cada analito mediante SBDLME-LC-MS/MS empleando $CoFe_2O_4$@OA-mentol:timol (1:5) obtenido de tres síntesis independientes, Las barras de error muestran la desviación estándar de los resultados (N=3)

Influencia de extracción

Anteriormente se habían empleado partículas magnéticas con ácido oleico en la determinación de filtros UV [43]. Por ello, se comprobó experimentalmente la mejora de las señales utilizando el ferrofluido. Como se puede apreciar en la **Figura 4.12**, para los filtros BZ3, IMC, MBC y BMDM, se produce un aumento significativo de la señal, lo que es de gran interés ya que se trata de los filtros UV cuyas determinaciones presentan menor sensibilidad.

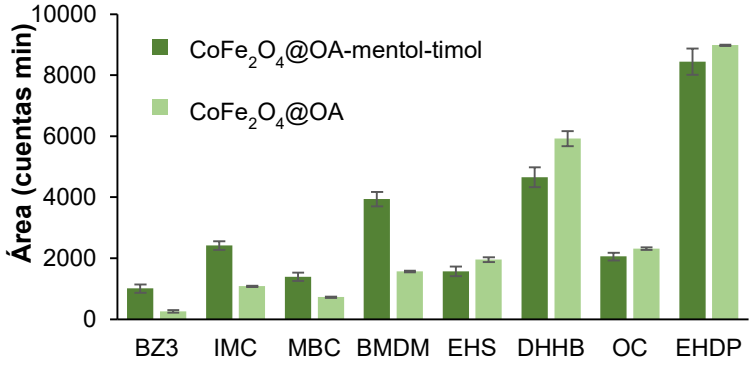

Figura 4.12. Comparación de la capacidad de extracción del ferrofluido $CoFe_2O_4$@OA-mentol:timol (1:5) con las partículas de $CoFe_2O_4$@OA. Las barras de error muestran la desviación estándar de los resultados (N=3)

Comparación con otros métodos de la bibliografía

El método se comparó con otros métodos encontrados en la bibliografía que utilizaban diferentes técnicas de microextracción con diferentes materiales sorbentes. Tal y como se observa en la **Tabla 4.6**, las técnicas dispersivas como la SBDLME y la SBSDME requieren tiempos más pequeños. Dentro de estos, los dos que utilizan extractantes líquidos son los que menor tiempo de extracción necesitan.

La diferencia entre los dos métodos de SBDLME radica en el tipo de material. Mientras que en el método previamente publicado se empleaba un MIL, con sus correspondientes consecuencias a nivel medioambiental y toxicidad, con el método que se presenta en este capítulo se obtienen resultados similares sin necesidad de síntesis complejas ni empleo de materiales de elevada toxicidad. Para corroborarlo, la síntesis de ambos materiales se comparó utilizando la aplicación ComplexGAPI.

Tabla 4.6. Comparación del método propuesto con otros métodos publicados en la bibliografía

Técnica de extracción	Técnica de medida	Fase de extracción[b]	Tiempo de extracción (min)	LOD (ng L^{-1})	Ref
SBSE	TD-GC-MS	PDMS	180	0.2-64	[139]
SBSDME	LC-UV	$CoFe_2O_4$@OA	20	2400-30000	[43]
SPME	GC-MS/MS	DVB/CAR/PDMS	30	2-1000	[140]
SBDLME	TD-GC-MS	$[P^+_{6,6,6,14}][Ni(hfacac)_3^-]$	10	9.9-27	[112]
SBDLME[a]	LC-MS/MS	$CoFe_2O_4$@OA-menthol:thymol	10	7-83	[141]

[a] Trabajo presentado en este capítulo

[a]**PDMS:** polidimetilsiloxano, **DVB/CAR/PDMS**: divinilbenceno-carboxeno-polidimetilsiloxano, **$[P^+_{6,6,6,14}][Ni(hfacac)_3^-]$**: trietilhexil(tetradecil)fosfonio níquel (II) hexafluoroacetilacetonato

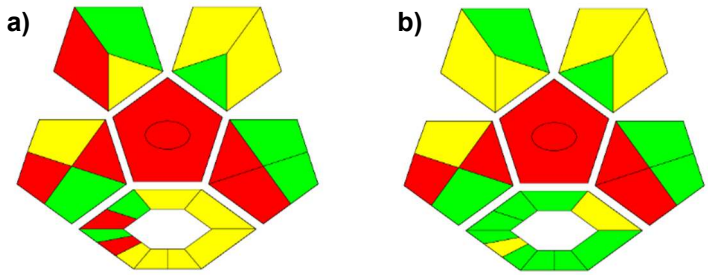

Figura 4.13. Evaluación de a) método empleando un MIL (Ref. [112]) b) método propuesto en este capítulo

Los pentágonos superiores corresponderían a la evaluación del muestreo, preparación de muestra y medida. Como se puede observar, en este sentido no hay mucha diferencia entre utilizar cualquiera de los dos métodos. Sin embargo, cuando se comparan los hexágonos, correspondientes a la evaluación de la síntesis del material, se puede apreciar una mayor

diferencia. El método para la obtención del ferrofluido es un método de síntesis más rápido, simple y seguro. Tampoco requiere de etapas de purificación, y el rendimiento obtenido es elevado. Por esa razón, el número de franjas verdes es mucho mayor que en el método basado en el empleo del MIL.

Evaluación de la seguridad y sostenibilidad del método

En la **Figura 4.14** se muestra un diagrama AGREEprep del método propuesto. De entre los tres métodos presentados en esta sección, este es el que mayor puntuación presenta. Esto se debe a que el empleo de disolventes verdes (como los DES) y la sustitución del MeOH por ACN, permite mejorar mucho su puntuación respecto a los anteriores. Otra ventaja respecto a los métodos de los **Capítulos 2** y **3**, es que en este caso no es necesario un acondicionamiento previo del material, gracias a la introducción de 200 µL de ACN que actúan a modo de dispersante, reduciendo el tiempo total de análisis.

No obstante, al igual que ocurría en los dos métodos de SBSDME, el volumen de muestra va a generar altos contenidos de residuos, impidiendo obtener una puntuación mayor.

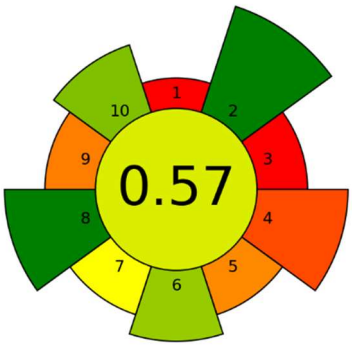

Figura 4.14. Evaluación del método propuesto empleando AGREEprep

Conclusiones

Se ha desarrollado un nuevo ferrofluido basado en un DES de baja toxicidad compuesto por timol y mentol para ser empleado en técnicas de microextracción en fase líquida.

Tanto el ferrofluido como sus componentes fueron caracterizados mediante diferentes técnicas para estudiar su correcta formación.

Este ferrofluido se aplicó con éxito en la determinación de filtros UV en aguas medioambientales empleando SBDLME.

El método presenta buenos resultados comparado con otros métodos publicados sin la necesidad de utilizar materiales tóxicos y/o de difícil obtención.

SECCIÓN 3

Capítulo 5: Microextracción en fase sólida dispersiva asistida por disolvente basada en sorbentes magnéticos modificada: Aplicación a la determinación de cortisol y cortisona en saliva

El contenido de este capítulo ha sido publicado en el artículo **Modified magnetic-based solvent-assisted dispersive solid-phase extraction: application to the determination of cortisol and cortisone in human saliva, Journal of chromatography A 1652 (2021) 462361** y presentado en formato póster en el congreso *"XXIII International Symposium on Advances in Extraction Technologies (ExTech)"* en Alicante (Online), 2021

Objetivo

Desarrollo de una nueva modalidad de microextración en fase sólida dispersiva asistida por disolvente basada en sorbentes magnéticos y su aplicación a la determinación de cortisona y cortisol en muestras de saliva.

Resumen

En este capítulo se presenta una modificación de la microextracción en fase sólida dispersiva asistida por disolvente basada en sorbentes magnéticos (***Magnetic Based Solvent Assisted Dispersive Solid Phase Extraction,* M-SA-DSPE**). La M-SA-DSPE se basa en el empleo de un disolvente orgánico para mejorar la dispersión del material sorbente y el contacto de este con la muestra. En estos métodos suelen emplearse equipamientos externos como agitador *vortex* y baño de ultrasonidos que reducen la portabilidad del método. Por esta razón, en el contexto de esta Tesis Doctoral, se propuso una nueva técnica basada en la DLLME pero trabajando con un material extractante sólido.

Esta modificación se aplicó a la determinación de cortisona y cortisol en muestras de saliva. La determinación conjunta de estos analitos constituye un excelente biomarcador para la diagnosis del síndrome de Cushing [142]. Para ello se empleó un polímero comercial en fase reversa (***Strata™ X-Polymeric Reversed Phase*, Strata™ X-RP**) con MNPs de $CoFe_2O_4$ incrustadas. Como técnica de medida tras la etapa de extracción se empleó LC-MS/MS.

Se estudiaron las variables del método y con las condiciones seleccionadas se obtuvieron límites de detección de 0.029 ng mL^{-1} para el cortisol y 0.018 ng mL^{-1} para la cortisona, con valores de RSD inferiores al 10 %. Los coeficientes de recuperación tras fortificar las muestras de saliva estuvieron comprendidos entre el 86 y el 111 %. Para demostrar la aplicabilidad de esta modificación, se analizaron cuatro muestras de saliva procedentes de distintos voluntarios.

Datos de interés del método

- Material sorbente: $CoFe_2O_4$-Strata^{TM} X-RP

- Volumen de muestra: 500 µL

- Técnica de microextracción empleada: M-SA-DSPE

- Tiempo extracción-desorción: 2 min

- Técnica de medida: LC-MS/MS

Compuestos estudiados

Tabla 5.1. Información sobre los compuestos objeto de estudio en este capítulo

Analito	Estructura química	Número CAS	Log P_{ow}
Cortisol	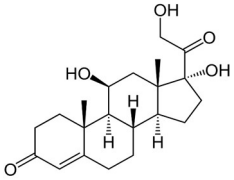	50-23-7	1.69
Cortisona	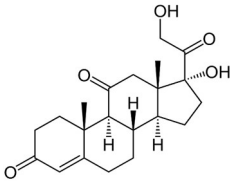	53-06-5	1.34

Se seleccionó prednisolona como patrón interno, ya que al tratarse de un glucocorticoide con una estructura semejante a los analitos, cuenta con propiedades muy similares a la cortisona y al cortisol. Además, no es endógena, por lo que no causa problemas de interferencias (salvo que se trate de una persona medicada con prednisona).

Selección y síntesis del material

Tanto el cortisol como la cortisona presentan la estructura de cuatro anillos propia de las hormonas esteroideas, además de poseer varios grupos funcionales como carbonilos e hidroxilos que les permiten establecer

interacciones dipolo-dipolo y formar puentes de hidrógeno. Por esa misma razón, se utilizó un polímero como el Strata™ X-RP. Este es un copolímero de estireno-divinilbenceno modificado con pirrolidona, lo que le confiere capacidad para producir interacciones de puente de hidrógeno e interacciones hidrofóbicas.

La síntesis de las MNPs se llevó a cabo de la misma forma que en el **Capítulo 2**. Las MNPs obtenidas se suspendieron para obtener una concentración final de 0.016 g mL^{-1}. Posteriormente, 9.4 mL de esta suspensión se mezclaron con 0.15 g de Strata™ X-RP para obtener una relación 1:1 (m/m). A continuación, se añadieron 50 mL de etanol y se agitó durante 3 días. Finalmente, se filtró a vacío empleando un filtro de nylon de 11 µm para separar las partículas magnéticas que no habían interaccionado. El sólido resultante se mantuvo toda la noche a 80 ºC para su secado.

Caracterización del material $CoFe_2O_4$-Strata™ X-RP

- **Estudio de las curvas de histéresis**

En la **Figura 5.1** se muestra la curva de histéresis para $CoFe_2O_4$-Strata™ X-RP

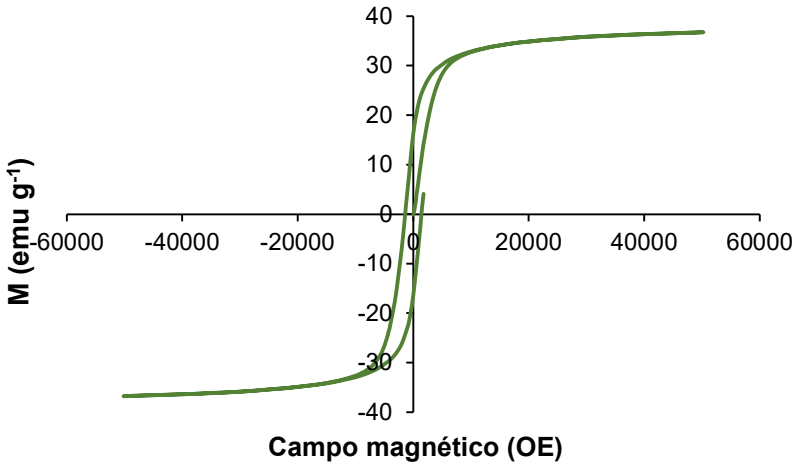

Figura 5.1. Curvas de histéresis del sorbente $CoFe_2O_4$.Strata™ X-RP

La magnetización obtenida para $CoFe_2O_4$-Strara™ X-RP fue 36.7 emu g^{-1}. Con estos niveles se permite un rápido aislamiento del material de la disolución de muestra empleando un campo magnético externo.

- **Imágenes SEM**

Se obtuvieron imágenes mediante SEM para los componentes individuales y para $CoFe_2O_4$-Strara™ X-RP. En la **Figura 5.2.a** se puede apreciar la forma esférica de las partículas magnéticas, y en la **Figura 5.2.b** se observa la forma, también esférica, del polímero comercial. Al realizar la unión entre ambos, las partículas magnéticas quedan incrustadas en la superficie del polímero como se puede ver en las **Figuras 5.2.c** y **5.2.d.**

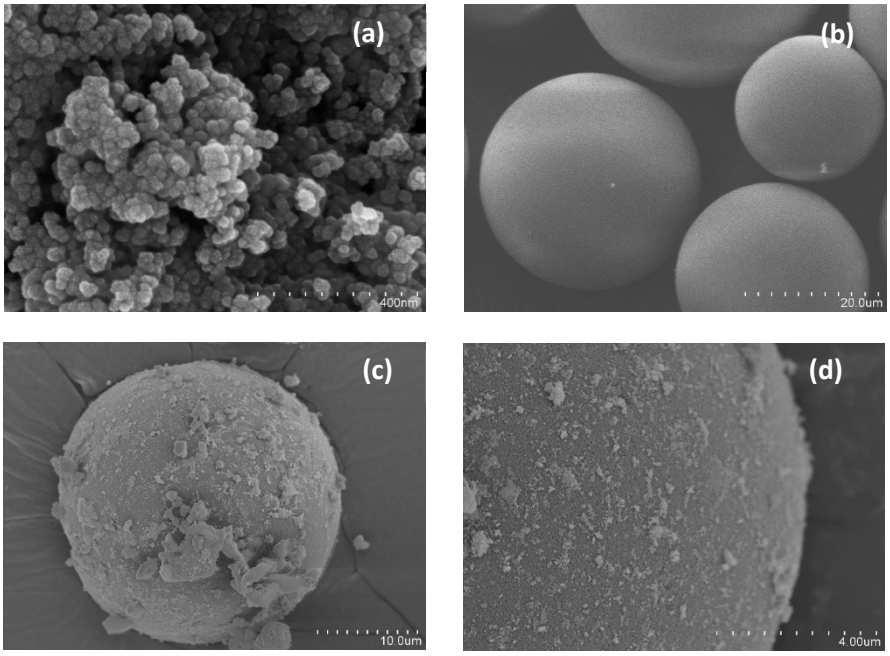

Figura 5.2. Imágenes SEM para a) $CoFe_2O_4$ a 120000 aumentos b) polímero Strata™ X-RP a 1200 aumentos c) $CoFe_2O_4$-Strata™ X-RP a 300 aumentos d) $CoFe_2O_4$-Strata™ X-RP a 10000 aumentos

- **Isoterma de adsorción/desorción**

La isoterma mostrada en la **Figura 5.3,** muestra un comportamiento de tipo IV, como demuestra también la existencia de mesoporos (en torno a los 6.6 nm). En cuanto al área superficial fue de 622.8 ± 0.8 m^2 g^{-1}.

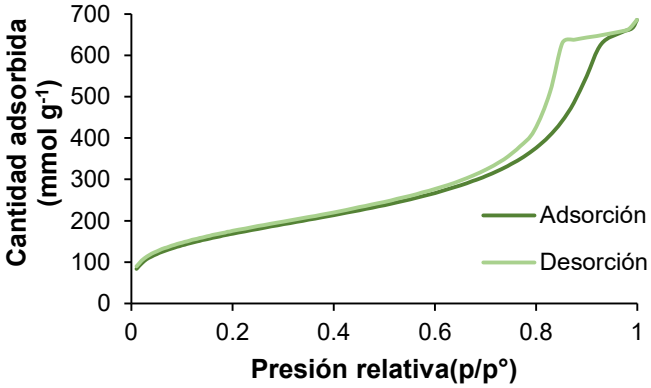

Figura 5.3. Isoterma de adsorción/desorción para el $CoFe_2O_4$-Strata™ X-RP

Pretratamiento de muestra

Se realiza un pretratamiento de la saliva para eliminar componentes no deseados que pudieran dificultar la aplicación de la técnica. Este tratamiento consiste primero en una etapa de centrifugación para eliminar las posibles flemas y los restos de alimentos. Posteriormente, las muestras son congeladas para producir la rotura de las cadenas de polisacáridos. Finalmente, se descongela y se centrifuga nuevamente.

Esquema del método analítico propuesto

En la **Figura 5.4,** se muestra un esquema del método analítico propuesto. En primer lugar, se añaden 50 µL de ACN sobre 1 mg del sorbente $CoFe_2O_4$-Strata™ X-RP.

La dispersión resultante se aspiró con una jeringa y se dispensa sobre 0.5 mL de muestra de saliva o de patrón (conteniendo 50 ng L^{-1} de prednisolona).

Esta dispersión se mantiene durante 1 min y, después, con ayuda de un imán externo se produce la separación entre disolución y material. La disolución de muestra o de patrón es entonces descartada. Por su parte, el material sorbente con los analitos se lava con 50 µL de agua ultrapura para eliminar los posibles restos de saliva y patrón.

Finalmente se añaden 60 µL de MeOH y se realizan 5 ciclos de aspiración/dispensación para producir la desorción de los analitos.

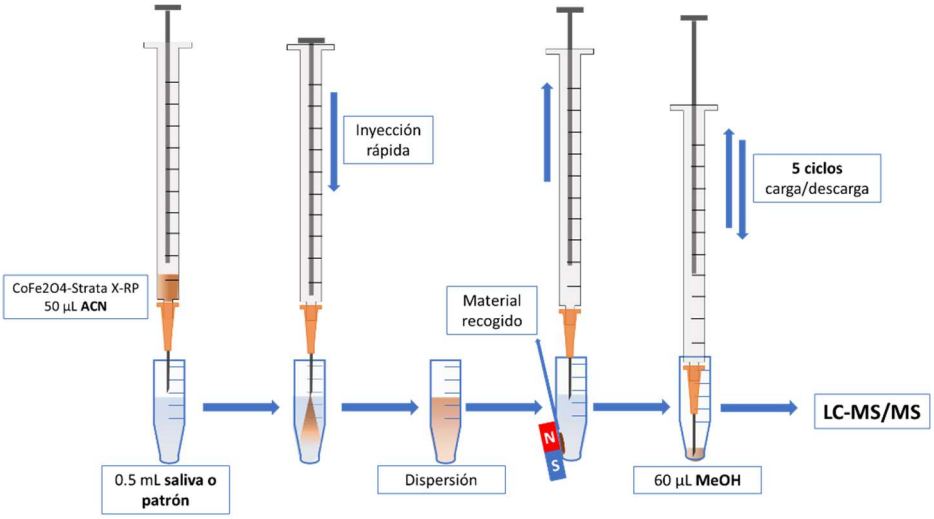

Figura 5.4. Método SA-DSPE-LC-MS/MS para la determinación de cortisona y cortisol en muestras de saliva

Condiciones cromatográficas

- Columna: Zorbax SB-C18, 50 mm longitud, 2.1 mm de diámetro interno y 1.8 µm de tamaño de partícula

- Fase móvil: H2O 0.1 % ácido fórmico y MeOH 0.1 % ácido fórmico (40:60 v:v)

- Flujo: 0.15 mL min^{-1}

- Temperatura de columna: 25 ºC

- Modo operacional MS/MS: ESI+

- Voltaje: 5000 V (ESI+)

- Temperatura de gas: 350 ºC

- Flujo del gas nebulizador: 11 L min^{-1}

- Presión de nebulizador: 50 psi

- Tiempo de cromatograma: 6 min

Tabla 5.2. Relaciones masa/carga (m/z) de los iones precursores y producto, energías de colisión y fragmentador para los distintos glucocorticoides determinados en este capítulo y el patrón interno

	Ion precursor (m/z)	Ion producto (m/z) [a]	CE (V)	Fragmentador (V)
Cortisol	363	**121**	21	155
		105	21	
Cortisona	361	**163**	26	140
		105	26	
Prednisolona	343	**325**	20	135
	361	163	26	140

[a]Marcados en negrita las m/z empleadas para la cuantificación

A modo de ejemplo, se muestran en **la Figura 5.5** los cromatogramas obtenidos para los analitos y el patrón interno tras la aplicación del método a una muestra de saliva.

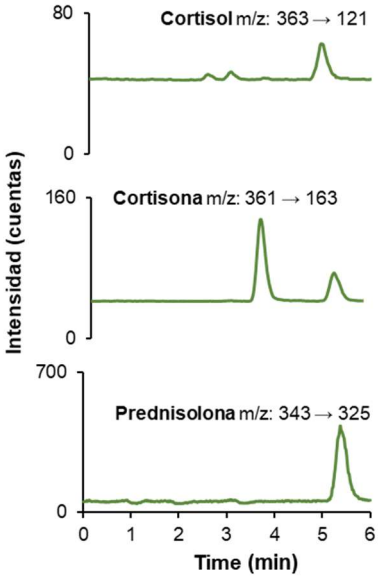

Figura 5.5. Cromatograma obtenido para una muestra de saliva tras la aplicación del método SA-DSPE-LC-MS/MS propuesto

Estudio de las variables implicadas en la etapa de extracción y desorción

Para el estudio se utilizó como señal analítica el área de los picos. Las variables estudiadas de las etapas de extracción y de desorción fueron:

- Cantidad de sorbente: 1-5 mg

- Tiempo de extracción: 0.5-20 min

- Fuerza iónica: 0-7 mg mL^{-1}

- Número de ciclos de desorción: 2-20

- **Cantidad de sorbente**

Se estudiaron cantidades entre 1 y 5 mg de sorbente. Como puede verse en la **Figura 5.6,** al aumentar la cantidad de sorbente la señal disminuye. Esto puede deberse a que la dispersión del sorbente durante la etapa de desorción puede verse dificultada cuando su masa es mayor.

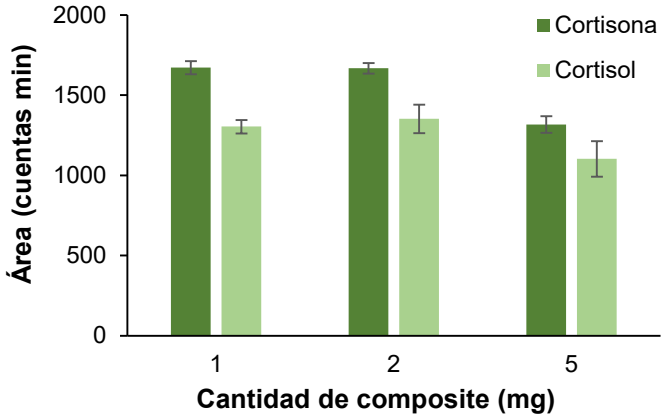

Figura 5.6. Estudio de la cantidad de sorbente. Las barras de error muestran la desviación estándar de los resultados (N=3)

- **Tiempo de extracción**

Se estudió el tiempo durante el que se mantuvo la dispersión para una completa extracción de los analitos. Se observa en la **Figura 5.7** que 0.5 min no fueron suficientes. Sin embargo, a partir de 1 min la señal se estabiliza. Por esa razón se seleccionó el mínimo tiempo, **1 min**.

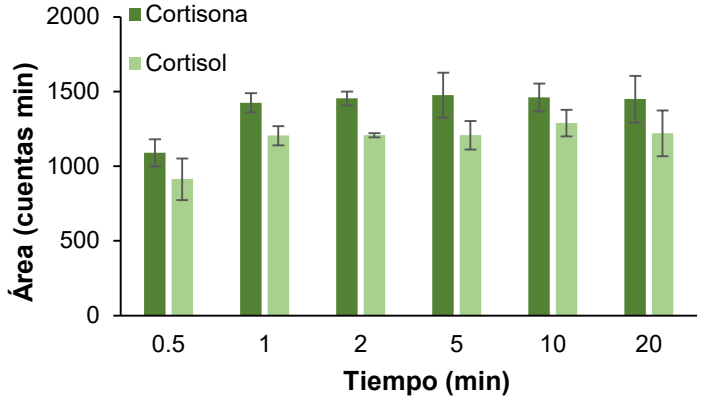

Figura 5.7. Estudio del tiempo de extracción. Las barras de error muestran la desviación estándar de los resultados (N=3)

- **Fuerza iónica**

Dado que las muestras de saliva pueden contener una cantidad variable de sales, se estudió la influencia de la fuerza iónica sobre la extracción. En la **Figura 5.8,** se observa que concentraciones entre 1 y 3.5 mg mL^{-1} proporcionan las máximas señales debido al efecto salino, mientras que con 7 mg mL^{-1} la viscosidad es tan grande que se dificulta la dispersión, reduciendo drásticamente la señal.

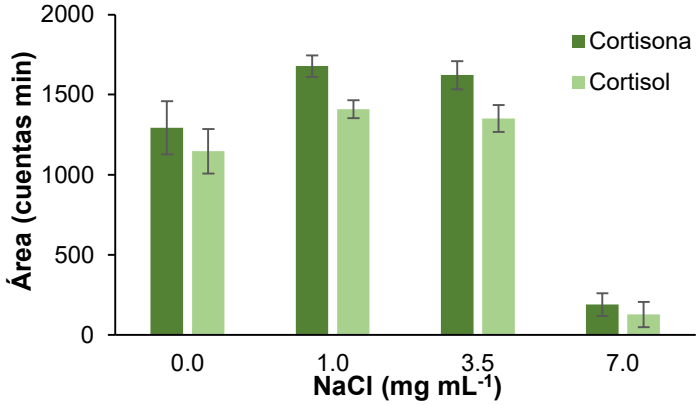

Figura 5.8. Estudio de la fuerza iónica (como concentración de NaCl) de la fase dadora. Las barras de error muestran la desviación estándar de los resultados (N=3)

Para estimar el contenido salino que se encuentra en las muestras de saliva, se realizaron medidas de conductividad de 10 salivas diferentes. Los resultados muestran que el contenido salino de la saliva se encontraba entre **1.20** y **3.15 mg mL^{-1}**, dentro del intervalo óptimo. Por lo que se optó por no modificar el contenido salino intrínseco de las muestras.

- **Ciclos de carga y descarga**

Para la desorción se estudió el número de ciclos de carga y descarga que se debían hacer con la jeringa para una correcta desorción de los analitos. Como se observa en la F**igura 5.9**, 2 ciclos no eran suficientes para conseguir una desorción completa. A partir de los **5 ciclos**, la señal se

estabilizaba, por lo que se seleccionó este valor para reducir al máximo el tiempo de análisis.

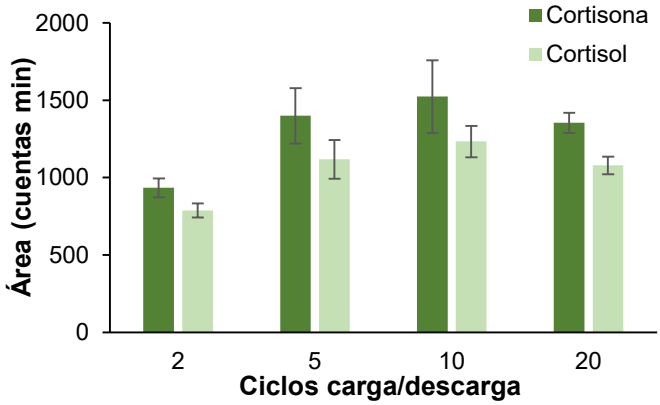

Figura 5.9. Estudio del número de los ciclos de carga/descarga. Las barras de error muestran la desviación estándar de los resultados (N=3)

Validación del método y análisis de muestras reales

Se validó el método estudiando la linealidad, los EFs, LODs y LOQs, además de la repetibilidad a partir de patrones acuosos. Para el estudio de los coeficientes de recuperación se empleó saliva de tres voluntarios fortificada a tres niveles de concentración. Los resultados se muestran en la **Tabla 5.3.**

Tabla 5.3. Propiedades analíticas del método propuesto

	LOD ($ng\ mL^{-1}$)	LOQ ($ng\ mL^{-1}$)	EF	Repetibilidad (% RSD)[a]			
				Intradía		Interdía	
				Nivel 1	Nivel 2	Nivel 1	Nivel 2
Cortisol	0.029	0.097	5.2 ± 0.2	4.2	6.1	10.0	6.3
Cortisona	0.018	0.060	5.6 ± 0.3	5.0	1.8	9.6	8.7

[a] Nivel 1: 1 $ng\ mL^{-1}$; Nivel 2: 10 $ng\ mL^{-1}$

- **Linealidad**

Se seleccionó un intervalo de trabajo entre 0.3 y 20 ng mL^{-1} basándose en los niveles medios de cortisol y cortisona en muestras de saliva. En este intervalo se obtuvieron niveles de linealidad con buenos coeficientes de regresión para los dos analitos (**R^2>0.999**).

- **Factor de enriquecimiento**

Para el cálculo de los EFs, se obtuvo el cociente entre las señales de un patrón de los analitos después de la extracción y antes de realizarla. Los resultados fueron de **5.2** para el cortisol y **5.6** para la cortisona.

- **Límites de detección y cuantificación**

El LOD y el LOQ se calcularon como la concentración mediante la que se obtenía una relación S/N de 3 y 10 respectivamente. Los LODs fueron de **0.029** y **0.018 ng mL^{-1}** y los LOQ de **0.097** y **0.06 ng mL^{-1}** para cortisol y cortisona, respectivamente.

- **Repetibilidad**

La repetibilidad se estableció calculando la RSD de 5 réplicas medidas el mismo día (repetibilidad intradía) y 5 réplicas medidas en distintos días (repetibilidad interdía). La RSD se calculó a tres niveles de concentración 1, 5 y 10 ng mL^{-1}, obteniéndose valores por debajo del **10 %** para ambos analitos.

- **Análisis de muestras reales**

En primer lugar, se fortificaron tres muestras de saliva a 1, 5 y 10 ng mL^{-1} para realizar el cálculo de los coeficientes recuperación. Los resultados se muestran en la **Tabla 5.4.** observándose coeficientes de recuperación entre **86** y **111 %** considerándose, por tanto, que no hay efecto matriz. De este modo, es posible trabajar con calibración externa con empleo de patrón interno.

Tabla 5.4. Coeficientes de recuperación obtenidos tras la aplicación del método propuesto a muestras de saliva fortificadas a tres niveles de concentración

Saliva	Cantidad añadida (ng mL^{-1})	Cantidad encontrada (ng mL^{-1})		Coeficiente de recuperación (%)	
		Cortisol	Cortisona	Cortisol	Cortisona
1	0	2.0 ± 0.2	8.1 ± 0.7	-	-
	1	2.86 ± 0.03	9.04 ± 0.05	87 ± 3	94 ± 5
	5	6.41 ± 0.05	12.9 ± 0.6	88 ± 5	96 ± 12
	10	11.7 ± 0.3	17.6 ± 0.3	97 ± 3	95 ± 3
2	0	1.03 ± 0.01	6.6 ± 0.5	-	-
	1	1.88 ± 0.06	7.61 ± 0.09	86 ± 6	96 ± 9
	5	5.5 ± 0.2	12.0 ± 0.7	89 ± 5	108 ± 13
	10	10.7 ± 0.7	17.7 ± 0.5	97 ± 3	111 ± 5
3	0	1.55 ± 0.01	4.3 ± 0.3	-	-
	1	2.44 ± 0.07	5.32 ± 0.09	89 ± 7	99 ± 9
	5	6.0 ± 0.4	9.6 ± 0.5	89 ± 9	107 ± 11
	10	12.1 ± 0.7	14.9 ± 0.2	106 ± 7	106 ± 2

Finalmente, se analizaron cuatro muestras procedentes de cuatro voluntarios sanos por el método M-SA-DSPE-LC-MS/MS propuesto. Todos los resultados mostrados en la **Tabla 5.5** se encontraron dentro de la normalidad.

Tabla 5.5. Concentraciones obtenidas de cortisona y cortisol en muestras procedentes de cuatro voluntarios

Compuesto	Concentración (ng mL^{-1})			
	Voluntario 1	Voluntario 2	Voluntario 3	Voluntario 4
Cortisol	0.54 ± 0.03	0.98 ± 0.09	1.81 ± 0.11	2.20 ± 0.07
Cortisona	3.8 ± 0.2	6.6 ± 0.5	7.5 ± 0.4	10.0 ± 0.2

Estudio de la repetibilidad de la síntesis

Para verificar la repetibilidad de la síntesis del material, se realizaron tres síntesis independientes y se procedió a la extracción de una disolución de cortisona y cortisol mediante el método propuesto. Los resultados se muestran en la **Figura 5.10.** No se observaron diferencias significativas en la señal analítica obtenida empleando los tres materiales.

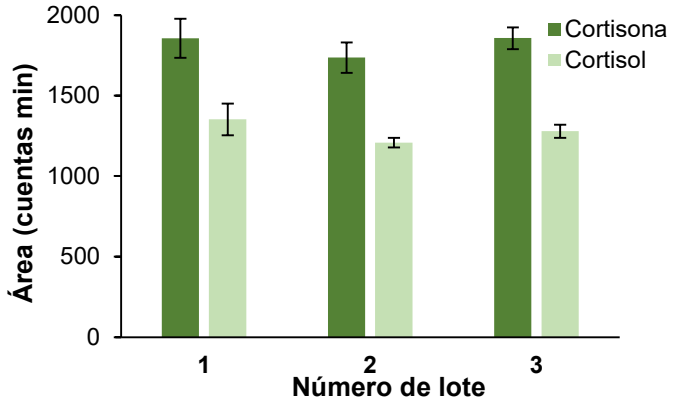

Figura 5.10. Comparación de las áreas obtenidas para cada analito mediante M-SA-DSPE-LC-MS/MS empleando $CoFe_2O_4$-Strata™ X-RP. Las barras de error muestran la desviación estándar de los resultados (N=3)

Influencia de extracción

Teniendo en cuenta las imágenes de SEM mostradas en las **Figuras 5.2.c** y **5.2.d,** donde se aprecia que las MNPs cubren parcialmente la superficie de las micropartículas de polímero, se sospechó que las MNPs pudieran tener influencia en la extracción.

Por ello, se comparó la capacidad de extracción del $CoFe_2O_4$-Strata™ X-RP con sus componentes por separado (polímero y MNPs). Debido a que el polímero no es magnético, para recogerlo fue necesario una etapa de centrifugación. Como se aprecia en la **Figura 5.11,** las partículas magnéticas apenas extraen el cortisol y la cortisona. Por otro lado, se observa que la diferencia de señales entre el polímero y el $CoFe_2O_4$-Strata™ X-RP no es significativa, probando que las partículas magnéticas situadas en la capa externa del $CoFe_2O_4$-Strata™ X RP no influyen en la extracción.

Por tanto queda patente que la extracción de los compuestos la realiza el polímero mientras que las MNPs se limitan a conferir magnetismo al primero.

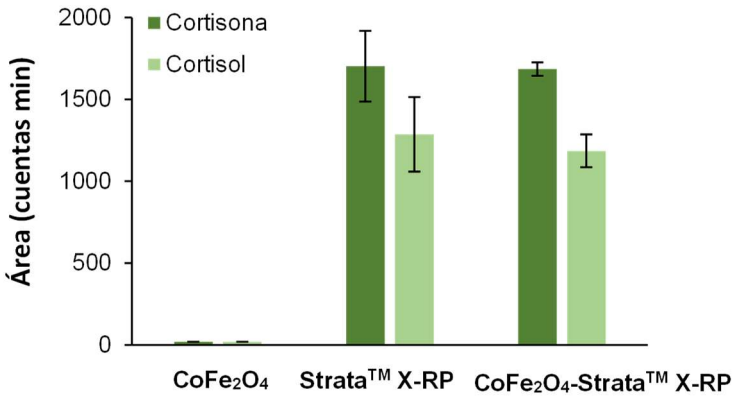

Figura 5.11. Comparación de la capacidad de extracción de las MNPs de $CoFe_2O_4$, el polímero Strata™ X-RP y $CoFe_2O_4$-Strata™ X-RP. Las barras de error muestran la desviación estándar de los resultados (N=3)

Comparación de la eficiencia de dispersión de la M-SA-DSPE

Para estudiar la eficiencia de dispersión de esta modificación de la M-SA-DSPE en comparación con otros métodos de agitación, se realizó la extracción de una misma muestra utilizando el presente método, asistida con agitador *vortex* (VA-DSPE) y por baño de ultrasonidos (USA-DSPE) manteniendo el mismo tiempo de extracción (1 min). Los resultados obtenidos en la **Figura 5.12** muestran como utilizando la M-SA-DSPE se obtienen valores muy superiores.

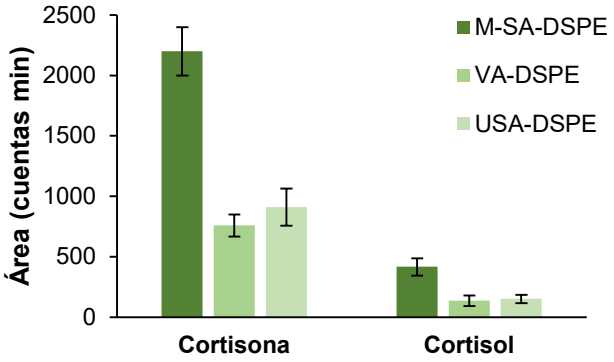

Figura 5.12. Comparación de M-SA-DSPE con VA-DSPE y USA-DSPE para la extracción de cortisona y cortisol en saliva. Las barras de error muestran la desviación estándar de los resultados (N=3)

El empleo de agitador *vortex* o de baño de ultrasonidos puede resultar agresivo para el composite, llegando a separar el sorbente del material magnético. Por ello, se realizó el mismo experimento pero finalizando con una etapa de recogida mediante centrifugación para recoger el posible sorbente que se hubiese separado de las partículas magnéticas. Como se aprecia en la **Figura 5.13,** las señales empleando agitador *vortex* (VA-DSPE) y empleando baño de ultrasonidos (USA-DSPE) aumentan, pero continúan siendo bastante inferiores a las obtenidas con M-SA-DSPE.

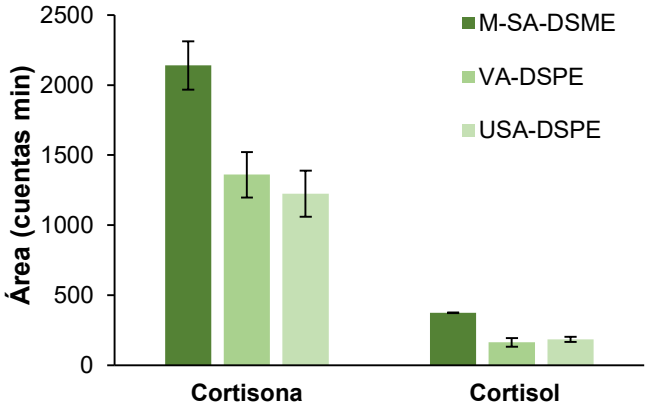

Figura 5.13. Comparación de M-SA-DSPE con VA-DSPE y USA-DSPE para la extracción de cortisona y cortisol en saliva con una etapa de centrifugación. Las barras de error muestran la desviación estándar de los resultados (N=3)

Comparación con otros métodos de la bibliografía

El método analítico propuesto se comparó con otros métodos existentes en la bibliografía empleando diferentes técnicas de extracción y microextracción. Como se aprecia en la **Tabla 5.5**, el método M-SA-DSPE-LC-MS/MS consigue alcanzar límites de detección muy bajos sin necesidad de derivatización.

Tabla 5.5. Comparación del método propuesto con otras metodologías presentes en la bibliografía.

Técnica de extracción	LOD (ng mL^{-1})		Coeficiente de recuperación (%)	Ref
	Cortisol	Cortisona		
SPE	0.060	0.300	68 – 98	[143]
SPE	0.185	0.128	90 – 115	[144]
SPE	0.002	0.005	80 – 120	[145]
SPE	0.043	0.085	96 – 114	[146]
IL-DLLME	0.162	0.111	83 – 116	[147]
M-SA-DSPE[a]	0.029	0.018	86 – 111	[148]

[a]Trabajo presentado en este capítulo

Evaluación de la seguridad y sostenibilidad del método

En la **Figura 5.14** se muestra el diagrama AGREEprep para el método propuesto. El primero de esta tesis doctoral en situarse por encima de 0.6. Esto se debe a la disminución en la cantidad de residuos derivado del empleo de pequeños volúmenes de muestra, disolventes orgánicos y sorbente. La puntuación de este método viene limitada, además, por la medida cromatográfica (punto 9) y el empleo de material no reutilizable (punto 3), por la falta de (semi)automatización de este proceso. Aspecto que se corregirá en los **Capítulos 6 y 7.**

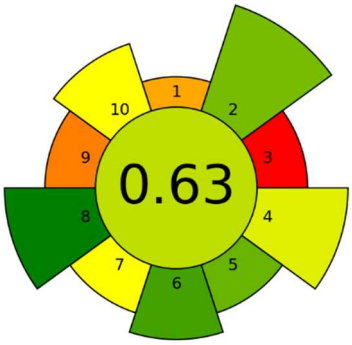

Figura 5.14. Evaluación del método propuesto empleando AGREEprep

Conclusiones

Se ha desarrollado una nueva modalidad de microextracción basada en la M-SA-DSPE que imita el mecanismo de la DLLME, permitiendo una dispersión mediante una jeringa, sin necesidad de agitadores externos (como agitador *vortex* o baño de ultrasonidos) y reduciendo el tiempo de extracción.

Esta modificación presenta un gran interés para el trabajo con pequeños volúmenes de muestra, reduciendo así también las cantidades de sorbente y disolventes orgánicos.

El método se aplicó a la determinación de cortisol y cortisona en saliva obteniendo excelentes resultados para ambos analitos.

El método desarrollado es fácil y rápido de aplicar, obteniendo resultados comparables con los de metodologías previas encontradas en la bibliografía.

Capítulo 6: Microextracción en fase sólida dispersiva magnética en punta de pipeta basada en sorbentes magnéticos como alternativa a técnicas en punta de pipeta convencionales: Aplicación a la determinación de testosterona en saliva

El contenido de este capítulo ha sido publicado en el artículo **A high-throughput magnetic-based pipette tip microextraction as an alternative to conventional pipette tip strategies: Determination of testosterone in human saliva as a proof-of-concept, Analytica Chimica Acta 1221 (2022) 340117** y presentado como comunicación oral en el congreso "XXIII Meeting of the Spanish Society of Analytical Chemistry" Oviedo, 2022

Objetivo

Desarrollo de una nueva técnica de microextracción en fase sólida dispersiva en punta de pipeta basada en el empleo de materiales magnéticos útil para el análisis de muestras de pequeño volumen.

Aplicación de esta técnica a la determinación de testosterona en muestras de saliva.

Resumen

En este capítulo se ha presentado una técnica híbrida llamada microextracción en punta de pipeta basada en sorbentes magnéticos (M-PTME) que combina la comodidad de las técnicas de microextracción en punta de pipeta y la eficacia de la DSPE con sorbentes magnéticos. En esta técnica, un pequeño imán de neodimio se introduce dentro de una punta de pipeta, con la que se toma la muestra y se dispensa abruptamente sobre el sorbente. De este modo, se forma una rápida dispersión del sorbente en la propia disolución de muestra produciendo la extracción de los analitos. Esta dispersión se recoge de nuevo con la propia punta, quedando el sorbente magnético conteniendo los analitos retenido en el imán, pudiéndose descartar fácilmente el resto de la matriz. Finalmente, se procede a etapas de lavado con agua y desorción con un disolvente apropiado.

Esta técnica se aplicó a la determinación de testosterona en saliva. Para ello, se empleó un material de sílice enlazada con cadenas C18 recubierto con MNPs de $CoFe_2O_4$ para conferirle magnetismo. Este método fue optimizado y validado, obteniendo un límite de detección de 7.5 ng L^{-1} para la testosterona, valores de RSD inferiores al 9 % y coeficientes de recuperación entre 82 y 106 %. Adicionalmente, se realizaron estudios en voluntarios antes y después de practicar ejercicio físico intenso para estudiar los cambios en los niveles de testosterona en saliva. Finalmente, se comparó esta técnica con las metodologías de microextracción con punta de pipeta más extendidas, como son la PT-SPE y la DPX, obteniendo resultados muy prometedores.

Datos de interés del método

- Material sorbente: $CoFe_2O_4$-C18

- Volumen de muestra: 400 µL

- Técnica de microextracción empleada: M-PTME

- Tiempo extracción-desorción: 0.5 min

- Técnica de medida: LC-MS/MS

Compuesto estudiado

Tabla 6.1. Información sobre el compuesto objeto de estudio en este capítulo

Analito	Estructura química	Número CAS	Log P_{ow}
Testosterona	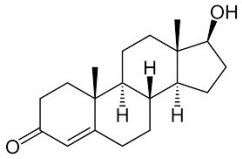	58-22-0	3.3

Se empleó testosterona deuterada (testosterona-d3) como patrón inteno. Al tratarse de la misma molécula pero sustituyendo tres átomos de hidrógeno por tres átomos de deuterio, presentan las mismas propiedades fisicoquímicas que la testosterona, pero con una señal m/z diferente para ser medido de forma independiente por MS/MS. Esto lo convierte en un excelente patrón interno para corregir, no solo los errores provocados durante la etapa de microextracción e inyección, sino también el efecto matriz que pudiera darse.

Selección y síntesis del material

La testosterona es un compuesto apolar (log P_{OW} = 3.3). Por esa razón, se seleccionó como material sorbente sílice recubierta con cadenas C18, dado que puede interaccionar con compuestos fuertemente hidrofóbicos como la testosterona, mientras que la mayoría de compuestos de carácter hidrofílico de la saliva son descartados.

También es necesario indicar que, debido a que uno de los puntos fundamentales de este trabajo era la comparación con otras técnicas comerciales, era necesario utilizar un material común. En este sentido cabe indicar que los productos comerciales suelen tener limitaciones en lo que a

variedad de materiales se refiere, siendo el C18 un material fácilmente accesible.

La síntesis de las MNPs $CoFe_2O_4$ se llevó a cabo de la misma forma que en el **Capítulo 3**. A continuación, 0.04 g de estas MNPs se mezclaron en tolueno con 0.4 g de C18. La mezcla se dejó agitar durante 3 días. El sólido resultante se filtró y se lavó dos veces con agua y una con etanol. Finalmente se mantuvo a 80 ºC toda la noche para secarlo.

Caracterización del material $CoFe_2O_4$-C18

- **Estudio de las curvas de histéresis**

En la **Figura 6.1**, se muestra la curva de histéresis para $CoFe_2O_4$-C18.

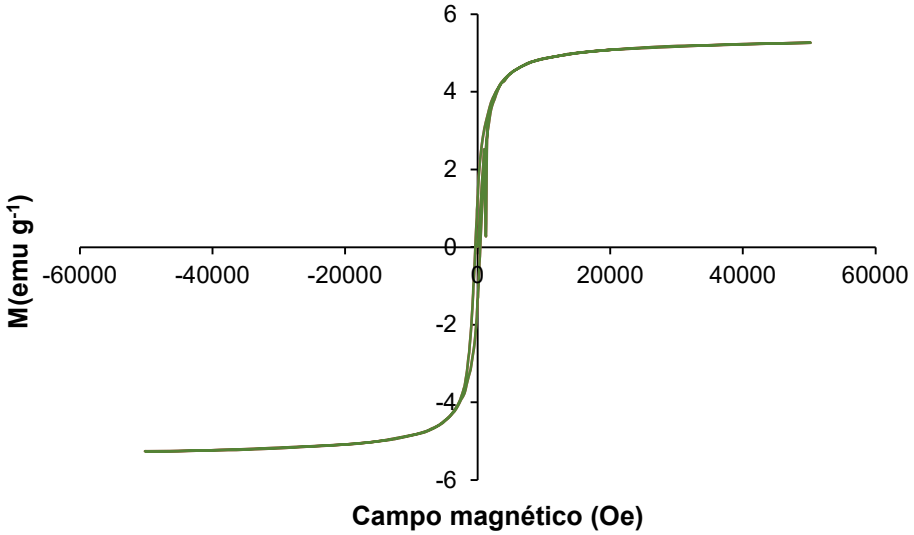

Figura 6.1. Curvas de histéresis del sorbente $CoFe_2O_4$-C18

La magnetización obtenida para $CoFe_2O_4$-C18 fue de 4.8 emu g^{-1}. La razón por la que este valor es muy inferior al compararla con los trabajos previos de esta tesis doctoral, es la reducción en la proporción de MNPs en esta síntesis (1:10 (m/m). No obstante, debido al poco volumen que se emplea

para esta técnica y, por tanto, la proximidad del material con el imán, no se requieren elevados valores de magnetismo para recuperar el material magnético, por lo que a pesar del aparente bajo carácter magnético, resulta apropiado para la técnica y permite reducir sustancialmente la cantidad de MNPs empleadas.

- **Imágenes SEM**

Se obtuvieron imágenes de SEM tanto para las micropartículas de C18 como para $CoFe_2O_4$-C18. En la **Figura 6.2.a** se pueden observar las micropartículas de C18 y en la **6.2.b y 6.2.c** recubiertas de las MNPs de $CoFe_2O_4$ tras la síntesis.

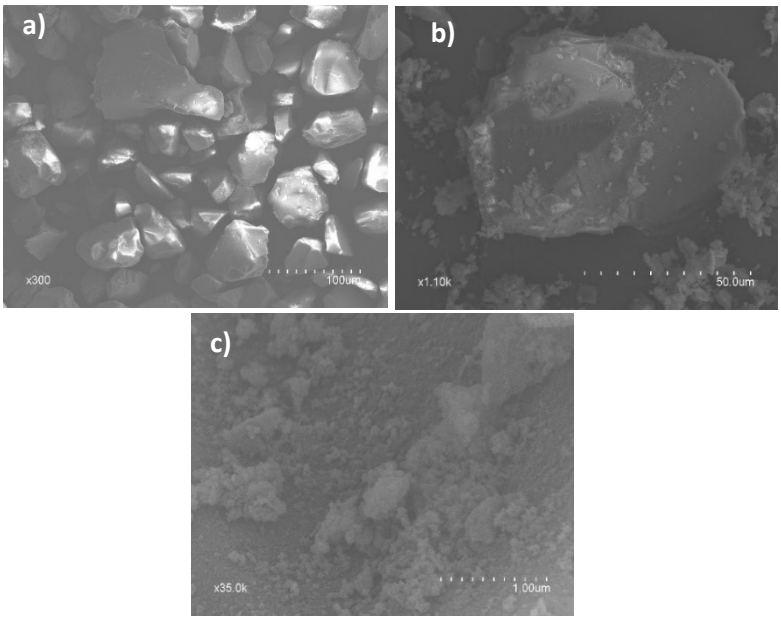

Figura 6.2. Imágenes SEM para a) C18 a 300 aumentos b) $CoFe_2O_4$-C18 a 1100 aumentos c) $CoFe_2O_4$-C18 a 35000 aumentos

- **Isoterma de adsorción/desorción**

En la **Figura 6.3** se muestra la isoterma de adsorción/desorción del material.

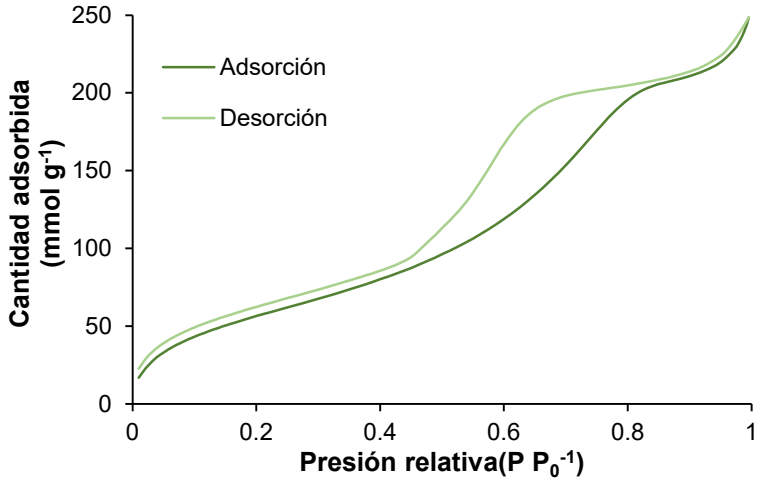

Figura 6.3. Isoterma de adsorción/desorción para $CoFe_2O_4$-C18

La isoterma muestra un comportamiento de tipo IV, con mesoporos de tamaño en torno a los 6.3 nm. Por otro lado, el área superficial obtenida fue de 233.8 ± 0.7 m^2 g^{-1}

- **Análisis termogravimétrico**

Se realizó también un estudio de la estabilidad del material en función de la temperatura. Como se puede apreciar en la **Figura 6.4,** a los 200 ºC se produce una pérdida progresiva (en torno a un 20 %) de masa hasta los 500 ºC. Esto se debe a la eliminación de las cadenas de C18 del material, quedando únicamente la sílice y las partículas magnéticas.

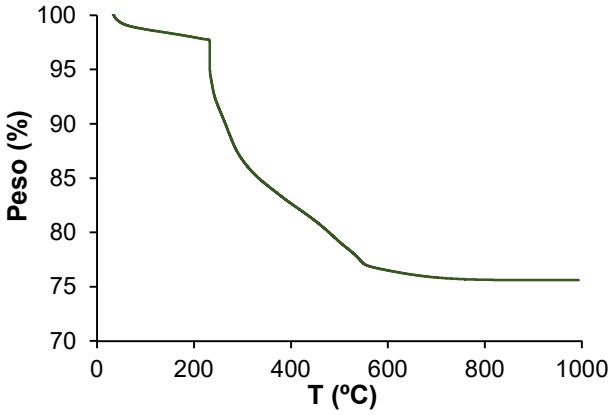

Figura 6.4. TGA para $CoFe_2O_4$-C18

- **Carga superficial**

Con el fin de medir la carga superficial del material sintetizado, se midió el potencial Z del material en una disolución de saliva sintética y 35 µL de metanol (condiciones de extracción). El valor obtenido fue ligeramente negativo (-6.9 mV), debido a que en esas condiciones las partículas magnéticas cuentan con una carga superficial positiva [149], mientras que el C18 está cargado negativamente [150], anulándose parcialmente.

Comparación de los dispositivos de extracción

Se comparó el empleo de dos dispositivos de microextracción diferentes. El primero utilizando una pipeta monocanal y el otro una multicanal de 12 posiciones.

El esquema del sistema monocanal se muestra en la **Figura 6.5.** En este modelo es necesario un imán externo para mantener fijo el imán interno durante las etapas de aspiración, además de evitar que caiga al fondo de la pipeta obstruyendo la punta. La presencia de un imán externo también permite modificar la altura del imán interno. Esto puede llegar a ser especialmente útil para cuando se utilizan muestras que requieran varios ciclos de extracción para mantener al imán separado de la dispersión mientras dure la extracción.

Figura 6.5. Esquema del montaje monocanal

Por otro lado, el sistema multicanal mostrado en la **Figura 6.6.** permite realizar doce análisis a la vez, reduciendo en gran medida el tiempo total de análisis. Además, en este caso los imanes interaccionan con los imanes de puntas adyacentes haciendo que la interacción magnética sea más débil que en el caso de la monocanal. Esto provoca que al aspirar la muestra, los imanes sean arrastrados hacia arriba reduciendo su distancia entre ellos, donde su interacción es más fuerte. Como consecuencia, los imanes se sitúan en una posición más elevada, siendo necesario, posteriormente, un volumen de disolvente orgánico mucho mayor para la etapa de desorción. De esta forma, se pierde gran parte del valor 'verde' de la técnica, a la vez que disminuyen la capacidad de preconcentración de la misma.

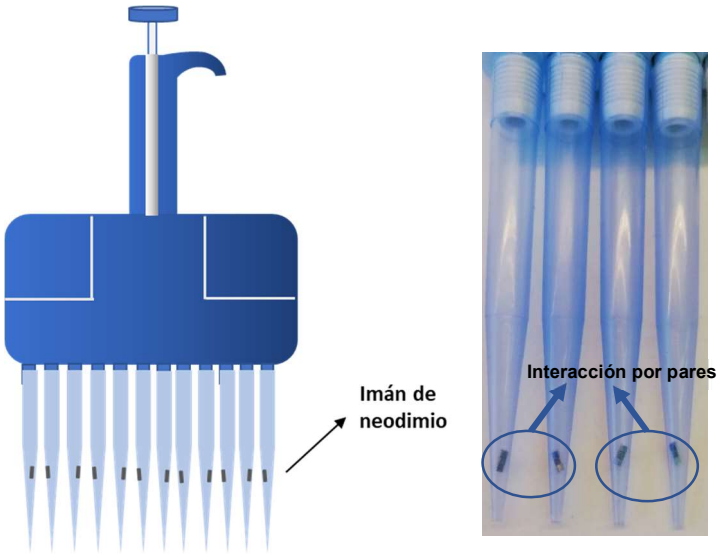

Figura 6.6. Esquema del montaje multicanal

Ante este inconveniente, se escogió el empleo de imanes más pequeños con forma cúbica, de modo que en cada punta se introducían 3 de estos imanes, obteniendo así una barra en forma de ortoedro. En este caso, como se observa en el **Vídeo 6.1**, los imanes son arrastrados por la corriente de aspiración y, llegado a cierto punto, interaccionan y vuelven a la posición inicial. Esto permite mantener fija la altura de los imanes aunque se muevan durante la aspiración de la muestra. Por otro lado, al ser imanes más pequeños es posible recubrirlos con menos cantidad de disolvente de elución, por lo que se reduce el volumen de disolvente orgánico. Además, debido a la forma cuadrada de la base del ortoedro, nunca llega a obstruir la punta.

Video 6.1. Comportamiento de los imanes en el sistema multicanal

No obstante, este dispositivo presenta un inconveniente, ya que al tratarse de imanes más pequeños sus capacidades magnéticas también lo son, por

lo que el sorbente magnético se retiene de forma menos eficiente. Por esta razón, son necesarias etapas de centrifugación adicionales para asegurar que el material sólido no se introduzca en el LC-MS/MS.

Por esta razón, se decidió emplear el modelo monocanal, mientras que se continuará con la mejora del dispositivo multicanal en futuros estudios.

Pretratamiento de muestra

Al igual que en el **Capítulo 5,** se realiza un pretratamiento de la saliva para eliminar componentes no deseados que pudieran dificultar la aplicación de la técnica. Este tratamiento consiste primero en una etapa de centrifugación para eliminar las posibles flemas y los restos de alimentos. Posteriormente, las muestras son congeladas para producir la rotura de las cadenas de polisacáridos. Finalmente, se descongela y se centrifuga nuevamente.

Esquema del método analítico propuesto

En la **Figura 6.7.** se muestra un esquema del método analítico propuesto. En primer lugar, 1 mg del material sorbente se dispersa en 35 µL de MeOH. Después, 400 µL de saliva o patrón conteniendo 100 µL del testosterona-d_3 (5 ng mL^{-1}) en agua ultrapura se dispensan abruptamente sobre esta mezcla para producir la dispersión del material en el seno de la disolución.

Inmediatamente después, la dispersión se aspira a través de la misma punta, quedando el material retenido en el pequeño imán de neodimio que se encuentra dentro de la misma. De este modo, la muestra se descarta fácilmente y se procede a lavar el imán aspirando 500 µL de agua ultrapura.

Finalmente se toman con la punta 35 µL de MeOH y se realizan 2 ciclos de aspiración/dispensación para provocar la desorción de los analitos.

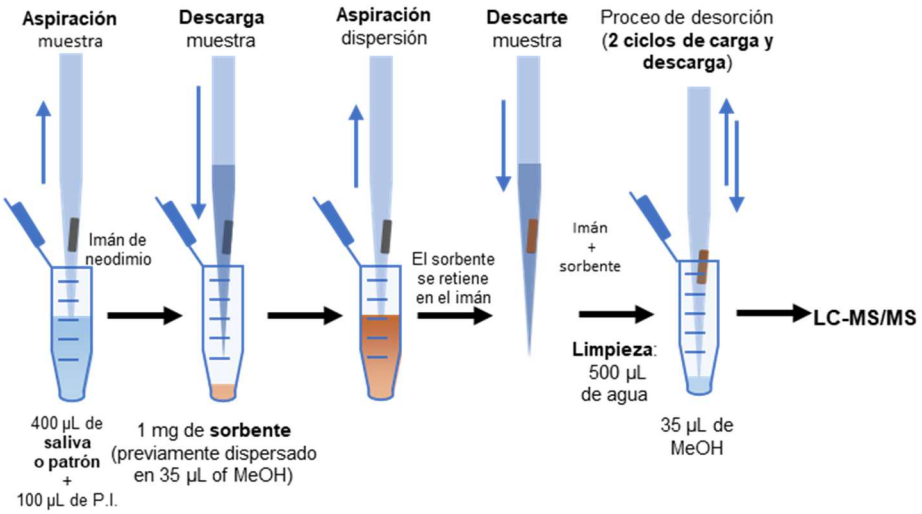

Figura 6.7. Método para la determinación de testosterona en muestras de saliva

Se muestra a continuación el **Vídeo 6.2,** donde se detalla la etapa de extracción.

Vídeo 6.2. Proceso de extracción empleando M-PTME

Condiciones cromatográficas

- Columna: Zorbax SB-C18, 50 mm longitud, 2.1 mm de diámetro interno y 1.8 µm de tamaño de partícula

- Fase móvil: H2O 0.1 % ácido fórmico y MeOH 0.1 % ácido fórmico (15:85 v/v)

- Flujo: 0.2 mL min^{-1}

- Temperatura de columna: 35 ºC

- Modo operacional MS/MS: ESI+

- Voltaje: 5000 V (ESI+)

- Temperatura de gas: 230 ºC

- Flujo del gas nebulizador: 13 L min^{-1}

- Presión de nebulizador: 35 psi

- Tiempo de cromatograma: 2.5 min

Tabla 6.2. Relaciones masa/carga (m/z) de los iones precursores y producto, energías de colisión y fragmentador para la testosterona y la testosterona d_3

Analito	Ion precursor (m/z)	Ion producto (m/z) [a]	CE (V)	Fragmentador (V)
Testosterona	289	**97**	21	132
		102	21	
Testosterona d_3	292	**97**	21	132

[a]En negrita las m/z empleadas para la cuantificación

En la **Figura 6.8** se muestra, a modo de ejemplo, los cromatogramas obtenidos para los analitos tras la aplicación del método a una muestra de saliva sin fortificar:

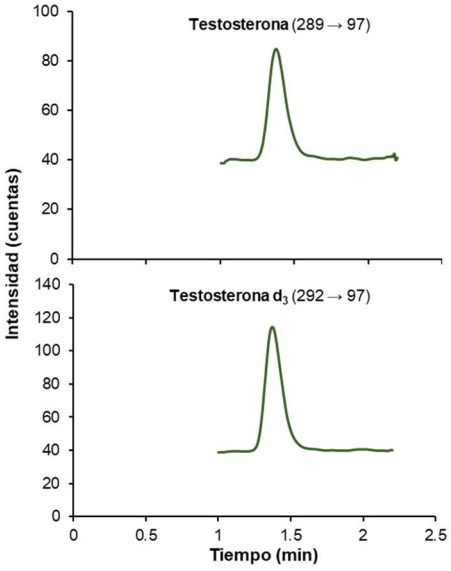

Figura 6.8. Cromatograma obtenido para una muestra de saliva tras la aplicación del método M-PTME-LC-MS/MS propuesto

Estudio de las variables implicadas en la etapa de extracción y desorción

Para la realización de este estudio se emplea el área relativa normalizada en lugar del área para el estudio de las variables de extracción y desorción. Esto es debido que proporciona una mayor facilidad para observar los cambios que se producen en una misma variable.

Las variables estudiadas de las etapas de extracción y de desorción fueron:

- Cantidad de sorbente: 1-5 mg

- Tiempo de extracción: 0-2 min

- **Volumen disolvente dispersante:** 25-100 µL

- Fuerza iónica: 0-1 %

- Volumen disolvente desorción: 35-150 µL

- Número de ciclos de desorción: 1-10 ciclos

▪ Cantidad de sorbente

Se estudiaron cantidades entre 1 y 5 mg de material. Como puede verse en la **Figura 6.9**, al aumentar la cantidad de sorbente la señal se reduce.

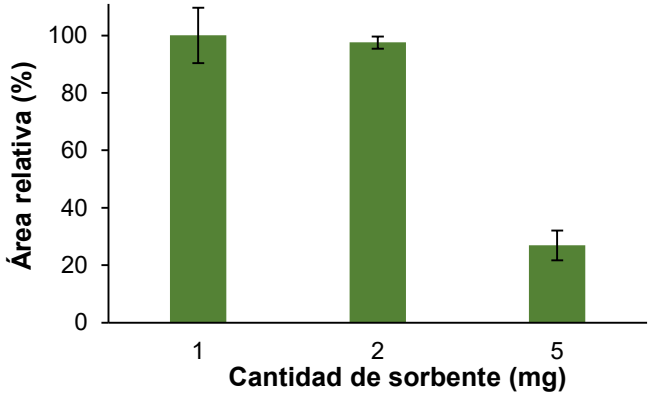

Figura 6.9. Estudio de la cantidad de sorbente. Las barras de error muestran la desviación estándar de los resultados (N=3)

Si se compara con la **Figura 5.6** del capítulo anterior**,** la disminución con 5 mg es incluso más pronunciada. Esto se debe a que, además de la peor dispersión durante la etapa de desorción, hay que añadir que tanta cantidad de sorbente es más difícil de retener por el imán interno, por lo que gran parte del material, conteniendo el analito, se pierde durante el descarte de la muestra, disminuyendo así la señal. En ese sentido, se seleccionó **1 mg** para emplear la menor cantidad de sorbente.

- **Tiempo de extracción y ciclos de carga/descarga**

Se optimizó el tiempo al que se mantuvo la dispersión para una completa extracción de los analitos. Se estudiaron tiempos de 0 a 2 min, observando en la **Figura 6.10** un descenso de la señal a medida que aumentaba el tiempo. Dada la poca afinidad que tiene el sorbente por la matriz de saliva, el sorbente se deposita al poco tiempo de haberse producido la dispersión. Así, cuanto más tiempo transcurre, más cantidad de sorbente se deposita y es más difícil de recoger. Así, se produce produciendo una pérdida parcial del analito, produciendo un descenso en la señal. En ese sentido, se optó por no dejar transcurrir ningún tiempo adicional tras la dispersión y aspirarla inmediatamente.

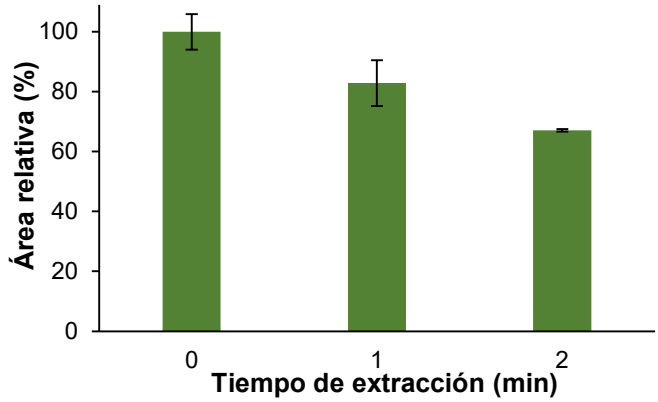

Figura 6.10. Estudio del tiempo de extracción. Las barras de error muestran la desviación estándar de los resultados (N=3)

Paralelamente, se estudió la influencia del número de ciclos de extracción sobre la señal analítica. La diferencia entre 1 y 5 ciclos no fue significativa, por lo que se decidió mantener **1 ciclo** de extracción.

- **Volumen de disolvente dispersante**

Como se puede apreciar en la **Figura 6.11,** hasta un volumen de 50 µL de disolvente dispersante no se observan grandes diferencias. Sin embargo, cuando se utilizaron 100 µL se produjo una disminución de la señal debido al incremento de la afinidad de la testosterona por la fase dadora. Se decidió entonces seleccionar el volumen de **35 µL** y no el de 25 µL ya que, con este último, la reproducibilidad del proceso se veía comprometida.

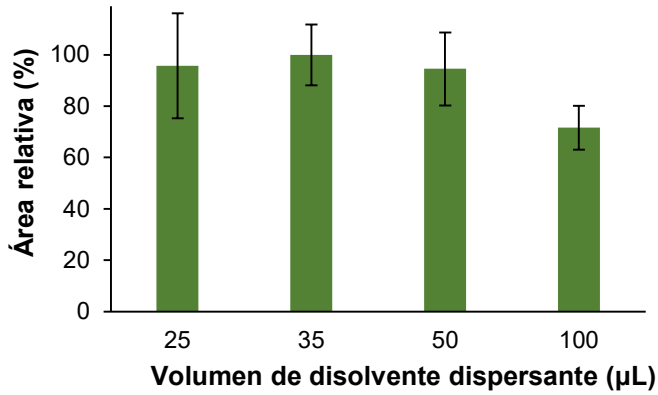

Figura 6.11. Estudio del volumen de disolvente dispersante. Las barras de error muestran la desviación estándar de los resultados (N=3)

- **Fuerza iónica**

Al igual que ocurría en el capítulo anterior, al trabajar con saliva, se estudió la influencia de la fuerza iónica en la extracción. Tal y como se puede ver en la **Figura 6.12**, valores bajos de fuerza iónica producen un incremento en la señal debido al efecto salino. No obstante, cuando la concentración de sal se incrementa más, la señal decrece debido al aumento de la viscosidad de la fase dadora y la reducción de transferencia de masa. De acuerdo al capítulo anterior, donde la fuerza iónica de la saliva se determinó entre 1 y 3.5 mg mL^{-1} (lo que equivale a 0.1-0.35 %), se decidió no modificar la fuerza iónica para futuros experimentos.

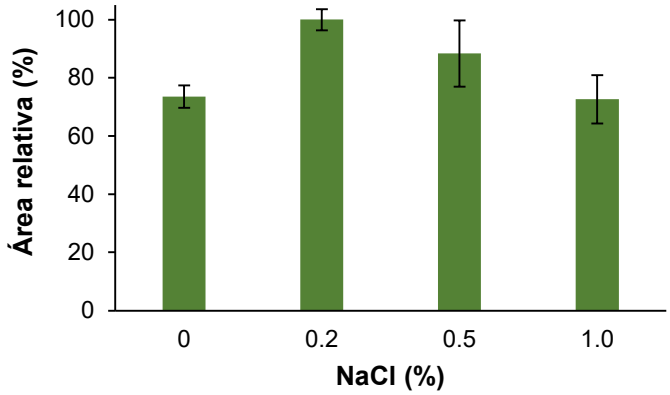

Figura 6.12. Estudio de la fuerza iónica (como concentración de NaCl %) de la fase dadora. Las barras de error muestran la desviación estándar de los resultados (N=3)

- **Volumen de disolvente de elución**

Se probaron diferentes volúmenes de MeOH, empleado como disolvente de desorción, para comprobar su efecto sobre la desorción de la testosterona. El volumen mínimo estudiado fue de 35 µL, que era el mínimo necesario para cubrir el imán. Los resultados se encuentran en la **Figura 6.13.** Como era de esperar, se produce una disminución de la señal a medida que se aumenta el volumen de desorción debido al efecto de la dilución. Pese a que las señales obtenidas con 35 y 50 µL eran muy similares, se decidió trabajar con **35 µL** para reducir la cantidad de disolvente orgánico empleado.

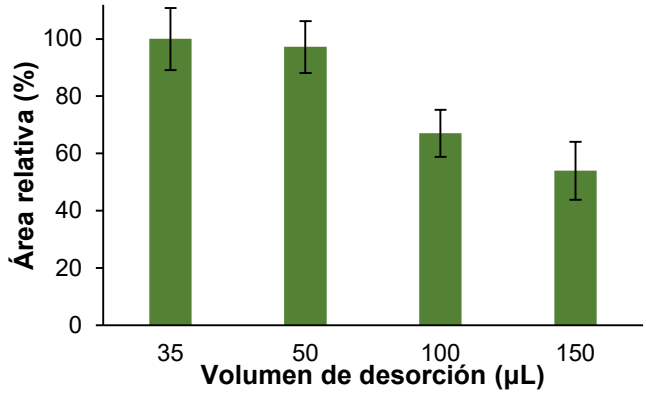

Figura 6.13. Estudio del volumen de disolvente de desorción (MeOH). Las barras de error muestran la desviación estándar de los resultados (N=3)

- **Ciclos de carga y descarga**

Por último, se comprobó cómo afectaba el número de ciclos de carga y descarga a la desorción de la testosterona. Los resultados se muestran en la **Figura 6.14.** El empleo de 1 ciclo no fue suficiente para una correcta desorción. En cambio, con 2 ciclos ya se produce una desorción cuantitativa del analito. Por lo tanto, se seleccionaron **2 ciclos** de desorción.

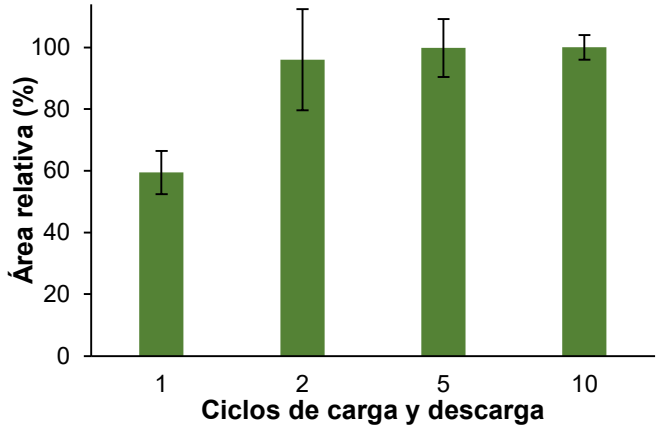

Figura 6.14. Estudio del tiempo de los ciclos de carga/descarga. Las barras de error muestran la desviación estándar de los resultados (N=3)

Validación del método y análisis de muestras reales

Se validó el método estudiando la selectividad, linealidad, EF, LOD y LOQ, además de la repetibilidad a partir de patrones preparados en saliva sintética. Para el estudio del coeficiente de recuperación se empleó saliva de tres voluntarios fortificada a tres niveles de concentración.

- **Selectividad**

Como se ha explicado anteriormente, el C18 permite extraer los compuestos hidrofóbicos de la saliva a la vez que excluye a aquellos hidrofílicos (como son urea, sacáridos, sales etc.). Este hecho, sumado a la determinación con LC-MS/MS, lo convierten en un método de elevada selectividad, tal y como se puede comprobar en la **Figura 6.9,** donde los cromatogramas únicamente muestran las señales producidas por la testosterona y testosterona deuterada.

- **Linealidad**

De acuerdo con los niveles habituales de testosterona en saliva, se seleccionó un intervalo de trabajo entre 25 y 2000 ng L^{-1}. En este intervalo se obtuvieron niveles de linealidad altos con buenos coeficientes de regresión (0.9993).

- **Factor de enriquecimiento**

Para el cálculo de los EFs, se obtuvo el cociente entre las señales de un patrón de los analitos después de la extracción y antes de realizarla. Se obtuvo un EF de **4.3** para la testosterona.

- **Límites de detección y cuantificación**

El LOD y el LOQ se calcularon mediante la concentración a la que se obtenía una relación de S/N de 3 y 10 respectivamente. El LOD para la testosterona fue de **7.5 ng L^{-1}** y el LOQ **24.8 ng L^{-1}**.

- **Repetibilidad**

La repetibilidad se estableció calculando la RSD de 5 réplicas medidas el mismo día (repetibilidad intradía) y 5 réplicas medidas en distintos días (repetibilidad interdía). La RSD se calculó a tres niveles de concentración (50, 250 y 1000 ng L^{-1}), obteniéndose valores de **7.8, 6.0** y **4.6 %** respectivamente para la repetibilidad interdía y de **8.5, 7.8** y **6.5 %** para la intradía.

- **Análisis de muestras reales**

Se fortificaron tres muestras de saliva con 50, 250 y 1000 ng L^{-1} de testosterona para realizar el cálculo de los coeficientes de recuperación. Los resultados se muestran en la **Tabla 6.3.** donde se observa que los coeficientes de recuperación estuvieron entre **82** y **106 %**, indicando que, en el caso de existir efecto matriz, el patrón interno utilizado lo corrige. De este modo, es posible el trabajar con calibración externa con empleo de patrón interno.

Tabla 6.3. Coeficientes de recuperación obtenidas tras la aplicación del método propuesto a muestras de saliva de diferentes voluntarios.

Voluntario[a]	Cantidad fortificada (ng L^{-1})	Cantidad encontrada (ng L^{-1})	Coeficiente de recuperación (%)
1 (H)	0	83 ±3	-
	50	127 ± 2	94 ± 10
	250	308 ± 20	90 ± 8
	1000	1090 ± 40	92 ± 4
2 (H)	0	98 ±5	-
	50	144 ± 5	82 ± 3
	250	360 ±10	88 ± 5
	1000	1140 ± 60	103 ± 6
3 (M)	0	60 ± 5	-
	50	110 ± 7	101 ± 14
	250	324 ± 10	106 ± 4
	1000	1100 ± 20	105 ± 3

[a](H): Hombre; (M): Mujer

Además, como aplicación del método, se determinó la testosterona en muestras de saliva de voluntarios antes y después de realizar ejercicio físico extenuante durante 1 h. Para todos los voluntarios se observó un incremento de la cantidad de testosterona tras el entrenamiento. Los resultados se muestran en la **Tabla 6.4**.

Tabla 6.4. Comparación de los niveles de testosterona antes y después de ejercicio físico

Voluntario[a]	Testosterona antes de entrenar (ng L^{-1})	Testosterona después de entrenar (ng L^{-1})	Incremento (%)
4 (M)	46 ± 6	58 ± 4	26
5 (M)	33 ± 2	41 ± 3	24
6 (H)	89 ± 1	99 ± 2	11
7 (H)	66 ± 2	75 ± 4	14

[a](M): Mujer; (H): Hombre

Estudio de la repetibilidad de la síntesis

Para verificar la repetibilidad de la síntesis del material se realizaron tres síntesis independientes y se procedió a la extracción de una disolución de testosterona. Tal y como se muestra en la **Figura 6.15**, no se observan diferencias significativas entre los tres materiales.

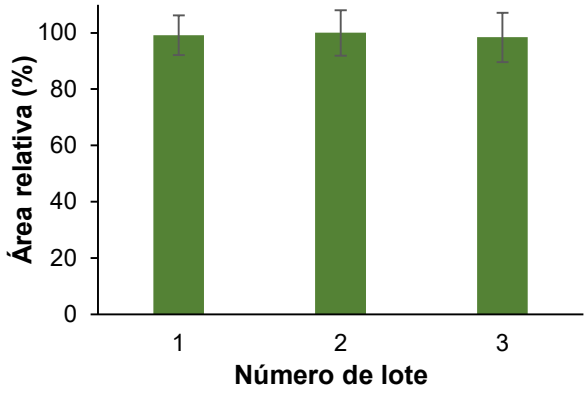

Figura 6.15. Comparación de las áreas obtenidas para cada síntesis mediante M-PTME empleando $CoFe_2O_4$-C18. Las barras de error muestran la desviación estándar de los resultados (N=3)

Influencia de extracción del $CoFe_2O_4$-C18

Como se aprecia en la **Figura 6.2**, las MNPs cubren parcialmente la superficie del C18. Por ello era necesario estudiar si estas MNPs tenían una influencia en la extracción de la testosterona. Por esa razón, se comparó la capacidad de extracción de $CoFe_2O_4$-C18 con sus componentes individuales (MNPs de $CoFe_2O_4$ y micropartículas de C18).

Tal y como se puede apreciar en la **Figura 6.16,** las MNPs tienen una influencia mínima en la extracción de testosterona, mientras que las señales obtenidas para el C18 y el $CoFe_2O_4$-C18 son comparables, lo que pone de manifiesto que el sorbente C18 es el responsable de la extracción de la testosterona y las MNPs de $CoFe_2O_4$ se limitan exclusivamente a conferirle magnetismo.

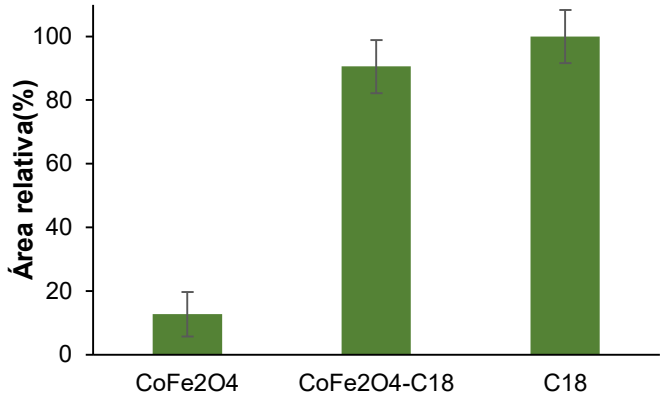

Figura 6.16. Comparación de la capacidad de extracción de las MNPs de $CoFe_2O_4$, las micropartículas C18 y el material $CoFe_2O_4$-C18. Las barras de error muestran la desviación estándar de los resultados (N=3)

Comparación con técnicas de microextracción basadas en puntas de pipeta

Finalmente, se realizó la comparación de esta nueva técnica con las dos técnicas de microextracción basadas en puntas de pipeta más empleadas, como son la PT-SPE y la DPX.

Para realizar esta comparación, se decidió mantener todas las condiciones lo más similares posibles. En ese sentido, se empleó la misma cantidad de

sorbente (1 mg), el mismo volumen de desorción (35 µL) y el mismo número de ciclos de carga y descarga para la etapa de extracción (1 ciclo), limpieza (1 ciclo) y de desorción (2 ciclos). A continuación, se detallan los procedimientos independientes para PT-SPE y DPX:

- **Procedimiento PT-SPE**

Para PT-SPE se optó por trabajar con puntas preparadas en nuestro laboratorio, en lugar de emplear puntas comerciales. Para ello, se selló 1 mg de C18 entre dos fritas en una punta de 1 mL convencional. Una vez fabricada la punta, se procedió a su acondicionamiento con los 35 µL de MeOH. Posteriormente, la muestra fue aspirada y descartada. Por último, se procedió al lavado y a la desorción con MeOH.

- **Procedimiento DPX**

Para la DPX fue necesario el empleo de puntas comerciales con sorbente C18. En este caso, para recoger todo el material disperso en la punta fueron necesarios varios ciclos de acondicionamiento con 300 µL de MeOH. A continuación, al igual que en los otros dos casos, se tomó la muestra y se descartó para proceder a las etapas de lavado y desorción.

- **Comparación de las técnicas**

Como se observa en la Figura **6.17,** las señales de las dos modalidades dispersivas (como son la técnica propuesta y la DPX) fueron comparables, mientras que la señal para la PT-SPE fue menor, dado su carácter estático.

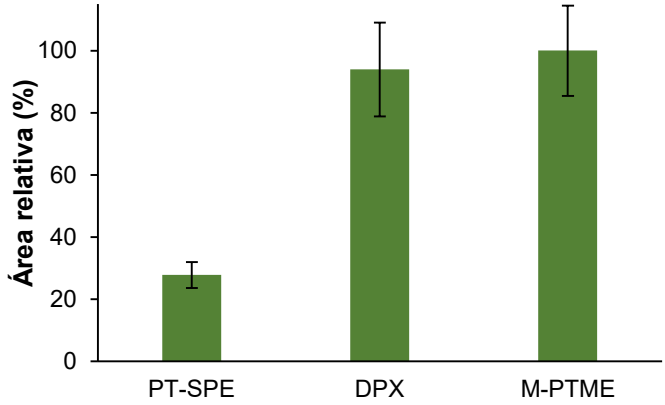

Figura 6.17. Comparación de la capacidad de extracción entre la PT-SPE, la DPX y la técnica propuesta

Además de la capacidad de extracción, se deben considerar otros factores, como son la manipulación por parte del operador y el precio.

En cuanto a la manipulación, la DPX y la técnica propuesta son similares. Sin embargo, al trabajar con PT-SPE y puntas caseras, se vieron algunos de los problemas mencionados en la bibliografía, como son obstrucción y pérdida de material [62]. Esto podría ser corregido mediante el empleo de puntas comerciales, aunque incrementaría considerablemente su precio. En cuanto al precio, las puntas comerciales para DPX son mucho más caras que las otras dos metodologías, sobrepasando los 150 euros por cada 100 análisis. En la **Tabla 6.5** se muestra, a modo de resumen, la comparación entre las tres técnicas.

Tabla 6.5. Comparación entre la PT-SPE, DPX y la M-PTME

Técnica de extracción	EF	Precio por 100 análisis (€)[b]	Ergonomía
PT-SPE[a]	1.2	1-2	+
DPX	4.0	100-160	+++
M-PTME	4.3	3-4	+++

[a]fabricadas en el laboratorio

[b] Los precios no incluyen gastos de envío

Además de estos factores, es necesario añadir que para el caso de la DPX se requiere más volumen de fase orgánica para la etapa de acondicionado reduciendo el carácter 'verde' de la misma comparado con la técnica propuesta.

Finalmente, otra ventaja de la técnica propuesta frente a las que emplean dispositivos comerciales, es que se puede emplear cualquier tipo de sorbente (siempre que sea magnético), aumentando en gran medida su versatilidad.

Evaluación de la seguridad y sostenibilidad del método

En la **Figura 6.18.** se muestra el diagrama AGREEprep del método propuesto. La puntuación es similar a la obtenida en el método anterior. Esto se debe a que las cantidades empleadas son muy similares a las encontradas en el **Capítulo 5.** A pesar de que respecto al capítulo anterior se corrige la falta de semi(automatización), el hecho de emplear MeOH como disolvente en lugar del ACN, hace que este método pierda puntuación. Por esta razón, para futuras aplicaciones, sería preciso adaptar los métodos a disolventes más seguros.

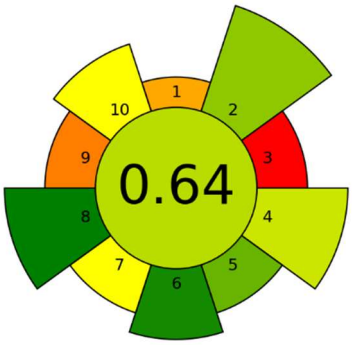

Figura 6.18. Evaluación del método propuesto empleando AGREEprep

Conclusiones

En este trabajo se ha desarrollado con éxito una nueva técnica basada en el empleo de puntas de pipeta y materiales magnéticos.

Esta permite el análisis rápido, simple y económico de pequeños volúmenes muestra. Además, permite reducir al máximo las cantidades de residuos y el uso de compuestos peligrosos y disolventes orgánicos.

Esta técnica fue aplicada con éxito al análisis de testosterona en muestras de saliva.

Comparado con técnicas previas basadas en puntas de pipeta, muestra resultados satisfactorios, probando ser una alternativa económica, eficaz y versátil para el análisis de muestras de bajo volumen.

SECCIÓN 4

Capítulo 7: Miniaturización de la microextracción en fase sólida dispersiva magnética en punta de pipeta basada en sorbentes magnéticos para el análisis de muestras de muy bajo volumen: determinación de cortisol en suero y orina de recién nacidos

Objetivo

Desarrollo de la miniaturización de la M-PTME para el análisis de muestras de muy bajo volumen.

Aplicación de esta técnica a la determinación de cortisol en muestras de suero y orina de recién nacidos prematuros.

Resumen

Como se indicó en **el Apartado 1.2.4** de la **Introducción**, en el caso de trabajar con pacientes enfermos y/o recién nacidos, es indispensable emplear el menor volumen de muestra posible.

No obstante, trabajar con cantidades muy pequeñas es complicado, por lo que es necesario el desarrollo de metodologías que permitan su fácil manipulación y que sean rápidas de aplicar. Por esta razón, en este capítulo se ha desarrollado una versión miniaturizada de la M-PTME descrita en el capítulo anterior. Esta modificación permite el trabajo con microvolúmenes de muestra a la vez que reduce al mínimo el consumo de disolventes y de material sorbente.

Para evaluar esta versión miniaturizada, se escogió la determinación de cortisol libre en muestras de suero y orina de recién nacidos. El cortisol libre en suero es un excelente indicador de insuficiencia suprarrenal en casos de pacientes críticos, mientras que en orina es un buen indicador para el diagnóstico del síndrome de Cushing.

Para esta tarea se empleó un inmunosorbente compuesto de micropartículas magnéticas recubiertas de proteína G para garantizar una correcta orientación durante la inmovilización del anticuerpo. Como técnica de medida y como herramienta de estudio de la reactividad cruzada del immunosorbente se empleó LC-MS/MS.

Se procedió al estudio de la síntesis del immunosorbente y de las variables del proceso de extracción y desorción. Bajo estos parámetros se validó el método obteniendo valores de LOD de 0.17 ng mL^{-1}, RSDs por debajo del 15 % y coeficientes de recuperación entre 91 y 111%.El el método se aplicó a muestras de suero y orina de recién nacidos prematuros de bajo peso.

Datos de interés del método

- Material sorbente: micropartículas magnéticas recubiertas de proteína G con anticuerpo de cortisol

- Volumen de muestra: 10 µL

- Técnica de microextracción empleada: M-PTME

- Tiempo extracción-desorción: 1 min

- Técnica de medida: LC-MS/MS

Compuesto estudiado

Tabla 7.1. Información sobre el compuesto objeto de estudio en este capítulo

Analito	Estructura química	Número CAS	Log P_{ow}
Cortisol	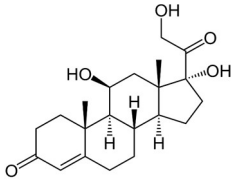	50-23-7	1.69

Para este trabajo no fue necesario el empleo de ningún tipo de patrón interno.

Selección y síntesis del material

Para este trabajo se decidió trabajar con un material de elevada selectividad, como son los anticuerpos. Estos se unieron a partículas magnéticas recubiertas de proteína G para garantizar una correcta orientación del anticuerpo, dejando más expuestas las zonas de unión al antígeno (compuesto de interés).

Su síntesis consistió en mezclar 2 µL de una suspensión de micropartículas de 35 mg mL^{-1} con 50 µL de una disolución de 10 µg mL^{-1} de anticuerpo en disolución '*Blind and Washing' (*disolución amortiguadora de fosfatos (***Phosphate Buffer Solution**, **PBS**) 0.1 M, 0.01% Tween 20, pH 8.2). La

mezcla se mantuvo en agitación durante 5 min tras lo cual se separó el sorbente y se lavó dos veces con PBS 0.1 M (pH 7.2).

Estudio de la síntesis del immunosorbente

Se estudiaron diferentes variables que afectan a la preparación del inmunosorbente:

- **Tiempo de inmovilización:** 5-45 min
- **Cantidad de micropartículas magnéticas:** 1-2 mg
- **Cantidad de anticuerpo:** 1-50 μg mL^{-1}

Este estudio se realizó mediante la extracción de una disolución de cortisol preparada en PBS con el método mostrado en el **Apartado 'Esquema del método analítico propuesto'.**

Tiempo de inmovilización

Se estudió el tiempo necesario para la inmovilización del anticuerpo. Tal y como se aprecia en la **Figura 7.1**, no se observaron diferencias significativas ente 5 y 45 min, por lo que seleccionaron 5 min.

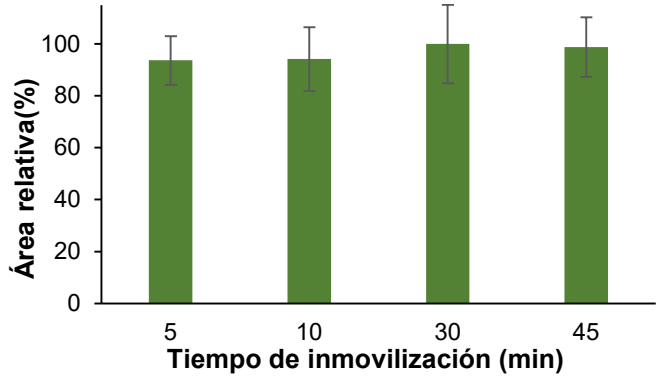

Figura 7.1. Estudio del tiempo de inmovilización

Cantidad de micropartículas magnéticas

La cantidad de micropartículas magnéticas viene limitada por la capacidad del imán para poder recogerlas íntegramente. En este sentido, cuando se emplean cantidades por encima de los 70-80 μg, parte de las partículas no

se anclan al imán, por lo que podrían llegar al extracto final y ser introducidas en el instrumento de LC-MS/MS. Para evitarlo, se limitó la cantidad a 60 µg. Entre las cantidades estudiadas, como se muestra en la **Figura 7.2**, a partir de **45 µg** no se conseguía un mayor incremento de señal, por lo que se seleccionó para futuros ensayos.

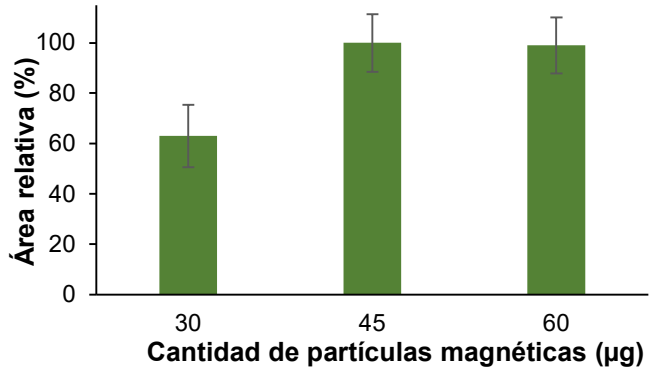

Figura 7.2. Estudio de la cantidad de micropartículas magnéticas

- **Cantidad de anticuerpo**

Finalmente, se estudiaron diferentes concentraciones de anticuerpo. En la **Figura 7.3** se observa un incremento de la señal a medida que aumenta la concentración. No obstante, a partir de 20 µg mL^{-1} se produce una disminución de la señal así como un incremento de la desviación estándar. Esto se produce debido a un aumento de la interacción del propio anticuerpo, lo que provoca una disminución en los huecos de unión del mismo reduciendo así los sitios activos para unirse con el analito, produciendo una disminución de la señal.

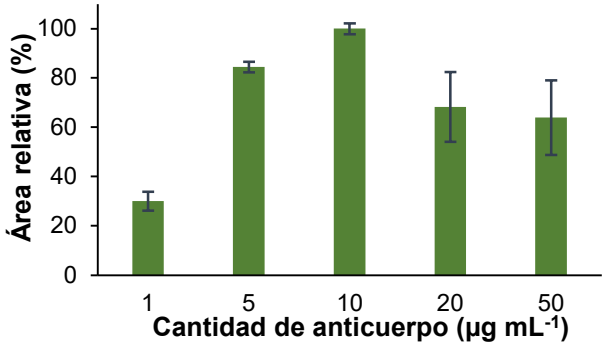

Figura 7.3. Estudio de la cantidad de anticuerpo

Dispositivo de microextracción

Para el trabajo con cantidades de muestra tan pequeñas, el dispositivo empleado en el capítulo anterior requería de una miniaturización todavía mayor. Por esa razón, se cambió el tipo de punta de 1 mL por una punta de 200 µL. Debido a su menor tamaño, el tamaño del imán también debía reducirse, por lo que el imán de 6x2 mm se sustituyó por un imán cúbico de 1x1 mm. En la **Figura 7.4** se muestra una comparación de los dos dispositivos.

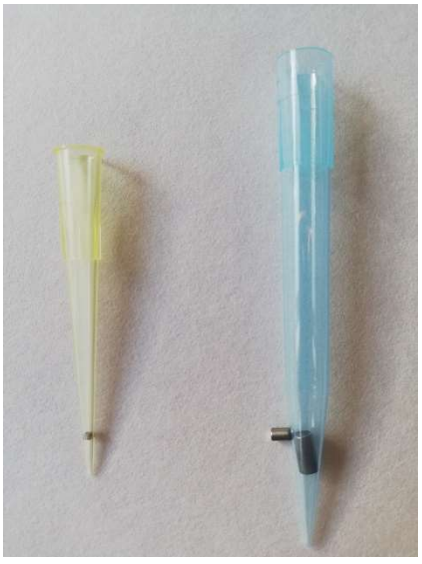

Figura 7.4. Comparación de los dispositivos de M-PTME actual (izquierda) y del Capítulo 6 (derecha)

Tal y como se muestra en la **Figura 7.5**, en este caso no es necesario un imán externo ya que, debido a la forma cúbica del imán y la forma cónica de la punta, se crean canales por lo que fluye la disolución y el flujo no queda obstruido. Por esa razón, en lugar del empleo de un imán externo que puede producir colisiones con las paredes del microtubo de centrífuga o la pared del pocillo, se prefirió incrustar el imán en el interior de la punta, de modo que, al aspirar o descargar las diferentes disoluciones por esta, el imán no se mueve.

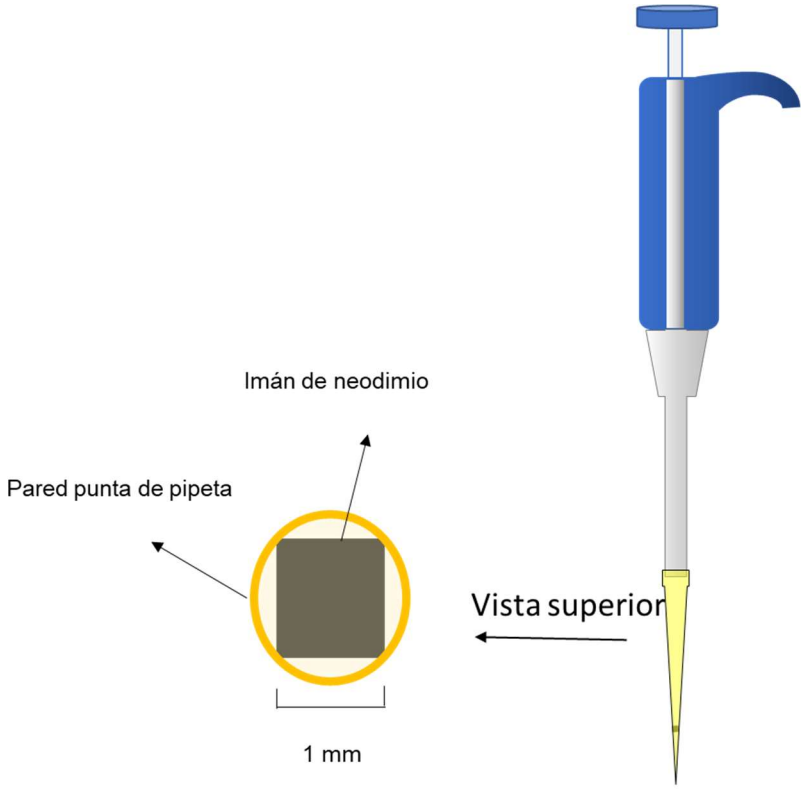

Figura 7.5. Esquema del dispositivo de M-PTME propuesto y de la vista superior del interior de la punta

Pretratamiento de muestra

Como el objetivo de este trabajo era la determinación de la fracción libre del cortisol, es necesario un pretratamiento previo de las muestras de suero para separar aquellas fracciones de cortisol que se encontraban unidas a macromoléculas como la transcortina, que se une al cortisol de forma

específica, u otras albúminas [151]. En este sentido, cuando se toma la muestra de suero, previamente se realiza una etapa de ultrafiltración [152], la cual consiste en centrifugar las muestras empleando tubos con un filtro de corte de 30 kDA. De este modo, las macromoléculas quedan retenidas en el filtro y el resto pasa al sobrenadante. Posteriormente, se tratan 200 µL de sobrenadante con ACN para precipitar proteínas de menor tamaño que pudieran estar presentes. Para el caso de la orina no es necesario ninguna de estas acciones.

Esquema del método analítico propuesto

En la **Figura 7.6** se muestra un esquema del método propuesto. Primero, se toman 60 µL de muestra diluida (1:5 con PBS) o patrón y se dispersan en el inmunosorbente magnético preparado en el **Apartado 'Selección y síntesis del material'** de este capítulo.

La dispersión se mantiene durante 30 s y, posteriormente, esta se aspira con la punta. Al igual que en el **Capítulo 6,** el material queda unido al imán interno, permitiendo un fácil descarte de la muestra o patrón. Después, se aspiran 60 µL de agua ultrapura para eliminar los restos de muestra o patrón.

Finalmente, los analitos se desorben empleando 5 ciclos de aspiración/dispensación con 10 µL de MeOH. Este volumen se diluye con 2.5 µL para una correcta resolución cromatográfica.

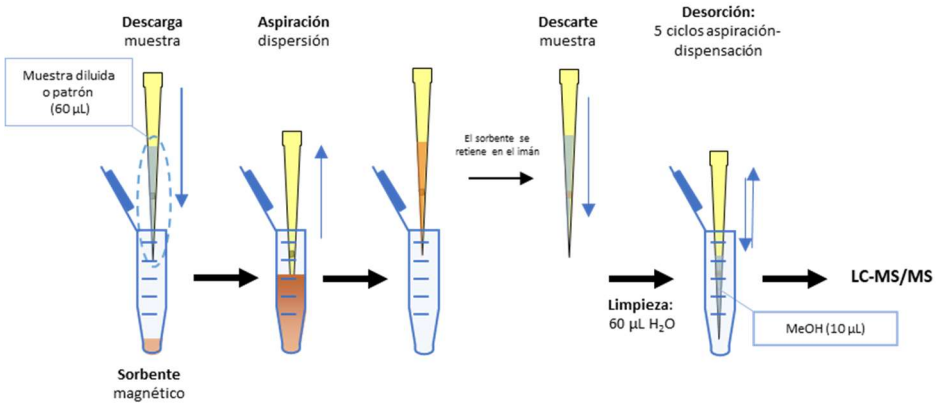

Figura 7.6. Método para la determinación de cortisol en muestras de suero y orina

Condiciones cromatográficas

- Columna: Zorbax SB-C18, 50 mm longitud, 2.1 mm de diámetro interno y 1.8 µm de tamaño de partícula

- Fase móvil: H2O 0.1 % ácido fórmico y MeOH 0.1 % ácido fórmico (30:70 v:v)

- Flujo: 0.15 mL min^{-1}

- Temperatura de columna: 40 ºC

- Modo operacional MS/MS: ESI+

- Voltaje: 5000 V (ESI+)

- Temperatura de gas: 350 ºC

- Flujo del gas nebulizador: 11 L min^{-1}

- Presión de nebulizador: 50 psi

- Tiempo de cromatograma: 2.5 min

Tabla 7.2. Relaciones masa/carga (m/z) de los iones precursores y producto, energías de colisión y fragmentador para el cortisol

Analito	Ion precursor (m/z)	Ion producto (m/z) [a]	CE (V)	Fragmentador (V)
Cortisol	363	**121**	21	155
		105	21	

[a] Marcados en negrita las m/z empleadas para la cuantificación

En la **Figura 7.7** se muestran, a modo de ejemplo, los cromatogramas obtenidos para el cortisol tras la aplicación del método a muestras de suero y orina sin fortificar:

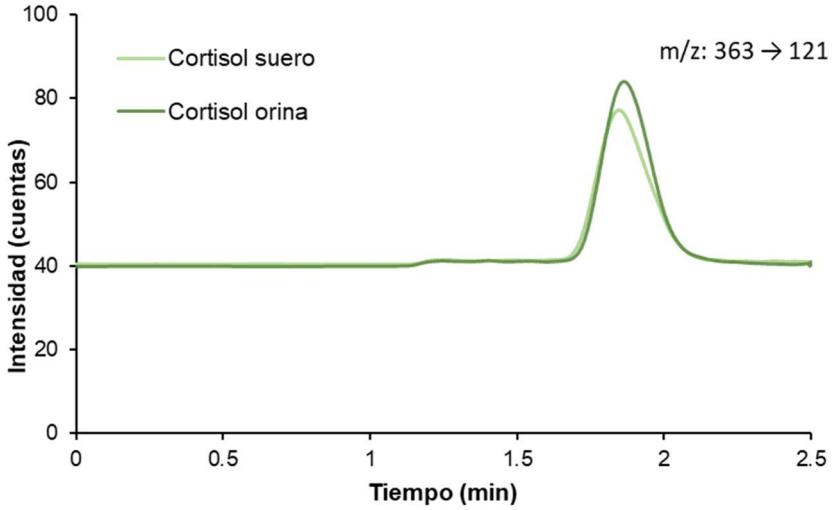

Figura 7.7. Cromatogramas obtenidos tras aplicar el método M-PTME-LC-MS/MS a una muestra de suero y orina

Estudio de las variables implicadas en la etapa de extracción y desorción

Para la realización de este estudio, al igual que en el **Capítulo 6**, se emplea el área relativa normalizada en lugar del área para el estudio de las variables de extracción y desorción. Esto es debido que proporciona una mayor facilidad para observar los cambios que se producen en una misma variable.

Las variables estudiadas de las etapas de extracción y de desorción fueron:

- Tiempo de extracción: 0-2 min

- Volumen disolvente desorción: 10-25 µL

- Número de ciclos de desorción: 2-10 ciclos

- **Tiempo de extracción**

Tras la dispersión del material se dejaron diferentes tiempos entre 0 y 120 s para estudiar como afectaba a la extracción. Tal y como se aprecia en la **Figura 7.8,** se produce un aumento a los 30 s, seguido de un ligero descenso progresivo. Esto se debe a que tras realizar la dispersión, esta se mantiene estable durante unos segundos, y después, se produce una

aglomeración del sorbente que termina depositándose en el fondo dificultando su aspiración. Por esta razón, se seleccionó un tiempo de **30 s**.

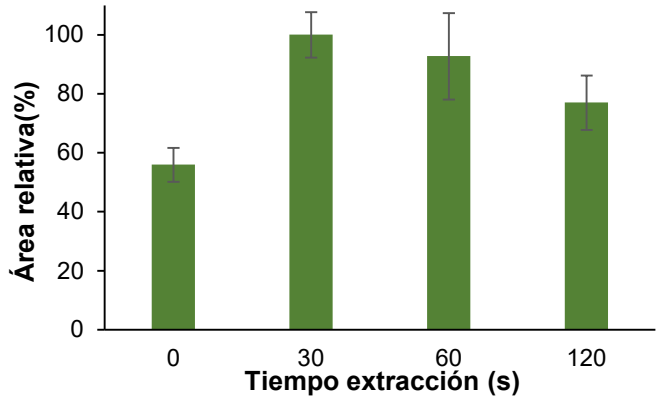

Figura 7.8. Estudio del tiempo de extracción

- **Volumen del disolvente de desorción**

Por otro lado, se estudiaron diferentes volúmenes de metanol en la etapa de desorción. En la **Figura 7.9** se muestra como al incrementar este volumen la señal va decreciendo. No se ensayaron volúmenes inferiores a **10 µL** para disponer de un volumen suficiente para su inyección en el instrumento LC-MS/MS.

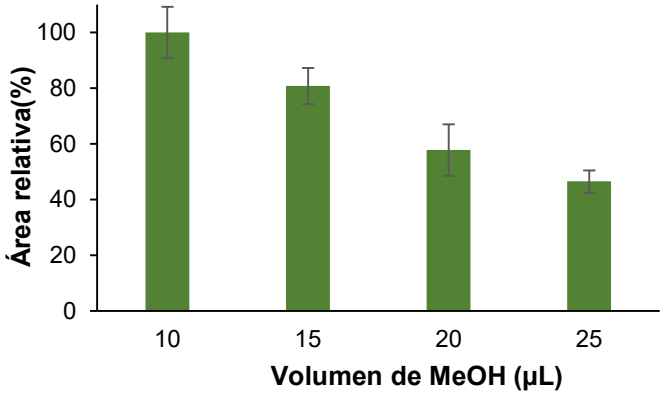

Figura 7.9. Estudio del disolvente de desorción

- **Número de ciclos de desorción**

Por último, se estudió el número de ciclos de carga y descarga durante la desorción. En la **Figura 7.10** se observa que 2 ciclos no son suficientes para producir una desorción cuantitativa de los analitos. Por otro lado, no hay diferencias entre usar 5 o 10 ciclos, por lo que se seleccionaron **5 ciclos.**

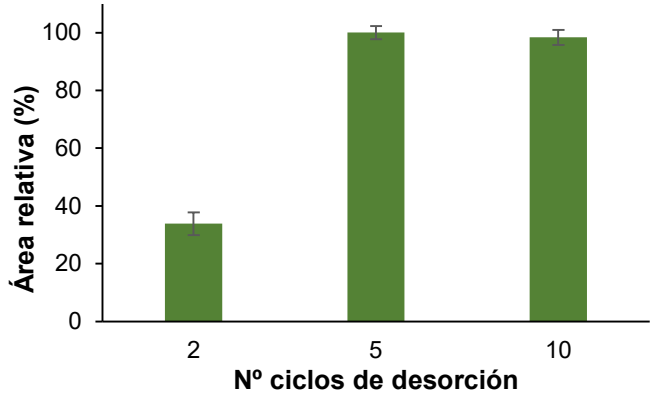

Figura 7.10. Estudio del número de ciclos de desorción

Validación del método y análisis de muestras reales

Se validó el método estudiando la selectividad, linealidad, LODs y LOQs, además de la repetibilidad a partir de patrones preparados en PBS. Para el estudio de la recuperación se emplearon muestras de suero y de orina previamente tratados para eliminar el cortisol.

- **Estudio previo del efecto matriz**

Debido a que el objetivo era determinar la parte libre del cortisol, previamente fue necesario una etapa de ultrafiltración [152] para separar la fracción unida a proteínas como la CBG y otras albúminas. Esta etapa de ultrafiltración consiste en centrifugar las muestras empleando un filtro con un corte de 30 KDa.

Se realizaron ensayos previos para comprobar el posible efecto matriz. La reducción de las señales comparados con el PBS fueron del 50 % para el caso del orina y de más del 90 % para el caso del suero. Para evitar este

efecto se llevó a cabo una etapa de dilución con PBS. Tras ensayar relaciones 1:1, 1:2 y 1:5, se optó por esta última, ya que era la única que conseguía eliminar totalmente el efecto matriz.

- **Selectividad**

Pese a que a los anticuerpos se les suele etiquetar como sorbentes específicos, pueden contar con interacciones cruzadas mediante las cuales interactúan con otro tipo de moléculas similares. En el caso concreto de los anticuerpos destinados a la determinación de cortisol, pueden darse este tipo de interacciones con otros corticoides como son la cortisona y la prednisolona. Para comprobar la especificidad del sorbente utilizado, se realizó la extracción de 10 ng mL^{-1} de cortisol en presencia de 10 ng mL^{-1} de cortisona y 10 ng mL^{-1} de prednisolona. Para la medida se empleó un método cromatográfico similar al utilizado en el **Capítulo 5**.

Como se puede comprobar en el cromatograma mostrado en la **Figura 7.11**, no se observó señal para la cortisona o para la prednisolona, verificándose la buena selectividad del inmunosorbente.

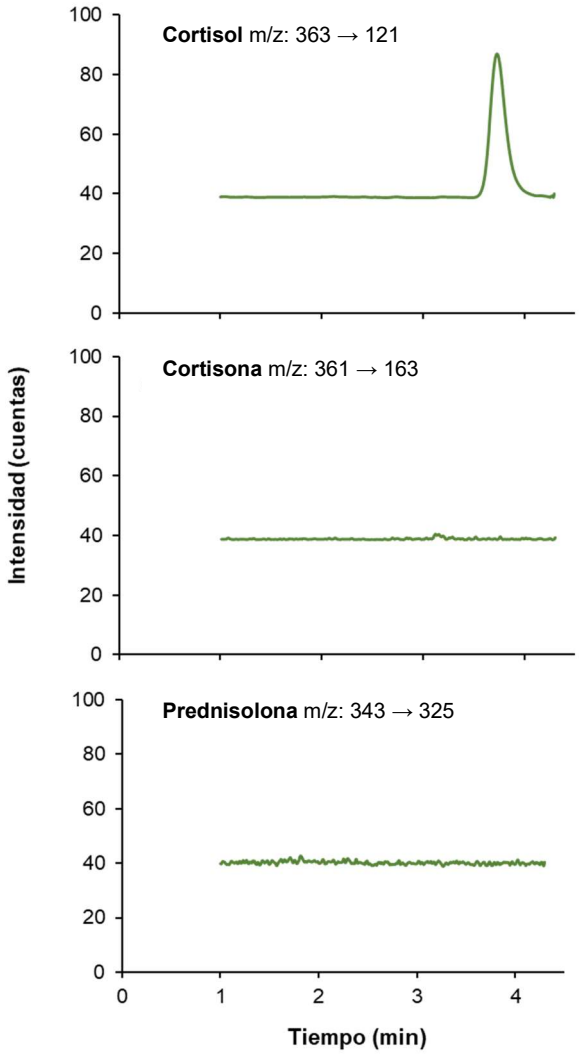

Figura 7.11. Cromatograma para la detección de cortisol, cortisona y prednisolona tras la aplicación del método propuesto

- **Linealidad**

Se optó por un intervalo lineal entre 1 y 50 ng mL^{-1}. En este intervalo se obtuvieron niveles de linealidad altos con buenos coeficientes de regresión de 0.9990.

- **Límites de detección y cuantificación**

El LOD y LOQ para el cortisol se calcularon mediante la concentración a la que se obtenía una relación de S/N de 3 y 10, respectivamente. El LOD fue de **0.08 ng mL^{-1}** mientras que el LOQ fue de **0.27 ng mL^{-1}**.

- **Repetibilidad**

La repetibilidad se estableció calculando la RSD de 5 réplicas medidas el mismo día (repetibilidad intradía) y 5 réplicas medidas en distintos días (repetibilidad interdía), a tres niveles de concentración (1, 10 y 20 ng mL^{-1}), obteniéndose valores por debajo de **10 %** para la repetibilidad interdía y del **15%** para la intradía.

- **Análisis de muestras reales**

Se trató una muestra de suero y otra de orina de adulto para eliminar el cortisol presente endógenamente empleando una columna de SPE (Strata^{TM} X-RP). A continuación, se fortificaron a 1, 10 y 20 ng mL^{-1} y se procedió a la extracción para calcular los coeficientes de recuperación. Los resultados de la **Tabla 7.3,** muestran coeficientes de recuperación entre el **91** y el **111 %.** De este modo, es posible trabajar con calibración externa.

Tabla 7.3. Coeficientes de recuperación obtenidoss tras la aplicación del método propuesto a muestras de suero y orina

Muestra	Cantidad fortificada (ng mL^{-1})	Coeficiente de recuperación (%)
Suero	1	100 ± 12
	10	111 ± 2
	20	91 ± 7
Orina	1	97 ± 11
	10	110 ± 3
	20	91 ± 5

Seguidamente, se procedió al análisis de muestras de cinco recién nacidos prematuros de bajo peso. Los resultados para suero y orina se muestran en la **Tabla 7.4.**

Tabla 7.4. Resultados obtenidos para 5 pacientes prematuros de bajo peso

	Edad gestacional (semanas + días)	Peso al nacer (g)	Cortisol libre en suero (μg L^{-1})	Cortisol libre en orina (μg L^{-1})
Paciente 1	27+4	900	1.5 ± 0.2	2.92 ± 0.14
Paciente 2	26+5	700	1.07 ± 0.12	0.49 ± 0.02
Paciente 3	27+3	950	0.36 ± 0.04	0.63 ± 0.04
Paciente 4	27+3	1100	1.39 ± 0.09	2.43 ± 0.19
Paciente 5	27+5	930	0.97 ± 0.12	0.35 ± 0.05

Los resultados fueron consistentes con estudios previos de la bibliografía llevados a cabo en recién nacidos [153].

Evaluación de la seguridad y sostenibilidad del método

En la **Figura 7.12** se muestra un diagrama AGREEprep para el método propuesto. Al tratarse de un análisis de microgotas, las cantidades empleadas de disolventes, muestra y sorbentes son mínimos. Esto provoca que su valoración sea la más alta de todos los trabajos presentados en esta tesis doctoral. Al igual que en los anteriores capítulos, este método sigue siendo mejorable desde un punto de vista 'verde', especialmente sustituyendo la técnica de medida (punto 9) por otra cuyo consumo de energía y de disolventes sea menor, así como empleando materiales más biodegradables (punto 3), que son las mayores penalizaciones que tiene el método presentado. Además, la búsqueda de otros dispositivos de medida más portátiles facilitará la realización de la ensayos *point-of-care,* muy necesario para el diagnóstico temprano de muchas enfermedades.

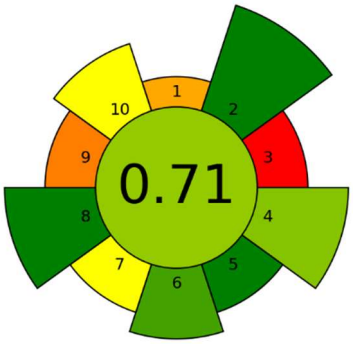

Figura 7.12. Evaluación del método propuesto empleando AGREEprep

Conclusiones

En este trabajo se ha modificado la M-PTME satisfactoriamente permitiendo el análisis de microvolúmenes de muestra.

Esta técnica es rápida, fácil de aplicar y permite reducir en gran medida el consumo de disolventes orgánicos y las cantidades de material sorbente, incluso más que su versión no miniaturizada, por lo que es una alternativa a tener en cuenta cuando se requiera trabajar con pequeñas cantidades de muestra.

La técnica se aplicó al análisis de cortisol en muestras cuya obtención presenta cierta complejidad, como son suero y orina de recién nacidos prematuros de bajo peso al nacer.

La combinación de esta técnica con LC-MS/MS lo convierte en una herramienta ideal para la determinación de interacciones cruzadas en inmunosorbentes.

Conclusiones finales

Conclusiones finales

En la presente tesis doctoral, se han desarrollado seis métodos basados en técnicas de microextracción haciendo uso de materiales magnéticos. Estos métodos pueden englobarse en tres grupos en función del volumen de muestra utilizado.

En este sentido, los **Capítulos 2, 3** y **4** mostraban tres aplicaciones empleando volúmenes de muestra elevados (15 - 25 mL). Por otro lado, en los **Capítulos 5** y **6** se explicaban metodologías para trabajar con volúmenes pequeños de muestra (0.4 y 0.5 mL). Por último, en el **Capítulo 7**, se exponía un método para el trabajo con microgotas de muestra (10 µL).

Dentro de los **Capítulos 2, 3** y **4**, se observa una mejoría del carácter 'verde' del método cuando se emplean disolventes de baja toxicidad como en el **Capítulo 4** o cuando se elimina el consumo de disolventes orgánicos como en el **Capítulo 3.** No obstante, al trabajar con volúmenes altos de muestra se terminan formando, de manera inevitable, una gran cantidad de residuos.

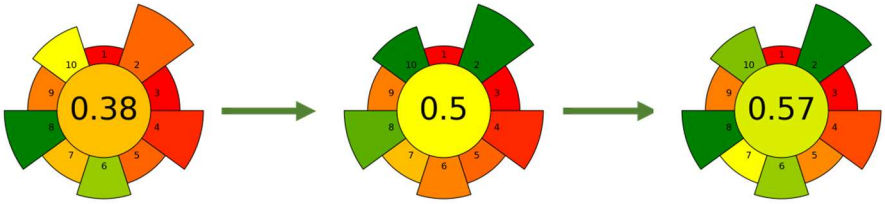

Por su parte, para los **Capítulos 5,6** y **7** se han desarrollado nuevas técnicas de microextracción adaptadas al trabajo con pequeños volúmenes de muestra. Estas técnicas están planteadas para conseguir una mínima invasividad del donante a la vez que se garantiza la sencillez de manipulación por parte del operador, siendo fácilmente aplicadas mediante el uso de una jeringa o una pipeta (semi)automática convencional. Además,

no requieren de sofisticados ni costosos mecanismos como ocurre en otros productos comerciales.

Se ha observado que la miniaturización del tamaño de muestra permite obtener múltiples ventajas en el ámbito de la preparación 'verde' de la muestra. Las metodologías con volúmenes pequeños requieren trabajar con tiempos menores de extracción, volúmenes menores de disolventes orgánicos y cantidades menores de sorbente. También favorecen el trabajo de campo al contar con sistemas de extracción más portátiles.

Si se comparan las evaluaciones obtenidas con la herramienta AGREEprep, se puede observar que las puntuaciones van aumentando a medida que se reduce el tamaño de muestra. Como se indicaba en la **Introducción**, a pesar de que directamente la disminución del volumen de muestra (punto 5) no tiene una influencia significativa, si atendemos a la figura siguiente, vemos que en los puntos 1 (lugar de preparación de muestra), 2 (volumen de sustancias peligrosas), 4 (residuos generados), también mejoran al reducir el volumen de muestra.

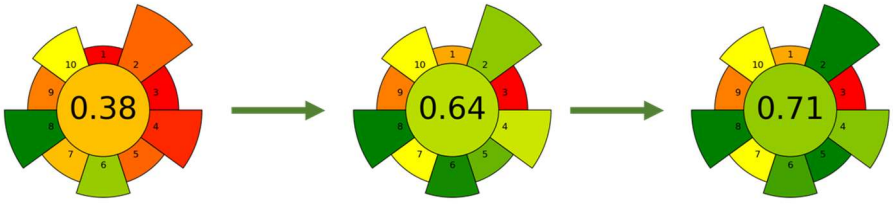

Capítulo 2 **Capítulo 6** **Capítulo 7**

En particular, el método del **Capítulo 7** destinado al análisis de volúmenes de muestra de muy bajo volumen, proporciona una valor de 0.71. Este valor, es excepcionalmente alto, pero todavía mejorable. Para ello, además del empleo de materiales biodegradables, es necesario el empleo de técnicas de medida que permitan un menor consumo de energía y de disolventes orgánicos. En este aspecto, el empleo de técnicas electroquímicas puede ser una gran alternativa debido a su elevada sensibilidad. Estas técnicas cuentan además con la ventaja adicional de ser portátiles, por lo que es posible el análisis *point-of-care*, el cual es de suma utilidad para la obtención temprana de diagnosis.

Además, estas metodologías, tal como se ha mencionado anteriormente, favorecen un muestreo menos invasivo al reducir drásticamente la cantidad

de muestra necesaria del paciente, lo que se convierte en un aspecto de vital importancia en el caso de los pacientes críticos o para bebés prematuros.

Cabe señalar que el camino a recorrer es todavía muy largo y hay algunos puntos clave, como son el empleo de materiales de plástico que deben de ser abordados cuanto antes. Es cierto que la reducción del tamaño de muestras también conlleva el uso de puntas y tubos más pequeños, pero estos siguen siendo difíciles de reciclar debido su uso con disolventes y muestras.

Por último indicar, a modo de conclusión final, que la miniaturización del volumen de muestra, a pesar de los enormes beneficios que alcanza, no necesariamente será siempre la solución óptima, ya que existen multitud de estrategias (y pueden ir surgiendo otras nuevas) para obtener métodos con un impacto muy reducido dependiendo del tipo de muestra, la concentración y/o la naturaleza de los analitos. Y por eso es importante entender que nunca hay un único camino correcto, pero siempre hay uno mejor y es nuestro deber como investigadores encontrarlo.

Final conclusions

Final conclusions

In this thesis, six different methods employing microextraction approaches with magnetic materials have been developed. These methods can be classified in three groups according to the sample volume.

In this sense, **Chapters 2,3** and **4** showed three applications employing relatively high sample volumes (15 - 25 mL). On the other side, in **Chapters 5** and **6** it was explained the use of new methodologies adapted to work with low sample volumes (0.4 and 0.5 mL). Finally, in **Chapter 7** it was shown a new method to work with microsamples (10 µL).

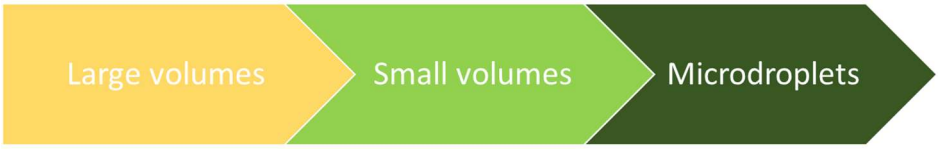

In **Chapters 2,3** and **4** it can be observed an improvement in the green character of the methods when low toxicity solvents are employed, as it happens in **Chapter 4,** or when the need of organic solvents is totally avoided, as it happens in **Chapter 3.** However, the use of high sample volumes produces big amounts of waste.

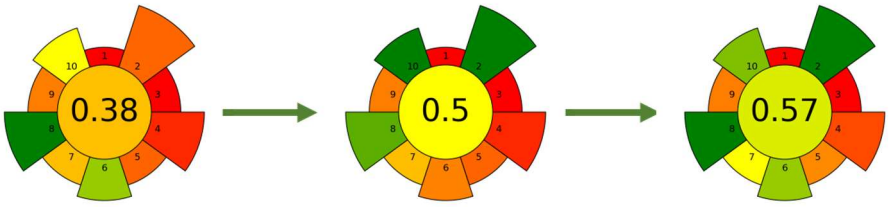

For **Chapters 5,6** and **7** new microextraction techniques have been developed to be employed with small sample volumes. These techniques have been proposed thinking on the ergonomics for the operator, avoiding complex and expensive mechanisms as it happen in other commercial strategies.

It has been observed how the miniaturization of the samples allows to obtain several benefits in the Green Sample Preparation field. Methodologies employing low sample volumes normally use lower extraction times and less

amounts of organic solvent and sorbents. Also facilitates the field work, creating more portable extraction devices.

If we compare the evaluation obtained from the app AGREEprep, it can be observed how the scores increase when the sample amount is reduced. As it was stablished in the **Introduction,** despite the reduction of the sample volume (point 5) will not have a high direct impact in the final evaluation. But, attending to the next figure, points 1 (sample preparation place), 2 (volume of hazardous substances), 4 (generated waster) and 5 (amount of sample), are highly improved with low sample strategies. Thus, the whole method becomes more sustainable and safer for the operator.

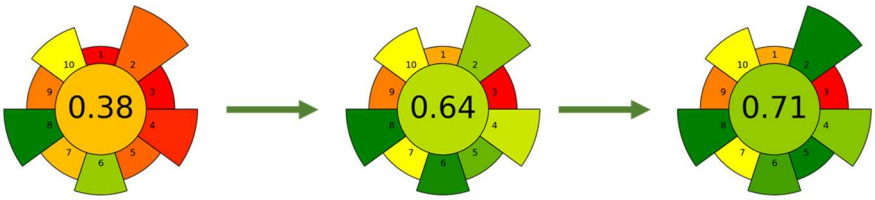

Chapter 2 **Chapter 6** **Chapter 7**

Particularly, the method developed in **Chapter 7,** intended for the analysis of sample microvolumes, obtained a final score of 0.71. This value is exceptionally high, but still improvable. In this sense, aside of the employment of renewable materials (point 3), it is necessary the use of measurement techniques that consume less organic solvents and less energy. In that aim, the use of electrochemical techniques may be a great alternative, due to their huge sensitivity. Moreover, these techniques are portable, making easier *point-of-care* analysis which are highly required for the obtention of early diagnosis.

Moreover, these methods, as it has been stablished before, allow to reduce the invasiveness of the sampling step, since the amount of sample needed from the patient is drastically reduced. Which is extremely necessary when samples from critical ill patients or preterm newborns are required.

It should be said that the path is still long and there are some ‘key points’, as are the huge employment of oil-based plastic materials, that must be solved as soon as possible. It is true that reducing the sample volume, the amount of plastic employed is also minimized. However, they are difficult to recycle due to their use with samples or solvents

Also is important to know, as a final statement, that the miniaturization of sample, despite of the multiple benefits that can achieve, is not always the optimum solution, since there are multiple strategies to obtain greener methods depending on the sample, the concentration and/or the nature of analyte. And that is why I think there is never only a good answer, but there is always a better one, and it is our duty as researchers to find it.

Bibliografía

[1] S. Armenta, S. Garrigues, F.A. Esteve-Turrillas, M. de la Guardia, Green extraction techniques in green analytical chemistry, TrAC - Trends Anal. Chem. 116 (2019) 248–253.

[2] S. Armenta, S. Garrigues, M. de la Guardia, The role of green extraction techniques in Green Analytical Chemistry, TrAC Trends Anal. Chem. 71 (2015) 2–8.

[3] A. Gałuszka, Z. Migaszewski, J. Namieśnik, The 12 principles of green analytical chemistry and the SIGNIFICANCE mnemonic of green analytical practices, TrAC - Trends Anal. Chem. 50 (2013) 78–84.

[4] H.M. Mohamed, Green, environment-friendly, analytical tools give insights in pharmaceuticals and cosmetics analysis, TrAC - Trends Anal. Chem. 66 (2015) 176–192.

[5] N. Li, T. Zhang, G. Chen, J. Xu, G. Ouyang, F. Zhu, Recent advances in sample preparation techniques for quantitative detection of pharmaceuticals in biological samples, TrAC - Trends Anal. Chem. 142 (2021) 116318.

[6] G.D.O. Silveira, A.M.F. Pego, J. Pereira E Silva, M. Yonamine, Green sample preparations for the bioanalysis of drugs of abuse in complex matrices, Bioanalysis. 11 (2019) 295–312.

[7] Á.I. López-Lorente, F. Pena-Pereira, S. Pedersen-Bjergaard, V.G. Zuin, S.A. Ozkan, E. Psillakis, The ten principles of green sample preparation, TrAC - Trends Anal. Chem. 148 (2022) 116530.

[8] F. Pena-Pereira, C. Bendicho, D.M. Pavlović, A. Martín-Esteban, M. Díaz-Álvarez, Y. Pan, J. Cooper, Z. Yang, I. Safarik, K. Pospiskova, M.A. Segundo, E. Psillakis, Miniaturized analytical methods for determination of environmental contaminants of emerging concern – A review, Anal. Chim. Acta. 1158 (2021) 238108.

[9] A. Agrawal, R. Keçili, F. Ghorbani-Bidkorbeh, C.M. Hussain, Green miniaturized technologies in analytical and bioanalytical chemistry, TrAC - Trends Anal. Chem. 143 (2021) 116383.

[10] H. Lord, J. Pawliszyn, Microextraction of drugs, J. Chromatogr. A. 902 (2000) 17–63.

[11] J. Grau, J.L. Benedé, A. Chisvert, Use of nanomaterial-based (micro) extraction techniques for the determination of cosmetic-related compounds, Molecules. 25 (2020) 2586.

[12] E.V.S. Maciel, A.L. de Toffoli, E.S. Neto, C.E.D. Nazario, F.M. Lanças, New materials in sample preparation: Recent advances and future trends, TrAC - Trends Anal. Chem. 119 (2019) 115633.

[13] L. Xu, X. Qi, X. Li, Y. Bai, H. Liu, Recent advances in applications of nanomaterials for sample preparation, Talanta. 146 (2016) 714–726.

[14] K. Murtada, Trends in nanomaterial-based solid-phase microextraction with a focus on environmental applications - A review, Trends Environ. Anal. Chem. 25

(2020) e00077.

[15] A. Pietroiusti, H. Stockmann-Juvala, F. Lucaroni, K. Savolainen, Nanomaterial exposure, toxicity, and impact on human health, Wiley Interdiscip. Rev. Nanomedicine Nanobiotechnology. 10 (2018) 1–21.

[16] A. Azzouz, S.K. Kailasa, S.S. Lee, A. J. Rascón, E. Ballesteros, M. Zhang, K.H. Kim, Review of nanomaterials as sorbents in solid-phase extraction for environmental samples, TrAC - Trends Anal. Chem. 108 (2018) 347–369.

[17] L. Xie, R. Jiang, F. Zhu, H. Liu, G. Ouyang, Application of functionalized magnetic nanoparticles in sample preparation, Anal. Bioanal. Chem. 406 (2014) 377–399.

[18] J.K. Oh, J.M. Park, Iron oxide-based superparamagnetic polymeric nanomaterials: Design, preparation, and biomedical application, Prog. Polym. Sci. 36 (2011) 168–189.

[19] C.W. Huck, G.K. Bonn, Recent developments in polymer-based sorbents for solid-phase extraction, J. Chromatogr. A. 885 (2000) 51–72.

[20] W. Jing, J. Wang, B. Kuipers, W. Bi, D.D.Y. Chen, Recent applications of graphene and graphene-based materials as sorbents in trace analysis, TrAC - Trends Anal. Chem. 137 (2021) 116212.

[21] A. Gutiérrez-Serpa, I. Pacheco-Fernández, J. Pasán, V. Pino, Metal–Organic Frameworks as Key Materials for Solid-Phase Microextraction Devices—A Review, Separations. 6 (2019) 47.

[22] P. Rocío-Bautista, P. González-Hernández, V. Pino, J. Pasán, A.M. Afonso, Metal-organic frameworks as novel sorbents in dispersive-based microextraction approaches, TrAC - Trends Anal. Chem. 90 (2017) 114–134.

[23] V. Pichon, A. Combès, N. Delaunay, Immunosorbents in microextraction, TrAC - Trends Anal. Chem. 113 (2019) 246–255.

[24] E. Turiel, A. Martín-Esteban, Molecularly imprinted polymers-based microextraction techniques, TrAC - Trends Anal. Chem. 118 (2019) 574–586.

[25] M. Arabi, A. Ostovan, A.R. Bagheri, X. Guo, L. Wang, J. Li, X. Wang, B. Li, L. Chen, Strategies of molecular imprinting-based solid-phase extraction prior to chromatographic analysis, TrAC - Trends Anal. Chem. 128 (2020) 115923.

[26] C.L. Arthur, J. Pawliszyn, Solid Phase Microextraction with Thermal Desorption Using Fused Silica Optical Fibers, Anal. Chem. 62 (1990) 2145–2148.

[27] Z. Zhang, J. Pawliszyn, Headspace Solid-Phase Microextraction, Anal. Chem. (1993) 1843–1852.

[28] E.A. Souza Silva, S. Risticevic, J. Pawliszyn, Recent trends in SPME concerning sorbent materials, configurations and in vivo applications, TrAC - Trends Anal. Chem. 43 (2013) 24–36.

[29] J. O'Reilly, Q. Wang, L. Setkova, J.P. Hutchinson, Y. Chen, H.L. Lord, C.M. Linton, J. Pawliszyn, Automation of solid-phase microextraction, J. Sep. Sci. 28 (2005) 2010–2022.

[30] E. Baltussen, P. Sandra, F. David, C. Cramers, Stir bar sorptive extraction (SBSE), a novel extraction technique for aqueous samples: Theory and principles, J. Microcolumn Sep. 11 (1999) 737–747.

[31] F. David, N. Ochiai, P. Sandra, Two decades of stir bar sorptive extraction: A retrospective and future outlook, TrAC - Trends Anal. Chem. 112 (2019) 102–111.

[32] M. He, Y. Wang, Q. Zhang, L. Zang, B. Chen, B. Hu, Stir bar sorptive extraction and its application, J. Chromatogr. A. 1637 (2021) 461810.

[33] M. Ghorbani, M. Aghamohammadhassan, M. Chamsaz, H. Akhlaghi, T. Pedramrad, Dispersive solid phase microextraction, TrAC - Trends Anal. Chem. 118 (2019) 793–809.

[34] M. Anastassiades, S.J. Lehotay, D. Štajnbaher, F.J. Schenck, Fast and easy multiresidue method employing acetonitrile extraction/partitioning and “dispersive solid-phase extraction” for the determination of pesticide residues in produce, J. AOAC Int. 86 (2003) 412–431.

[35] M.S. Cárdenas Aranzana, Dispersive Solid-Phase (Micro)Extraction, Encycl. Anal. Chem. (2010) 1–13.

[36] S. Büyüktiryaki, R. Keçili, C.M. Hussain, Functionalized nanomaterials in dispersive solid phase extraction: Advances & prospects, TrAC - Trends Anal. Chem. 127 (2020) 115893.

[37] H.Y. Shen, Y. Zhu, X.E. Wen, Y.M. Zhuang, Preparation of Fe3O4-C18 nano-magnetic composite materials and their cleanup properties for organophosphorous pesticides, Anal. Bioanal. Chem. 387 (2007) 2227–2237.

[38] A. Chisvert, S. Cárdenas, R. Lucena, Dispersive micro-solid phase extraction, TrAC - Trends Anal. Chem. 112 (2019) 226–233.

[39] M. Faraji, M. Shirani, H. Rashidi-Nodeh, The recent advances in magnetic sorbents and their applications, TrAC - Trends Anal. Chem. 141 (2021) 116302.

[40] L. Soltys, O. Olkhovyy, T. Tatarchuk, M. Naushad, Green Synthesis of Metal and Metal Oxide Nanoparticles: Principles of Green Chemistry and Raw Materials, Magnetochemistry. 7 (2021) 145.

[41] A. Gutiérrez-Serpa, R. González-Martín, M. Sajid, V. Pino, Greenness of magnetic nanomaterials in miniaturized extraction techniques: A review, Talanta. 225 (2021) 122053.

[42] V.C. Karade, P.P. Waifalkar, T.D. Dongle, S.C. Sahoo, P. Kollu, P.S. Patil, P.B. Patil, Greener synthesis of magnetite nanoparticles using green tea extract and their magnetic properties, Mater. Res. Express. 4 (2017) 096102.

[43] J.L. Benedé, A. Chisvert, D.L. Giokas, A. Salvador, Development of stir bar sorptive-dispersive microextraction mediated by magnetic nanoparticles and its analytical application to the determination of hydrophobic organic compounds in aqueous media, J. Chromatogr. A. 1362 (2014) 25–33.

[44] V. Vállez-Gomis, J. Grau, J.L. Benedé, D.L. Giokas, A. Chisvert, A. Salvador, Fundamentals and applications of stir bar sorptive dispersive microextraction: A

tutorial review, Anal. Chim. Acta. 1153 (2021) 338271.

[45] M.M. Delgado-Povedano, M.D. Luque de Castro, The 'in medium virtus' assessment of green analytical chemistry, Curr. Opin. Green Sustain. Chem. 19 (2019) 8–14.

[46] M. Llompart, M. Celeiro, C. García-Jares, T. Dagnac, Environmental applications of solid-phase microextraction, TrAC - Trends Anal. Chem. 112 (2019) 1–12.

[47] A. Chisvert, J.L. Benedé, A. Salvador, Current trends on the determination of organic UV filters in environmental water samples based on microextraction techniques – A review, Anal. Chim. Acta. 1034 (2018) 22–38.

[48] M.D. Luque de Castro, F. Priego Capote, Miniaturisation of analytical steps: necessity and snobbism, Anal. Bioanal. Chem. 390 (2008) 67–69.

[49] S.M. Daryanavard, H. Zolfaghari, A. Abdel-Rehim, M. Abdel-Rehim, Recent applications of microextraction sample preparation techniques in biological samples analysis, Biomed. Chromatogr. 35 (2021) 1–31.

[50] F.G. Bellagambi, T. Lomonaco, P. Salvo, F. Vivaldi, M. Hangouët, S. Ghimenti, D. Biagini, F. Di Francesco, R. Fuoco, A. Errachid, Saliva sampling: Methods and devices. An overview, TrAC Trends Anal. Chem. 124 (2020) 115781.

[51] D.P. Lima, D.G. Diniz, S.A.S. Moimaz, D.H. Sumida, A.C. Okamoto, Saliva: reflection of the body, Int. J. Infect. Dis. 14 (2010) 184–188.

[52] J.M. Yoshizawa, C.A. Schafer, J.J. Schafer, J.J. Farrell, B.J. Paster, D.T.W. Wong, Salivary biomarkers: Toward future clinical and diagnostic utilities, Clin. Microbiol. Rev. 26 (2013) 781–791.

[53] D.A. Granger, E.A. Shirtcliff, A. Booth, K.T. Kivlighan, E.B. Schwartz, The "trouble" with salivary testosterone, Psychoneuroendocrinology. 29 (2004) 1229–1240.

[54] D. Turoňová, L. Kujovská Krčmová, F. Švec, Application of microextraction in pipette tips in clinical and forensic toxicology, TrAC Trends Anal. Chem. 143 (2021) 116404.

[55] S. Seidi, M. Tajik, M. Baharfar, M. Rezazadeh, Micro solid-phase extraction (pipette tip and spin column) and thin film solid-phase microextraction: Miniaturized concepts for chromatographic analysis, TrAC - Trends Anal. Chem. 118 (2019) 810–827.

[56] Z. Wang, Y. Liao, L. Chen, X. Huang, On-site sample preparation of trace aromatic amines in environmental waters with monolith-based multichannel in-tip microextraction apparatus followed by HPLC determination, Talanta. 220 (2020) 121423.

[57] T. Sun, M.M. Ali, D. Wang, Z. Du, On-site rapid screening of benzodiazepines in dietary supplements using pipette-tip micro-solid phase extraction coupled to ion mobility spectrometry, J. Chromatogr. A. 1610 (2020) 460547.

[58] J. Grau, J.L. Benedé, A. Chisvert, A. Salvador, A high-throughput magnetic-based pipette tip microextraction as an alternative to conventional pipette tip strategies: Determination of testosterone in human saliva as a proof-of-concept,

Anal. Chim. Acta. 1221 (2022) 340117.

[59] J.W. Holm, O.S. Mortensen, F. Gyntelberg, Upper limb disorders among biomedical laboratory workers using pipettes, Cogent Med. 3 (2016) 1256849.

[60] S.C. Tan, H.K. Lee, Fully automated graphitic carbon nitride-based disposable pipette extraction-gas chromatography-mass spectrometric analysis of six polychlorinated biphenyls in environmental waters, J. Chromatogr. A. 1637 (2021) 461824.

[61] J.X. Shen, C.I. Tama, R.N. Hayes, Evaluation of automated micro solid phase extraction tips (μ-SPE) for the validation of a LC-MS/MS bioanalytical method, J. Chromatogr. B Anal. Technol. Biomed. Life Sci. 843 (2006) 275–282.

[62] S. Wang, Z. He, W. Li, J. Zhao, T. Chen, S. Shao, H. Chen, Reshaping of pipette tip: A facile and practical strategy for sorbent packing-free solid phase extraction, Anal. Chim. Acta. 1100 (2020) 47–56.

[63] D.C.M. Bordin, M.N.R. Alves, E.G. de Campos, B.S. De Martinis, Disposable pipette tips extraction: Fundamentals, applications and state of the art, J. Sep. Sci. 39 (2016) 1168–1172.

[64] E. Carasek, L. Morés, R.D. Huelsmann, Disposable pipette extraction: A critical review of concepts, applications, and directions, Anal. Chim. Acta. 1192 (2022) 339383.

[65] Z. Lu, N. Fang, Z. Zhang, Z. Hou, Z. Lu, Y. Li, Residue analysis of fungicides fenpicoxamid, isofetamid, and mandestrobin in cereals using zirconium oxide disposable pipette extraction clean-up and ultrahigh-performance liquid chromatography-tandem mass spectrometry, J. Chromatogr. A. 1620 (2020) 461004.

[66] G.S. Tomasin, W.R. Silva, B.E. dos Santos Costa, N.M.M. Coelho, Highly sensitive determination of Cu(II) ions in hemodialysis water by F AAS after disposable pipette extraction (DPX) using Moringa oleifera as solid phase, Microchem. J. 161 (2021) 105749.

[67] G. Corazza, J. Merib, H.A. Magosso, O.R. Bittencourt, E. Carasek, A hybrid material as a sorbent phase for the disposable pipette extraction technique enhances efficiency in the determination of phenolic endocrine-disrupting compounds, J. Chromatogr. A. 1513 (2017) 42–50.

[68] F.C. Turazzi, L. Morés, E. Carasek, J. Merib, G.M. De Oliveira Barra, A rapid and environmentally friendly analytical method based on conductive polymer as extraction phase for disposable pipette extraction for the determination of hormones and polycyclic aromatic hydrocarbons in river water samples using high-performance l, J. Environ. Chem. Eng. 7 (2019) 103156.

[69] A.L. Oenning, J. Merib, E. Carasek, An effective and high-throughput analytical methodology for pesticide screening in human urine by disposable pipette extraction and gas chromatography – mass spectrometry, J. Chromatogr. B Anal. Technol. Biomed. Life Sci. 1092 (2018) 459–465.

[70] R.D. Huelsmann, C. Will, E. Carasek, Novel strategy for disposable pipette extraction (DPX): Low-cost Parallel-DPX for determination of phthalate migration

from common plastic materials to saliva simulant with GC-MS, Talanta. 221 (2021) 121443.

[71] INTip Solid Phase Extraction - DPX Technologies, (n.d.).

[72] M.R. Jamali, A. Firouzjah, R. Rahnama, Solvent-assisted dispersive solid phase extraction, Talanta. 116 (2013) 454–459.

[73] M. Abbasghorbani, A. Attaran, M. Payehghadr, Solvent-assisted dispersive micro-SPE by using aminopropyl-functionalized magnetite nanoparticle followed by GC-PID for quantification of parabens in aqueous matrices, J. Sep. Sci. 36 (2013) 311–319.

[74] P. Mohammadi, M. Masrournia, Z. Es'haghi, M. Pordel, Determination of four antiepileptic drugs with solvent assisted dispersive solid phase microextraction – Gas chromatography–mass spectrometry in human urine samples, Microchem. J. 159 (2020) 105542.

[75] Á. Molinero-Fernández, M. Moreno-Guzmán, M.Á. López, A. Escarpa, An array-based electrochemical magneto-immunosensor for early neonatal sepsis diagnostic: Fast and accurate determination of C-reactive protein in whole blood and plasma samples, Microchem. J. 157 (2020) 104913.

[76] L. García-Carmona, M.C. González, A. Escarpa, Nanomaterial-based electrochemical (bio)-sensing: One step ahead in diagnostic and monitoring of metabolic rare diseases, TrAC - Trends Anal. Chem. 118 (2019) 29–42.

[77] M.A. Jeannot, F.F. Cantwell, Solvent microextraction into a single drop, Anal. Chem. 68 (1996) 2236–2240.

[78] A.L. Theis, A.J. Waldack, S.M. Hansen, M.A. Jeannot, Headspace solvent microextraction, Anal. Chem. 73 (2001) 5651–5654.

[79] M. Rezaee, Y. Assadi, M.-R. Milani Hosseini, E. Aghaee, F. Ahmadi, S. Berijani, Determination of organic compounds in water using dispersive liquid–liquid microextraction, J. Chromatogr. A. 1116 (2006) 1–9.

[80] E. Psillakis, Vortex-assisted liquid-liquid microextraction revisited, TrAC - Trends Anal. Chem. 113 (2019) 332–339.

[81] P. Viñas, N. Campillo, I. López-García, M. Hernández-Córdoba, Dispersive liquid-liquid microextraction in food analysis. A critical review Microextraction Techniques, Anal. Bioanal. Chem. 406 (2014) 2067–2099.

[82] G. Li, K.H. Row, Utilization of deep eutectic solvents in dispersive liquid-liquid micro-extraction, TrAC - Trends Anal. Chem. 120 (2019) 115651.

[83] A. Zgoła-Grześkowiak, T. Grześkowiak, Dispersive liquid-liquid microextraction, TrAC - Trends Anal. Chem. 30 (2011) 1382–1399.

[84] M.I. Leong, S. Da Huang, Dispersive liquid-liquid microextraction method based on solidification of floating organic drop combined with gas chromatography with electron-capture or mass spectrometry detection, J. Chromatogr. A. 1211 (2008) 8–12.

[85] S. Şahin, Tailor-designed deep eutectic liquids as a sustainable extraction media: An alternative to ionic liquids, J. Pharm. Biomed. Anal. 174 (2019) 324–329.

[86] N. Adawiyah, M. Moniruzzaman, S. Hawatulaila, M. Goto, Ionic liquids as a potential tool for drug delivery systems, Medchemcomm. 7 (2016) 1881–1897.

[87] E. Aguilera-Herrador, R. Lucena, S. Cárdenas, M. Valcárcel, The roles of ionic liquids in sorptive microextraction techniques, TrAC - Trends Anal. Chem. 29 (2010) 602–616.

[88] K. Yavir, K. Konieczna, Ł. Marcinkowski, A. Kloskowski, Ionic liquids in the microextraction techniques: The influence of ILs structure and properties, TrAC Trends Anal. Chem. 130 (2020) 115994.

[89] N. V. Plechkova, K.R. Seddon, Applications of ionic liquids in the chemical industry, Chem. Soc. Rev. 37 (2008) 123–150.

[90] A. Chisvert, I.P. Román, L. Vidal, A. Canals, Simple and commercial readily-available approach for the direct use of ionic liquid-based single-drop microextraction prior to gas chromatography. Determination of chlorobenzenes in real water samples as model analytical application, J. Chromatogr. A. 1216 (2009) 1290–1295.

[91] J.L. Benedé, J.L. Anderson, A. Chisvert, Trace determination of volatile polycyclic aromatic hydrocarbons in natural waters by magnetic ionic liquid-based stir bar dispersive liquid microextraction, Talanta. 176 (2018) 253–261.

[92] E. Aguilera-Herrador, R. Lucena, S. Cárdenas, M. Valcárcel, Direct coupling of ionic liquid based single-drop microextraction and GC/MS, Anal. Chem. 80 (2008) 793–800.

[93] F.-Q. Zhao, J. Li, B.-Z. Zeng, Coupling of ionic liquid-based headspace single-drop microextraction with GC for sensitive detection of phenols, J. Sep. Sci. 31 (2008) 3045–3049.

[94] F. Zhao, S. Lu, W. Du, B. Zeng, Ionic liquid-based headspace single-drop microextraction coupled to gas chromatography for the determination of chlorobenzene derivatives, Microchim. Acta. 165 (2009) 29–33.

[95] L. Vallecillos, E. Pocurull, F. Borrull, Fully automated ionic liquid-based headspace single drop microextraction coupled to GC-MS/MS to determine musk fragrances in environmental water samples, Talanta. 99 (2012) 824–832.

[96] M. De Boeck, G. Damilano, W. Dehaen, J. Tytgat, E. Cuypers, Evaluation of 11 ionic liquids as potential extraction solvents for benzodiazepines from whole blood using liquid-liquid microextraction combined with LC-MS/MS, Talanta. 184 (2018) 369–374.

[97] G.P. Jackson, D.C. Duckworth, Electrospray mass spectrometry of undiluted ionic liquids, Chem. Commun. 4 (2004) 522–523.

[98] M.A. Farajzadeh, M.R. Afshar Mogaddam, M. Aghanassab, Deep eutectic solvent-based dispersive liquid-liquid microextraction, Anal. Methods. 8 (2016) 2576–2583.

[99] M.Q. Farooq, N.M. Abbasi, J.L. Anderson, Deep eutectic solvents in separations: Methods of preparation, polarity, and applications in extractions and capillary electrochromatography, J. Chromatogr. A. 1633 (2020) 461613.

[100] Q. Zhang, K. De Oliveira Vigier, S. Royer, F. Jérôme, Deep eutectic solvents: Syntheses, properties and applications, Chem. Soc. Rev. 41 (2012) 7108–7146.

[101] L. Ramos, Chapter 5: Greening sample preparation: New solvents, new sorbents, 2020.

[102] H. Musarurwa, N.T. Tavengwa, Emerging green solvents and their applications during pesticide analysis in food and environmental samples, Talanta. 223 (2021) 121507.

[103] S.C. Cunha, J.O. Fernandes, Extraction techniques with deep eutectic solvents, TrAC - Trends Anal. Chem. 105 (2018) 225–239.

[104] M. de los Á. Fernández, J. Boiteux, M. Espino, F.J.V. Gomez, M.F. Silva, Natural deep eutectic solvents-mediated extractions: The way forward for sustainable analytical developments, Anal. Chim. Acta. 1038 (2018) 1–10.

[105] J. Grau, C. Azorín, J.L. Benedé, A. Chisvert, A. Salvador, Use of green alternative solvents in dispersive liquid-liquid microextraction: A review, J. Sep. Sci. 45 (2022) 210–222.

[106] J. Płotka-Wasylka, M. Rutkowska, M. de la Guardia, Are deep eutectic solvents useful in chromatography? A short review, J. Chromatogr. A. 1639 (2021).

[107] S. Hayashi, H.O. Hamaguchi, Discovery of a magnetic ionic liquid [bmim]FeCl4, Chem. Lett. 33 (2004) 1590–1591.

[108] K.D. Clark, O. Nacham, J.A. Purslow, S.A. Pierson, J.L. Anderson, Magnetic ionic liquids in analytical chemistry: A review, Anal. Chim. Acta. 934 (2016) 9–21.

[109] M. Sajid, K. Kalinowska, J. Płotka-Wasylka, Ferrofluids based analytical extractions and evaluation of their greenness, J. Mol. Liq. 339 (2021) 116901.

[110] R. Nayebi, F. Shemirani, Ferrofluids-based microextraction systems to process organic and inorganic targets: The state-of-the-art advances and applications, TrAC - Trends Anal. Chem. 138 (2021) 116232.

[111] R. González-Martín, A. Gutiérrez-Serpa, V. Pino, The use of ferrofluids in analytical sample preparation: A review, Separations. 8 (2021) 1–14.

[112] A. Chisvert, J.L. Benedé, J.L. Anderson, S.A. Pierson, A. Salvador, Introducing a new and rapid microextraction approach based on magnetic ionic liquids: Stir bar dispersive liquid microextraction, Anal. Chim. Acta. 983 (2017) 130–140.

[113] M.J. Trujillo-Rodríguez, J.L. Anderson, In situ generation of hydrophobic magnetic ionic liquids in stir bar dispersive liquid-liquid microextraction coupled with headspace gas chromatography, Talanta. 196 (2019) 420–428.

[114] A.R. Zarei, M. Nedaei, S.A. Ghorbanian, Deep eutectic solvent based magnetic nanofluid in the development of stir bar sorptive dispersive microextraction: An efficient hyphenated sample preparation for ultra-trace nitroaromatic explosives

extraction in wastewater, J. Sep. Sci. 40 (2017) 4757–4764.

[115] W. Wojnowski, M. Tobiszewski, F. Pena-Pereira, E. Psillakis, AGREEprep – Analytical greenness metric for sample preparation, TrAC Trends Anal. Chem. 149 (2022) 116553.

[116] F. Pena-Pereira, W. Wojnowski, M. Tobiszewski, AGREE - Analytical GREEnness Metric Approach and Software, Anal. Chem. 92 (2020) 10076–10082.

[117] J. Płotka-Wasylka, W. Wojnowski, Complementary green analytical procedure index (ComplexGAPI) and software, Green Chem. 23 (2021) 8657–8665.

[118] J. Płotka-Wasylka, A new tool for the evaluation of the analytical procedure: Green Analytical Procedure Index, Talanta. 181 (2018) 204–209.

[119] G. Cano-Sancho, A. Smith, M.A. La Merrill, Triphenyl phosphate enhances adipogenic differentiation, glucose uptake and lipolysis via endocrine and noradrenergic mechanisms, Toxicol. Vitr. 40 (2017) 280–288.

[120] E. Mendelsohn, A. Hagopian, K. Hoffman, C.M. Butt, A. Lorenzo, J. Congleton, T.F. Webster, H.M. Stapleton, Nail polish as a source of exposure to triphenyl phosphate, Environ. Int. 86 (2016) 45–51.

[121] K. Maaz, A. Mumtaz, S.K. Hasanain, A. Ceylan, Synthesis and magnetic properties of cobalt ferrite (CoFe2O4) nanoparticles prepared by wet chemical route, J. Magn. Magn. Mater. 308 (2007) 289–295.

[122] E.M. Cooper, A. Covaci, A.L.N. Van Nuijs, T.F. Webster, H.M. Stapleton, Analysis of the flame retardant metabolites bis(1,3-dichloro-2-propyl) phosphate (BDCPP) and diphenyl phosphate (DPP) in urine using liquid chromatography-tandem mass spectrometry, Anal. Bioanal. Chem. 401 (2011) 2123–2132.

[123] N. Van den Eede, H. Neels, P.G. Jorens, A. Covaci, Analysis of organophosphate flame retardant diester metabolites in human urine by liquid chromatography electrospray ionisation tandem mass spectrometry, J. Chromatogr. A. 1303 (2013) 48–53.

[124] G. Su, R.J. Letcher, H. Yu, Determination of organophosphate diesters in urine samples by a high-sensitivity method based on ultra high pressure liquid chromatography-triple quadrupole-mass spectrometry, J. Chromatogr. A. 1426 (2015) 154–160.

[125] I. Kosarac, C. Kubwabo, W.G. Foster, Quantitative determination of nine urinary metabolites of organophosphate flame retardants using solid phase extraction and ultra performance liquid chromatography coupled to tandem mass spectrometry (UPLC-MS/MS), J. Chromatogr. B Anal. Technol. Biomed. Life Sci. 1014 (2016) 24–30.

[126] S.S.E. Petropoulou, M. Petreas, J.S. Park, Analytical methodology using ion-pair liquid chromatography-tandem mass spectrometry for the determination of four di-ester metabolites of organophosphate flame retardants in California human urine, J. Chromatogr. A. 1434 (2016) 70–80.

[127] J. Grau, J.L. Benedé, J. Serrano, A. Segura, A. Chisvert, Stir bar sorptive-

dispersive microextraction for trace determination of triphenyl and diphenyl phosphate in urine of nail polish users, J. Chromatogr. A. 1593 (2019) 9–16.

[128] Regulation (EC) No. 1223/2009 of the European Parliament and of the Council of 30 November 2009 on Cosmetic Products, and Its Successive Amendments, (2009).

[129] T. Luckenbach, D. Epel, Nitromusk and polycyclic musk compounds as long-term inhibitors of cellular xenobiotic defense systems mediated by multidrug transporters, Environ. Health Perspect. 113 (2005) 17–24.

[130] J. Cavalheiro, A. Prieto, O. Zuloaga, H. Preudhomme, D. Amouroux, M. Monperrus, Evaluation of preconcentration methods in the analysis of synthetic musks in whole-water samples, J. Sep. Sci. 38 (2015) 2298–2304.

[131] M.G. Pintado-Herrera, E. González-Mazo, P.A. Lara-Martín, Atmospheric pressure gas chromatography-time-of-flight-mass spectrometry (APGC-ToF-MS) for the determination of regulated and emerging contaminants in aqueous samples after stir bar sorptive extraction (SBSE), Anal. Chim. Acta. 851 (2014) 1–13.

[132] W.-H. Chung, S.-H. Tzing, M.-C. Huang, W.-H. Ding, Dispersive Micro Solid-phase Extraction Coupled with Ultrasound-assisted Solvent Desorption for Determination of Synthetic Polycyclic and Nitro-aromatic Musks in Aqueous Samples, J. Chinese Chem. Soc. 61 (2014) 1031–1038.

[133] M. López-Nogueroles, A. Chisvert, A. Salvador, A. Carretero, Dispersive liquid-liquid microextraction followed by gas chromatography-mass spectrometry for the determination of nitro musks in surface water and wastewater samples, Talanta. 85 (2011) 1990–1995.

[134] L. Guo, N. Binte Nawi, H.K. Lee, Fully Automated Headspace Bubble-in-Drop Microextraction, Anal. Chem. 88 (2016) 8409–8414.

[135] J. Regueiro, M. Llompart, C. Garcia-Jares, J.C. Garcia-Monteagudo, R. Cela, Ultrasound-assisted emulsification-microextraction of emergent contaminants and pesticides in environmental waters, J. Chromatogr. A. 1190 (2008) 27–38.

[136] O. Posada-Ureta, M. Olivares, P. Navarro, A. Vallejo, O. Zuloaga, N. Etxebarria, Membrane assisted solvent extraction coupled to large volume injection-gas chromatography-mass spectrometry for trace analysis of synthetic musks in environmental water samples, J. Chromatogr. A. 1227 (2012) 38–47.

[137] J. Grau, J.L. Benedé, A. Chisvert, Polydopamine-coated magnetic nanoparticles for the determination of nitro musks in environmental water samples by stir bar sorptive-dispersive microextraction, Talanta. 231 (2021) 122375.

[138] S.A. Mat Hussin, P. Varanusupakul, S. Shahabuddin, B. Yih Hui, S. Mohamad, Synthesis and characterization of green menthol-based low transition temperature mixture with tunable thermophysical properties as hydrophobic low viscosity solvent, J. Mol. Liq. 308 (2020) 113015.

[139] R. Rodil, M. Moeder, Development of a method for the determination of UV filters in water samples using stir bar sorptive extraction and thermal desorption-gas chromatography-mass spectrometry, J. Chromatogr. A. 1179 (2008) 81–88.

[140] M. Vila, M. Celeiro, J.P. Lamas, C. Garcia-Jares, T. Dagnac, M. Llompart, Simultaneous in-vial acetylation solid-phase microextraction followed by gas chromatography tandem mass spectrometry for the analysis of multiclass organic UV filters in water, J. Hazard. Mater. 323 (2017) 45–55.

[141] A. Duque, J. Grau, J.L. Benedé, R.M. Alonso, M.A. Campanero, A. Chisvert, Low toxicity deep eutectic solvent-based ferrofluid for the determination of UV filters in environmental waters by stir bar dispersive liquid microextraction, Talanta. 243 (2022) 123378.

[142] A. Garrahy, H. Forde, P. O'Kelly, K. McGurren, H.M. Zia-ul-Hussnain, E. Noctor, W.P. Tormey, D. Smith, M.C. Dennedy, M. Bell, M. Javadpour, A. Agha, The diagnostic utility of late night salivary cortisol (LNSF) and cortisone (LNSE) in Cushing's syndrome, Ir. J. Med. Sci. 190 (2021) 615–623.

[143] M. Mezzullo, F. Fanelli, A. Fazzini, A. Gambineri, V. Vicennati, G. Di Dalmazi, C. Pelusi, R. Mazza, U. Pagotto, R. Pasquali, Validation of an LC–MS/MS salivary assay for glucocorticoid status assessment: Evaluation of the diurnal fluctuation of cortisol and cortisone and of their association within and between serum and saliva, J. Steroid Biochem. Mol. Biol. 163 (2016) 103–112.

[144] G. Antonelli, F. Ceccato, C. Artusi, M. Marinova, M. Plebani, Salivary cortisol and cortisone by LC-MS/MS: Validation, reference intervals and diagnostic accuracy in Cushing's syndrome, Clin. Chim. Acta. 451 (2015) 247–251.

[145] B. Magda, Z. Dobi, K. Mészáros, É. Szabó, Z. Márta, T. Imre, P.T. Szabó, Charged derivatization and on-line solid phase extraction to measure extremely low cortisol and cortisone levels in human saliva with liquid chromatography–tandem mass spectrometry, J. Pharm. Biomed. Anal. 140 (2017) 223–231.

[146] I. Perogamvros, L.J. Owen, J. Newell-Price, D.W. Ray, P.J. Trainer, B.G. Keevil, Simultaneous measurement of cortisol and cortisone in human saliva using liquid chromatography-tandem mass spectrometry: Application in basal and stimulated conditions, J. Chromatogr. B Anal. Technol. Biomed. Life Sci. 877 (2009) 3771–3775.

[147] F. Abujaber, A.I. Corps Ricardo, Á. Ríos, F.J. Guzmán Bernardo, R.C. Rodríguez Martín-Doimeadios, Ionic liquid dispersive liquid-liquid microextraction combined with LC-UV-Vis for the fast and simultaneous determination of cortisone and cortisol in human saliva samples, J. Pharm. Biomed. Anal. 165 (2019) 141–146.

[148] J. Grau, J.L. Benedé, A. Chisvert, A. Salvador, Modified magnetic-based solvent-assisted dispersive solid-phase extraction: application to the determination of cortisol and cortisone in human saliva, J. Chromatogr. A. 1652 (2021) 462361.

[149] A. Zielińska-Jurek, Z. Bielan, S. Dudziak, I. Wolak, Z. Sobczak, T. Klimczuk, G. Nowaczyk, J. Hupka, Design and Application of Magnetic Photocatalysts for Water Treatment. The Effect of Particle Charge on Surface Functionality, Catalysts. 7 (2017) 360.

[150] K. Krzemińska, S. Bocian, R. Pluskota, B. Buszewski, Surface properties of stationary phases with embedded polar group based on secondary interaction, zeta potential measurement and linear solvatation energy relationship studies, J. Chromatogr. A. 1637 (2021) 461853.

[151] I. Perogamvros, D.W. Ray, P.J. Trainer, Regulation of cortisol bioavailability - Effects on hormone measurement and action, Nat. Rev. Endocrinol. 8 (2012) 717–727.

[152] C.J. Pretorius, J.P. Galligan, B.C. McWhinney, S.E. Briscoe, J.P.J. Ungerer, Free cortisol method comparison: Ultrafiltation, equilibrium dialysis, tracer dilution, tandem mass spectrometry and calculated free cortisol, Clin. Chim. Acta. 412 (2011) 1043–1047.

[153] J.J. Zimmerman, R.M. Barker, R. Jack, Initial observations regarding free cortisol quantification logistics among critically ill children, Intensive Care Med. 36 (2010) 1914–1922.

Lista de abreviaturas

Lista de abreviaturas

AGREE
Analytical GREEnes metric

AGREEprep
Analyticial GREEnes metric for sample preparation

AW
Intercambiador aniónico débil

BMDM
Butil metoxidibenzoilmetano

BZ3
Benzofenona-3

CAR
Carboxeno

ComplexGAPI
Complementary green analytical procedure index

C18
Octadecil

DBP
Dibencilfosfato

DES
Disolvente eutéctico profundo

DHHB
Dietilamino hydroxibenzoil hexil benzoato

DLLME
Microextracción líquido-líquido dispersiva

DPP
Difenilfosfato

DPX
Extracción dispersiva con pipeta

DSPE
Eextracción en fase sólida dispersiva

DVB
Divinilbenceno

EF
Factor de enriquecimiento o preconcentración

EHDP
Etillhexil dimetil para-aminobenzoato

EHS
Etilhexil salicilato

ESI
Ionización por electrospray

GAC
Química analítica ‘verde’

GC-MS
Cromatografía de gases acoplada a espectrometría de masas

GO
Óxido de grafeno

GSP
Preparación de muestra ‘verde’

HBA
Aceptor de puentes de hidrógeno

HBD
Dador de puentes de hidrógeno

HCB
Hexaclorobenceno

IL
Líquido iónico

IMC
Isoamil p-metoxicinamato

LC-MS/MS
Cromatografía de líquidos acoplada a espectrometría de masas en tándem

LC-UV
Cromatografía de líquidos con detección ultravioleta

LLE
Extracción líquido-líquido

LOD
Límite de detección

LOQ
Límite de cuantificación

LT-DES
Disolvente eutéctico profundo de baja toxicidad

MA
Almizcle ambreta

MBC
4-metilbenciliden canfor

MIL
Líquido iónico magnético

MIP
Polímero de impresión molecular

MK
Almizcle cetona

MM
Almizcle muscado

MNP
Nanopartícula magnética

MOF
Red metal-orgánica

M-PTME
microextracción dispersiva magnética mediante puntas de pipeta

MS
Espectrometría de masas

MT
Almizcle tibetano

MX
Almizcle xileno

NADES
Disolventes eutécticos profundos naturales

OA
Ácido oleico

OC
Octocrileno

PBS
Disolución amortiguadora de fosfatos

PDA
Polidopamina

PDMS
polidimetilsiloxano

PT-SPE
Extracción en fase sólida basada en puntas de pipeta

$[P^{+}_{6,6,6,14}][Ni(hfacac)_3^{-}]$
Trietilhexil(tetradecil)fosfonio níquel (II) hexafluoroacetilacetonato

---

rGO
Óxido de grafeno reducido

RP
Fase reversa

RSD
Desviación estándar relativa

SA-DSPE
Extracción en fase sólida dispersiva asistida por disolvente

SBDLME
microextracción en fase líquida dispersiva sobre barra agitadora

SBSDME
Microextracción en fase sólida dispersiva sobre barra agitadora

SBSE
Extracción sobre barra agitadora

SDME
microextracción en gota

SEM
Microscopía electrónica de barrido

SFOD
Solidificación de gota orgánica flotante

S/N
Relación señal ruido

SPE
Extracción en fase sólida

SPME
Microextracción en fase sólida

TD
Desorción térmica

TEM
Microscopía electrónica de transmisión

TGA
Análisis termogravimétrico

TPP
Trifenilfosfato

Tris
Tris(hidroximetil) aminometano

ANEXO I: PUBLICACIONES DERIVADAS DIRECTAMENTE DE LA PRESENTE TESIS DOCTORAL

Use of nanomaterial-based (micro)extraction techniques for the determination of cosmetic-related compounds

Molecules 25 (2020) 2586

DOI: 10.3390/molecules25112586

molecules

MDPI

Review

Use of Nanomaterial-Based (Micro)Extraction Techniques for the Determination of Cosmetic-Related Compounds

José Grau, Juan L. Benedé and Alberto Chisvert *

Department of Analytical Chemistry, University of Valencia, Burjassot, 46100 Valencia, Spain; jose.grau-escribano@uv.es (J.G.); benede@uv.es (J.L.B.)
* Correspondence: alberto.chisvert@uv.es

Academic Editors: Rafael Lucena, Soledad Cárdenas and Guillermo Lasarte Aragonés
Received: 14 May 2020; Accepted: 29 May 2020; Published: 2 June 2020

Abstract: The high consumer demand for cosmetic products has caused the authorities and the industry to require rigorous analytical controls to assure their safety and efficacy. Thus, the determination of prohibited compounds that could be present at trace level due to unintended causes is increasingly important. Furthermore, some cosmetic ingredients can be percutaneously absorbed, further metabolized and eventually excreted or bioaccumulated. Either the parent compound and/or their metabolites can cause adverse health effects even at trace level. Moreover, due to the increasing use of cosmetics, some of their ingredients have reached the environment, where they are accumulated causing harmful effects in the flora and fauna at trace levels. To this regard, the development of sensitive analytical methods to determine these cosmetic-related compounds either for cosmetic control, for percutaneous absorption studies or for environmental surveillance monitoring is of high interest. In this sense, (micro)extraction techniques based on nanomaterials as extraction phase have attracted attention during the last years, since they allow to reach the desired selectivity. The aim of this review is to provide a compilation of those nanomaterial-based (micro)extraction techniques for the determination of cosmetic-related compounds in cosmetic, biological and/or environmental samples spanning from the first attempt in 2010 to the present.

Keywords: cosmetic-related compounds; microextraction techniques; nanomaterials; sample preparation

1. Introduction

The growing social concern about beauty has encouraged in last decades a remarkable increase in the use of cosmetic products. These products are used daily by many consumers, contributing to the improvement of their well-being. To ensure their safety, these products are regulated worldwide, so that the different regulations in force in each country prohibit and restrict (in terms of concentration, type of product, users, etc.) the use of certain compounds [1]. In this sense, analytical methods to perform the control of cosmetic products, not only to monitor the prohibited substances but also the allowed ingredients, to ensure their efficacy are demanded by authorities and by the cosmetic industry itself [2].

It is important to note that, given the high responsibility of the cosmetic industry, the presence of prohibited substances in the cosmetic products as consequence of their intentional use is not expected. Therefore, their presence at trace level could be due to unintended causes (e.g., impurities from raw materials, degradation of some ingredients, migration of compounds from the containers, or even undesired reactions between cosmetic ingredients during the manufacturing or storage processes).

Moreover, different studies have shown that after the application of a cosmetic product, some of its ingredients might be percutaneously absorbed into the organism [3]. Then, they are distributed

throughout the organism by blood where they can be altered producing different metabolites that might cause adverse effects on health [4–6] due to their endocrine disrupting and/or carcinogenic properties [7]. To this regard, analytical methods are needed to carry out studies of percutaneous absorption, metabolism and/or excretion of these cosmetic ingredients and their metabolites.

Likewise, due to the increasing use of cosmetic products, some of their ingredients have reached the environment by direct and indirect sources, and they are being accumulated in surface waters or sediments, having a negative effect on the different ecosystems even at trace levels [8–10]. Here again, analytical methods are needed to allow the environmental surveillance of cosmetic ingredients.

For all the above reasons, it has been necessary to develop analytical methods of high selectivity and sensitivity for the determination of traces of these cosmetic-related compounds in these three scenarios: cosmetic, biological and environmental matrices.

In this regard, extraction techniques are required for enrichment purposes. Traditional liquid–liquid extraction (LLE) and solid-phase extraction (SPE) are time-consuming and use high quantities of organic solvents. Thus, the employment of the so-called microextraction techniques have been considered as better alternatives because they not only reduce the use of solvents and extraction times but also allow to obtain lower limits of detection (LODs).

On this matter, sorbent-based microextraction techniques have a huge impact nowadays. In these techniques, in the first step, the analytes are adsorbed by the extractant phase. Subsequently, compounds are selectively desorbed into a small amount of solvent (liquid desorption) or introduced directly in the GC system for thermal desorption (TD).

Among the sorbent-based microextraction techniques, those based on the use of nanomaterials as extraction phase have attracted attention during the last years. Their higher surface area, compared with macroscopic materials, and their easy surface modification, which allows to synthesize a great diversity of superficially modified sorbents and thus to increase their selectivity with regard to the target analytes [11], make them interesting alternatives for sorbent-based microextraction techniques.

This review presents a comprehensive compilation of those published papers on the application of nanomaterial-based (micro)extraction techniques to the determination of cosmetic-related compounds in different matrices, such as cosmetic products, biological and environmental samples, spanning from the first attempt in 2010 to the present.

2. (Nano)Materials in Sorbent-Based Microextraction Approaches

In sorbent-based extraction approaches, sorbents play a crucial role to get selective, precise and accurate enrichment of the analytes. Several sorbents with different compositions and physicochemical properties have been used. Moreover, combination of different materials, including nanometric and micrometric materials, gives rise to hybrid nanomaterials or composites. An important feature of these resulting sorbents is that they maintain the properties of both original materials. Some of those materials used in microextraction techniques are briefly presented below.

Regarding to nanometric materials, one of the most popular materials are the nanoparticles (NPs). NPs are small spheres between 1 and 100 nm of a wide range of metallic and metallic oxide materials. In this group, NPs of noble metals (i.e., AuNPs and AgNPs) [12] are commonly used due to their chemical stability, elevated adsorption and high ratio surface/volume. Most recently, magnetic NPs (MNPs) have gained a considerably interest. They present similar properties to nonmagnetic NPs, such as high surface and huge adsorption capacity, but their main advantage compared with the nonmagnetic ones is the easy retrieval after the extraction, since only an external magnetic field is necessary [13]. Moreover, the MNPs can be easily coated with other materials maintaining the nanometric size or can be embedded on the surface of the material to obtain magnetic composites [14]. Traditionally, ferrite NPs (Fe_3O_4) have been preferred, but its low stability and its facility to form aggregates make a coating step (e.g., with silica shell) necessary to protect them from oxidation. On the other side, cobalt ferrite MNPs ($CoFe_2O_4$) have proved to be more stable, and no additional steps are needed in order to protect them [15].

Carbonaceous nanomaterials such as carbon nanotubes (CNTs), either single-walled (SWCNTs) or multiwalled (MWCNTs), graphene oxide (GO), reduced graphene oxide (rGO) or carbon dots (CDs) are also widely used as sorbents. MWCNTs can be used as sorbent themselves due to their high surface area and their ability to have hydrophobic, π-π and/or electrostatic interactions [16] or can be used to create composite materials maximizing the specific surface area of the original sorbent material [17]. Graphene derivatives (GO or rGO) are preferred than graphene mainly for economic reasons. GO is obtained by the oxidation of graphite, whereas rGO is prepared by the reduction of GO. GO is preferred to analyse polar compounds since its surface has polar groups (i.e., alcoholic, carboxyl and epoxy groups). In contrast, when the reduction is produced to obtain rGO, most of these groups disappear, which makes rGO an ideal sorbent for non-polar analytes. Both GO and rGO show high surface area and thermal and chemical stability that make them really efficient sorbents [18]. Finally, CDs are nanoparticles that possess unique optical properties similar to the well-known quantum dots, but they are safer and less harmful for the environment [19].

Metal–organic frameworks (MOFs) are nanomaterials recently employed as sorbents in microextraction approaches. They are three-dimensional inorganic–organic crystalline structures formed by the assembly of metal ions and organic ligands by coordinative bonds or different polymers with different interactions for the extraction of different analytes. Their properties vary depending on the ligands used and/or their geometry. They present interesting properties to be used as sorbents, such as high chemical and thermal stability, large porosity and huge surface area. In fact, the high stability allows some of them to be reused more than 100 times [20]. On the other hand, covalent organic frameworks (COFs), most recently used as sorbents in extraction techniques, consist in the assembly between different units by covalent bonds, and their structures may adopt a two- to three-dimensional form depending on the application. Similar to MOFs, they have large surface area, high chemical stability and high porosity. Furthermore, they present other properties such as low density and tunable pore size and structure [21,22].

Finally, layered double hydroxides (LDH) are two-dimensional nanosorbents composed by two layers of divalent and trivalent cations with an anionic interphase. The anions in the interlayer can be easily exchanged by other anions [23] and, for that reason, they are normally employed for the determination of anionic compounds.

Along with nanomaterials, non-nanometric sorbents are usually employed to enhance the selectivity and the extraction capability.

In this regard, polymers are micrometric structures synthetized either from the same type of monomer or employing two or more types of monomers (copolymerization) [24]. Different polymers have been widely used as sorbents due to their good extraction properties. Moreover, composite materials made of polymers combined with NPs present higher porosity when compared to the naked polymers [16].

When copolymerization of functional monomers and a cross-linker is performed in the presence of a template molecule, the so-called molecularly imprinted polymers (MIPs) are obtained. The cavities formed by this template allow to have a very selective sorbent, since they are complementary in size, shape and chemical environment to the analyte. MIPs can be synthetized for just one analyte, if only one template is used or can be prepared with multiple templates to recognize different analytes, enhancing its versatility [25].

Finally, ionic liquids (ILs), which are melt salts at temperature below 100 °C made of a combination between organic cations and different inorganic or organic anions, have been widely used in analytical methods due to their interesting properties, such as high extractability, elevated thermal stability and negligible vapor pressure. Besides those mentioned before, their viscosity and miscibility can be modified for specific applications [26,27].

3. Nanomaterials-Based Microextraction Approaches Used for the Determination of Cosmetic-Related Compounds

In this review, those published articles employing nanomaterials for the extraction (or determination) of cosmetic-related compounds in cosmetic, biological or/and environmental samples are compiled and briefly discussed. From the first one in 2010 up to the present, more than 70 articles have been published, with a clear increase every year, representing a trend within the analytical chemistry field. Figure 1 shows a histogram of all these research articles according to year of publication.

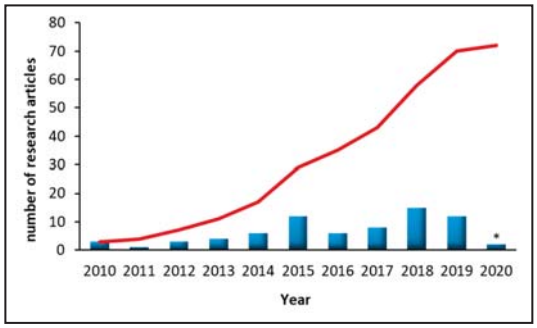

Figure 1. Number of research articles published in the last 10 years about the use of nanomaterial-based (micro)extraction techniques for the determination of cosmetic-related compounds (red line represents the accumulated number; * current year).

3.1. Solid Phase Extraction

Briefly, classical solid-phase extraction (SPE) process consists of percolating the sample solution through a cartridge (or disc) containing the solid sorbent that retains the target analytes, whereas the rest of the sample is discarded. After a cleaning step, an elution solvent is passed to desorb and to retrieve the analytes.

As it can be seen in Table 1, different nanomaterials have been packed in SPE-cartridges for the determination of cosmetic-related compounds. In this sense, Márquez-Sillero et al. [28] employed MWCNTs for the determination of four parabens in cosmetic products, previously lixiviated with water. Wang et al. [29] developed a GO sponge for the determination of six benzotriazole compounds in sewage and cosmetic samples. The use of MIPs in SPE for cosmetic analysis was first proposed by Zhu et al. [30], who used MIP-coated silica nanoparticles for the determination of bisphenol A (BPA) in shampoos and bath lotions, which were previously lixiviated with toluene before introducing them into the cartridge. Later, Wang et al. [31] functionalized MWCNT with a prednisone-template MIP for the determination of this glucocorticoid. Zhong et al. [32] employed carboxylated GO with polyvinyl chloride (PVC) as sorbent to determine different sulphonamides as contaminants in cosmetics products, and Abdolmohammad-Zadeh et al. [33] created a LDH cartridge with nickel and zinc for the analysis of p-aminobenzoic acid in cosmetic samples, which was dissolved in a proper water or ethanol amount before the extraction.

It should be noticed that SPE is not in fact a microextraction technique, but the use of nanomaterials as sorbents allows to achieve low LODs (from ng mL^{-1} to ng L^{-1}), which are suitable for the trace analysis of cosmetic-related compounds in the different matrices considered.

Table 1. Published papers on cosmetic-related compounds determination by nanomaterials-based solid phase extraction.

Analyte(s) [a]	Matrix	Extraction Technique [b]	Material/Composite [c]	Instrumental Technique [d]	LOD (ng L^{-1})	RSD (%)	RR (%)	Year	Ref.
Parabens	Cosmetic	SPE	MWCNT	C-CAD	500–2100	<7.6	96–104	2010	[28]
GCCs	Cosmetic	SPE	MWCNT-MIP	LC-UV	5000	<2.1	83–106	2010	[30]
p-aminobenzoic acid	Cosmetic	SPE	NI-Zn-LDH	UV	3780	1.2	96–101	2014	[33]
Sulphonamides	Cosmetic	SPE	GO-PVC	LC-UV	3400–7100	<7.6	88–102	2015	[32]
Benzotriazole UV stabilizers	Cosmetic and environmental	SPE	GO	LC-UV	20–80	<8.1	89–105	2018	[29]
BPA	Cosmetic	SPE	SiO_2@MIP	LC-FLD	229	<9	87–97	2018	[31]

[a] BPA: bisphenol A; GCCs: glucocorticoids. [b] SPE: solid-phase extraction. [c] GO: graphene oxide; LDH: layered double hydroxides; MIP: molecularly imprinted polymer; MWCNT: multiwalled carbon nanotube; PVC: polyvinyl chloride. [d] C-CAD: corona-charge aerosol detector; FLD: fluorescence detector; LC: liquid chromatography; UV: ultraviolet detector.

3.2. Solid Phase Microextraction

Solid phase microextraction (SPME) was developed by Arthur and Pawliszyn in 1990 [34]. In this technique, analytes are retained on a fibre coated with the sorbent material. The extraction can be performed by direct immersion into the sample or, if the analytes are volatile enough, by setting the fibre in the head space. After the extraction, analytes are, usually, thermally desorbed, although in a minor extent, liquid desorption in an appropriate solvent has also been used. Several methods based on SPME have been employed for the extraction of cosmetic-related compounds from different matrices. They are all listed in Table 2.

With that aim, different works for determination of parabens in different matrices have been reported. Ara et al. [35] modified mesoporous silica nanoparticles with polyaniline (PANI) and p-toluene sulphonic acid to coat the fibre for the determination of three of these target compounds in various cosmetics creams and wastewater. Yazdi et al. [36] determined the same parabens in wastewater samples employing AgNPs embedded on polypyrrole. First of all, pyrrole was polymerized on the hollow fibre, and then, it was introduced in a suspension of AgNPs for bounding.

For the determination of UV filters in environmental samples, different titanium oxide-based fibres have been used due to their excellent properties, such as high chemical and thermal stability, low cost and toxicity and good biocompatibility. In this sense, Du and coworkers used PANI-coated titania nanotubes (NTs) [37], ZrO_2-based fibre [38] and TiO_2 NPs functionalized with phenyl groups [39] for the analysis of different UV filters in river water and wastewater. The same authors also used electrodeposited AuNPs onto a stainless-steel wire followed by a coating step with 1,8-octanedithiol [40] for the same purpose. Moreover, Mei et al. [41] synthesized a polymeric ionic liquid (PIL) with MNPs to enhance the extraction capability of diamagnetic UV filters employing magnetic field gradients. This method was applied to lake and river waters and wastewater.

In addition to parabens and UV filters, extraction of other cosmetic-related compounds has been also performed by SPME. Wu et al. [42] employed a graphitic carbon nitride (g-C_3N_4) modified with rGO for the analysis of six polycyclic aromatic hydrocarbons (PAHs) in cosmetic products previously diluted in water. Tong et al. [43] synthesized a polymeric monolith by copolymerization of butyl methacrylate (BMA) and ethylene dimethacrylate (EDMA), followed by the addition of rGO nanosheets for the analysis of nine glucocorticoids (GCCs). In this methodology, GCCs were first extracted with acetonitrile (ACN) and then, SPME was performed. Finally, Wang et al. [44] used hydroxyapatite (HAP) NPs to coat a titanium fibre for the analysis of different chlorophenols, BPA and triclosan (TCS) in river water and sewage.

All the analyses reported with SPME show a great sensitivity, proving to be one of the most appropriate techniques for the analysis of traces. As shown in Table 2, the lowest LODs are achieved for those methods focused on the analysis of environmental samples (mostly waters). Since cosmetic matrices are usually difficult matrices, a clean-up step with organic solvents is usually required, which reduces the sensitivity of the method due to the dilution effect, but in any case, the achieved LODs are low enough to analyse the cosmetic samples.

Table 2. Published papers on cosmetic-related compounds determination by nanomaterials-based solid phase microextraction.

Analyte(s) [a]	Matrix	Extraction Technique [b]	Material/Composite [c]	Instrumental Technique [d]	LOD (ng L^{-1})	RSD (%)	RR (%)	Year	Ref.
GCCs	Cosmetic	SPME	BMA-EDMA-rGO	LC-MS	130–1930	<14	84–104	2012	[43]
UV filters	Environmental	SPME	Ti-TiO_2/ZrO2	LC-UV	32–82	<11	77–114	2014	[38]
UV filters	Environmental	SPME	Co-S-AuNPs	LC-UV	25–56	<9.4	92–106	2014	[40]
Parabens	Cosmetic and environmental	SPME	SBA-15/PANI-p-TSA	GC-FID	80–400	<7	82–108	2015	[35]
UV filters	Environmental	SPME	Ph-TiO_2-Ti	LC-UV	0.1–50	<9.1	86–106	2015	[39]
UV filters	Environmental	SPME	PANI/TiO_2NTs/Ti	LC-UV	30–50	<7.7	86–113	2017	[37]
UV filters	Environmental	SPME	PIL-MCC/MNPs	LC-UV	40–260	<10	71–119	2017	[41]
PAHs	Cosmetic	SPME	g-C_3N_4@rGO	GC-MS	1.0–2.0	<12	70–118	2017	[42]
Parabens	Environmental	SPME	PPY-AgNPs	LC-UV	10	<4.5	94–104	2018	[36]
TCS, BPA and CPs	Environmental	SPME	HAP@SiO_2	LC-UV	12–14	<8.2	90–110	2018	[44]

[a] BPA: bisphenol A; CPs: chlorophenols; GCCs: glucocorticoids; PAHs: polycyclic aromatic hydrocarbons, TCS: triclosan. [b] SPME: solid-phase microextraction. [c] AP: aminopropyl; BMA: butyl methacrylate; EDMA: ethylene dimethacrylate; g-C_3N_4: graphitic carbon nitride; MCC: monolithic capillary column; MNPs: magnetic nanoparticles; NPs: nanoparticles; NTs: nanotubes; PANI: polyaniline; Ph: phenyl; PIL: polymeric ionic liquid; PPY: polypyrrole; rGO: reduced graphene oxide; SBA-15: mesoporous silica nanoparticles; TSA: toluene sulphonic acid. [d] FID: flame ionization detector; GC: gas chromatography; LC: liquid chromatography; MS: mass spectrometry detector; UV: ultraviolet detector.

3.3. Stir Bar Sorptive Extraction

Stir bar sorptive extraction (SBSE), introduced at the end of the 1990s by Baltussen et al. [45], consists on a stir bar coated with the extractant material. This functionalized stir bar is then introduced in the sample and stirred in order to extract the analytes. As it is shown in Table 3, just four articles employing nanomaterials-coated stir bars have been reported. Wang et al. [46] immobilized MIL-68 MOF onto the stir bar surface for the analysis of three parabens from pretreated sunscreen and plasma samples. Fresco-Cala et al. [47] developed a hybrid monolith composed by carbon nanohorns and a polymer formed by methacrylate monomers for the analysis of five benzophenone-type UV filters in urine and water samples. Siritham et al. [48] extracted butylated hydroxytoluene (BHT), butylated hydroxyanisole (BHA) and other antioxidants from different cosmetic products, such as conditioners, hair shampoos and mouthwash. First, samples were treated due to their high viscosity. Then, a composite based on GO, polyethylene glycol and natural latex was added for the microextraction procedure. Finally, Zang et al. [49] determined four chlorophenols employing a stir bar fabricated by filling a hollow tube with a Fe_3O_4-rGO-g-C_3N_4 composite.

Similar to SPME, excellent LODs are achieved by SBSE for all those analysed matrices. However, despite the simplicity of this technique, the necessity of higher extraction times, sometimes more than 2 h, makes it less attractive for this application, and other techniques based on the dispersion of the sorbent, as discussed below, are preferred.

Table 3. Published papers on cosmetic-related compounds determination by nanomaterials-based stir bar sorptive extraction.

Analyte(s) [a]	Matrix	Extraction Technique [b]	Material/Composite [c]	Instrumental Technique [d]	LOD (ng L^{-1})	RSD (%)	RR (%)	Year	Ref.
Parabens	Cosmetic and biological	SBSE	MIL-68	LC-MS/MS	1–2	<9.7	73–104	2018	[46]
UV filters	Environmental	SBSE	CNH/MA	LC-UV	100–1000	<7.9	71–124	2018	[47]
MI, BHT, BHA	Cosmetic	SBSE	GO-PEG-PANNL	GC-MS	500–5000	<3	84–107	2018	[48]
CPs	Cosmetic	SBSE	Fe_3O_4-rGO/g-C_3N_4	LC-UV	200–300 ng kg^{-1}	<12	85–104	2018	[49]

[a] BHA: butylated hydroxyanisole; BHT: butylated hydroxytoluene; CPs: chlorophenols; MI: 2-methyl-3-isothiazolinone. [b] SBSE: stir bar sorptive extraction. [c] CNH: carbon nanohorns; GO: graphene oxide; g-C_3N_4: graphitic carbon nitride; MA: methacrylate; PANNL: natural latex; PEG: polyethylene glycol; rGO: reduced graphene oxide. [d] GC: gas chromatography; LC: liquid chromatography; MS: mass spectrometry detector; UV: ultraviolet detector.

3.4. Dispersive Solid Phase Extraction

Dispersive solid phase extraction (DSPE) has become a widely used extraction technique since its proposal by Anastassiades et al. in 2003 [50]. Traditionally, the sorbent is introduced and dispersed into the sample. When the extraction is completed, the sorbent is recovered by means of centrifugation and decantation. However, nowadays, this technique has gained more interest due to the introduction of magnetic materials as sorbents, allowing an easy recovery of the sorbent by employing an external magnetic field, which considerably reduces the analysis time.

As can be seen in Table 4, 38 articles employing DSPE for the determination of cosmetic-related compounds have been reported, and only 6 of them resort to nonmagnetic sorbents, which shows the high impact that magnetic materials have caused in this extraction technique. In this sense, Rocío-Bautista et al. [51] used the MOF HKUST-1 in vortex-assisted DSPE for the extraction of a group of seven parabens in cosmetic creams, urine and environmental waters. Rashvand et al. [52] also analysed two parabens in wastewater samples by employing a GO-PANI composite. Li et al. [53] dispersed the MOF MIL-101 (Cr) in toner samples for the determination of different benzophenones. Gao et al. [54] synthesized a TCS-based MIP on CNTs in order to extract this analyte from lake and river waters. Zhai et al. [55] developed a method for the determination of hormones employing the MOF MIL-101 that was dispersed into the cosmetic sample after its dilution in a saline solution. Finally, Liu et al. [56] achieved the extraction of Hg(II) from cosmetic samples by measuring the fluorescence of CDs obtained from grass carps after their interaction with the analyte.

On the other hand, several magnetic composites have been reported, especially focused on the study of parabens and TCS in different matrixes and UV filters in environmental samples. With that aim, Tahmasebi et al. [57] used PANI-coated Fe_3O_4 MNPs for the determination of three parabens in wastewaters, cosmetic creams and toothpaste. Ghambari et al. [58] employed recycled polystyrene (PS) to synthesize a composite with $CoFe_2O_4$ MNPs to determine a group of four parabens in river, creek and tap waters by using vortex to disperse the composite. Abbasghorbani et al. [59] used a magnetic composite of aminopropyl (AP) and Fe_3O_4 MNPs for the determination of five parabens in different aqueous samples. Ariffin et al. functionalized the Fe_3O_4 with different surfactants, such as Sylgard 309 [60] and DC193C [61], for the extraction of different parabens in lake, river and sea waters. Casado-Carmona et al. [62] created a hybrid material based on MNPs and an IL (i.e., $MIMPF_6$) for the determination of four parabens along with some benzophenones and BPA in pool waters. The extraction was performed by dispersing the Fe_3O_4@$MIMPF_6$ by ultrasounds and employing vortex agitation to achieve the adsorption of the analytes. Mehdinia et al. [63] immobilized self-doped PANI on a Fe_3O_4-rGO composite for the determination of various parabens in different cosmetics (sunscreen, toothpaste and moisturizing cream) pretreated with MeOH. Later, the same authors [64] compared different silica-based magnetic nanocomposites for the extraction of parabens from various cosmetic samples. Feng et al. [65] also worked with rGO for determination of two parabens in cosmetic samples. In this case, Fe_3O_4 MNPs were embedded into the rGO surface, and then, it was covered by layers of mesoporous silica ($mSiO_2$) with phenyl-functionalized pore walls. Ultrasounds were employed for the dispersion of the material.

Jalilian et al. [66] modified the MOF MIL-101 surface with Fe_3O_4 MNPs and MWCNTs for the determination of two parabens along with three phthalates in both cosmetic creams and tap water. Cosmetic products were previously dissolved in MeOH:H_2O before the extraction. The use of a COF as sorbent was proposed by Shavar et al. [67], who functionalized Fe_3O_4 MNPs with a covalent triazine-based COF for the determination of a group of four parabens in water, cosmetic products and breastmilk. Yusoff et al. [68] synthesized a magnetic composite with Fe_3O_4 MNPs coated with the IL 1-butyl-3-methylimidazolium chloride. This sorbent was applied to the extraction of four parabens in river, pond and lake waters and in MeOH pretreated cosmetic creams. Pastor-Belda et al. [69] precipitated Fe_3O_4 MNPs on MWCNTs surface for the analysis of several parabens in water and urine. Ghasemi et al. [70] employed γ-Fe_2O_3 MNPs coated with HAP to determine six parabens in soils, water and urine assisted by ultrasounds. Before DSPE procedure, soil samples were lixiviated in water.

Regarding the analysis of UV filters in environmental samples, Wang et al. [71] performed the extraction of three benzophenones in soils with Fe_3O_4 MNPs combined with MOF-1210 (Zr/Cu). Piovesana et al. [72] employed graphitized carbon black (GCB) prepared with MNPs for the extraction of 10 UV filters in different surface waters. Cheng et al. [73] used polydopamine-coated Fe_3O_4 MNPs for the analysis of 11 UV filters in wastewaters. Román-Falcó et al. [74] covered the $CoFe_2O_4$ MNPs surface with oleic acid. The extraction and subsequent determination of six UV filters was accomplished in tap, river and sea waters. Giokas et al. [75] developed a method for the determination of four UV filters, consisting a cloud-point (CP) extraction followed by a DSPE step in the micellar phase using core–shell Fe_2O_3@C coated with polysiloxane (PSx).

Regarding to TCS determination, Yang et al. [76] performed the microextraction in toothpastes previously lixiviated in MeOH. For the DSPE step, MIL-101 MOF was functionalized with Fe_3O_4. Li et al. [77] analysed TCS and triclocarban (TCC) in biological samples employing a magnetic COF formed by the condensation of 1,3,5-tris(4-aminophenyl) benzene (TAPB) and terephthaldicarboxaldehyde (TPA) on the surface of the MNPs. Li et al. [78] employed GO embedded with magnetic iron nanowires for the analysis of TCS in lake water and wastewater along with BPA, and Jiang et al. [79] synthesized a Fe_3O_4-PANI composite for the extraction of TCS, BPA and 2,4-dichlorophenol from water samples.

Besides those compounds mentioned before, other analytes have been also determined using nanomaterials. Three works have been reported on the analysis of GCCs in cosmetic products. Du et al. [80] employed Fe_3O_4 coated with a MIP for the determination of dexamethasone in skincare products. Liu et al. [81] prepared a magnetic composite based on MNPs coated with a dual template MIP for the determination of hydrocortisone and dexamethasone from different cosmetic products (lotions, masks and toners), which were previously treated with a saturated NaCl solution and acetonitrile (ACN). Finally, Li et al. [82] determined five GCCs in facial masks previously sonicated in ultrapure water, employing magnetically functionalized g-C_3N_4 bonded to MIL-101 MOF.

Moreover, the determination of the dye rhodamine B in different matrices has been also performed. In this regard, Khani et al. [83] worked with γ-Fe_2O_3 MNPs coated with imino-pyridine on hand washing soaps. Before the DSPE step, the samples were dissolved in water. Bagheri et al. [84] used Fe_3O_4 MNPs functionalized with poly(aniline-naphthylamide) (PAN) for its determination in shampoos, eye shadows and hand washing products.

Tarigh et al. [85] worked with lipstick samples for the determination of lead and manganese employing a composite of Fe_3O_4 MNPs and MWCNT. Before the extraction, samples were mineralized at 450 °C, and subsequently, the ashes were dissolved with nitric acid. Xia et al. [86] determined whitening agents working with Fe_3O_4 MNPs coated with a polymeric COF based on benzidine and 1,3,5-triformylphloroglucinol. Liu et al. [87] synthesized a MIP-coated Fe_3O_4 MNPs for the determination of metronidazole in cosmetic creams, lotions and powders, previously lixiviated with MeOH. Finally, Maidatsi et al. [88] prepared a magnetic composite of Fe_3O_4 MNPs and rGO functionalized with octylamine to determine different musks, allergens and phthalates in water samples. More recently, Zhang et al. [89] employed halloysite nanotubes (HNTs) that where first filled with $CoFe_2O_4$ MNPs and later assembled with Au-NPs on its surface using APTES. This composite was applied for the determination of 4,4′–thioaniline in hair dyes.

As described in Table 4, LODs between μg mL^{-1} and ng L^{-1} are achieved in DSPE-based methods, although as expected, the instrumental technique has a huge impact on this parameter. In this sense, despite LC-UV has been extensively used, it might be not enough sensitive for the determination of trace levels of some of the cosmetic-related compounds. For this reason, other options, such as LC-MS/MS, have been preferred.

Extraction times are similar regardless of the use of magnetic materials or not. However, the use of the magnetic ones avoids centrifugation steps to recover the sorbent in the extraction and desorption steps, which redounds in the reduction of the total time of analysis.

Table 4. Published papers on cosmetic-related compounds determination by nanomaterials-based dispersive solid phase extraction.

Analyte(s) [a]	Matrix	Extraction Technique [b]	Material/Composite [c]	Instrumental Technique [d]	LOD (ng L^{-1}) [e]	RSD (%)	RR (%)	Year	Ref.
TCS	Environmental	DSPE	MWCNT@MIP	LC-UV	n.r.	<12	91–95	2010	[54]
UV filters	Environmental	(M) DSPE	$CoFe_2O_4$@oleic acid	GC-MS	0.2–6	<16	74–119	2011	[74]
Parabens	Environmental	(M) DSPE	Fe_3O_4@PANI	LC-UV	300–400	<2.4	86–109	2012	[57]
UV filters	Environmental	CP (M) DSPE	Fe_2O_3@C-PSx	LC-UV	1430–7500	<14.9	89–97	2012	[75]
Parabens	Environmental	(M) DSPE	Fe_3O_4-AP	GC-PID	50–300	<8	87–103	2013	[59]
Rhodamine B	Cosmetic and environmental	(M) DSPE	Fe_3O_4@PAN	Fl	100	<8.2	94–99	2013	[84]
Pb (II) Mn (II)	Cosmetic and biological	(M) DSPE	Fe_3O_4-MWCNTs	AA	600–1000	<4.3	n.r.	2013	[85]
Hormones	Cosmetic	DSPE	MIL-101(Cr)	LC-UV	360–910	<6.1	93–102	2014	[55]
Parabens	Cosmetic, biological and environmental	DSPE	HKUST-1	LC-UV	1500–2600	<15	57–101	2015	[51]
UV filters	Cosmetics	DSPE	MIL-101	LC-UV	900–1200	<10	94–105	2015	[53]
Parabens	Cosmetic	(M) DSPE	Fe_3O_4@PANI-rGO	GC-FID	1200–2800	<7.9	89–101	2015	[63]
Parabens	Cosmetic	(M) DSPE	Fe_3O_4-G-mSiO_2-Ph	LC-UV	10,000–25,000	<5.61	79–106	2015	[64]
TCS and BPA	Environmental	(M) DSPE	Fe-Fe_2O_3/GO	LC-UV	80–100	<7.5	85–93	2015	[78]
TCS, BPA and CPs	Environmental	(M) DSPE	Fe_3O_4@PANI	LC-UV	100–130	<6.6	85–107	2015	[79]
Metronidazole	Cosmetic	(M) DSPE	Fe_3O_4@MIP	LC-UV	3000	<5.20	91–104	2015	[87]
Musks, phthalates and allergens	Environmental	(M) DSPE	Fe_3O_4-rGO-OCT	GC-MS	0.29–3.2	<9.4	83–105	2015	[88]
Parabens	Environmental	DSPE	GO-PANI	LC-UV	50–1800	<11.5	74–120	2016	[52]
Parabens and UV filters	Environmental	(M) DSPE	Fe_3O_4@MIM-PF6	LC-MS/MS	260–1350	<8.3	87–99	2016	[62]
Parabens	Cosmetic	(M) DSPE	Fe_3O_4@SiO_2	GC-FID	200–900	<5.6	85–107	2016	[65]
TCS	Cosmetic	(M) DSPE	Fe_3O_4-MIL-100	LC-UV	30,000 ng Kg^{-1}	<5.5	91–101	2016	[76]
Parabens	Environmental	(M) DSPE	$CoFe_2O_4$-PS	LC-MS	50–150	<8.5	81–105	2017	[58]
Parabens	Cosmetic and environmental	(M) DSPE	Fe_3O_4@βCD-BMIM-Cl	LC-UV	20–90	<14.9	80–117	2017	[68]
UV filters	Environmental	(M) DSPE	Fe_3O_4-GCB	LC-MS/MS	1–4	<15	81–115	2017	[72]
GCCs	Cosmetic	(M) DSPE	Fe_3O_4@dtMIP	LC-UV	15,000	<2.6	87–102	2017	[81]
Parabens	Cosmetic, biological and environmental	(M) DSPE	Fe_3O_4@COF	LC-UV	20	<4.9	86–102	2018	[67]

Table 4. *Cont.*

Analyte(s) [a]	Matrix	Extraction Technique [b]	Material/Composite [c]	Instrumental Technique [d]	LOD (ng L^{-1}) [e]	RSD (%)	RR (%)	Year	Ref.
Parabens	Biological and environmental	(M) DSPE	Fe_3O_4-MWCNTs	GC-MS	30–2000	<9.2	81–119	2018	[69]
UV filters	Environmental	(M) DSPE	Fe_3O_4@PDA	LC-MS	60–130	<3	95–104	2018	[73]
GCCs	Cosmetic	(M) DSPE	Fe_3O_4@MIP	LC-UV	50,000	<2.7	94–98	2018	[80]
Whitening agents	Cosmetic	(M) DSPE	Fe_3O_4@COF	LC-FLD	0.1	<5.5	78–105	2018	[86]
Hg(II)	Cosmetic and environmental	DSPE	CDs	Fl	2800	<3.4	91–117	2019	[56]
Parabens	Environmental	(M) DSPE	Fe_3O_4@sylgard 309	LC-UV	20,000–30,000	<11.4	60–120	2019	[60]
Parabens	Environmental	(M) DSPE	Fe_3O_4@DC193C	LC-UV	2300–6300	<10.2	86–118	2019	[61]
Parabens and phthalates	Environmental	(M) DSPE	Fe_3O_4-MWCNTs-MIL-101	LC-UV	30–150	<7.5	38–71	2019	[66]
Parabens	Biological and environmental	(M) DSPE	γ-Fe_2O_3@HAP	GC-MS	5000–10,000	<4.2	95–106	2019	[70]
UV filters	Environmental	(M) DSPE	Fe3O4-1210 (Zr/Cu)	LC-UV	10–20	<3.6	88–114	2019	[71]
TCS and TCC	Biological	(M) DSPE	Fe_3O_4@COF	UPLC-MS/MS	5–20	n.r.	93–109	2019	[77]
GCCs	Cosmetic	(M) DSPE	Fe_3O_4-MIL-101/g-C_3N_4	UPLC-MS/MS	2	<5.5	77–113	2019	[82]
Rhodamine B	Cosmetic	(M) DSPE	γ-Fe_2O_3@imino-pyridine	Fl	1600	<2.7	91–97	2019	[83]
4,4′-thioaniline	Cosmetic	(M) DSPE	$CoFe_2O_4$@HNTs-Au-NPs	SERS	26,000	<10	72–104	2020	[89]

[a] BPA: bisphenol A; CPs: chlorophenols; GCCs: glucocorticoids; TCC: triclocarban TCS: triclosan. [b] CP: cloud-point; DSPE: dispersive solid-phase extraction; (M): magnetic-based. [c] AP: aminopropyl; BMIM-Cl: 1-butyl-3-methylimidazolium chloride; βCD: β-cyclodextrin; CDs: carbon dots; COF: covalent organic framework; dtMIP: dual template MIP; GCB: graphitized carbon black; GO: graphene oxide; g-C_3N_4: graphitic carbon nitride; HAP: hydroxyapatite; HNT: halloysite nanotubes; LDH: layered double hydroxides; MIM-PF6: methylimidazolium hexafluorophosphate; MIP: molecularly imprinted polymer; mSiO_2: mesoporous silica; MWCNT: multiwalled carbon nanotube; NPs: nanoparticles; PAN: poly(aniline-naphthylamide); PANI: polyaniline; PDA: polydopamine; Ph: phenyl; PS: polystyrene; PSx: polysiloxane; OCT: octylamine; rGO: reduced graphene oxide; TSA: toluene sulphonic acid. [d] AA: atomic absorption; FID: flame ionization detector; Fl: fluorimetry; FLD: fluorescence detector; GC: gas chromatography; LC: liquid chromatography; MS: mass spectrometry detector; SERS: surface-enhanced Raman scattering UPLC: ultraperformance liquid chromatography; UV: ultraviolet detector. [e] n.r.: not reported.

Compared with other techniques, DSPE combined with nanosorbents allows excellent LODs, many times comparable with SPME and SBSE, but with the advantage of shortest extraction times, usually under 20 min.

3.5. Stir Bar Sorptive-Dispersive Microextraction

A hybrid approach combining DSPE and SBSE, termed stir bar sorptive-dispersive microextraction (SBSDME), was introduced in 2014 by Benedé et al. [90]. In this technique, a magnetic sorbent coats the stir bar by means of magnetic interactions. When the stirring rate is high enough, the sorbent is dispersed in the sample until the stirring is stopped; at that moment, the magnetic composite containing the analytes is retrieved by the stir bar. This approach has been also employed for the determination of cosmetic-related compounds in different matrices (Table 5). Benedé et al. developed different strategies for determination of UV filters in environmental samples employing $CoFe_2O_4$ MNPs coated with oleic acid for the analysis of eight hydrophobic UV filters in environmental samples [90–92]. Later, the same authors developed a method based on $CoFe_2O_4$ MNPs embedded on nylon-6 polymer for the determination of six hydrophilic UV filters [93].

Recently, SBSDME has been applied for the determination of other types of analytes in different matrices. Grau et al. [94] applied this technique for the study of triphenyl phosphate (TPP) and its metabolite, diphenyl phosphate (DPP), in urine samples by means of $CoFe_2O_4$ incrusted onto a weak anion exchanger (Strata X-AW). Miralles et al. [95] functionalized MIL-101 MOF with $CoFe_2O_4$ for the determination of eight N-nitrosamines in cosmetic products. In this methodology, N-nitrosamines were first pre-extracted in hexane and then preconcentrated with SBSDME. Finally, Vállez-Gomis et al. [96] determined 10 PAHs in cosmetic creams employing rGO covered with $CoFe_2O_4$ MNPs, where samples were previously extracted with hexane, and then, SBSDME was performed on the hexane solution.

As can be seen in Table 5, similar LODs are obtained for SBSDME and DSPE with comparable extraction times. The main difference between these two approaches relies where the magnet is positioned, i.e., outside the solution in DSPE and inside the solution in SBSDME; thus, this last one does not require an external magnet to retrieve the sorbent. This fact alleviates losses of the extractant material in the different steps due to the reduction of sorbent and sample manipulation.

Table 5. Published papers on cosmetic-related compounds determination by nanomaterials-based stir bar sorptive dispersive microextraction.

Analyte(s) [a]	Matrix	Extraction Technique [b]	Material/Composite [c]	Instrumental Technique [d]	LOD (ng L^{-1})	RSD (%)	RR (%) [e]	Year	Ref.
UV filters	Environmental	SBSDME	$CoFe_2O_4$@oleic acid	LC-UV	2400–30,600	<11	79–120	2014	[90]
UV filters	Environmental	SBSDME	$CoFe_2O_4$@oleic acid	LC-UV	1600–2900	<12	90–115	2016	[91]
UV filters	Environmental	SBSDME	$CoFe_2O_4$-nylon 6	TD-GC-MS	13–148	<11	0–116	2016	[93]
UV filters	Environmental	SBSDME	$CoFe_2O_4$@oleic acid	GC-MS	10–550 ng kg^{-1}	<14	91–110	2019	[92]
TPP and DPP	Biological	SBSDME	$CoFe_2O_4$-Strata X-AW	LC-MS/MS	1.9–6.3	<8	81–111	2019	[94]
N-Nitrosamines	Cosmetic	SBSDME	$CoFe_2O_4$-MIL-101	LC-MS/MS	60–300	<13.9	96–109	2019	[95]
PAHs	Cosmetic	SBSDME	$CoFe_2O_4$-rGO	GC-MS	20–2500	<10	n.r.	2020	[96]

[a] DPP: dipheny lphosphate; PAHs: polycyclic aromatic hydrocarbons, TPP: triphenyl phosphate. [b] SBSDME: stir bar sorptive dispersive microextraction; SBSE: stir bar sorptive extraction; SPE: solid-phase extraction; SPME: solid-phase microextraction. [c] AW: anion weak exchanger; rGO: reduced graphene oxide. [d] GC: gas chromatography; LC: liquid chromatography; MS: mass spectrometry detector; TD: thermal desorption UV: ultraviolet detector. [e] n.r.: not reported.

3.6. Other Sorbent-Based Microextraction Approaches

Besides the most used microextraction techniques described above, other extraction approaches using nanomaterials for the determination of cosmetic-related compounds have been published. These methods are summarized in Table 6. Makkliang et al. [97] proposed rotative SPME using a multistir-rod microextractor based on MWCNT functionalized with carboxyl groups, which was applied for parabens determination in cosmetic samples previously dissolved in MeOH. Alcudia-León et al. [98] also determined parabens in pool and sea waters by magnetically confined hydrophobic nanoparticles microextraction. In this method, a magnetic device made of a magnet, a PTFE septum and a magnetic nanocomposite (Fe_3O_4@C18) is employed for the microextraction. Wang et al. [99] determined five parabens and TCS in biological samples, using a magnetic μSPE chip connected directly with the chromatographic system. Fresco-Cala and Cárdenas [100] synthetized a composite based on carbon nanohorns inside pipette tips for the determination of a group of four parabens in urine. Wang et al. [101] developed a device with GO packed into polyamide organic membrane for the analysis of different parabens in water, and finally, Montesdeoca-Esponda et al. [102] analysed benzotriazole UV stabilizers in sewage water by fabric phase sorptive extraction (FPSE), with a PDMS nanocomposite bonded on a polystyrene support as extraction device.

Table 6. Published papers on cosmetic-related compounds determination by other nanomaterials-based (micro)extraction techniques.

Analyte(s) [a]	Matrix	Extraction Technique [b]	Material/Composite [c]	Instrumental Technique [d]	LOD (ng L^{-1})	RSD (%)	RR (%)	Year	Ref.
Parabens	Environmental	MCE	Fe_3O_4-C18	GC-MS	23.2–86.1	<7.1	96–106	2013	[98]
Parabens	Environmental	µSPE	GO	GC-MS	5–10	<9.5	85–106	2014	[101]
Benzotriazole UV stabilizers	Environmental	FPSE	PDMS	UPLC-MS/MS	6.01–60.7	<29.2	35–99	2015	[102]
Parabens + TCS	Biological	Microflow injection	magnetic SPE PANI chip	LC-UV	1100–4500	<11	84–117	2017	[99]
Parabens	Cosmetic	Rotative SPME	MWCNTs-COOH	LC-UV	630–800	<5.8	83–103	2018	[97]
Parabens	Biological	DPX	CNH monolith	LC-UV	1000–7000	<16	80–116	2019	[100]

[a] TCS: triclosan. [b] DPX: disposable pipette extraction; FPSE: fabric phase sorptive extraction; MCE: magnetically confined hydrophobic nanoparticles microextraction; µSPE: micro solid-phase extraction. [c] CNH: carbon nanohorns; GO: graphene oxide; MWCNT: multiwalled carbon nanotube; PANI: polyaniline; PDMS: polydimethylsiloxane. [d] GC: gas chromatography; LC: liquid chromatography; MS: mass spectrometry detector; UPLC: ultraperformance liquid chromatography; UV: ultraviolet detector.

As summary, we would like to emphasize that, regarding to the nanomaterials-based microextraction techniques used for the determination of cosmetic-related compounds, those based on the dispersion of the sorbent (i.e., DSPE and SBSDME) represent more than half of the published articles, as it is shown in Figure 2a. As commented before, the reduction of the extraction time, most probably, is the reason behind this trend.

With regard to the target analytes, authors paid attention during many years to the determination of parabens and UV filters, which gather about half of the published articles, as it is shown in Figure 2b.

Finally, with regard to the use of nonmagnetic or magnetic materials, Figure 2c shows that they are practically on par, but the observed trend is an increase in the use of magnetic materials in the last years.

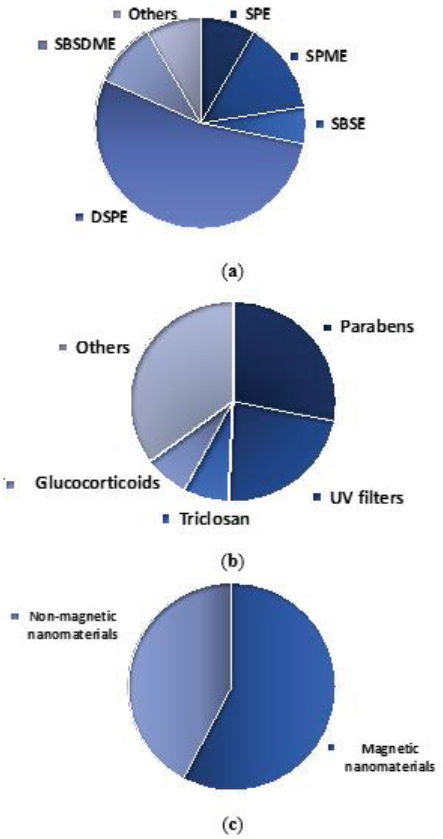

Figure 2. (**a**) Distribution of nanomaterials-based (micro)extraction techniques used in the determination of cosmetic-related compounds. SPE (solid-phase extraction); SPME (solid-phase microextraction); SBSE (stir bar sorptive extraction); DSPE (dispersive solid-phase extraction); SBSDME (stir bar sorptive dispersive microextraction). (**b**) Distribution of analytes studied. (**c**) Distribution of the materials employed.

4. Conclusions and Future Trends

In the last years, new analytical methods have been developed in order to control the presence of nonintended prohibited compounds in cosmetics products. Moreover, the presence of cosmetic ingredients and/or their metabolites in biological and environmental samples has also been studied. After an exhaustive revision of these methods, a clear trend in the use of nanomaterials for the determination of these cosmetic-related compounds has been observed, in line with the general trend observed within the analytical chemistry field. The high surface area, in addition to the thermal and chemical stability, and the easy fabrication/functionalization, make nanomaterials as excellent sorbents for any matrix.

In this review, the evolution of the impact of the use of nanomaterials for the extraction of cosmetic-related compounds has been studied. It should be noted that in the early 2010s (i.e., from 2010 to 2013), only eleven articles about this topic were published. By contrast, only in this last year, more than 10 articles were published, proving the high interest in this issue.

Moreover, focusing on the type of microextraction technique, DSPE has been highly employed reaching more than half of the reported articles. Its simplicity and low cost compared with other well-stablished techniques such as SPME or SBSE, in addition to the possibility of reducing the total analysis time employing magnetic nanomaterials, have increased its popularity in recent years, and its use with novel magnetic materials is a clear trend. It should be noticed that 42 of the 72 articles reported in this review employ novel magnetic sorbents to achieve the extraction.

Regarding the target analytes, the major research of the published articles is performed on the extraction of parabens and/or UV filters, either in cosmetics, biological or environmental samples. These analytes are probably the most controversial ingredients in cosmetic products, along with potentially allergenic perfumes, and this might be the reason for the attention that has been given to them. However, in our opinion, other compounds have received less attention from the analytical chemistry community. We are referring to all those compounds not allowed in cosmetics due to its harmful effects, but that could be present at trace level due to unintended causes, e.g., impurities from raw materials, degradation of some ingredients, migration from the containers, cross reactions between ingredients, etc. For this reason, it is necessary to focus our attention on them, e.g., N-nitrosamines and polycyclic aromatic hydrocarbons, among others. Fortunately, there are already a few incipient efforts in this regard, but in our opinion, more efforts should be performed and most probably, it will be established as one of the future trends in this field. With regard to biological matrices, it is difficult to predict a future trend, since the cosmetic industry is continuously innovating cosmetic ingredients, but it is sure that both percutaneous absorption and metabolism studies should be conducted on new ingredients. Finally, from an environmental surveillance point of view, the researchers should focus their attention to all those cosmetic ingredients that easily reach the environment and cause a negative impact on flora and fauna. So, besides UV filters, which have been extensively studied, preservatives other than parabens (which are being less used due to the bad opinion from the consumers and the recent prohibition on some of them) could constitute a good choice.

Author Contributions: Writing original draft, J.G.; review and editing, J.L.B. and A.C. and supervision A.C. All authors have read and agreed to the published version of the manuscript.

Funding: J.G. and J.L.B. would like to thank the Generalitat Valenciana and the European Social Fund for their predoctoral and postdoctoral grants, respectively. This research received no external funding. APC was sponsored by MDPI.

Acknowledgments: This article is based upon work from the Sample Preparation Task Force and Network, supported by the Division of Analytical Chemistry of the European Chemical Society.

Conflicts of Interest: The authors declare no conflict of interest.

References

1. Dorato, S. General concepts: Current legislation on cosmetics in various countries. In *Analysis of Cosmetics Products*, 2nd ed.; Salvador, A., Chisvert, A., Eds.; Elsevier: Amsterdam, The Netherlands, 2018; pp. 3–37. ISBN 9780444635082.
2. Mildau, G. General review of official methods of analysis of cosmetics. In *Analysis of Cosmetics Products*, 2nd ed.; Salvador, A., Chisvert, A., Eds.; Elsevier: Amsterdam, The Netherlands, 2018; pp. 67–83. ISBN 9780444635082.
3. Bronaugh, R.L.; Maibach, H.I. Percutaneous absorption: Drugs-cosmetics-mechanisms-methodology. In *Percutaneous Penetration as It Relates to the Safety Evaluation of Cosmetic Ingredients*, 3rd ed.; Yourick, J.J., Bronaugh, R.L., Eds.; Taylor and Francis: Abingdon, UK, 1999; pp. 659–673. ISBN 0-8247-1966-2.
4. Hewitt, N.J.; Grégoire, S.; Cubberley, R.; Duplan, H.; Eilstein, J.; Ellison, C.; Lester, C.; Fabian, E.; Fernandez, J.; Géniès, C.; et al. Measurement of the penetration of 56 cosmetic relevant chemicals into and though human skin using a standardized protocol. *J. Appl. Toxicol.* **2019**, *40*, 403–415. [CrossRef] [PubMed]
5. Nohynek, G.J.; Antignac, E.; Re, T.; Toutain, H. Safety assessment of personal care products/cosmetics and their ingredients. *Toxicol. Appl. Pharm.* **2010**, *243*, 239–259. [CrossRef] [PubMed]
6. Fransway, A.F.; Fransway, P.J.; Belsito, D.V.; Yiannias, J.A. Paraben toxicology. *Dermatitis* **2019**, *30*, 32–45. [CrossRef] [PubMed]
7. Nicolopoulou-Stamati, P.; Hens, L.; Sasco, A.J. Cosmetics as endocrine disruptors: Are they a health risk? *Rev. Endocr. Metab. Disord.* **2015**, *16*, 373–383. [CrossRef] [PubMed]
8. Sánchez-Quiles, D.; Tovar-Sánchez, A. Are sunscreens a new environmental risk associated with coastal tourism? *Environ. Int.* **2015**, *83*, 158–170. [CrossRef]
9. Haman, C.; Dauchy, X.; Rosin, C.; Munoz, J.F. Occurrence, fate and behaviour of parabens in aquatic environments: A review. *Water Res.* **2015**, *68*, 1–11. [CrossRef]
10. Giokas, D.L.; Chisvert, A.; Salvador, A. Environmental monitoring of cosmetics ingredients. In *Analysis of Cosmetics Products*, 2nd ed.; Salvador, A., Chisvert, A., Eds.; Elsevier: Amsterdam, The Netherlands, 2018; pp. 435–547. ISBN 9780444635082.
11. Murtada, K. Trends in nanomaterial-based solid-phase microextraction with a focus on environmental applications—A review. *Trend. Environ. Anal. Chem.* **2020**, *25*, e00077. [CrossRef]
12. Zhao, X.; Zhao, H.; Yan, L.; Li, N.; Shi, J.; Jiang, C. Recent developments in detection using noble metal nanoparticles. *Crit. Rev. Anal. Chem.* **2020**, *50*, 97–110. [CrossRef]
13. Azzouz, A.; Kailasa, S.K.; Lee, S.S.; Rascón, A.J.; Ballesteros, E.; Zhang, M.; Kim, K.H. Review of nanomaterials as sorbents in solid-phase extraction for environmental samples. *TrAC Trend. Anal. Chem.* **2018**, *108*, 347–369. [CrossRef]
14. Reyes-Gallardo, E.M.; Lucena, R.; Cárdenas, S.; Valcárcel, M. Magnetic nanoparticles-nylon 6 composite for the dispersive micro solid phase extraction of selected polycyclic aromatic hydrocarbons from water samples. *J. Chomatogr. A* **2014**, *1345*, 43–49. [CrossRef]
15. Maaz, K.; Mumtaz, A.; Hasanain, S.K.; Ceylan, A. Synthesis and magnetic properties of cobalt ferrite (CoFe2O4) nanoparticles prepared by wet chemical route. *J. Magn. Magn. Mater.* **2007**, *308*, 289–295. [CrossRef]
16. Chisvert, A.; Cárdenas, S.; Lucena, R. Dispersive micro-solid phase extraction. *TrAC Trend. Anal. Chem.* **2019**, *112*, 226–233. [CrossRef]
17. Yang, S.J.; Choi, J.Y.; Chae, H.K.; Cho, J.H.; Nahm, K.S.; Park, C.R. Preparation and enhanced hydro stability and hydrogen storage capacity of CNT@MOF-5 hybrid composite. *Chem. Mater.* **2009**, *21*, 1893–1897. [CrossRef]
18. Reinholds, I.; Jansons, M.; Pugajeva, I.; Bartkevics, V. Recent applications of carbonaceous nanosorbents in solid phase extraction for the determination of pesticides in food sample. *Crit. Rev. Anal. Chem.* **2019**, *49*, 439–458. [CrossRef] [PubMed]
19. Muk, S. Carbon dots optical nanoprobes for biosensors. In *Nanobiosensors for Biomolecular Targeting*; Gopinath, S.C., Lakshmiriya, T., Eds.; Elsevier: Amsterdam, The Netherlands, 2019; pp. 269–300. ISBN 9780128139004.
20. Gutiérrez-Serpa, A.; Pacheco-Fernández, I.; Pasán, J.; Pino, V. Metal-organic frameworks as key materials for solid-phase microextraction devices—A review. *Separations* **2019**, *6*, 47. [CrossRef]

21. Ding, S.Y.; Wang, W. Covalent organic frameworks (COFs): From design to applications. *Chem. Soc. Rev.* **2013**, *42*, 548–568. [CrossRef]
22. Li, N.; Du, J.; Wu, D.; Liu, J.; Li, N.; Sun, Z.; Li, G.; Wu, Y. Recent advances in facile synthesis and applications of covalent organic framework materials as superior adsorbents in sample pretreatment. *TrAC Trend. Anal. Chem.* **2018**, *108*, 154–166. [CrossRef]
23. Sajid, M.; Basheer, C. Layered double hydroxides: Emerging sorbent materials for analytical extractions. *TrAC Trend. Anal. Chem.* **2016**, *75*, 174–182. [CrossRef]
24. Young, I.R.; Lovell, P.A. *Introduction to Polymers*, 3rd ed.; CRC Press: Boca Raton, FL, USA, 2011; pp. 205–233. ISBN 9781439894156.
25. Haupt, K.; Linares, A.V.; Bompart, M.; Bui, B.T.S. Molecularly imprinted polymers. In *Molecular Imprinting Polymers*; Haupt, K., Ed.; Springer: Berlin/Heidelberg, Germany, 2012; pp. 1–28. ISBN 978-3-642-28420-5.
26. Ho, T.D.; Canestraro, A.J.; Anderson, J.L. Ionic liquids in solid-phase microextraction: A review. *Anal. Chim. Acta* **2011**, *695*, 18–43. [CrossRef]
27. Trujillo-Rodríguez, M.J.; Rocío-Bautista, P.; Pino, V.; Afonso, A.M. Ionic liquids in dispersive liquid-liquid microextraction. *TrAC Trend. Anal. Chem.* **2013**, *51*, 87–106. [CrossRef]
28. Márquez-Sillero, I.; Aguilera-Herrador, E.; Cárdenas, S.; Valcárcel, M. Determination of parabens in cosmetic products using multi-walled carbon nanotubes as solid phase extraction sorbent and corona-charged aerosol detection system. *J. Chromatogr. A* **2010**, *1217*, 1–6. [CrossRef] [PubMed]
29. Wang, X.; Wang, J.; Du, T.; Kou, H.; Du, X.; Lu, X. Determination of six benzotriazole ultraviolet filters in water and cosmetic samples by graphene sponge-based solid-phase extraction followed by high-performance liquid chromatography. *Anal. Bioanal. Chem.* **2018**, *410*, 6955–6962. [CrossRef]
30. Zhu, R.; Zhao, W.; Zhai, M.; Wei, F.; Cai, Z.; Sheng, N.; Hu, Q. Molecularly imprinted layer-coated silica nanoparticles for selective solid-phase extraction of bisphenol A from chemical cleansing and cosmetics samples. *Anal. Chim. Acta* **2010**, *658*, 209–216. [CrossRef] [PubMed]
31. Wang, F.; Li, X.; Li, J.; Zhu, C.; Liu, M.; Wu, Z.; Liu, L.; Tan, X.; Lei, F. Preparation and application of a molecular capture for safety detection of cosmetics based on surface imprinting and multi-walled carbon nanotube. *J. Colloid Interface Sci.* **2018**, *527*, 124–131. [CrossRef] [PubMed]
32. Zhong, Z.; Li, G.; Luo, Z.; Liu, Z.; Shao, Y.; He, W.; Deng, J.; Luo, X. Carboxylated graphene oxide/polyvinyl chloride as solid-phase extraction sorbent combined with ion chromatography for the determination of sulfonamides in cosmetics. *Anal. Chim. Acta* **2015**, *888*, 75–84. [CrossRef] [PubMed]
33. Abdolmohammad-Zadeh, H.; Falaghi, S.; Rahimpout, E. An innovative nano-sorbent for selective solid-phase extraction and spectrophotometric determination of p-amino benzoic acid in cosmetic products. *Int. J. Cosmet. Sci.* **2014**, *36*, 140–147. [CrossRef] [PubMed]
34. Arthur, C.L.; Pawliszyn, J. Solid phase microextraction with thermal desorption using fused silica optical fibers. *Anal. Chem.* **1990**, *62*, 2145–2148. [CrossRef]
35. Ara, K.M.; Pandidan, S.; Aliakbari, A.; Raofie, F.; Amini, M.M. Porous-membrane-protected polyaniline-coated SBA-15 nanocomposite micro-solid-phase extraction followed by high-performance liquid chromatography for the determination of parabens in cosmetic products and wastewater. *J. Sep. Sci.* **2015**, *38*, 1213–1224. [CrossRef] [PubMed]
36. Yazdi, M.N.; Yamini, Y.; Asiabi, H. Fabrication of polypyrrole-silver nanocomposite for hollow fiber solid phase microextraction followed by HPLC/UV analysis for determination of parabens in water and beverages samples. *J. Food Compost. Anal.* **2018**, *74*, 18–26. [CrossRef]
37. Ma, M.; Wang, H.; Zhen, Q.; Zhang, M.; Du, X. Development of nitrogen-enriched carbonaceous material coated titania nanotubes array as a fiber coating for solid-phase microextraction of ultraviolet filters in environmental water. *Talanta* **2017**, *167*, 118–125. [CrossRef]
38. Li, Y.; Yang, Y.; Liu, H.; Wang, X.; Du, X. Fabrication of a novel Ti–TiO_2–ZrO_2 fiber for solid phase microextraction followed by high performance liquid chromatography for sensitive determination of UV filters in environmental water samples. *Anal. Methods* **2014**, *6*, 8519–8525. [CrossRef]
39. Li, L.; Guo, R.; Li, Y.; Guo, M.; Wang, X.; Du, X. In situ growth and phenyl functionalization of titania nanoparticles coating for solid-phase microextraction of ultraviolet filters in environmental water samples followed by high performance liquid chromatography–UV detection. *Anal. Chim. Acta* **2015**, *867*, 38–46. [CrossRef] [PubMed]

40. Yang, Y.; Li, Y.; Liu, H.; Wang, X.; Du, X. Electrodeposition of gold nanoparticles onto an etched stainless steel wire followed by a self-assembled monolayer of octanedithiol as a fiber coating for selective solid-phase microextraction. *J. Chromatogr. A* **2014**, *1372*, 25–33. [CrossRef] [PubMed]
41. Mei, M.; Huang, X. Online analysis of five organic ultraviolet filters in environmental water samples using magnetism-enhanced monolith-based in-tube solid phase microextraction coupled with high-performance liquid chromatography. *J. Chromatogr. A* **2017**, *1525*, 1–9. [CrossRef] [PubMed]
42. Wu, T.; Wuang, J.; Liang, W.; Zang, X.; Wang, C.; Wu, Q.; Wang, Z. Single layer graphitic carbon nitride-modified graphene composite as a fiber coating for solid-phase microextraction of polycyclic aromatic hydrocarbons. *Microchim. Acta* **2017**, *184*, 2171–2180. [CrossRef]
43. Tong, S.; Liu, Q.; Li, Y.; Zhou, W.; Jia, Q.; Duan, T. Preparation of porous polymer monolithic column incorporated with graphene nanosheets for solid phase microextraction and enrichment of glucocorticoids. *J. Chromatogr. A* **2012**, *1253*, 22–31. [CrossRef]
44. Wang, Z.; Jin, P.; Zhou, S.; Wang, X.; Du, X. Controlled growth of a porous hydroxyapatite nanoparticle coating on a titanium fiber for rapid and efficient solid-phase microextraction of polar chlorophenols, triclosan and bisphenol A from environmental water. *Anal. Methods* **2018**, *10*, 3237–3247. [CrossRef]
45. Baltussen, E.; Sandra, P.; David, F.; Cramers, C.A. Stir bar sorptive extraction (SBSE), a novel extraction technique for aqueous samples: Theory and principles. *J. Microcolumn Sep.* **1999**, *11*, 737–747. [CrossRef]
46. Wang, C.; Zhou, W.; Liao, X.; Wang, X.; Chen, Z. Covalent immobilization of metal organic frameworks onto chemical resistant poly(ether ketone) jacket for stir bar extraction. *Anal. Chim. Acta* **2018**, *1025*, 124–133. [CrossRef]
47. Fresco-Cala, B.; Cárdenas, S. Nanostructured hybrid monolith with integrated stirring for the extraction of UV-filters from water and urine samples. *Talanta* **2018**, *182*, 391–395. [CrossRef]
48. Siritham, C.; Thammakhet-Buranachai, C.; Thavarungkul, P.; Kanatharana, P. A stir foam composed of graphene oxide, poly(ethylene glycol) and natural latex for the extraction of preservatives and antioxidant. *Microchim. Acta* **2018**, *185*, 148–156. [CrossRef] [PubMed]
49. Zang, X.; Chang, Q.; Liang, W.; Wu, T.; Wang, C.; Wang, Z. Micro-solid phase extraction of chlorophenols using reduced graphene oxide functionalized with magnetic nanoparticles and graphitic carbon nitride as the adsorbent. *Microchim. Acta* **2018**, *185*, 18–26. [CrossRef] [PubMed]
50. Anastassiades, M.; Lehotay, S.J.; Stajnbaher, D.; Schenk, F.J. Fast and easy multiresidue method employing acetonitrile extraction/partitioning and "dispersive solid-phase extraction" for determination of pesticide residues in produce. *J. Aoac Int.* **2003**, *86*, 412–431. [CrossRef] [PubMed]
51. Rocío-Bautista, P.; Martínez-Benito, C.; Pino, V.; Pasán, J.; Ayala, J.H.; Ruiz-Pérez, C.; Alfonso, A.M. The metal–organic framework HKUST-1 as efficient sorbent in a vortex-assisted dispersive micro solid-phase extraction of parabens from environmental waters, cosmetic creams, and human urine. *Talanta* **2015**, *139*, 13–20. [CrossRef] [PubMed]
52. Rashvand, M.; Vosough, M. Graphene oxide–polyaniline nanocomposite as a potential sorbent for dispersive solid-phase extraction and determination of selected pharmaceutical and personal care products in wastewater samples using HPLC with a diode-array detector. *Anal. Methods* **2016**, *8*, 1898–1907. [CrossRef]
53. Li, N.; Zhu, Q.; Yang, Y.; Huang, J.; Dang, X.; Chen, H. A novel dispersive solid-phase extraction method using metal-organic framework MIL-101 as the adsorbent for the analysis of benzophenones in toner. *Talanta* **2015**, *132*, 713–718. [CrossRef]
54. Gao, R.; Kong, X.; Su, F.; He, X.; Chen, L.; Zhang, Y. Synthesis and evaluation of molecularly imprinted core–shell carbon nanotubes for the determination of triclosan in environmental water samples. *J. Chromatogr. A* **2010**, *1217*, 8095–8102. [CrossRef]
55. Zhai, Y.; Li, N.; Lei, L.; Yang, X.; Zhang, H. Dispersive micro-solid-phase extraction of hormones in liquid cosmetics with metal-organic framework. *Anal. Methods* **2014**, *6*, 9435–9445. [CrossRef]
56. Liu, G.; Jia, H.; Li, N.; Li, X.; Yu, Z.; Wang, J.; Song, Y. High-fluorescent carbon dots (CDs) originated from China grass carp scales (CGCS) for effective detection of Hg(II) ions. *Microchem. J.* **2019**, *145*, 718–728. [CrossRef]
57. Tahmasebi, E.; Yamini, Y.; Mehdinia, A.; Rouhi, F. Polyaniline-coated Fe_3O_4 nanoparticles: An anion exchange magnetic sorbent for solid-phase extraction. *J. Sep. Sci.* **2012**, *35*, 2256–2265. [CrossRef]

58. Ghambari, H.; Reyes-Gallardo, E.M.; Lucena, R.; Saraji, M.; Cárdenas, S. Recycling polymer residues to synthesize magnetic nanocomposites for dispersive micro-solid phase extraction. *Talanta* **2017**, *170*, 451–456. [CrossRef]
59. Abbasghorbani, M.; Attaran, A.; Payehghadr, M. Solvent-assisted dispersive micro-SPE by using aminopropyl-functionalized magnetite nanoparticle followed by GC-PID for quantification of parabens in aqueous matrices. *J. Sep. Sci.* **2013**, *36*, 311–319. [CrossRef] [PubMed]
60. Ariffin, M.M.; Sohaime, N.M.; Yih, B.S.; Saleh, N.M. Magnetite nanoparticles coated with surfactant Sylgard 309 and its application as an adsorbent for paraben extraction from pharmaceutical and water samples. *Anal. Methods* **2019**, *11*, 4126–4136. [CrossRef]
61. Ariffin, M.M.; Azmi, A.H.; Saleh, N.M.; Mohamad, S.; Rozi, S.K. Surfactant functionalization of magnetic nanoparticles: A greener method for parabens determination in water samples by using magnetic solid phase extraction. *Microchem. J.* **2019**, *147*, 930–940. [CrossRef]
62. Casado-Carmona, F.A.; Alcudia-León, M.C.; Lucena, R.; Cárdenas, S.; Valcárcel, M. Magnetic nanoparticles coated with ionic liquid for the extraction of endocrine disrupting compounds from waters. *Microchem. J.* **2016**, *128*, 347–353. [CrossRef]
63. Mehdinia, A.; Esfandiarnejad, R.; Jabbari, A. Magnetic nanocomposite of self-doped polyaniline–graphene as a novel sorbent for solid-phase extraction. *J. Sep. Sci.* **2015**, *38*, 141–147. [CrossRef]
64. Mehdinia, A.; Bahrami, M.; Mozaffari, S. A comparative study on different functionalized mesoporous silica nanomagnetic sorbents for efficient extraction of parabens. *J. Iran Chem. Soc.* **2015**, *12*, 1543–1552. [CrossRef]
65. Feng, J.; He, X.; Liu, X.; Sun, X.; Li, Y. Preparation of magnetic graphene/mesoporous silica composites with phenyl-functionalized pore-walls as the restricted access matrix solid phase extraction adsorbent for the rapid extraction of parabens from water-based skin toners. *J. Chromatogr. A* **2016**, *1465*, 20–29. [CrossRef] [PubMed]
66. Jalilian, N.; Ebrahimzadeh, H.; Asgharinezhad, A.A. Preparation of magnetite/multiwalled carbon nanotubes/metal-organic framework composite for dispersive magnetic micro solid phase extraction of parabens and phthalate esters from water samples and various types of cream for their determination with liquid chromatography. *J. Chromatogr. A* **2019**, *1608*, 460426. [CrossRef]
67. Shavar, A.; Soltani, R.; Saraji, M.; Dinari, M.; Alijani, S. Covalent triazine-based framework for micro solid-phase extraction of parabens. *J. Chromatogr. A* **2018**, *1565*, 48–56. [CrossRef]
68. Yusoff, M.M.; Raoov, M.; Yahaya, N.; Salleh, N.M. An ionic liquid loaded magnetically confined polymeric mesoporous adsorbent for extraction of parabens from environmental and cosmetic samples. *RSC Adv.* **2017**, *7*, 35832–35844. [CrossRef]
69. Pastor-Belda, M.; Marín-Soler, L.; Campillo, N.; Viñas, P.; Hernández-Córdoba, M. Magnetic carbon nanotube composite for the preconcentration of parabens from water and urine samples using dispersive solid phase extraction. *J. Chromatogr. A* **2018**, *1564*, 102–109. [CrossRef] [PubMed]
70. Gashemi, E.; Sillanpää, M. Ultrasound-assisted solid-phase extraction of parabens from environmental and biological samples using magnetic hydroxyapatite nanoparticles as an efficient and regenerable nanosorbent. *Microchim. Acta* **2019**, *186*, 622–628. [CrossRef] [PubMed]
71. Li, W.; Wang, R.; Chen, Z. Metal-organic framework-1210(zirconium/cuprum) modified magnetic nanoparticles for solid phase extraction of benzophenones in soil samples. *J. Chromatogr. A* **2019**, *1607*, 460403. [CrossRef]
72. Piovesana, S.; Capriotti, A.L.; Cavaliere, C.; La Barbera, G.; Samperi, R.; Chiozzi, R.Z.; Laganà, A. A new carbon-based magnetic material for the dispersive solid-phase extraction of UV filters from water samples before liquid chromatography–tandem mass spectrometry analysis. *Anal. Bioanal. Chem.* **2017**, *409*, 4181–4194. [CrossRef] [PubMed]
73. Cheng, J.; Kong, X.; Liu, S.; Che, D.; Sun, Z.; Li, G.; Ping, M.; Tang, J.; You, J. Determination of ultraviolet filters in domestic wastewater by LC–MS coupled with polydopamine-based magnetic solid-phase extraction and isotope-coded derivatization. *Chromatographia* **2018**, *81*, 1673–1684. [CrossRef]
74. Román, I.P.; Chisvert, A.; Canals, A. Dispersive solid-phase extraction based on oleic acid-coated magnetic nanoparticles followed by gas chromatography-mass spectrometry for UV-filter determination in water samples. *J. Chromatogr. A* **2011**, *1218*, 2467–2475. [CrossRef]

75. Giokas, D.L.; Zhu, Q.; Pan, Q.; Chisvert, A. Cloud point–dispersive μ-solid phase extraction of hydrophobic organic compounds onto highly hydrophobic core–shell Fe_2O_3@C magnetic nanoparticles. *J. Chromatogr. A* **2012**, *1251*, 33–39. [CrossRef]
76. Yang, Y.; Ma, X.; Feng, F.; Dang, X.; Huang, J.; Chen, H. Magnetic solid-phase extraction of triclosan using core-shell Fe_3O_4@MIL-100 magnetic nanoparticles, and its determination by HPLC with UV detection. *Microchim. Acta* **2016**, *183*, 2467–2472. [CrossRef]
77. Li, Y.; Zhang, H.; Chen, Y.; Huang, L.; Lin, Z.; Cai, Z. Core-shell structured magnetic covalent organic framework nanocomposites for triclosan and triclocarban adsorption. *ACS Appl. Mater. Interfaces* **2019**, *11*, 22492–22500. [CrossRef]
78. Li, F.; Cai, C.; Cheng, J.; Zhou, H.; Ding, K.; Zhang, L. Extraction of endocrine disrupting phenols with iron-ferric oxide core-shell nanowires on graphene oxide nanosheets, followed by their determination by HPLC. *Microchim. Acta* **2015**, *182*, 2503–2511. [CrossRef]
79. Jiang, X.; Cheng, J.; Zhou, H.; Li, F.; Wung, W.; Ding, K. Polyaniline-coated chitosan-functionalized magnetic nanoparticles: Preparation for the extraction and analysis of endocrine-disrupting phenols in environmental water and juice samples. *Talanta* **2015**, *141*, 239–246. [CrossRef] [PubMed]
80. Du, W.; Zhang, B.; Guo, P.; Chen, G.; Chang, C.; Fu, Q. Facile preparation of magnetic molecularly imprinted polymers for the selective extraction and determination of dexamethasone in skincare cosmetics using HPLC. *J. Sep. Sci.* **2018**, *41*, 2441–2452. [CrossRef]
81. Liu, M.; Li, X.; Li, J.; Wu, Z.; Wang, F.; Liu, L.; Tan, X.; Lei, F. Selective separation and determination of glucocorticoids in cosmetics using dual-template magnetic molecularly imprinted polymers and HPLC. *J. Colloid Interf. Sci.* **2017**, *504*, 124–133. [CrossRef] [PubMed]
82. Li, Y.; Chen, X.; Xia, L.; Xiao, X.; Li, G. Magnetic metal-organic frameworks-101 functionalized with graphite-like carbon nitride for the efficient enrichment of glucocorticoids in cosmetics. *J. Chromatogr. A* **2019**, *1606*, 460382. [CrossRef]
83. Khani, R.; Sobhani, S.; Yari, T. Magnetic dispersive micro solid-phase extraction of trace Rhodamine B using imino-pyridine immobilized on iron oxide as nanosorbent and optimization by Box–Behnken design. *Microchem. J.* **2019**, *146*, 471–478. [CrossRef]
84. Bagheri, H.; Daliri, R.; Roostaie, A. A novel magnetic poly(aniline-naphthylamine)-based nanocomposite for micro solid phase extraction of rhodamine B. *Anal Chim. Acta* **2013**, *794*, 38–46. [CrossRef]
85. Tarigh, G.D.; Shemirani, F. Magnetic multi-wall carbon nanotube nanocomposite as an adsorbent for preconcentration and determination of lead (II) and manganese (II) in various matrices. *Talanta* **2013**, *115*, 744–750. [CrossRef]
86. Xia, L.; Chen, X.; Xiao, X.; Li, G. Magnetic-covalent organic polymer solid-phase extraction coupled with high-performance liquid chromatography for the sensitive determination of fluorescent whitening agents in cosmetics. *J. Sep. Sci.* **2018**, *41*, 3733–3741. [CrossRef]
87. Liu, M.; Li, X.Y.; Li, J.J.; Su, X.M.; Wu, Z.Y.; Li, P.F.; Lei, F.H.; Tan, X.C.; Shi, Z.W. Synthesis of magnetic molecularly imprinted polymers for the selective separation and determination of metronidazole in cosmetic samples. *Anal. Bioanal. Chem.* **2015**, *407*, 3875–3880. [CrossRef]
88. Maidatsi, K.V.; Chatzimitakos, T.G.; Sakkas, V.A.; Stalikas, C.D. Octyl-modified magnetic graphene as a sorbent for the extraction and simultaneous determination of fragrance allergens, musks and phthalates in aqueous samples by gas chromatography with mass spectrometry. *J. Sep. Sci.* **2015**, *38*, 3758–3765. [CrossRef] [PubMed]
89. Zhang, H.; Lai, H.; Li, G.; Hu, Y. $CoFe_2O_4$@HNT/AuNPs for rapid magnetic solid-phase extraction and efficient SERS detection of complex samples all-in-one. *Anal. Chem.* **2020**, *92*, 4607–4613. [CrossRef] [PubMed]
90. Benedé, J.L.; Chisvert, A.; Giokas, D.L.; Salvador, A. Development of stir bar sorptive-dispersive microextraction mediated by magnetic nanoparticles and its analytical application to the determination of hydrophobic organic compounds in aqueous media. *J. Chromatogr. A* **2014**, *1362*, 25–33. [CrossRef] [PubMed]
91. Benedé, J.L.; Chisvert, A.; Giokas, D.L.; Salvador, A. Determination of ultraviolet filters in bathing waters by stir bar sorptive–dispersive microextraction coupled to thermal desorption–gas chromatography–mass spectrometry. *Talanta* **2016**, *147*, 246–252. [CrossRef] [PubMed]

92. Benedé, J.L.; Chisvert, A.; Moyano, C.; Giokas, D.L.; Salvador, A. Expanding the application of stir bar sorptive-dispersive microextraction approach to solid matrices: Determination of ultraviolet filters in coastal sand samples. *J. Chromatogr. A* **2019**, *1564*, 25–33. [CrossRef] [PubMed]
93. Benedé, J.L.; Chisvert, A.; Giokas, D.L.; Salvador, A. Stir bar sorptive-dispersive microextraction mediated by magnetic nanoparticles–nylon 6 composite for the extraction of hydrophilic organic compounds in aqueous media. *Anal. Chim. Acta* **2016**, *926*, 63–71. [CrossRef]
94. Grau, J.; Benedé, J.L.; Serrano, J.; Segura, A.; Chisvert, A. Stir bar sorptive-dispersive microextraction for trace determination of triphenyl and diphenyl phosphate in urine of nail polish users. *J. Chromatogr. A* **2019**, *1593*, 9–16. [CrossRef]
95. Miralles, P.; van Gemert, I.; Chisvert, A.; Salvador, A. Stir bar sorptive-dispersive microextraction mediated by magnetic nanoparticles-metal organic framework composite: Determination of N-nitrosamines in cosmetic products. *J. Chromatogr. A* **2019**, *1604*, 460465. [CrossRef]
96. Vállez-Gomis, V.; Grau, J.; Benedé, J.L.; Chisvert, A.; Salvador, A. Reduced graphene oxide-based magnetic composite for trace determination of polycyclic aromatic hydrocarbons in cosmetics by stir bar sorptive dispersive microextraction. *J. Chromatogr. A* **2020**, *1624*, 461229. [CrossRef]
97. Makkliang, F.; Kanatharana, P.; Thavarungkul, P.; Thammakhet-Buranachai, C. A miniaturized monolith-MWCNTs-COOH multi-stir-rod micro extractor device for trace parabens determination in cosmetic and personal care products. *Talanta* **2018**, *184*, 429–436. [CrossRef]
98. Alcudia-León, M.C.; Lucena, R.; Cárdenas, S.; Valcárcel, M. Determination of parabens in waters by magnetically confined hydrophobic nanoparticle microextraction coupled to gas chromatography/mass spectrometry. *Microchem. J.* **2013**, *110*, 643–648. [CrossRef]
99. Wang, H.; Cocovi-Solberg, D.J.; Hu, B.; Miró, M. 3D-Printed microflow injection analysis platform for online magnetic nanoparticle sorptive extraction of antimicrobials in biological specimens as a front end to liquid chromatographic assays. *Anal. Chem.* **2017**, *89*, 12541–12549. [CrossRef] [PubMed]
100. Fresco-Cala, B.; Cárdenas, S. Preparation of macroscopic carbon nanohorn-based monoliths in polypropylene tips by medium internal phase emulsion for the determination of parabens in urine samples. *Talanta* **2019**, *198*, 295–301. [CrossRef]
101. Wang, L.; Zang, X.; Wang, C.; Wang, Z. Graphene oxide as a micro-solid-phase extraction sorbent for the enrichment of parabens from water and vinegar samples. *J. Sep. Sci.* **2014**, *37*, 1656–1662. [CrossRef] [PubMed]
102. Montesdeoca-Esponda, S.; Sosa-Ferrera, Z.; Kabir, S.; Furton, K.G.; Santana-Rodríguez, J.J. Fabric phase sorptive extraction followed by UHPLC-MS/MS for the analysis of benzotriazole UV stabilizers in sewage samples. *Anal. Bioanal. Chem.* **2015**, *407*, 8137–8150. [CrossRef] [PubMed]

Use of green alternative solvents in dispersive liquid-liquid microextraction: A review

J. Sep. Sci. 45 (2022) 210-222

DOI: 0.1002/jssc.202100609

Received: 30 July 2021 | Revised: 1 September 2021 | Accepted: 1 September 2021

DOI: 10.1002/jssc.202100609

REVIEW ARTICLE

JOURNAL OF SEPARATION SCIENCE

Use of green alternative solvents in dispersive liquid-liquid microextraction: A review

José Grau | **Cristian Azorín** | **Juan L. Benedé** | **Alberto Chisvert** | **Amparo Salvador**

Department of Analytical Chemistry, GICAPC Research group, University of Valencia, Burjassot, Spain

Correspondence
Alberto Chisvert, Department of Analytical Chemistry, GICAPC Research group, University of Valencia, 50 Doctor Moliner St., 46100 Burjassot, Valencia, Spain.
Email: alberto.chisvert@uv.es

Funding information
Spanish Ministry of Science and Innovation, Grant/Award Number: PID2020-118924RB-I00

Dispersive liquid-liquid microextraction is one of the most widely used microextraction techniques currently in the analytical chemistry field, mainly due to its simplicity and rapidity. The operational mode of this approach has been constantly changing since its introduction, adapting to new trends and applications. Most of these changes are related to the nature of the solvent employed for the microextraction. From the classical halogenated solvents (e.g., chloroform or dichloromethane), different alternatives have been proposed in order to obtain safer and non-pollutants microextraction applications. In this sense, low-density solvents, such as alkanols, switchable hydrophobicity solvents, and ionic liquids were the first and most popular replacements for halogenated solvents, which provided similar or better results than these classical dispersive liquid-liquid microextraction solvents. However, despite the good performances obtained with low-density solvents and ionic liquids, researchers have continued investigating in order to obtain even greener solvents for dispersive liquid-liquid microextraction. For that reason, in this review, the evolution over the last five years of the three types of solvents already mentioned and two of the most promising solvent alternatives (i.e., deep eutectic solvents and supramolecular solvents), have been studied in detail with the purpose of discussing which one provides the greenest alternative.

KEYWORDS
deep eutectic solvents, dispersive liquid-liquid microextraction, green chemistry, supramolecular solvents

Article Related Abbreviations: ChCl, choline chloride; DES, deep eutectic solvent; DLLME, dispersive liquid-liquid microextraction; IL, Ionic liquid; HFIP, hexafluoroisopropanol; LDS, low-density solvent; LTTM, low transition temperature material; NADES, natural deep eutectic solvent; SHS, switchable hydrophobicity solvent; SFOD, solidification of floating organic drop; SSME, supramolecular solvent microextraction; SUPRAs, supramolecular solvents; TBAB, tetrabutylammonium bromide; THF, tetrahydrofuran

1 | INTRODUCTION

The use of microextraction techniques has grown substantially during the last decades over classical extraction techniques such as SPE and liquid-liquid extraction. The high demand for obtaining low limits of detection, but reducing the analysis time and the consumption of organic solvents, have increased the interest in employing this kind of approach [1,2].

In this sense, dispersive liquid-liquid microextraction (DLLME), introduced by Rezaee et al. in 2006 [3], quickly became one of the most widespread microextraction techniques, taking advantage of its simplicity, rapidity, low cost, and the high enrichment factors achieved with this approach. Originally, a hydrophobic and high-density extraction solvent (e.g., dichloromethane, chloroform, tetrachloroethylene, among others) was quickly dispersed into a conical tube containing the aqueous sample as donor phase by means of the so-called dispersant solvent, which is miscible in both the extraction solvent and sample (e.g., acetone, ethanol, acetonitrile, among others). The microemulsion formed by hundreds of microdroplets allows a large surface area to exist between the different phases, favoring the instant transfer of the analytes from the donor phase to the extraction solvent. After extraction, phase separation is achieved by centrifugation, where the settled phase is easily collected with a syringe for later measurement in the analytical instrument. This is the reason for using high-density organic solvents as extraction solvents. A scheme of the DLLME approach is presented in Figure 1.

Since its introduction, the interest in DLLME has only grown. As can be seen in Figure 2, the number of applications of DLLME-based approaches has increased substantially during the last years, reaching over 400 DLLME applications just in 2020. These values reflect its high potential and the great attention that the scientific community has paid to this approach in the last years. As already stated, the popularity of this approach can be easily explained due to its simplicity and the reduced analysis times.

In order to reduce the volume of organic solvents, different modifications of the original DLLME procedure, where the dispersion of the extraction solvent is assisted by external energy sources, were introduced (e.g., vortex-assisted [4] and ultrasound-assisted [5]). However, the main drawback of conventional DLLME is the use of high-density halogenated solvents that are commonly employed as extraction solvents. Even though the employed volume of these solvents for DLLME is in the microliter range, its use in routine analysis, where hundreds of analyses can be performed per day, should not be recommended due to the environmental and healthy point of view, since the generated wastes are usually higher than the pollutants that are being monitored in most of the DLLME-based applications.

For that reason, during the last years, greener alternatives have been proposed in order to be less harmful to the environment and the researcher [6]. In this context, the aim of this review is to compile and discuss the state of the art in the use of greener solvents as extraction solvents in DLLME. Due to the vast number of published analytical methods employing DLLME-based approaches, this review does not provide an exhaustive revision of all of them, but only emphasizes the developments and trends in the field.

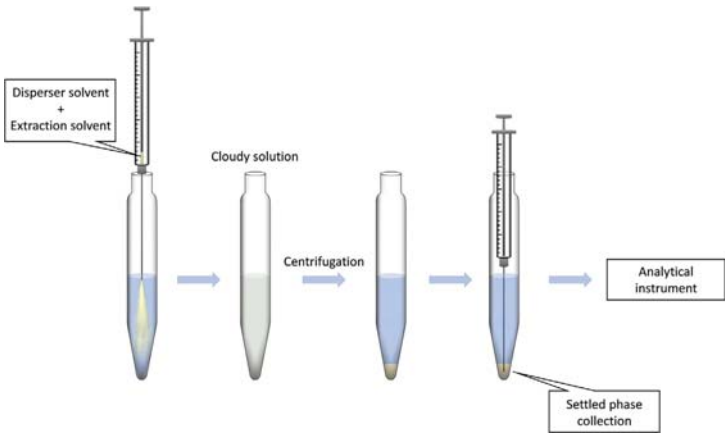

FIGURE 1 Scheme of the traditional procedure of dispersive liquid-liquid microextraction (DLLME)

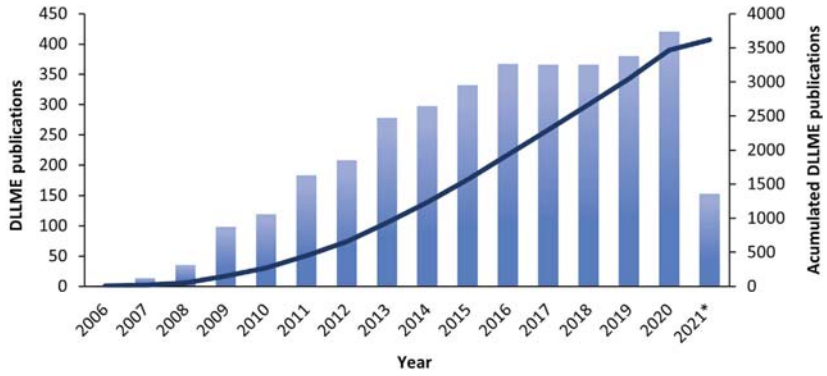

FIGURE 2 Publications on dispersive liquid-liquid microextraction (DLLME) approaches since its introduction (line represents the accumulated number; *current year)

2 | FIRST STEPS IN GREEN DLLME

2.1 | Low-density solvents

As said before, in conventional DLLME, the high-density halogenated solvents are recovered from the bottom of a conical tube. The small volume of the bottom of the conical tubes allows the solvent to be settled in a small drop making it easy to retrieve small volumes of extraction solvent. However, when low-density solvents (LDSs), i.e., all those conventional non-halogenated solvents that are less denser than water, are employed, the situation is different. In this case, the extraction solvent remains at the top of the sample after the phase separation, thus forming a thin film difficult and tedious to collect. In order to correct this limitation, Leong and Huang [7] made use of the solidification of floating organic drop (SFOD) approach [8] to collect it. In this operational mode, both the disperser and the LDS are introduced as in conventional DLLME but, after the phase separation, the LDS containing the target analytes is frozen by introducing the flask in an ice bath. Then, the drop-shaped solid formed is easily retrieved from the top of the solution with a spatula.

In these approaches, fatty alcohols, such as decanol, undecanol, or dodecanol, are usually employed as extraction solvents. Nevertheless, despite these LDSs are less harmful than halogenated solvents, and the employed amounts are small, they are still organic solvents that must be treated after use due to their pollutant behavior [9,10].

2.2 | Switchable hydrophilicity solvents

Recently, a new kind of LDS named switchable-hydrophilicity solvents (SHSs) [11] have been introduced in microextraction approaches. Although they have not been used exactly as extraction solvents in DLLME, their performance is similar to this approach in terms of dispersion. SHSs are solvents consisting of amidines, secondary/tertiary amines, or saturated fatty acids that show the capability of changing their hydrophilicity and, therefore, change from slightly miscible to completely miscible with water by means of a simple change in the aqueous medium. This change in miscibility is usually driven by an acid-base equilibrium after the addition of CO_2 for basic SHSs or CO_3^{2-} for acidic SHSs [12].

In general, the pH change enhances the formation of a water-soluble salt, hence solubilizing the SHS. After that, the reaction is forced backward producing the separation of the two phases. In this sense, the employment of SHSs is based on the principles of the classical homogeneous liquid-liquid extraction [13], achieving an extremely large contact area and, therefore, improving the extraction efficiency. Moreover, this is achieved without the use of disperser organic solvents, avoiding the centrifugation step [11].

Despite all the above, SHSs have not attracted the interest compared with other alternative solvents used in liquid-phase microextraction techniques. First of all, in spite of employing CO_2 for the solubilization step, the subsequent pH change is normally performed with strong acids [14–16] or strong bases [17,18]. Second, about their safety, some SHSs (especially, those formed from secondary amines) are expected to be safer than traditional solvents in some terms like flammability or smog formation [19]. However, some of these amines are compounds with well-known toxic properties [20,21]. On the other hand, alkanoic acids, even though their environmental impact has been discussed [22,23], some of them (e.g., dodecanoic acid, also known as lauric acid) are relatively harmless to the environment

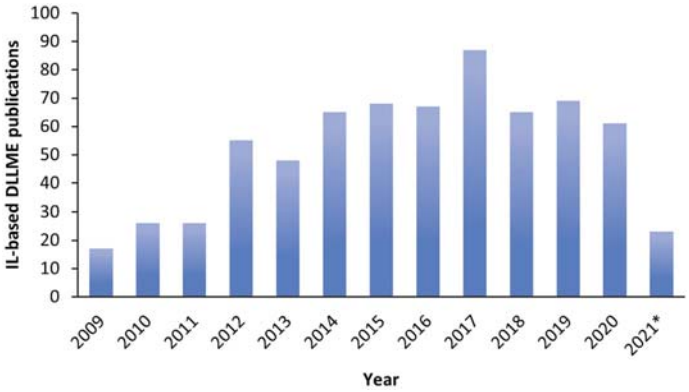

FIGURE 3 Publications on ionic liquid (IL)-based dispersive liquid-liquid microextraction (DLLME) approaches (*current year)

and non-toxic. Moreover, LDSs are still simple solvents and their extraction versatility and efficiency cannot compete with more complex 'tailor-made' extraction solvents described in the following sections [24,25].

2.3 | Ionic liquids

Ionic liquids (ILs) are defined as substances composed of ions whose melting point is less than 100°C, which result from the combination of an organic cation and an organic or inorganic anion [26].

ILs present exceptional attributes to be employed as microextraction solvents, and moreover, they possess high thermal stability and low vapor pressure. Moreover, some of their properties such as viscosity, density, and solubility can be tuned by combining properly the different cations and anions available [26,27]. Furthermore, they can be modified and functionalized to empower specific interactions with the analyte, promoting extraction efficiency. Then, it is obvious that they were a good alternative to be used in DLLME in place of conventional solvents.

The employment of ILs in DLLME was introduced for the first time in 2009 by Liu et al. [28], who used the ionic liquid 1-hexyl-3-methylimidazolium hexafluorophosphate ($[C_6MIM][PF_6]$) as an extraction solvent for the extraction of heterocyclic insecticides in water samples prior to LC-UV visible analysis. Since then, many types of ILs have been incorporated into the different microextraction techniques beyond DLLME, seeking to exploit their tuneable properties, becoming very popular in the sample preparation step [29,30].

In Figure 3, the evolution of the employment of ILs in DLLME approaches is shown. It can be observed how the number of publications increased during the first years. However, since 2014 it has remained constant.

This fact could be explained by observing the main limitations of ILs. On one hand, they have problems to be coupled with chromatographic devices and atomic absorption instrumentation. Their lack of volatility is incompatible with GC [31], although different approaches were proposed to overcome this limitation [32–35]. Besides, as a result of their low volatility and high viscosity, they are also incompatible with LC–MS systems, since the formation of the electrospray is highly affected, which redounds in serious matrix effects and signal drift [36,37]. High viscosity may also be difficult in handling, diffusion, and mass transfer. Finally, their high thermal stability should also be considered, because the elevated temperatures needed in electrothermal atomic absorption spectroscopy during the pyrolysis step can involve analyte loss [31].

On the other hand, the environmental aspects of most of these ILs should be discussed. ILs are usually called green solvents due to their low vapor pressure, which avoids ILs to reach the atmosphere or to be inhaled by the operator. However, usually, the components of the synthesis or the final products are toxic, and thus, they cannot be considered green [38]. Therefore, in spite of the great properties of ILs, Deetlefs and Seddon [39] concluded that they are 'green, but not green enough.'

3 | POTENTIAL GREEN SOLVENTS

Attending to the disadvantages presented by the previous solvents, and despite the improvements compared to halogenated solvents, other alternatives have been emerged in order to obtain tailorable green solvents with huge extraction capabilities. In this regard, the objective of this review has focused on the evaluation of two potential alternative solvents for DLLME and their evolution from 2016.

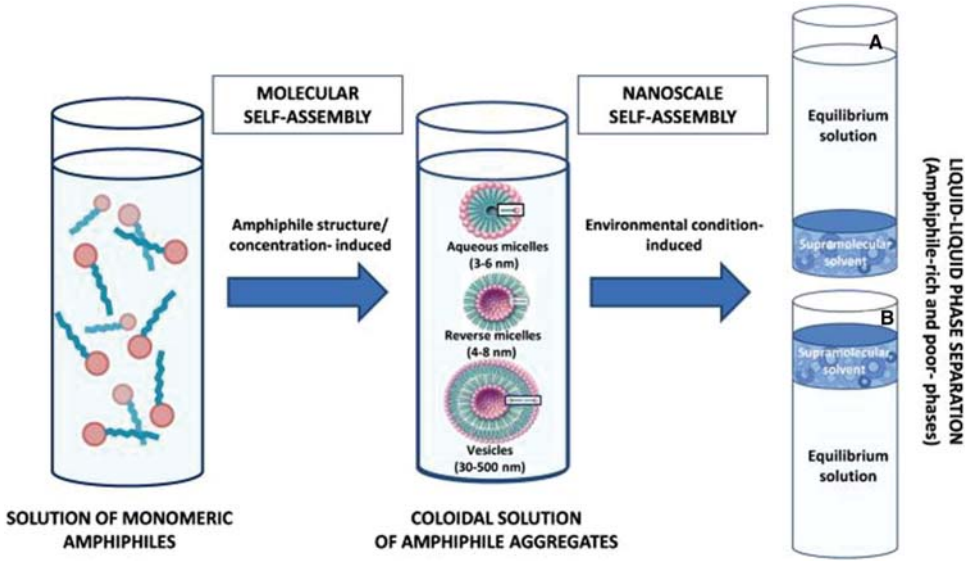

FIGURE 4 Self-assembly processes in supramolecular solvent formation. *Reproduced with permission from* [40]

3.1 | Supramolecular solvents

Supramolecular solvents (SUPRAs) are solvents generated after the coacervation of previously formed micelles in a solution. First, amphiphiles are added to the solution, and when the critical aggregation concentration is achieved the amphiphiles groups are reorganized in micelles. Once micelles are formed, a change in the environment of the solution is produced in order to reduce the repulsion interaction between the amphiphiles forming the micelle. This action allows more amphiphile groups to be introduced into the micelles, forming bigger aggregates, that will interact with other aggregates forming the supramolecular solvent [40]. A scheme of coacervation of SUPRAs is presented in Figure 4.

The environmental disruption to produce the coacervation process will depend on the class of amphiphile employed. On one hand, for ionic amphiphiles, neutralization of the charge driven by the addition of a counterion, or a change of the pH will reduce the electrostatic repulsion. On the other hand, for non-ionic SUPRAs, the addition of an organic solvent to produce the desolvation of the hydrophilic heads is the most usual approach [41].

These SUPRAs possess exceptional extraction capabilities due to their great surface and their different polarity environments. Moreover, they can be synthesized in situ during the analysis and they do not need extra treatment to be introduced in LC systems (as it happens with ILs) [41], making them really attractive for microextraction approaches.

The first time that SUPRAs were employed for DLLME (also called supramolecular solvent microextraction (SSME) when these solvents are employed as extraction solvent) was in 2009. In this application, Ballesteros-Gómez et al. [42] employed a SUPRA formed by decanoic acid, which was organized in reversed micelles, and tetrahydrofuran (THF) as coacervation agent for the determination of benzo[a]pyrene, bisphenol A, and ochratoxin from beverages. After the microextraction process, the SUPRA phase was directly injected into the LC system.

Since 2016, more than 100 works have been published on the use of SUPRAs in DLLME. Nonetheless, no big steps have been made since most of the works published employed similar approaches, using alkanoic acids (i.e., decanoic acid and octanoic acid) as amphiphilic substances and THF as coacervation agent. In 2016, Gemini surfactants were proposed as an alternative in SSME [43]. These Gemini-based SUPRAs have the advantages of possessing a lower critical micelle concentration than the single-chain surfactants and a better dispersive capability [44].

In 2017, Seebunrueng et al. [45] employed tetrabutylammonium bromide (TBAB) as an amphiphilic counter ion and aluminum chloride ($AlCl_3$) in contradistinction to the previous methods employing THF. In this work, the surfactant employed for the microextraction was sodium

dodecyl sulfate instead of the classical fatty compounds. During the same year, Salatti-Dorado et al. [46] used a restricted access SUPRA composed of hexanol and THF for the analysis of bisphenol A in urine. This restricted access SUPRA can be obtained by modifying the environment (i.e., THF-water composition) to obtain the appropriate hydrophilic cavity of the reversed micelles increasing their capability of macromolecule exclusion and thus, reducing the matrix effect. Moreover, the presence of hexanol and THF allows the precipitation of proteins in urine obtaining a cleaner sample.

In 2018, Zong et al. [47] used hexafluoroisopropanol (HFIP) to develop a SUPRA with octanoic acid for the determination of six steroids in urine. One of the main advantages of HFIP is its huge density compared with water, generating a high-density SUPRA that was deposited in the bottom of the flask after the microextraction, allowing to use of smaller amounts of sorbent without the need for extra processes for solvent recovery (i.e., SFOD), unlike the previous SUPRAs employed. Furthermore, HFIP has great extraction capabilities for analytes with hydrogen bond interactions.

During 2019, Chen et al. [48] created a SUPRA of Brij 35 to extract parabens from different types of matrices due to its different hydrophobic and hydrophilic binding sites. In this work, HFIP was used to reduce the cloud point temperature of Brij 35 and to increase the density of the resulting SUPRA. Later that year, Gissawong et al. [49] employed dodecyltrimethylammonium bromide and didodecyldimethylammonium bromide as amphiphiles and sodium chloride as a coacervation agent, for the determination of tetracyclines in food samples. The extraction was performed in alkaline pH, where these compounds are negatively charged improving the electrostatic interactions with the cationic extraction solvent.

In 2020, Najafi et al. [50] employed a surfactant obtained from nonylphenol tetra-ethoxylate. This non-ionic surfactant formed by ethoxylated nonylphenols allows a wide range of interactions (i.e., π-π, hydrogen bonding and hydrophobic, among others). This SUPRA was employed to analyze orthophosphate in water samples using THF for coacervation.

More recently, in 2021, Accioni et al. [51] employed heptafluorobutyric acid as an amphiphilic substance to prepare a SUPRA in order to extract amino acids and oligopeptides. To prepare this SUPRA, the coacervation step was performed in hydrochloric media to protonate the heptafluorobutyric acid to reduce the electrostatic repulsion. After vortexing, the obtained SUPRA with the analytes was separated from the bottom of the flask due to its high density and directly measured with LC-MS/MS.

3.2 | Deep eutectic solvents

Deep eutectic solvents (DESs) are formed by two or three components combined by hydrogen bond interactions, creating a eutectic mixture with a melting point lower than the original parts. A diagram of a eutectic mixture is shown in Figure 5.

The formed DESs share some of the properties with ILs [53], such as thermal stability, low vapor pressure, and low flammability. Moreover, in analogy to ILs, DESs can be tailorable in the function of the behavior of the analytes. However, the starting materials (i.e., a hydrogen bond acceptor and a hydrogen bond donor) differs from those used in ILs (i.e., an organic cation and an (in)organic anion). In addition, their mode of obtention is usually cheaper and safer for the environment and the operator due to their low toxicity and biodegradability [54,55], making DESs ideal solvents for microextraction approaches [56,57].

Regarding DLLME, the first time that was combined with DESs was in 2016 by Farajzadeh et al. [58] for the determination of pesticides in fruit juices and vegetables. In this work, first choline chloride (ChCl) and chlorophenol were mixed and heated for 10 min at 75°C to obtain the DES. Then, the formed DES was quickly injected into the sample solution to obtain a cloudy dispersion. Finally, the mixture was centrifuged, and the sedimented DES was used for subsequent GC analysis.

Since then, the number of papers employing DESs in DLLME has increased substantially. During 2016 and 2017, different strategies were performed in order to improve the dispersion of the DES. In this regard, DES-based vortex-assisted DLLME was introduced by Zeng et al. [59] that also employed SFOD for the simple separation of the extraction solvent upper phase. Moreover, in the same year, Zounr et al. [60] employed ultrasounds to improve the dispersion efficiency of the DES in the sample matrix. Also in 2017, Farajzadeh et al. [61] used air steam as a dispersant agent of the DES.

However, during this first period, the DESs employed cannot be cataloged as 'green'. These were composed of hazardous components such as phenols and halogenated phenols, pollutants as alkanols, or ILs which, at the same time, need a previous synthesis step. Moreover, unlike it happens with SUPRAs, most of DESs cannot be directly introduced in the chromatographic system without a pretreatment with organic solvents.

During the next years, safer components such as menthol [62] and betaine [63] were employed in order to produce greener extraction solvents. However, it was not until 2018 when Panhwar et al. [64] employed a DES formed by two harmless components such as ChCl and ethylene glycol for the analysis of chromium in

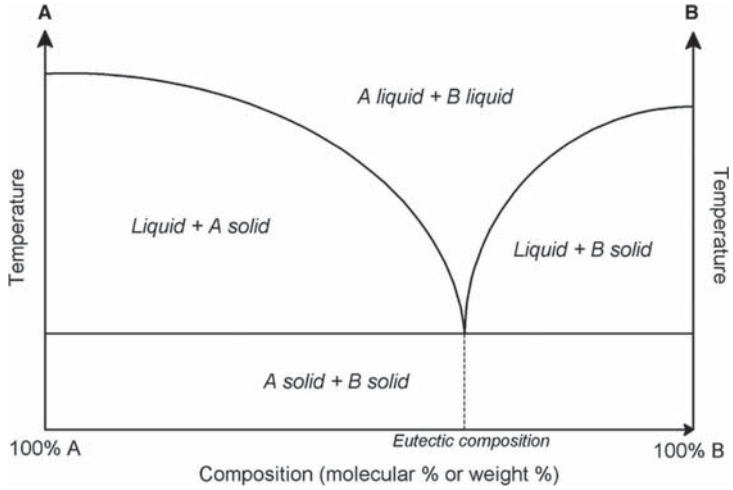

FIGURE 5 Scheme of a eutectic mixture. *Reproduced with permission from* [52]

environmental samples. The DES was obtained by mixing both components and heating at 80°C until the formation of a clear liquid. For the microextraction procedure, first, azadipyrromethene as a chelating agent and the DES were dissolved in the sample. Later, the DES was separated from the water sample employing THF.

In 2019, Altunay et al. [65] employed for the first time a DESs synthesized by 'natural' components, termed as 'natural DES' (NADES) [66], for a DLLME application. In this work, citric acid and sucrose were used in order to extract some metals from honey. In this method, THF was employed as an aprotic disperser solvent. Finally, the extract was diluted to reduce the viscosity of the DES prior to its measurement by flame atomic absorption spectroscopy. Also in 2019, Shishov et al. [67] employed TBAB and heptanol to generate a DES to extract estradiol from water. The importance of this work is the introduction of DES decomposition that can be employed to fix one of the main drawbacks of DES, that is, the combination with chromatographic techniques due to its high viscosity. First, the DES was synthesized and then introduced in the aqueous sample, where the DES is decomposed into its original components. Thus, TBAB remains in the water solution meanwhile heptanol is easily separated by centrifugation and no extra solvents are needed. However, due to the high viscosity of heptanol, it was necessary to dilute it before the chromatographic process.

Furthermore, Tomai et al. [68] employed a low transition temperature material (LTTM). LTTMs are similar to DESs but the difference between them is that DESs present lower melting points than the original components and LTTMs present lower glass transitions instead of melting points [69]. In this work, ChCl and acetylsalicylic acid were combined for the determination of pesticides in water employing THF as disperser solvent and then diluting the extract with MeOH to be introduced in the LC system.

In 2020, Shishov et al. [70] used the DES decomposition step described above. In this sense, the first lixiviation with a DES composed of hexanoic acid, TBAB, and malonic acid was performed. Then, water was added to decompose the DES. In this sense, TBAB and malonic acid remained in the water and hexanoic acid is separated on the top of the water solution and it can be separated and be introduced directly into the LC system. During the same year, Ge et al. [71] synthesized a DES composed of menthol and polyethylene glycol for the determination of parabens in different kinds of samples. Polyethylene glycol has the potential to substitute classical solvents due to its low toxicity to humans and the environment [72].

Mogaddam et al. [73] performed an in situ synthesis of a ChCl and butyric acid DES into the sample during the microextraction of phytosterols from edible oil. First, both components were introduced in the sample extract (i.e., ethanol with the analyte after a dispersive SPE process diluted with water), and then was heated at 75°C for 5 min. After the phase separation, the mixture was introduced in an ice bath to solidify the formed DES to be easily separated.

Finally, in 2020, two ferrofluids were prepared with DESs. The first one was proposed by Dil et al. [74], who

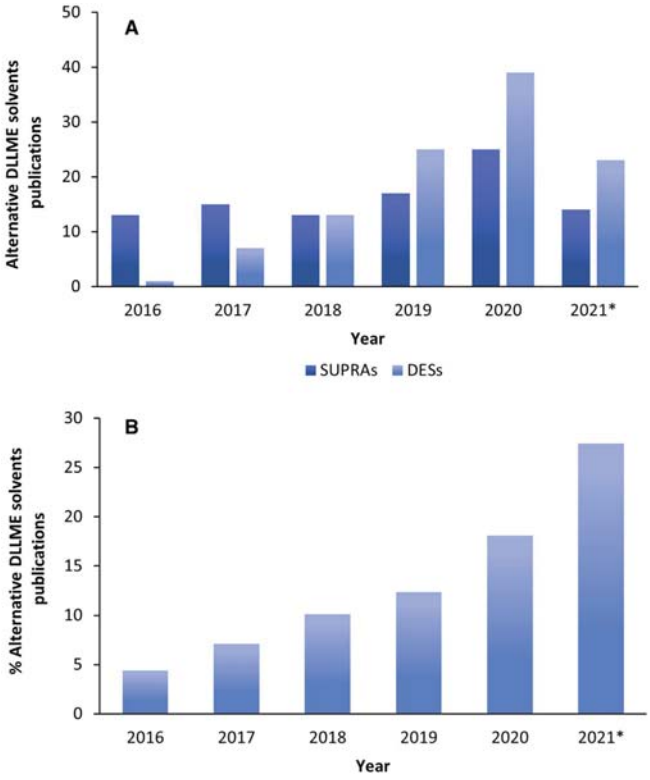

FIGURE 6 (A) Publications on supramolecular solvents (SUPRAs) and deep eutectic solvents (DESs) used in dispersive liquid-liquid microextraction (DLLME). (B) Percentage of alternative solvents used in DLLME over the total of DLLME-based methods (*current year)

mixed oleic acid-coated Fe_3O_4 magnetic nanoparticles with a menthol-octanoic acid DES for the determination of doxycycline in different types of samples. The resultant ferrofluid was introduced in the sample and shaken using a vortex agitator. The ferrofluid was then separated employing an external magnet. Later, Jouyban et al. [75] also employed Fe_3O_4 magnetic nanoparticles, in this case, coated with TEOS, combined with menthol, ChCl, and octanoic acid DES for the analysis of polycyclic aromatic hydrocarbons in meat samples.

In this year 2021, Masrouri et al. [76] combined diethyl amine chloride and carvacrol to obtain a DES for the determination of aflatoxin M1 in cheese samples. This DES can interact with the polar groups and the aromatic rings of aflatoxin. For its synthesis, despite being performed at a relatively high temperature (80°C), the time needed was only 45 min. Moreover, in this method, the amount of organic solvent employed for diluting the DES before the LC process was 5 μl. Later this year, Hussin et al. [77] used an LTTM composed of sesamol and ChCl (obtained by heating for 5 min at 50°C) for the analysis of pesticides in urine using ethyl acetate as disperser solvent. After the phase separation, the upper DES phase was introduced directly into the LC system.

4 | DISCUSSION

As discussed in previous sections, the use of alternative solvents has increased substantially in DLLME during the last 5 years, mainly due to the introduction of DESs. As shown in Figure 6A, the number of DESs-based applications have increased from just one paper in 2016 to 40 in 2020. In fact, in the first half of 2021, the number of DES-based DLLME publications has reached the number of publications about IL-based DLLME, proving the high impact of DESs. On the other hand, the use of SUPRAs has also increased the number of applications during the years 2019 and 2020. In Figure 6B, it is shown the percentage of both SUPRAs and DESs compared with the total DLLME applications. These percentiles have been growing since 2016 obtaining the maximum percentile (i.e., 25%) in 2021, proving the

increasing interest in this kind of solvents by the Analytical Chemistry community.

Nevertheless, notwithstanding being called 'alternative' solvents, researchers should know that this is not necessarily a synonym of green or harmless. It is true that DESs and SUPRAs have 'greener' properties than their predecessors (i.e., LDSs and ILs). However, in many cases, the components employed for their synthesis are toxic for humans and the environment.

For example, as it has been said in Section 3.1, SUPRAs have great extraction capabilities and are less toxic and contaminant than original halogenated solvents. Nevertheless, most of them are generated employing alkanols, toxic to the aquatic environment, and usually employing THF for coacervation step. THF is flammable and is suspected of being carcinogenic [78]. Different alternatives to these SUPRAs have been tried, but these new SUPRAs are often more toxic despite improving the extraction efficiency [79–81]. Moreover, despite its compatibility with different analytical instruments, SUPRAs cannot be directly introduced into a GC system without a pre-treatment step [41].

Regarding DESs, the situation is quite different. The evolution of the type of DES employed in DLLME since 2016 has changed from the halogenated phenols employed in the first papers to the use of greener components such as urea, citric acid, sucrose, and menthol among many others, making of DESs the solvents with more green possibilities in DLLME.

These types of non-toxic DESs are often cataloged as 'natural' (i.e., NADES), although in our opinion this name is not completely accurate. First, natural is not a synonym of harmless since, just as an example, it is well-known that some of the most dangerous poisons are 'natural'. Second, even if some of the components can be presented naturally (e.g., urea in urine), they are probably obtained by synthesis. For that reason, we propose the term 'low-toxicity DES' instead of NADES in order to be more consistent. This term also includes other DESs, which, despite having low toxicity for the environment and humans, were not incorporated in the term NADES.

However, some drawbacks have to be emended before considering DESs as the 'ideal' DLLME solvent. Their main problem is its viscosity, as it happens with ILs, which makes difficult its direct connection to measurement devices without a previous dilution step in many cases. Some works have employed the DES decomposition after the microextraction, thus, one of the original components containing the analytes can be directly introduced into the measurement system. Moreover, unlike SUPRAs, DESs usually need a previous synthesis step. However, this synthesis, even though sometimes can be considered time-consuming, the conditions are softer than those employed in most IL syntheses.

5 | CONCLUSION AND FUTURE TRENDS

Since its development in 2006, DLLME has attracted the attention of the analytical community due to its simplicity and good analytical features. However, since its first use, conventional DLLME has dragged one drawback, that is, the use of high-density halogenated solvents. In spite of the good results obtained, these halogenated solvents are quite toxic and a method employing this kind of solvent cannot be considered as a green method.

For that reason, researchers have been looking for solvents that were not only safe for the environment and operators but also able to improve the extraction efficiency of DLLME-based methods. In this sense, many alternatives have been proposed. In this review, the evolution over the last 5 years of the different types of solvents used in DLLME has been exposed. Special emphasis on the two of the most promising ones (i.e., SUPRAs and DESs) has been discussed in detail. Both types of solvents have extraordinary properties for microextraction purposes and some benefits to being considered as green solvents. SUPRAs can be synthesized in situ and do not need additional steps to be introduced into most of the measurement devices (i.e., LC, flame atomic absorption spectroscopy, etc.), but most of them are generated with organic solvents (i.e., THF) and amphiphilic groups with high environmental impact. On the other side, DESs can be generated with solvents with low toxicity for the operator and the environment, notwithstanding they cannot be introduced directly in the measurement instruments without a previous dilution step. Furthermore, they normally need a previous synthesis step.

As has been discussed in this review, big steps have been walked in order to obtain greener solvents in DLLME approaches. Nevertheless, the world of chemistry tends to be conservative in some aspects and many of the DLLME works still use conventional halogenated solvents obeying the rule. We are aware of the obvious advantages of these solvents, such as their easy employment and high density, but it should not be ignored the huge impact that this kind of solvents has on health and the environment.

For that reason, the employment of newer and greener solvents must be the objective during the next years of DLLME, focused on tailorable green solvents with great extraction capabilities and easy and harmless synthesis.

In this sense, new amphiphilic substances, besides the lauric acid, with higher biodegradability should be investigated to obtain SUPRAs with low environmental impact

[82,83] in order to make even more versatile the SSME and, moreover, it is mandatory to reduce the organic solvent (i.e., THF) needed for the coacervation step.

On the other hand, it is necessary to continue developing low toxicity-DESs with new strategies to accomplish the coupling with measurements devices without further steps and using cleaner and safer dispersant procedures.

Finally, although this review has been focused on the extraction solvent, to achieve a 'green DLLME' other aspects such as the dispersant solvent should be studied. In this sense, during the last years, some works have reported the use of DESs as dispersant solvents [84,85], opening the door to future DLLME applications with dispersant DESs.

ACKNOWLEDGMENTS

Financial support from the Spanish Ministry of Science and Innovation (PID2020-118924RB-I00) is gratefully acknowledged. The authors also thank the Spanish Ministry of Education and Vocational Training for the predoctoral grant of Cristian Azorín and the Generalitat Valenciana and the European Social Fund for the postdoctoral grant of Juan L. Benedé. This article is based upon work from the National Thematic Network on Sample Treatment (RED-2018-102522-T) of the Spanish Ministry of Science, Innovation and Universities, and the Sample Preparation Study Group and Network supported by the Division of Analytical Chemistry of the European Chemical Society.

CONFLICT OF INTEREST

The authors have declared no conflict of interest.

ORCID

Cristian Azorín https://orcid.org/0000-0003-3472-6857
Alberto Chisvert https://orcid.org/0000-0003-1349-0478
Amparo Salvador https://orcid.org/0000-0003-1248-4076

REFERENCES

1. Armenta S, Garrigues S, de la Guardia M. The role of green extraction techniques in Green Analytical Chemistry. TrAC Trends Anal Chem. 2015;71:2–8.
2. Jalili V, Barkhordari A, Ghiasvand A. New extraction media in microextraction techniques. A review of reviews. Microchem J. 2020;153:104386.
3. Rezaee M, Assadi Y, Milani Hosseini MR, Aghaee E, Ahmadi F, Berijani S. Determination of organic compounds in water using dispersive liquid-liquid microextraction. J Chromatogr A. 2006;1116:1–9.
4. Psillakis E. Vortex-assisted liquid-liquid microextraction revisited. TrAC Trends Anal Chem. 2019;113:332–9.
5. Albero B, Tadeo JL, Pérez RA. Ultrasound-assisted extraction of organic contaminants. TrAC Trends Anal Chem. 2019;118:739–50.
6. An J, Trujillo-Rodríguez MJ, Pino V, Anderson JL. Non-conventional solvents in liquid phase microextraction and aqueous biphasic systems. J Chromatogr A. 2017;1500:1–23.
7. Leong MI, Huang SD. Dispersive liquid-liquid microextraction method based on solidification of floating organic drop combined with gas chromatography with electron-capture or mass spectrometry detection. J Chromatogr A. 2008;1211:8–12.
8. Zanjani MRK, Yamini Y, Shariati S, Jönsson JÅ. A new liquid-phase microextraction method based on solidification of floating organic drop. Anal Chim Acta. 2007;585:286–93.
9. Musarurwa H, Tavengwa NT. Deep eutectic solvent-based dispersive liquid-liquid micro-extraction of pesticides in food samples. Food Chem. 2021;342:127943.
10. Food E, Authority S. Conclusion on the peer review of the pesticide risk assessment of the active substance 1-decanol. EFSA J. 2010;8:1–42.
11. Alshana U, Hassan M, Al-Nidawi M, Yilmaz E, Soylak M. Switchable-hydrophilicity solvent liquid-liquid microextraction. TrAC Trends Anal Chem. 2020;131:116025.
12. Bazel Y, Rečlo M, Chubirka Y. Switchable hydrophilicity solvents in analytical chemistry. Five years of achievements. Microchem J. 2020;157:105115.
13. Murata K, Yokoyama Y, Ikeda S. Homogeneous liquid-liquid extraction method: extraction of iron(III) thenoyltrifluoroacetonate by propylene carbonate. Anal Chem. 1972;44:805–10.
14. Vakh C, Pochivalov A, Andruch V, Moskvin L, Bulatov A. A fully automated effervescence-assisted switchable solvent-based liquid phase microextraction procedure: Liquid chromatographic determination of ofloxacin in human urine samples. Anal Chim Acta. 2016;907:54–9.
15. Pochivalov A, Vakh C, Garmonov S, Moskvin L, Bulatov A. An automated in-syringe switchable hydrophilicity solvent-based microextraction. Talanta 2020;209:120587.
16. Behpour M, Nojavan S, Asadi S, Shokri A. Combination of gel-electromembrane extraction with switchable hydrophilicity solvent-based homogeneous liquid-liquid microextraction followed by gas chromatography for the extraction and determination of antidepressants in human serum, breast milk and wastewater. J Chromatogr A. 2020;1621:461041.
17. Reclo M, Yilmaz E, Soylak M, Andruch V, Bazel Y. Ligandless switchable solvent based liquid phase microextraction of nickel from food and cigarette samples prior to its micro-sampling flame atomic absorption spectrometric determination. J Mol Liq. 2017;237:236–41.
18. Erarpat S, Bodur S, Er EÖ, Bakırdere S. Combination of ultrasound-assisted ethyl chloroformate derivatization and switchable solvent liquid-phase microextraction for the sensitive determination of L-methionine in human plasma by GC–MS. J Sep Sci. 2020;43:1100–6.
19. Vanderveen JR, Durelle J, Jessop PG. Design and evaluation of switchable-hydrophilicity solvents. Green Chem. 2014;16:1187–97.
20. Guest I, Varma DR. Developmental toxicity of methylamines in mice. J Toxicol Environ Health. 1991;32:319–30.
21. Zeiger E. Review of toxicological literature. Integrated laboratory systems. 1997;1–63.

22. Regulation (EU) no 528/2012 concerning the making available on the market and use of biocidal products. Assesment Report: Octanoic acid; 2012.
23. Regulation (EU) no 528/2012 concerning the making available on the market and use of biocidal products. Assesment Report: Decanoic acid; 2012.
24. Aguilera-Herrador E, Lucena R, Cárdenas S, Valcárcel M. The roles of ionic liquids in sorptive microextraction techniques. TrAC Trends Anal Chem. 2010;29:602–16.
25. Han D, Tang B, Ri Lee Y, Ho Row K. Application of ionic liquid in liquid phase microextraction technology. J Sep Sci. 2012;35:2949–61.
26. Yavir K, Konieczna K, Marcinkowski Ł, Kloskowski A. Ionic liquids in the microextraction techniques: the influence of ILs structure and properties. TrAC Trends Anal Chem. 2020;130:115994.
27. Trujillo-Rodríguez MJ, Rocío-Bautista P, Pino V, Afonso AM. Ionic liquids in dispersive liquid-liquid microextraction. TrAC Trends Anal Chem. 2013;51:87–106.
28. Liu Y, Zhao E, Zhu W, Gao H, Zhou Z. Determination of four heterocyclic insecticides by ionic liquid dispersive liquid-liquid microextraction in water samples. J Chromatogr A. 2009;1216:885–91.
29. Feng J, Loussala HM, Han S, Ji X, Li C, Sun M. Recent advances of ionic liquids in sample preparation. TrAC Trends Anal Chem. 2020;125:115833.
30. Carda-Broch S, Ruiz-Ángel MJ. *Ionic liquids in analytical chemistry*. 1st ed. Elsevier: Amsterdam; 2021.
31. Marcinkowska R, Konieczna K, Marcinkowski Ł, Namieśnik J, Kloskowski A. Application of ionic liquids in microextraction techniques: current trends and future perspectives. TrAC Trends Anal Chem. 2019;119:115614.
32. Chisvert A, Román IP, Vidal L, Canals A. Simple and commercial readily-available approach for the direct use of ionic liquid-based single-drop microextraction prior to gas chromatography. Determination of chlorobenzenes in real water samples as model analytical application. J Chromatogr A. 2009;1216:1290–5.
33. Aguilera-Herrador E, Lucena R, Cárdenas S, Valcárcel M. Direct coupling of ionic liquid based single-drop microextraction and GC/MS. Anal Chem. 2008;80:793–800.
34. Zhao FQ, Li J, Zeng BZ. Coupling of ionic liquid-based headspace single-drop microextraction with GC for sensitive detection of phenols. J Sep Sci. 2008;31:3045–9.
35. Zhao F, Lu S, Du W, Zeng B. Ionic liquid-based headspace single-drop microextraction coupled to gas chromatography for the determination of chlorobenzene derivatives. Microchim Acta. 2009;165:29–33.
36. De Boeck M, Damilano G, Dehaen W, Tytgat J, Cuypers E. Evaluation of 11 ionic liquids as potential extraction solvents for benzodiazepines from whole blood using liquid-liquid microextraction combined with LC-MS/MS. Talanta 2018;184:369–74.
37. Jackson GP, Duckworth DC. Electrospray mass spectrometry of undiluted ionic liquids. Chem Commun. 2004;4:522–3.
38. Plechkova NV, Seddon KR. Applications of ionic liquids in the chemical industry. Chem Soc Rev. 2008;37:123–50.
39. Deetlefs M, Seddon KR. Assessing the greenness of some typical laboratory ionic liquid preparations. Green Chem. 2010;12:17–30.
40. Ballesteros-Gómez A, Sicilia MD, Rubio S. Supramolecular solvents in the extraction of organic compounds. A review. Anal Chim Acta. 2010;677:108–30.
41. Rubio S. Twenty years of supramolecular solvents in sample preparation for chromatography: achievements and challenges ahead. Anal Bioanal Chem. 2020;412:6037–58.
42. Ballesteros-Gómez A, Rubio S, Pérez-Bendito D. Potential of supramolecular solvents for the extraction of contaminants in liquid foods. J Chromatogr A. 2009;1216:530–9.
43. Feizi N, Yamini Y, Moradi M, Ebrahimpour B. Nano-structured gemini-based supramolecular solvent for the microextraction of cyhalothrin and fenvalerate. J Sep Sci. 2016;39:3400–9.
44. Moradi M, Yamini Y, Feizi N. Development and challenges of supramolecular solvents in liquid-based microextraction methods. TrAC Trends Anal Chem. 2021;138:116231.
45. Seebunrueng K, Dejchaiwatana C, Santaladchaiyakit Y, Srijaranai S. Development of supramolecular solvent based microextraction prior to high performance liquid chromatography for simultaneous determination of phenols in environmental water. RSC Adv. 2017;7:50143–9.
46. Salatti-Dorado JÁ, Caballero-Casero N, Sicilia MD, Lunar ML, Rubio S. The use of a restricted access volatile supramolecular solvent for the LC/MS-MS assay of bisphenol A in urine with a significant reduction of phospholipid-based matrix effects. Anal Chim Acta. 2017;950:71–9.
47. Zong Y, Chen J, Hou J, Deng W, Liao X, Xiao Y. Hexafluoroisopropanol-alkyl carboxylic acid high-density supramolecular solvent based dispersive liquid-liquid microextraction of steroid sex hormones in human urine. J Chromatogr A. 2018;1580:12–21.
48. Chen J, Deng W, Li X, Wang X, Xiao Y. Hexafluoroisopropanol/Brij-35 based supramolecular solvent for liquid-phase microextraction of parabens in different matrix samples. J Chromatogr A. 2019;1591:33–43.
49. Gissawong N, Boonchiangma S, Mukdasai S, Srijaranai S. Vesicular supramolecular solvent-based microextraction followed by high performance liquid chromatographic analysis of tetracyclines. Talanta 2019;200:203–11.
50. Najafi A, Hashemi M. Feasibility of liquid phase microextraction based on a new supramolecular solvent for spectrophotometric determination of orthophosphate using response surface methodology optimization. J Mol Liq. 2020;297:111768.
51. Accioni F, García-Gómez D, Rubio S. Exploring polar hydrophobicity in organized media for extracting oligopeptides: application to the extraction of opiorphin in human saliva. J Chromatogr A. 2021;1635:461777.
52. Durand E, Lecomte J, Villeneuve P. From green chemistry to nature: the versatile role of low transition temperature mixtures. Biochimie 2016;120:119–23.
53. Zhang Q, De Oliveira Vigier K, Royer S, Jérôme F. Deep eutectic solvents: syntheses, properties and applications. Chem Soc Rev. 2012;41:7108–46.
54. Musarurwa H, Tavengwa NT. Emerging green solvents and their applications during pesticide analysis in food and environmental samples. Talanta 2021;223:121507.
55. Plotka-Wasylka J, de la Guardia M, Andruch V, Vilková M. Deep eutectic solvents vs ionic liquids: similarities and differences. Microchem J 2020;159:105539.
56. Makoś P, Słupek E, Gębicki J. Hydrophobic deep eutectic solvents in microextraction techniques–a review. Microchem J. 2020;152:104384.
57. Li X, Row KH. Development of deep eutectic solvents applied in extraction and separation. J Sep Sci. 2016;39:3505–20.

58. Farajzadeh MA, Mogaddam MRA, Aghanassab M. Deep eutectic solvent-based dispersive liquid-liquid microextraction. Anal Methods. 2016;8:2576–83.
59. Zeng H, Qiao K, Li X, Yang M, Zhang S, Lu R, Li J, Gao H, Zhou W. Dispersive liquid–liquid microextraction based on the solidification of deep eutectic solvent for the determination of benzoylureas in environmental water samples. J Sep Sci. 2017;40:4563–70.
60. Zounr RA, Tuzen M, Khuhawar MY. Ultrasound assisted deep eutectic solvent based on dispersive liquid liquid microextraction of arsenic speciation in water and environmental samples by electrothermal atomic absorption spectrometry. J Mol Liq. 2017;242:441–6.
61. Farajzadeh MA, Sattari Dabbagh M, Yadeghari A. Deep eutectic solvent based gas-assisted dispersive liquid-phase microextraction combined with gas chromatography and flame ionization detection for the determination of some pesticide residues in fruit and vegetable samples. J Sep Sci. 2017;40:2253–60.
62. Ge D, Zhang Y, Dai Y, Yang S. Air-assisted dispersive liquid–liquid microextraction based on a new hydrophobic deep eutectic solvent for the preconcentration of benzophenone-type UV filters from aqueous samples. J Sep Sci 2018;41:1635–43.
63. Ferrone V, Genovese S, Carlucci M, Tiecco M, Germani R, Preziuso F, Epifano F, Carlucci G, Taddeo VA. A green deep eutectic solvent dispersive liquid-liquid micro-extraction (DES-DLLME) for the UHPLC-PDA determination of oxyprenylated phenylpropanoids in olive, soy, peanuts, corn, and sunflower oil. Food Chem. 2018;245:578–85.
64. Panhwar AH, Tuzen M, Deligonul N, Kazi TG. Ultrasonic assisted deep eutectic solvent liquid–liquid microextraction using azadipyrromethene dye as complexing agent for assessment of chromium species in environmental samples by electrothermal atomic absorption spectrometry. Appl Organomet Chem. 2018;32:1–9.
65. Altunay N, Elik A, Gürkan R. Monitoring of some trace metals in honeys by flame atomic absorption spectrometry after ultrasound assisted-dispersive liquid liquid microextraction using natural deep eutectic solvent. Microchem J. 2019;147:49–59.
66. Pacheco-Fernández I, González-Martín R, Silva FAE, Freire MG, Pino V. Insights into coacervative and dispersive liquid-phase microextraction strategies with hydrophilic media–a review. Anal Chim Acta. 2021;1143:225–49.
67. Shishov A, Chromá R, Vakh C, Kuchár J, Simon A, Andruch V, Bulatov A. In situ decomposition of deep eutectic solvent as a novel approach in liquid-liquid microextraction. Anal Chim Acta. 2019;1065:49–55.
68. Tomai P, Lippiello A, D'Angelo P, Persson I, Martinelli A, Di Lisio V, Curini R, Fanali C, Gentili A. A low transition temperature mixture for the dispersive liquid-liquid microextraction of pesticides from surface waters. J Chromatogr A. 2019;1605:360329.
69. Francisco M, Van Den Bruinhorst A, Kroon MC. New natural and renewable low transition temperature mixtures (LTTMs): screening as solvents for lignocellulosic biomass processing. Green Chem. 2012;14:2153–7.
70. Shishov A, Gerasimov A, Nechaeva D, Volodina N, Bessonova E, Bulatov A. An effervescence-assisted dispersive liquid–liquid microextraction based on deep eutectic solvent decomposition: determination of ketoprofen and diclofenac in liver. Microchem J. 2020;156:104837.
71. Ge D, Gao Y, Cao Y, Dai E, Yuan L. Preparation of a new polymeric deep eutectic solvent and its application in vortex-assisted liquid-liquid microextraction of parabens in foods, cosmetics and pharmaceutical products. J Braz Chem Soc. 2020;31:2120–8.
72. Soni J, Sahiba N, Sethiya A, Agarwal S. Polyethylene glycol: A promising approach for sustainable organic synthesis. J Mol Liq. 2020;315:113766.
73. Mogaddam MRA, Farajzadeh MA, Azadmard Damirchi S, Nemati M. Dispersive solid phase extraction combined with solidification of floating organic drop–liquid–liquid microextraction using in situ formation of deep eutectic solvent for extraction of phytosterols from edible oil samples. J Chromatogr A. 2020;1630:461523.
74. Dil EA, Ghaedi M, Asfaram A, Tayebi L, Mehrabi F. A ferrofluidic hydrophobic deep eutectic solvent for the extraction of doxycycline from urine, blood plasma and milk samples prior to its determination by high-performance liquid chromatography-ultraviolet. J Chromatogr A. 2020;1613:460695.
75. Jouyban A, Farajzadeh MA, Mogaddam MRA, Nemati M, Alizadeh Nabil AA. Ferrofluid-based dispersive liquid-liquid microextraction using a deep eutectic solvent as a support: applications in the analysis of polycyclic aromatic hydrocarbons in grilled meats. Anal Methods. 2020;12:1522–31.
76. Masrouri M, Mogaddam MRA, Farajzadeh MA, Nemati M, Lotfipour F. Combination of solvent extraction with deep eutectic solvent based dispersive liquid–liquid microextraction for the analysis of aflatoxin M1 in cheese samples using response surface methodology optimization. J Sep Sci. 2021;44:1501–9.
77. Hussin SAM, Varanusupakul P, Shahabuddin S, Yih Hui B, Mohamad S. Synthesis and characterization of green menthol-based low transition temperature mixture with tunable thermophysical properties as hydrophobic low viscosity solvent. J Mol Liq. 2020;308:113015.
78. Sanders JM, Bucher JR, Peckham JC, Kissling GE, Hejtmancik MR, Chhabra RS. Carcinogenesis studies of cresols in rats and mice. Toxicology 2009;257:33–9.
79. Garcia MT, Kaczerewska O, Ribosa I, Brycki B, Materna P, Drgas M. Biodegradability and aquatic toxicity of quaternary ammonium-based gemini surfactants: Effect of the spacer on their ecological properties. Chemosphere 2016;154:155–60.
80. Sirisattha S, Momose Y, Kitagawa E, Iwahashi H. Toxicity of anionic detergents determined by Saccharomyces cerevisiae microarray analysis. Water Res. 2004;38:61–70.
81. Lee MY, Wang WL, Xu ZB, Ye B, Wu QY, Hu HY. The application of UV/PS oxidation for removal of a quaternary ammonium compound of dodecyl trimethyl ammonium chloride (DTAC): the kinetics and mechanism. Sci Total Environ. 2019;655:1261–9.
82. Atta DY, Negash BM, Yekeen N, Habte AD. A state-of-the-art review on the application of natural surfactants in enhanced oil recovery. J Mol Liq. 2021;321:114888.
83. Kurpiers M, Wolf JD, Spleis H, Steinbring C, Jörgensen AM, Matuszczak B, Bernkop-Schnürch A. Lysine-based biodegradable surfactants: increasing the lipophilicity of insulin by hydrophobic ion paring. J Pharm Sci. 2021;110:124–34.

84. Shishov A, Volodina N, Nechaeva D, Gagarinova S, Bulatov A. Deep eutectic solvents as a new kind of dispersive solvent for dispersive liquid-liquid microextraction. RSC Adv. 2018;8:38146–9.
85. Shishov A, Terno P, Moskvin L, Bulatov A. In-syringe dispersive liquid-liquid microextraction using deep eutectic solvent as disperser: determination of chromium (VI) in beverages. Talanta 2020;206:120209.

How to cite this article: Grau J, Azorín C, Benedé JL, Chisvert A, Salvador A. Use of green alternative solvents in dispersive liquid-liquid microextraction: A review. J Sep Sci. 2022;45:210–222.
https://doi.org/10.1002/jssc.202100609

Stir bar sorptive-dispersive microextraction for trace determination of triphenyl and diphenyl phosphate in urine of nail polish users

Journal of Chromatography A 1593 (2019) 9-16

DOI: 10.1016/j.chroma.2019.02.014

Journal of Chromatography A, 1593 (2019) 9–16

Contents lists available at ScienceDirect

Journal of Chromatography A

journal homepage: www.elsevier.com/locate/chroma

Stir bar sorptive-dispersive microextraction for trace determination of triphenyl and diphenyl phosphate in urine of nail polish users☆

José Grau, Juan L. Benedé, Javier Serrano, Andrea Segura, Alberto Chisvert*

Department of Analytical Chemistry, University of Valencia, 46100, Burjassot, Valencia, Spain

ARTICLE INFO

Article history:
Received 31 October 2018
Received in revised form 18 January 2019
Accepted 6 February 2019
Available online 7 February 2019

Keywords:
Cosmetics
Endocrine disruptors
Magnetic composite
Nail polish
Stir bar sorptive-dispersive microextraction
Urine samples

ABSTRACT

This work describes a new analytical method useful for monitoring the human exposure to the endocrine-disrupting plasticizer triphenyl phosphate (TPP) via nail polish use. The method allows trace determination of this parent compound and its main metabolite, namely diphenyl phosphate (DPP), in urine samples of nail polish users. The method is based on a novel microextraction technique termed stir bar sorptive-dispersive microextraction (SBSDME) using a magnetic composite made of $CoFe_2O_4$ magnetic nanoparticles embedded into a mixed-mode weak anion exchange polymer (Strata™-X-AW), followed by liquid chromatography-tandem mass spectrometry (LC–MS/MS). The main parameters involved in the extraction procedure were evaluated and optimized. Under the optimized conditions, the method was successfully validated showing good linearity (at least up to 100 ng mL^{-1}) and enrichment factors (17 and 30), limits of detection and quantification in the low ng L^{-1} range (1.9–17.1 ng L^{-1} and 6.3–57.1 ng L^{-1}, respectively) and good intra- and inter-day precision (RSD < 8%). Excellent recoveries (81–112 %) were achieved by using matrix-matched calibration for quantification. Finally, the method was applied to the determination of both the parent compound and the metabolite in human urine samples from volunteers who applied themselves a nail polish containing TPP. Detectable amounts of the parent compound were found just in the first urination, whereas quantifiable amounts of DPP were found in the low ng mL^{-1} range even 24 h after application of the nail polish, thus suggesting a rapid biotransformation and a low excretion, and showing DPP as excellent biomarker of human exposure to TPP. This work expands the analytical potential of the novel SBSDME, and the proposed methodology contributes to the study of the absorption/excretion levels of endocrine disruptors present in cosmetic products.

1. Introduction

New substances are continuously incorporated in the elaboration of cosmetic products, mainly due to the constant need for innovation in the cosmetic sector. Triphenyl phosphate (TPP), a well-known plasticizer and flame retardant commonly used in polyurethane foam in furniture and baby products [1], is added as cosmetic ingredient to nail polishes [2,3] in order to confer them higher flexibility and durability. Different studies have shown neurotoxic effects and endocrine-disrupting properties of TPP in aquatic biota and mice [4–7], and other studies have postulated that TPP could cause similar toxic effects in humans [8], in such a way it could affect the thyroid hormone causing an increase in weight in women and a decrease of fertility in men [9,10]. To this regard, this compound has been included in the current *The Endocrine Disruption Exchange* (TEDX) list of endocrine disruptors [11], since it might be a potential risk for human health. However, according to the European regulation on cosmetic products [12], its use is neither prohibited nor restricted despite its direct exposure through the cuticle and paronychial edge or even through the nail plate [2].

Once absorbed, *in vitro* experiments carried out in hepatic cell lines have shown that this compound is rapidly transformed into several metabolites [13–15], of which diphenyl phosphate (DPP) constitutes an excellent biomarker of human exposure to TPP since it can be found in urine at ng mL^{-1} levels [2,16,17]. Taking into account that urine is a complex matrix where DPP is found at trace level, solid-phase extraction (SPE) is usually employed with the aim of preconcentrate the target analyte and/or to eliminate potentially interfering compounds [18–22].

Commercial SPE cartridges of different nature has been assayed for the extraction of DPP, such as reversed-phase [18–21], weak anion exchange [18–20], strong anion exchange [18,19,21], mixed-mode weak anion exchange [18–22], and tailor-made molecularly imprinted polymer [18]. Since DPP is strongly acid (pKa 1.12) [23],

☆ Selected paper from the 20th International Symposium on Advances in Extraction Technologies (ExTech 2018), June 19–22, 2018, in Ames, Iowa.

* Corresponding author.
E-mail address: alberto.chisvert@uv.es (A. Chisvert).

https://doi.org/10.1016/j.chroma.2019.02.014
0021-9673/

it is permanently charged unless under extremely pH conditions, in such a way the strong anion exchanger retains it strongly making difficult its elution [18,19,21]. However, the weak anion exchanger and reversed-phase retains DPP poorly and therefore considerable leaks are observed during the loading and/or washing steps [18–21]. The best results are obtained with the mixed-mode weak anion exchanger containing both anion-exchange moieties in a reversed-phase backbone, since DPP contains lipophilic aromatic rings besides the negatively charged phosphate moiety [18–20]. Molecularly imprinted polymers-based cartridges show higher selectivity than mixed-mode weak anion exchange-based ones but the formers suffer of lower extraction efficiency [18].

It should be pointed out that no evidences of the use of the highly-potential microextraction techniques for similar purposes have been found in the literature, which might increase the sensitivity and reduce the used solvent amounts. Among all the current microextraction approaches, stir bar sorptive dispersive microextraction (SBSDME) is a promising hybrid solid phase-based microextraction approach presented by our group that consists in the use of a neodymium stir bar coated with a magnetic material as extraction device [24]. This novel approach combines the principles of stir bar sorptive extraction (SBSE) [25] and dispersive solid-phase extraction (DSPE) [26], in such a way at low stirring rate the magnetic material remains onto the surface of the stir bar like in (SBSE), whereas at high stirring rate the material is completely dispersed into the donor solution like in (DSPE). Once the stirring is ceased, the magnetic material containing the target analytes is retrieved by the stir bar without requiring any additional magnetic field. Later, the analytes can be either desorbed in an appropriate solvent for further injection into a liquid chromatographic (LC) instrument [24,27], or directly thermally desorbed (TD) into a GC system [28]. In this manner, SBSDME presents advantages over both SBSE (i.e., lower extraction time and more versatile sorbents by using different coated MNPs) and DSPE (i.e., easier extraction and post-extraction treatment and minimum manual intervention) [24,27,28]. Up to now, this approach has only been applied to the analysis of environmental waters [24,27,28] and recently to sand samples [29].

To this regard, it is worthy to mention that the dispersion of magnetic materials (e.g., functionalized nanoparticles, or composite materials made of nanoparticles embedded in polymeric sorbents) have gained great popularity in microextraction techniques, due to the facility to retrieve them by applying a magnetic field [30–32].

In this work, the analytical potential of SBSDME has been applied to the study of the absorption/excretion levels of the endocrine-disrupting plasticizer TPP via nail polish use, which is metabolized into DPP and excreted by means of urine. As sorbent material, a magnetic composite made of $CoFe_2O_4$ magnetic nanoparticles (MNPs) embedded into a mixed-mode weak anion exchange polymer (Strata™-X-AW) (i.e., $CoFe_2O_4$-Strata™ X—AW) is used to entrap both the parent compound (TPP) by means of hydrophobic interactions and Π-Π bonding, and the metabolite (DPP) by, moreover, weak anion exchange interactions. The main parameters involved in the extraction procedure were evaluated and optimized, and it was then applied to samples from four volunteers after application of a nail polish containing TPP.

2. Experimental

2.1. Reagents and samples

All reagents and solvents were obtained from major suppliers. Triphenyl phosphate (TPP) ≥99% and diphenyl phosphate 99% (DPP) from Sigma-Aldrich (Steinheim, Germany) were used as standards. Dibenzyl phosphate (DBP) 98% from Alfa Aesar (Kandel, Germany) was used as surrogate.

For the synthesis of cobalt ferrite nanoparticles, cobalt (II) chloride hexahydrate ($CoCl_2{\cdot}6H_2O$) and iron (III) chloride hexahydrate ($FeCl_3{\cdot}6H_2O$) were purchased from Acros Organics (New Jersey, USA), and sodium hydroxide (reagent grade) was purchased from Scharlau (Barcelona Spain). A commercial polymeric mixed-mode weak anion sorbent from Phenomenex (Torrance, USA) (Strata™-X-AW) was used as the polymeric network for the synthesis of the composite.

Gradient-grade methanol, LC-grade ethanol and nitric acid 65% were acquired from VWR chemicals (Fontenay-sous-Bois, France). Deionized water was obtained from a Connect water purification system provided by Adrona (Riga, Latvia). Sodium chloride (99.5%, analytical grade) that was used as ionic strength regulator was purchased from Scharlau (Barcelona, Spain).

LC–MS grade methanol and LC–MS grade water from VWR Chemicals (Fontenay-sous-Bois, France) and reagent grade ammonium acetate from Panreac (Barcelona, Spain) were used for the mobile phase.

Nitrogen used as nebulizer and curtain gas in the MS/MS ion source was obtained by a NiGen LCMS 40 nitrogen generator from Claind S.r.l. (Lenno, Italy). Extrapure nitrogen (>99.999%), used as collision gas in the MS/MS collision cell, was provided by Praxair (Madrid, Spain).

Blank urine samples used for the method development and validation were obtained from different healthy volunteers who were known not to use cosmetic products containing TPP. Moreover, urine samples from other healthy volunteers who topically applied a commercial nail polish containing TPP were employed for method application. All urine samples were kept at 4 °C in the fridge until analysis. Each volunteer gave written informed consent to participate in this study, which was conformed to the ethical guidelines of the Declaration of Helsinki, and was approved by the Ethical Committee of the University of Valencia (Spain).

2.2. Apparatus and materials

An Agilent 1100 Series comprised of a degasser, a quaternary pump, an autosampler and a thermostatic column oven, coupled to an Agilent 6410B Tripe Quad MS/MS was employed throughout the study. Separations were carried out in a Zorbax SB-C18 (50 mm length, 4 mm I.D., 1.8 μm).

Magnetic stirring hotplates (Stuart Scientific, Staffordshire, United Kingdom) were used as stirrers in the extraction procedure, and NdFeB (45 MGOe) magnetic tumble stir cylinders (3 mm diameter x 12 mm long, nickel coated) from Superimanes S.L. (Sevilla, Spain) were used as stir bars for the extraction. A Basic 20 pH meter from Crison (Alella, Spain) was used for the adjustment of pH. Hydrophobic PTFE syringe filters from Labbox (Barcelona, Spain) were used to filter the solutions prior to LC–MS/MS analysis.

All those instruments used for characterization of the sorbent material are listed in Supplementary Material.

2.3. Synthesis of $CoFe_2O_4$@Strata-X™-AW magnetic composite

The synthesis of the $CoFe_2O_4$@Strata-X™-AW composite consisted of two steps: the synthesis of the magnetic nanoparticles by wet chemical co-precipitation according to an adapted protocol [33], and subsequent insertion of the $CoFe_2O_4$ MNPs into the polymeric network [34].

First, 100 mL of a 0.4 M $FeCl_3$ aqueous solution and 100 mL of a 0.2 M $CoCl_2$ aqueous solution were mixed, and then 100 mL of a 3 M sodium hydroxide aqueous solution were added dropwise under continuous stirring for one hour at 80 °C.

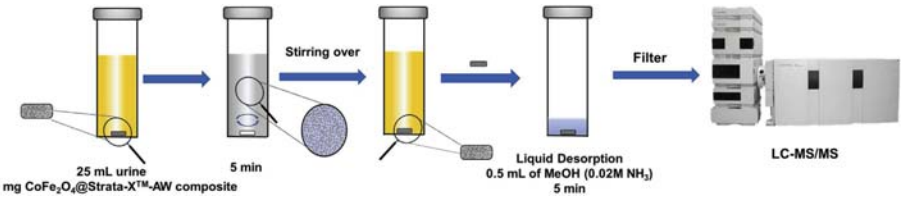

Fig. 1. Schematic diagram of the proposed SBSDME approach.

Afterwards, a magnetic decantation was performed in which the MNPs were deposited on the bottom with the help of an external magnetic field. The supernatant was then discarded. Next, the MNPs were resuspended in 100 mL of 1 M HCl put into the refrigerator (4 °C) for 2 h. After that, the mixture was decanted with the aid of the magnet, and the solid was resuspended in water for 3 days. The suspension was filtered with a 0.45 μm pore size nylon filter. From the resulting suspension, a 1 mL aliquot was separated and dried overnight at 100 °C to determine the concentration of MNPs in the final suspension.

For the preparation of the polymeric network with the MNPs embedded, 0.25 g of Strata-X^{TM}-AW were weighed and the corresponding volume of the MNPs suspension was added so that finally the polymer and MNPs ratio was 1:1 (w/w). The mixture was kept under stirring for 1 day.

Finally, the precipitate was filtered through a Whatman® filter paper with a pore size of 11 μm, dried overnight at 100 °C and pulverized into a fine powder with a mortar.

2.4. Proposed method

2.4.1. Matrix-matched calibration

A stock solution containing 500 μg mL^{-1} of TPP and DPP was prepared in ethanol. Then, an aliquot of this solution was properly diluted with deionized water to prepare a multicomponent solution with 500 ng mL^{-1} of both analytes. A stock solution of DBP (as surrogate) was prepared in ethanol at 125 μg mL^{-1}.

Matrix-matched calibration solutions were prepared by transferring six aliquots of 25 mL of a free-analyte pool of urine to 30-mL vials, which were respectively spiked with the multicomponent solution to achieve concentrations of the target analytes from 0.5 to 5 ng mL^{-1}. The surrogate was added at 100 ng mL^{-1} into all the calibration solutions.

2.4.2. SBSDME procedure

For preconditioning and physical coating of the stir bars, 10 mg of dried $CoFe_2O_4$@Strata-X^{TM}-AW composite were dispersed in 2 mL of methanol. A neodymium stir bar (45 MGOe, 3 mm diameter x 12 mm long) was introduced and stirred for 3 min at high stirring rate to solvate the composite. By stopping the stirrer, the composite was strongly attracted by the neodymium stir bar and then the composite-coated stir bar was removed from the solution with the aid of plastic thumb forceps.

For the extraction procedure, the coated stir bar was immersed into the vials containing the 25 mL working standard solutions (described in Section 2.4.1) or 25 mL of urine sample. Then, each solution was magnetically stirred for 5 min at room temperature at a high stirring rate to disperse the $CoFe_2O_4$@Strata-X^{TM}-AW composite. After stirring was stopped, the magnetic composite was collected onto the magnetic stir bar, and then the coated stir bar was removed with plastic thumb forceps, gently rinsed with deionized water and placed into a glass vial containing 0.5 mL of methanol (with 0.02 M NH_3) for 5 min to accomplish the liquid desorption of the analytes. Finally, the extracts were filtered through 0.45 μm PTFE-filters and transferred into inserts placed inside 1.5 mL injection vials for LC–MS/MS analysis. Fig. 1 shows a schematic diagram of the experimental procedure.

After each use, the composite-coated stir bars were sequentially soaked in ethanol and acetone to prevent possible background contamination and carryover, and then dried at room temperature. The glass material was soaked in an aqueous solution of HNO_3 at 50% in order to clean it.

2.4.3. LC–MS/MS analysis

Three microliters of each extract were injected into the chromatographic system. Mobile phase consisted of solvent A (0.01 M ammonium acetate buffer) and solvent B (MeOH), by isocractic elution at a mixing ratio of 20:80% (v/v). The flow was 0.30 mL min^{-1} and the column temperature was maintained constant at 45 °C. The run time was below 2 min. Calibration curves were constructed by plotting A_i/A_{sur} (where A_i is the peak area of the target analyte and A_{sur} that of the surrogate (i.e. DBP)) versus target analyte concentration.

The triple quadrupole MS operated in positive or negative electrospray ionization mode (ESI), depending on the compound, by multiple reaction monitoring (MRM). Specifically, positive polarity (ESI^+, capillary voltage at 2 kV) was used to measure TPP, and negative polarity (ESI^-, capillary voltage at −3 kV) was used to measure DPP and the surrogate. The other conditions were: gas temperature at 350 °C, nebulizer gas flow rate at 11 L min^{-1}, nebulizer gas at 50 psi and collision energy at 53, 26 and 20 for TPP, DPP and DBP (as surrogate), respectively. The *m/z* precursor→product ion transitions for quantification were 327→152 for TPP, 249→93 for DPP, and 277→107 for DBP.

3. Results and discussion

3.1. Selection of the composite and characterization

The selection of $CoFe_2O_4$@Strata-X^{TM}-AW as sorbent material was based on the ability of the commercial Strata-X^{TM}-AW polymeric network to interact with the analytes by weak anion exchange, Π-Π bonding and/or hydrophobic interactions, as described previously. The $CoFe_2O_4$ MNPs confer to this sorbent the magnetism needed for an easy recovery. $CoFe_2O_4$ MNPs were preferred rather than classical Fe_3O_4 due to their higher chemical stability [35].

With the aim of obtaining $CoFe_2O_4$@Strata-X^{TM}-AW with maximum magnetization, different synthetic strategies were carried out. On one hand, previously synthetized MNPs were added to a polymer solution, which was previously swelled by using N-methyl-2-pyrrolidone according to Chung and Lee [36] and Lin et al. [34] (synthesis approach #1), or not swelled (synthesis approach #2). On the other hand, the possibility of carrying out the synthesis of the magnetic nanoparticles in situ was also studied by mixing a polymer solution (previously swelled (synthesis approach

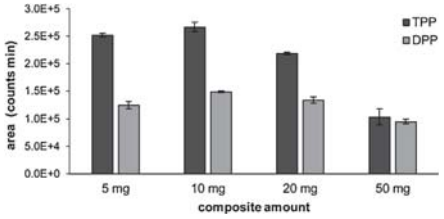

Fig. 2. Effect of the composite amount. Extraction conditions: 25 mL of sample, 5 min extraction time. Desorption conditions: 0.5 mL MeOH, 5 min desorption time.

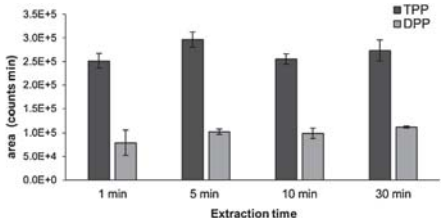

Fig. 3. Effect of the extraction time. Extraction conditions: 25 mL of sample, 10 mg composite. Desorption conditions: 0.5 mL MeOH, 5 min desorption time.

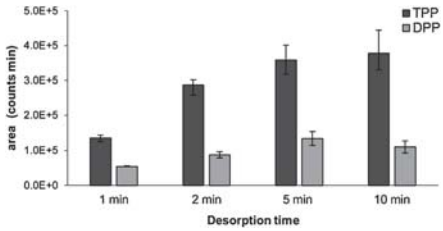

Fig. 4. Effect of the desorption time. Extraction conditions: 25 mL of sample, 10 mg composite, 5 min extraction time. Desorption conditions: 0.5 mL MeOH.

#3) or not (synthesis approach #4)) with Fe(III) and Co(II) solutions and then increasing the pH up to form the MNPs, similar to Reyes-Gallardo et al. [37]. The experimental details are described in Supplementary Material. Based on the magnetization curves observed for those four different synthesis (see Fig. S1 in Supplementary Material), the best results were obtained when previously synthetized MNPs were incorporated to the polymer rather than *in situ* synthesis, where a lower specific magnetization (Ms) was observed. Between the two syntheses using previously synthetized MNPs, differences were not significant (i.e., 22.2 emu g^{-1} when the polymer was swelled and 25.0 emu g^{-1} without swelling the polymer). Therefore, the synthesis approach #2, which avoids an additional swelling step, was finally selected.

Dynamic light scattering (DLS) was applied to the $CoFe_2O_4$@Strata-X^{TM}-AW selected composite (i.e., synthesis approach #2) in order to measure the particle size. The results demonstrated that the sorbent had an average size of 32 ± 1 μm (see Fig. S2 in Supplementary Material), similar to the naked polymer provided by the manufacturer (i.e., 31 ± 3 μm). Other characterization techniques were also applied to confirm the morphology of the composite, and to determine the surface area and porosity (see Supplementary Material). Briefly, the selected composite has an average pore diameter of 29.54 nm and a surface area of 406.6 ± 0.7 m^2/g. Representative transmission electronic microscopy (TEM) micrographs of the MNPs and the composite were also recorded as it is shown in Supplementary Material, showing MNPs with a spherical shape and a diameter around 20 nm, and how these spherical $CoFe_2O_4$ MNPs are embedded into the polymeric network

3.2. Optimization of the SBSDME variables

Different parameters may affect the overall extraction process: the amount of composite, the extraction, deposition and desorption times, the ionic strength and the pH. In this sense, these variables were carefully studied and evaluated by extracting aqueous standard solutions containing the target analytes at 100 ng mL^{-1} in terms of the peak area of each analyte (A_i). All the experiments were performed in triplicate. The sample volume was set at 25 mL. MeOH was used as elution solvent, and its volume was set at 0.5 mL, which is the minimum amount to cover the coated stir bar.

3.2.1. Amount of $CoFe_2O_4$@Strata-X^{TM}-AW composite

Different amounts of composite from 5 to 50 mg were studied in order to obtain the highest signals. As can be seen in Fig. 2, no significant differences were observed between 5 and 20 mg of composite. In the case of 50 mg, a decrease in the signal for both compounds was observed. Due to the small volume of MeOH (0.5 mL) used as desorption solvent for the relatively high mass of composite, the sorbent containing the extracted analytes might not be dispersed correctly and thus the analytes might not be properly eluted. Since higher solvent volumes were discarded in order to avoid excessive dilution, 10 mg of composite was finally selected for further experiments.

3.2.2. Extraction time

The time during which the composite is stirred inside the sample solution was also studied. Different times (1–30 min) were tested. The obtained results (Fig. 3) showed that the signal was slightly higher for 1 min. For this reason, an extraction time of 5 min was selected for further experiments.

3.2.3. Deposition time

When the stirring is over, the composite is retrieved by the magnetic stir bar due to the magnetic field. The deposition time was ranged between 1 and 30 min (data not shown). For DPP, the optimum time was observed at 5 min, but for TPP the signal gradually increased with time. A desorption time of 5 min was finally selected in order to do not extend excessively the extraction process.

3.2.4. Desorption time

After the extraction process, the analytes need to be eluted from the sorbent. Different desorption times were studied from 1 to 10 min. The results are shown in Fig. 4. The signals for both target compounds increased from 1 to 5 min, but at higher values the differences were not significant. Thus, 5 min of desorption time was selected for further experiments.

3.2.5. pH of the donor phase

The pH of the donor phase was ranged from 3 to 12 (Fig. 5). As expected, the TPP extraction, and thus the signal, was not affected by the pH, since this compound is not ionizable. However, as it can be seen, the pH did affect the DPP extraction. According to the Strata-X^{TM}-AW manufacturer, this polymer has a $pK_a = 9$, so at pH > 9 it is less and less protonated and thus it is less positively charged, in such a way that the weak anion exchange interactions between DPP and Strata-X^{TM}-AW are less achieved.

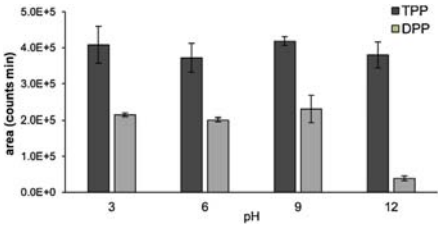

Fig. 5. Effect of the pH of the donor solution. Extraction conditions: 25 mL of sample, 10 mg composite, 5 min extraction time. Desorption conditions: 0.5 mL MeOH, 5 min desorption time.

3.2.6. Ionic strength of the donor phase

The amount of salt in the donor solution may affect the extraction of the analytes. On one hand, the well-known 'salting out' effect has a positive effect promoting the leaving of organic compounds from the water solutions, but on the other hand, the ions compete for the active sites of the anionic exchanger thus producing a negative effect. In order to study this variable, different concentrations of NaCl were tested (up to 2.5% (w/w)). Results (not shown) revealed that no significant changes were observed for TPP, whereas DPP signals were lower compared to without salt addition, which could be attributed to chloride anions competing for active sites of the sorbent and diminishing the extraction of DPP via the anion exchanger mechanism. According to these results, no adjustment of the salt content was carried out in further experiments. This could affect the results when urine samples, containing higher salt content than water, were analysed. For this reason, a surrogate such as dibenzyl phosphate (DBP) was used.

3.3. Study of matrix effects

In order to determine the influence of the matrix in the analysis, the signals (i.e., peak areas) obtained for an aqueous standard solution and for an analyte-free urine sample from a volunteer who did not use cosmetics containing TPP (urine A), both of them containing the target analytes at 5 ng mL^{-1}, were compared. Both solutions also contained the surrogate (i.e., DBP) at 100 ng mL^{-1}. The areas were compared for a 5% significance level (n = 3) by applying a Student's *t*-test, and the results were not statistically comparable. This showed the presence of a significant negative matrix effect (80% for DPP and 44% for TPP), and thus the quantification of the analytes would not be reliable through an external calibration prepared in deionized water despite using the extraction step. Fig. 6 shows a comparison between a chromatogram of an aqueous standard solution containing TPP at 40 ng L^{-1} and DPP at 400 ng L^{-1} and a real urine sample spiked with the target analytes at the same concentrations.

Then, different calibration sets were prepared in urine coming from four different volunteers (urines A, B, C and D). An additional calibration set was prepared by using pooled urine obtained mixing these four urines. The slopes were compared within volunteers and the pooled urine, and the results (see Table 1) showed that no significant differences were observed for a 5% significance level. Therefore, the quantification of the analytes in the samples can be carried out by means of the so-called matrix-matched calibration [38], i.e., by using spiked blank urine samples as calibration standards, which is a less tedious and time-consuming calibration methodology than standard addition calibration.

3.4. Analytical performance of the proposed method

Method validation was performed studying different parameters, such as the linearity and working range, the limits of detection

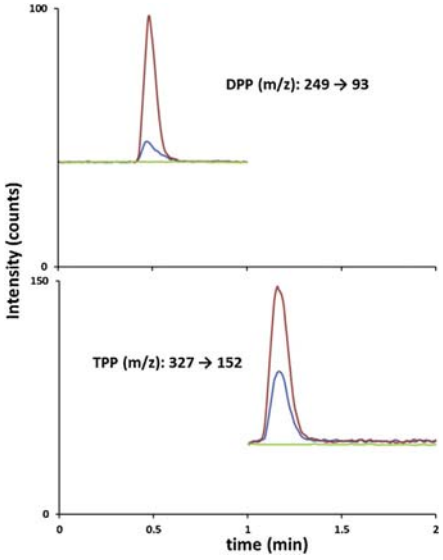

Fig. 6. Chromatogram of an aqueous standard solution containing TPP at 40 ng L^{-1} and DPP at 400 ng L^{-1} (red line), a real urine sample spiked with the target analytes at the same concentrations (blue line), and a blank urine solution (green line) (For interpretation of the references to colour in this figure legend, the reader is referred to the web version of this article).

Table 1
Comparison of slopes of each volunteer urine with a pool of all urine samples for TPP and DPP.

Compound	Standard matrix	Slope ± Deviation[a] (Counts min ng mL^{-1})	Student's *t*-test[b]	
			t_{exp}	Equality
TPP	Urine pool	10.5 ± 0.1	–	–
	Urine A	11.5 ± 0.4	2.41	Yes
	Urine B	11.0 ± 0.3	1.34	Yes
	Urine C	10.3 ± 0.3	0.80	Yes
	Urine D	10.3 ± 0.3	0.67	Yes
DPP	Urine pool	0.098 ± 0.003	–	–
	Urine A	0.094 ± 0.004	0.73	Yes
	Urine B	0.092 ± 0.005	1.16	Yes
	Urine C	0.089 ± 0.003	2.09	Yes
	Urine D	0.108 ± 0.004	2.26	Yes

[a] Concentration range: 0.5–5 ng mL^{-1}. Number of calibration points: 6.
[b] Student's *t*-test for slopes comparison between aqueous and each individually urine with the urine pool ($t_{crit}(0.05,4) = 2.77$).

(LOD) and limits of quantification (LOQ), the enrichment factor (EF) and extraction efficiency (EE) and the repeatability (expressed as relative standard deviation (% RSD). All these parameters are shown in Table 2.

A high level of linearity was achieved, reaching at least up to 100 ng mL^{-1}. Nevertheless, taking into account the expected low concentration levels in the samples, the working range was stablished from 0.5 to 5 ng mL^{-1}.

Both analytes showed good regression coefficients in all samples ($R^2 > 0.99$). The instrumental LODs and LOQs were calculated as the concentration value corresponding to a value of signal-to-noise of 3 and 10, respectively. Low LODs were obtained for both compounds (i.e., 1.9 ng L^{-1} for TPP and 17.1 ng L^{-1} for DPP). The method LODs and LOQs (MLOD and MLOQ), i.e., in urine samples, were 6.7 and 22.1 ng L^{-1} for TPP, respectively, and 77.2 and 254.8 ng L^{-1} for DPP.

Table 2
Main quality parameters of the proposed SBSDME-LC–MS/MS method.

Compound	EF[a]	EE (%)[b]	LOD[c] (ng L^{-1})	LOQ[c] (ng L^{-1})	MLOD[d] (ng L^{-1})	MLOQ[d] (ng L^{-1})	Repeatability[e] (% RSD)				
							Intra-day 0.05 ng mL^{-1}	0.5 ng mL^{-1}	2 ng mL^{-1}	Inter-day 0.05 ng mL^{-1}	0.5 ng mL^{-1}	2 ng mL^{-1}
TPP	30 ± 1	60	1.9	6.3	6.7	22.1	2.8	2.1	4.3	7.5	5.9	8.0
DPP	17 ± 1	34	17.1	57.1	77.2	254.8	–	2.2	2.4	–	3.6	5.3

[a] EF: Enrichment factor, as the mean of three replicates (± standard deviation) of an aqueous standard solution containing 5 ng mL^{-1} of the target analytes.
[b] EE: Extraction efficiency.
[c] LOD: Limit of detection; LOQ: Limit of quantification; calculated as 3 times and 10 times, respectively, the signal-to-noise ratio.
[d] MLOD: Method limit of detection and MLOQ: Method limit of quantification (i.e., in urine sample), calculated as 3 and 10 times, respectively, the signal-to-noise ratio.
[e] Relative standard deviation (RSD), five replicate analysis of an aqueous standard solution containing 0.05 (for TPP) and 0.5 and 2 ng mL^{-1} of the target analytes.

Fig. 7. Kinetic profiles of DPP in urine samples from volunteers (two male, M1 and M2; two female, F1 and F2) after application of a commercial nail polish containing TPP.

The EF was calculated as the ratio of the concentration of a standard solution of 5 ng mL^{-1} before ($[A]_{before}$) and after ($[A]_{after}$) applying the proposed method (i.e., EF = $[A]_{after}/[A]_{before}$). The EF was 30 for TPP and 17 for the DPP. These values correspond to EE of 60% and 34%, respectively, which were calculated as EE = EF·$V_{final}/V_{initial}$, where V_{final} is the final volume (i.e., the volume of the elution solvent, 0.5 mL), and $V_{initial}$ is the initial volume (i.e., the volume of sample, 25 mL).

The repeatability of the proposed method was studied by analysing 5 replicates of a standard solution (i.e., analytes-free pooled urine) containing the target analytes at a concentration of 0.05 (for TPP), 0.5 and 2 ng mL^{-1} (for TPP and DPP) in the same day (intra-day) and in different consecutive days (inter-day), showing RSD < 8% for both analytes, and thus demonstrating the good precision of the method.

Finally, the accuracy of the proposed method was established measuring three analytes-free urine samples coming from three volunteers (volunteers 1, 2 and 3) spiked with three concentrations levels for TPP (i.e., 0.05, 0.5 and 2.5 ng mL^{-1}) and two concentrations levels for DPP (i.e., 0.5 and 2.5 ng mL^{-1}). The results are shown in Table 3. As can be seen, good recovery values (between 81 and 112% for TPP, and from 93 to 111% for DPP) were obtained, thus showing that the matrix-matched calibration approach works in a reliable way.

A comparison of the proposed SBSDME with other analytical methods based on SPE for the determination of DPP in urine samples is shown in Table 4. It can be seen that the analytical performance in terms of LODs and relative recoveries is comparable or even better than those obtained by SPE. Moreover, the reduction in the consumption of organic solvents, and the avoidance of derivatization steps facilitate the procedure considerably.

3.5. Application to the analysis of urine samples

A commercial nail polish containing 4% of TPP was applied to four volunteers (two male (M1 and M2) and two female (F1 and F2)). The mean amount of the nail polish applied to the nails was approximately 0.1 g, which means that ca. 0.004 g of TPP was applied. Urine samples were collected before and after application at different time intervals for a period of 24 h. Then, they were kept at 4 °C until analyzed by the SBSDME-LC–MS/MS proposed method.

The results obtained in all the volunteers were similar. Detectable amounts of TPP (but below LOQ) were found in the first hours after the application (i.e., 1–2 h), but its concentration rapidly decreased probably due to its rapid metabolization being undetectable after that. Regarding to DPP, Fig. 7 shows the kinetic profiles. As expected, the concentration values increased over time reaching its maximum after 6–16 h, depending on the volunteer. After this time, the DPP concentration decreased although considerable amounts were still present at least 24 h after the nail polish application. The mean concentration levels found were 1.2,

Table 3
Recoveries values obtained by applying the proposed method via matrix-matched calibration to three analyte-free urine samples spiked at two concentration level concentration.

Compound	Volunteer 1			Volunteer 2			Volunteer 3		
	Added (ng mL^{-1})	Found amount after spiking (ng mL^{-1})	Relative recovery (%)	Added (ng mL^{-1})	Found amount after spiking (ng mL^{-1})	Relative recovery (%)	Added (ng mL^{-1})	Found amount after spiking (ng mL^{-1})	Relative recovery (%)
TPP	0.05	0.046	91 ± 6	0.05	0.044	88 ± 4	0.05	0.056	112 ± 7
	0.50	0.44	88 ± 3	0.50	0.40	81 ± 4	0.50	0.53	105 ± 8
	2.50	2.13	85 ± 5	2.50	2.02	81 ± 8	2.50	2.60	104 ± 5
DPP	0.50	0.51	103 ± 3	0.50	0.51	103 ± 7	0.50	0.46	93 ± 5
	2.50	2.47	99 ± 2	2.50	2.78	111 ± 2	2.50	2.60	104 ± 5

Table 4
Comparison of the proposed SBSDME approach with other methods coupled to LC–MS/MS for determination of DPP in urine samples.

Extractiontechnique[a]	Sorbent phase	MLOD[b] (ng mL^{-1})	Derivatization	Relative recovery (%)	Ref.
SPE	Strata-X-AW	0.20	no	71 - 97	[19]
SPE	Oasis Wax	0.09	yes	102 - 105	[20]
SPE	Isolute aminopropyl	0.05	yes	95 - 108	[21]
SPE	Oasis Wax	0.13	no	108	[22]
SPE	Strata-X-AW	0.2	no	n.r.[c]	[39]
SBSDME	$CoFe_2O_4$@Strata™-X-AW composite	0.08	no	93 - 111	This work

[a] SPE: Solid-phase extraction; SBSDME: Stir bar sorptive dispersive microextraction.
[b] MLOD: Method limit of detection (i.e., in the urine sample).
[c] n.r.: not reported.

1.7, 0.8 and 1.5 ng mL-1, for volunteer 1, 2, 3 and 4, respectively. Taking into account these values and that the mean urinary rate for adults in 24 h is ca. 1.5 L, and assuming that all the TPP percutaneously absorbed is metabolized to DPP and it is excreted by the urinary tract, means that 0.045, 0.064, 0.030 and 0.056% of the TPP applied is percutaneously absorbed, which gives an average of 0.049 ± 0.015%. These data provides an estimation of the percutaneous absorption, which are consistent with previous reported results [2]. It should be said that, in order to have a more consistent idea about the percutaneous absorption of TPP into the human organism, it would be necessary to extend the number of samples from different people and during longer periods of time.

4. Conclusions

In the present work, a new analytical method useful for monitoring the human exposure to the endocrine-disrupting plasticizer triphenyl phosphate (TPP) via nail polish use is proposed. The method allows trace determination of this parent compound and of its main metabolite, namely diphenyl phosphate (DPP), in urine samples of nail polish users.

The method is based on SBSDME as extraction technique prior to LC–MS/MS analysis, and it shows good analytical properties, such as accuracy, precision and sensitivity. In addition, the proposed method is fast and employs small amounts of organic solvents when compared with SPE-based methods previously used for the same purpose. In order to avoid matrix effects, matrix-matched calibration was used for quantification, by employing an analytes-free pooled urine.

This method would be useful for the study of the absorption/metabolism/excretion levels of this endocrine-disrupting cosmetic ingredient, with the aim of safeguard the user's health.

Finally, the presented study expands the analytical potential of SBSDME to other matrices and analytes.

Acknowledgements

Authors acknowledge the financial support of the Spanish Ministry of Economy and Competitiveness (Project CTQ2015-70301R). J.G. also thanks the Generalitat Valenciana and the European Social Fund for his predoctoral grant.

Appendix A. Supplementary data

Supplementary material related to this article can be found, in the online version, at doi: https://doi.org/10.1016/j.chroma.2019.02.014.

References

[1] H.M. Stapleton, S. Klosterhaus, A. Keller, P.L. Ferguson, S. Van Bergen, E. Cooper, T.L. Webster, A. Blum, Identification of flame retardants in polyurethane foam collected from baby products, Environ. Sci. Technol. 12 (2011) 5323–5331.
[2] E. Mendelsohn, A. Hagopian, K. Hoffman, C.M. Butt, A. Lorenzo, J. Congleton, T.F. Webster, H.M. Stapleton, Nail polish as a source of exposure to triphenyl phosphate, Environ. Int. 86 (2016) 45–51.
[3] A.S. Young, J.G. Allen, U. Kim, S. Seller, T.F. Webster, K. Kannan, D.M. Ceballos, Phthalate and Organophosphate Plasticizers in Nail Polish: Evaluation of Labels and Ingredients, Environ. Sci. Technol. 52 (2018) 12841–12850, http://dx.doi.org/10.1021/acs.est.8b04495, in press.
[4] X. Liu, K. Ji, K. Choi, Endocrine disruption potentials of organophosphate flame retardants and related mechanisms in H295R and MVLN cell lines and in zebrafish, Aquat. Toxicol. 114 (2012) 173–181.
[5] X. Liu, K. Ji, A. Jo, H.B. Moon, K. Choi, Effects of TDCPP or TPP on gene transcriptions and hormones of HPG axis, and their consequences on reproduction in adult zebrafish, Aquat. Toxicol. 134 (2013) 104–111.
[6] S. Yuan, H. Li, Y. Dang, C. Liu, Effects of triphenyl phosphate on growth, reproduction and transcription of genes of Daphnia magna, Aquat. Toxicol. 195 (2018) 58–66.
[7] D. Wang, W. Zhu, L. Chen, J. Yan, M. Teng, Z. Zhou, Neonatal triphenyl phosphate and its metabolite diphenyl phosphate exposure induce sex- and dose-dependent metabolic disruptions in adult mice, Environ Pollut. 237 (2018) 10–17.
[8] I. Van der Veen, J. de Boer, Phosphorus flame retardants: properties, production, environmental occurrence, toxicity and analysis, Chemosphere 88 (2012) 1119–1153.
[9] J.D. Meeker, H.M. Stapleton, House dust concentrations of organophosphate flame retardants in relation to hormone levels and semen quality parameters, Environ. Health Perspect. 118 (2010) 318–323.
[10] J.D. Meeker, E.M. Cooper, H.M. Stapleton, R. Hauser, Exploratory analysis of urinary metabolites of phosphorus-containing flame retardants in relation to markers of male reproductive health, Endocr. Disruptors 1 (2013) e26306.
[11] The Endocrine Disruption Exchange (TEDX) https://endocrinedisruption.org.
[12] European Commission, Regulation EC N^{o} 1223/2009 of the European Parliament and of the Council of 30 November 2009 on Cosmetic Products.

[13] N. Van den Eede, W. Maho, C. Erratico, H. Neels, A. Covaci, First insights in the metabolism of phosphate flame retardants and plasticizers using human liver fractions, Toxicol. Lett. 223 (2013) 9–15.
[14] G. Su, R.L. Letcher, D. Crump, D.M. Gooden, H.M. Stapleton, In vitro metabolism of the flame retardant triphenyl phosphate in chicken embryonic hepatocytes and the importance of the hydroxylation pathway, Environ. Sci. Technol. 4 (2015) 100–104.
[15] N. Van den Eede, I. de Meester, W. Maho, H. Neels, A. Covaci, Biotransformation of three phosphate flame retardants and plasticizers in primary human hepatocytes: untargeted metabolite screening and quantitative assessment, J. Appl. Toxicol. 11 (2016) 1401–1408.
[16] J.D. Meeker, E.M. Cooper, H.M. Stapleton, R. Hauser, Urinary metabolites of organophosphate flame retardants: temporal variability and correlations with house dust concentrations, Environ. Health Perspect. 121 (2013) 580–585.
[17] K. Hoffman, J.L. Daniels, H.M. Stapleton, Urinary metabolites of organophosphate flame retardants and their variability in pregnant women, Environ. Int. 63 (2014) 169–172.
[18] K. Möller, C. Crescenzi, U. Nilsson, Determination of a flame retardant hydrolysis product in human urine by SPE and LC-MS. Comparison of molecularly imprinted solid-phase extraction with a mixed-mode anion exchanger, Anal. Bioanal. Chem. 378 (2004) 197–204.
[19] E.M. Cooper, A. Covaci, A.L. Van Nuijs, T.F. Webster, H.M. Stapleton, Analysis of the flame retardant metabolites bis(1,3-dichloro-2-propyl) phosphate (BDCPP) and diphenyl phosphate (DPP) in urine using liquid chromatography-tandem mass spectrometry, Anal. Bioanal. Chem. 401 (2011) 2123–2132.
[20] N. Van den Eede, H. Neels, P.G. Jorens, A. Covaci, Analysis of organophosphate flame retardant diester metabolites in human urine by liquid chromatography electrospray ionisation tandem mass spectrometry, J. Chromatogr. A 1303 (2013) 48–53.
[21] G. Su, R.J. Letcher, H. Yu, Determination of organophosphate diesters in urine samples by a high-sensitivity method based on ultra-high pressure liquid chromatography-triple quadrupole-mass spectrometry, J. Chromatogr. A 1426 (2015) 154–160.
[22] I. Kosarac, C. Kubwabo, W.G. Foster, Quantitative determination of nine urinary metabolites of organophosphate flame retardants using solid phase extraction and ultra-performance liquid chromatography coupled to tandem mass spectrometry (UPLC-MS/MS), J. Chromatogr. B 1014 (2016) 24–30.
[23] Chemical Abstracts Service: pKa value calculated using Advanced Chemistry Development (ACD/Labs) Software V11.02 (1994-2018 ACD/Labs).
[24] J.L. Benedé, A. Chisvert, D.L. Giokas, A. Salvador, Development of stir bar sorptive-dispersive microextraction mediated by magnetic nanoparticles and its analytical application to the determination of hydrophobic organic compounds in aqueous media, J. Chromatogr. A 1362 (2014) 25–33.
[25] E. Baltussen, P. Sandra, F. David, C.A. Cramers, Stir bar sorptive extraction (SBSE), a novel extraction technique for aqueous samples: theory and principles, J. Microcol. 11 (September) (1999) 737–747.
[26] M. Anastassiades, S.J. Lehotay, D. Stajnbaher, F.J. Schenck, Fast and easy multiresidue method employing acetonitrile extraction/partitioning and dispersive solid-phase extractionfor the determination of pesticide residues in produce, J. AOAC Int. 86 (2003) 412–431.
[27] J.L. Benedé, A. Chisvert, D.L. Giokas, A. Salvador, Stir bar sorptive-dispersive microextraction mediated by magnetic nanoparticles-nylon 6 composite for the extractioin of hydrophilic organic compounds in aqueous media, Anal. Chim. Acta 926 (2016) 63–71.
[28] J.L. Benedé, A. Chisvert, D.L. Giokas, A. Salvador, Determination of ultraviolet filters in bathing waters by stir bar sorptive-dispersive microextraction coupled to thermal desorption-gas chromatography-mass spectrometry, Talanta 147 (2016) 246–252.
[29] J.L. Benedé, A. Chisvert, C. Moyano, D.L. Giokas, A. Salvador, Expanding the application of stir bar sorptive-dispersive microextraction approach to solid matrices: determination of ultraviolet filters in coastal sand samples, J. Chromatogr. A 1564 (2018) 25–33.
[30] K. Aguilar-Arteaga, J.A. Rodriguez, E. Barrado, Magnetic solids in analytical chemistry: a review, Anal. Chim. Acta 674 (2010) 157–165.
[31] X. Li, G. Zhu, Y. Luo, B. Yuan, Y. Feng, Synthesis and applications of functionalized magnetic materials in sample preparation, Trends Anal. Chem. 45 (2013) 233–247.
[32] Á. Ríos, M. Zougagh, Recent advances in magnetic nanomaterials for improving analytical processes, Trends Anal. Chem. 84 (2016) 72–83.
[33] K. Maaz, A. Mumtaz, S.K. Hasanain, A. Ceylan, Synthesis and magnetic properties of cobalt ferrite (CoFe2O4) nanoparticles prepared by wet chemical route, J. Magn. Magn. Mater. 308 (2007) 289–295.
[34] Y.Z. Lin, T.H. Wang, Y.S. Lin, W.C. Kuan, W.C. Lee, A novel method to prepare magnetic polymer-based anion exchangers and their application, J. Appl. Polym. Sci. 131 (2014) 40725.
[35] I.P. Román, A. Chisvert, A. Canals, Dispersive solid-phase extraction based on oleic acid-coated magnetic nanoparticles followed by gas chromatography–mass spectrometry for UV-filter determination in water samples, J. Chromatogr. A 1218 (2011) 2467–2475.
[36] T. Chung, W. Lee, Preparation of styrene-based, magnetic polymer microspheres by a swelling and penetration proces, React. Funct. Pol. 68 (2008) 1441–1447.
[37] E.M. Reyes-Gallardo, G. Lasarte-Aragonés, R. Lucena, S. Cárdenas, M. Valcárcel, Hybridization of commercial polymeric microparticles and magnetic nanoparticles for the dispersive micro-solid phase extraction of nitroaromatic hydrocarbons from water, J. Chromatogr. A 1271 (2013) 50–55.
[38] L. Cuadros-Rodríguez, M.G. Bagur-González, M. Sánchez-Viñas, A. González-Casado, A.M. Gómez-Sáez, Principles of analytical calibration/quantification for the separation sciences, J. Chromatogr. A 1158 (2007) 33–46.
[39] S.-S.E. Petropoulou, M. Petreas, J.-S. Park, Analytical methodology using ion-pair liquid chromatography-tandem mass spectrometry for the determination of four di-ester metabolites of organophosphate flame retardants in California human urine, J. Chromatogr. A 1434 (2016) 70–80.

Stir bar sorptive-dispersive microextraction for trace determination of triphenyl and diphenyl phosphate in urine of nail polish users

José Grau, Juan L. Benedé, Javier Serrano, Andrea Segura, Alberto Chisvert*
Department of Analytical Chemistry, University of Valencia, 46100 Burjassot, Valencia, Spain

Department of Analytical Chemistry, University of Valencia, 46100 Burjassot, Valencia, Spain

* Corresponding author:
e-mail address: alberto.chisvert@uv.es (A. Chisvert)

Instruments for composite characterization

Different techniques were applied to characterize the $CoFe_2O_4$@Strata-X^{TM}-AW composite.

A Quantum Design (CA, USA) MPMS-XL-5 superconducting quantum interference device (SQUID) magnetometer was used to measure the magnetic properties of the composite materials

Particle size distribution curve of the $CoFe_2O_4$@Strata-X^{TM}-AW composite was performed using a Malvern Mastersizer 2000 particle size analyzer.

Zeta potential measurements in order to determine the point of zero charge of the composite were performed using a Malvern Zetasizer ZS instrument.

A JEOL JEM-1010 transmission electron microscopy (TEM) operating at 100 kV equipped with an AMT RX80 (8.0 Mpx) digital camera and a S4100 scanning electron microscopy (SEM) were used to observe the morphology of the composite.

Nitrogen adsorption-desorption isotherms were measured on a ASAP 2010 analyzer from Micromeritics (GA, USA), in order to determine the surface area and pore size.

Magnetization curves

Different synthetic strategies were carried out. On one hand, previously synthetized MNPs were added to a polymer solution, which was previously swelled by using N-methyl-2-pyrrolidone (synthesis approach #1), or not swelled (synthesis approach #2). On the other hand, the possibility of carrying out the synthesis of the magnetic nanoparticles in situ was also studied by mixing a polymer (previously swelled (synthesis approach #3) or not (synthesis approach #4))

solution with Fe(III) and Co(II) solutions and then increasing the pH up to form the MNPs. These four synthetic strategies are described below.

Synthesis approach #1

For this synthesis 0.25 g of Strata-X^{TM}-AW polymer was weighted and mixed with 15 mL of pyrrolidone and 20 mL of water. The mix was stirred 24 hours. After that, the swelled polymer was mixed with 10 mL of a solution of 2,5 mg mL^{-1} in MNPs. 1M NaOH was added to obtain a alkaline pH. After 36 hours stirring, the dispersion was filtered (11µm) and dried overnight at 100 ºC.

Synthesis approach #2

0.25 g of Strata-X^{TM}-AW was suspended in 25 mL of water. 10 mL of a solution of 2,5 mg mL^{-1} in MNPs was then added. 1 M NaOH was added to obtain a alkaline pH. After 36 hours stirring, the dispersion was filtered (11µm) and dried overnight at 100 ºC.

Synthesis approach #3

0.25 g of Strata-X^{TM}-AW polymer was weighted and mixed with 15 mL of pyrrolidone and 20 mL of water. The mix was stirred 24 hours. Then, 0.50 g of $FeCl_3$ and 0.21 g of $CoCl_2$ were weighted and dissolved in 10 mL of water. 4 mL of a 3 M NaOH solution was added drop by drop in order to obtain an alkaline pH. The resultant solution was heated an hour at 80 ºC. The obtained dispersion was stirred during 48 hours at room temperature. The dispersion was filtered (11µm) and dried overnight at 100 ºC.

Synthesis approach #4

0.25 g of Strata-X^{TM}-AW was suspended in 25 mL of water. Then, 0.50 g of $FeCl_3$ and 0.21 g of $CoCl_2$ were weighted and dissolved in 10 mL of water. 4 mL of a 3 M NaOH solution was added drop by drop in order to obtain an alkaline pH. The resultant solution was heated an hour at 80 ºC. The obtained dispersion was stirred during 48 hours at room temperature. The dispersion was filtered (11µm) and dried overnight at 100 ºC.

Fig. S1 shows the magnetization curves for these four synthesis approaches. The first and the second approach have similar M_s values. Nevertheless, the second approach was selected as the swollen step was not necessary.

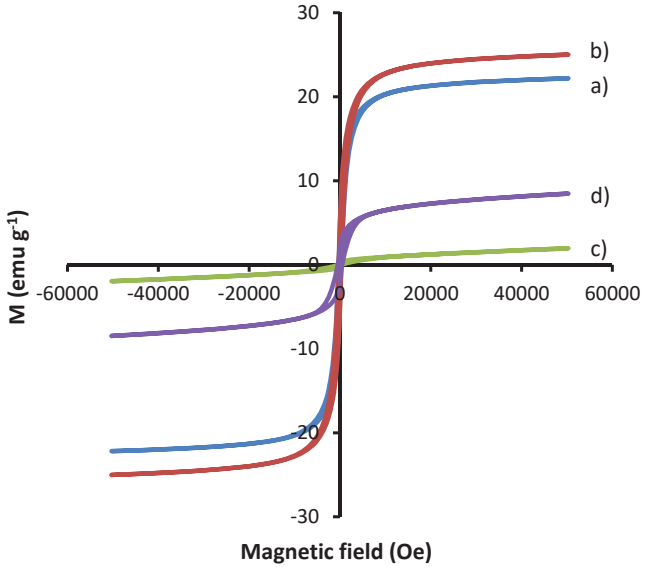

Fig. S1. Magnetization curves of (a) synthesis approach #1, (b) synthesis approach #2, (c) synthesis approach #3 and (d) synthesis approach #4.

Particle size

Particle size was determined by the number distribution method measured by the dynamic light scattering (DLS) technique. Fig. S2 shows the particle size distribution of the selected composite (i.e., according to the synthesis approach #2). The mean size obtained from this representation was 32 ± 1 μm.

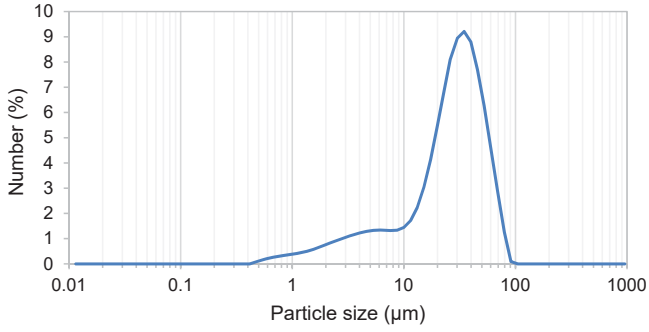

Fig. S2. Particle size distribution of the $CoFe_2O_4$@Strata-X^{TM}-AW composite.

Zeta potential - point of zero charge

Fig. S3 shows the pH versus zeta potential plot for a suspension of composite (2 mg/mL) in different 1 mM o-phosphoric acid solutions adjusted to different pH values (i.e. 3, 6, 9 and 12) with sodium hydroxide. The responses at pH < 3 were not satisfactory due to the high conductivity of the sample at this pH value. As can be seen, pH_{pzc} was determined to be 6.

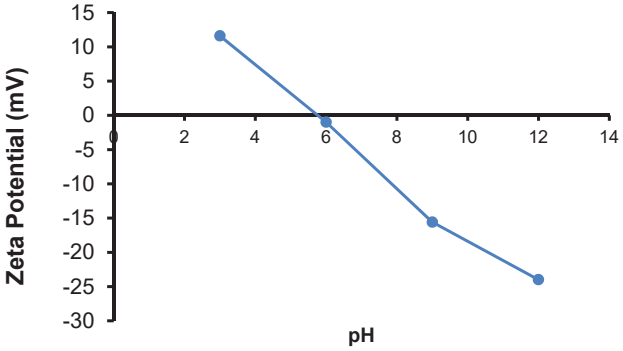

Fig. S3. Zeta potential of the $CoFe_2O_4$@Strata-X^{TM}-AW composite.

Morphology

Morphology of the $CoFe_2O_4$ MNPs and the $CoFe_2O_4$@Strata-X^{TM}-AW composite was determined by TEM microscopy operating at 100 kV. Representative TEM micrographs of the MNPs and the composite are shown in Fig. S4. Fig. S4a) shows MNPs with a spherical shape and a diameter around 20 nm, whereas Fig. S4b) shows the spherical $CoFe_2O_4$ MNPs embedded into the polymeric network.

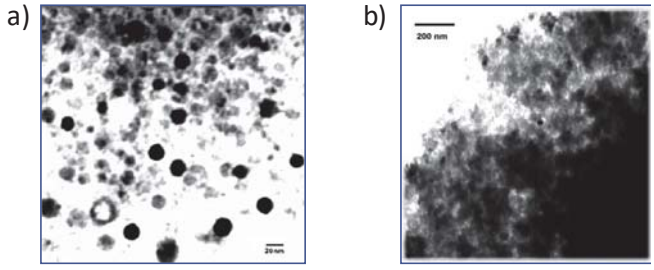

Fig. S4. TEM micrographs of (a) $CoFe_2O_4$ MNPs and (b) $CoFe_2O_4$@Strata-X^{TM}-AW composite.

Moreover, a typical SEM image showing the amorphous aggregates of the $CoFe_2O_4$@Strata-X^{TM}-AW composite is shown in Fig. S5.

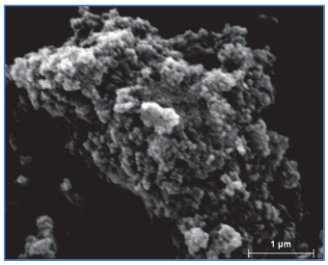

Fig. S5. A SEM micrograph of the $CoFe_2O_4$@Strata-X^{TM}-AW composite.

The specific surface area and the porosity of the $CoFe_2O_4$@Strata-X^{TM}-AW composite were also measured in order to demonstrate the adsorption capacity of this material. The obtained isotherm (see Fig. S6) can be considered as essentially type-IV curve, which demonstrates the presence of mesopores, with an average pore diameter of 29.54 nm according to Fig. S7. The BET specific surface area value was 406.6 ± 0.7 m^2/g.

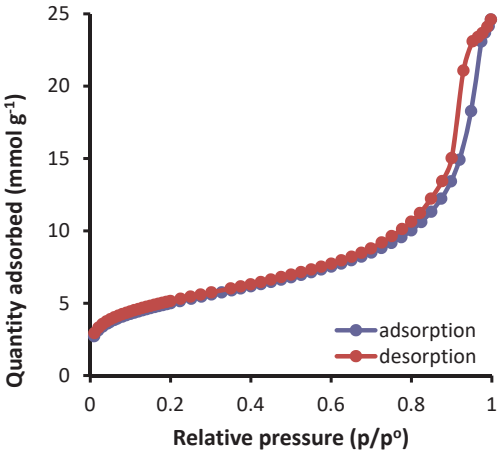

Fig. S6. Isotherm linear plot of the $CoFe_2O_4$@Strata-X^{TM}-AW composite.

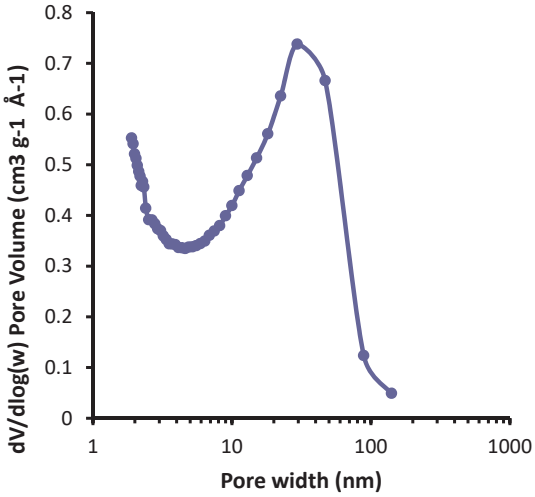

Fig. S7. Barrett-Jolner-Halenda (BJH) pore-size distribution plot of the $CoFe_2O_4$@Strata-X^{TM}-AW composite.

Polydopamine-coated magnetic nanoparticles for the determination of nitro musks in environmental water samples by stir bar sorptive-dispersive microextraction

Talanta 231 (2021) 122375

DOI: 10.1016/j.talanta.2021.122375

Talanta 231 (2021) 122375

Contents lists available at ScienceDirect

Talanta

journal homepage: www.elsevier.com/locate/talanta

Polydopamine-coated magnetic nanoparticles for the determination of nitro musks in environmental water samples by stir bar sorptive-dispersive microextraction

José Grau, Juan L. Benedé, Alberto Chisvert *

Department of Analytical Chemistry, University of Valencia, 46100, Burjassot, Valencia, Spain

ARTICLE INFO

Keywords:
Environmental water analysis
Magnetic composite
Nitro musks
Polydopamine
Stir bar sorptive-dispersive microextraction

ABSTRACT

Magnetic-based microextraction approaches have gained popularity in recent years due to the magnetic properties of the extraction phases allowing to handle them easier and more efficiently. This work describes a magnetic-based analytical method for the determination of the family of nitro musks in environmental water samples. These compounds have been of great concern due to their environmental impacts and potential health effects. The method is based on stir bar sorptive-dispersive microextraction (SBSDME) as extraction approach, prior to thermal desorption coupled to gas chromatography-mass spectrometry analysis (TD-GC-MS). For this purpose, polydopamine-coated cobalt ferrite magnetic nanoparticles ($CoFe_2O_4$@PDA) were used as extraction material. The main parameters involved in the extraction procedure (i.e., sorbent amount, extraction time and ionic strength) as well as in the thermal desorption step (i.e., temperature and desorption time) were evaluated in order to obtain the highest sensitivity. Under the selected conditions, the method showed good linearity, limits of detection and quantification in the low ng L^{-1} range, intra- and inter-day repeatability with RSD <15%, and high enrichment factors (178–640). Finally, the method was applied to four environmental water samples of different origin. Relative recovery values ranging from 91 to 120% highlighted that the matrices under consideration do not affect the extraction process. This work constitutes the first time in which nitro musks compounds were selectively extracted by taking advantage the high potential that magnetic-based microextraction techniques offer, specially SBSDME.

1. Introduction

Musk compounds have been widely used as valuable fragrance ingredients in daily consumer products such as cosmetics and household products, among others. Natural musks are obtained from glands of certain animals, such as deer, but their use is nowadays scarce due to ethical and economic reasons [1]. However, synthetic musks are a group of compounds having totally different chemical structures than natural ones but possessing musk-like odour properties [2]. More specifically, nitro musks are a group of these synthetic musks whose structure consists of dinitro and trinitro substituted benzene derivatives. The nitro musk family (see Table S1) is constituted by musk ambrette (MA), musk ketone (MK), musk moskene (MM), musk tibetene (MT) and musk xylene (MX). However, despite their pleasant aroma and extensive use, they have shown eco-toxicity and human health risks related to dermatitis, carcinogenic effects and endocrine disruption [3,4].

It should be said that some studies show that nitro musks are released into the environment through household water and wastewater [5–7]. These compounds are not easily biodegradable but they are highly persistent, since they are not completely removed in wastewater treatment plants [7,8]. For these reasons, and due to their habitual use in many daily products, they are very widespread in the environment, especially in aquatic and marine ecosystems [3,9]. Therefore, it is important to develop analytical methods from the point of view of environmental surveillance, and thus assess the human exposures to these compounds, as well as to evaluate its potential for bioaccumulation on the environment and their ecotoxicological effects in the flora and fauna.

Several methodologies, mostly based on gas chromatography (GC) coupled to mass spectrometry (MS), are available in the literature for the determination of these five compounds in environmental surface waters [10,11]. Moreover, due to the low concentration of these compounds in

* Corresponding author.
E-mail address: alberto.chisvert@uv.es (A. Chisvert).

https://doi.org/10.1016/j.talanta.2021.122375
Received 30 November 2020; Received in revised form 28 February 2021; Accepted 18 March 2021
Available online 31 March 2021

this type of samples and the relative complexity of the matrix involved, (micro)extraction techniques are commonly applied in order to improve the method sensitivity and/or to eliminate potentially interfering compounds. In this way, solid-phase extraction (SPE) [12,13], and its miniaturization approaches like solid-phase microextraction (SPME) [14,15], stir bar sorptive extraction (SBSE) [16–19], dispersive solid-phase extraction (DSPE) [20] and microextraction by packed sorbent (MEPS) [21] have been employed for this purpose. Regarding liquid-phase based microextraction techniques, dispersive liquid-liquid microextraction (DLLME) [16,17,22,23], single-drop microextraction (SDME) [24,25], ultrasounds-assisted emulsification microextraction (USAEME) [26], and membrane-assisted solvent extraction (MASE) [15,27] have been also reported with the same purposes but to a lesser extent.

Among the vast array of developed microextraction techniques which can be found in the literature, those based on the dispersion of the solid extraction phase (i.e., DSPE) within the donor phase have attracted considerable attention. The main purpose of dispersion is to accomplish a higher surface contact of the sorbent with the liquid sample, or its extract or solution, resulting in more favorable extraction kinetics and lower extraction times [28]. Moreover, magnetic-based DSPE has gained popularity in recent years due to the magnetic properties of the extraction phases that allow their facile and fast retrieval by means of an external magnet, overcoming the tedious handling of non-magnetic sorbents, typically used in conventional DSPE [29]. Other potential advantages are the good sorbent reusability and the high extraction efficiencies achieved due to the nanoscale of these materials [30–32]. However, to the best of our knowledge, the high potential of magnetic materials has never been used before for the determination of the complete family of nitro musks compounds despite the advantages above mentioned. Only one publication has reported the application of a magnetic material for the extraction of other synthetic musks (namely, polycyclic musk) [33].

In this context, our group developed a hybrid dispersive-based microextraction approach which uses magnetic materials as extraction phase, termed stir bar sorptive-dispersive microextraction (SBSDME) [34]. In this technique, a magnetic sorbent material (e.g., functionalized magnetic nanoparticles (MNPs) or composite materials made of MNPs and polymers) is added to a vial containing a neodymium bar-shaped magnet, in such a way it is attracted by the magnet. At high stirring rate, the material is released and dispersed into the donor solution, thus increasing the contact area between the sample and the extraction phase. When stirring is over, the neodymium stir bar rapidly retrieves the magnetic sorbent containing the extracted analytes. Then, the magnetic material-coated stir bar is easily taken from the sample solution and the analytes can be either desorbed in an appropriate solvent for further injection into a liquid chromatographic (LC) or a GC instrument, or directly thermally desorbed (TD), as solvent-free desorption, into a GC system. The fundamentals of this approach, and an overview of the published papers concerning analytical methods based on the use of the SBSDME approach have been very recently compiled in a tutorial review [35].

The aim of this work is to develop, for the first time, a highly sensitive magnetic-based analytical method for the determination of the nitro musks family in environmental water samples. This method is based on SBSDME as extraction technique followed by TD-GC-MS analysis, presenting a great clean-up and enrichment potential. Polydopamine-coated cobalt ferrite MNPs (i.e., $CoFe_2O_4$@PDA) is proposed here as sorbent material due to the great ability of PDA to interact with the analytes through hydrophobic and π–π interactions. This ability and their chemical and environmental stability have increased their use as sorbent in the last decade [36], being employed for the extraction of a wide range of analytes. As far as we know, this work constitutes the first time in which these analytes have been selectively extracted taking advantage of the use of magnetic materials. Additionally, this work expands the analytical potential of SBSDME to compounds not yet determined by this approach [35], as well as the use of other magnetic sorbents (i.e., polydopamine-based materials).

2. Experimental

2.1. Reagents and samples

All reagents and solvents were obtained from major suppliers. 1-*tert*-butyl-3-methyl-2,4-dinitroanisole (Musk Tibetene, MT) 99%, 1,1,3,3,5-pentamethyl-4,6-dinitroindane (Musk Moskene, MM) 99%, 6-*tert*-butyl-3-methyl-2,4-dinitroanisole (Musk Ambrette, MA) 99% and a cyclohexane solution of 100 mg mL^{-1} of 1-*tert*-butyl-3,5-dimethyl-2,4,6-trinitrobenzene (Musk Xylene, MX) from LGC standards (Lancashire, United Kingdom), and 4-*tert*-butyl-2,6-dimethyl-3,5-dinitro-acetophenone (Musk Ketone, MK) 98% from Dr. Ehrenstorfer (Augsburg, Germany) were used as standards. Hexachlorobenzene (HCB) 99% from Sigma-Aldrich (Steinheim, Germany) was used as surrogate. The chemical structure and some relevant information are given in Table S1.

For the synthesis of $CoFe_2O_4$ MNPs, cobalt (II) chloride hexahydrate ($CoCl_2{\cdot}6H_2O$) and iron (III) chloride hexahydrate ($FeCl_3{\cdot}6H_2O$) were purchased from Acros Organics (New Jersey, USA), and sodium hydroxide (reagent grade) was purchased from Scharlau (Barcelona Spain). Dopamine hydrochloride from Sigma-Aldrich (Steinheim, Germany) and tris(hydroxymethyl)-aminomethane-hydrochloride from Merck (Darmstadt, Germany) were used for the functionalization of the $CoFe_2O_4$ MNPs.

HPLC-grade ethanol (EtOH) was purchased from Scharlau (Barcelona, Spain). Deionized water was obtained from a Connect water purification system provided by Adrona (Riga, Latvia). Sodium chloride (99.5%, analytical grade) that was used as ionic strength regulator was purchased from Scharlau (Barcelona, Spain). High purity helium (99.9999%) from Carburos Metálicos S.A. (Paterna, Spain) was used as carrier gas in the GC-MS system.

Water samples were collected from Malvarrosa Beach (Valencia, Spain), Mijares River (Castellón, Spain), a drinking water treatment plant (Picassent, Spain), and a cleaning water from a cosmetic company from the same region. All samples were collected in 1 L topaz glass bottles and stored in the dark at 4 °C. Before analysis, the samples were left to reach room temperature.

2.2. Apparatus and materials

A Focus GC gas chromatograph coupled to a DSQ II mass spectrometry detector (operated in positive electron ionization mode at an ionization energy of 70 eV) from Thermo Fisher Scientific (Austin, TX, USA) was employed. Thermal desorption was performed with a UNITY 2™ thermodesorption system from Markes International Limited (Llantrisant, UK).

A multi-position magnetic stirrer from DLAB Scientific Europe S.A.S (Schiltigheim, France) was used for the extraction procedure, and NdFeB (45 MGOe) magnetic tumble stir cylinders (3 mm diameter x 12 mm long, nickel coated) from Superimanes S.L. (Sevilla, Spain) were used as stir bars for the extraction.

A Quantum Design (CA, USA) MPMS-XL-5 superconducting quantum interference device (SQUID) magnetometer was used to measure the magnetic properties of the material.

A JEOL JEM-1010 transmission electron microscopy (TEM) operating at 80 kV equipped with an AMT RX80 (8.0 Mpx) digital camera and a HITACHI S4800 scanning electron microscopy (SEM) operating at 10 kV equipped with an RX Bruker nackscattered electron detector, were used to observe the morphology of the material.

Nitrogen adsorption-desorption isotherms were measured on a ASAP 2010 analyzer from Micromeritics (GA, USA) in order to determine the surface area and pore size.

Thermogravimetric analysis (TGA) was accomplished using a PerkinElmer TGA-7 thermobalance by heating from room temperature to

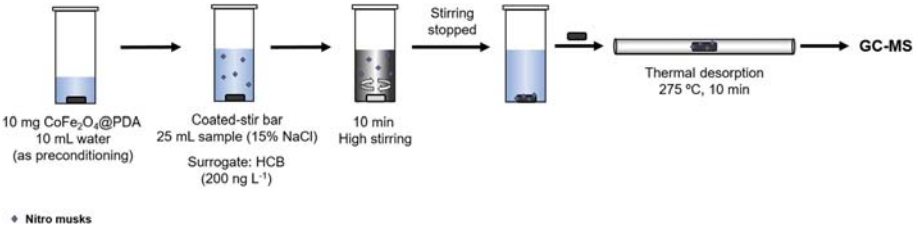

Fig. 1. Schematic diagram of the proposed SBSDME approach.

1000 °C under nitrogen atmosphere.

2.3. Synthesis of $CoFe_2O_4$@PDA MNPs

The synthesis of the $CoFe_2O_4$@PDA MNPs consisted of two steps: the synthesis of bare $CoFe_2O_4$ MNPs by wet chemical co-precipitation according to an adapted protocol [37], and subsequent coating with dopamine [38].

First, 100 mL of a 0.4 M $FeCl_3$ aqueous solution and 100 mL of a 0.2 M $CoCl_2$ aqueous solution were mixed, and then 100 mL of a 3 M sodium hydroxide aqueous solution were added dropwise under continuous stirring. The black precipitate product was slowly cooled to room temperature and washed several times with ultrapure water and ethanol. Finally, the precipitate was dried overnight at 100 °C and then pulverized into a fine powder. The yield of this step is ca. 78%.

For the functionalization of the MNPs, 250 mg of the above-obtained $CoFe_2O_4$ MNPs were homogeneously dispersed into 100 mL Tris buffer (10 mM, pH = 8.5). Then, 500 mg of dopamine monomer were added and the mixture was magnetically stirred for 12 h at room temperature. The resultant $CoFe_2O_4$@PDA MNPs were washed with ultrapure water and ethanol, dried overnight at 80 °C and finally pulverized into a fine powder. The yield of this step is ca. 40%.

2.4. Proposed method

2.4.1. Standards preparation

A stock solution containing 500 μg mL^{-1} of all five nitro musks was prepared in ethanol. A stock solution of HCB (as surrogate) was prepared in ethanol at 200 μg mL^{-1}. Working solutions (20–100 ng L^{-1}) containing HCB at 200 ng L^{-1} were prepared by appropriate dilution with deionized water.

2.4.2. SBSDME procedure

For preconditioning and physical coating of the stir bars, 10 mg of dried $CoFe_2O_4$@PDA MNPs were dispersed in 10 mL of deionized water and a bare neodymium stir bar (45 MGOe, 3 mm diameter x 12 mm long) was introduced and stirred for 5 min at high stirring rate to solvate the composite. The MNPs were strongly attracted by the bar-shaped neodymium magnet by stopping the stirrer, and then the MNPs-coated stir bar was taken out from water with the aid of plastic thumb forceps.

For the extraction procedure, the coated stir bar was immersed in a vial containing 25 mL of an aqueous standard working solution or sample (both adjusted to 15% NaCl (w/v)). Then, the solution was magnetically stirred for 10 min at room temperature at a high stirring rate (ca. 1000 rpm) to completely disperse the $CoFe_2O_4$@PDA MNPs. After stirring stopped, the MNPs were collected onto the magnetic stir bar (ca. 2 min), and then the coated stir bar was removed with plastic thumb forceps, gently rinsed with deionized water and placed into a glass desorption tube (89 mm long x 6.4 mm o.d.) to accomplish the

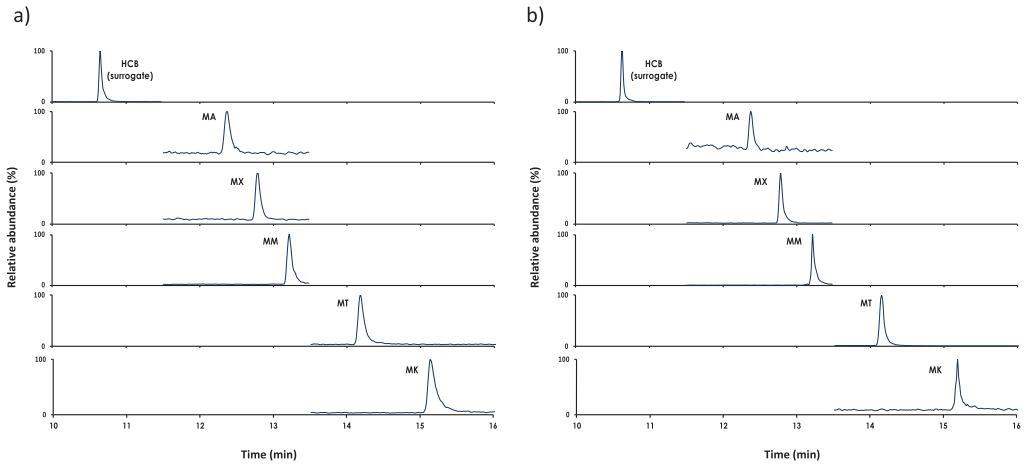

Fig. 2. Chromatograms obtained by the optimized SBSDME-TD-GC-MS approach to (a) a standard solution containing 100 ng L^{-1} of the target analytes and (b) a sample spiked with the analytes at the same concentration, both containing 200 ng L^{-1} of the surrogate.

thermal desorption of the analytes. Fig. 1 shows a schematic diagram of the experimental procedure.

After each use, the MNPs were removed from the surface of the stir bars with the help of a stronger neodymium magnet, and then the stir bars and the glass desorption tubes were cleaned with water and sequentially soaked in ethanol and acetone to prevent possible background contamination and carryover. Then, the desorption tubes and the stir bars were dried at room temperature.

2.4.3. TD-GC-MS analysis

First, a pre-purge for 1 min was carried out. Afterwards, the tube containing the coated stir bar was heated at 50 °C for 2 min to remove any possible water residues originating from the SBSDME step. The analytes were desorbed from the coated stir bar at 275 °C for 10 min using helium as carrier gas in splitless mode. Then the desorbed compounds were cryo-focused at −10 °C in the cold trap (graphitized carbon) during desorption. Finally, trap temperature was programmed to increase from −10 °C to 275 °C (held for 3 min) at 16 °C s^{-1} to inject the trapped compounds into the GC column. The TD transfer line was maintained at 200 °C.

Chromatographic separations were carried out in a HP-5MS Ultra Inert (95% dimethyl-5% diphenylpolysiloxane, 30 m length, 0.25 mm i.d., 0.25 μm film thickness) column from Agilent Technologies (Palo Alto, CA, USA). The separations were run at a 1 mL min^{-1} constant flow rate using helium as carrier gas. The oven temperature program was: from 60 °C (1 min) to 120 °C at 20 °C min^{-1}, then to 180 °C at 10 °C min^{-1} and finally to 280 °C (1 min) at 25 °C min^{-1}. The MS transfer line and ion source temperatures were set at 280 and 250 °C respectively. The chromatograms were recorded in selected ion monitoring (SIM) mode at the mass/charge (m/z) ratios for each analyte shown in Table S1. Calibration was performed by plotting A_i/A_{sur} (where A_i is the peak area of the target analyte and A_{sur} is that of the surrogate) versus the target analyte concentration. Fig. 2 shows chromatograms of (a) a standard solution containing the target analytes at 100 ng L^{-1} and (b) a sample spiked with the analytes at the same concentration, both containing the surrogate at 200 ng L^{-1}.

3. Results and discussion

3.1. Selection of the sorbent material

The selection of $CoFe_2O_4$@PDA composite as sorbent material was based on the ability of PDA to interact with the analytes by hydrophobic and π−π interactions due to its highly delocalized π−π conjugated system, in addition to having a large specific surface area and good dispersibility in water [36].

Moreover, the synthesis requirement of PDA is simple and mild with no need for organic solvent owing to its unique non-covalent self-assembly and covalent polymerization in alkaline aqueous media [39,40]. The easy synthesis of PDA-coated cobalt ferrite MNPs is simply executed via stirring dopamine hydrochloride in a Tris-HCl buffer saline solution at pH 8.5 (see Section 2.3). The $CoFe_2O_4$ MNPs confer to the active sorbent (i.e., PDA) the magnetism needed to be used in SBSDME. $CoFe_2O_4$ MNPs were preferred rather than to Fe_3O_4 MNPs due to its higher chemical stability [41].

In order to minimize the variability not only of the SBSDME procedure but also of the TD-GC stage, HCB was used as surrogate. This compound was selected since it potentially presents the same interactions with the sorbent than nitro musks (i.e., π−π and hydrophobic interactions), and thus it is extractable in a similar way. Moreover, its volatility is suitable to be measured by TD-GC.

3.2. Characterization of $CoFe_2O_4$@PDA MNPs

3.2.1. Magnetization curve

Fig. S1 shows the magnetization curve for (a) $CoFe_2O_4$ MNPs and (b) the synthesized $CoFe_2O_4$@PDA MNPs. As can be seen below, the saturation magnetization (M_s) value for the bare MNPs was 65.0 emu g^{-1}, the residual magnetism (B_r) was 28.5 emu g^{-1} and the coercivity (H_c) was 0.99 kOe. Regarding the $CoFe_2O_4$@PDA MNPs, the obtained M_S was about 46.2 emu g^{-1}, B_r was 27.4 emu g^{-1} and H_C value to demagnetize the material after its magnetization was 3 kOe. As expected, $CoFe_2O_4$@PDA was less magnetic than $CoFe_2O_4$ MNPs, but its Ms value is high enough for SBSDME application. Moreover, these results showed the $CoFe_2O_4$@PDA composite as a soft ferromagnetic material.

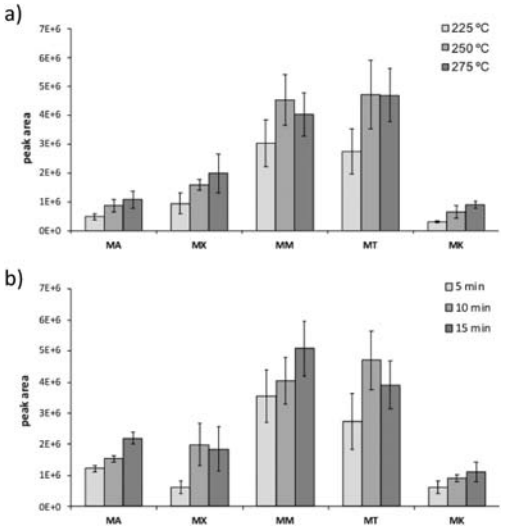

Fig. 3. Effect of the thermal desorption conditions: a) temperature, b) desorption time. Extraction conditions: 20 ng mL^{-1} of target analytes, 25 mL sample volume, 10 mg $CoFe_2O_4$@PDA MNPs, 5 min extraction time (n = 3).

3.2.2. Morphology

Morphology of the $CoFe_2O_4$@PDA MNPs was studied by TEM operating at 80 kV and SEM operating at 10 kV. Representative TEM and SEM micrographs of this material are shown in Fig. S2 and Fig. S3, respectively. The results demonstrated the spherical shape of the $CoFe_2O_4$ MNPs covered by an outer layer of polydopamine (around 20–50 nm).

Moreover, estimations of the surface are and pore size of the magnetic material were performed by nitrogen adsorption isotherm measurement. The obtained isotherm (Fig. S4) can be considered as a type-IV curve, and the pore diameter (7.50 nm) confirms the mesoporous size of the material. Furthermore, BET surface area was also studied obtaining a value of 10.544 ± 0.008 m^2 g^{-1}.

3.2.3. Thermogravimetric analysis

Fig. S5 shows the TGA curve of $CoFe_2O_4$@PDA MNPs under N_2 atmosphere. The thermal stability of the material is maintained up to ca. 300 °C, from which a weight lost is observed until 650 °C, due to the decomposition of organic matter (i.e., PDA). From 650 °C the mass percentage (weight, %) is approximately 69.2%, which means that the PDA content in the $CoFe_2O_4$@PDA MNPs is 30.8%. According to this information, $CoFe_2O_4$@PDA MNPs are stable during the TD process, where the highest temperature reached is 275 °C.

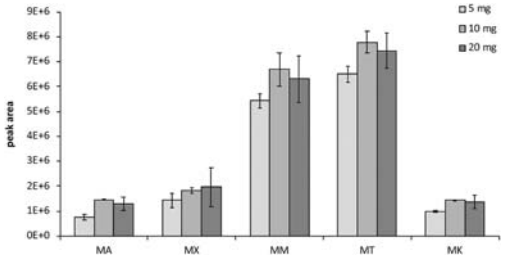

Fig. 4. Effect of the $CoFe_2O_4$@PDA MNPs amount on the extraction process. Extraction conditions: 20 ng mL^{-1} of target analytes, 25 mL aqueous phase, 5 min extraction time. Desorption conditions: 275 °C for 10 min (n = 3).

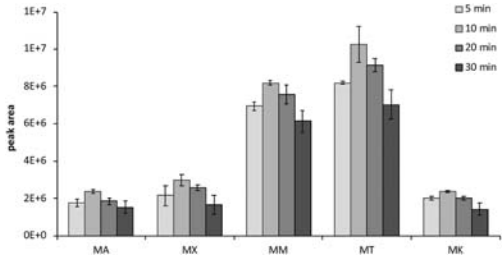

Fig. 5. Effect of the extraction time on the extraction process. Extraction conditions: 20 ng mL^{-1} of target analytes, 25 mL aqueous phase, 10 mg $CoFe_2O_4$@PDA MNPs. Desorption conditions: 275 °C for 10 min (n = 3).

3.3. Study of the experimental variables

The main parameters involved in the thermal desorption step (i.e., temperature and desorption time) as well as in the extraction procedure (i.e., sorbent amount, extraction time and ionic strength) were evaluated in order to obtain the highest enrichment factors, and therefore the lowest limits of detection. For this purpose, the influence of these variables was evaluated by extracting an aqueous standard solution containing 20 ng mL^{-1} of each target nitro musk. All experiments were carried out in triplicate and the peak area of each analyte (A_i) was used as the analytical response. The surrogate (i.e., HCB) was not used in the optimization step since it could be affected in the same or different extension (either negatively or positively) than the analytes, which could lead to wrong conclusions.

3.3.1. TD conditions

The effect of the desorption temperature was studied in the range from 225 to 275 °C, at a hold time set at 10 min. As can be seen in Fig. 3a, the TD temperature profiles increased up to 250–275 °C, depending on the analyte. Higher temperatures were not recommended since baseline perturbations acquired high relevance, since the thermal stability of the material endangers above 300 °C, as previously stated. Regarding the effect of desorption time (5–15 min), an evident improvement between the signals obtained at 5 min and 10 min was observed (Fig. 3b), and in some cases a desorption time of 15 min did not contribute to any improvement in the peak areas. Therefore, 275 °C for 10 min were selected as the best conditions for performing the desorption step. This results are in agreement with previous works in which some of these nitro musks were also thermally desorbed after to SBSE [18,42].

Before the desorption step, it was considered to include an additional step to eliminate possible water residues that remained after the SBSDME, thus preventing their introduction into the GC-MS system. Thus, the tube was heated at mild conditions (i.e., 50 °C for 2 min), which allowed to eliminate the residual water without a significant loss of the target analytes.

No significative carryover among repeated desorptions on the same coated stir bar was observed, since the relative amount of analytes measured in a second desorption experiment was less than 3%, thus suggesting that desorption was quantitative and no additional desorption steps were necessary to recover the analytes.

3.3.2. Amount of $CoFe_2O_4$@PDA sorbent

In order to obtain the maximum signal of all analytes, the $CoFe_2O_4$@PDA MNPs amount was varied in the range of 5–20 mg, whereas the volume of the donor phase was maintained constant at 25 mL. Higher amounts were not tested so that not surpass the weight limitations of the TD sample tube. As can be seen in Fig. 4, the signals increased up 10 mg, while they remained constant at higher amounts. Based on these results, 10 mg of sorbent were selected for further experiments.

3.3.3. Extraction time

Extraction time depends on the equilibrium time, which is associated with the distribution coefficient of the analytes between the donor phase and the sorbent material. To this regard, different times (1–30 min) were tested. The obtained results (Fig. 5) showed that the signal was higher at 10 min, while longer extraction times produced a negative effect. Although there is no exhaustive study to justify this phenomenon, it may be attributed to incomplete retrieval of the sorbent after the extraction due to $CoFe_2O_4$@PDA MNPs were partially disassembled under vigorous stirring for long periods. For this reason, an extraction time of 10 min was selected.

3.3.4. Ionic strength

The ionic strength of the donor phase was studied in the range 0–25% of NaCl (w/v %). A clear improvement was observed up to 15% (Fig. 6), mainly due to the salting-out effect, which has a positive effect promoting the extraction of organic compounds from water solutions. A decrease was observed at 25%, due to the viscosity of the solution was so high that prevented the properly dispersion of the MNPs into the donor phase.

3.4. Analytical performance of the proposed method

Analytical parameters of the proposed method, such as linearity, enrichment factors (EFs), extraction efficiencies (EE), method limits of detection (MLOD) and quantification (MLOQ), and repeatability were evaluated under selected conditions. The results are summarized in Table 1.

Due to SBSDME approach is not an exhaustive extraction one,

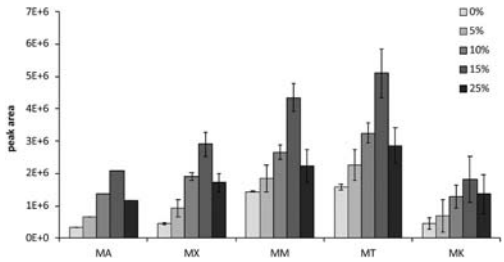

Fig. 6. Effect of the ionic strength of the donor aqueous phase on the extraction process. Extraction conditions: 20 ng mL^{-1} of target analytes, 25 mL aqueous phase, 10 mg $CoFe_2O_4$@PDA MNPs, 10 min extraction time. Desorption conditions: 275 °C for 10 min (n = 3).

Table 1
Main analytical features of the proposed SBSDME-TD-GC-MS method.

Nitro musk	Determination coefficient R^2[a]	MLOD[b] (ng L^{-1})	MLOQ[b] (ng L^{-1})	EF[c]	EE[c] (%)	Repeatability[d] (% RSD)			
						Intra-day		Inter-day	
						20 ng L^{-1}	40 ng L^{-1}	20 ng L^{-1}	40 ng L^{-1}
MA	0.997	5.6	18.6	284 ± 10	1.1 ± 0.1	3.9	4.5	9.7	10.2
MX	0.999	3.8	13.0	178 ± 10	0.7 ± 0.1	4.8	5.4	8.6	9.6
MM	0.998	0.3	1.0	640 ± 70	2.6 ± 0.4	3.5	3.7	7.8	12.3
MT	0.999	1.8	6.0	303 ± 30	1.2 ± 0.2	5.8	6.6	9.8	11.5
MK	0.995	0.6	2.0	378 ± 30	1.5 ± 0.2	5.3	5.9	10.5	10.1

[a] Working range: 20–100 ng L^{-1}.
[b] MLOD: Method limit of detection; MLOQ: Method limit of quantification; calculated as 3 times and 10 times, respectively, the signal-to-noise ratio.
[c] EF: Enrichment factor, EE: extraction efficiency, as the mean of three replicates (±standard deviation) of an aqueous standard solution (adjusted to 15% NaCl (w/v)) containing 100 ng L^{-1} of the target analytes.
[d] Relative standard deviation (RSD), five replicate analysis of an aqueous standard solution containing 20 and 40 ng L^{-1} of the target analytes.

Table 2
Comparison of the proposed SBSDME approach with other approaches coupled to GC-MS for determination of nitro musks in environmental waters.

Nitro musks	Extraction technique	Extraction time (min)[a]	EF[b]	MLOD (ng L^{-1})	Relative recovery (%)[b]	Ref.
MK, MM, MT, MX	SPME	900	n.r.	0.05–60	42–119	[15]
MA, MK, MM, MT, MX	SBSE	240	n.r.	0.02–1.4	n.r.	[43]
MK, MX	DSPE	10	n.r.	0.5–2.0	70–97	[20]
MA, MK, MM, MT, MX	DLLME	–	230–314	4–33	87–116	[22]
MA, MK, MM, MT, MX	BID-SDME	20	65–92	12–42	92–105	[25]
MK, MM, MX	USAEME	10	n.r.	9.2–10	80–114	[26]
MA, MK, MM, MT, MX	MASE	240	n.r.	4–25	47–138	[27]
MA, MK, MM, MT, MX	SBSDME	10	172–640	0.1–2.8	92–120	This work

[a] BID-SDME: bubble-in-drop single drop microextraction; DLLME: dispersive liquid-liquid microextraction; DSPE: dispersive solid-phase extraction; MASE: membrane-assisted solvent extraction; SBSDME: stir bar sorptive dispersive microextraction; SBSE: stir bar sorptive extraction; SPME: solid-phase microextraction; USAEME: ultrasound assisted-emulsification microextraction.
[b] n.r.: not reported.

standard solutions were prepared in deionized water (adjusted to 15% NaCl (w/v)) and subjected to the extraction procedure like samples. The experiments showed that linearity reached at least 20 μg L^{-1}, but the working range employed was set from 20 to 100 ng L^{-1}, with coefficients of determination (R^2) equal or greater than 0.995.

The MLODs, calculated as 3-folds the signal-to-noise ratio, ranged from 0.3 to 5.6 ng L^{-1}, and the MLOQs, calculated as 10-folds the signal-to-noise ratio, ranged from 1.0 to 18.6 ng L^{-1}.

The estimated EFs were calculated as the ratio of the concentration of the target compound after extraction (obtained by external calibration, introducing 1 μL of unextracted standard solutions into the glass tube to carry out the TD) to the initial concentration of the same compound in the aqueous phase before the extraction. For this purpose, three independent aqueous standard solution containing 100 ng L^{-1} of the target analytes were extracted, showing EFs between 178 and 640, depending on the analyte, which correspond to EE values between 0.7 and 2.6%.

The repeatability, expressed as relative standard deviation (RSD), was evaluated by applying the whole proposed SBSDME method to five independent aqueous standard solutions (adjusted to 15% NaCl (w/v)) containing 20 and 40 ng L^{-1} of the target compounds. Repeatability (intra-day precision) ranged from 3.5% to 6.6%, whereas reproducibility (inter-day precision) was less than 13%, illustrating the good precision of the procedure.

3.5. Reproducibility and reusability of $CoFe_2O_4$@PDA material

The inter-batch repeatability for the synthesis of the $CoFe_2O_4$@PDA MNPs was evaluated by comparing three different batches of the magnetic sorbent synthesized as in Section 2.3. RSD values for the five analytes were under 15%, proving the good repeatability during the synthesis process.

Reusability of $CoFe_2O_4$@PDA MNPs were also tested, proving to be reusable at least once (RSD values from 3.2 to 6.3%, depending on the analyte). However, the difficult handling of the small amount of material on the stir bar (i.e., 10 mg), in addition to possible losses during the material collection process, make reuse of the material tedious and not essential, since the synthesis process is easy and allows to obtain a relatively high quantity of material for several extractions.

3.6. Comparison of the SBSDME proposed method with other microextraction approaches

The proposed method was compared with some reported studies for determination of these nitro musks in environmental water samples by using other microextraction techniques (both liquid-based and solid-based). In order to make a more realistic comparison in terms of instrumental sensitivity, only works using GC-MS have been selected. The results are summarized in Table 2, which satisfactorily confirm that the analytical performance in terms of MLODs and relative recoveries are comparable or even better than some of these previous works. Moreover, the SBSDME approach offers important improvements over other techniques. On one hand, SBSDME allows to achieve a significant reduction in the extraction time from hours to just 10 min compared to other static techniques, such as SPME, SBSE or MASE, mainly due to the dispersion of the extraction phase. On the other hand, SBSDME allows easier extraction and post-extraction handling due to the use of magnetic materials, thus reducing the manual intervention when compared to conventional DSPE. Furthermore, the possibility to extract water samples that contain salt, such as seawater, is an advantage of the proposed method compared to other microextraction approaches where the addition of salt had a negative effect on the extraction [22]. Finally, the possibility of coupling the SBSDME approach with the TD allows to obtain high enrichment factors, since it enables direct insertion of the entire quantity of the extracted analytes into the analytical instrument, and not just a portion as in liquid desorption.

Table 3
Relative recovery values obtained by applying the developed SBSDME-TD-GC-MS method to two water samples spiked at 20 and 40 ng L^{-1}.

Nitro musk	Relative recoveries (%)			
	Sea water[a]		River water[b]	
	20 ng L^{-1}	40 ng L^{-1}	20 ng L^{-1}	40 ng L^{-1}
MA	103 ± 12	114 ± 6	111 ± 12	101 ± 9
MX	106 ± 10	102 ± 6	101 ± 5	98 ± 7
MM	118 ± 10	97 ± 10	101 ± 3	109 ± 14
MT	91 ± 2	99 ± 8	108 ± 6	110 ± 4
MK	110 ± 14	110 ± 10	108 ± 11	90 ± 11

[a] Malvarrosa Beach (Valencia, Spain).
[b] Mijares River (Castellón, Spain).

3.7. Application to the analysis of environmental water samples

Once the method was optimized, two environmental water samples (i.e., sea and river) obtained from areas burdened with recreational activities, and therefore with a high possible human exposure to these compounds, a cleaning water from a cosmetic company, and water from a drinking water treatment plant were analyzed in triplicate by the proposed SBSDME-TD-GC-MS method. Previously, the ionic strength of the samples was regulated to 15% by adding NaCl, taking into account the initial salt content in each sample (i.e., ca. 0.05% in river water, and 3–5% in seawater). The results showed that all the target compounds were below the MLODs. Then, to test the reliability of the proposed method and evaluate matrix effects, recovery studies were carried out on two of the above-mentioned water samples. To this end, the samples were spiked with the target analytes at 20 and 40 ng L^{-1} and the surrogate (200 ng L^{-1}) and subjected to the proposed method. As can be seen in Table 3, the obtained relative recoveries ranged from 92 to 120%, showing the good accuracy of the method and the lack of matrix effects from representative environmental water samples.

4. Conclusions

A highly sensitive magnetic-based method for the determination of the complete family of nitro musks in environmental waters is presented in this work. The proposed approach, based on stir bar sorptive dispersive microextraction (SBSDME), presents a great clean-up and enrichment potential, whose main advantage is the use of a magnetic sorbent as extraction phase that is dispersed by magnetic stirring and retrieved again due to its magnetic susceptibility. The dispersion of the material, in addition to its nanometric size, considerably increases the surface area and thus reduces the extraction time. Moreover, it involves minimum sample manipulation, and the preparation of the sorbent is simple and uses low-cost commercially available materials. Likewise, the proposed method shows good analytical properties, such as accuracy, precision and sensitivity. To the best of our knowledge, this is the first time in which these compounds have been extracted by means of magnetic materials.

Declaration of competing interest

The authors declare that they have no known competing financial interests or personal relationships that could have appeared to influence the work reported in this paper.

Acknowledgements

J.G. and J.L.B would like to thank the Generalitat Valenciana and the European Social Fund for their predoctoral and postdoctoral grant, respectively. This article is based upon work from the National Thematic Network on Sample Treatment (RED-2018-102522-T) of the Spanish Ministry of Science, Innovation and Universities, and the Sample Preparation Study Group and Network supported by the Division of Analytical Chemistry of the European Chemical Society.

Appendix A. Supplementary data

Supplementary data to this article can be found online at https://doi.org/10.1016/j.talanta.2021.122375.

Credit author statement

J. Grau, Investigation, Data treatment, Writing – original draft.; J.L. Benedé;: Conceptualization, Methodology, Investigation, Data treatment, Writing – original draft; A. Chisvert, Supervision, Methodology, Project organization, Funding acquisition, Writing - reviewing and editing.

References

[1] Cosmetics and fragrances, in: T. Mitsui (Ed.), New Cosmet. Sci., Elsevier Science, 1997, pp. 99–120.
[2] A. Chisvert, M. López-Nogueroles, P. Miralles, A. Salvador, Perfumes in cosmetics: regulatory aspects and analytical methods, in: Analysis of Cosmetics Products, second ed., Elsevier B.V., 2018, pp. 225–248, https://doi.org/10.1016/B978-0-444-63508-2.00010-2.
[3] Y. Gao, G. Li, Y. Qin, Y. Ji, B. Mai, T. An, New theoretical insight into indirect photochemical transformation of fragrance nitro-musks: mechanisms, eco-toxicity and health effects, Environ. Int. 129 (2019) 68–75, https://doi.org/10.1016/j.envint.2019.05.020.
[4] K.M. Taylor, M. Weisskopf, J. Shine, Human exposure to nitro musks and the evaluation of their potential toxicity: an overview, Environ. Health Global Access Sci. Source 13 (2014) 14, https://doi.org/10.1186/1476-069X-13-14.
[5] D.A. Chase, A. Karnjanapiboonwong, Y. Fang, G.P. Cobb, A.N. Morse, T. A. Anderson, Occurrence of synthetic musk fragrances in effluent and non-effluent impacted environments, Sci. Total Environ. 416 (2012) 253–260, https://doi.org/10.1016/j.scitotenv.2011.11.067.
[6] K. Bester, Analysis of musk fragrances in environmental samples, J. Chromatogr. A 1216 (2009) 470–480, https://doi.org/10.1016/j.chroma.2008.08.093.
[7] K. Juksu, Y.S. Liu, J.L. Zhao, L. Yao, C. Sarin, S. Sreesai, P. Klomjek, A. Traitangwong, G.G. Ying, Emerging contaminants in aquatic environments and coastal waters affected by urban wastewater discharge in Thailand: an ecological risk perspective, Ecotoxicol. Environ. Saf. 204 (2020) 110952, https://doi.org/10.1016/j.ecoenv.2020.110952.
[8] S. Ren, F. Tan, Y. Wang, H. Zhao, Y. Zhang, M. Zhai, J. Chen, X. Wang, In situ measurement of synthetic musks in wastewaters using diffusive gradients in thin film technique, Water Res. 185 (2020) 116239, https://doi.org/10.1016/j.watres.2020.116239.
[9] S. Rainieri, A. Barranco, M. Primec, T. Langerholc, Occurrence and toxicity of musks and UV filters in the marine environment, Food Chem. Toxicol. 104 (2017) 57–68, https://doi.org/10.1016/j.fct.2016.11.012.
[10] A. Chisvert, D. Giokas, J.L. Benedé, A. Salvador, Environmental monitoring of cosmetic ingredients. Analysis of Cosmetic Products, second ed., Elsevier B.V., 2018, pp. 435–547, https://doi.org/10.1016/B978-0-444-63508-2.00016-3.
[11] L. Vallecillos, F. Borrull, E. Pocurull, Recent approaches for the determination of synthetic musk fragrances in environmental samples, TrAC Trends Anal. Chem. 72 (2015) 80–92, https://doi.org/10.1016/j.trac.2015.03.022.
[12] L.I. Osemwengie, S. Steinberg, On-site solid-phase extraction and laboratory analysis of ultra-trace synthetic musks in municipal sewage effluent using gas chromatography-mass spectrometry in the full-scan mode, J. Chromatogr. A 932 (2001) 107–118, https://doi.org/10.1016/S0021-9673(01)01216-X.
[13] M. Lopez-Nogueroles, S. Lordel-Madeleine, A. Chisvert, A. Salvador, V. Pichon, Development of a selective solid phase extraction method for nitro musk compounds in environmental waters using a molecularly imprinted sorbent, Talanta 110 (2013) 128–134, https://doi.org/10.1016/j.talanta.2013.02.023.
[14] M. Polo, C. Garcia-Jares, M. Llompart, R. Cela, Optimization of a sensitive method for the determination of nitro musk fragrances in waters by solid-phase microextraction and gas chromatography with micro electron capture detection using factorial experimental design, Anal. Bioanal. Chem. 388 (2007) 1789–1798, https://doi.org/10.1007/s00216-007-1359-z.
[15] J. Cavalheiro, A. Prieto, O. Zuloaga, H. Preudhomme, D. Amouroux, M. Monperrus, Evaluation of preconcentration methods in the analysis of synthetic musks in whole-water samples, J. Sep. Sci. 38 (2015) 2298–2304, https://doi.org/10.1002/jssc.201500192.
[16] V. Homem, A. Alves, A. Alves, L. Santos, Ultrasound-assisted dispersive liquid-liquid microextraction for the determination of synthetic musk fragrances in aqueous matrices by gas chromatography-mass spectrometry, Talanta 148 (2016) 84–93, https://doi.org/10.1016/j.talanta.2015.10.049.
[17] S. Ramos, V. Homem, L. Santos, Simultaneous determination of synthetic musks and UV-filters in water matrices by dispersive liquid-liquid microextraction followed by gas chromatography tandem mass-spectrometry, J. Chromatogr. A 1590 (2019) 47–57, https://doi.org/10.1016/j.chroma.2019.01.013.

[18] N. Ramírez, F. Borrull, R.M. Marcé, Simultaneous determination of parabens and synthetic musks in water by stir-bar sorptive extraction and thermal desorption-gas chromatography-mass spectrometry, J. Sep. Sci. 35 (2012) 580–588, https://doi.org/10.1002/jssc.201100887.
[19] M. Arbulu, M.C. Sampedro, N. Unceta, A. Gómez-Caballero, M.A. Goicolea, R. J. Barrio, A retention time locked gas chromatography-mass spectrometry method based on stir-bar sorptive extraction and thermal desorption for automated determination of synthetic musk fragrances in natural and wastewaters, J. Chromatogr. A 1218 (2011) 3048–3055, https://doi.org/10.1016/j.chroma.2011.03.012.
[20] W.H. Chung, S.H. Tzing, M.C. Huang, W.H. Ding, Dispersive micro solid-phase extraction coupled with ultrasound-assisted solvent desorption for determination of synthetic polycyclic and nitro-aromatic musks in aqueous samples, J. Chin. Chem. Soc. 61 (2014) 1031–1038, https://doi.org/10.1002/jccs.201300666.
[21] J. Cavalheiro, A. Prieto, M. Monperrus, N. Etxebarria, O. Zuloaga, Determination of polycyclic and nitro musks in environmental water samples by means of microextraction by packed sorbents coupled to large volume injection-gas chromatography-mass spectrometry analysis, Anal. Chim. Acta 773 (2013) 68–75, https://doi.org/10.1016/j.aca.2013.02.036.
[22] M. López-Nogueroles, A. Chisvert, A. Salvador, A. Carretero, Dispersive liquid-liquid microextraction followed by gas chromatography-mass spectrometry for the determination of nitro musks in surface water and wastewater samples, Talanta 85 (2011) 1990–1995, https://doi.org/10.1016/j.talanta.2011.07.048.
[23] S.V.M.d. Sá, J.O. Fernandes, S.C. Cunha, In situ acetylation dispersive liquid–liquid microextraction followed by gas chromatography–mass spectrometry for the simultaneous determination of musks, triclosan and methyl-triclosan in wastewaters, Int. J. Environ. Anal. Chem. 99 (2019) 1–15, https://doi.org/10.1080/03067319.2019.1566955.
[24] L. Vallecillos, E. Pocurull, F. Borrull, Fully automated ionic liquid-based headspace single drop microextraction coupled to GC-MS/MS to determine musk fragrances in environmental water samples, Talanta 99 (2012) 824–832, https://doi.org/10.1016/j.talanta.2012.07.036.
[25] L. Guo, N. Binte Nawi, H.K. Lee, Fully automated headspace bubble-in-drop microextraction, Anal. Chem. 88 (2016) 8409–8414, https://doi.org/10.1021/acs.analchem.6b01543.
[26] J. Regueiro, M. Llompart, C. Garcia-Jares, J.C. Garcia-Monteagudo, R. Cela, Ultrasound-assisted emulsification-microextraction of emergent contaminants and pesticides in environmental waters, J. Chromatogr. A 1190 (2008) 27–38, https://doi.org/10.1016/j.chroma.2008.02.091.
[27] O. Posada-Ureta, M. Olivares, P. Navarro, A. Vallejo, O. Zuloaga, N. Etxebarria, Membrane assisted solvent extraction coupled to large volume injection-gas chromatography-mass spectrometry for trace analysis of synthetic musks in environmental water samples, J. Chromatogr. A 1227 (2012) 38–47, https://doi.org/10.1016/j.chroma.2011.12.104.
[28] A. Chisvert, S. Cárdenas, R. Lucena, Dispersive micro-solid phase extraction, TrAC Trends Anal. Chem. 112 (2019) 226–233, https://doi.org/10.1016/j.trac.2018.12.005.
[29] S. Di, T. Ning, J. Yu, P. Chen, H. Yu, J. Wang, H. Yang, S. Zhu, Recent advances and applications of magnetic nanomaterials in environmental sample analysis, TrAC Trends Anal. Chem. 126 (2020) 115864, https://doi.org/10.1016/j.trac.2020.115864.
[30] K. Aguilar-Arteaga, J.A. Rodriguez, E. Barrado, Magnetic solids in analytical chemistry: a review, Anal. Chim. Acta 674 (2010) 157–165, https://doi.org/10.1016/j.aca.2010.06.043.
[31] A.S. de Dios, M.E. Díaz-García, Multifunctional nanoparticles: analytical prospects, Anal. Chim. Acta 666 (2010) 1–22, https://doi.org/10.1016/j.aca.2010.03.038.
[32] X.S. Li, G.T. Zhu, Y.B. Luo, B.F. Yuan, Y.Q. Feng, Synthesis and applications of functionalized magnetic materials in sample preparation, TrAC Trends Anal. Chem. 45 (2013) 233–247, https://doi.org/10.1016/j.trac.2012.10.015.
[33] K.V. Maidatsi, T.G. Chatzimitakos, V.A. Sakkas, C.D. Stalikas, Octyl-modified magnetic graphene as a sorbent for the extraction and simultaneous determination of fragrance allergens, musks, and phthalates in aqueous samples by gas chromatography with mass spectrometry, J. Sep. Sci. 38 (2015) 3758–3765, https://doi.org/10.1002/jssc.201500578.
[34] J.L. Benedé, A. Chisvert, D.L. Giokas, A. Salvador, Development of stir bar sorptive-dispersive microextraction mediated by magnetic nanoparticles and its analytical application to the determination of hydrophobic organic compounds in aqueous media, J. Chromatogr. A 1362 (2014) 25–33, https://doi.org/10.1016/j.chroma.2014.08.024.
[35] V. Vállez-Gomis, J. Grau, J.L. Benedé, D.L. Giokas, A. Chisvert, A. Salvador, Fundamentals and applications of stir bar sorptive dispersive microextraction: a tutorial review, Anal. Chim. Acta 1153 (2021) 338271, https://doi.org/10.1016/j.aca.2021.338271.
[36] D. Che, J. Cheng, Z. Ji, S. Zhang, G. Li, Z. Sun, J. You, Recent advances and applications of polydopamine-derived adsorbents for sample pretreatment, TrAC Trends Anal. Chem. 97 (2017) 1–14, https://doi.org/10.1016/j.trac.2017.08.002.
[37] K. Maaz, A. Mumtaz, S.K. Hasanain, A. Ceylan, Synthesis and magnetic properties of cobalt ferrite (CoFe2O4) nanoparticles prepared by wet chemical route, J. Magn. Magn. Mater. 308 (2007) 289–295, https://doi.org/10.1016/j.jmmm.2006.06.003.
[38] Y. Wang, S. Wang, H. Niu, Y. Ma, T. Zeng, Y. Cai, Z. Meng, Preparation of polydopamine coated Fe3O4 nanoparticles and their application for enrichment of polycyclic aromatic hydrocarbons from environmental water samples, J. Chromatogr. A 1283 (2013) 20–26, https://doi.org/10.1016/j.chroma.2013.01.110.
[39] C. Ye, Y. Wu, Z. Wang, Modification of cellulose paper with polydopamine as a thin film microextraction phase for detection of nitrophenols in oil samples, RSC Adv. 6 (2016) 9066–9071, https://doi.org/10.1039/C5RA23232E.
[40] S. Hong, Y.S. Na, S. Choi, I.T. Song, W.Y. Kim, H. Lee, Non-covalent self-assembly and covalent polymerization co-contribute to polydopamine formation, Adv. Funct. Mater. 22 (2012) 4711–4717, https://doi.org/10.1002/adfm.201201156.
[41] I.P. Román, A. Chisvert Alberto, A. Canals, Dispersive solid-phase extraction based on oleic acid-coated magnetic nanoparticles followed by gas chromatography-mass spectrometry for UV-filter determination in water samples, J. Chromatogr. A 1218 (2011) 2467–2475, https://doi.org/10.1016/j.chroma.2011.02.047.
[42] J. Aguirre, E. Bizkarguenaga, A. Iparraguirre, L.Á. Fernández, O. Zuloaga, A. Prieto, Development of stir-bar sorptive extraction-thermal desorption-gas chromatography-mass spectrometry for the analysis of musks in vegetables and amended soils, Anal. Chim. Acta 812 (2014) 74–82, https://doi.org/10.1016/j.aca.2013.12.036.
[43] M.G. Pintado-Herrera, E. González-Mazo, P.A. Lara-Martín, Atmospheric pressure gas chromatography-time-of-flight-mass spectrometry (APGC-ToF-MS) for the determination of regulated and emerging contaminants in aqueous samples after stir bar sorptive extraction (SBSE), Anal. Chim. Acta 851 (2014) 1–13, https://doi.org/10.1016/j.aca.2014.05.030.

Polydopamine-coated magnetic nanoparticles for the determination of nitro musks in environmental water samples by stir bar sorptive-dispersive microextraction

José Grau, Juan L. Benedé, Alberto Chisvert*

Department of Analytical Chemistry, University of Valencia, 46100 Burjassot, Valencia, Spain

* Corresponding author:

E-mail address: alberto.chisvert@uv.es (A. Chisvert)

TABLE OF CONTENTS

Table S1. Chemical structure and relevant data of the target compounds and the surrogate.

Nitro musk	Chemical structure	Molecular formula	CAS number	Boiling point (ºC)	m/z value [a]
Musk Ambrette (MA)	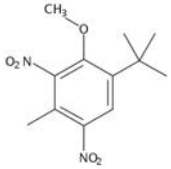	$C_{12}H_{16}N_2O_5$	83-66-9	369	**253**, 263, 282
Musk Xylene (MX)	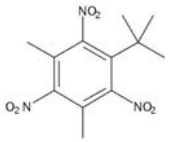	$C_{12}H_{15}N_3O_6$	81-15-2	392	253, 263, **282**
Musk Moskene (MM)	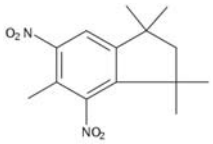	$C_{14}H_{18}N_2O_4$	116-66-5	351	253, **263**, 282
Musk Tibetene (MT)	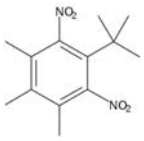	$C_{13}H_{18}N_2O_4$	145-39-1	391	**251**, 279
Musk Ketone (MK)	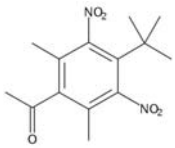	$C_{14}H_{18}N_2O_5$	81-14-1	369	251, **279**
Hexachlorobenzene (HCB)	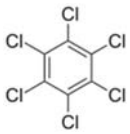	C_6Cl_6	118-74-1	324	**284**

[a] The m/z values used as quantifiers are shown in bold.

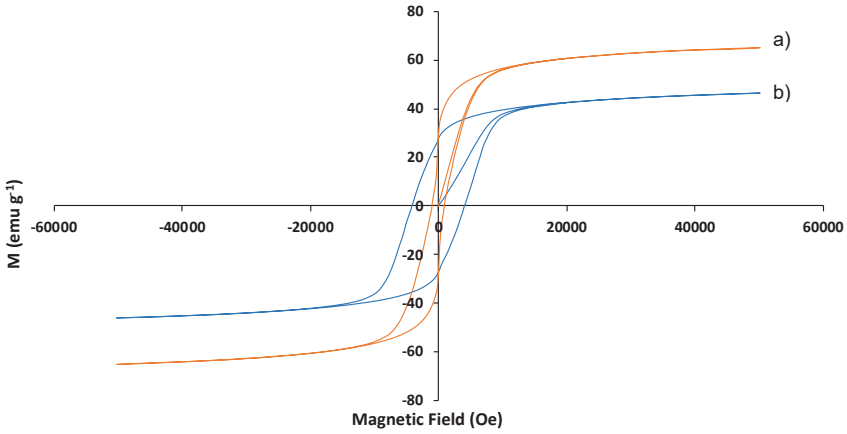

Fig. S1. Magnetization curve of a) $CoFe_2O_4$ MNPs and (b) $CoFe_2O_4$@PDA MNPs

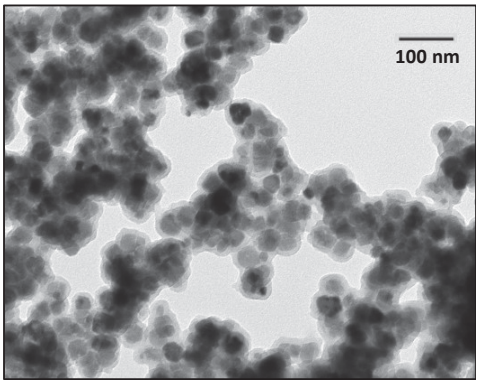

Fig. S2. TEM micrograph observation of $CoFe_2O_4$@PDA MNPs

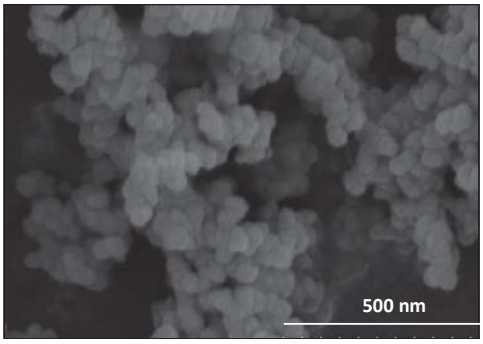

Fig. S3. SEM micrograph observation of the $CoFe_2O_4$@PDA MNPs at a magnification 120000

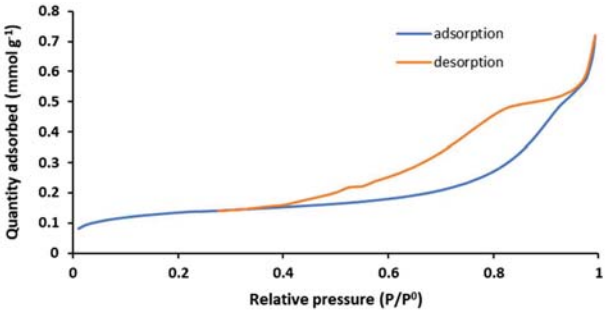

Fig. S4. Isotherm linear plot of $CoFe_2O_4$@PDA MNPs

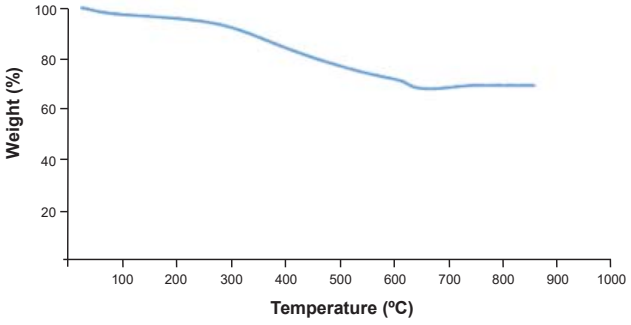

Fig. S5. TGA curve of $CoFe_2O_4$@PDA MNPs

Low toxicity deep eutectic solvent-based ferrofluid for the determination of UV filters in environmental waters by stir bar dispersive liquid microextraction

Talanta 243 (2022) 123378

DOI: 10.1016/j.talanta.2022.123378

Talanta 243 (2022) 123378

Contents lists available at ScienceDirect

Talanta

journal homepage: www.elsevier.com/locate/talanta

Low toxicity deep eutectic solvent-based ferrofluid for the determination of UV filters in environmental waters by stir bar dispersive liquid microextraction

Alaine Duque [a,1], José Grau [b,1], Juan L. Benedé [b], Rosa M. Alonso [c], Miguel A. Campanero [a], Alberto Chisvert [b,*]

[a] A3Z Advanced Analytical Consulting Services, 48160, Derio, Vizcaya, Spain
[b] GICAPC Research Group, Department of Analytical Chemistry, University of Valencia, 46100, Burjassot, Valencia, Spain
[c] FARMARTEM Group, Department of Analytical Chemistry, Faculty of Science and Technology, University of the Basque Country (UPV/EHU), 48940, Leioa, Vizcaya, Spain

ARTICLE INFO

Keywords:
Deep eutectic solvent
Ferrofluid
Liquid chromatography-tandem mass spectrometry
Stir bar dispersive liquid microextraction
UV filters
Water samples

ABSTRACT

In this work, a low toxicity deep eutectic solvent-based ferrofluid is presented for the first time as magnetic fluid to be used as an efficient solvent in liquid-based microextraction techniques. This ferrofluid is made of a hydrophobic deep eutectic solvent, composed by menthol and thymol in a 1:5 molar ratio as carrier solvent, and oleic acid-coated cobalt ferrite ($CoFe_2O_4$@oleic acid) magnetic nanoparticles. This material was characterized via magnetism measurement, scanning electron microscopy, infrared spectroscopy and density measurement. The determination of UV filters in environmental water samples was selected as model analytical application to test the extraction performance of this new ferrofluid by employing stir bar dispersive liquid microextraction, prior to liquid chromatography-tandem mass spectrometry analysis. The response surface methodology was used as a multivariate optimization method for extraction step. Under the optimized conditions, good analytical features were obtained, such as low limits of detection between 7 and 83 ng L^{-1}, good repeatability (relative standard deviations, RSD (%) below 15%), enrichment factors between 46 and 101 and relative recoveries between 80 and 117%, proving the good extraction capability of this ferrofluid. Finally, the method was successfully applied to three environmental waters (beach and river waters), finding trace amounts of the target UV filters. The presented low toxicity deep eutectic solvent-based ferrofluid results to be a good alternative to conventional solvents used in liquid-phase microextraction techniques.

1. Introduction

The evolution of Analytical Chemistry has been traditionally focused on the development of new analytical methods able to achieve lower and lower limits of detection in an efficient way. In addition, due to the social concern for the environment, researchers have prioritized the development of greener strategies to reduce, not only their impact on the environment, but also the risks to the operator [1].

In this context, the implementation of liquid-phase microextraction techniques and sorbent-based microextraction techniques allowed to reduce drastically the amount of organic solvents employed in each analysis. From these two, those liquid phase-based microextraction techniques usually needs higher amounts of organic solvents, although in the microliter range, including, in some cases, hazardous halogenated ones [2]. Moreover, these solvents employed as extractant phase present a lack of selectivity compared with the tailor-made sorbents used in solid phase-based microextraction techniques [3,4]. In any case, the employment of this kind of solvents is not recommended by the principles of the Green Analytical Chemistry [5] and the Green Sample Preparation [6], since they are not safe neither for environment nor for operators.

For this reason, in order to reduce the impact caused by these solvents when liquid-phase microextraction techniques are used, new greener tailor-made solvents, such as ionic liquids (ILs) and deep

* Corresponding author.
E-mail address: alberto.chisvert@uv.es (A. Chisvert).
[1] These authors contributed equally to this work.

https://doi.org/10.1016/j.talanta.2022.123378
Received 3 February 2022; Received in revised form 9 March 2022; Accepted 9 March 2022
Available online 11 March 2022

eutectic solvents (DESs), have been incorporated to these microextraction techniques [7]. These solvents are made from two individual components, which can be selected from different possibilities resulting in very interesting tunable properties that can be exploited for carrying out targeted extractions [8].

Concretely, DESs have attracted the attention of researchers during the recent years [9,10] due to different reasons. They are easily formed by mixing a hydrogen bond acceptor (HBA) and a hydrogen bond donor (HBD), which interact forming strong hydrogen bonds, resulting in the formation of a eutectic mixture with a lower melting temperature than that of each individual component [11]. Consequently, DESs may be liquids at room temperature, even if the original components are solid [12]. In addition, their preparation is easy to perform and can be done in a matter of minutes, just mixing the HBA and HBD, even *in situ* in the donor phase [13,14].

It should be noted that DESs share several properties with ILs, such as low vapour pressure, high thermal stability and low flammability. Nevertheless, the individual components of DESs are usually cheaper and quite less harmful than those for ILs, and generally, their preparation is easier and consumes less energy [15].

Although DESs boast of having high greenness and low toxicity, some individual components used to prepare them may be toxic. For this reason, the term natural DES (NADES) has been usually employed to distinguish those non-harmful DES [16,17]. However, NADES definition is an inaccurate term since it may not include all non-toxic DES. In this sense, the term low toxicity DESs (LT-DESs) should be more appropriate [7].

However, DESs and LT-DESs are not exempted from issues, since their lack of volatility may affect their introduction in some measurement devices such as in a gas chromatography system, of course, but also in a mass spectrometer [18]. Moreover, their lower density than water makes their retrieval after the extraction process tedious unless additional steps are conducted (e.g., solidification of floating organic droplet [19]).

The use of magnetic nanoparticles (MNPs) to form ferrofluids has allowed to easily retrieve low density solvents in microextraction techniques by applying magnetic forces [20–22]. Ferrofluids are stable colloidal and homogenous dispersions of MNPs in a carrier solvent [23]. Dispersive agents, such as surfactants (e.g., oleic acid (OA)) are usually employed to avoid the agglomeration of the MNPs in the bosom of the solvent [22,24]. In this sense, ferrofluids are easily prepared by simple sonication of OA-coated MNPS (i.e., MNPs@OA) with the carrier solvent.

During the last years, several liquid-phase microextraction strategies have been developed employing ferrofluids or other magnetic fluids such as magnetic ionic liquids (MILs) as extraction phase. Most of these strategies employ dispersive-based techniques, in such a way that tiny droplets of the fluid are formed in the sample solution, increasing the contact area between the sample and the extraction phase, and thus enhancing the extraction speed [25]. Finally, after the extraction, the fluid can be easily retrieved by applying an external magnetic field.

In this regard, some techniques, such as modifications of the well-known dispersive liquid-liquid microextraction (DLLME) [26,27] and other novels like stir bar dispersive liquid microextraction (SBDLME) [28], have been proposed as magnetic fluid-based extraction approaches. Although the applications of SBDLME are scarce so far, its simplicity and good extraction performance [29,30], in addition to the no-need of an external magnetic field [28], makes it a good alternative to DLLME.

In SBDLME, a magnetic fluid and a neodymium-core magnetic stir bar are introduced into the sample allowing the magnetic fluid to coat the stir bar due to magnetic interactions. When low stirring rates are applied, the liquid is retained onto the neodymium magnet. However, when the stirring rate is increased, the rotational forces surpass the magnetic field and the material is dispersed into the sample. After extraction period, the stirring is stopped and the magnetic fluid containing the analytes is attracted again by magnetic interactions onto the stir bar [28].

Up to now, only MILs [29,30] and just a DES [31] have been used as extraction phases in SBDLME. However, LT-DES-based ferrofluid may be a greener alternative. For that reason, the aim of this work was to develop a LT-DES-based ferrofluid for SBDLME, thus avoiding the use of toxic compounds and tedious synthesis processes, in addition to reduce the analysis cost.

In this work, an innovative ferrofluid is presented as a green and efficient solvent for liquid-phase microextraction techniques. This one is formed by a low toxicity menthol and thymol DES as carrier solvent and OA-coated cobalt ferrite ($CoFe_2O_4$@OA) MNPs. This ferrofluid not only has the advantage of being quite safe and harmless for the environment, but also it can be easily separated into their volatile components employing a small amount of organic solvent, thus allowing it to be introduced in the mass spectrometer without harming it. As far as we know, this is the first time that this ferrofluid has been employed for analytical purposes.

As model analytical application of this new ferrofluid, the determination of UV filters in environmental waters by liquid chromatography-tandem mass spectrometry (LC-MS/MS) was selected. The high concern about the impact of solar radiation in human health has caused an increase of the use of cosmetic products containing UV filters. Consequently, high amounts of these compounds are able to reach the environment by direct or indirect sources and hence, to be bioaccumulated in environment [32]. Once there, these UV filters can alter aquatic fauna and flora. For that reason, these compounds are considered as emerging pollutants, and the development of sensitive analytical methods for their environmental monitoring is mandatory.

2. Experimental

2.1. Reagents and preparation of standard solutions

All reagents and solvents were purchased from major suppliers. Benzophenone-3 (BZ3) 98% and ethylhexyl salicylate (EHS) 99% from Sigma-Aldrich (Barcelona, Spain), isoamyl p-methoxycinnamate (IMC) 99.3% from Haarmann and Reimer (Parets del Vallés, Spain), 4-methylbenzylidene camphor (MBC) 99.7% from Guinama S.L. (Valencia, Spain), octocrylene (OC) > 98% from F. Hoffmann-La Roche Ltd. (Basel, Switterland), ethylhexyl dimethyl PABA (EHDP) 100%, butyl methoxydibenzoylmethane (BMDM) 98% from Merck (Darmstadt, Germany), and diethylamino hydroxybenzoyl hexyl benzoate (DHHB) 99.8% from BASF (Barcelona, Spain) were used as standards. The chemical structures and relevant information are given in Table S1. Octocrylene (2-ethyl-d_5-hexyl-2,3,3,4,4,5,5,6,6,6-d_{10}) (OC-d_{15}) from Sigma-Aldrich (Barcelona, Spain) was used as surrogate.

To perform the synthesis of $CoFe_2O_4$@OA MNPs, cobalt (II) chloride hexahydrate ($CoCl_2{\cdot}6H_2O$) and iron (III) chloride hexahydrate ($FeCl_3{\cdot}6H_2O$), both for analysis, were obtained from Acros Organics (New Jersey, USA), while oleic acid (OA) (90%) was acquired from Sigma-Aldrich (Steinheim, Germany). Thymol 99% and (±)-menthol 98% from Sigma-Aldrich (Steinheim, Germany) were used for the preparation of DES.

HPLC-grade ethanol and acetonitrile were purchased from Panreac (Barcelona, Spain). Deionized water was obtained from a Connect water purification system provided by Adrona (Riga, Latvia). Sodium chloride (NaCl, 99.5%, analytical grade), ortho-phosphoric acid (85%, analytical grade), di-sodium hydrogen phosphate dodecahydrate (reagent grade), hydrochloric acid (37%, reagent grade) and sodium hydroxide (analytical reagent grade) used as ionic strength and pH regulators, were acquired from Scharlau (Barcelona, Spain).

To prepare the chromatographic mobile phase, LC-MS grade methanol and LC-MS grade water were obtained from VWR Chemicals (Fontenay-sous-Bois, France), whereas formic acid (98%, for mass spectrometry) was purchased from Fluka (Steinheim, Germany).

Nitrogen used as nebulizer and curtain gas in the MS/MS ion source was obtained by means of a NiGen LCMS nitrogen generator from Claind S.r.l. (Lenno, Italy). Extra pure nitrogen (>99.999%) from Praxair (Madrid, Spain) was used as collision gas in the MS/MS collision cell.

Different stock solutions of the target compounds were prepared in ethanol at 500 μg mL^{-1}. From them, a multicomponent stock solution was prepared in ethanol at different concentration for each UV filter depending on their limits of detection (see Section 3.3): 50 μg mL^{-1} for DHHB and EHDP, 100 μg mL^{-1} for BZ3, IMC and OC, 200 μg mL^{-1} for MBC and BMDM and 500 μg mL^{-1} for EHS. This solution was kept at 4 °C and protected from UV radiation by using amber glassware. From this solution, an intermediate 1:1000 v/v solution was prepared also in ethanol. Afterwards, from this intermediate solution, working solutions between 30 and 750 ng L^{-1} for DHHB and EHDP, 70–1750 ng L^{-1} for BZ3, IMC and OC, 130–3250 ng L^{-1} for MBC and BMDM and 300–7500 ng L^{-1} for EHS were prepared by proper dilution with a 6% NaCl w/v aqueous solution. In addition, a 500 μg mL^{-1} OC-d_{15} stock solution (as surrogate) was prepared in ethanol and then diluted in ultrapure water at a concentration of 150 ng L^{-1}. All these solutions were kept at 4 °C and protected from UV radiation by using amber glassware. Under these conditions, these solutions were stable at least one month.

2.2. Sample collection and pretreatment

Three different water samples were analyzed. In this sense, sea water from Puzol beach (Puzol, Spain) and Patacona beach (Valencia, Spain), and river water from Mijares River (Montanejos, Spain) were collected during the summer season in a 1 L amber glass bottle and were kept at 4 °C until their analysis, as it will be described further on. Prior to analysis, they were filtered and their ionic strength was regulated to NaCl 6% w/v after measurement of their conductivity.

2.3. Apparatus

An Agilent 1100 Series HPLC system equipped with a G1379B degasser, a G1312A binary pump, a G1367A autosampler and a G1330B thermostatic column oven, coupled to an Agilent 6410B Triple Quad MS/MS was employed in the present study. MassHunter version B.08.00 was used as software for data acquisition. Separations were carried out in an Agilent Zorbax SB-C18 (50 mm × 2.1 mm, 1.8 μm) purchased to Agilent Technologies (Waldbronn, Germany).

For the preparation of MNPs, DESs and ferrofluids, a ZX3 vortex mixer from VELP Scientifica (Usmate Velate, Italy), an Incudigit lab stove, a Tectron water bath and an ultrasound bath (50 Hz, 360 W) all from J.P. Selecta (Barcelona, Spain) were employed.

A 10-position multiple stirring plate model MS-M-S10 from Labbox (Barcelona, Spain) and NdFeB magnets (54 MGO, 10 mm length x 3 mm diameter) from Supermagnete (Gottmadingen, Germany) were employed to perform the SBDLME process.

A Basic 30 conductimeter from Crison (Barcelona, Spain) was used for the study of the salt content in water samples, and a Basic 20 pH meter from Crison (Alella, Spain) was used for the adjustment of the pH of the solutions.

A Jasco FTIR 4100 Fourier transform infrared spectrometer (FT-IR) from Jasco Europe S.r.l. (Cremella, Italy) was used to confirm the preparation of menthol:thymol 1:5 DES. The surface morphology of the MNPs were provided by a HITACHI S-4800 field emission scanning electron microscope (SEM) operating at 10 kV and equipped with a RX Bruker backscattered electron detector (Krefeld, Germany). The magnetic measurements were assessed by a homemade vibrating sample magnetometer (VSM) fabricated by the Magnetism Unit of SGIker of University of the Basque Country (UPV/EHU).

2.4. Synthesis of the $CoFe_2O_4$@OA magnetic nanoparticles

The synthesis of the $CoFe_2O_4$@OA MNPs included two different steps. First, $CoFe_2O_4$ MNPs were synthesized by wet chemical coprecipitation according to an adapted protocol [33] and then, they were coated with OA.

In this sense, 100 mL of a 0.4 M $FeCl_3$ aqueous solution and 100 mL of a 0.2 M $CoCl_2$ aqueous solution were mixed. Then, 100 mL of a 3 M sodium hydroxide aqueous solution were added dropwise under continuous stirring at 80 °C. After that, 2 mL of OA were added and the reaction mixture was stirred at 80 °C for 1 h. The black precipitate product was slowly cooled to room temperature and the MNPs were washed twice with ultrapure water and once with ethanol. Finally, the precipitate was dried overnight at 100 °C and pulverized into a fine powder.

2.5. Preparation of low toxicity menthol:thymol deep eutectic solvent

The menthol:thymol 1:5 DES was prepared by weighing separately 0.47 g of menthol, as HBA, and 2.76 g of thymol, as HBD, in two 15 mL polystyrene Falcon™ tubes. Then, they were heated at 60 °C in a water bath for 10 min, and mixed and vortexed for 1 min until a homogeneous transparent liquid was obtained. The resultant DES was left to reach room temperature before the synthesis of the ferrofluid.

2.6. Preparation of low toxicity deep eutectic solvent-based ferrofluid

To prepare the $CoFe_2O_4$@OA-menthol:thymol ferrofluid, 25 mg of $CoFe_2O_4$@OA MNPs were weighed in a microcentrifuge tube and 1 mL of DES was added. The resultant mixture was sonicated for 40 min leading to the formation of a stable ferrofluid.

2.7. SBDLME procedure

Firstly, a neodymium stir bar was introduced into a clean and dry 40-mL extraction vial. Then, 100 μL of ferrofluid, 15 mL of a standard solution or a sample, 200 μL of acetonitrile as dispersant agent, and 100 μL of 150 ng mL^{-1} OC-d_{15} solution (as surrogate) were added into the vial and vigorously stirred (ca. 1000 rpm) for 10 min at room temperature to achieve the total dispersion of the ferrofluid throughout the aqueous donor solution. When stirring was stopped, the magnetic ferrofluid was collected on the stir bar. Subsequently, the stir bar was removed with plastic forceps, and it was introduced into a 5-mL desorption vial containing 100 μL of acetonitrile to accomplish the liquid desorption of the analytes. Finally, after 2 min of slow stirring rate (ca. 250 rpm), the acetonitrile extract was collected with a syringe, passed through a 0.22 μm nylon filter and transferred to a chromatographic vial for LC-MS/MS analysis. Fig. 1 shows a schematic diagram of the experimental SBDLME procedure.

2.8. LC-MS/MS analysis

The chromatographic method was carried out with a mobile phase consisted of solvent A (H_2O, 0.1% formic acid) and solvent B (methanol, 0.1% formic acid), by isocratic elution at a mixing ratio of 15:85 (v/v). The injection volume was 5 μL. The flow rate was set 0.2 mL min^{-1} and the column temperature was kept constant at 35 °C. The run time was 6 min.

The triple quadrupole MS detector operated in positive electrospray ionization mode (ESI^+, capillary voltage at 6 kV), by multiple reaction monitoring (MRM). The other conditions were: gas temperature at 230 °C, nebulizer gas flow rate at 13 L min^{-1}, nebulizer gas pressure at 35 psi, and dwell time at 50 ms. The *m/z* precursor → product ion transitions for quantification and for identification, the collision energies and fragmentor values for each analyte are shown in Table S2.

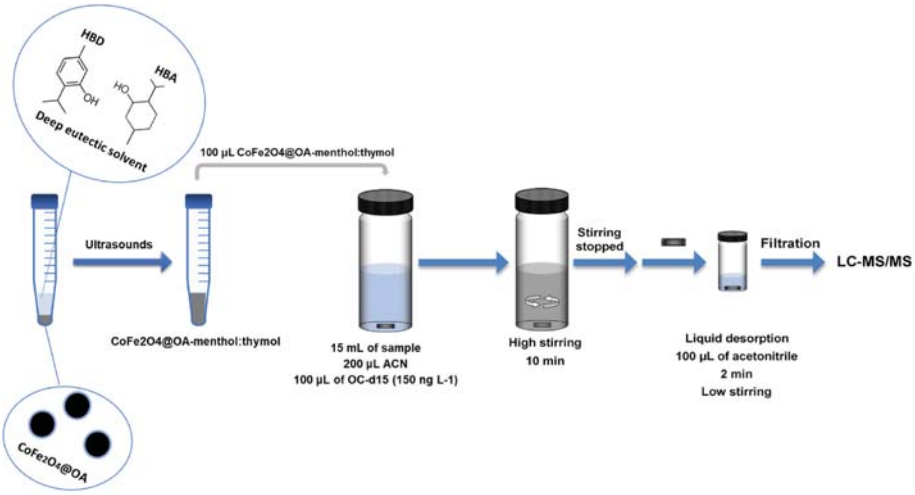

Fig. 1. Schematic diagram of proposed SBDLME-LC-MS/MS method.

3. Results and discussion

3.1. Selection of the ferrofluid and characterization

The combination of menthol and thymol was selected for the formation of the ferrofluid due to their hydrophobic character and aromaticity, improving the interactions with the analytes. Furthermore, both HBA and HBD are volatile, thus after decomposing the DES into the original components it can be introduced into the mass spectrometer system without risk of fouling it.

Three different molar ratios of menthol:thymol (i.e., 1:1, 1:2 and 1:5) were tested in order to select which resulting ratio provided the best extraction of the analytes. The extractions were performed in 5 mL of aqueous standard solution with 2 ng mL^{-1} of the target analytes, and 50 µL of the ferrofluid. Higher molar ratios of menthol were not tested in order to favor π-π interactions between thymol and UV filters. The DES with 1:1 ratio was not properly formed and then it was discarded. Between 1:2 and 1:5, the latter provided better results in terms of extraction capability (Fig. S1), due to their major number of aromatic rings provided by thymol molecules. Thus, the 1:5 ratio was selected for further experiments.

Afterwards, different amounts of $CoFe_2O_4$@OA MNPs (i.e., 6, 12, 25, 50 and 100 mg) to form the ferrofluid were studied in 1 mL of menthol:thymol 1:5 DES. The assay was performed in 5 mL of aqueous standard solution with 2 ng mL^{-1} of the target analytes, and 50 µL of the ferrofluid. Higher presence of MNPs (i.e., >25 mg) formed ferrofluids with huge viscosity hindering their aspiration with conventional micropipettes, impairing the repeatability. Lower amounts were not enough to form the $CoFe_2O_4$@OA-menthol:thymol ferrofluid properly making it less magnetic and thus reducing its retrieval, as it was visually observed. Then, the ferrofluid was prepared with 25 mg of $CoFe_2O_4$@OA MNPs per 1 mL of menthol:thymol 1:5 DES.

3.1.1. Characterization of menthol:thymol 1:5 DES

The preparation of menthol:thymol 1:5 DES was studied by FT-IR analysis. The spectra of DES and its individual components are presented in (Fig. S2). As it is shown in Fig. S2a, the stretching vibration bands at 3158 cm^{-1} (O–H), 2866-1956 cm^{-1} (C–H), 1584-1619 cm^{-1} (aromatic C═C) and 1239 cm^{-1} (C–O) of thymol can be identified. In the FT-IR spectra of menthol (Fig. S2b) it is possible to identify the stretching vibrations of 3291 cm^{-1} (O–H), 2843-2948 cm^{-1} (C–H) and 1023 and 1042 cm^{-1} (C–O). However, as can be seen in the DES spectra (Fig. S2c), the band corresponding to the O–H stretching in menthol:thymol 1:5 DES is wider than the individual O–H stretching bands of thymol and menthol and, moreover, it appears shifted. Likewise, the stretching vibration band of C–O in menthol appears shifted in DES spectra, proving the existence of strong interactions between the protons on the hydroxyl groups from menthol and thymol, thus inferring that hydrogen bonds were formed between these hydroxyl groups [34]. Therefore, it suggests the successful formation of menthol:thymol 1:5 DES.

The density of menthol:thymol 1:5 DES was also determined, measuring it at room temperature by weighing 500 µL of DES, resulting in a density of 0.905 g cm^{-3}.

3.1.2. Characterization of $CoFe_2O_4$@OA MNPs

The surface morphology of $CoFe_2O_4$@OA MNPs was investigated with SEM. Fig. S3 shows the spherical and uniform shape of the MNPs with a particle size around 50 nm.

3.1.3. Characterization of $CoFe_2O_4$@OA-menthol:thymol ferrofluid

For the characterization of the ferrofluid, the magnetization curve of the $CoFe_2O_4$@OA MNPs and the resultant $CoFe_2O_4$@OA-menthol:thymol ferrofluid were measured at room temperature (Fig. S4). A hysteresis loop may be observed in $CoFe_2O_4$@OA MNPs, showing a residual magnetism when the magnetic field is stopped [35]. The magnetic saturation (Ms) of the ferrofluid was 24 emu g^{-1}, which, as expected, is lower than the Ms obtained for $CoFe_2O_4$@OA MNPs (i.e., 57 emu g^{-1}). It could be attributed to, for one hand, the less amount of the magnetic component (i.e., MNPs) per gram of material, and on the other hand, to the shielding that DES produces in the MNPs. This shielding may also be responsible of the observed loss of retentivity and coercivity. Even though, its magnetic behavior is enough to efficiently retrieve the ferrofluid from an aqueous solution employing a magnetic field and thus to be employed in SBDLME.

3.2. Optimization of the SBDLME variables

Before the multivariate optimization of the conditions of the extraction step (see Section 3.2.1.), preliminary studies were performed to evaluate the employment of acetonitrile as disperser solvent. It was observed that adding 200 μL of acetonitrile the ferrofluid was more efficiently dispersed. It should be emphasized that under these conditions, the DES was not decomposed and maintained its structure, since there are not significant differences between the IR spectra after (Fig. S2d) and before (Fig. S2c) the extraction.

Afterwards, the desorption solvent and sample volume were also evaluated using a univariate approach. In this regard, 250 μL of different organic solvents (namely methanol, ethanol and acetonitrile) were evaluated as desorption solvents. The extractions were performed intra-day in 5 mL of aqueous standard solution with 2 ng mL^{-1} of the target analytes, and 50 μL of the ferrofluid. The peak area was considered as response function. Results in Fig. S5 show that acetonitrile significantly increased the signals of the analytes with lower sensitivity (BMDM and EHS) and the signals of BZ3 and IMC. Furthermore, acetonitrile decomposes the DES into the individual volatile components (i.e., menthol and thymol). This can be observed in Fig. S2d, where the O–H stretching band of the DES after the desorption in pure acetonitrile is narrower than in Fig. S2c. This gives rise to the dissolution of the analytes into the desorption solvent and the introduction of the extract into the LC-MS/MS without risk of fouling it as might happen if the DES was introduced. Consequently, acetonitrile was selected as desorption solvent for the next experiments.

Regarding to sample volume, 5, 10, 15 and 20 mL were evaluated. In general terms, the highest signals were obtained at a sample volume of 15 mL (Fig. S6). The lower signals observed employing 20 mL may be produced because part of the ferrofluid was accumulated in the topper face of the sample solution and the magnetic forces were insufficient to recover it. Thus, 15 mL was chosen as sample volume to enhance the efficiency of the analysis.

3.2.1. Multivariate optimization of the extraction conditions

The factors of influence in the extraction procedure were optimized using the response surface methodology (RSM). In this sense, Box-Behnken design was performed to evaluate four significant extraction variables, performing 27 experimental runs with three levels for each factor (see Supplementary Material). The StatGraphics Centurion XVI software from StatGraphics Technologies, Inc. (The Plains, VA, USA) was employed for the statistical analysis. The studied independent factors were the ferrofluid volume (20–200 μL), the extraction time (2–20 min), pH of the donor phase (2–10) and the ionic strength of the donor phase (0–10% NaCl (w/v)). All experiments are summarized in Table S3 and were carried out intra-day in 15 mL of aqueous standard solution at a concentration of 2 ng mL^{-1}; and the desorption was accomplished with 250 μL of acetonitrile for 5 min. The adequacy of the model was evaluated by the coefficient of determination (R^2), which was ≥0.81 for all the UV filters. This value indicates that the designed model is efficient for the prediction of response.

Fig. 2 shows the response surface plots in terms of desirability (estimated as described in Supplementary Material) for the four factors. In Fig. 2a, it can be observed that the best responses were obtained using 100–140 μL of ferrofluid, getting the proper dispersion of the whole material and the highest elution of the analytes. For that reason, 100 μL was established for further experiments in order to minimise the use of ferrofluid. In addition, when the amount of ferrofluid was higher than 140 μL, the extraction capacity decreased because huge amounts of

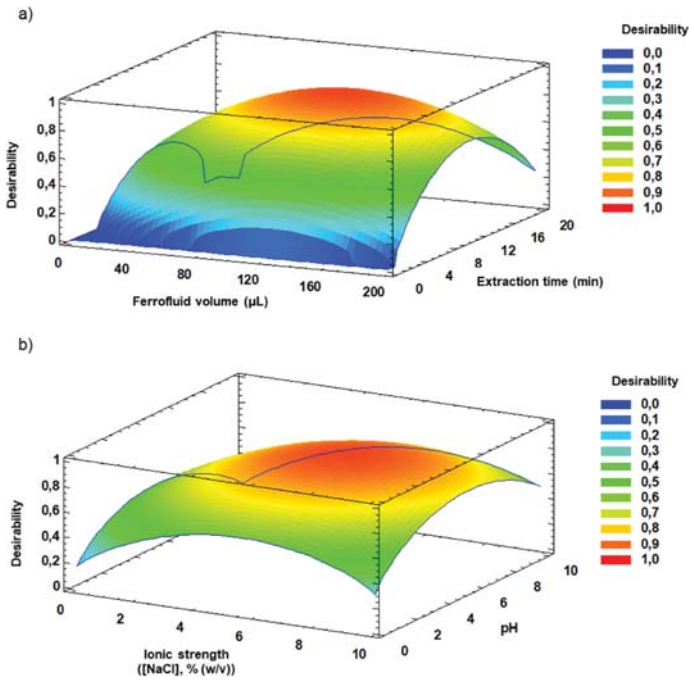

Fig. 2. Response surface of the desirability function representing the relation between the different variables: a) ferrofluid volume vs extraction time, and b) ionic strength vs pH.

ferrofluid may have difficulties to be retrieved by the magnet, thus decreasing the signal.

Regarding the extraction time, in Fig. 2a it is observed that the signal increased until ca. 10 min. At longer times, the signal decreased probably because the ferrofluid was partially separated into the $CoFe_2O_4$@OA MNPs and the DES under vigorous stirring. This phenomenon is known as leaching effect [36]. In consequence, the stir bar only retrieved the remaining ferrofluid and the naked MNPs, but not the released DES and the analytes it contained.

On the other side, as it is shown in Fig. 2b, an improvement was observed working in the pH range of 4–6 due to the pK_a values of the UV filters (see Table S1). In this pH range, the UV filters remain in their neutral form, increasing the interaction with the hydrophobic DES and, thus, favouring their extraction.

Finally, the optimal extraction efficiency was achieved employing 6% NaCl (w/v) due to the known salting-out effect (see Fig. 2b). The extraction capacity increased at low-medium amounts of salt (i.e., 1–6%), however it decreased at high amounts. This may be produced due to the fact that the aqueous medium becomes highly ionic and viscous, causing the bad dispersion of the ferrofluid in the aqueous samples.

In summary, the optimized method consisted of 100 μL of ferrofluid, 10 min of stirring time and NaCl adjustment to 6%. The pH was not adjusted since the normal pH in environmental waters is within the optimum interval.

3.2.2. Optimization of the desorption variables

Different desorption times (0, 2, 5 and 10 min) were tested. The obtained results (Fig. 3a) show that 2 min were enough to complete the desorption of UV filters from the extraction phase showing the maximum signals at this time. Therefore, this desorption time was selected.

The effect of the desorption solvent volume (i.e., acetonitrile) was explored. Different acetonitrile volumes (100, 250 and 500 μL) were tested. As it is shown in Fig. 3b the best results were obtained employing 100 μL. Volumes below 100 μL were insufficient to cover the neodymium magnet so they were discarded. Therefore, 100 μL of acetonitrile was selected as the appropriate volume for the desorption solvent.

3.3. Extraction performance of $CoFe_2O_4$@OA and ferrofluid

The extraction efficiency of $CoFe_2O_4$@OA MNPs and the ferrofluid (i.e., $CoFe_2O_4$@OA-menthol:thymol) were compared in order to study the influence of the DES in the extraction performance. Fig. 4 shows how the extraction with the ferrofluid increased the signals of the analytes with lower sensitivity such as BZ3, IMC, MBC and BMDM. For OC, EHDP and

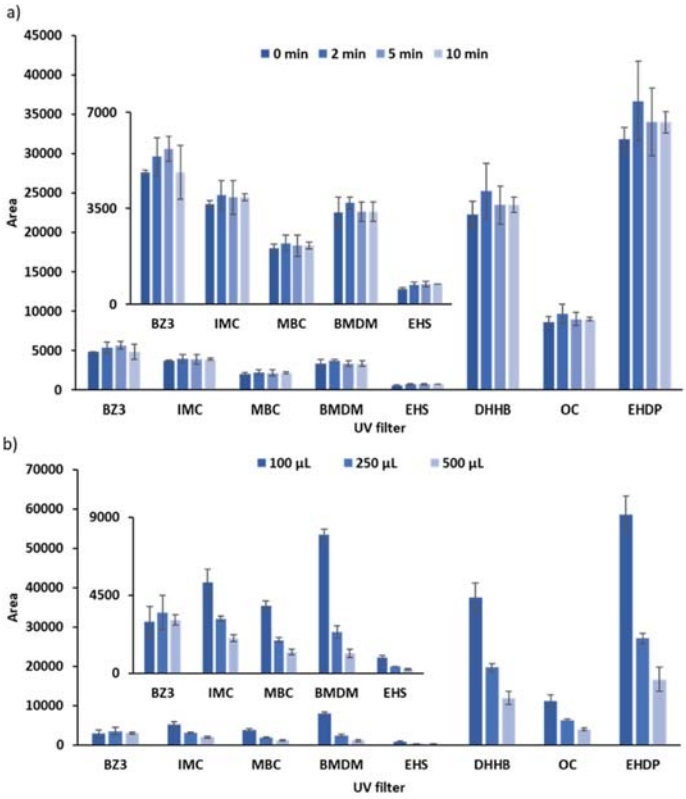

Fig. 3. a) Effect of the desorption time. Extraction conditions: 10 mL aqueous solution with 2 ng mL^{-1} of the target analytes at pH 5, 100 μL of ferrofluid and 6% NaCl (w/v). Error bars show the standard deviation of the results (n = 3). b) Effect of the desorption volume. Extraction conditions: 10 mL aqueous solution with 2 ng mL^{-1} of the target analytes at pH 5, 100 μL of ferrofluid and 6% NaCl (w/v). Error bars show the standard deviation of the results (n = 3).

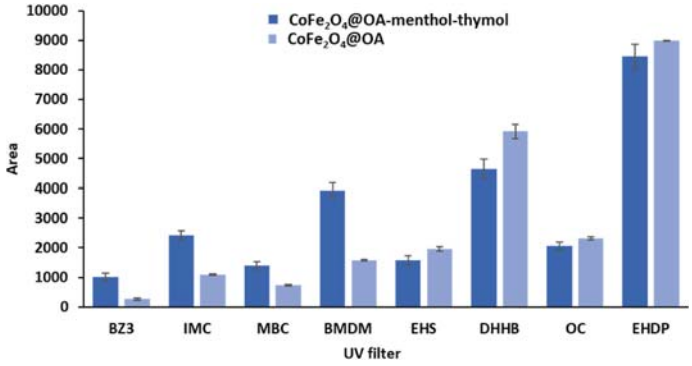

Fig. 4. Comparison of the extraction performance of the $CoFe_2O_4$@OA MNPs and the ferrofluid. Extraction conditions: 10 mL aqueous solution with 3 ng mL^{-1} of EHS, 0.6 ng mL^{-1} of BZ3, IMC and OC, 1.2 ng mL^{-1} of MBC and BMDM, and 0.03 ng mL^{-1} of DHHB and EHDP at pH 5, 100 μL of ferrofluid and 6% NaCl (w/v). Error bars show the standard deviation of the results (n = 3).

EHS, there were not great differences employing the ferrofluid or the $CoFe_2O_4$@OA MNPs.

Therefore, it can be concluded that the addition of the DES to the $CoFe_2O_4$@OA provides a synergistic effect improving, in overall terms, the extraction efficiency for the UV filters, which increases the sensitivity of the method.

3.4. Inter-batch repeatability of the synthesis of the ferrofluid

The inter-batch repeatability of the synthetized ferrofluid was evaluated by comparing the extraction capacity of three different synthesis batches on the extraction of a 750 ng L^{-1} standard solution under the optimized conditions. Results in Fig. 5 show that there were not significant differences ($p < 0.05$) between the three batches proving the good repeatability of the synthesis process.

3.5. Method validation

Limits of detection (LOD) and quantification (LOQ), linear working range (LR), repeatability (expressed as relative standard deviation (RSD (%)) and enrichment factors (EF) were evaluated for method validation. In order to correct for the variability during the SBDLME process, OC-d_{15} was used as surrogate. As consequence, the calibration was performed by plotting A_i/A_{sur} (where A_i is the peak area of the target analyte and A_{sur} is that of the surrogate) versus the target analyte concentration. The results are presented in Table 1.

The LODs and LOQs were estimated by measuring 3 and 10 times the signal to noise ratio from a 1000 ng L^{-1} multicomponent aqueous standard solution. Then, standard solutions were injected at different concentrations after the SBDLME approach in order to find the signal with a S/N = 3 (for LOD) and S/N = 10 (for LOQ). The LODs and LOQs ranged from 7 to 83 ng L^{-1} and from 24 to 276 ng L^{-1}, respectively, depending of the analyte.

This method provided good linearity until 20 ng mL^{-1}. However, due the low levels of UV filters expected in environmental waters, working ranges were set at different ng L^{-1} levels according to the LOQs obtained for each UV filter and the samples requirements. Thus, 30–750 ng L^{-1} was selected for EHDP and DHHB, 70–1750 ng L^{-1} for BZ3, IMC and OC, 130–3250 ng L^{-1} for BMDM and MBC and 300–7500 ng L^{-1} for EHS. In this sense, good determination coefficients ($R^2 > 0.998$) were obtained

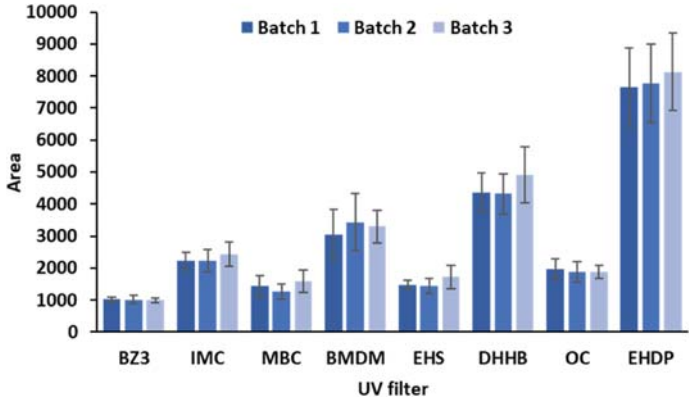

Fig. 5. Inter-batch repeatability of the synthesis process of the ferrofluid. Extraction conditions: 10 mL aqueous solution with 3 ng mL^{-1} of EHS, 0.6 ng mL^{-1} of BZ3, IMC and OC, 1.2 ng mL^{-1} of MBC and BMDM, and 0.03 ng mL^{-1} of DHHB and EHDP at pH 5, 100 μL of ferrofluid and 6% NaCl (w/v). Error bars show the standard deviation of the results (n = 3).

Table 1
Figures of merit of the proposed SBDLME method.

UV filter	R^2[a]	EF[b]	LOD[c] (ng L^{-1})	LOQ[c] (ng L^{-1})	Repeatability (RSD (%))[d]					
					Intra-day			Inter-day		
					Level 1[e]	Level 2[f]	Level 3[g]	Level 1[e]	Level 2[f]	Level 3[g]
BZ3	0.9999	93	20	67	4.5	13.8	9.6	12.2	12.7	5.6
IMC	0.9998	75	16	54	6.6	6.1	5.0	9.9	12.8	14.2
MBC	0.9993	80	39	130	5.2	9.3	5.0	12.5	8.0	4.8
DHHB	0.9998	73	8	25	8.3	8.8	2.7	12.8	14.9	10.7
OC	0.9999	46	18	60	10.8	9.5	3.2	7.3	2.8	4.5
EHDP	0.9993	101	7	24	12.8	10.1	1.8	8.6	11.1	9.1
BMDM	0.9993	71	36	116	8.6	9.1	4.5	13.0	4.9	8.6
EHS	0.998	78	83	276	6.0	10.7	3.4	12.5	11.1	10.8

[a] Coefficient of determination; Number of calibration points: 5.
[b] EF: Enrichment factor.
[c] LOD: Limit of detection (S/N = 3); LOQ: Limit of quantification (S/N = 10).
[d] RSD: relative standard deviation (%) (n = 5).
[e] Level 1: 30 ng L^{-1} for DHHB and EHDP; 70 ng L^{-1} for BZ3, IMC and OC; 130 ng L^{-1} for MBC and BMDM; 300 ng L^{-1} for EHS.
[f] Level 2: 190 ng L^{-1} for DHHB and EHDP; 340 ng L^{-1} for BZ3, IMC and OC; 690 ng L^{-1} for MBC and BMDM; 1875 ng L^{-1} for EHS.
[g] Level 3: 750 ng L^{-1} for DHHB and EHDP; 1350 ng L^{-1} for BZ3, IMC and OC; 2750 ng L^{-1} for MBC and BMDM; 7500 ng L^{-1} for EHS.

for all the analytes.

The intra- and inter-day repeatability was established by the extraction of five aqueous standard solutions at three different concentration levels in the same day (n = 5) and in five consecutive days (n = 5), respectively. The resultant RSD (%) were under 15% in all cases, proving the good repeatability of the proposed method.

The EFs were calculated as the ratio of the signal obtained before and after the extraction of a 2000 ng L^{-1} aqueous standard solution, and they ranged from 46 to 101.

3.6. Analysis of environmental water samples

Three environmental waters (beach and river water) were analyzed to determine the amount of UV filters in these samples in order to evaluate this method in a real case application. Prior to analysis, the conductivity of the samples was measured to estimate their ionic strength value (i.e., 0.05% in river water, and 4% in seawater). Then, it was regulated to 6% w/v by adding NaCl. Table 2 shows the results after the SBDLME-LC-MS/MS method. As can be seen, the measured concentrations in beach 1 were noticeable higher than in beach 2, likely due to the fact it was a more crowded area for bathers and thus higher quantities of sunscreen arrive to the nearshore. On the contrary, most UV filters were not detected in river water despite it was sampled from a bathing area, probably due to the constant circulation of the water stream. As example, a chromatogram of sample beach 1 is shown in Figure S7.

Anyway, it should be added that the concentration of UV filters in that kind of aquatic samples depends on several factors, such as number of swimmers, water tide and water recirculation rates along the day.

Table 2
Concentration of UV filters in three environmental water samples. Results are presented as the average value ± the standard deviation of three replicates (n = 3).

UV Filter	Found concentration (ng L^{-1})		
	Beach 1	Beach 2	River
BZ3	225 ± 25	<67[b]	<20[a]
IMC	<16[a]	<16[a]	<16[a]
MBC	148 ± 13	<130[b]	<39[a]
DHHB	58 ± 6	<25[b]	<25[b]
OC	78 ± 9	84 ± 7	208 ± 2
EHDP	<24[b]	<24[b]	<7[a]
BMDM	240 ± 20	<116[b]	<36[a]
EHS	<276[b]	<276[b]	<83[a]

[a] < limit of detection.
[b] < limit of quantification.

Finally, for the study of the accuracy of the method, these three samples were spiked at three different concentration levels in order to calculate the relative recoveries for each analyte. As can be seen in Table 3, good relative recoveries were obtained (80–117%), proving the absence of a significant matrix effect.

3.7. Comparison with previously reported methods

A comparison between the proposed method and some previously reported methods based on the determination of the same UV filters in environmental waters is presented in Table 4. As can be seen, the analytical performance is comparable or better than these previous methods. In general terms, compared to non-dispersive techniques (i.e., SPME and SBSE), the dispersive-based techniques (i.e., SBSDME and SBDLME) require lower extraction times. Nevertheless, SBDLME present even lower extraction times compared with those employing solid sorbents. Moreover, comparing the two SBDLME-based methods, similar results were obtained (the high limit of detection obtained for EHS attributed to its low signal employing LC-MS/MS and not to the extraction technique), proving that this new LT-DES-based ferrofluid can be employed as a cheaper and greener alternative to MILs.

Additionally, a greenness study of the presented method and the previous MIL-based SBDLME method is presented in Supplementary Material employing the ComplexGAPI [37] and AGREEprep [38] apps. As can be seen, employing complexGAPI (Fig. S8), there are not significant differences in the analysis (5 upper pentagons). However, if the synthesis of the materials is included (hexagon), a huge difference employing the MIL (Fig. S8a) and the LT-DES-based ferrofluid (Fig S8b) can be noticed, thus proving the greener synthesis of the menthol: thymol ferrofluid.

On the other side, according to AGREEprep (Fig. S9), minimum differences are observed employing the MIL (Fig. S9a) or the LT-DES-based ferrofluid (Fig. S9b), since the synthesis process is not included and it is mainly focused on the sample preparation.

4. Conclusions

A new low toxicity deep eutectic solvent (LT-DES)-based ferrofluid has been presented as an extraction phase for microextraction purposes. This ferrofluid, composed by $CoFe_2O_4$@OA MNPs and a 1:5 ratio of menthol and thymol DES, has two main advantages over other magnetic fluids (i.e., MILs). First of all, its components are quite less toxic and less harmful to the environment. Moreover, the synthesis is simple and safe, since only a water bath was needed for the preparation of the DES and a

Table 3
Relative recoveries after the application of the SBDLME method on three environmental water samples spiked at three concentration levels. Results are presented as the average value ± the standard deviation of three replicates (n = 3).

UV Filter	Beach 1			Beach 2			River		
	Level 1[a]	Level 2[b]	Level 3[c]	Level 1[a]	Level 2[b]	Level 3[c]	Level 1[a]	Level 2[b]	Level 3[c]
BZ3	104 ± 13	105 ± 9	91 ± 9	113 ± 15	83 ± 2	87 ± 7	100 ± 4	109 ± 16	91 ± 12
IMC	96 ± 15	112 ± 11	94 ± 7	83 ± 3	80 ± 3	93 ± 7	84 ± 1	85 ± 6	98 ± 14
MBC	120 ± 1	91 ± 8	80 ± 8	109 ± 10	84 ± 7	82 ± 6	116 ± 4	80 ± 2	96 ± 5
DHHB	109 ± 7	115 ± 4	111 ± 10	89 ± 7	104 ± 8	101 ± 3	114 ± 8	107 ± 3	96 ± 6
OC	96 ± 6	107 ± 1	98 ± 4	107 ± 1	112 ± 9	112 ± 8	91 ± 3	86 ± 10	98 ± 2
EHDP	116 ± 4	101 ± 5	88 ± 7	97 ± 3	107 ± 4	102 ± 3	115 ± 6	100 ± 4	91 ± 8
BMDM	104 ± 8	94 ± 16	97 ± 13	107 ± 14	112 ± 13	104 ± 3	106 ± 3	115 ± 3	102 ± 6
EHS	80 ± 7	90 ± 10	84 ± 12	81 ± 1	103 ± 14	102 ± 2	98 ± 9	97 ± 11	96 ± 8

[a] Level 1: 30 ng L^{-1} for DHHB and EHDP; 70 ng L^{-1} for BZ3, IMC and OC; 130 ng L^{-1} for MBC and BMDM; 300 ng L^{-1} for EHS.
[b] Level 2: 190 ng L^{-1} for DHHB and EHDP; 340 ng L^{-1} for BZ3, IMC and OC; 690 ng L^{-1} for MBC and BMDM; 1875 ng L^{-1} for.
[c] Level 3: 750 ng L^{-1} for DHHB and EHDP; 1350 ng L^{-1} for BZ3, IMC and OC; 2750 ng L^{-1} for MBC and BMDM; 7500 ng L^{-1} for EHS.

Table 4
Comparison of the proposed SBDLME method and other methods focused on the determination of UV filters in environmental waters.

UV filters[a]	Extraction technique[b]	Measurement technique[c]	Extraction phase[d]	Extraction time (min)	Sample volume (mL)	LOD (ng L^{-1})	RR%	Ref.
BZ3, MBC, IMC, OC, EHMC, EHDP, BMDM, EHS, HMS	SBSE	TD-GC-MS	PDMS	180	20	0.2–64	75–116	[39]
BZ3, MBC, IMC, OC, EHMC, EHDP, EHS, HMS	SBSDME	LC-UV	$CoFe_2O_4$@OA	20	25	2400–30000	87–120	[40]
BZ1, BZ3, BZ4, BZ8, MBC, IMC, OC, EHMC, EHDP, EHS, HMS, BS, Eto, MA	SPME	GC-MS/MS	DVB/CAR/PDMS	30	10	2–1000	80–106	[41]
BZ3, MBC, IMC, OC, EHMC, EHDP, EHS, HMS	SBDLME	TD-GC-MS	$[P^{+}_{6,6,6,14}][Ni(hfacac)_3^{-}]$	10	25	9.9–27	87–117	[28]
BZ3, MBC, IMC, DHHB, OC, EHDP, BMDM, EHS	SBDLME	LC-MS/MS	$CoFe_2O_4$@OA-menthol:thymol	10	15	7–83	80–117	This work

[a] BZ: benzophenone; MBC: methybenzylidene camphor; IMC: isoamyl p-methoxycinnamate; OC: octocrylene; EHMC: ethylhexyl methoxycinnamate; EHDP: ethylhexyl dimethyl PABA; EHS: ethylhexyl salicylate; HMS: homosalate; BMDM: butyl methoxydibenzoylmethane; BS: benzyl salicylate; Eto: etocrylene; MA: menthyl anthranilate.
[b] SBSE: stir bar sorptive extraction; SBSDME: stir bar sorptive-dispersive microextraction; SPME: solid phase microextraction; SBDLME: stir bar dispersive liquid microextraction.
[c] TD-GC-MS: thermal desorption-gas chromatography-mass spectrometry; LC-UV: liquid chromatography-ultraviolet spectrometry; GC-MS/MS: gas chromatography-tandemmass spectrometry; LC-MS/MS: liquid chromatography-tandem mass spectrometry.
[d] PDMS: polydimethylsiloxane; $CoFe_2O_4$@OA: oleic acid-coated cobalt ferrite nanoparticles; DVB/CAR/PDMS: divinylbenzene-carboxen-polydimethylsiloxane; $[P^{+}_{6,6,6,14}][Ni(hfacac)_3^{-}]$: trihexyl(tetradecyl)phosphonium nickel(II) hexafluoroacetylacetonate ionic liquid; $CoFe_2O_4$@OA-menthol:thymol: oleic acid-coated cobalt ferrite nanoparticles-menthol:thymol deep eutectic solvent ferrofluid.

sonication step to form the ferrofluid.

This new ferrofluid was tested in the determination of UV filters in environmental waters employing SBDLME as microextraction technique obtaining good analytical features. This method was compared with the previous SBDLME methodology used for the same purpose, but employing a MIL as an extraction phase [28]. The proposed method showed similar results, proving the potential of this ferrofluid as a cheaper and greener alternative of MILs to be employed in future analytical approaches.

Credit author statement

A. Duque: Investigation, Data treatment, Writing – original draft; J. Grau: Investigation, Data treatment, Writing – original draft; J.L. Benedé; : Methodology, Writing - reviewing and editing; R.M. Alonso: Conceptualization, Supervision, Methodology, Writing - reviewing and editing; M.A. Campanero: Conceptualization, Supervision, Methodology, Writing - reviewing and editing; A. Chisvert: Conceptualization, Supervision, Methodology, Project organization, Funding acquisition, Writing - reviewing and editing.

Declaration of competing interest

The authors declare that they have no known competing financial interests or personal relationships that could have appeared to influence the work reported in this paper.

Acknowledgements

J.L.B. thanks the Generalitat Valenciana and the European Social Fund for his postdoctoral grant, and A.D. thanks the Basque Country Government for her predoctoral contract (Bikaintek 2020 Program from the Regional Minister for Economic Development and Infrastructures (order 2021–1353, file number 021-B2/2020)). Authors also thank to the Magnetism Unit of SGIker of University of Basque Country (UPV/EHU) for kindly carrying out the magnetism measurements. This article is based upon work from the National Thematic Network on Sample Treatment (RED-2018-102522-T) of the Spanish Ministry of Science, Innovation and Universities, and the Sample Preparation Study Group and Network supported by the Division of Analytical Chemistry of the European Chemical Society.

Appendix A. Supplementary data

Supplementary data to this article can be found online at https://doi.org/10.1016/j.talanta.2022.123378.

References

[1] S. Armenta, S. Garrigues, F.A. Esteve-Turrillas, M. de la Guardia, Green extraction techniques in green analytical chemistry, TrAC Trends Anal. Chem. (Reference Ed.) 116 (2019) 248–253.

[2] G. Li, K.H. Row, Utilization of deep eutectic solvents in dispersive liquid-liquid micro-extraction, TrAC Trends Anal. Chem. (Reference Ed.) 120 (2019) 115651.

[3] S. Peng, X. Huang, Y. Huang, Y. Huang, J. Zheng, F. Zhu, J. Xu, G. Ouyang, Novel solid-phase microextraction fiber coatings: a review, J. Separ. Sci. 45 (2022) 282–304.

[4] P. Ścigalski, P. Kosobucki, Recent materials developed for dispersive solid phase extraction, Molecules 25 (2020) 1–27.

[5] A. Gałuszka, Z. Migaszewski, J. Namieśnik, The 12 principles of green analytical chemistry and the SIGNIFICANCE mnemonic of green analytical practices, TrAC Trends Anal. Chem. (Reference Ed.) 50 (2013) 78–84.

[6] A.I. López-Lorente, F. Pena-Pereira, S. Pedersen-Bjergaard, V.G. Zuin, S.A. Ozkan, E. Psillakis, The ten principles of green sample preparation, TrAC Trends Anal. Chem. (Reference Ed.) 148 (2022) 116530.

[7] J. Grau, C. Azorín, J.L. Benedé, A. Chisvert, A. Salvador, Use of green alternative solvents in dispersive liquid-liquid microextraction: a review, J. Separ. Sci. 45 (2022) 210–222.

[8] P. Makoś, E. Słupek, J. Gębicki, Hydrophobic deep eutectic solvents in microextraction techniques–A review, Microchem. J. 152 (2020) 104384.

[9] Á. Santana-Mayor, R. Rodríguez-Ramos, A.V. Herrera-Herrera, B. Socas-Rodríguez, M.Á. Rodríguez-Delgado, Deep eutectic solvents. The new generation of green solvents in analytical chemistry, TrAC Trends Anal. Chem. (Reference Ed.) 134 (2021) 116108.

[10] A. Shishov, A. Pochivalov, L. Nugbienyo, V. Andruch, A. Bulatov, Deep eutectic solvents are not only effective extractants, TrAC Trends Anal. Chem. (Reference Ed.) 129 (2020) 115956.

[11] M.Q. Farooq, N.M. Abbasi, J.L. Anderson, Deep eutectic solvents in separations: methods of preparation, polarity, and applications in extractions and capillary electrochromatography, J. Chromatogr., A 1633 (2020) 461613.

[12] Q. Zhang, K. De Oliveira Vigier, S. Royer, F. Jérôme, Deep eutectic solvents: syntheses, properties and applications, Chem. Soc. Rev. 41 (2012) 7108–7146.

[13] B.B. Hansen, S. Spittle, B. Chen, D. Poe, Y. Zhang, J.M. Klein, A. Horton, L. Adhikari, T. Zelovich, B.W. Doherty, B. Gurkan, E.J. Maginn, A. Ragauskas, M. Dadmun, T.A. Zawodzinski, G.A. Baker, M.E. Tuckerman, R.F. Savinell, J. R. Sangoro, Deep eutectic solvents: a review of fundamentals and applications, Chem. Rev. 121 (2021) 1232–1285.

[14] H. Musarurwa, N.T. Tavengwa, Emerging green solvents and their applications during pesticide analysis in food and environmental samples, Talanta 223 (2021) 121507.

[15] O.E. Plastiras, E. Andreasidou, V. Samanidou, Microextraction techniques with deep eutectic solvents, Molecules 25 (2020) 6026.

[16] M. de los Á Fernández, J. Boiteux, M. Espino, F.J.V. Gomez, M.F. Silva, Natural deep eutectic solvents-mediated extractions: the way forward for sustainable analytical developments, Anal. Chim. Acta 1038 (2018) 1–10.

[17] J. Płotka-Wasylka, M. Rutkowska, K. Owczarek, M. Tobiszewski, J. Namiesnik, Extraction with environmentally friendly solvents, TrAC Trends Anal. Chem. (Reference Ed.) 91 (2017) 12–25.

[18] J. Płotka-Wasylka, M. Rutkowska, M. de la Guardia, Are deep eutectic solvents useful in chromatography? A short review, J. Chromatogr., A 1639 (2021) 461918.

[19] J. Lee, D. Jung, K. Park, Hydrophobic deep eutectic solvents for the extraction of organic and inorganic analytes from aqueous environments, TrAC Trends Anal. Chem. (Reference Ed.) 118 (2019) 853–868.

[20] R. Nayebi, F. Shemirani, Ferrofluids-based microextraction systems to process organic and inorganic targets: the state-of-the-art advances and applications, TrAC Trends Anal. Chem. (Reference Ed.) 138 (2021) 116232.

[21] M.Á. Aguirre, A. Canals, Magnetic deep eutectic solvents in microextraction techniques, TrAC Trends Anal. Chem. (Reference Ed.) 146 (2022) 116500.

[22] M. Sajid, K. Kalinowska, J. Płotka-Wasylka, Ferrofluids based analytical extractions and evaluation of their greenness, J. Mol. Liq. 339 (2021) 116901.

[23] M. Ebrahimi, A short review on ferrofluids surface modification by natural and biocompatible polymers, Nanomedicine J 3 (2016) 155–158.

[24] R. González-Martín, A. Gutiérrez-Serpa, V. Pino, The use of ferrofluids in analytical sample preparation: a review, Separations 8 (2021) 1–14.

[25] E. Psillakis, Vortex-assisted liquid-liquid microextraction revisited, TrAC Trends Anal. Chem. (Reference Ed.) 113 (2019) 332–339.

[26] M. Sajid, Magnetic ionic liquids in analytical sample preparation: a literature review, TrAC Trends Anal. Chem. (Reference Ed.) 113 (2019) 210–223.

[27] B. Hashemi, P. Zohrabi, K.H. Kim, M. Shamsipur, A. Deep, J. Hong, Recent advances in liquid-phase microextraction techniques for the analysis of environmental pollutants, TrAC Trends Anal. Chem. (Reference Ed.) 97 (2017) 83–95.

[28] A. Chisvert, J.L. Benedé, J.L. Anderson, S.A. Pierson, A. Salvador, Introducing a new and rapid microextraction approach based on magnetic ionic liquids: stir bar dispersive liquid microextraction, Anal. Chim. Acta 983 (2017) 130–140.

[29] J.L. Benedé, J.L. Anderson, A. Chisvert, Trace determination of volatile polycyclic aromatic hydrocarbons in natural waters by magnetic ionic liquid-based stir bar dispersive liquid microextraction, Talanta 176 (2018) 253–261.

[30] M.J. Trujillo-Rodríguez, J.L. Anderson, In situ generation of hydrophobic magnetic ionic liquids in stir bar dispersive liquid-liquid microextraction coupled with headspace gas chromatography, Talanta 196 (2019) 420–428.

[31] A.R. Zarei, M. Nedaei, S.A. Ghorbanian, Deep eutectic solvent based magnetic nanofluid in the development of stir bar sorptive dispersive microextraction: an efficient hyphenated sample preparation for ultra-trace nitroaromatic explosives extraction in wastewater, J. Separ. Sci. 40 (2017) 4757–4764.

[32] A. Chisvert, J.L. Benedé, A. Salvador, Current trends on the determination of organic UV filters in environmental water samples based on microextraction techniques – a review, Anal. Chim. Acta 1034 (2018) 22–38.

[33] K. Maaz, A. Mumtaz, S.K. Hasanain, A. Ceylan, Synthesis and magnetic properties of cobalt ferrite ($CoFe_2O_4$) nanoparticles prepared by wet chemical route, J. Magn. Magn Mater. 308 (2007) 289–295.

[34] S.A.M. Hussin, P. Varanusupakul, S. Shahabuddin, B.Y. Hui, D. Mohamad, Synthesis and characterization of green menthol-based low transition temperature mixture with tunable thermophysical properties as hydrophobic low viscosity solvent, J. Mol. Liq. 308 (2020) 113015.

[35] L. Kafi-ahmadi, S. Khademinia, M.N. Nansa, A.A. Alemi, M. Mahdavi, A.P. Marjani, Co-precipitation synthesis, characterization of $CoFe_2O_4$ nanomaterial and evaluation of its toxicity behavior on human leukemia cancer K562 cell line, J. Chil. Chem. Soc. 65 (2020) 4845–4848.

[36] V. Vállez-Gomis, J. Grau, J.L. Benedé, D.L. Giokas, A. Chisvert, A. Salvador, Fundamentals and applications of stir bar sorptive dispersive microextraction: a tutorial review, Anal. Chim. Acta 1153 (2021) 338271.

[37] J. Płotka-Wasylka, W. Wojnowski, Complementary green analytical procedure index (ComplexGAPI) and software, Green Chem. 23 (2021) 8657–8665.

[38] W. Wojnowski, M. Tobiszewski, F. Pena-Pereira, E. Psillakis, AGREEprep – analytical greenness metric for sample preparation, TrAC Trends Anal. Chem. (Reference Ed.) 149 (2022) 116553.

[39] R. Rodil, M. Moeder, Development of a method for the determination of UV filters in water samples using stir bar sorptive extraction and thermal desorption-gas chromatography-mass spectrometry, J. Chromatogr., A 1179 (2008) 81–88.

[40] J.L. Benedé, A. Chisvert, D.L. Giokas, A. Salvador, Development of stir bar sorptive-dispersive microextraction mediated by magnetic nanoparticles and its analytical application to the determination of hydrophobic organic compounds in aqueous media, J. Chromatogr., A 1362 (2014) 25–33.

[41] M. Vila, M. Celeiro, J.P. Lamas, C. Garcia-Jares, T. Dagnac, M. Llompart, Simultaneous in-vial acetylation solid-phase microextraction followed by gas chromatography tandem mass spectrometry for the analysis of multiclass organic UV filters in water, J. Hazard Mater. 323 (2017) 45–55.

Low toxicity deep eutectic solvent-based ferrofluid for the determination of UV filters in environmental waters by stir bar dispersive liquid microextraction

Alaine Duque[a] #, José Grau[b] #, Juan L. Benedé[b], Rosa M. Alonso[c], Miguel A. Campanero[a], Alberto Chisvert[b] *

[a] A3Z Advanced Analytical Consulting Services, 48160 Derio, Vizcaya, Spain

[b] GICAPC Research group, Department of Analytical Chemistry, University of Valencia, 46100 Burjassot, Valencia, Spain

[c] FARMARTEM Group, Department of Analytical Chemistry, Faculty of Science and Technology, University of the Basque Country (UPV/EHU), 48940 Leioa, Vizcaya, Spain

* Corresponding author: Alberto Chisvert (alberto.chisvert@uv.es)

# These authors contributed equally to this work

TABLE OF CONTENTS

Table S1. Chemical structure and relevant data of the target compounds.

UV filter	Chemical structure	CAS	$logP_{ow}$ [a]	pK_a [b]
Benzophenone-3 (BZ3)	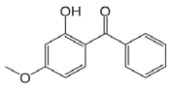	131-57-7	3.79	7.1
Isoamyl p-methoxycinnamate (IMC)	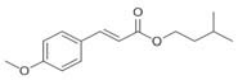	71617-10-2	3.25	-
4-methylbenzylidene camphor (MBC)	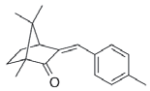	36861-47-9	4.95	-
Diethylamino hydroxybenzoyl hexyl benzoate (DHHB)	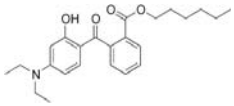	302776-68-7	6.20	7.6
Octocrylene (OC)	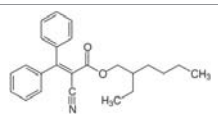	6197-30-4	7.04	-
Ethylhexyl dimethyl PABA (EHDP)	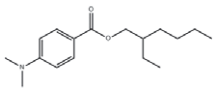	21245-02-3	5.77	2.9
Butyl methoxydibenzoylmethane (BMDM)	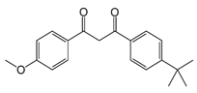	70356-09-1	4.51	9.7
Ethylhexyl salicylate (EHS)	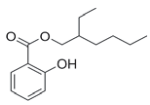	118-60-5	5.77	8.1

[a] Pow: Octanol-water partition coefficient; [b] Ka: Acid-base dissociation constant

Table S2. Tandem mass spectrometry parameters for the target analytes.

UV filter	Precursor ion (m/z)	Product ion (m/z) [a]	Collision energy (V)	Fragmentor (V)
BZ3	229	**151**	17	100
		105	17	
IMC	249	**179**	5	100
		161	13	
MBC	255	**105**	29	100
		91	53	
DHHB	398	**149**	13	100
		93	69	
OC-d_{15}	377	**251**	21	100
OC	362	**250**	21	100
		232	21	
EHDP	278	**166**	21	150
		151	33	
BMDM	311	**161**	25	100
		135	25	
EHS	251	**139**	1	100
		121	21	

[a] The m/z values used as quantifiers are marked in bold

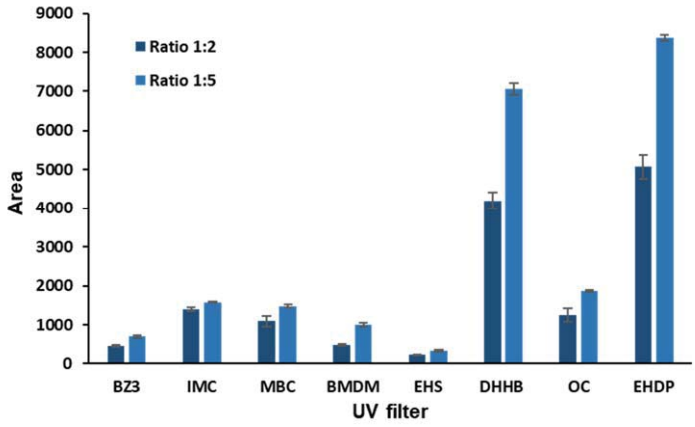

Fig. S1. Effect of the menthol:thymol molar ratio. Extraction conditions: 5 mL aqueous solution with 2 ng mL^{-1} of the target analytes and 50 µL of ferrofluid. Error bars show the standard deviation of the results (n = 3).

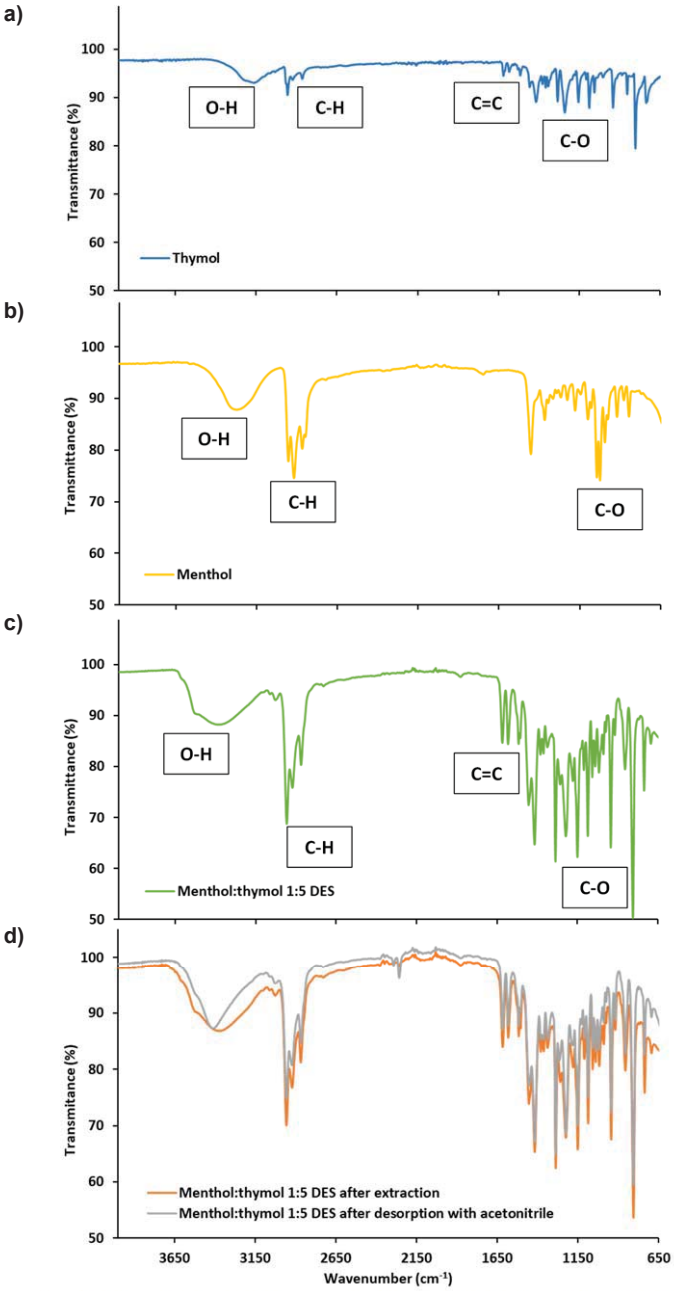

Fig. S2. FT-IR spectra of a) thymol, b) menthol, c) menthol:thymol 1:5 DES and d) menthol:thymol 1:5 DES after extraction and menthol:thymol 1:5 DES after desorption with acetonitrile.

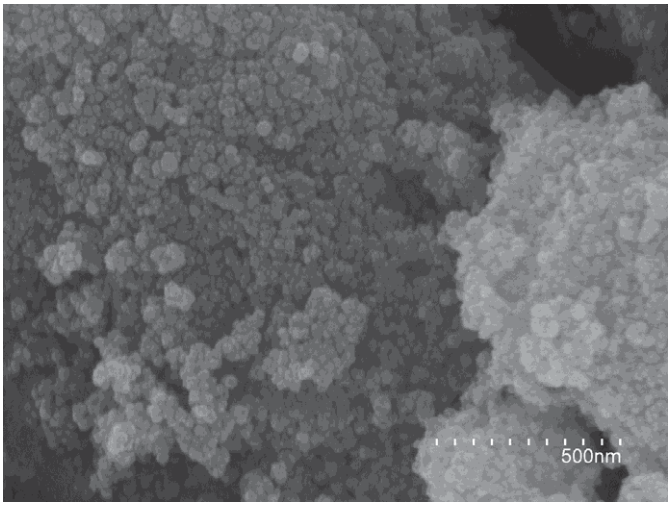

Fig. S3. SEM image of the synthetized $CoFe_2O_4$@OA MNPs.

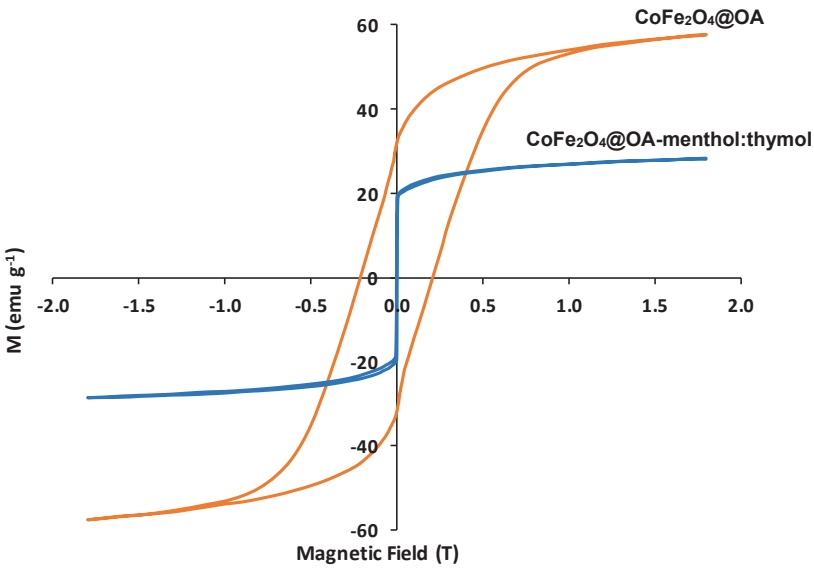

Fig. S4. Magnetization curves of $CoFe_2O_4$@OA MNPs and $CoFe_2O_4$@OA-menthol:thymol ferrofluid.

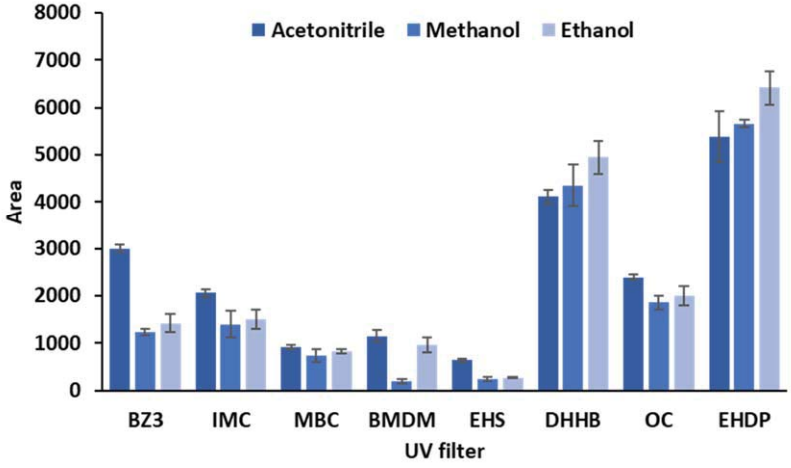

Fig. S5. Effect of the desorption solvent. Extraction conditions: 5 mL aqueous solution with 2 ng mL^{-1} of the target analytes and 50 µL of ferrofluid. Error bars show the standard deviation of the results (n = 3).

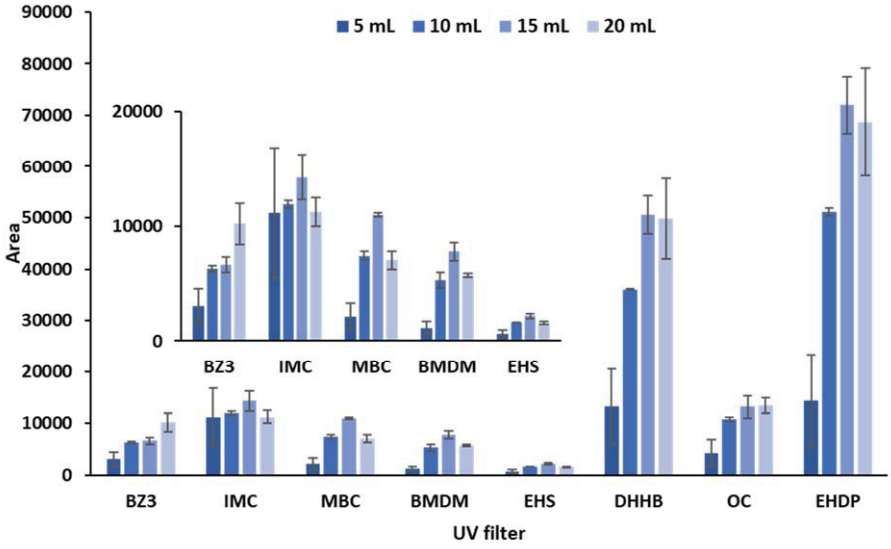

Fig. S6. Effect of the sample volume. Extraction conditions: 5, 10, 15 and 20 mL aqueous solution with 2 ng mL^{-1} of the target analytes and 50 µL of ferrofluid. Error bars show the standard deviation of the results (n = 3).

Box-Benhken design

Box-Benhken designs are used to generate higher order response surfaces using fewer required runs than a normal factorial technique. The total number of experiments for the Box-Benhken design is defined from the following equation:

$$N = 2 \cdot \mathrm{k} \cdot (\mathrm{k} - 1) + Cp \qquad (1)$$

where N is the total number of experiments to perform, k is the number of factors (i.e., 4), and CP is the number of replicates of the central point. According to the Equation (1), 27 experiments were necessary, selecting 3 replicates of the central point. The range of each factor was defined between a high and low value, as shown in Table S3. The following quadratic polynomial equation was applied to evaluate the multiple linear regression for each response:

$$Y = \beta_o + \sum \beta_i X_i + \sum \beta_{ii} X_i^2 + \sum \beta_{ij} X_i X_j + \varepsilon \qquad (2)$$

where Y is the analytical response; β0 refers the constant term; βi, βii and βij represent the regression coefficients of the design; χi and χj are the different variables; and ε is the residual error.

Then, the global desirability of the experiment (D) was applied to assess the different responses and to obtain the optimal extraction conditions to maximize the analytical signals of the target analytes:

$$D = (d_1(Y_1) \cdot d_2(Y_2) \cdots d_n(Y_n))^{1/n} \qquad (3)$$

where n is the number of responses in the optimization process, and di(Yi) is the individual desirability of each response in the experiment. The individual desirability is calculated as:

$$di = \frac{Yi - Ymin}{Ymax - Ymin} \qquad (4)$$

Responses are ranged between 0 and 1, respectively, in order to define the undesirable responses and fully desirable responses.

Table S3. Box-Behnken design for multivariate optimization of the critical variables.

Step	Volume of ferrofluid (µL)		Extraction time (min)		Ionic strength (%NaCl, w/v)		pH	
	Uncoded	Coded	Uncoded	Coded	Uncoded	Coded	Uncoded	Coded
1	20	-1	2	-1	5	0	6	0
2	200	1	2	-1	5	0	6	0
3	20	-1	20	1	5	0	6	0
4	200	1	20	1	5	0	6	0
5	110	0	11	0	0	-1	2	-1
6	110	0	11	0	10	1	2	-1
7	110	0	11	0	0	-1	10	1
8	110	0	11	0	10	1	10	1
9	20	-1	11	0	5	0	2	-1
10	200	1	11	0	5	0	2	-1
11	20	-1	11	0	5	0	10	1
12	200	1	11	0	5	0	10	1
13	110	0	2	-1	0	-1	6	0
14	110	0	20	1	0	-1	6	0
15	110	0	2	-1	10	1	6	0
16	110	0	20	1	10	1	6	0
17	20	-1	11	0	0	-1	6	0
18	200	1	11	0	0	-1	6	0
19	20	-1	11	0	10	1	6	0
20	200	1	11	0	10	1	6	0
21	110	0	2	-1	5	0	2	-1
22	110	0	20	1	5	0	2	-1
23	110	0	2	-1	5	0	10	1
24	110	0	20	1	5	0	10	1
25	110	0	11	0	5	0	6	0
26	110	0	11	0	5	0	6	0
27	110	0	11	0	5	0	6	0

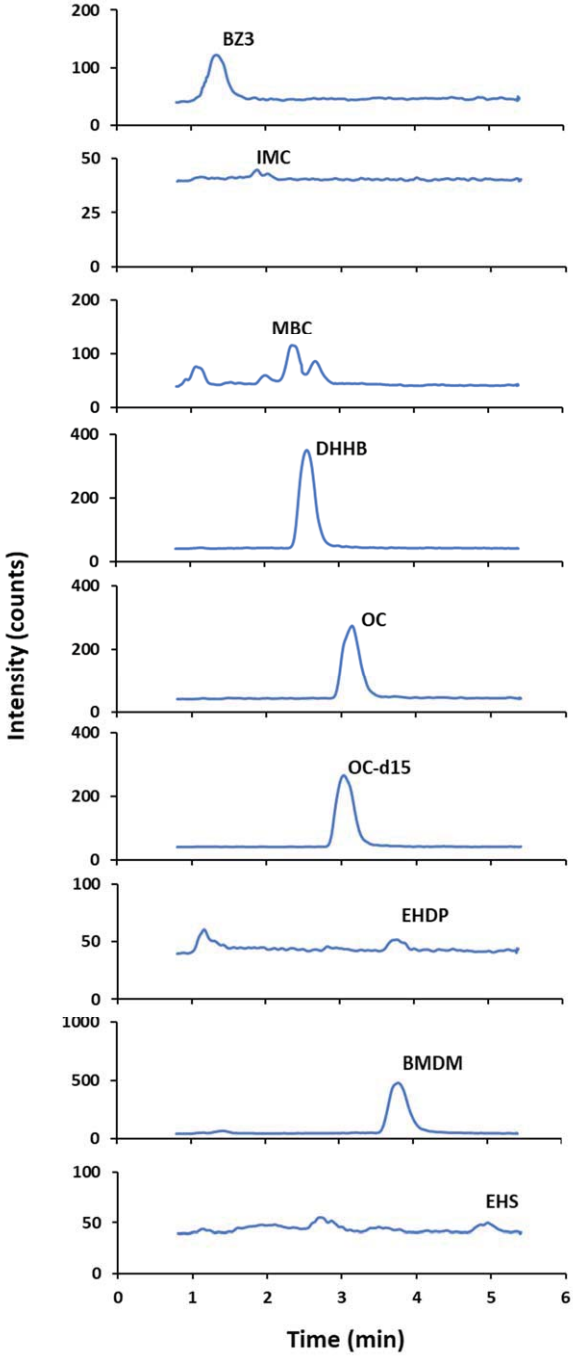

Fig S7. Chromatogram of an extracted water sample (i.e. beach 1)

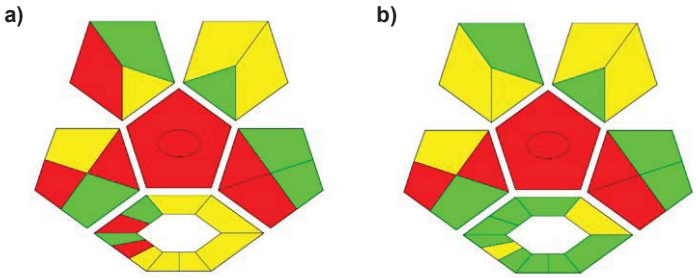

Fig S8. Evaluation of greenness with ComplexGAPI of a) SBDLME using a MIL [28] and b) using the proposed LT-DES-based ferrofluid.

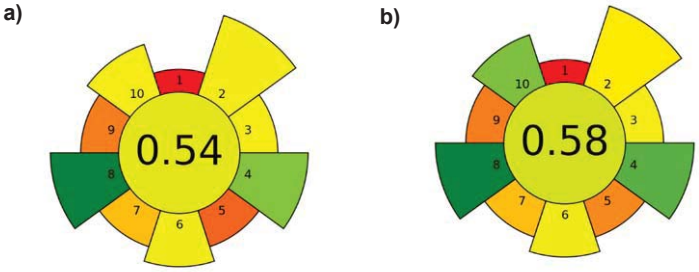

Fig S9. Evaluation of greenness with AGREEprep of a) SBDLME using a MIL [28] and b) using the proposed LT-DES-based ferrofluid.

Modified magnetic-based solvent-assisted dispersive solid-phase extraction: application to the determination of cortisol and cortisone in human saliva

Journal of chromatography A 1652 (2021) 462361

DOI: 10.1016/j.chroma.2021.462361

Journal of Chromatography A 1652 (2021) 462361

Contents lists available at ScienceDirect

Journal of Chromatography A

journal homepage: www.elsevier.com/locate/chroma

Modified magnetic-based solvent-assisted dispersive solid-phase extraction: application to the determination of cortisol and cortisone in human saliva

José Grau, Juan L. Benedé, Alberto Chisvert*, Amparo Salvador

Department of Analytical Chemistry, University of Valencia, 46100 Burjassot, Valencia, Spain

ARTICLE INFO

Article history:
Received 2 February 2021
Revised 17 June 2021
Accepted 22 June 2021
Available online 28 June 2021

Keywords:
Biomarkers
Dispersive-based microextraction
Liquid chromatography-tandem mass spectrometry
Magnetic sorbent
Saliva samples

ABSTRACT

A modification of magnetic-based solvent-assisted dispersive solid-phase extraction (M-SA-DSPE) has been employed for the determination of the biomarkers cortisol and cortisone in saliva samples. M-SA-DSPE is based on the dispersion of the sorbent material by using a disperser solvent like in dispersive solid phase extraction (SA-DSPE) but a magnetic sorbent is used like in magnetic dispersive solid-phase extraction (M-DSPE). Thus, the magnetic sorbent containing the target analytes is retrieved using an external magnet like in M-DSPE. Finally, the analytes are desorbed into a small volume of organic solvent for the subsequent chromatographic analysis. To this regard, a M-SA-DSPE-based method was developed using a magnetic composite as sorbent, made of $CoFe_2O_4$ magnetic nanoparticles embedded into a reversed phase polymer (Strata-X^{TM}-RP), which exhibits affinity to the target analytes. Then, liquid chromatography coupled to tandem mass spectrometry (LC-MS/MS) was used to measure both analytes in the M-SA-DSPE extract. Under the optimized conditions, good analytical features were obtained: limits of detection of 0.029 ng mL^{-1} for cortisol and 0.018 ng mL^{-1} for cortisone, repeatability (as RSD) $\leq$ 10 %, and relative recoveries between 86 and 111 %, showing no significant matrix effects. Finally, the proposed method was applied to the analysis of saliva from different volunteers. This new methodology allows a fast and non-invasive determination of cortisol and cortisone, and it employs small amounts of sample, organic solvent and sorbent. Likewise, the sample treatment is minimum, since any supporting equipment (vortex, centrifuge, ultrasounds, etc.) is required.

1. Introduction

Sample preparation is one of the most hot-spot research trends in Analytical Chemistry, especially in trace analysis, where it is usually necessary to perform a preconcentration of the analytes and/or a cleaning-up step to eliminate potentially interfering compounds [1].

In recent years, different approaches have been developed for extraction of analytes in samples of a very different nature employing a wide range of extraction phases (either liquids or solids). Those in which the acceptor phase is dispersed have gained special interest due to the high surface contact area between sample and acceptor phase, which redounds in a considerably reduction of the extraction time [2]. In relation to dispersive liquid-based microextraction techniques, the so-called dispersive liquid-liquid microextraction (DLLME) [3], and its different variants [4], is one of the most extended microextraction approaches due to its easy handling [5]. DLLME consists of dispersing a small volume of an extraction solvent into the liquid sample by forming a microemulsion in a conical tip tube. After centrifugation, the extraction solvent is generally retrieved from the bottom of the tube. Dispersion is usually achieved by using a disperser solvent, miscible in both the donor phase and the extraction phase, or by mechanical assistance (e.g., vortex or ultrasounds). This approach has been used in different types of matrices [5-7]. Regarding dispersive solid-based microextraction approaches, dispersive solid phase extraction (DSPE) [8] has been widely used in several samples employing different sorbent materials [9–11]. In this methodology, the sorbent is usually dispersed into the sample by vortex stirring or ultrasounds [10–12].

A hybrid technique combining both DLLME and DSPE was first proposed by Jamali et al. [13], who called it solvent-assisted dispersive solid-phase extraction (SA-DSPE). In this approach, an organic

* Corresponding author.
E-mail address: alberto.chisvert@uv.es (A. Chisvert).

https://doi.org/10.1016/j.chroma.2021.462361

solid like benzophenone is used as sorbent by solving it in a water-miscible organic solvent like methanol, and then it is dispersed into the aqueous matrix thereby precipitating in-situ, by forming a cloudy-solution. Finally, the solidified sorbent containing the analytes is retrieved by means of centrifugation. However, the need of centrifuge to recover the sorbent makes this process tedious and increases the analysis time. To this regard, it should be said that magnetic DSPE (M-DSPE), which makes use of sorbents with magnetic properties, presents notable advantages since it allow an easy manipulation of the magnetic sorbents by using external magnets [14–17].

Different works have been previously reported about the use of magnetic materials in SA-DSPE. In this sense, Abbasghorbani et al [18] used hexyl acetate in order to improve the extraction efficiency of parabens in aqueous matrices employing vortex. Later, Jullakan et al. [19] performed a previous step where their polypyrrole magnetic composite was mixed with dichloromethane to increase its affinity with the organophosphorus pesticides. Finally, Mohammadi et al. [20] performed a previous dispersion of their silica magnetic sorbent in methanol and then the mix was dispersed it in the sample employing ultrasounds.

In this work, a modification of these magnetic-based SA-DSPE (M-SA-DSPE) approaches is presented. This new modification imitates the conventional DLLME performance but using a magnetic solid as extractant sorbent and thus avoiding the use of halogenated solvents. The dispersion is produced by the quick injection of a mixture of the sorbent material and the disperser solvent with a syringe. This modification allows obtaining low extraction times and avoids the use of external sources (i.e., vortex, ultrasounds etc.). Once the extraction is accomplished, the magnetic sorbent containing the analytes is easily retrieved by means of an external magnet. Finally, analytes are desorbed into a small volume of organic solvent for liquid desorption. The main advantages of this new approach compared with the original SA-DSPE are the use of magnetic (nano)materials that allow an easier handling. Compared to M-DSPE, the sorbent is more efficiently dispersed by using the disperser solvent.

This methodology has been applied to the determination of cortisol and cortisone in human saliva. Abnormal levels of cortisol provide information about the malfunction of the adrenal gland, the pituitary and the hypothalamus, and also can be an indicator of Cushing disease [21], stress [22]. Study of serum cortisol has been traditionally employed for years in clinical analysis. However, nowadays, the measurement of salivary cortisol is preferred because it is a relatively non-invasive method, and it shows a good correlation with serum cortisol [23] and some studies demonstrate that salivary cortisol can be employed instead of serum cortisol as a sepsis biomarker [24]. Moreover, the action of enzyme 11-β hydroxysteroid-2 dehydrogenase (11-β HSD2) present in the parotid gland turns part of free cortisol into cortisone [25], and thus, the concentration of salivary cortisone is usually higher than salivary cortisol. For this reason, measurement of salivary cortisone has gained interest in recent years as a marker of the amount of free cortisol in serum [26]. Simultaneous determination of salivary cortisol and cortisone can be used as a part of the diagnosis of Cushing's syndrome [27] or to determine the activity of 11-β HSD2 [25].

Different methods for the determination of cortisol and/or cortisone in saliva have been published in the literature. In this context, electrochemical methods employing a graphene oxide biosensor [28,29], and enzyme-linked immunosorbent assay [30] have been performed for the determination of cortisol. Methods for simultaneous determination of both analytes can also be found, such as liquid-liquid extraction (LLE) [21], or on-line solid-phase extraction (SPE) [31-34] followed by liquid chromatography-tandem mass spectrometry (LC-MS/MS), or ionic liquid-based DLLME followed by LC with ultraviolet (UV) detection [35].

The aim of this work was to present a modification of the M-SA-DSPE approach for the determination of cortisol and cortisone in saliva using acetonitrile as disperser solvent to efficiently disperse a magnetic sorbent formed by cobalt ferrite ($CoFe_2O_4$) magnetic nanoparticles (MNPs) embedded into a commercial pyrrolidone-modified styrene-divinylbenzene copolymer (i.e., Strata-X^{TM}-RP) employing LC-MS/MS as measurement technique. To our knowledge, this is the first time that M-SA-DSPE has been employed for the determination of cortisol and/or cortisone. Moreover, this modification of the M-SA-DSPE approach, unlike the previous of M-SA-DSPE, avoid the use of external agitators, such as ultrasounds, vortex, etc.

2. Experimental

2.1. Reagents

All reagents and solvents were obtained from major suppliers. Cortisol (1 mg mL^{-1} in methanol) and cortisone (99 %) as analytes, and prednisolone ($\geq$ 99 %) as surrogate, were provided by Sigma-Aldrich (Steinheim, Germany).

For the synthesis of $CoFe_2O_4$ MNPs, cobalt (II) chloride hexahydrate ($CoCl_2{\cdot}6H_2O$) and iron (III) chloride hexahydrate ($FeCl_3{\cdot}6H_2O$) were purchased from Acros Organics (New Jersey, USA), and sodium hydroxide (reagent grade) was purchased from Scharlau (Barcelona Spain). A commercial pyrrolidone-modified styrene-divinylbenzene copolymer (Strata-X^{TM}-RP) from Phenomenex (Torrance, USA) was used as the polymeric network for the synthesis of the composite.

Gradient-grade acetonitrile was acquired from VWR Chemicals (Fontenay-sous-Bois, France). Deionized water was obtained from a Connect water purification system provided by Adrona (Riga, Latvia). Sodium chloride (NaCl) (99.5%, analytical grade) used as ionic strength regulator was purchased from Scharlau (Barcelona, Spain).

LC-MS grade methanol and LC-MS grade water from VWR Chemicals (Fontenay-sous-Bois, France) and formic acid 98% (for mass spectrometry) from Fluka (Steinheim, Germany) were used to prepare the mobile phase.

Nitrogen used as nebulizer and curtain gas in the MS/MS ion source was obtained by a NiGen LCMS nitrogen generator from Claind S.r.l. (Lenno, Italy). Extra pure nitrogen (>99.999 %), used as collision gas in the MS/MS collision cell, was provided by Praxair (Madrid, Spain).

For the preparation of synthetic saliva, sodium chloride (NaCl), potassium chloride (KCl), calcium chloride ($CaCl_2{\cdot}H_2O$), potassium thiocyanate (KSCN) and di-sodium hydrogen phosphate ($Na_2HPO_4{\cdot}H_2O$) from Panreac (Barcelona, Spain), sodium sulfide (Na_2S) from Scharlau (Barcelona, Spain) and urea from VWR Chemicals (Fontenay-sous-Bois, France) were used.

2.2. Sample collection

To obtain saliva samples from the different volunteers, Salivette® tubes from Sarstedt (Nümbrecht, Germany) were employed. Seven samples (four male and three female) were collected at different moments of the day.

Each volunteer gave written informed consent to participate in this study, which was conformed to the ethical guidelines of the Declaration of Helsinki.

2.3. Apparatus and materials

An Agilent 1100 Series chromatography system comprised of a degasser, a programmable pump, an autosampler and a thermostatic column oven, coupled to an Agilent 6410B Triple Quad

MS/MS was employed throughout the study. Separations were carried out in a Zorbax SB-C18 (50 mm length, 2.1 mm I.D., 1.8 µm) column.

A Basic 30 conductimeter from Crison (Barcelona, Spain) was employed for the study of salt content in saliva.

A ZX3 vortex mixer from VELP Scientifica (Usmate Velate, Italy), a Hettich® (Tuttlingem, Germany) EBA 21 centrifuge (provided with a rotor of 9.7 cm radius), and an Ultrasons-HD ultrasonic bath from J.P. Selecta (Barcelona, Spain) were also employed for the comparison of the proposed method with other approaches.

All those instruments used for characterization of sorbent material are listed in Supplementary Material.

2.4. Preparation of synthetic saliva

Synthetic saliva employed in the study of accuracy was prepared according to an adapted protocol [36]. For that aim, 250 mL of an aqueous solution containing NaCl (400 mg L^{-1}), KCl (400 mg L^{1}), $CaCl_2{\cdot}H_2O$ (795 mg L^{-1}), $Na_2HPO_4{\cdot}H_2O$ (690 mg L^{-1}), KSCN (300 mg L^{-1}), Na_2S (5 mg L^{-1}), and urea (1000 mg L^{-1}) in ultrapure water was prepared.

2.5. Synthesis of $CoFe_2O_4$-Strata-X^{TM}-RP magnetic composite

The synthesis of the $CoFe_2O_4$-Strata-X^{TM}-RP composite consisted of two steps: the synthesis of the magnetic nanoparticles by wet chemical co-precipitation according to an adapted protocol [37], and subsequent incrustation of the $CoFe_2O_4$ MNPs on the polymeric surface.

First, 100 mL of a 0.4 M $FeCl_3$ aqueous solution and 100 mL of a 0.2 M $CoCl_2$ aqueous solution were mixed, and then 100 mL of a 3 M sodium hydroxide aqueous solution were added dropwise under continuous stirring for one hour at 80 °C.

Afterwards, a magnetic decantation was performed. In this sense, MNPs were deposited on the bottom with the help of an external magnet, and the supernatant was then discarded. Next, the MNPs were suspended in 100 mL of 1 M HCl and kept in the refrigerator (4 °C) for 2 hours. After that, the mixture was decanted again with the aid of the external magnet, and the solid was suspended in water for 3 days. Finally, the suspension was filtered with a 0.45 µm pore size nylon filter. From the resulting suspension, a 1 mL-aliquot was separated and dried overnight at 100 °C to gravimetrically determine the concentration of MNPs in the final suspension, which was 0.016 g mL^{-1}.

For the preparation of the composite in which MNPs are embedded into the polymeric network, 0.15 g of Strata-X^{TM}-RP were weighed and 9.4 mL of the MNPs suspension were added so that the polymer and MNPs ratio was 1:1 (w/w). Then, 50 mL of ethanol were added and the mixture was stirred for 3 days to ensure that nanoparticles were embedded in the pores of the polymer.

Finally, the precipitate was filtered under vacuum through a Whatman filter paper with a pore size of 11 µm to discard the free MNPs, dried overnight at 80 °C and pulverized into a fine powder with a mortar.

2.6. Preparation of standard and sample solutions

A stock solution containing 100 µg mL^{-1} of cortisol and another one containing 500 µg mL^{-1} of cortisone, both in methanol, were prepared. After that, an aliquot of each solution was diluted in water to obtain a multicomponent solution containing 1 µg mL^{-1} of each compound. Moreover, a stock solution containing 200 µg mL^{-1} of prednisolone (used as surrogate) was prepared in methanol and diluted to 1 µg mL^{-1} with water. Six working standard solutions (0.5 – 20 ng mL^{-1}) were prepared by adding directly to an Eppendorf® tube the corresponding volume of the multicomponent solution and 1 mL of a NaCl solution (1.5 mg mL^{-1}).

Each saliva sample was obtained by means of the Salivette® tubes. After centrifugation, saliva was kept at 4 °C until the analysis. Saliva can be storage up to 3 months at 5 °C [38]. An aliquot of 1 mL, by triplicate, was transferred to three Eppendorf® tubes, respectively.

To all above solutions, 50 μL of prednisolone aqueous solution (1 μg mL^{-1}) and 450 μL of deionized water were added prior to the M-SA-DSPE procedure.

2.7. M-SA-DSPE procedure

For the extraction procedure, 1 mg of $CoFe_2O_4$-Strata-X^{TM}-RP was weighted and suspended into 50 µL of acetonitrile. The resultant suspension was injected into the standard or saliva solution described previously. After 1 min, the supernatant was removed from the vial by placing an external magnet at the bottom in order to prevent any loss of the magnetic composite containing the target compounds. Then, 50 μL of water (containing 0.5 % of NaCl) were added for clean-up purposes. Then, water was discarded employing an external magnet, and 60 µL of methanol were added subsequently 5 pull push cycles were used for the liquid desorption of the target compounds employing a 1 mL plastic syringe provided with a needle. Finally, the magnetic composite was separated by means of a magnet, and the whole supernatant was taken using a syringe and transferred to an injection vial, where 40 µL of water were added before being injected into the LC-MS/MS to ensure a correct chromatographic performance reducing the eluotropic strength. Fig. 1 shows a schematic diagram of the proposed method.

2.8. LC-MS/MS analysis

Ten microliters of each solution were injected into the chromatographic system. Mobile phase consisted of solvent A (H_2O, 0.1% formic acid) and solvent B (MeOH, 0.1% formic acid), by isocratic elution at a mixing ratio of 40(A):60(B) % (v/v). The flow rate was 0.15 mL min^{-1} and the column temperature was kept constant at 25 °C. Calibration curves were constructed by plotting A_i/A_{sur} (where A_i is the peak area of the target analyte and A_{sur} is the peak area of the surrogate (i.e., prednisolone)) versus target analyte concentration.

The triple quadrupole MS detector operated in positive electrospray ionization mode (ESI^+), by multiple reaction monitoring (MRM). Specifically, positive polarity (ESI^+, capillary voltage at 5 kV) was used to measure cortisol, cortisone and prednisolone. The other conditions were gas temperature at 350°C, nebulizer gas flow rate at 11 L min^{-1}, nebulizer gas pressure at 50 psi, collision energies at 21, 26 and 20 V and fragmentor at 155, 140, 135 V for cortisol, cortisone and prednisolone, respectively, and dwell time at 400 s for cortisol and cortisone and 200 s for prednisolone. The m/z precursor → product ion transitions for quantification and for identification were, respectively, 363 → 121 and 363 → 105 for cortisol, 361 → 163 and 361 → 105 for cortisone, and 343 → 325 and 361→ 163 for prednisolone. Fig. 2 shows a chromatogram for a standard and for a saliva sample obtained after applying the M-SA-DSPE. The run time was 6 min.

3. Results and discussion

3.1. Selection of the composite and characterization

Both cortisol and cortisone present a hydrophobic steroid skeleton and hydroxyl and carbonyl moieties. In this sense, the selection

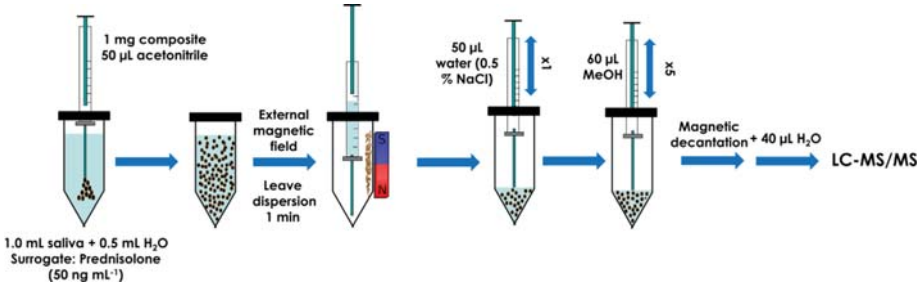

Fig. 1. Schematic diagram of proposed M-SA-DSPE-LC-MS/MS method.

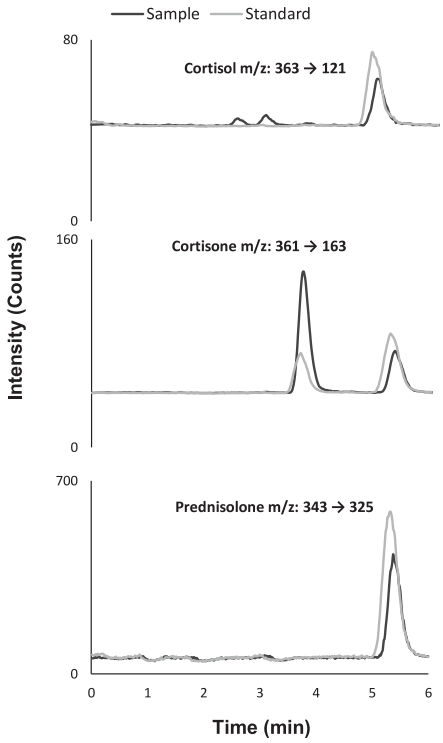

Fig. 2. Chromatogram of a standard (1 ng mL^{-1}) and a human saliva sample (volunteer 3) after application of M-SA-DSPE-LC-MS/MS. Surrogate concentration 30 ng mL^{-1}

of $CoFe_2O_4$-Strata-X^{TM}-RP as sorbent material was based on the ability of the pyrrolidone-modified styrene-divinylbenzene copolymer (Strata-X^{TM}-RP) to interact with the analytes by hydrophobic interactions and hydrogen bonding, which fits with hydrophobic molecules with hydroxyl and carbonyl groups as cortisol and cortisone. The $CoFe_2O_4$ MNPs confer to this sorbent the magnetism needed for an easy retrieval by means of a magnet. $CoFe_2O_4$ MNPs were preferred rather than to usually-employed Fe_3O_4 MNPs due to its higher chemical stability [39].

Experimental details from characterization are shown in Supplementary Material. Magnetization, particle size distribution, morphology, specific surface area and pore size were established. In addition, energy dispersive X-ray spectroscopy (EDS) was performed for elemental analysis.

3.2. Optimization of the M-SA-DSPE variables

Different parameters may affect the overall extraction process. In this sense, the amount of composite, the extraction time, the pull-push cycles used for desorption process and the ionic strength of the donor phase were carefully studied and evaluated.

In addition to these variables, other parameters were set for the analysis based on practical considerations or preliminary experiments. Thus, the donor phase was set at 1 mL taking into consideration that it is an easy and accessible volume for saliva samples. Previous experiments showed that acetonitrile dispersed the sorbent more effectively than methanol and therefore it was selected as disperser solvent. The volume of acetonitrile was set at 50 µL since it was the minimum volume that provided a suitable dispersion of the magnetic composite. On the other hand, both methanol and acetonitrile provided good results as desorption solvents, but methanol was selected because the mobile phase contained this same solvent. Its volume was set at 60 µL, since lower volumes were difficult to handle during the desorption process.

Taking into account that saliva is mainly water (ca. 99%) [40], all the experiments were performed by extracting aqueous standard solutions, by triplicate, containing the target analytes at 20 ng mL^{-1}, and the results were considered in terms of the peak area of each analyte (A_i).

3.2.1. Amount of composite

Different amounts of $CoFe_2O_4$-Strata-X^{TM}-RP were tested to obtain maximum sensitivity. As can be seen in Fig. 3a, small amounts of composite (1-2 mg) achieved maximum signals. Higher amounts may affect the correct dispersion of composite during the desorption process due to the small volume of methanol (60 µL) used as desorption volume. In order to check this hypothesis, an additional experiment was carried out with 5 mg of composite and 120 µL of methanol, which was enough to achieve a correct dispersion, in order to see if the results improved when compared with 5 mg of composite and 60 µL of desorption volume. A similar signal was obtained, thus suggesting that the concentration in the extract was similar. In other words, higher amounts of the analytes are extracted with 5 mg when compared to 1-2 mg, but the desorption volume needed to effectively disperse such amount (i.e., 120 µL) did not offset the dilution effect. With all these results, the minimum quantity of sorbent (1 mg) and the minimum amount of desorption solvent (60 µL) were selected for further experiments.

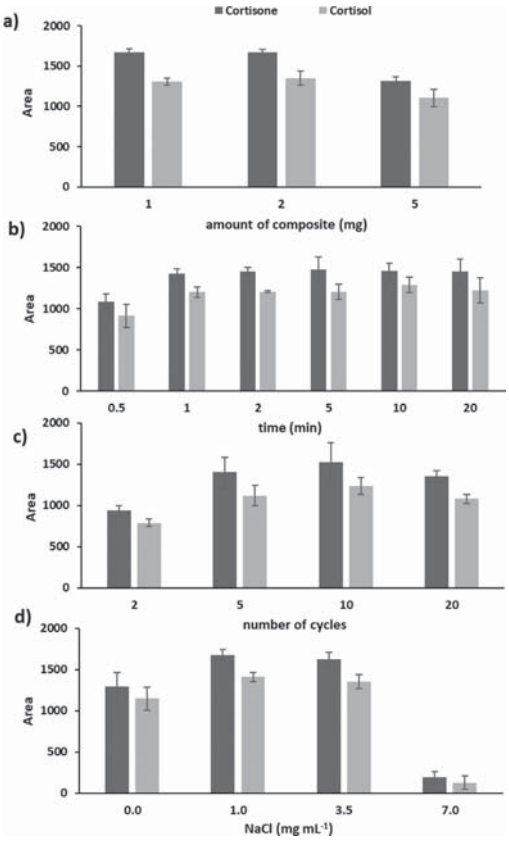

Fig. 3. Study of the experimental variables for M-SA-DSPE: a) Effect of the amount of composite. Extraction conditions: 1 mg mL^{-1} of NaCl, 5 minutes of extraction time, 10 pull-push cycles; b) Effect of the extraction time. Extraction conditions: 1 mg of composite, 1 mg mL^{-1} of NaCl, 10 pull-push cycles; c) Effect of the number of pull-push cycles in the desorption process. Extraction conditions: 1 mg of composite, 1 mg mL^{-1} of NaCl, 1 min of extraction time; d) Effect of the amount of salt in the donor solution. Extraction conditions: 1 mg of composite, 1 min of extraction time, 5 pull-push cycles. Error bars show the standard deviation of the results (N=3).

3.2.2. Extraction time

After injection of the composite, the obtained dispersion was left unaltered during different times. The obtained results (Fig. 3b) showed that maximum signal was obtained after 1 min. After this time, differences were not significant (one-way ANOVA p-values > 0.05 for both cortisol and cortisone). It should be noted that dispersion was no longer stable after ca. two minutes so higher times did not improve the extraction efficiency. In this sense, 1 min was selected in order to reduce the extraction time.

3.2.3. Number of pull-push cycles

For the desorption process, the dispersion of the composite into methanol was conducted by applying different number of pull-push cycles (i.e., consecutive aspiration-injection of the composite into the desorption solvent). As can be seen in Fig. 3c, more than 5 cycles did not provide any benefit, and the areas were statistically comparable (one-way ANOVA p-values > 0.05 for both cortisol and cortisone). Thus, 5 cycles were selected in order to minimize the total analysis time.

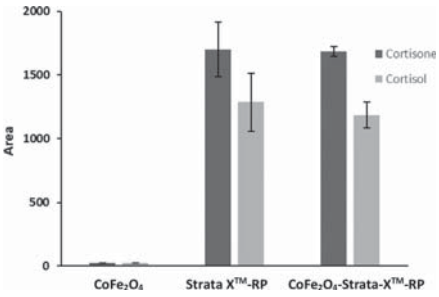

Fig. 4. Comparison of the extraction performance of $CoFe_2O_4$ MNPs, Strata-X^{TM}-RP and $CoFe_2O_4$-Strata-X^{TM}-RP. Error bars show the standard deviation of the results (N=3).

3.2.4. Ionic strength

The extraction of organic compounds from aqueous samples may be improved by the well-known salting-out effect. Then, in order to check if the extraction process was affected by the ionic strength of the donor phase, different aqueous standard solutions of the target analytes containing different amounts of sodium chloride were extracted. As it can be seen in Fig. 3d, the signal increased at low-medium amounts, whereas it decreased sharply at high amounts since the dispersion of the composite was not achieved satisfactorily. Thus, ionic strength of standard and sample solutions should be adjusted by adding sodium chloride up to 1 – 3 mg mL^{-1}.

However, human saliva may contain different amounts of salts [35] that need to be established in order to adjust the ionic strength conveniently. In this sense, the salinity of human saliva was established by measuring ten saliva samples from different volunteers by direct conductometry using standard solutions of sodium chloride (1 – 10 mg mL^{-1}). Results were between 1.20 and 3.15 mg mL^{-1}, which suggest that normal levels of salt in saliva are in the optimum interval, and none additional amount of salt is needed to perform the extraction.

3.3. Extraction performance of *$CoFe_2O_4$ MNPs, Strata-X^{TM}-RP and $CoFe_2O_4$-Strata-X^{TM}-RP*

In order to study the extraction performance of $CoFe_2O_4$-Strata-X^{TM}-RP, different experiments were carried out employing bare $CoFe_2O_4$ MNPs, Strata-X^{TM}-RP copolymer and $CoFe_2O_4$-Strata-X^{TM}-RP composite. For Strata-X^{TM}-RP, as is not magnetic, the retrieval of the material was performed by centrifugation for 5 min. Fig. 4 shows that the extraction performance of $CoFe_2O_4$ MNPs was negligible, whereas both Strata-X^{TM}-RP and $CoFe_2O_4$-Strata-X^{TM}-RP provided comparable results (one-way ANOVA p-values > 0.05 for both cortisol and cortisone). Therefore, it can be concluded that the responsible for the extraction of the analytes is the polymeric material. The presence of $CoFe_2O_4$ MNPs is to confer the magnetism needed to efficiently handle it.

3.4. Analytical performance of the proposed method

Method validation was performed studying different parameters, such as linear and working ranges, limits of detection (LOD)

Table 1
Main quality parameters of the proposed M-SA-DSPE-LC-MS/MS method.

Compound	Calibration curves[a]	R^2	MLOD[b] (ng mL^{-1})	MLOQ[b] (ng mL^{-1})	EF[c]	Repeatability (% RSD)			
						Intra-day		Inter-day	
						1 ng mL^{-1}	10 ng mL^{-1}	1 ng mL^{-1}	10 ng mL^{-1}
Cortisol	A_i/A_{sur} = 0.184 (± 0.004)C + 0.13 (± 0.02)	0.9990	0.029	0.097	5.2 ± 0.2	4.2	6.1	10.0	6.3
Cortisone	A_i/A_{sur} = 0.240 (± 0.003)C + 0.08 (± 0.02)	0.9995	0.018	0.060	5.6 ± 0.3	5.0	1.8	9.6	8.7

[a] A_i: peak area of the target analyte; A_{sur}: peak area of the surrogate; number of calibration points: 7; working range: 0.3-20 ng mL^{-1}
[b] MLOD: Method limit of detection; MLOQ: Method limit of quantification
[c] EF: Enrichment factor

Table 2
Relative recoveries obtained from spiked real samples.

Sample	Amount spiked (ng mL^{-1})	Amount found (ng mL^{-1})		Relative recovery (%)	
		Cortisol	Cortisone	Cortisol	Cortisone
1	0	2.0 ± 0.2	8.1 ± 0.7	-	-
	1	2.86 ± 0.03	9.04 ± 0.05	87 ± 3	94 ± 5
	5	6.41 ± 0.05	12.9 ± 0.6	88 ± 5	96 ± 12
	10	11.7 ± 0.3	17.6 ± 0.3	97 ± 3	95 ± 3
2	0	1.03 ± 0.01	6.6 ± 0.5	-	-
	1	1.88 ± 0.06	7.61 ± 0.09	86 ± 6	96 ± 9
	5	5.5 ± 0.2	12.0 ± 0.7	89 ± 5	108 ± 13
	10	10.7 ± 0.7	17.7 ± 0.5	97 ± 3	111 ± 5
3	0	1.55 ± 0.01	4.3 ± 0.3	-	-
	1	2.44 ± 0.07	5.32 ± 0.09	89 ± 7	99 ± 9
	5	6.0 ± 0.4	9.6 ± 0.5	89 ± 9	107 ± 11
	10	12.1 ± 0.7	14.9 ± 0.2	106 ± 7	106 ± 2

and limits of quantification (LOQ), enrichment factor (EF), repeatability (expressed as relative standard deviation (% RSD)) and accuracy.

High linearity range was observed, up to 20 ng mL^{-1}. Working range was set at 0.3-20 ng mL^{-1} as an approximated range taking into account the expected levels of cortisol and cortisone in saliva. Calibration curves for both analytes (see Table 1) exhibited good regression coefficients ($R^2 \geq 0.999$).

LODs and LOQs were calculated by measuring 3 and 10 times the signal-to-noise ratio criteria (S/N), respectively, from a solution containing 0.5 ng mL^{-1} of cortisol and cortisone. As it is shown in Table 1, LODs were found below ng mL^{-1} range.

The EF was estimated comparing the signal obtained of an unextracted standard and the signal obtained after performing the extraction process.

Repeatability of the method, which was established by the RSD values for five replicates analyzed in the same day (intra-day) and five replicates analyzed in different days (inter-day), was ≤ 10 % for both compounds.

For the study of the accuracy of the method, firstly, a synthetic saliva sample, containing the target analytes at two concentration levels (i.e., 1 and 10 ng mL^{-1}), was prepared according to section 2.4 and analysed. Results obtained were 0.98 ± 0.08 and 10.5 ± 0.05 ng mL^{-1} for cortisol and 0.97 ± 0.08 and 10.5 ± 0.7 ng mL^{-1} for cortisone, showing a good correlation between employing synthetic saliva and aqueous solutions with relative errors below 6 %. In a subsequent experiment, three different human saliva samples were spiked at three concentration levels (i.e., 1, 5 and 10 ng mL^{-1}) to evaluate the matrix effects by means of the relative recoveries (% RR) values. These results are presented in Table 2, where it can be seen that relative recovery values between 86 and 111 % were obtained, thus proving that matrix effects were negligible, and then external calibration is suitable for quantification.

A comparison between the proposed method and other previously published methods for the determination of cortisol and cortisone in saliva samples is shown in Table 3. As can be seen, results obtained using M-SA-DSPE provided good analytical features, with lower LODs than these other methods based on traditional extraction techniques (i.e., LLE o SPE), with an easy and rapid sample treatment and without the need of a derivatization step.

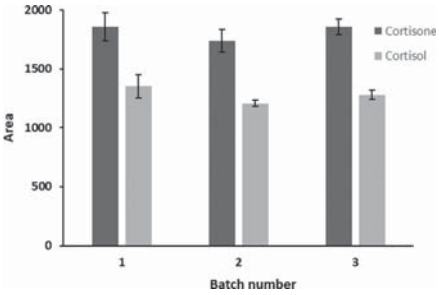

Fig. 5. Inter-batch repeatability of the synthesis process of $CoFe_2O_4$-Strata-X^{TM}-RP composite. Error bars show the standard deviation of the results (N=3).

3.5. Inter-batch repeatability of $CoFe_2O_4$-Strata X^{TM}-RP

The inter-batch repeatability of the synthetized $CoFe_2O_4$-Strata-X^{TM}-RP composite was evaluated by comparing the extracted amount (20 ng mL^{-1} of both compounds) by three different synthesis batches. Results in Fig. 5 show that there are not significantly differences between the three batches (one-way ANOVA p-values > 0.05 for both cortisol and cortisone), proving the good repeatability of the synthesis process.

3.6. Application to real saliva samples

Saliva samples obtained from four different volunteers were treated by the proposed M-SA-DSPE approach and the extracts were measured by LC-MS/MS. The obtained results are presented

Table 3
Comparison between M-SA-DSPE and other methods for the determination of cortisol and cortisone in saliva

Extraction technique	Instrumental technique	MLOD[b] (ng mL^{-1})		RSD (%)	Relative Recoveries (%)	EF [c]		Reference
		Cortisol	Cortisone			Cortisol	Cortisone	
LLE	LC-MS/MS	0.060	0.300	<8.6	68 - 98	n.r.[d]	n.r.[d]	[31]
SPE	LC-MS/MS	0.185	0.128	<10.0	90 - 115	n.r.[d]	n.r.[d]	[32]
SPE [a]	LC-MS/MS	0.002	0.005	<6.5	80 - 120	n.r.[d]	n.r.[d]	[33]
SPE	LC-MS/MS	0.043	0.085	<10.3	96 - 114	n.r.[d]	n.r.[d]	[34]
IL-DLLME	LC-UV	0.162	0.111	<7.8	83 - 116	5.0	6.3	[35]
M-SA-DSPE	LC-MS/MS	0.029	0.018	<10.0	86 – 111	5.2	5.6	This work

[a] Derivatization of the analytes was needed
[b] MLOD: Method limit of detection
[c] Enrichment factor
[d] Not reported

Table 4
Concentration obtained by applying the M-SA-DSPE-LC-MS/MS method to real saliva samples from different volunteers.

Compound	Concentration (ng mL^{-1})			
	Volunteer 1	Volunteer 2	Volunteer 3	Volunteer 4
Cortisol	0.54 ± 0.03	0.98 ± 0.09	1.81 ± 0.11	2.20 ± 0.07
Cortisone	3.8 ± 0.2	6.6 ± 0.5	7.5 ± 0.4	10.0 ± 0.2

in Table 4, showing the application of the method to obtain data about the salivary levels of cortisol and cortisone.

3.7. M-SA-DSPE dispersion efficiency

In order to study the dispersion efficiency of M-SA-DSPE approach, it was compared to other conventional dispersion modes like vortex-assisted (VA) and ultrasound-assisted (USA) by analysing the same human saliva sample. The extraction time for USA-DSPE (50 Hz frequency) and VA-DSPE (40 Hz agitation speed) was arbitrarily set to one minute to maintain the overall extraction time in the three approaches compared, while the rest of conditions were kept as in M-SA-DSPE. As can be seen in Fig. 6a, the analytical signal obtained employing M-SA-DSPE were 2 to 3 times higher than those obtained by VA-DSPE and USA-DSPE. This is attributed to the fact that the sorbent was less efficiently dispersed employing ultrasounds or vortex when compared by using a disperser solvent. In order to check this hypothesis and discard that it could be attributed to leaching of $CoFe_2O_4$ MNPs from the $CoFe_2O_4$-Strata X^{TM}-RP composite during the VA-DSPE and/or USA-DSPE procedures, which might cause that the active sorbent containing the target analytes (i.e., the Strata-X^{TM}-RP) was partially retrieved, a comparison between the three procedures was made again, but the sorbent was retrieved by centrifugation. In this way all the sorbent material is retrieved, and not just that maintaining the magnetism. Fig. 6b shows how signals are enhanced for VA-DSPE and USA-DSPE, but they are still lower than M-SA-DSPE.

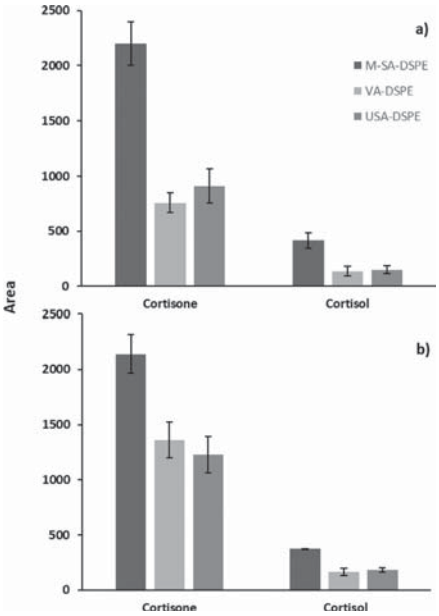

Fig. 6. a) Comparison between the signals obtained by M-SA-DSPE, VA-DSPE and USA-DSPE; b) Comparison between the signals obtained by M-SA-DSPE, VA-DSPE and USA-DSPE using centrifugation instead of magnetic retrieval. Error bars show the standard deviation of the results (N=3).

4. Conclusions

In this work, a modification of M-SA-DSPE has been employed for the determination of cortisol and cortisone in human saliva. This methodology, termed magnetic-based solvent-assisted dispersive solid-phase extraction (M-SA-DSPE), allows a rapid determination of target analytes employing small amounts of sample, organic solvents and sorbent without any supporting equipment (vortex, centrifuge, ultrasounds, etc.).

This approach has been successfully applied to the determination of both biomarkers employing LC-MS/MS as measurement technique. Good analytical features were obtained for both analytes. This method was applied to monitor the cortisol and cortisone levels in saliva samples from different volunteers, proving its potential as new sample preparation technique for the analysis of these biomarkers in saliva.

Declaration of Competing Interest

The authors declare that they have no known competing financial interests or personal relationships that could have appeared to influence the work reported in this paper.

CRediT authorship contribution statement

José Grau: Data curation, Formal analysis, Investigation, Methodology, Validation, Writing – original draft. **Juan L. Benedé:** Methodology, Supervision, Writing – original draft. **Alberto Chisvert:** Conceptualization, Funding acquisition, Supervision, Writing – review & editing. **Amparo Salvador:** Funding acquisition, Supervision, Writing – review & editing.

Acknowledgements

J.G. and J.L.B. thank the Generalitat Valenciana and the European Social Fund for their predoctoral and postdoctoral grant, respectively. This article is based upon work from the National Thematic Network on Sample Treatment (RED-2018-102522-T) of the Spanish Ministry of Science, Innovation and Universities, and the Sample Preparation Study Group and Network supported by the Division of Analytical Chemistry of the European Chemical Society.

Supplementary materials

Supplementary material associated with this article can be found, in the online version, at doi:10.1016/j.chroma.2021.462361.

References

[1] V. Jalili, A. Barkhordari, A. Ghiasvand, New extraction media in microextraction techniques. A review of reviews, Microchem. J. 153 (2020) 104386.
[2] M. Cruz-Vera, R. Lucena, S. Cárdenas, M. Valcárcel, Sample treatments based on dispersive (micro)extraction, Anal. Methods 3 (2011) 1719–1728.
[3] M. Reazee, Y. Assadi, M.M. Hosseini, E. Aghaee, F. Ahmadi, S. Berijani, Determination of organic compounds in water using dispersive liquid-liquid microextraction, J. Chromatogr. A 1116 (2006) 1–9.
[4] M.I Leong, M.R Fuh, S.D. Hang, Beyond liquid-liquid microextraction, J. Chromatogr. A 1335 (2014) 2–14.
[5] F.R Mansour, M.A. Khairy, Pharmaceutical and biomedical application of dispersive liquid-liquid microextraction, J. Chromatogr. B 1061-1062 (2017) 382–391.
[6] E.G. Primel, S.S. Caldas, L.C. Marube, A.L.V. Escarrone, An overview of advances in dispersive liquid-liquid microextraction for the extraction of pesticides and emerging contaminants from environmental samples, Trends. Environ. 14 (2017) 1–18.
[7] P. Viñas, N. Campillo, I. López-García, M. Hernández-Córdoba, Dispersive liquid-liquid microextraction in food analysis. A critical review, Anal. Bioanal. Chem. 406 (2014) 2067–2099.
[8] M. Anastassiades, S.J. Lehotay, D. Stajnbaher, F.J. Schenk, Fast and easy multiresidue method employing acetonitrile extraction/partitioning and "dispersive solid-phase extraction" for determination of pesticide residues in produce, J. AOAC Int. 86 (2003) 412–431.
[9] A. Chisvert, J.L. Benedé, A. Salvador, Current trends on the determination of organic UV filters in environmental water samples based on microextraction techniques-A review, Anal. Chim. Acta 1034 (2018) 22–38.
[10] A. Chisvert, S. Cárdenas, R. Lucena, Dispersive micro-solid phase extraction, Trends Anal. Chem. 112 (2019) 226–233.
[11] M. Ghorbani, M. Aghamohammadhassan, M. Chamsaz, H. Akhlaghi, T. Pedramrad, Dispersive solid phase microextraction, Trends Anal. Chem. 118 (2019) 793–809.
[12] T. Khezeli, A. Daneshfar, Development of dispersive micro-solid phase extraction based on micro and nano sorbents, Trends Anal. Chem. 89 (2017) 99–118.
[13] M.R. Jamali, A. Firouzjah, R. Rahnama, Solvent-assisted dispersive solid phase extraction, Talanta 116 (2013) 454–459.
[14] A.L. Capriotti, C. Cavaliere, G. La Barbera, A. Laganà, Recent applications of magnetic solid-phase extraction for sample preparation, Chromatographia. 82 (2019) 1251–1274.
[15] K. Aguilar-Arteaga, J.A. Rodriguez, E. Barrado, Magnetic solids in analytical chemistry: A review, Anal. Chim. Acta 674 (2010) 157–165.
[16] M. Yu, L. Wang, L. Hu, Y. Li, D. Luo, S. Mei, Recent applications of magnetic composites as extraction adsorbents for determination of environmental pollutants, Trends Anal. Chem. 119 (2019) 115611.
[17] S. Di, T. Ning, J. Yu, P. Chen, H. Yu, J. Wang, H. Yang, S. Zhu, Recent advances and applications of magnetic nanomaterials in environmental sample analysis, Trends Anal. Chem. 126 (2020) 115864.
[18] M. Abbasghorbani, A. Attaran, M. Payehghadr, Solvent-assisted dispersive micro-SPE by using aminopropyl-functionalized magnetite nanoparticle followed by GC-PID for quantification of parabens in aqueous matrices, J. Sep. Sci. 36 (2013) 311–319.
[19] S. Jullakan, O. Bunkoed, S. Pinsrithong, Solvent-assisted dispersive liquid-solid phase extraction of organophosphorus pesticides using a polypirrole thin film–coated porous composite magnetic sorbent prior to their determination with GC-MS/MS, Microchim. Acta 187 (2020) 677.
[20] P. Mohammadi, M. Masrournia, Z. Es'haghi, M. Pordel, Determination of four antiepileptic drugs with solvent assisted dispersive solid phase microextraction-gas chromatography-mass spectrometry in human urine samples, Microchem. J. 159 (2020) 105542.
[21] M.S. Starkman, S.S. Gebarski, S. Berent, D.E. Schteingart, Hippocampal formation volume, memory dysfunction, and cortisol levels in patients with Cushing's syndrome, Biol. Psychiatry 32 (1992) 756–765.
[22] M.J. Aguilar-Cordero, A.M. Sánchez-López, N. Mur-Villar, I. García-García, M.A. Roodríguez-López, A. Ortegón-Piñero, E- Cortés-Castell, Salivary cortisol as an indicator of phycological stress in children and adults; a systematic review, Nutr. Hosp. 29 (2014) 960–968.
[23] R.F Vining, R.A. McGinley, J.J. Maksvytis K. Y Ho, Salivary cortisol: a better measure of adrenal cortical function than serum cortisol, Ann. Clin. Biochem. 20 (1983) 329–335.
[24] R.M Estrada-Y-Martin, P.R. Orlander, Salivary cortisol can replace free serum cortisol measurements in patients with septic shock, Chest. 140 (2011) 1216–1222.
[25] M. Quinkler, P.M. Stewart, Hypertension and the Cortisol-Cortisone Shuttle, J. Clin. Endocrinol. Metab. 88 (2003) 2384–2392.
[26] I. Perogamvros, B.G. Keevil, D.W. Ray, P.J. Trainer, Salivary cortisone is a potential biomarker for serum free cortisol, J. Clin. Endocrinol. Metab. 95 (2010) 4951–4958.
[27] A. Garrahy, H. Forde, P. O'Kelly, K. McGurren, H.M. Zia-ul-Hussnain, E. Noctor, W.P. Tormey, D. Smith, M.C. Dennedy, M. Bell, M. Javadpour, A. Agha, The diagnostic utility of late night salivary cortisol (LNSF) and cortisone (LNSE) in Chusing's syndrome, Ir. J. Med. Sci. (2020) 1971–1979.
[28] Y.H. Kim, K. Lee, H. Jung, H.K. Kang, J. Jo, I.K. Park, H.H. Lee, Direct immune-detection of cortisol by chemiresitor graphene oxide sensor, Biosens. Bioelectron. 98 (2017) 473–477.
[29] N. Dhull, G. Kaur, V. Gupta, M. Tomar, Highly sensitive and non-invasive electrochemical immunosensor for salivary cortisol detection, Sens. Actuators B 293 (2019) 281–288.
[30] G. Spano, S. Cavalera, F. Di Nardo, C. Giovannoli, Development of a biomimetic enzyme-linked immunosorbent assay on a molecularly imprinted polymer for the detection of cortisol in human saliva, Anal. Methods 11 (2019) 2320–2326.
[31] M. Mezzullo, F. Fanelli, A. Fazzini, A. Gambineri, V. Vicennati, G. Di Dalmazi, C. Pelusi, R. Mazza, U. Pagotto, R. Pasquali, Validation of an LC-MS/MS salivary assay for glucocorticoid status assessment: Evaluation of the diurnal fluctuation of cortisol and cortisone and of their association within and between serum and saliva, J. Steroid Biochem. Mol. Biol. 163 (2016) 103–112.
[32] G. Antonelli, F. Ceccato, C. Artusi, M. Marinova, M- Plebani, Salivary cortisol and cortisone by LC-MS/MS: validation, reference intervals and diagnotisc accuracy in Cushing's syndrome, Clin. Chim. Acta 451 (2015) 247–251.
[33] B. Magda, Z. Dobi, K. Meszaros, E. Szabo, Z. Marta, T. Imre, P.T. Szabo, Charged derivatization and on-line solid phase extraction to measure extremely low cortisol and cortisone levels in human saliva with liquid chromatography-tandem mass spectrometry, J. Pharm. Biomed. Anal. 140 (2017) 223–231.
[34] I. Perogamvros, L.J. Owen, J. Newell-Price, D.W. Ray, P.J. Trainer, B.G. Keevil, Simultaneous measurement of cortisol and cortisone in human saliva using liquid chromatography–tandem mass spectrometry: Application in basal and stimulated conditions, J. Chromatogr. B 877 (2009) 3771–3775.
[35] F. Abujaber, A.I. Corps-Ricardo, A. Ríos, F.J. Guzmán Bernardo, R.C. Rodríguez, Ionic liquid dispersive liquid-liquid microextraction combined with LC-UV-Vis for the fast simultaneous determination of cortisone and cortisol in human saliva samples, J. Pharm. Biomed. Anal. 165 (2019) 141–146.
[36] T. Fusayama, T. Katayori, S. Nomoto, Corrosion of gold and amalgam placed with each other, J. Dent. Res. 42 (1963) 1183–1197.
[37] K. Maaz, A. Mumtaz, S.K. Hasanain, A. Ceylan, Synthesis and magnetic properties of cobalt ferrite (CoFe2O4) nanoparticles prepared by wet chemical route, J. Magn. Magn. Mater. 308 (2007) 289–295.
[38] A.H. Garde, Å.M. Hansen, Long-term stability of salivary cortisol, Scand. J. Clin. Lab. Invest. 65 (2005) 433–436.
[39] I.P. Román, A. Chisvert, A. Canals, Dispersive solid-phase extraction based on oleic acid-coated magnetic nanoparticles followed by gas chromatography-mass spectrometry for UV-filter determination in water samples, J. Chromatogr. A. 1218 (2011) 2467–2475.
[40] S.P. Humphrey, R.T. Williamson, A review of saliva: Normal composition, flow and function, J. Prosthet. Dent. 85 (2001) 162.

Modified magnetic-based solvent-assisted dispersive solid-phase extraction: application to the determination of cortisol and cortisone in human saliva

José Grau, Juan L. Benedé, Alberto Chisvert*, Amparo Salvador

Department of Analytical Chemistry, University of Valencia, 46100 Burjassot, Valencia, Spain

* Corresponding author:

e-mail address: alberto.chisvert@uv.es

TABLE OF CONTENTS

Instruments for composite characterization

Different techniques were applied to characterize the $CoFe_2O_4$-Strata-X^{TM}-RP composite. A Quantum Design (CA, USA) MPMS-XL-5 superconducting quantum interference device (SQUID) magnetometer was used to measure the magnetic properties of the composite material.

Particle size distribution curve of the $CoFe_2O_4$-Strata-X^{TM}-RP composite was performed using a Malvern Mastersizer 2000 particle size analyser.

A HITACHI S-4800 scanning electron microscopy (SEM) operating at 10 kV equipped with an RX Bruker backscattered electron detector, was used to observe the morphology and to perform energy-dispersive X-ray spectroscopy (EDS) of the composite.

Nitrogen adsorption-desorption isotherms were measured on a ASAP 2010 analyser from Micromeritics (GA, USA), in order to determine the surface area and pore size.

Magnetization curves

Fig. S1 shows magnetization curve for (a) $CoFe_2O_4$ MNPs and (b) $CoFe_2O_4$-Strata-X^{TM}-RP composite. The saturation magnetization (M_s) value for the MNPs was 65.0 emu g^{-1}, the residual magnetism (B_r) was 28.5 emu g^{-1} and the coercivity (H_c) was 0.99 kOe. Regarding the composite, M_s value was 36.7 emu g^{-1}, B_r value was 20.72 emu g^{-1} and the H_c was 1.5 kOe. These results shown the $CoFe_2O_4$-Strata-X^{TM}-RP composite as a soft ferromagnetic material.

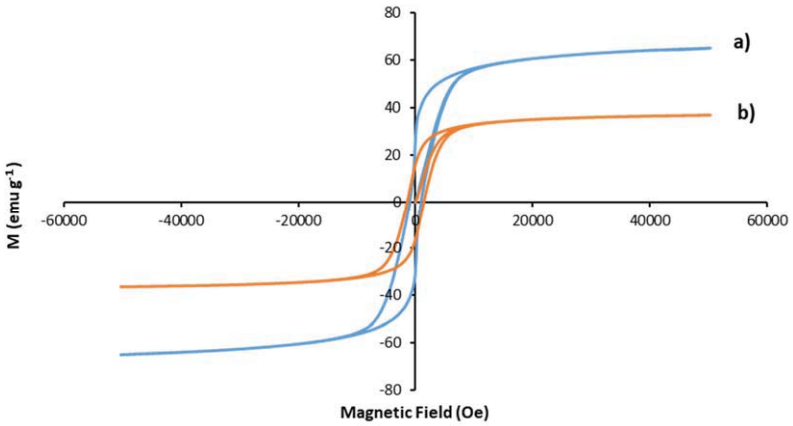

Fig. S1. Magnetization curve for (a) $CoFe_2O_4$ MNPs and (b) $CoFe_2O_4$@Strata-X^{TM}-RP composite

Particle size distribution

Particle size was determined by the number distribution method measured by dynamic light scattering (DLS). Fig. S2 shows the particle size distribution of the $CoFe_2O_4$-Strata-X^{TM}-RP composite. The mean size obtained from this representation was 23.7 ± 0.5 µm.

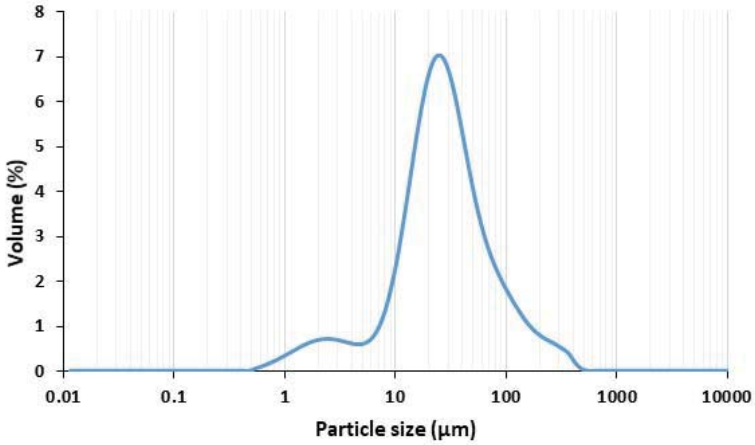

Fig. S2. Particle size distribution of $CoFe_2O_4$-Strata-X^{TM}-RP composite

Morphology

Morphology of the $CoFe_2O_4$-Strata-X^{TM}-RP was studied by SEM operating at 10 kV. Results are showed in Fig. S3. Specifically, a) and b) for the individual materials (i.e., $CoFe_2O_4$ MNPs and Strata-X^{TM}-RP polymer, respectively), and c) and d) for the resulting $CoFe_2O_4$-Strata-X^{TM}-RP composite at different magnification. In these latter two images it can also be observed how the Strata-X^{TM}-RP polymer is covered by the $CoFe_2O_4$ MNPs.

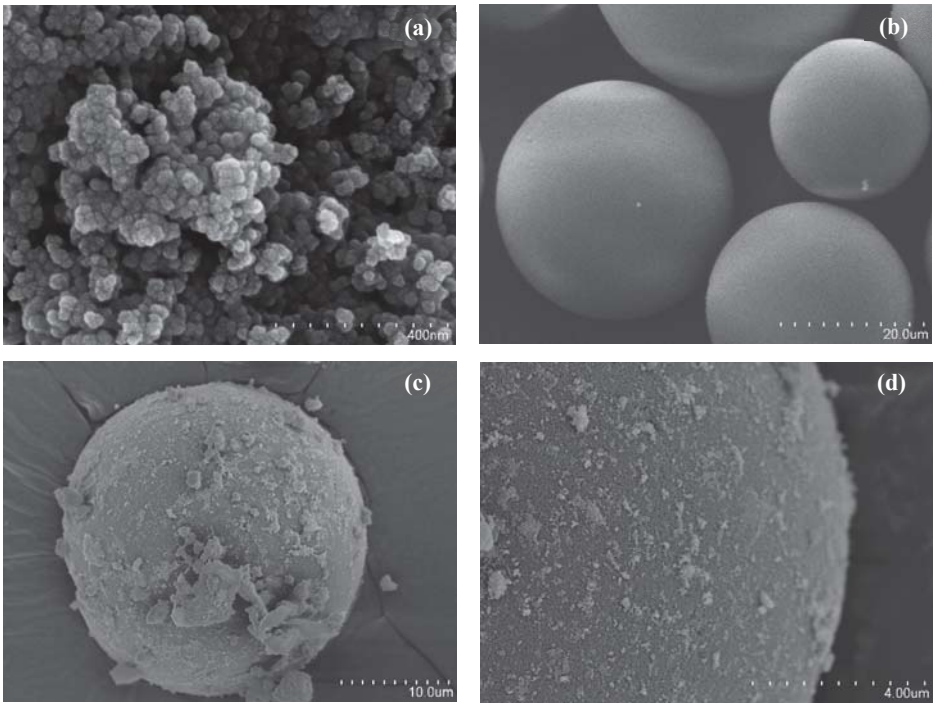

Fig. S3. (a) SEM micrograph of $CoFe_2O_4$ nanoparticles at magnification 120000; (b) SEM micrograph of Strata-X^{TM}-RP polymer at magnification 1200; (c) and (d) SEM micrographs of $CoFe_2O_4$-Strata-X^{TM}-RP composite at magnification 3000 (c) 10000 (d)

Regarding the study of the adsorption capacity of the material, the specific surface area was measured. The obtained isotherm (see Fig. S4**)** shows a Type-IV behaviour, which demonstrates the presence of mesopores with an average pore diameter of 6.6 nm**.** The BET surface area was 622.8 ± 0.8 $m^2\ g^{-1}$.

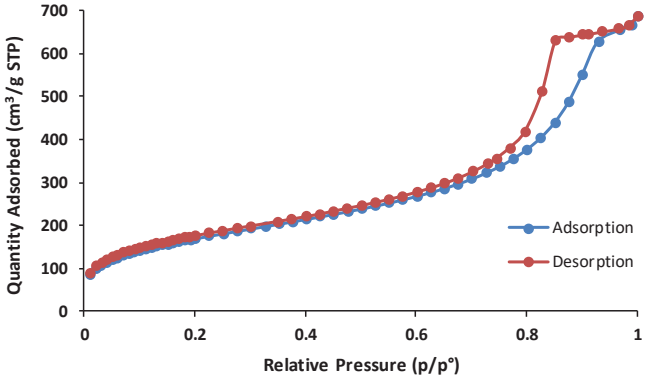

Fig. S4. Isotherm linear plot of the $CoFe_2O_4$-Strata-X^{TM}-RP composite

Energy dispersive X-ray analysis

Fig. S5 shows the EDS spectra for $CoFe_2O_4$ MNPs, the Strata-X^{TM}-RP polymer and the $CoFe_2O_4$-Strata-X^{TM}-RP composite. Signals produced by oxygen, iron and cobalt are observed in $CoFe_2O_4$ and composite spectra, while the peak produced by carbon is only appreciated in polymer and composite spectra. In other words, the EDS spectra of the composite match well with spectra of both individual components.

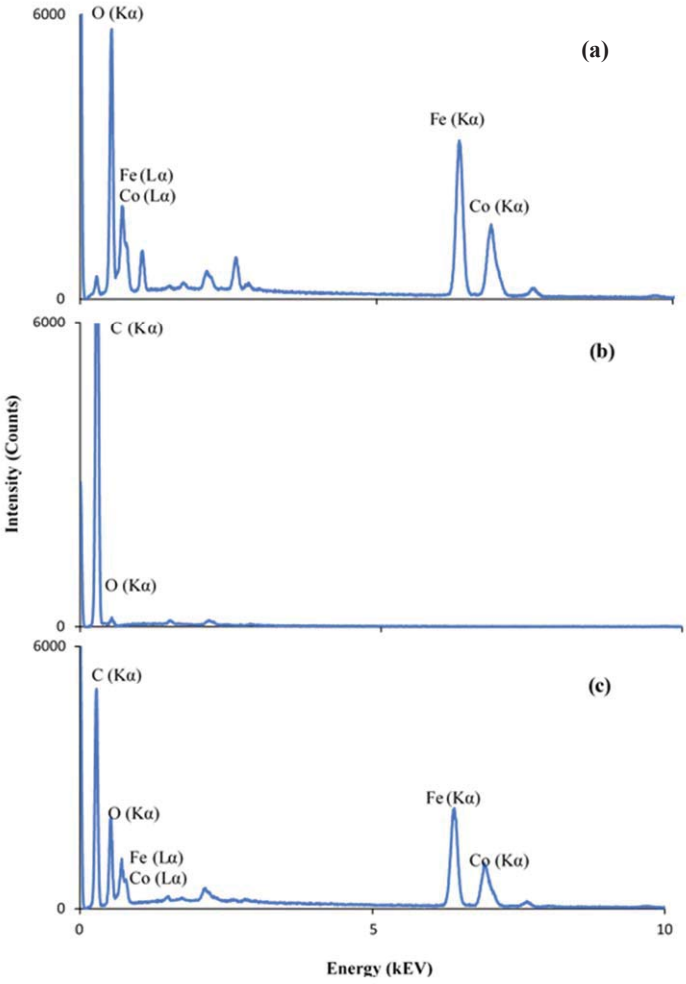

Fig. S5. EDS spectra. (a) $CoFe_2O_4$ magnetic nanoparticles, (b) Strata-X^{TM}-RP polymer and (c) $CoFe_2O_4$-Strata-X^{TM}-RP composite.

A high-throughput magnetic-based pipette tip microextraction as an alternative to conventional pipette tip strategies: Determination of testosterone in human saliva as a proof-of-concept

Analytica Chimica Acta 1221 (2022) 340117

Analytica Chimica Acta 1221 (2022) 340117

Contents lists available at ScienceDirect

Analytica Chimica Acta

journal homepage: www.elsevier.com/locate/aca

A high-throughput magnetic-based pipette tip microextraction as an alternative to conventional pipette tip strategies: Determination of testosterone in human saliva as a proof-of-concept

José Grau, Juan L. Benedé, Alberto Chisvert *, Amparo Salvador

GICAPC Research Group, Department of Analytical Chemistry, University of Valencia, 46100, Burjassot, Valencia, Spain

HIGHLIGHTS

- A high-throughput dispersive pipette tip microextraction approach is presented.
- The use of a magnetic sorbent reduces significantly manipulation and analysis time.
- Good results are obtained when compared with other pipette tip-based strategies.
- The sample throughput is further increased with a multichannel pipette.
- Salivary testosterone is selected as proof-of-concept to test the proposed approach.

GRAPHICAL ABSTRACT

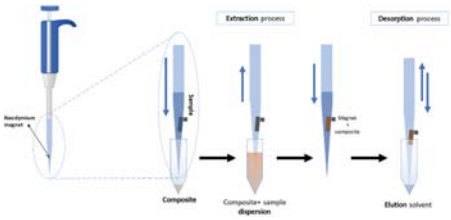

ARTICLE INFO

Keywords:
Magnetic sorbent
Bioanalysis
Dispersive-based microextraction
Pipette tip-based microextraction
Saliva sample
Testosterone

ABSTRACT

In this work, a lab-made and affordable high-throughput pipette tip microextraction strategy is presented. In this approach, a magnetic sorbent is quickly dispersed in the sample by means of a disperser solvent and the resulting dispersion is immediately aspirated into a pipette tip containing a small neodymium magnet inside, which entraps the magnetic sorbent containing the analytes. The sample is then discarded, and the subsequent cleaning and desorption steps are conducted by aspirating/dispensing the suitable solvents. This methodology provides satisfactory results when compared with previous pipette tip extraction strategies (i.e., pipette-tip solid-phase extraction and dispersive pipette extraction). Furthermore, it requires a minimum number of aspirating/dispensing cycles, thus benefiting the ergonomics for the operator, and it is not commercially dependent. This new approach has been tested by measuring testosterone levels in saliva of volunteers as a proof-of-concept. In this regard, a magnetic composite made of $CoFe_2O_4$ magnetic nanoparticles embedded in octadecyl bonded silica microparticles was employed as sorbent material. Testosterone was quantified by liquid chromatography coupled to tandem mass spectrometry. Under the optimized conditions, low limits of detection and quantification (7.5 ng L^{-1} and 24.8 ng L^{-1}, respectively), good repeatability (RSD <9%) and relative recoveries between 82 and 106% were obtained with just one adsorption and two desorption cycles, which requires few seconds per sample. In order to increase even more the sample throughput, a multichannel pipette was also evaluated.

* Corresponding author.
E-mail address: alberto.chisvert@uv.es (A. Chisvert).

https://doi.org/10.1016/j.aca.2022.340117
Received 8 April 2022; Received in revised form 20 June 2022; Accepted 22 June 2022
Available online 24 June 2022

1. Introduction

Sample preparation is usually considered the most limiting step of an analytical process, since it usually requires long times and high sample manipulation. This becomes especially critical when trace analysis and complicated matrices converge, given that high efforts are needed to isolate the target compounds from the matrix and to concentrate them [1]. Classical extraction techniques like liquid-liquid extraction (LLE) and solid-phase extraction (SPE), despite being extensively used in the past, are being replaced by microextraction techniques, respectively [2–4].

These miniaturized sample preparation techniques are aligned with some of the principles of the so-called Green Sample Preparation (GSP) [5], since they require less amounts of solvent and sorbent, thus generating less waste. Furthermore, those approaches based on sample flow through the acceptor phase (e.g., pipette-tip solid-phase extraction (PT-SPE) or microextraction by packed sorbents (MEPS)), and those based on dispersing the acceptor phase into the sample (e.g., dispersive liquid-liquid microextraction (DLLME) or dispersive solid-phase extraction (DSPE)), allow to accelerate the extraction kinetics [6,7] and therefore to reduce the extraction times. Nevertheless, some of the static approaches such as, for example, solid-phase microextraction (SPME) or thin-film microextraction (TFME), enable a high level of automation that counteracts the low sample throughput obtained. In this sense, the complete retention-elution-measurement procedure can be performed by means of robotized autosamplers [8]. The implementation of multi-well (usually 96-well) format workstations notably increases the sample treatment throughput [9]. The 96-well format has been also implemented for miniaturized SPE [10] and PT-SPE [11] by using pipetting workstations.

Leaving aside robotic workstations, which are not affordable for most of the laboratories, it should be emphasized the (semi)automation degree achieved when PT-SPE is used, since the aspirating/dispensing operations are conducted easily by using a manual pipette [12]. Moreover, PT-SPE allows on-site sampling and the tips are disposable, thus reducing carryover and cross-contamination [13]. However, tens of aspirating/dispensing cycles are needed in order to achieve a high extraction/elution efficiency, which may cause upper limb disorders. Furthermore, problems associated with clogging usually appear [14]. In this sense, monoliths presenting high permeability [15], paper-based sorbents rolled inside the tip [16] or, more recently, a sorbent packing-free approach based on functionalized-inner wall pipette tips [17], have been proposed to alleviate clogging problems, however they still require long extraction times.

The so-called disposable pipette extraction (DPX) [18], later rebranded as dispersive pipette extraction [19], can be considered as a hybrid technique between DSPE and PT-SPE. Unlike PT-SPE, the sorbent is not packed between two frits but it is placed loosely, in such a way when the sample is aspirated the sorbent is dispersed like in DSPE. All this increases the extraction kinetics thus increasing the sample throughput compared to PT-SPE at the same time it avoids the problems associated with clogging. However, it has been observed that the aspiration rate is not high enough to achieve an efficient dispersion, and different pipette-tip designs have been proposed to improve it. Based on this, commercially-available tips can be found incorporating a baffle system inside that is shaped to disrupt the flow of aspirated sample and thus force the dispersion [19]. It should be emphasized that the lab-made manufacture of these tips is not easy, and in any case, the design is under patent [20], which makes the commercial dependence indisputable. Besides this commercial dependence and high cost, the amount of extracting phases commercially available is limited [18].

Changing the subject to other issues, it should be emphasized that the use of magnetic (nano)materials in microextraction techniques, especially in DSPE, has been extensively exploited due to their easy retrieval by using an external magnet [21]. If the magnet is placed inside the sample and acts as stirring engine and sorbent retrieval, as occurs in stir bar sorptive dispersive microextraction (SBSDME) [22], both the retrieval and sample handling are further facilitated.

All this inspired us to propose a high-throughput, operator-friendly and cost-effective approach, based on the (semi)automated character of pipettes and the advantages of magnetic (nano)materials. To this regard, a conventional pipette tip with a small neodymium magnet inside is proposed as an alternative to PT-SPE and DPX tips. First, a magnetic sorbent is quickly dispersed in the sample in a 1.5 mL microcentrifuge tube by means of a disperser solvent and, immediately, the resulting dispersion is aspirated into the tip, in such a way the magnetic sorbent entrapping the analytes is retained by the magnet. Then, the sample is discarded, and finally, a small amount of desorption solvent is aspirated/dispensed to desorb the analytes, thus providing an extract ready to be measured.

A previous work combining a magnetic sorbent with a pipette tip was published as clean-up method [23]. In this work, an annular magnet was surrounding the pipette tip, in such a way it was manually moved up and down continuously for a defined period of time (2 min) to ensure the contact between the sorbent and the solution. However, in this approach the sorbent is not efficiently dispersed and the manual intervention by the operator is unavoidable, thus decreasing the degree of (semi)automatitation provided by the employment of pipette-tip strategies, such as PT-SPE, DPX and the presented approach.

To test the proposed approach, a magnetic composite made of $CoFe_2O_4$ magnetic nanoparticles (MNPs) embedded on octadecyl silica (C18) microparticles (i.e., $CoFe_2O_4$–C18) has been selected for the determination of testosterone in saliva as a proof-of-concept. Testosterone levels can be used as a biomarker of different diseases [24–26]. In addition, testosterone is widely employed by professional athletes in doping [27]. Saliva samples have the advantage of not being as stressful and invasive as serum or urine [28], and it has been demonstrated that salivary testosterone, despite being quite lower than in serum, presents good correlation [28]. To overcome the issue of low concentration levels, a sensitive technique like liquid chromatography-tandem mass spectrometry (LC-MS/MS) is proposed as measurement technique.

2. Experimental

2.1. Reagents

All reagents were acquired from major suppliers. Testosterone (purity ≥99% (HPLC)) and 16,16,17-d_3-testosterone (testosterone-d3) were obtained from Sigma Aldrich (Steinheim, Germany).

For the preparation of the cobalt ferrite ($CoFe_2O_4$) magnetic nanoparticles (MNPs), cobalt (II) chloride hexahydrate ($CoCl_2{\cdot}6H_2O$) and iron (III) chloride hexahydrate ($FeCl_3{\cdot}6H_2O$) were obtained from Acros Organics (New Jersey, NJ, USA), and ethanol was purchased from Panreac (Barcelona, Spain). These MNPs were embedded in commercial octadecyl silica (C18) microparticles (50 μm average diameter) from Sigma Aldrich (Steinheim, Germany) using toluene from Fischer Scientific (Loughborough, United Kingdom).

Deionized water was obtained from a Connect water purification system provided by Adrona (Riga, Latvia).

To prepare the chromatographic mobile phase, LC-MS grade methanol (MeOH) from Honeywell (Seelze, Germany), LC-MS grade water from Panreac (Barcelona, Spain) and formic acid 98% (for mass spectrometry) from Fluka (Steinheim, Germany) were used. Nitrogen used as nebulizer and curtain gas in the MS/MS ion source was obtained by a NiGen LCMS 40-1 nitrogen generator from Claind S.r.l. (Lenno, Italy). Extra pure nitrogen (>99.999%), used as collision gas in the MS/MS collision cell, was provided by Praxair (Madrid, Spain).

For the preparation of synthetic saliva, sodium chloride (NaCl) from Fisher Scientific (Loughborough, United Kingdom), potassium chloride (KCl), calcium chloride ($CaCl_2{\cdot}H_2O$), potassium thiocyanate (KSCN) and di-sodium hydrogen phosphate ($Na_2HPO_4{\cdot}H_2O$) from Panreac (Barcelona, Spain), sodium sulfide (Na_2S) from Scharlau (Barcelona, Spain)

and urea from VWR Chemicals (Fontenay-sous-Bois, France) were used.

2.2. Sample collection and pre-treatment

Passive drooling was employed to collect the samples, since commercial sampling devices may affect the concentration of testosterone in saliva [29].

In this sense, three samples from different volunteers (one female and two male) were analysed and used for recovery studies. Other four samples (two female and two male) were collected before and after physical exercise. All samples were first centrifuged (5 min, 6000 rpm) to separate saliva from leftovers and/or phlegm, and the supernatant was frozen at −20 °C to break the polysaccharides. To be analysed, samples were thawed at room temperature and centrifuged again (5 min, 18000 rpm).

2.3. Apparatus and materials

An Ultrasons-HD ultrasonic bath from J.P. Selecta (Barcelona, Spain) and a EBA 21 centrifuge (provided with a rotor of 15 cm radius for centrifuge tubes and a rotor of 9.7 cm radius for microcentrifuge tubes) were used.

For the extraction devices, a single-channel EHP pipette from VWR (Radnor, PA, USA) and a multichannel pipette P8X1200L from Gilson (Middleton, WI, USA), and neodymium magnets (6 mm length x 2 mm diameter, 3 mm × 1 mm, and 1 × 1 mm) from Supermagnete (Uster, Switzerland) were acquired. DPX XTR tips were kindly provided by DPX technologies (Columbia, SC, USA).

Those instruments employed for characterization of the sorbent material are listed in Supplementary Material.

2.4. Preparation of synthetic saliva

For the validation of the method, synthetic saliva was prepared according to an adapted protocol [30]. In this sense, an aqueous solution of ultrapure water (250 mL) containing NaCl (400 mg L^{-1}), KCl (400 mg L^{-1}), $CaCl_2{\cdot}H_2O$ (795 mg L^{-1}), $Na_2HPO_4{\cdot}H_2O$ (690 mg L^{-1}), KSCN (300 mg L^{-1}), Na_2S (5 mg L^{-1}) and urea (1000 mg L^{-1}) was prepared.

2.5. Synthesis of $CoFe_2O_4$–C18 magnetic sorbent

The synthesis of $CoFe_2O_4$ MNPs was performed by wet chemical co-precipitation following an adapted protocol [31]. In this sense, 100 mL of a 0.4 M aqueous solution of $FeCl_3$ and 100 mL of a 0.2 M aqueous solution of $CoCl_2$ were mixed. Afterwards, 100 mL of a sodium hydroxide 3 M solution was slowly added under vigorous stirring at 80 °C and the mixture was kept stirring at this temperature for 1 h. The resultant MNPs were isolated by magnetic decantation and washed twice with ultrapure water and once with ethanol. Finally, MNPs were dried overnight at 80 °C.

For the preparation of the $CoFe_2O_4$–C18 composite, 0.04 g of the previous synthesized MNPs were mixed with 0.4 g of C18 microparticles suspended in 10 mL of toluene, and the mixture was stirred for 2 days at room temperature. The yield obtained in this part was 70%, obtaining ca. 0.3 g for each synthesis, allowing to perform over 300 analyses per synthesis.

2.6. Preparation of standard and sample solutions

Firstly, stock solutions of testosterone at 500 μg mL^{-1} and testosterone-d_3 (surrogate) at 1000 μg mL^{-1} were separately prepared in MeOH. These stock solutions proved to be stable at least for one month.

Then, an intermediate solution at 2 μg L^{-1} of testosterone was prepared in synthetic saliva (see Section 2.4), whereas a surrogate solution at 5 μg L^{-1} was prepared by proper dilution of its stock solution in ultrapure water.

The working standard solutions (N = 7) between 25 and 2000 ng L^{-1} were prepared directly in a 96-well plate, employing the proper volume of the testosterone intermediate solution (2 μg L^{-1}) and adding the corresponding volume of synthetic saliva up to 400 μL. Finally, 100 μL of the surrogate intermediate solution were added (i.e., 1 μg L^{-1} in the final solution).

Saliva samples were also prepared in a 96-well plate, similar to the working standard solutions, i.e., 400 μL of sample were mixed with 100 μL of the surrogate intermediate solution.

2.7. Scheme of the microextraction device

For the preparation of the single-channel microextraction device, a neodymium magnet (6 mm length x 2 mm diameter) was placed inside a 1 mL pipette tip. Then, a smaller magnet (1× 1 mm) was placed outside the tip in order to attach the inner magnet to the wall of the tip and avoid its movement. Otherwise, the magnet would fall plugging the orifice of the pipette tip, and thus hindering the flow of solutions. Fig. 1a shows a scheme of this device. Likewise, a picture of the system is shown in Fig. 1c.

On the other hand, a multichannel device was also tested by employing a 12-channel pipette. In this case, as can be seen in Fig. 1b and d, no external magnet is employed, since the inner magnets themselves interact in pairs between consecutive pipette tips. In this way, they are suspended on the side of the wall of the pipette tip, allowing the correct flow of the solutions. For this second system, the magnets employed were smaller (3× 1 mm) than those in the single-channel approach (as discussed in Section 3.2.2).

2.8. Extraction procedure

To carry out the extraction, 1 mg of $CoFe_2O_4$–C18 magnetic sorbent was first dispersed in 35 μL of MeOH by 10 s of sonication. 500 μL of each working standard or sample solution (prepared as described in Section *2.6.*) were aspirated into the pipette tip of the extraction device, and they were dispensed over the dispersed sorbent. The resultant dispersion was immediately aspirated into the pipette tip where the sorbent was retained by the inner magnet, and the remaining solution was discarded. Later, ca. 500 μL of ultrapure water were aspirated and discarded as a clean-up step to eliminate the leftovers of saliva inside the tip. Finally, testosterone was desorbed by aspirating/dispensing 35 μL of MeOH twice, and the extract was transferred into a 250 μL insert placed inside a 2-mL injection vial.

Fig. 2 shows a scheme of the extraction procedure, whereas Supplementary Video S1 shows the steps of dispersion and the retention of the magnetic material by the magnet.

Supplementary data related to this article can be found at https://doi.org/10.1016/j.aca.2022.340117.

2.9. LC-MS/MS analysis

An Agilent 1100 Series chromatography system comprised of a degasser, a programmable pump, an autosampler and a thermostatic column oven with a Zorbax SB-C18 (50 mm length, 2.1 mm I.D., 1.8 μm) column, coupled to an Agilent 6410B Triple Quad MS/MS was employed throughout the study.

For the LC-MS/MS analysis, each extract was injected (10 μL) into the chromatographic system. The mobile phase was composed of 0.1% formic acid and 2 mM ammonium acetate aqueous solution and MeOH containing 0.1% formic acid with isocratic elution at a mixing ratio of 15:85% (v/v) employing a flow rate of 0.2 mL min^{-1}. The column temperature was set constant at 35 °C.

The triple quadrupole MS detector operated in electrospray ionization mode (ESI), by multiple reaction monitoring (MRM). Specifically, positive polarity (ESI^+, capillary voltage at 5 kV) was used to measure testosterone and testosterone-d_3. The other conditions were: gas

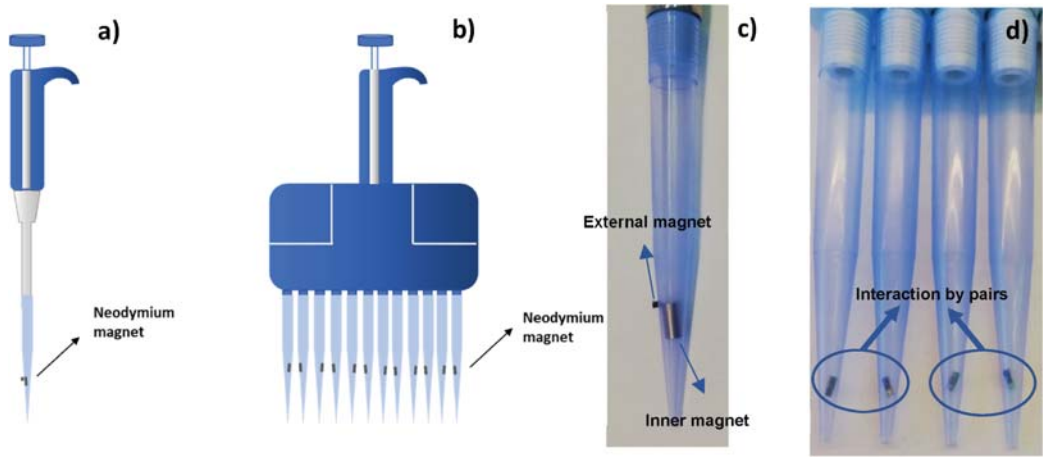

Fig. 1. Scheme of the extraction devices: a) single-channel device, b) multichannel device, c) detail of the tip for the single-channel device with both the external and the inner magnets, and d) detail of the tip for the multichannel device showing the magnetic interaction between adjacent magnets.

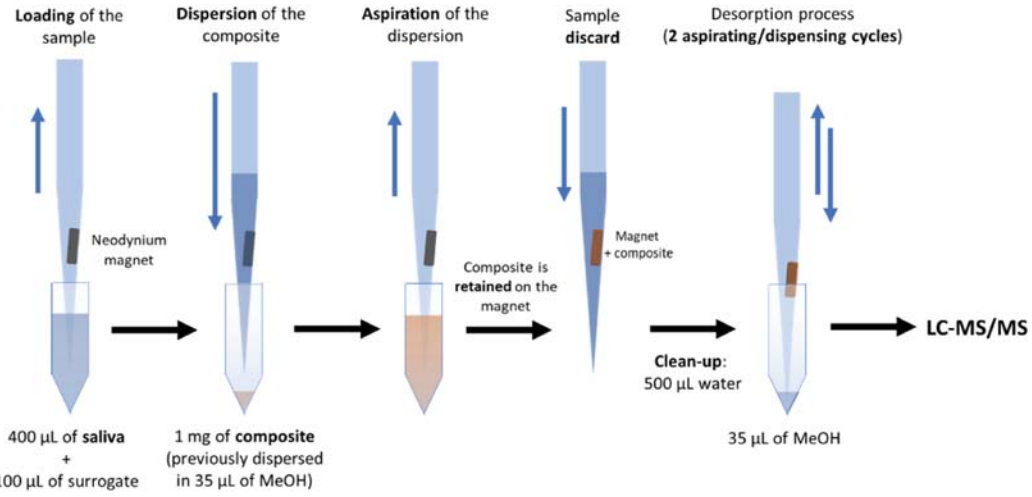

Fig. 2. Scheme of the proposed analytical method.

temperature at 230 °C, nebulizer gas flow rate at 13 L min^{-1}, nebulizer gas pressure at 35 psi, collision energy at 21 V, fragmentor at 132 V, and dwell time at 200 s. The *m/z* precursor → product ion transitions for quantification and identification of testosterone were 289 → 97 and 289 → 102, respectively. For testosterone-d_3, only the transition 292 → 97 was selected. Total run time was 2.5 min.

3. Results and discussion

3.1. Selection and characterization of $CoFe_2O_4$–C18 magnetic sorbent

As one of the purposes of this work was the comparison with commercial pipette tip-based techniques, it was necessary to employ a common material, which is limited due to the lack of variety of sorbents that commercial brands present. Among the few available sorbents, octadecyl (C18) was selected, since it allows strong hydrophobic interactions with highly hydrophobic compounds like testosterone (Log $K_{o/w}$ = 3.3). To provide the magnetism needed to be used in the presented approach, a magnetic composite was prepared (as described in Section 2.5) by embedding $CoFe_2O_4$ MNPs on the pores of silica C18 end-capped microparticles by non-covalent bonds.

Different properties of the synthesized $CoFe_2O_4$–C18 magnetic composite such as magnetization, morphology, specific surface area, pore diameter, surface charge, and thermogravimetry stability were studied. The inter-batch comparison and the extraction performance of the composite material and its individual components were also

evaluated. All these results are presented in Supplementary Material.

3.2. Selection of the microextraction device

Two different devices, i.e., the single-channel and the multichannel, have been tested. Despite their similarity, they present some differences that are commented below.

3.2.1. Single-channel device

The single-channel device employs an external magnet to fix the height of the inner magnet and thus avoiding the obstruction of the pipette tip. Since the inner and the external magnet are very close, the magnetic interaction is so strong that the magnets do not move during the sample aspiration/dispensing processes.

The height of the inner magnet can be easily modified by just displacing the external magnet according to the analysis requirements. The recommended height was the minimum to avoid flow obstruction of the pipette tip. If the inner magnet is placed too high, the magnetic sorbent containing the analytes would not be retrieved and it would be discarded along with the sample.

However, sometimes it could be useful to change the height of the magnet. This is especially important when it is necessary more than one cycle to obtain a proper dispersion, as it could happen for viscous samples. In these cases, the inner magnet can be placed in the upper part of the pipette tip to not disturb during the extraction process, otherwise the magnet would retrieve all the magnetic sorbent during the first aspiration of the dispersion provoking that during the further aspiration/dispensing cycles the system would work as PT-SPE. Once the extraction step is over, the magnet could be easily moved back to the bottom of the pipette tip for the subsequent steps.

3.2.2. Multichannel device

Compared to the single-channel device, the multichannel system has the advantage of treating multiple samples at the same time, which allows to significantly reduce the total analysis time. In this device, the external magnet is not needed since the inner magnet is held by the closest magnet from the adjacent pipette tip. In this case, during the aspiration of the sample, the magnets could be slightly displaced to an upper position, where the distance between both magnets is lower. In this case, as said before, it would be necessary to increase the volume of the desorption solvent. The use of external magnets like in the single-channel mode is not possible since they would hit the wall of the 96-well plate and they would be displaced to higher place resulting in the same described problem. To solve it, the employment of square-shape magnets (3 mm length x 1 mm width) provided satisfactory results. With this new configuration, the interaction between adjacent magnets is lower and they remain at the bottom of the pipette tip. Then, when the sample is aspirated, their square form does not obstruct the flow, but the magnets are dragged by the sample up to a determined height where they increase the interaction and thus the ascension is stopped. When the aspiration is stopped, the magnets fall down to the original position allowing to retrieve the magnetic material. A video showing this behaviour is shown in Supplementary Video S2. It should be said that this movement of the magnets only occurs during the sample aspiration. During the desorption process, where small volumes are employed (i.e., 25 μL), the magnets remain on their original positions. A great advantage of this system is that since the magnets are smaller, it is necessary less volume of organic solvent during the desorption process. Nevertheless, the magnetic interactions with sorbent employing these small magnets are weaker, causing that not all the magnetic material is retrieved during the desorption step. In this case, it would be necessary a centrifugation step to avoid the introduction of solid particles in the chromatographic system. In order to evade the centrifugation step, the multichannel device will be improved for future applications.

Supplementary data related to this article can be found at https://doi.org/10.1016/j.aca.2022.340117.

Taking into account these observations, single-channel system was selected for further experiments.

3.3. Study of the extraction and desorption variables

The amount of composite, the extraction time, the number of dispensing cycles, the disperser solvent volume, the ionic strength (% NaCl (w/v)) and the sample dispensing speed were evaluated as critical variables during the microextraction process using the single-channel device. A univariate optimization was selected in order to study each variable independently. Considering that human saliva is mainly composted of water (ca. 99%), each experiment was performed by triplicate extracting 500 μL of aqueous standard solution with 1 μg L^{-1} of testosterone during the same working session. Discussion of these results are presented in the Supporting Information. The selected conditions were 1 mg of composite, no additional extraction time, one dispensing cycle, 35 μL of disperser solvent and 0.2% of NaCl. Regarding the sample dispensing speed, it was used as rapid as possible to increase the dispersion of the sorbent.

Moreover, the desorption variables, such as the elution solvent volume and the number of aspirating/dispensing cycles were examined. Discussion of these results are included in Supporting Information. The selected desorption conditions were two aspirating/dispensing cycles and 35 μL of elution solvent.

3.4. Analytical performance

Different parameters were evaluated in order to validate the proposed method.

3.4.1. Selectivity

As it was stablished in Section 3.1, the strong hydrophobicity of C18 allows to separate non-polar trace compounds (such as testosterone), while the major components present in saliva (saccharides, salts, urea, proteins, etc.) are not retained by this composite due to their high hydrophilicity and they are discarded with the rest of the sample. In this sense, the biological matrix is removed and the analytes can be introduced into the MS without harming it or affecting the signal [32]. Furthermore, the subsequent LC-MS/MS analysis allows to separate testosterone from other possible interferences that could be extracted. The testosterone identity was stablished in terms of the retention time and the *m/z* transitions compared with a standard. According to the chromatogram obtained (shown in Fig. S9) after the application of the method to a real sample, no additional peaks besides the target analyte and surrogate were observed, proving the good selectivity of the overall proposed method.

3.4.2. Linearity

High levels of linearity were obtained up to 5 μg L^{-1}. However, according to the usual levels of testosterone, the working range was set from 25 to 2000 ng L^{-1}. The obtained calibration curve was $A/A_{sur} = (1.534 \pm 0.022)\cdot C + (0.110 \pm 0.019)$ with a regression coefficient (R^2) of 0.9993 for $N = 7$, where A is the peak area of the testosterone, A_{sur} is the peak area of the surrogate and C is the testosterone concentration in ng L^{-1}. Moreover, the difference between calculated and experimental values (residuals) was less than 10%.

The heteroscedasticity was also tested with the Breusch-Pagan test [33], the tabulated value for χ_0^2 for 1° of freedom and a significance level of 0.05 was 3.84, and the calculated value for χ^2 was 2.98. As $\chi^2 < \chi_0^2$, it can be concluded that the regression is homoscedastic.

3.4.3. Limit of detection and quantification

The limit of detection (LOD) and the limit of quantification (LOQ) were estimated with the 3 and 10 signal-to-noise ratio (S/N) criteria respectively, by measuring different concentrations after the extraction in order to find which one provides the closest S/N to 3 (LOD) and to 10

(LOQ), respectively. Values for LOD and LOQ were 7.5 ± 0.4 and 24.8 ± 1.3 ng L^{-1} respectively.

3.4.4. Repeatability

For the study of repeatability of the proposed method, five independent replicate standard solutions containing the analyte at three concentration levels (50, 250 and 1000 ng L^{-1}) were measured during the same day (intra-day repeatability) obtaining RSD values of 7.8, 6.0 and 4.6% respectively, and five independent replicates were measured on different days (inter-day repeatability) with RSD values of 8.5, 7.8 and 6.5% respectively.

3.4.5. Enrichment factor and extraction efficiency

The enrichment factor (EF) was calculated as the ratio of the signal obtained before and after the extraction of a 250 ng L^{-1} solution, obtaining a value of 4.3 ± 0.4.

The extraction efficiency is related with EF, in such a way it was calculated as the product of the EF and the ratio between final (i.e., 35 μL) and initial volume (i.e., 400 μL) in %. The obtained value was 37 ± 3%.

3.5. Comparison with other pipette tip-based analytical strategies

In order to study if this new pipette tip-based approach provides advantages over PT-SPE and DPX strategies, the extraction of a 1 μg L^{-1} aqueous solution of testosterone was performed using these three strategies.

For comparative purposes, all processes employed the same amounts of composite (i.e., 1 mg) and desorption solvent (i.e., 35 μL), and the same number of aspirating/dispensing cycles for the extraction (i.e., one cycle), for the clean-up (i.e., one cycle) and for the desorption (i.e., two cycles) steps. The detailed processes for PT-SPE and DPX are described in Supplementary Material.

As it can be observed in Fig. 3, similar results were obtained employing DPX and the presented approach. However, for PT-SPE the signal obtained was quite lower, thus demonstrating the higher extraction efficiency of the dispersion approaches versus the static one.

Additionally, a comparison of some of the crucial aspects of the approaches (i.e., analytical performances, prices and ergonomics for the operator) is presented in Table 1. As it was discussed before, the performance of DPX and the presented approach was similar. Nevertheless, the price of the commercialized DPX pipette tips is quite higher.

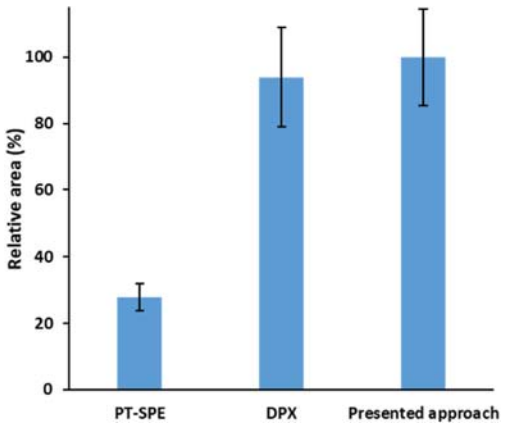

Fig. 3. Comparison between the analytical performance of PT-SPE, DPX and the presented approach. Errors bars show the standard deviation (N = 3).

Table 1
Comparison between PT-SPME, DPX and the presented method.

Extraction technique	EF	Price per 100 analysis (€)[b]	Ergonomics
PT-SPE[a]	1.2	1–2	+
DPX	4.0	100–160	+++
This approach	4.3	3–4	+++

[a] Home-made PT-SPE tips.
[b] Prices do not include shipment charges.

Moreover, DPX required more volume of organic solvent (i.e., 300 μL of MeOH) for preconditioning the sorbent. In terms of comfort and ergonomics, both are quite grateful with the operator, unlike PT-SPE that needs more cycles to achieve the same extraction efficiency as the others. On the other side, the lab-made PT-SPE is the cheapest method, but its analytical performance was lower than the other competitors, also experimenting some of the problems mentioned in the bibliography [16] such as clogging, material loses, etc. It is true that part of these complications would be diminished with commercial tips; however, the prices of each pipette tip would be increased.

According to these aspects, it can be concluded that the presented technique is the best alternative due to its low cost, simplicity, reduced consumption of organic solvents and non-commercial dependence compared with the other two approaches.

Additionally, another advantage of the presented approach over those employing commercial tips is the possibility of using a wide variety of sorbents tailored to the analytes, unlike the commercial ones that present a lack of variety of available sorbents, which significantly reduces their versatility.

3.6. Accuracy and analysis of real samples

For the study of the accuracy, the matrix effects were evaluated. For this purpose, three samples from three different volunteers (a female and two males) were analysed before and after being spiked at three levels of concentration (50, 250 and 1000 ng L^{-1}). As shown in Table 2, good relative recoveries (between 82 and 106%) were obtained, thus proving matrix effects were not significant and, therefore, standard addition calibration was not necessary. The employment of a deuterated internal standard (i.e., testosterone-d_3) that has the same behaviour as the target analyte during the extraction process and the measurement, corrects the matrix effects.

Just as a proof-of-concept, saliva from four volunteers (two females and two males) were analysed before and after physical exercise to see if there was an enhance of the salivary testosterone levels. As expected, an increase in the levels of salivary testosterone after the activity was observed for all volunteers. The growth was higher for females (26 and 40%) than for males (around 10%). Results are presented in Table 3.

Table 2
Relative recoveries of the proposed method.

Volunteer[a]	Amount spiked (ng L^{-1})	Amount found (ng L^{-1})	Relative recovery (%)
1 (M)	0	83 ± 3	–
	50	127 ± 2	94 ± 10
	250	308 ± 20	90 ± 8
	1000	1090 ± 40	92 ± 4
2 (M)	0	98 ± 5	–
	50	144 ± 5	82 ± 3
	250	360 ± 10	88 ± 5
	1000	1140 ± 60	103 ± 6
3 (F)	0	60 ± 5	–
	50	110 ± 7	101 ± 14
	250	324 ± 10	106 ± 4
	1000	1100 ± 20	105 ± 3

[a] **(M):** Male; **(F):** Female.

Table 3
Comparison of levels of testosterone before and after physical exercise.

Volunteer[a]	Testosterone before training (ng L^{-1})	Testosterone after training (ng L^{-1})	Increase (%)
4 (F)	46 ± 6	58 ± 4	26
5 (F)	33 ± 2	41 ± 3	40
6 (M)	89 ± 1	99 ± 2	11
7 (M)	66 ± 2	75 ± 4	14

[a] **(M)**: Male; **(F)**: Female.

4. Conclusions

In this paper, a high-throughput approach that combines the quickness of dispersive solid phase extraction, the easy retrieval of the magnetic sorbents, and the simplicity of pipette tip-based microextraction techniques has been presented. The preparation of the extraction device just requires the incorporation of small neodymium magnets inside pipette tips. In order to test the viability of this new approach, the determination of salivary testosterone was selected obtaining good analytical features in terms of linearity, enrichment factor, LODs and LOQs, repeatability, and accuracy. Compared with other pipette tip-based microextraction techniques, this one using lab-made tips allows to obtain similar extraction and analysis times than those using expensive commercialized pipette tips that also present a lack of sorbent versatility. Moreover, it requires less amounts of organic solvents per analysis than other pipette tip-based approaches, being in compliance with the principles of Green Sample Preparation (e.g., low volumes of non-toxic organic solvents, minimization of waste, etc). Additionally, a multichannel pipette was tested to increase, even more, the sample throughput, reducing the analysis time. However, this version needs some adjustments in order to avoid centrifugation and it will be improved for future applications. The obtained results prove the excellent properties of this new approach as a low-cost and user-friendly alternative over conventional pipette tip-based strategies for the on-site analysis of small volumes of samples.

CRediT authorship contribution statement

José Grau: Investigation, Data treatment, Writing – original draft. **Juan L. Benedé:** Methodology, Writing – review & editing. **Alberto Chisvert:** Conceptualization, Supervision, Methodology, Project organization, Funding acquisition, Writing – review & editing. **Amparo Salvador:** Supervision, Methodology, Writing – review & editing.

Declaration of competing interest

The authors declare that they have no known competing financial interests or personal relationships that could have appeared to influence the work reported in this paper.

Data availability

Data will be made available on request.

Acknowledgments

Grant PID2020-118924RB-I00 funded by Spanish Ministry of Science and Innovation (MCIN/AEI/10.13039/501100011033) is greatly appreciated. This article is based upon work from the National Thematic Network on Sample Treatment (RED-2018–102522-T) of the Spanish Ministry of Science, Innovation and Universities, and the Sample Preparation Study Group and Network supported by the Division of Analytical Chemistry of the European Chemical Society.

Appendix A. Supplementary data

Supplementary data to this article can be found online at https://doi.org/10.1016/j.aca.2022.340117.

References

[1] M. Arabi, A. Ostovan, A.R. Bagheri, X. Guo, L. Wang, J. Li, X. Wang, B. Li, L. Chen, Strategies of molecular imprinting-based solid phase extraction prior to chromatographic analysis, TrAC, Trends Anal. Chem. 128 (2020), 115923.
[2] M. Rutkowska, J. Płotka-Wasylka, M. Sajid, V. Andruch, Liquid–phase microextraction: a review of reviews, Microchem. J. 149 (2019), 103989.
[3] M.J. Trujillo-Rodríguez, I. Pacheco-Fernández, I. Taima-Mancera, J.H.A. Díaz, V. Pino, Evolution and current advances in sorbent-based microextraction configurations, J. Chromatogr. A 1634 (2020), 461670.
[4] J. Płotka-Wasylka, N. Szczepańska, M. de la Guardia, J. Namieśnik, Modern trends in solid phase extraction: new sorbent media, TrAC, Trends Anal. Chem. 77 (2016) 23–43.
[5] Á.I. López-Lorente, F. Pena-Pereira, S. Pedersen-Bjergaard, V.G. Zuin, S.A. Ozkan, E. Psillakis, The ten principles of green sample preparation, TrAC, Trends Anal. Chem. 148 (2022), 116530.
[6] E. Psillakis, Vortex-assisted liquid-liquid microextraction revisited, TrAC, Trends Anal. Chem. 113 (2019) 332–339.
[7] A. Chisvert, S. Cárdenas, R. Lucena, Dispersive micro-solid phase extraction, TrAC, Trends Anal. Chem. 112 (2019) 226–233.
[8] J. O'Reilly, Q. Wang, L. Setkova, J.P. Hutchinson, Y. Chen, H.L. Lord, C.M. Linton, J. Pawliszyn, Automation of solid-phase microextraction, J. Sep. Sci. 28 (2005) 2010–2022.
[9] N. Reyes-Garcés, E. Gionfriddo, G.A. Gómez-Ríos, M.N. Alam, E. Boyacl, B. Bojko, V. Singh, J. Grandy, J. Pawliszyn, Advances in solid phase microextraction and perspective on future directions, Anal. Chem. 90 (2018) 302–360.
[10] R.F. Venn, J. Merson, S. Cole, P. Macrae, 96-Well solid-phase extraction: a brief history of its development, J. Chromatogr. B 817 (2005) 77–80.
[11] M. Abdel-Rehim, C. Persson, Z. Altun, L. Blomberg, Evaluation of monolithic packed 96-tips and liquid chromatography-tandem mass spectrometry for extraction and quantification of pindolol and metoprolol in human plasma samples, J. Chromatogr. A 1196–1197 (2008) 23–27.
[12] H. Sun, J. Feng, S. Han, X. Ji, C. Li, J. Feng, M. Sun, Recent advances in micro- and nanomaterial-based adsorbents for pipette-tip solid-phase extraction, Microchim. Acta 188 (2021) 189.
[13] S. Seidi, M. Tajik, M. Baharfar, M. Rezazadeh, Micro solid-phase extraction (pipette tip and spin column) and thin film solid-phase microextraction: miniaturized concepts for chromatographic analysis, TrAC, Trends Anal. Chem. 118 (2019) 810–827.
[14] B. Hashemi, P. Zohrabi, K.H. Kim, M. Shamsipur, A. Deep, J. Hong, Recent advances in liquid-phase microextraction techniques for the analysis of environmental pollutants, TrAC, Trends Anal. Chem. 97 (2017) 83–95.
[15] M. Vergara-Barberán, E.J. Carrasco-Correa, M.J. Lerma-García, E.F. Simó-Alfonso, J.M. Herrero-Martínez, Current trends in affinity-based monoliths in microextraction approaches: a review, Anal. Chim. Acta 1084 (2019) 1–20.
[16] J. Ríos-Gómez, R. Lucena, S. Cárdenas, Paper supported polystyrene membranes for thin film microextraction, Microchem. J. 133 (2017) 90–95.
[17] S. Wang, Z. He, W. Li, J. Zhao, T. Chen, S. Shao, H. Chen, Reshaping of pipette tip: a facile and practical strategy for sorbent packing-free solid phase extraction, Anal. Chim. Acta 1100 (2020) 47–56.
[18] D.C.M. Bordin, M.N.R. Alves, E.G. de Campos, B.S. De Martinis, Disposable pipette tips extraction: fundamentals, applications and state of the art, J. Sep. Sci. 39 (2016) 1168–1172.
[19] INTip Solid Phase Extraction - DPX Technologies, (n.d.).
[20] W. Brewer, Dispersive Pipette Extraction Tip and Methods for Use, 2013.
[21] K. Aguilar-Arteaga, J.A. Rodriguez, E. Barrado, Magnetic solids in analytical chemistry: a review, Anal. Chim. Acta 674 (2010) 157–165.
[22] V. Vállez-Gomis, J. Grau, J.L. Benedé, D.L. Giokas, A. Chisvert, A. Salvador, Fundamentals and applications of stir bar sorptive dispersive microextraction: a tutorial review, Anal. Chim. Acta 1153 (2021), 338271.
[23] H.L. Cheng, F.L. Wang, Y.G. Zhao, Y. Zhang, M.C. Jin, Y. Zhu, Simultaneous determination of fifteen toxic alkaloids in meat dishes and vegetable dishes using double layer pipette tip magnetic dispersive solid phase extraction followed by UFLC-MS/MS, Anal. Methods 10 (2018) 1151–1162.
[24] J.E. Michaud, K.L. Billups, A.W. Partin, Testosterone and prostate cancer: an evidence-based review of pathogenesis and oncologic risk, Ther. Adv. Urol. 7 (2015) 378–387.
[25] C. Carnegie, Diagnosis of hypogonadism: clinical assessments and laboratory tests, Rev. Urol. 6 (Suppl 6) (2004) S3–S8.
[26] L.M. Demers, Androgen deficiency in women; Role of accurate testosterone measurements, Maturitas 67 (2010) 39–45.
[27] D. Thieme, C. Rautenberg, J. Grosse, M. Schoenfelder, Significant increase of salivary testosterone levels after single therapeutic transdermal administration of testosterone: suitability as a potential screening parameter in doping control, Drug Test. Anal. 5 (2013) 819–825.
[28] M. Schönfelder, H. Hofmann, T. Schulz, T. Engl, D. Kemper, B. Mayr, C. Rautenberg, R. Oberhoffer, D. Thieme, Potential detection of low-dose transdermal testosterone administration in blood, urine, and saliva, Drug Test. Anal. 8 (2016) 1186–1196.

[29] P. Celec, D. Ostatníková, Saliva collection devices affect sex steroid concentrations, Clin. Chim. Acta 413 (2012) 1625–1628.
[30] T. Fusayama, T. Katayori, S. Nomoto, Corrosion of gold and amalgam placed in contact with each other, J. Dent. Res. 42 (1963) 1183–1197.
[31] K. Maaz, A. Mumtaz, S.K. Hasanain, A. Ceylan, Synthesis and magnetic properties of cobalt ferrite ($CoFe_2O_4$) nanoparticles prepared by wet chemical route, J. Magn. Magn. Mater. 308 (2007) 289–295.
[32] M. Abdel-Rehim, S. Pedersen-Bjergaard, A. Abdel-Rehim, R. Lucena, M. Mahdi, S. Cárdenas, M. Miró, Microextraction approaches for bioanalytical applications: an overview, J. Chromatogr. A 1616 (2020), 460790.
[33] T.S. Breusch, A.R. Pagan, A simple test for heteroscedasticity and random coefficient variation, Econometrica 47 (1979) 1287–1294.

A high-throughput magnetic-based pipette tip microextraction as an alternative to conventional pipette tip strategies: determination of testosterone in human saliva as a proof-of-concept

José Grau, Juan L. Benedé, Alberto Chisvert*, Amparo Salvador

Department of Analytical Chemistry, University of Valencia, 46100 Burjassot, Valencia, Spain

* Corresponding author:

e-mail address: alberto.chisvert@uv.es

Table of contents

Sorbent characterization

Instruments for sorbent characterization. A Quantum Design (CA, USA) MPMS-XL-5 superconducting quantum interference device (SQUID) magnetometer was used to measure the magnetic properties of the composite material.

A HITACHI S-4800 scanning electron microscopy (SEM), operating at 10 kV and equipped with an RX Bruker backscattered electron detector, was used to observe the morphology. Nitrogen adsorption-desorption isotherms were measured on an ASAP 2010 analyser from Micromeritics (GA, USA), in order to determine the surface area and pore size.

Zeta potential measurements in order to determine the surface charge of the synthetized composite material were performed using a Malvern Zetasizer ZS instrument.

Thermogravimetric analysis (TGA) was accomplished using a PerkinElmer TGA-7 thermobalance.

Magnetization curves. Magnetism is an important factor when this new approach is applied. If the material is not magnetic enough, the retrieval of the composite is slow and increases the analysis time. Fig S1 shows the magnetization curve for $CoFe_2O_4$-C18 composite. The saturation magnetization (Ms) value for this composite was 5.26 emu g^{-1}, the residual magnetism (Br) was 1.37 emu g^{-1} and the coercivity (Hc) was 408 Oe.

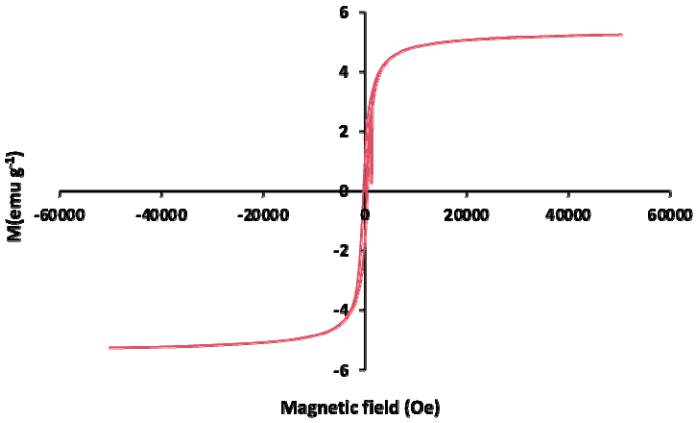

Fig S1. Magnetization curve for $CoFe_2O_4$-C18 sorbent.

Compared with previous works of the research group [1], where the magnetism of the naked $CoFe_2O_4$ MNPs was measured, values of Ms around 60 emu g^{-1} were obtained. These huge differences between the two materials can be easily explained by the small amount of MNPs that have been embedded on the C18 microparticles surface (ratio C18:MNPs 10:1). However, the levels of magnetism obtained for the $CoFe_2O_4$-C18 composite are more than enough to be retrieved by the inner magnet.

Morphology. Morphology of the $CoFe_2O_4$-C18 was studied by SEM operating at 10 kV. Results are shown in Fig. S2, where it can be observed the irregular blocks of C18 commercial polymer (Fig. S2a) and how the MNPs are embedded on its surface (Fig. S2b and S2c), conferring magnetic properties on it.

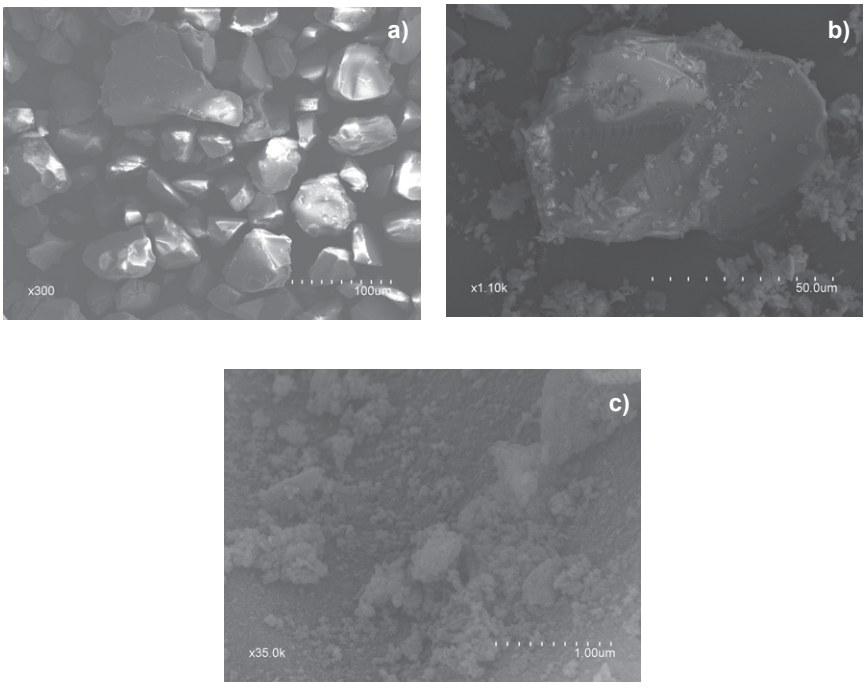

Fig S2. a) SEM micrograph of C18 microparticles (magnification 300); b) SEM micrograph of $CoFe_2O_4$-C18 composite (magnification 1100); c) SEM micrograph of $CoFe_2O_4$-C18 composite (magnification 35000).

On the other side, the adsorption capacity of the material was studied. As can be seen in Fig. S3, the isotherm shows a Type IV behaviour, which demonstrates the presence of mesopores with an average pore diameter of 6.3 nm**.** The BET surface area obtained was 233.8 ± 0.7 m^2 g^{-1}.

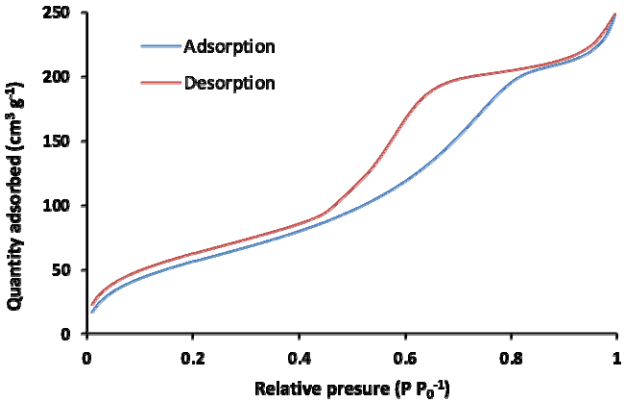

Fig S3. Isotherm linear plot of the $CoFe_2O_4$-C18 composite.

Zeta potential. The surface charge of the composite was studied at the extraction conditions (35 µL of MeOH as disperser solvent and 500 µL of synthetic saliva as donor phase). The resultant value was -6.9 ± 0.9 mV. At these conditions the MNPs of the surface of the composite are charged positively [2], however the C18 is negatively charged [3]. As a consequence, the resultant value was slightly negative.

Thermogravimetric analysis (TGA). Results obtained in Fig S4 shows how the weight is drastically reduced up to 75% from 200 to 550 ºC, owing to the progressive elimination of the C18 chains bonded to silica microparticles.

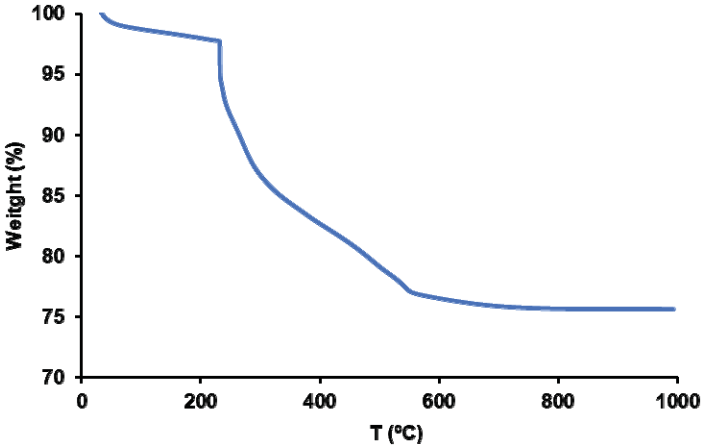

Fig S4. TGA of the $CoFe_2O_4$-C18 composite.

Inter-batch repeatability of $CoFe_2O_4$-C18 magnetic sorbent. In order to study the repeatability of the synthesis process, three different batches of $CoFe_2O_4$-C18 were synthesized and applied to the optimized extraction process. These batches were employed to extract the same concentration of testosterone (i.e., 1 μg L^{-1}) in synthetic saliva. As can be seen in Fig. S5, non-significant differences were observed employing any of the three batches, confirming the good repeatability of the synthesis process. Results are presented as relative area, which was established by dividing each area by the maximum area obtained in each experiment (as %).

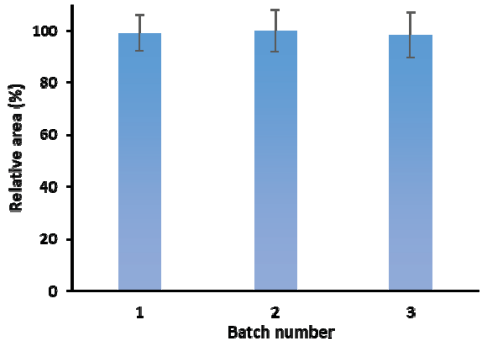

Fig. S5. Study of the inter-batch repeatability. Errors bars show the standard deviation (N=3).

Extraction efficiency of $CoFe_2O_4$-C18 magnetic sorbent. Firstly, a complete extraction process was performed with a bare neodymium magnet, just to prove that this one does not participate actively in the extraction process. The experiment was performed by triplicate, and no signal after the whole process was observed, thus proving that the magnet is not involved in the extraction.

On the other side, from Fig. S2, it can be noticed that the C18 surface is partially covered by the MNPs, which could influence the extraction process. In this regard, different extraction experiments were separately performed with 1 mg of $CoFe_2O_4$ MNPs, 1 mg of C18 microparticles and 1 mg of $CoFe_2O_4$-C18 composite.

For the magnetic composite and the MNPs, the experimental process was the same as described in the Section 2.8. For the extraction with C18, as it is not a magnetic material, it was necessary to perform various centrifugation steps to separate the sorbent during the extraction, clean-up and desorption steps. In this sense, 1 mg of C18 microparticles were weighed and dispersed in MeOH. Later, sample was dispensed. In this case, for its isolation, the suspension was centrifuged 5 min at 6000 rpm. Then the supernatant was discarded and the C18 was washed with 500 µL of water. After that, another centrifuge step was needed (5 min, 6000 rpm). Finally, the desorption was performed by two aspirating-dispensing cycles with 35 µL of MeOH and again centrifuged (5 min, 6000 rpm). The supernatant was then introduced into the chromatographic vial.

As it can be seen in Fig. S6, non-significant differences were observed between using C18 and the magnetic composite. However, the reduction of analysis time employing a magnetic sorbent was considerable due to its magnetic behaviour facilitating its handling. On the other hand, a minimum signal was found when the extraction was performed with only bare MNPs as extraction phase. As expected, these results show that the extraction was accomplished by C18, and the $CoFe_2O_4$ MNPs embedded on the surface of the C18 just provided the magnetic behaviour to handle it.

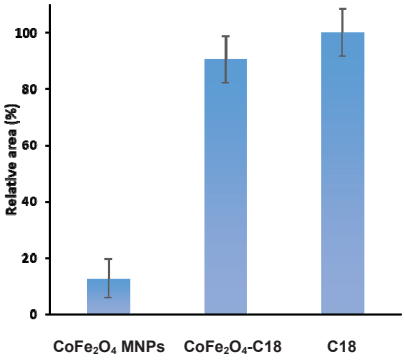

Fig. S6. Study of the extraction efficiency of the $CoFe_2O_4$-C18 magnetic composite. Errors bars show the standard deviation (N=3).

Optimization of extraction variables

Each variable was studied during the same working session. Results are presented as relative area, which was established by dividing each area by the maximum area obtained in each group of experiment (as %). Relative peak area is proportional to the extracted amount and thus to the extraction efficiency, and it shows how a change in a variable affects relatively with respect to the optimum value.

Amount of composite. Three different amounts of $CoFe_2O_4$-C18 magnetic composite (i.e., 1, 2 and 5 mg) were tested. As can be seen in Fig. S7a, no significant differences were observed between 1 and 2 mg. However, an important decrease of the signal was observed when 5 mg of composite were employed. In the latter case, a substantial part of the sorbent was not retrieved during the deposition on the magnet and it was discarded with the rest of the sample, thus loosing part of the extracted analyte. However, when working with 1 or 2 mg most of the sorbent was easily retrieved. In this sense, 1 mg was selected in order to reduce the amount of composite.

Extraction time and dispensing cycles. The number of dispensing cycles was found to have a minimum influence, and one cycle provided the same extraction efficiency than five (data not

shown). As it can be observed in Video S1, this first cycle is enough to produce the dispersion of the composite, increasing the extraction kinetics hugely.

Moreover, it was also studied how the extraction time (i.e., the time that the dispersion of the sorbent in the donor phase is maintained unaltered) could affect the extraction. As can be seen in Fig. S7b, the longer the extraction time, the less the extraction performance. As the dispersion is only stable during a few seconds, higher times than 1 min produced the deposition of the material on the bottom of the plate, hindering its retrieval and thus loosing part of the target compound.

Disperser solvent volume. Different volumes of MeOH (i.e., 25, 35, 50 and 100 µL) to enhance the dispersion of the sorbent in the donor solution were studied. As it can be seen in Fig. S7c, there were not significant differences, except for 100 µL where the signal decreased. It could be attributed to high amounts of organic solvent affect the partition coefficient of testosterone thus triggering more affinity of testosterone for the liquid phase (donor solution plus disperser solvent) rather than for the sorbent. Based on these results, 35 µL was selected for further experiments, as the dispersion with 25 µL was sometimes not achieved correctly.

Ionic strength. Different amounts of NaCl (0, 0.2, 0.5 and 1% (w/v)) were tested. A maximum value was observed at 0.2% (w/v) (Fig. S7d), due to the salting-out effect. Higher ionic strength values hindered the proper dispersion of the composite, decreasing the amount of testosterone extracted. In a previous work [4], it was found that the salt content of the saliva samples was between 0.12 and 0.35%. For that reason, no additional salt was added to the samples.

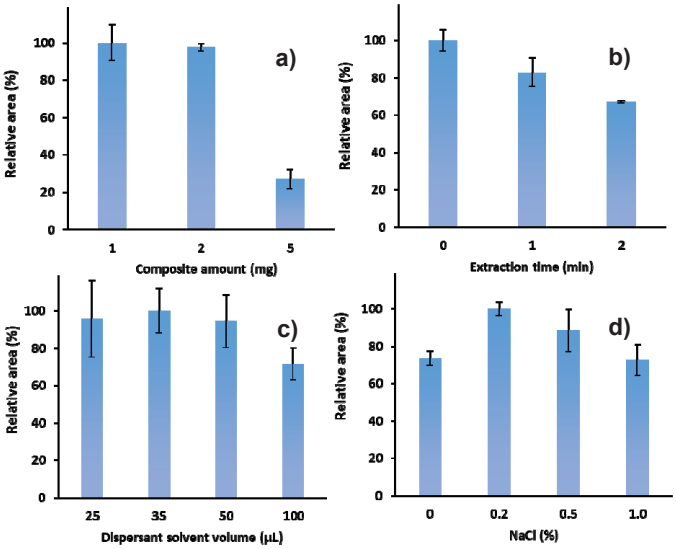

Fig. S7. Optimization of the extraction variables: a) Composite amount; b) Extraction time; c) Disperser solvent volume; d) Amount of NaCl. Errors bars show the standard deviation (N=3).

Sample dispensing speed. Some tests were performed in order to study the influence of the sample dispensing speed. Since it is a parameter with several difficulties to be measured, it was unmanageable to stablish an accurate value. Nevertheless, it can be said that low dispensing speeds (e.g., more than 1 second for the dispensation) did not achieve a correct dispersion of the sorbent. Thereby, it is necessary to increase the speed by means of a quick pulse as it is shown in Video S1.

Optimization of desorption variables

As can be seen in Fig. S8a, when higher volumes of MeOH were employed, more dilution was applied and thus the signal decreased. No significant differences were obtained between using 35 or 50 µL. However, in order to reduce the volume of organic solvents, 35 µL was selected. Lower volumes were not studied since it would have been difficult to reach the height of the magnet, not allowing analytes to be desorbed.

On the other hand, the number of aspirating/dispensing cycles during the desorption process was also studied. In this sense, 1, 2, 5 and 10 cycles were tested and, as can be observed in Fig. S8b, one cycle was not enough to complete the desorption of the testosterone. However, there was not a significant difference from 2 to 10 cycles, so the minimum number of cycles (i.e., 2 cycles) was selected.

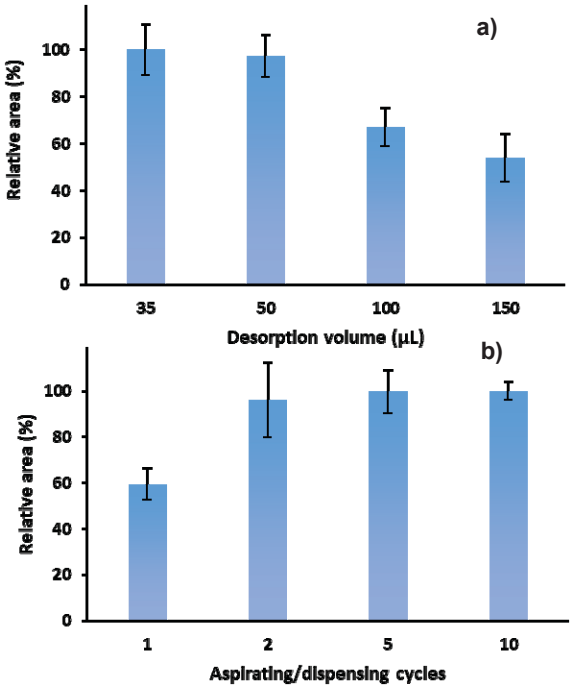

Fig. S8. Optimization of the desorption variables: a) Desorption solvent volume; b) Number of aspirating/dispensing cycles. Errors bars show the standard deviation (N=3).

Chromatogram

A chromatogram obtained for a saliva sample (volunteer 1) by applying the proposed method is included in Fig. S9.

Some robustness considerations should be mentioned about the LC-MS/MS methodology (data not shown). Parameters such as the flow rate (0.15 – 0.3 mL min^{-1}) and the column temperature (25 – 45 ºC) can modify the retention time and the peak shape, however the signals are not

significantly affected. The composition of the mobile phase has more influence, since the presence of buffer salts such as ammonium acetate increased the analytical signal compared with those mobile phases with just formic acid. Finally, the concentration of the ammonium acetate does not affect the signal between 2 and 10 mM.

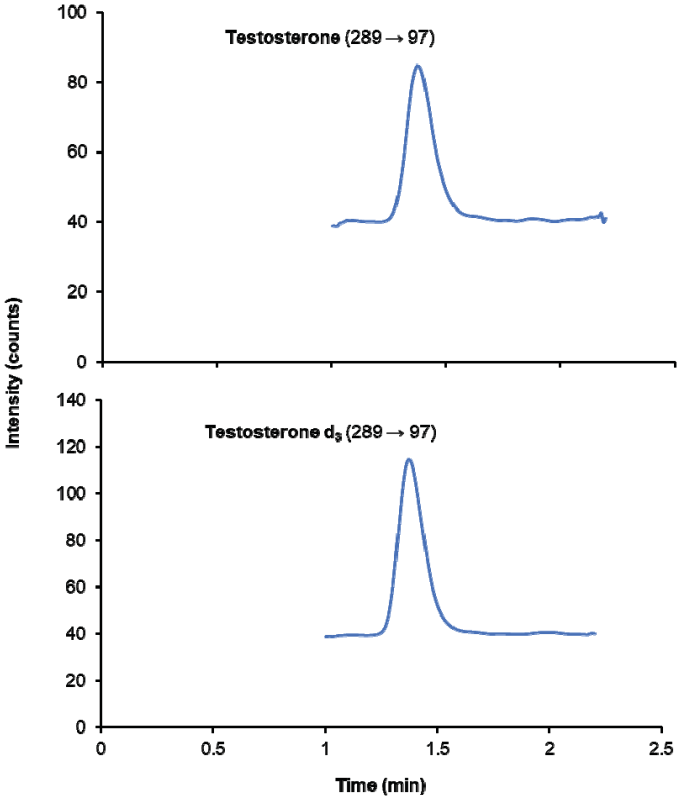

Fig S9. Chromatogram obtained for a saliva sample (volunteer 1) by applying the proposed method.

PT-SPE and DPX processes

PT-SPE. Pipette tips for PT-SPE were lab-made by introducing 1 mg of C18 between two SPE frites. For PT-SPE process, 35 µL of MeOH as conditioning solvent was used. After that, sample was aspirated and discarded once. Then, one aspirating/dispensing cycle with water

was employed for clean-up purposes, and two cycles with 35 µL of MeOH were used for desorption.

DPX process. For DPX, commercial tips with 1 mg of sorbent were employed. First, 300 µL of MeOH were aspirated and dispensed to collect all the sorbent that was on the upper parts of the pipette tip. Then, the sample was aspirated and the dispersion was performed. Finally, the sample was discarded, and one clean up step with 500 µL of ultra-pure water and two desorption cycles with 35 µL of MeOH were employed.

References

[1] A. Duque, J. Grau, J.L. Benedé, R.M. Alonso, M.A. Campanero, A. Chisvert, Low toxicity deep eutectic solvent-based ferrofluid for the determination of UV filters in environmental waters by stir bar dispersive liquid microextraction, Talanta. 243 (2022) 123378.

[2] A. Zielińska-Jurek, Z. Bielan, S. Dudziak, I. Wolak, Z. Sobczak, T. Klimczuk, G. Nowaczyk, J. Hupka, Design and application of magnetic photocatalysts for water treatment. The effect of particle charge on surface functionality, Catalysts. 7 (2017) 360.

[3] K. Krzemińska, S. Bocian, R. Pluskota, B. Buszewski, Surface properties of stationary phases with embedded polar group based on secondary interaction, zeta potential measurement and linear solvatation energy relationship studies, J. Chromatogr. A. 1637 (2021) 461853.

[4] J. Grau, J.L. Benedé, A. Chisvert, A. Salvador, Modified magnetic-based solvent-assisted dispersive solid-phase extraction: application to the determination of cortisol and cortisone in human saliva, J. Chromatogr. A. 1652 (2021) 462361.

Analysis of microsamples by miniaturized magnetic-based pipette tip microextraction: determination of free cortisol in serum and urine from very low birth weight preterm newborns

Enviado y pendiente de publicación

Analytica Chimica Acta

Analysis of microsamples by miniaturized magnetic-based pipette tip microextraction: determination of free cortisol in serum and urine from very low birth weight preterm newborns

--Manuscript Draft--

Manuscript Number:	
Article Type:	Full Length Article
Section/Category:	EXTRACTION & SAMPLE HANDLING
Keywords:	Magnetic immunosorbent; LC-MS/MS; Neonatal samples; Cortisol; Dispersive-based microextraction; Microsample
Corresponding Author:	Alberto Chisvert, Ph.D. University of Valencia: Universitat de Valencia Burjassot, Vaencia SPAIN
First Author:	José Grau
Order of Authors:	José Grau
	María Moreno-Guzmán
	Luis Arruza
	Miguel Ángel López
	Alberto Escarpa
	Alberto Chisvert, Ph.D.
Manuscript Region of Origin:	SPAIN
Abstract:	Miniaturized magnetic-based pipette tip microextraction is presented as a sample preparation approach for microsamples. It consists of the quick dispersion of a tiny amount of a magnetic sorbent material in a low-volume sample (10 µL) to entrap the target analytes. Next, the dispersion is aspirated using a (semi)automatic pipette through a pipette tip with a small cubic neodymium magnet inside that retrieves the magnetic sorbent containing the analytes. After discarding the rest of the sample, the sorbent is properly rinsed by aspirating/dispensing water, and then, the analytes are eluted by aspirating/dispensing an appropriate solvent. This approach was employed for the determination of free cortisol in serum and urine from very low birth weight preterm newborns, a vulnerable patient group who present low availability for sampling biological fluids. A magnetic immunosorbent made of cortisol antibody was employed for the selective extraction, followed by liquid chromatography-tandem mass spectrometry. Good analytical features were obtained, such as limits of detection and quantification of 0.08 and 0.27 ng mL-1 respectively, RSDs values under 15% and relative recoveries between 91-111%. The cross-reactivity of the used antibody was evaluated to show the selectivity of the method. Finally, the method applicability was demonstrated towards the determination of free cortisol in serum and urine samples from low weight birth preterm newborns.
Suggested Reviewers:	Elia Psillakis Technical University of Crete epsillakis@tuc.gr Prof. Psillakis have a lot of experience with the use microextraction approaches in different kind of matrices
	Audrey Combès audrey.combes@espci.fr Dr. Combès has published several works about the use of microextraction techniques in biological samples
	Antonio Martín-Esteban National Institute for Agricultural and Food Research and Technology amartin@inia.csic.es

	Victoria Samanidou Aristotle University of Thessaloniki samanidu@chem.auth.gr
	Jared L Anderson Iowa State University andersoj@iastate.edu Prof. Anderson works with different kind of sorbent for the analysis of multiple kind of samples
	Verónica Pino University of La Laguna veropino@ull.edu.es Prof. Pino has published many papers related with microextraction techniques most of them in biological samples

Analysis of microsamples by miniaturized magnetic-based pipette tip microextraction: determination of free cortisol in serum and urine from very low birth weight preterm newborns

José Grau[a], María Moreno-Guzmán[b], Luis Arruza[c], Miguel Ángel López[d,e], Alberto Escarpa[d,e*] Alberto Chisvert[a,*]

[a] GICAPC Research Group, Department of Analytical Chemistry, University of Valencia, 46100 Burjassot, Valencia, Spain

[b] Department of Chemistry in Pharmaceutical Sciences, Analytical Chemistry, Faculty of Pharmacy, Complutense University of Madrid, Plaza Ramón y Cajal s/n, 28040 Madrid, Spain

[c] Division of Neonatology, Child and Teenager Institute, Clínico San Carlos Hospital IdISCC, Madrid, Spain

[d] Department of Analytical Chemistry, Physical Chemistry and Chemical Engineering, University of Alcala, Ctra. Madrid-Barcelona, Km. 33.600, Alcalá de Henares, 28802 Madrid, Spain

[e] Chemical Research Institute "Andres M. Del Río", University of Alcala, Ctra. Madrid-Barcelona, Km. 33.600, Alcala de Henares, 28802 Madrid, Spain

ABSTRACT

Miniaturized magnetic-based pipette tip microextraction is presented as a sample preparation approach for microsamples. It consists of the quick dispersion of a tiny amount of a magnetic sorbent material in a low-volume sample (10 µL) to entrap the target analytes. Next, the dispersion is aspirated using a (semi)automatic pipette through a pipette tip with a small cubic neodymium magnet inside that retrieves the magnetic sorbent containing the analytes. After discarding the rest of the sample, the sorbent is properly rinsed by aspirating/dispensing water, and then, the analytes are eluted by aspirating/dispensing an appropriate solvent. This approach was employed for the determination of free cortisol in serum and urine from very low birth weight preterm newborns, a vulnerable patient group who present low availability for sampling biological fluids. A magnetic immunosorbent made of cortisol antibody was employed for the selective extraction, followed by liquid chromatography-tandem mass spectrometry. Good analytical features were obtained, such as limits of detection and quantification of 0.08 and 0.27 ng mL^{-1} respectively, RSDs values under 15 % and relative recoveries between 91-111 %. The cross-reactivity of the used antibody was evaluated to show the selectivity of the method. Finally, the method

applicability was demonstrated towards the determination of free cortisol in serum and urine samples from low weight birth preterm newborns.

Keywords: Magnetic immunosorbent, LC-MS/MS, Neonatal samples, Cortisol, Dispersive-based microextraction, microsample

*Corresponding authors:

Email addresses: alberto.chisvert@uv.es (A. Chisvert); alberto.escarpa@uah.es (A. Escarpa)

1. Introduction

The analysis of biological samples is usually a challenge. First of all, because of the complexity of the matrices that need a rigorous sample treatment and, secondly, the sample volume limitation to guarantee the health of the patient under study [1,2]. This becomes specially struggling in the diagnosis of pathologies of critical ill patients and/or newborns, even more in those with very low birth weight [3,4]. Due to the fragility of these groups, the sample amount available is reduced drastically to a few microliters. To this regard, the development of analytical methodologies to handle low-volume samples are demanded.

Microextraction techniques do not completely solve this problem, since the efforts on this field have been traditionally focused on the miniaturization of the amounts of sorbents and/or on the volumes of organic solvents employed, leaving aside the reduction of the sample volume. Nevertheless, the reduction of the extracting phase enables, indirectly, the reduction of the sample volume but not to the level that is required in the scenarios commented above. Furthermore, it should be said, that reducing the sample volumes presents also benefits according to the Green Analytical Chemistry [5] and Green Sample Preparation principles [6] (i.e., minimizing extractant amounts, reducing analysis times and creating portable devices for on-site sample preparation).

At this point, it is worth to emphasize that a few methodologies have been adapted to work with small sample amounts. Between them, it should be mentioned pipette tip-based solid phase extraction (PT-SPE) [7], dispersive pipette tip extraction (DPX) [8,9] and, more recently, magnetic-based pipette tip microextraction [10]. These approaches are characterized by being intuitive for the operator, just needing aspirating/dispensing cycles with a (semi)automatic pipette to produce the extraction of the analytes and easily discard the sample for further steps (i.e., washing and desorption).

Nevertheless, all these pipette tip-based approaches normally work with volumes between 0.2-5 mL, amounts that, despite of being quite low, are not recommendable in case of critical ill patients, especially when newborns are involved. In this regard, the main objective of the present work was to develop a miniaturized version of the magnetic-based pipette tip microextraction for the analysis of microsamples (10 µL). For this purpose, a simple device, consisting of a cubic

neodymium magnet incrusted in a conventional pipette tip, is designed. It is easy to build, affordable and portable for the performance of on-site sample preparation. Moreover, the quickness of the method allows to perform several analysis in a small amount of time, increasing the sample throughput and allowing the implementation in point-of-care analysis for the obtention of faster diagnosis [11]. To show the real applicability of this device, the determination of free cortisol in serum and urine from low weight birth preterm newborns, where the amount of sample is extremely limited, has been selected as a proof-of-concept.

It should be said that serum cortisol is a good biomarker of adrenal malfunction in critically ill patients. Preterm neonates are at high risk of developing absolute or relative adrenal insufficiency in the first weeks of life. This blunted response to situations of stress, such as sepsis, is the main underlying factor in the pathophysiology of severe arterial hypotension unresponsive to vasopressor therapy [12]. In these sick babies, treatment with corticosteroids can contribute to normalise blood pressure and facilitate weaning from vasopressors. Diagnosis of this emergency situation is challenging and ideally requires the demonstration of low baseline cortisol levels and an insufficient response to adrenocorticotropin hormone (ACTH) stimulation (<12% increase from baseline) [13]. However, the need for relatively large blood sample volumes and the long processing times frequently makes the diagnosis of this condition impractical prior to initiation of treatment. Therefore, steroid therapy is usually started before or even without laboratory results. This strategy is not without risks because given the potential side effects of postnatal steroids in the preterm infant, they should only be used if clearly indicated. A similar situation can be found in adult patients with septic shock. In this scenario, treatment with steroids is indicated when fluid resuscitation and vasopressors do not restore hemodynamic stability [14]. While only unbound cortisol is active, the levels of serum cortisol have been traditionally obtained through the determination of total cortisol [15], being the most bonded to cortisol-binding globulin (CBG) [16]. In recent years, determination of free cortisol has been proposed as a better alternative for the diagnosis of adrenal insufficiency in critical ill patients. In this purpose, different alternatives have been employed to separate the bounded cortisol from the sample, being the ultrafiltration one of the easiest and most employed methodologies [17]. One of the few studies available that measured free cortisol in sick preterm infants found a reference value of 1.37 ng mL^{-1} for this

population [18]. On the other hand, the analysis of urinary free cortisol (UFC), may be a good biomarker for the diagnosis of Cushing's syndrome [19].

These analysis have been commonly performed by means of immunoassays [20]. However, some immunosorbents could present cross-reactivity with similar compounds obtaining non-specific signals as it has been discussed by Raff et al. [21]. In the case of the determination of cortisol, there is a possible cross-reactivity due to the structural similitudes with other glucocorticoids (e.g. cortisone).

All this motivated us to develop a fast and reliable analytical method with the aim of finding a quick diagnosis in these fragile patients from which urine, and specially serum, are scarce. Thus, a miniaturized version of magnetic-based pipette tip microextraction with a magnetic immunosorbent made of cortisol antibody followed by liquid chromatography-tandem mass spectrometry (LC-MS/MS) is proposed.

2. Experimental

2.1. Reagents and samples

All reagents and solvents were purchased from major suppliers. Cortisol (1 mg mL^{-1} in methanol) was obtained from Sigma Aldrich (Steinheim, Germany). For the magnetic immunosorbent, a suspension of 30 mg mL^{-1} Dynabeads® (magnetic beads, MBs) covered with protein G were obtained from Thermo Fisher Scientific (Waltham, MA, USA), whereas cortisol antibody 4.35 mg mL^{-1} was purchased from East Coast Bio (Maryland Heighs, MO, USA).

For buffer preparation, sodium chloride (NaCl) was obtained from Fischer Chemicals (Loughborough, UK), sodium dihydrogen phosphate monohydrate ($NaH_2PO_4 \cdot H_2O$) and di-sodium hydrogen phosphate dodecahydrate ($Na_2HPO_4 \cdot 12H_2O$) were acquired from Scharlau (Barcelona, Spain), potassium chloride (KCl) was purchased from Panreac (Barcelona, Spain) and Tween 20 was obtained from Sigma-Aldrich (Steinheim, Germany). Finally, sodium hydroxide (NaOH) from Scharlau (Barcelona, Spain) was employed to adjust the pH.

LC-MS grade methanol (MeOH) from Honeywell (Seelze, Germany), LC-MS grade water from Panreac (Barcelona, Spain) and ammonium fluoride (for mass spectrometry) from Acros Organics (Geel, Belgium) were employed to prepare the mobile phase. Nitrogen used as nebulizer and

curtain gas in the MS/MS ion source was obtained by a NiGen LCMS 40-1 nitrogen generator from Claind S.r.l. (Lenno, Italy). On the other side, extra pure nitrogen (>99.999%), used as collision gas in the MS/MS collision cell, was provided by Praxair (Madrid, Spain).

2.2. Apparatus and materials

Strata X™-RP cartridges for the preparation of blank samples were obtained from Phenomenex (Torrance, USA). Ultrafiltration tubes (0.5 mL, 30 kDA cut-off) for sample pre-treatment were obtained from Sigma Aldrich (Steinheim, Germany).

A Basic 20 pH meter from Crison (Alella, Spain) was used for the adjustment of pH.

An IMMULITE 2000 immunoassay system from Siemens Healthcare (Munich, Germany) was employed for the analysis of total cortisol.

A TS-100 thermo-shaker purchased from Biosan (Riga, Latvia) was employed for the immunosorbent preparation.

For the extraction devices, cubic neodymium magnets (1 x 1 mm) from Supermagnete (Gottmadingen, Germany) and 1-200 µL pipette tips from VWR (Radnor, PA, USA) were acquired.

An Agilent 1100 Series chromatography system comprised of a degasser, a programmable pump, an autosampler and a thermostatic column oven with a Zorbax SB-C18 (50 mm length, 2.1 mm I.D., 1.8 µm) column, coupled to an Agilent 6410B Triple Quad MS/MS was employed throughout the study.

2.3. Sample collection and pre-treatment

Serum and urine samples from a healthy adult volunteer were employed in the development and validation of the method. Serum and urine samples from healthy preterm neonates were provided by the Clínico San Carlos Hospital (Madrid, Spain), and parental informed consent was obtained before the collections of samples. The premature newborns were included in this study because their samples were needed as part of the standard care in the intensive care unit and not for the only purpose of the present study. This study was approved by the Ethics Committee of both University of Valencia and the Clínico San Carlos Hospital. Total cortisol was measured in the hospital laboratory to obtain reference values. Serum volume required was 10 µL but at least 100

µL more were needed for the sample cup. Although results can be obtained in 30 minutes, hospital samples are analyzed once daily, therefore results can be delayed for several hours.

For the analysis of free cortisol, blood samples were first centrifuged (15 min, 6000 rpm) in order to isolate the serum. Serum was then ultrafiltrated (30 kDA cut-off, 10 min, 18000 rpm) to separate the non-free cortisol. After that, 50 µL of sample were treated with 25 µL of ACN to separate the low-molecular weight proteins present in serum. Finally, samples were centrifuged (5 min, 18000 rpm) and the supernatant was frozen at -80 ºC until its analysis.

On the other side, urine samples were centrifuged (5 min, 6000) rpm and kept at 4 ºC until its analysis.

2.4. Preparation of standard and samples

250 mL of phosphate buffered saline (PBS) solution 0.1 M (pH 7.2) was prepared. Bind and washing (B&W) solution (pH 8.2) for the preparation of the immunosorbent was prepared with Tween 20 (0.01% in PBS).

A standard solution of 100 µg mL^{-1} of cortisol was prepared in methanol and kept at -20ºC. 10 µL of this solution was employed to prepare a 1 µg mL^{-1} intermediate solution in PBS. Then, working solutions were prepared from 1-50 µg L^{-1} in PBS.

Samples for validation studies were obtained from a healthy adult volunteer and were treated with Strata X^{TM}-RP to remove the endogenous cortisol. First, cartridges were conditioned with 5 mL of MeOH and equilibrated with 10 mL of H_2O. Then, around 20 mL of sample were loaded and the percolated sample was frozen at -20ºC until the moment of the analysis.

2.5. Preparation of the immunosorbent

To prepare the immunosorbent, firstly, 1.5 µL of MBs (30 mg mL^{-1}) were added to a 0.5 mL microcentrifuge tube and washed with 50 µL of B&W, then the MBs were isolated by employing an external magnet and the supernatant was discarded. Afterwards, a solution of 10 µg mL^{-1} of cortisol antibody prepared in B&W solution was added and shaken at 1400 rpm at 25 ºC for 30 minutes. After this time, the immunosorbent was washed twice with 50 µL of PBS (pH 7.2).

The prepared immunosorbent proved to be stable at 4 ºC in PBS (pH 7.2) at least one week after being prepared. In this sense, several batches of immunosorbent can be prepared during the first day of the week and they can be employed during the whole week.

2.6. Scheme of the microextraction device

The microextraction was performed using a modified pipette tip. This one consists of a conventional pipette tip (2-200µL) with an internal cubic neodymium magnet (1 x 1 mm) incrusted. Compared with the previous designed device [10], there is no need of an external magnet to avoid the dragging of the internal magnet during the sample aspiration. The cubic geometry within the inverted conical shape of the tip allows to create channels between the magnet and the tip wall thus preventing clogging. A scheme of this device is presented in Fig. 1.

Once the microextraction has been finished, the neodymium magnet can be retrieved pushing it with a needle or a similar object.

2.7. Microextraction procedure

For the microextraction process 10 µL of standard or sample were first diluted with 50 µL of PBS. Then, 60 µL of the diluted standard or sample solution were aspirated by the microextraction device described in Section 2.5. After that, the solution was dispensed over the immunosorbent (prepared in Section 2.4). The resultant dispersion was kept unaltered between 30 and 60 s thus, within this time, it was aspirated by the microextraction device in such a way the magnetic immunosorbent containing the entrapped analyte was retained on the magnet. The sample solution was then discarded and the pipette tip containing the retained immunosorbent with cortisol was washed with 60 µL of water by two aspirating/dispensing cycles. Finally, 5 aspirating/dispensing cycles were performed with 10 µL of MeOH to desorb the analytes. Fig. 2 shows a scheme of the proposed method.

2.8. LC-MS/MS analysis

Before its introduction into the LC-MS/MS, the 10 µL of the methanolic extract were diluted with 2.5 µL of water to ensure a subsequent good analytical performance. Then, 5 µL were injected into the chromatographic system. Mobile phase was composed of solvent A (H_2O, 0.5 mM ammonium fluoride) and solvent B (MeOH), by isocratic elution employing a ratio of 30:70 (A:B)

(v/v). The flow rate was set as 0.15 mL min^{-1} and the column temperature was kept at 40 °C. The total run time was 2.5 min.

On the other side, triple quadrupole MS detector operated in positive electrospray ionization mode (ESI+), by multiple reaction monitoring (MRM). To measure cortisol, positive polarity (ESI+, capillary voltage at 5 kV) was used. The gas temperature was set at 350°C, nebulizer gas flow rate at 11 L min^{-1}, nebulizer gas pressure at 50 psi, collision energies at 21 V and fragmentor at 155 V, the dwell time used was 400 s. The m/z precursor → product ion transitions for quantification and for identification were 363 → 121 and 363 → 105, respectively.

3. Results and discussion

3.1. Optimization of the preparation of the immunosorbent

The immobilization time, the amount of antibody and MBs were studied to optimize the immunosorbent preparation. Each experiment was performed by triplicate extracting 60 µL of a solution of 10 ng mL^{-1} of cortisol prepared in PBS (pH 7.2). Results are expressed as relative area (%). Performance of each experiment were performed during the same working session.

As it can be seen in Fig. 3a, increasing the immobilization time did not increase the analytical signal. Thus, it can be concluded that 5 min was time enough to produce the immobilization of the antibody on the surface of the MBs and thus 5 min were selected.

The amount of MBs employed were also studied. In this case, looking at Fig. 3b the signal increases when 45 µg of MBS (i.e., 1.5 µL MBs suspension) were employed. However, there was no significant differences employing 45 or 60 µg. Higher amounts of MBS were not studied since the small magnet could not retain those amounts thus introducing solid particles into the LC-MS/MS. Consequently, the lesser amount (i.e., 45 µg) was selected for further experiments.

Finally, as it can be observed in Fig. 3c, increasing the amount of cortisol antibody until 10 µg mL^{-1} increases the extraction capacity of the immunosorbent. Nevertheless, higher amounts of cortisol antibody produce a diminution of the signal. Since all the protein G have interacted with the antibody, the molecules of antibody begin to interact between them reducing the active spots of the antibody and thus, decreasing the signal. According to these results, 10 µg mL^{-1} was selected, since provided the highest signal.

3.2. Optimization of the extraction/desorption variables

Once the preparation of the immunosorbent was concluded, different variables of the extraction/desorption method were studied. In this sense, the extraction time, the aspirating/dispensing cycles, and the desorption volume were tested. Each experiment was performed by triplicate extracting 60 µL of a solution of 10 ng mL^{-1} of cortisol prepared in PBS (pH 7.2).

The suspension of the immunosorbent in the sample was assayed at different times to see how the extraction/suspension time affected the extraction of cortisol. As it is observed in Fig. 4a, times between 30 and 60 s obtained the maximum signal. After this time, part of the sorbent begins to be deposited at the bottom of the microcentrifuge tube, making difficult its retrieval for further steps. According to these results, the minimum time (i.e., 30 s) was selected in order to reduce the total analysis time.

The desorption volume was also studied. Results in Fig. 4b show that, as it was expected, using more amount of desorption solvent (i.e., MeOH) caused a decrease in the signal. 10 µL was then selected since lower volumes were not recommended to ensure the correct intake of the injection volume by the LC-MS/MS instrument (i.e., 5 µL).

Finally, the number of aspirating/dispensing cycles were investigated. As it is shown in Fig. 4c, 2 cycles were not enough to produce a quantitative desorption. In this sense, 5 cycles were selected.

3.3. Analytical performance

The selectivity, working range, linearity, limit of detection (LOD) and limit of quantification (LOQ), the repeatability and the accuracy were studied to validate the analytical method.

Previously, some experiments were performed in blank urine and blank serum to study the presence of matrix effect. Huge matrix effect was observed for both matrices. Different dilution ratios with PBS (pH 7.2) were tested, thus showing that the matrix effect was negligible whit a 1:5 dilution ratio.

One of the advantages of working with LC-MS/MS is the possibility to study the cross-reactivity of the antibody, since some cortisol antibodies may interact with other glucocorticoids such as cortisone. To this end, the affinity of the immunosorbent with cortisol against other glucocorticoids,

a mixed solution of 10 ng mL^{-1} cortisone and prednisolone was prepared in PBS (pH 7.2) and then this solution was extracted with the proposed method. The LC-MS/MS method from a previous work [22] was employed for the simultaneous measurement of cortisol, cortisone and prednisolone. As can be seen in Fig. 5, no peaks were observed for cortisone and prednisolone, thus proving the good selectivity of the immunosorbent against cortisone and prednisolone.

The working range was set between 0.3 and 50 ng mL^{-1} to cover the expected content in both healthy children (ca. 1 ng mL^{-1}) and critical ill children (where the contents can be increased several times) [23]. In this range, good linearity was found with a regression coefficient (R^2) of 0.9990.

LOD and LOQ were obtained after the extraction of a 1 ng mL^{-1} of a PBS standard and calculating which concentration provided 3 (LOD) and 10 (LOQ) times the signal-to-noise ratio. Values were 0.08 ng mL^{-1} and 0.27 ng mL^{-1}, respectively.

For the study of repeatability, the RSD of five replicates extracted and analyzed during the same day (intraday), and five replicates in five different days (interday) at three levels of concentration (i.e., 1, 10 and 20 ng mL^{-1}) were measured. Values of RSD were under 10 % for intraday and under 15 % for interday.

Two blank samples (i.e., serum and urine) from a healthy adult were spiked at three levels of concentration (i.e., 1, 10 and 20 ng mL^{-1}) and analyzed by the proposed method under optimized conditions. Results are presented in Table 1 showing relative recoveries between 91 and 111% for both samples, thus showing no matrix effects.

3.4. Analysis of real samples

Finally, five serum and five urine samples from very low birth weight preterm infants were analyzed to obtain the levels of free cortisol. Results from serum cortisol were compared with the amount of total cortisol obtained in the Clínico San Carlos Hospital. Results are shown in Table 2. Fig. 6 shows the chromatogram obtained for a serum and for a urine sample from one of the preterm newborns participating in this study. Levels of free cortisol were found to be around one hundred times lower. It should be said that the determination of free cortisol levels by the proposed method makes use of different strategies to avoid potential interferences. On one side,

the ultrafiltration separates the bounded cortisol, thus ensuring that the signal obtained is only due to the free cortisol, whereas on the other side, the use of an immunosorbent in the extraction step followed by LC-MS/MS avoids the non-specific interferences. Additionally, the levels of urinary free cortisol were also measured in the same children, obtaining similar values between them. Our results are in agreement with previous studies in sick preterm infants [18] that found population reference values of 1.37 ng mL^{-1}. Urinary free cortisol levels were also in the normal range for newborn children [24] . Unfortunately, serum free cortisol was not measured in these newborns at the Clínico San Carlos Hospital and therefore comparison was not possible. Nevertheless, the total cortisol levels reported by the hospital were in accordance with reference values for this population [12].

4. Conclusions

In this paper, a miniaturized magnetic-based pipette-tip microextraction approach has been successfully developed as a new way for the analysis of small sample volumes (10 µL), thus opening new insights in the analysis of microsamples. This technique allows to reduce, not only the sample volume, but also the amount of organic solvents and sorbents, minimizing thus the quantity of wastes in accordance with the ten principles of Green Sample Preparation. The proposed method has been successfully validated and applied to the determination of free cortisol in serum and urine samples from low weight birth preterm newborns obtaining excellent results. The analysis of this kind of samples is critical due to the restricted volume available from these vulnerable patients. The combination of the employment of immunosorbents, LC-MS/MS and ultrafiltration have proved to eliminate the non-specific interaction and the interferences from non-free cortisol. In this sense, this new technique is an excellent strategy for the analysis of reduced sample volumes due to its simplicity, greenness, low price and quickness, thus offering a feasible tool in the diagnosis of disorders by means of the analysis of microsamples.

Acknowledgements

Grant PID2020-118924RB-I00 funded by Spanish Ministry of Science and Innovation (MCIN/AEI/ 10.13039/501100011033) is greatly appreciated. This article is based upon work from the National Thematic Network on Sample Treatment (RED-2018-102522-T) of the Spanish Ministry of Science, Innovation and Universities, and the Sample Preparation Study Group and Network

supported by the Division of Analytical Chemistry of the European Chemical Society. Authors are very grateful to Dr. María José Torrejón from Clínico San Carlos Hospital for processing the clinical samples and obtain the total cortisol levels.

Declaration of interest

The authors declare that they have no known competing financial interests or personal relationships that could have appeared to influence the work reported in this paper.

References

[1] M. Abdel-Rehim, S. Pedersen-Bjergaard, A. Abdel-Rehim, R. Lucena, M.M. Moein, S. Cárdenas, M. Miró, Microextraction approaches for bioanalytical applications: An overview, J. Chromatogr. A. 1616 (2020) 460790.

[2] Z. Niu, W. Zhang, C. Yu, J. Zhang, Y. Wen, Recent advances in biological sample preparation methods coupled with chromatography, spectrometry and electrochemistry analysis techniques, TrAC - Trends Anal. Chem. 102 (2018) 123–146.

[3] A. Molinero-Fernandez, M.A. Lopez, A. Escarpa, Electrochemical Microfluidic Micromotors-Based Immunoassay for C-Reactive Protein Determination in Preterm Neonatal Samples with Sepsis Suspicion, Anal. Chem. 92 (2020) 5048–5054.

[4] L. García-Carmona, M.C. González, A. Escarpa, Nanomaterial-based electrochemical (bio)-sensing: One step ahead in diagnostic and monitoring of metabolic rare diseases, TrAC - Trends Anal. Chem. 118 (2019) 29–42.

[5] A. Gałuszka, Z. Migaszewski, J. Namieśnik, The 12 principles of green analytical chemistry and the SIGNIFICANCE mnemonic of green analytical practices, TrAC - Trends Anal. Chem. 50 (2013) 78–84.

[6] Á.I. López-Lorente, F. Pena-Pereira, S. Pedersen-Bjergaard, V.G. Zuin, S.A. Ozkan, E. Psillakis, The ten principles of green sample preparation, TrAC - Trends Anal. Chem. 148 (2022) 116530.

[7] S. Seidi, M. Tajik, M. Baharfar, M. Rezazadeh, Micro solid-phase extraction (pipette tip and spin column) and thin film solid-phase microextraction: Miniaturized concepts for chromatographic analysis, TrAC - Trends Anal. Chem. 118 (2019) 810–827.

[8] D.C.M. Bordin, M.N.R. Alves, E.G. de Campos, B.S. De Martinis, Disposable pipette tips extraction: Fundamentals, applications and state of the art, J. Sep. Sci. 39 (2016) 1168–1172.

[9] E. Carasek, L. Morés, R.D. Huelsmann, Disposable pipette extraction: A critical review of concepts, applications, and directions, Anal. Chim. Acta. 1192 (2022) 339383.

[10] J. Grau, J.L. Benedé, A. Chisvert, A. Salvador, A high-throughput magnetic-based pipette tip microextraction as an alternative to conventional pipette tip strategies: Determination of testosterone in human saliva as a proof-of-concept, Anal. Chim. Acta. 1221 (2022) 340117.

[11] B.M. Cummins, F.S. Ligler, G.M. Walker, Point-of-care diagnostics for niche applications, Biotechnol. Adv. 34 (2016) 161–176.

[12] N. Kumbhat, S. Noori, Corticosteroids for Neonatal Hypotension, Clin. Perinatol. 47 (2020) 549–562.

[13] O. Hochwald, L. Holsti, H. Osiovich, The use of an early ACTH test to identify hypoadrenalism-related hypotension in low birth weight infants, J. Perinatol. 32 (2012) 412–417.

[14] L. Evans, A. Rhodes, W. Alhazzani, M. Antonelli, C.M. Coopersmith, C. French, F.R. MacHado, L. McIntyre, M. Ostermann, H.C. Prescott, C. Schorr, S. Simpson, W. Joost Wiersinga, F. Alshamsi, D.C. Angus, Y. Arabi, L. Azevedo, R. Beale, G. Beilman, E. Belley-Cote, L. Burry, M. Cecconi, J. Centofanti, A.C. Yataco, J. De Waele, R.P. Dellinger, K. Doi, B. Du, E. Estenssoro, R. Ferrer, C. Gomersall, C. Hodgson, M.H. Møller, T. Iwashyna, S. Jacob, R. Kleinpell, M. Klompas, Y. Koh, A. Kumar, A. Kwizera, S. Lobo, H. Masur, S. McGloughlin, S. Mehta, Y. Mehta, M. Mer, M. Nunnally, S. Oczkowski, T. Osborn, E. Papathanassoglou, A. Perner, M. Puskarich, J. Roberts, W. Schweickert, M. Seckel, J. Sevransky, C.L. Sprung, T. Welte, J. Zimmerman, M. Levy, Executive Summary: Surviving Sepsis Campaign: International Guidelines for the Management of Sepsis and Septic Shock 2021, Crit. Care Med. 49 (2021) 1974–1982.

[15] N. Molenaar, A.B. Johan Groeneveld, H.M. Dijstelbloem, M.F.C. De Jong, A.R.J. Girbes, A.C. Heijboer, A. Beishuizen, Assessing adrenal insufficiency of corticosteroid secretion using free versus total cortisol levels in critical illness, Intensive Care Med. 37 (2011) 1986–1993.

[16] I. Perogamvros, D.W. Ray, P.J. Trainer, Regulation of cortisol bioavailability - Effects on hormone measurement and action, Nat. Rev. Endocrinol. 8 (2012) 717–727.

[17] C.J. Pretorius, J.P. Galligan, B.C. McWhinney, S.E. Briscoe, J.P.J. Ungerer, Free cortisol method comparison: Ultrafiltation, equilibrium dialysis, tracer dilution, tandem mass spectrometry and calculated free cortisol, Clin. Chim. Acta. 412 (2011) 1043–1047.

[18] H.E. Vezina, C.M. Ng, D.M. Vazquez, J.D. Barks, V. Bhatt-Mehta, Population pharmacokinetics of unbound hydrocortisone in critically ill neonates and infants with vasopressor-resistant hypotension, Pediatr. Crit. Care Med. 15 (2014) 546–553.

[19] A. Luo, E.T.M. El Gierari, L.M. Nally, L.R. Sturmer, D. Dodd, R.Z. Shi, Clinical utility of an ultrasensitive urinary free cortisol assay by tandem mass spectrometry, Steroids. 146 (2019) 65–69.

[20] U. Turpeinen, E. Hämäläinen, Determination of cortisol in serum, saliva and urine, Best Pract. Res. Clin. Endocrinol. Metab. 27 (2013) 795–801.

[21] H. Raff, R.J. Auchus, J.W. Findling, L.K. Nieman, Urine free cortisol in the diagnosis of Cushing's syndrome: Is it worth doing and, if so, how?, J. Clin. Endocrinol. Metab. 100 (2015) 395–397.

[22] J. Grau, J.L. Benedé, A. Chisvert, A. Salvador, Modified magnetic-based solvent-assisted dispersive solid-phase extraction: application to the determination of cortisol and cortisone in human saliva, J. Chromatogr. A. 1652 (2021) 462361.

[23] P. Poomthavorn, R. Lertbunrian, A. Preutthipan, A. Sriphrapradang, P. Khlairit, P. Mahachoklertwattana, Serum free cortisol index, free cortisol, and total cortisol in critically ill children, Intensive Care Med. 35 (2009) 1281–1285.

[24] R. Wang, M.F. Hartmann, S.A. Wudy, Targeted LC–MS/MS analysis of steroid glucuronides in human urine, J. Steroid Biochem. Mol. Biol. 205 (2021) 105774.

Figure captions

Figure 1. Scheme of the microextraction device, showing a cross-section with the incrusted magnet and the channels.

Figure 2. Scheme of the proposed analytical method.

Figure 3. Optimization of the immunosorbent preparation a) Immobilization time; b) MBs amount; c) Antibody concentration. Errors bars show the standard deviation (N=3).

Figure 4. Optimization of the extraction and desorption variables: a) Extraction time; b) Volume of MeOH; c) Nº of dispersion aspirating/dispensing cycles. Errors bars show the standard deviation (N=3).

Figure 5. Chromatogram of a PBS solution spiked with 10 ng mL^{-1} of cortisol, cortisone and prednisolone after the magnetic-based pipette tip microextraction extraction method.

Figure 6. Chromatogram of urine and serum sample from a preterm newborn after the magnetic-based pipette tip microextraction method.

Fig. 1.

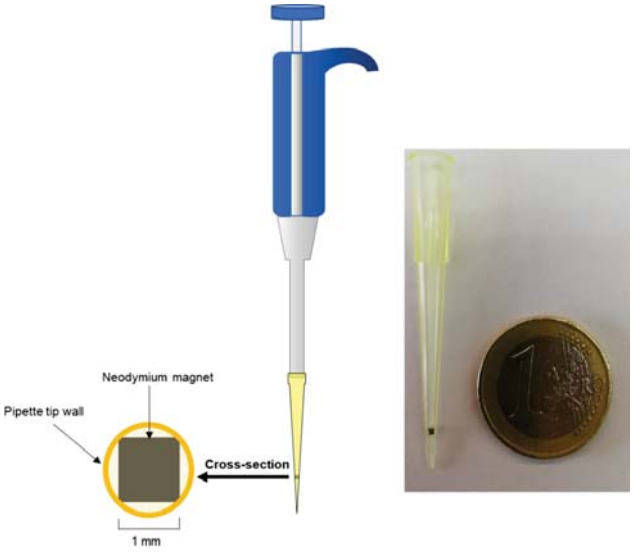

Fig. 2

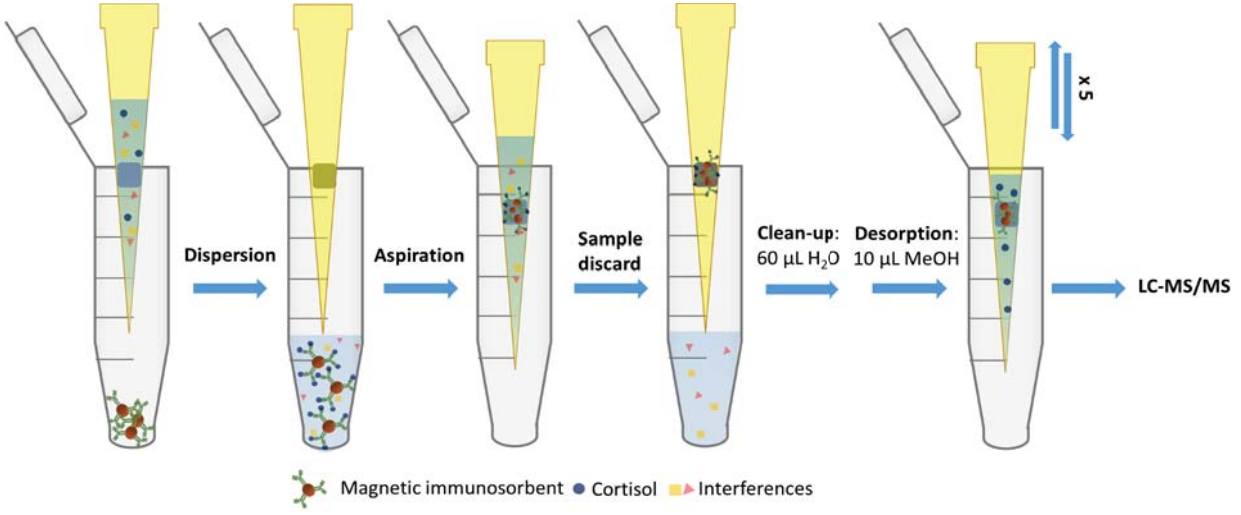
Dispersion
Aspiration
Sample discard
Clean-up: 60 µL H_2O
Desorption: 10 µL MeOH
x 5
LC-MS/MS
Magnetic immunosorbent
Cortisol
Interferences

Fig. 3.

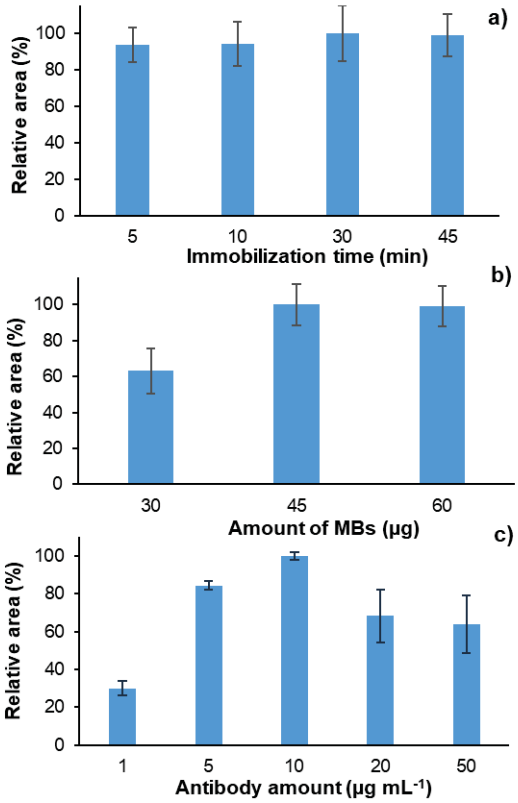
a)
Relative area (%)
0
20
40
60
80
100
5
10
30
45
Immobilization time (min)
b)
Relative area (%)
0
20
40
60
80
100
30
45
60
Amount of MBs (µg)
c)
Relative area (%)
0
20
40
60
80
100
1
5
10
20
50
Antibody amount (µg mL-1)

Fig. 4.

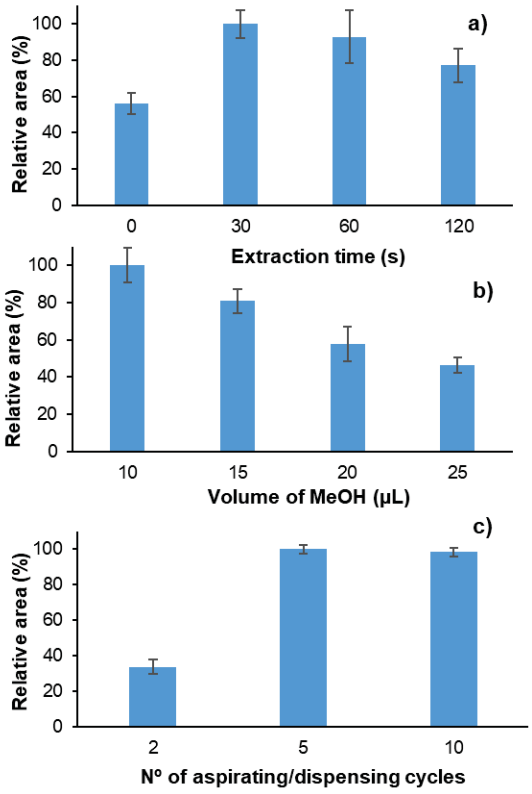
a)
Relative area (%)
100
80
60
40
20
0
0
30
60
120
Extraction time (s)
b)
Relative area (%)
100
80
60
40
20
0
10
15
20
25
Volume of MeOH (µL)
c)
Relative area (%)
100
80
60
40
20
0
2
5
10
Nº of aspirating/dispensing cycles

Fig. 5

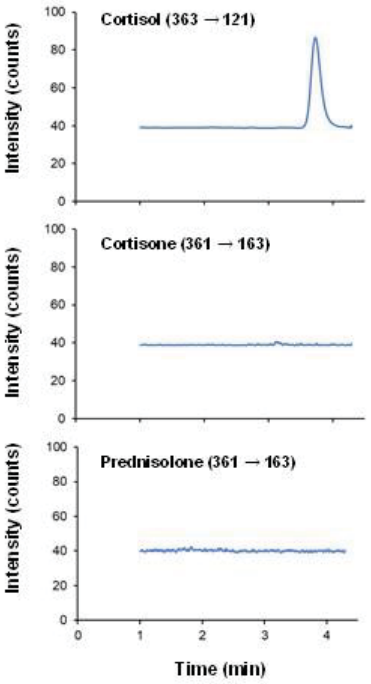
Cortisol (363 → 121)
Cortisone (361 → 163)
Prednisolone (361 → 163)
Intensity (counts)
Time (min)
0
20
40
60
80
100
1
2
3
4

Fig. 6

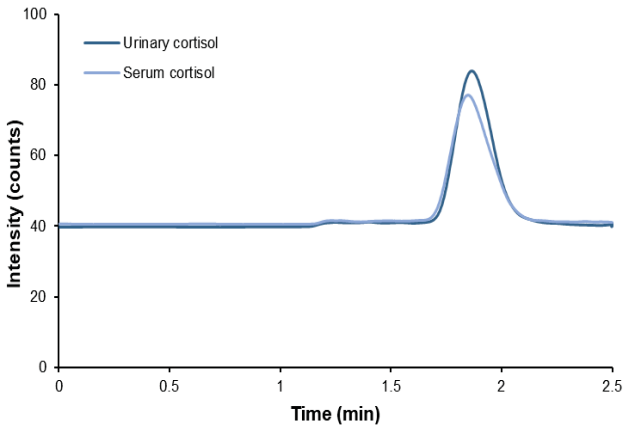
Urinary cortisol
Serum cortisol
Intensity (counts)
Time (min)
0
20
40
60
80
100
0
0.5
1
1.5
2
2.5

Table 1. Relative recoveries of the proposed method obtained from blank samples of serum and urine

Sample	Amount spiked (ng mL^{-1})	Relative recovery (%)
Serum	1	100 ± 12
	10	111 ± 2
	20	91 ± 7
Urine	1	97 ± 11
	10	110 ± 3
	20	91 ± 5

Table 2. Results obtained from five low weight birth preterm newborns

Patient	**Gestational age (weeks + days)**	**Birthweight (g)**	**Serum free cortisol (ng mL^{-1})**	**Serum total cortisol (ng mL^{-1})**	**Urinary free cortisol (ng mL^{-1})**
1	27+4	900	1.5 ± 0.2	106	2.9 ± 0.1
2	26+5	700	1.1 ± 0.1	126	0.49 ± 0.02
3	27+3	950	0.36 ± 0.04	60	0.63 ± 0.04
4	27+3	1100	1.39 ± 0.09	104	2.4 ± 0.2
5	27+5	930	1.0 ± 0.1	138	0.35 ± 0.05